THIRD AUSTRALIA – NEW ZEALAND CONFERENCE ON GEOMECHANICS

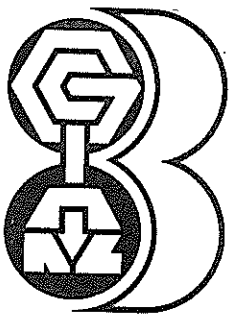

Wellington
May 12–16, 1980

Organised by
The New Zealand Geomechanics Society

Organisation Committee

CONVENOR

J. A. Webster
School of Architecture, Victoria University of Wellington.

FINANCE/NATIONAL COMMITTEE LIAISON

J. H. H. Galloway
Ministry of Works and Development, Wellington.

TECHNICAL PROGRAMME

M. J. Pender
Department of Civil Engineering, Auckland University.
G. Ramsay
Ministry of Works and Development, Wellington.

PUBLICITY

P. E. Salt
Ministry of Works and Development, Wellington.
T. J. Kayes
Tonkin and Taylor, Wellington.

SOCIAL PROGRAMME

P. Millar
Central Laboratories, Ministry of Works and Development, Lower Hutt.

Published by the New Zealand Institution of Engineers,
101 Molesworth Street, Wellington, New Zealand.

Printed by Bryce Francis Ltd, 11a Marion Street, Wellington.

Preface

The Third Australia New Zealand Conference on Geomechanics continues the sequence of conferences previously held in Melbourne (1971) and Brisbane (1975). The conference is related to the three main fields of geomechanics; soil mechanics, rock mechanics and engineering geology.

The conference is jointly sponsored by the New Zealand Institution of Engineers, The Institution of Engineers (Australia) and the Australasian Institute of Mining and Metallurgy and has been organised in conjunction with the Australian Geomechanics Society.

The conference proceedings are presented in three volumes, the first two volumes comprising papers submitted for presentation and the third volume reports of discussion at conference sessions and keynote addresses delivered by invited speakers. The papers are arranged in the two volumes in order of presentation at the technical sessions of the conference.

PAPERS: VOLUME ONE

PAPERS: VOLUME TWO

Investigations into the Deformability of Rockfill

A. J. BOWLING
Geomechanics Engineer, Hydro-Electric Commission, Tasmania

SUMMARY The Hydro-Electric Commission, Tasmania is currently involved in the design and construction of four major concrete decked rockfill dams. Although the concrete deck in this type of dam is designed to accommodate some movements in the rockfill it is important that the rockfill should not be too deformable. This paper describes a laboratory confined compression test from which the Young's modulus of a rockfill sample can be determined as an index of the deformability of the rolled rockfill. The results of tests on 77 rock samples are summarized and compared with the results of other mechanical tests on the rocks involved and with some results obtained from the observed settlements in two completed rockfill dams.

1 INTRODUCTION

The Hydro-Electric Commission, Tasmania is currently involved in the design and construction of four major concrete faced rockfill dams in the West of Tasmania. These dams will form part of the Pieman River Power Development and will range in size from the 75 m high Mackintosh and Bastyan Dams to the 118 m high Lower Pieman Dam (Jeffries, 1972).

These four dams follow the Commission's successful completion of four similar concrete faced rockfill dams in earlier hydro-electric developments, Wilmot Dam (34 m high completed in 1970), Cethana Dam (110 m, 1971), Paloona Dam (40 m, 1972) and Serpentine Dam (40 m, 1972).

The integrity of a concrete-faced rockfill dam depends on the ability of the concrete face to accommodate instantaneous and time dependent (i.e. creep) movements in the rockfill due to its own weight and due to the reservoir water loading (Wilkins, 1968, Fitzpatrick, 1971). Whilst the inclusion of flexible water stops along joints in the face, particularly along the perimetral joint, allows for some rockfill movement it is important that such movements should not be excessive.

In order to assess the deformational characteristics of a proposed rockfill material a laboratory confined compression test has been developed. This paper describes the confined compression test and the results which have been obtained for a variety of rockfill materials. The test results are also compared with the observed deformations of two completed rockfill dams.

2 THE DEFORMATIONAL BEHAVIOUR OF ROCKFILL

The relationship between applied stress and resultant deformation in rockfill is dependent on a number of physical characteristics of the rockfill including rock type and degree of weathering, grading, particle shape, compacted void ratio and moisture content. These physical characteristics are not entirely independent of each other as, for example, grading and particle shape will depend to some extent on rock type and compacted void ratio will depend on grading and moisture content.

The deformational behaviour of rockfill is also dependent on the stress history of the material. Thus at any point in a rockfill dam, stresses will change in magnitude and direction both during construction and during subsequent reservoir filling. As a consequence the relationship between stress and deformation at such a point will also change during these phases.

Whilst it is thus difficult to establish a simple specific relationship between stress and strain for rockfill it became apparent, during laboratory investigations, that a comparatively simple standard test could be used to index the deformational properties of rockfill. This test could be used to compare different types of rock material which might be under consideration for rockfill, even though a modulus value for predicting the deformation of a rockfill embankment is not necessarily obtained from the test.

The test which has evolved is the confined compression test in which a sample of rockfill is compressed whilst confined in a steel cylinder and from which the Young's modulus on initial loading of the confined material is the main deduced parameter.

3 THE STANDARD CONFINED COMPRESSION TEST

The rock sample obtained from the site can be in the form of either rock pieces or drill core. It is crushed in a laboratory jaw crusher to a 19 mm maximum size and then prepared to a prescribed grading (see Fig. 1). The coordinates of this grading curve are as follows: 9.5 mm 48%, 4.75 mm 25.4%, 2.36 mm 17.7%, 1.18 mm 11%, 600 μm 7.2%, 300 μm 4.8%, 150 μm 3.2% and 75 μm 2.2%. This initial grading was arrived at by averaging the as-crushed gradings of a number of materials investigated in the early stages of the investigation and is coarser than the maximum density gradings of Wilhelmi (Fig. 1). Although this initial grading is otherwise arbitrary it is similar in shape to many prototype rockfill grading curves.

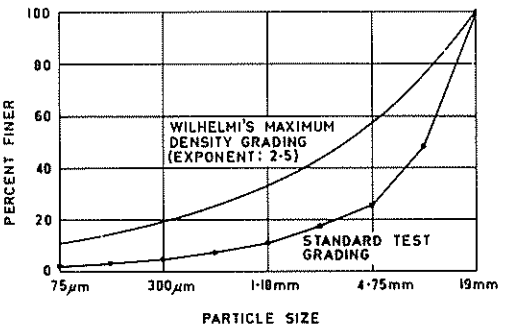

Figure 1 Confined compression test standard grading

A portion of the graded rockfill sample is mixed with water to give a moisture content of approximately 2.5%. This moisture content has been found to be convenient for the grading and types of rock tested. A standard compaction test is carried out on this portion to establish the approximate compacted density so that the amount of graded rockfill to fill the test cell to a depth of about 140 mm can be calculated.

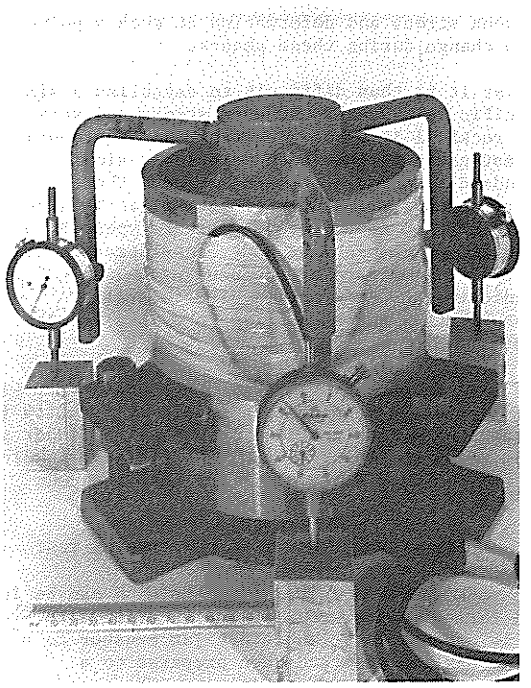

Figure 2 The confined compression test cell

The test cell consists of a steel cylinder, 150 mm in internal diameter 180 mm high and with a wall thickness of 10 mm (Fig. 2). This cylinder is closed at the bottom by a freely fitting chamfered disc attached to a base plate and at the top by a chamfered loading head equipped with three arms to hold dial gauges. These dial gauges are to measure the longitudinal strain in the confined rockfill within the cylinder and have a least reading of 20 μm. Two bonded wire electric resistance circumferential strain gauges around the outside of the steel cylinder allow lateral pressures exerted by the rockfill to be measured. The steel cylinder is equipped with three external lugs so that it can be bolted to the base plate whilst being filled with rockfill.

Prior to filling the test cell, the internal walls are greased with graphite grease and the steel cylinder is clamped with a 10 mm gap between the bottom edge of the steel cylinder and the base plate.

The appropriate amount of graded rockfill at approximately 2.5% moisture content is compacted into the test cell using the equivalent of standard compaction which for the cell is 18 blows with a 4.5 kg hammer falling through 455 mm for each of four layers. The loading head is placed on top of the compacted rockfill and the dial gauges are set up. The steel cylinder clamps are then released so that during subsequent loading the steel cylinder is floating.

The cell is placed in a testing machine and the initial readings of the three dial gauges and the two circumferential strain gauges are taken. Load is applied to the cell and gauge readings are taken at applied stresses of 100 kPa, 500 kPa and then at steps of 500 kPa up to 3000 kPa. The loading rate is controlled at 250 kPa per minute. At 3000 kPa the load is held for 15 minutes. Gauge readings are then taken at similar steps of stress back to zero. The loading rate is based on convenience but is otherwise arbitrary. The maximum stress of 3000 kPa is approximately the stress that could be expected under 150 m of rockfill. After unloading, the tested rockfill is ovendried and sieved to determine the new particle size distribution. Following Marsal (1967) the breakage of the rockfill (B) due to compaction and testing is calculated as the sum of the increases in percents passing the eight sieves used in testing (i.e. 9.5, 4.75, 2.36 and 1.18 mm, 600, 300, 150 and 75 μm).

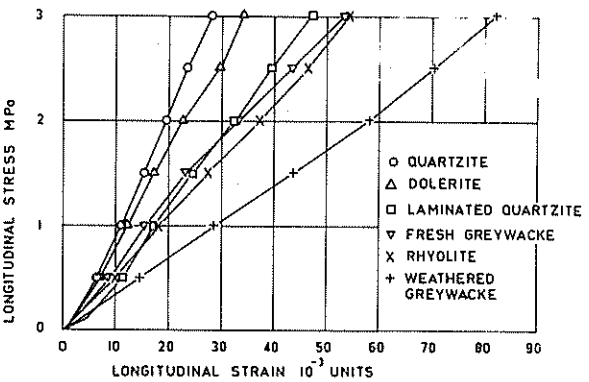

Figure 3 Typical plots of longitudinal stress against longitudinal strain

The plot of applied stress against longitudinal strain for the loading part of the test is effectively linear (see Fig. 3) and the slope is equal to the confined modulus (M) of the sample. The plot of applied stress against external circumferential strain is also linear (Fig. 4) and from the slope (N) of this plot the Poisson's ratio (ν) of the confined rockfill can be obtained from

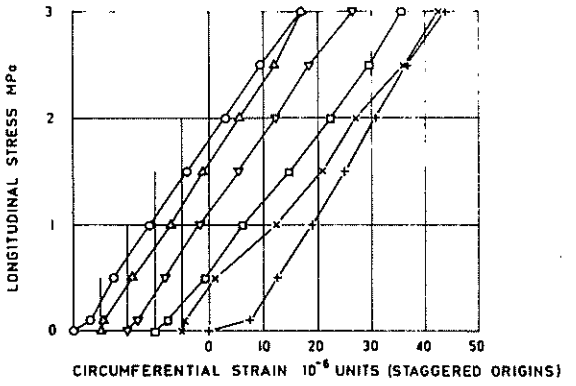

Figure 4 Typical plots of longitudinal stress against circumferential strain. See Figure 3 for symbols

$$\nu = \frac{1}{1 + KN} \quad (1)$$

where $$K = \frac{1}{2k\ (1 + k)\ Es} \quad (2)$$

Es = Young's modulus of steel

and k = ratio of wall thickness to internal diameter of the cell

The Young's modulus (E) of the confined rockfill can be calculated from the confined modulus and the Poisson's ratio using the equation

$$E = M \frac{(1 + \nu)\ (1 - 2\nu)}{(1 - \nu)} \quad (3)$$

Two other parameters deduced from the test are the 15 minute creep and the recovery on unloading. These are given by

$$\text{15 minute creep} = \frac{\varepsilon_{15} - \varepsilon_1}{\varepsilon_1} \quad (4)$$

$$\text{recovery on unloading} = \frac{\varepsilon_{15} - \varepsilon_o}{\varepsilon_1} \quad (5)$$

in which ε_1 is the initial longitudinal strain at 3000 kPa

ε_{15} is the longitudinal strain after 15 minutes at 3000 kPa

ε_o is the longitudinal strain when just unloaded

The repeatability of the confined compression test has been assessed from the results obtained for a number of rock samples in which separate confined compression tests on two or three subsamples of the same sample have been carried out. From these results the coefficients of variation listed in Table I for five of the confined compression test experimental parameters have been deduced.

4 RESULTS OF TESTS ON VARIOUS ROCK MATERIALS

To the time of writing, seventy-seven tests have been carried out on ten types of rock. Rockfill Young's modulus values for these various rock types range from about 25 MPa for weathered greywacke to just over 100 MPa for fresh quartzite. Although rockfill Young's modulus is the principal parameter deduced from the confined compression test four other experimental parameters of interest are also determined.

TABLE I

COEFFICIENTS OF VARIATION OF FIVE PARAMETERS MEASURED IN THE CONFINED COMPRESSION TEST

Experimental Parameter	Coefficient of Variation (%)
Rockfill Young's Modulus	12
Rockfill Poisson's Ratio	4
Breakage	12
15 minute Creep	13
Recovery on Unloading	15

The rockfill Poisson's ratio is much less variable than the Young's modulus, with an average value of 0.27 and with 90% of the 77 values lying between 0.23 and 0.31. It is of interest that these values agree quite well with a theoretical value of 0.26 for an ideal clastic material (Trollope, 1968).

Of the three other parameters derived from the confined compression test, breakage and recovery on unloading correlate satisfactorily with rockfill Young's modulus, with low modulus rocks yielding high breakage and low recovery values (Figs. 5 and 6). However the 15 minute creep values gave almost no correlation with rockfill Young's modulus. The average of this creep value for the 77 tests was 7.2% with 90% of values lying between 4.5% and 12.5%.

Whilst almost all the materials tested displayed the trend between rockfill Young's modulus and breakage shown in Fig. 5, one material (foliated quartzite used in the construction of the Serpentine Dam) gave anomalous breakage values. Three out of the four samples of this material which were tested, whilst giving high values for Young's modulus and recovery on unloading, also gave high breakage values (see Fig. 5). Samples of this material also gave significantly finer gradings, when crushed in the laboratory, than all the other materials. However the high rockfill Young's modulus of this material indicated by the confined compression tests has been confirmed by the small settlements observed in the Serpentine Dam.

The correlations of rockfill Young's modulus with other mechanical properties of the rock have been investigated for a number of the materials. For most of the rock materials the porosity of the rock fabric has been measured. For the drill core samples, RQD (Rock Quality Designation), dynamic Young's modulus, uniaxial compressive strength, and in some cases point load strength index values have been determined. For some of the rock piece samples point load strength, Los Angeles abrasion resistance and sodium sulphate soundness tests have been carried out.

Because of the variety of these various test results and their intrinsic scatter, the correlation of the rockfill Young's modulus with other rock properties has been made using ranking methods (Moroney, 1956). For a group of samples for which the same set of rock properties are available, the samples in the group have been ranked according to each of the rock properties. An average ranking has then been determined from the rank totals for each sample. Spearman rank correlation coefficients have been

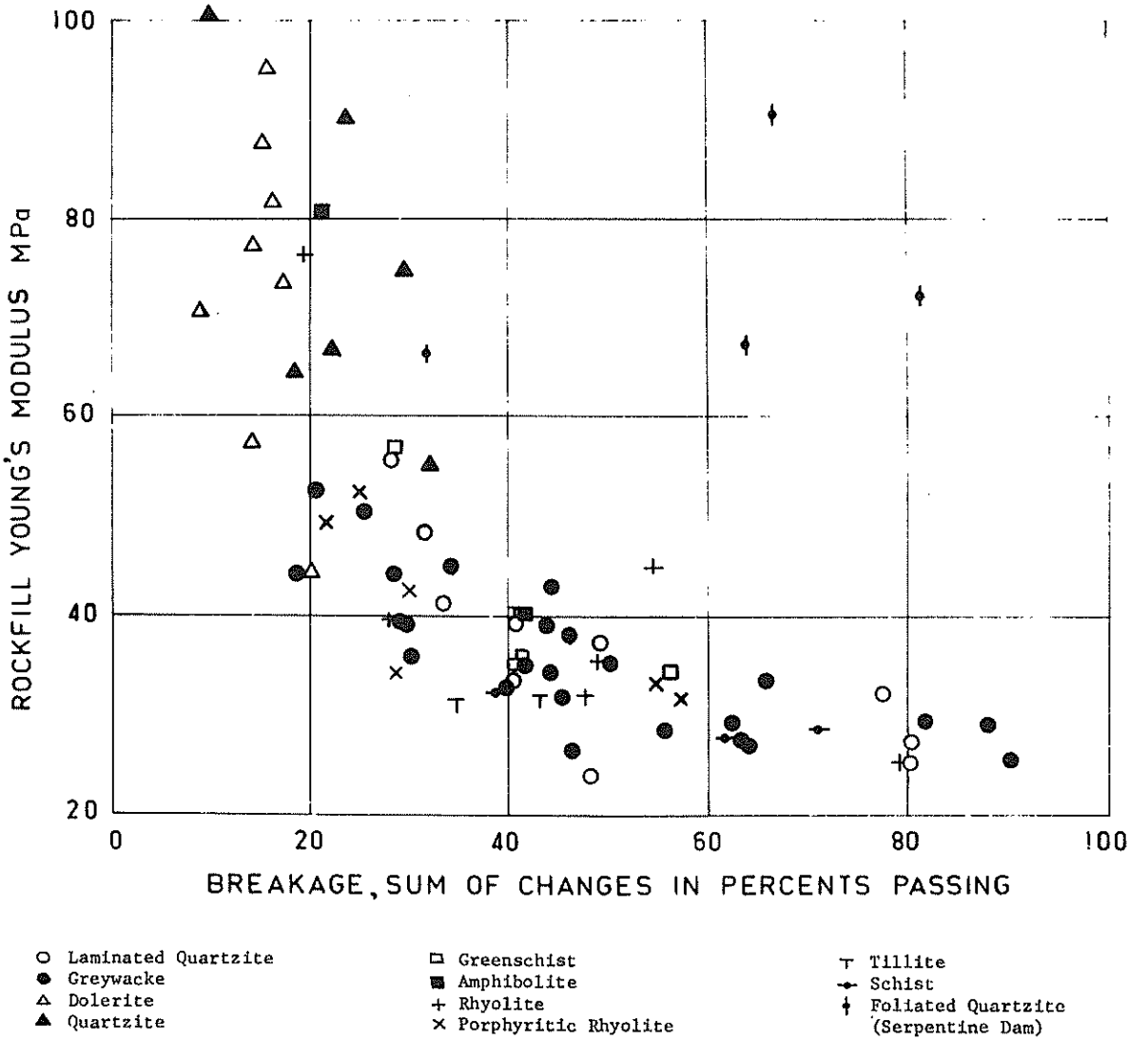

Figure 5 Plot of rockfill Young's modulus against breakage

determined between the ranking according to the rockfill Young's modulus and the ranking according to the other rock properties and between the average ranking and the ranking according to the various rock properties. The results of such analyses are shown in Table II for three groups of samples.

From this table it will be seen that breakage in the confined compression test correlates well with rockfill Young's modulus (rank correlation coefficient close to plus one) as would be expected from Fig. 5. However the rank correlation of other rock properties with rockfill Young's modulus is not particularily good. On the other hand the rockfill Young's modulus correlates quite well with the average rank. Since average rank would appear to be a reasonable indication of the overall quality of the rock, it is deduced that the rockfill Young's modulus is dependent on overall rock quality.

The effects of variations in some of the test conditions which are controlled in the standard confined compression test have been investigated in a number of supplementary tests. The standard test is basically for crushed rock in which particle to particle contact is at sharp points or edges. However tests on rounded quartzite river gravels have yielded rockfill Young's modulus values of up to 175 MPa, about twice those obtained for crushed quartzite although the Poisson's ratio value for these rounded gravels was 0.265, close to the overall average. In the extreme case rockfill Young's modulus values of up to 180 MPa were obtained for a collection of 14 mm steel ball bearings, although for this material Poisson's ratio was 0.45.

Tests on a few of the rock materials have indicated that if maximum density gradings are used, such as those of Wilhelmi (Fig. 1), the rockfill Young's modulus is increased by about 40%, breakage is decreased by about 30% and recovery on unloading is increased by about 50%. If single size material is used (passing 19 mm and retained at 9.5 mm) the rockfill Young's modulus is decreased by about 40%, breakage is again decreased, this time by about 20%, and recovery on unloading is also again increased by about 50%.

TABLE II

SPEARMAN RANK CORRELATION COEFFICIENTS BETWEEN ROCKFILL YOUNG'S MODULUS AND OTHER MECHANICAL PROPERTIES AND (IN BRACKETS) BETWEEN AVERAGE RANK AND MECHANICAL PROPERTIES

Rock Property	14 Drill Core Samples subjected to 8 tests Various rock types	26 Drill Core Samples subjected to 7 tests Various rock types	12 Rock Piece Samples subjected to 7 tests Greywacke
Rockfill Young's Modulus	1.00 (0.94)	1.00 (0.86)	1.00 (0.69)
Breakage	0.90 (0.84)	0.88 (0.88)	0.73 (0.79)
Recovery on Unloading	0.66 (0.70)	0.54 (0.28)	0.18 (-0.06)
Rock Fabric Porosity	0.48 (0.61)	0.37 (0.73)	0.10 (0.69)
RQD	0.57 (0.76)	0.35 (0.62)	
Dynamic Young's Modulus	0.81 (0.84)	0.50 (0.77)	
Uniaxial Compressive Strength	0.67 (0.64)	0.54 (0.66)	
Point Load Strength Index	0.71 (0.87)		0.09 (0.57)
Los Angeles Abrasion Resistance			0.39 (0.87)
Sodium Sulphate Soundness			0.46 (0.60)

A few tests with crushed rhyolite, in which the moisture content was varied, suggest that if the moisture content is increased from dry to about 6% the rockfill Young's modulus is decreased by about 20%, breakage is increased by about 40% and recovery on unloading is decreased by about 30%. In this case also Poisson's ratio decreased by about 25%.

5 MODULUS VALUES DEDUCED FROM THE DEFORMATIONS OF COMPLETED DAMS

Although, as pointed out above, the confined compression test is not intended to provide a Young's modulus value for the deformational analysis of a prototype structure, it is of interest to compare the results of confined compression tests with the measurements of settlement in completed dams.

The five completed concrete faced rockfill dams of the Tasmanian Hydro-Electric Commission contain hydrostatic settlement gauges installed during construction. Similar gauges will be installed in the three dams which are yet to be constructed in the Pieman River Power Development. The principle of the hydrostatic settlement gauge has been described by Russell (1960). These gauges provide information on settlement during construction as well as during reservoir filling and subsequent operation.

Whilst it is proposed to publish eventually an analysis of the settlements observed in a number of the Commission's dams, settlements in Cethana Dam and in Mackintosh Dam have already been analysed to determine Young's modulus values for comparison with the results of confined compression tests on samples of the rockfill materials involved.

The 110 m high Cethana Dam was commenced in September, 1968, and reached a height of 98 m in November, 1969. The final 12 m of rockfill were added in October, 1970 (Wilkins et al, 1973). Rockfill was quarried quartzite which was placed in 0.9 m layers, sluiced and rolled. Four hydrostatic settlement cells were located at two levels on the maximum section of the dam (Fitzpatrick et al, 1973). As strains due to increasing self weight during construction are most nearly equivalent to those produced in the confined compression test, only the settlements between the time of gauge installation and the time of commencing reservoir filling (a period of 22 months for the two lower gauges and 19 months for the two upper gauges) have been analysed.

In the analysis, creep settlements have been assumed to be proportional to the product of stress and the logarithm of the time under stress. The analysis yields a value for the constant of proportionality for such a creep relationship together with the Young's modulus of the rockfill.

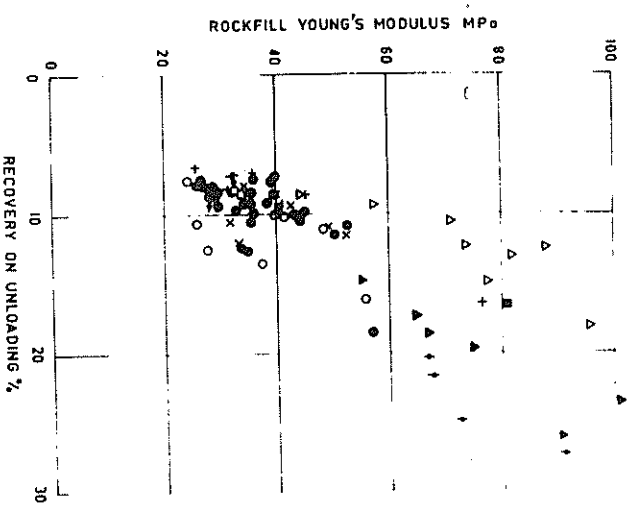

Figure 6 Plot of rockfill Young's modulus against recovery on unloading. See Figure 5 for symbols.

Although the analysis cannot be detailed in this paper, the values obtained for the Young's modulus of the Cethana quartzite rockfill ranged from 160 to 210 MPa. By comparison confined compression tests on two laboratory samples of the quartzite gave values of 90 and 67 MPa for the rockfill Young's modulus.

Rockfill placing for the 75 m high Mackintosh Dam was commenced in September, 1977, and was completed one year later (Paterson et al 1979). At the time of writing the concrete face is nearing completion and water storage should commence in the second half of 1980. The rockfill material was a quarried greywacke some of which contained minor amounts of interfoliated slate. As for Cethana Dam the rockfill was placed in 0.9 m layers and was sluiced and rolled. Six hydrostatic settlement cells were installed at three levels on the maximum section of the dam and two others were installed towards the left abutment.

As for the Cethana Dam settlement gauges, settlements indicated by the six gauges on the maximum section have been analysed from the time of their installation to July, 1979, a period ranging between 11 and 16 months. From this analysis rockfill Young's modulus values of between 34 and 47 MPa have been deduced. Confined compression tests have been carried out on 20 samples of rockfill material used in the dam and values of rockfill Young's modulus ranging from 27 MPa to 53 MPa have been obtained from these tests.

Good agreement has thus been obtained between rockfill Young's modulus values deduced from laboratory confined compression tests and from measured prototype settlements for the Mackintosh greywacke. The agreement between the two sets of modulus values for the Cethana quartzite has not been so good. However it should be noted that the Cethana Dam is located in a narrow valley with steep sides. Arching of the rockfill may thus have occurred, reducing settlements in the dam and leading to higher deduced rockfill Young's modulus values. Notwithstanding, the confined compression test results have satisfactorily predicted that the Cethana quartzite rockfill is a significantly less deformable material than the Mackintosh greywacke.

Whilst the laboratory confined compression test does not necessarily aim at predicting a prototype Young's modulus value directly, the accumulation of data from the behaviour of prototype structures should lead eventually to a correlation between confined compression test modulus and prototype modulus.

6 CONCLUSIONS

The confined compression test procedure described in this paper appears to provide a rockfill Young's modulus value which is a suitable index of the deformation properties of the rockfill. This rockfill Young's modulus value correlates well with the average quality of the rock as indicated by a number of other rock properties including RQD, point load strength, rock fabric porosity and dynamic modulus of rock core specimens.

Although the deformation behaviour of rockfill in a prototype structure is dependent on various factors such as grading, compacted density and stress history, it seems likely that, with the accumulation of data on the deformational behaviour of prototype rockfill structures, a satisfactory relationship between confined compression test modulus and prototype modulus will be established.

7 ACKNOWLEDGEMENTS

The author wishes to thank the Commissioner of the Hydro-Electric Commission, Tasmania, Mr. J.R. Ashton, for permission to publish the information contained in this paper.

8 REFERENCES

FITZPATRICK, M.D. (1971). Concrete Face Design, Contribution to a Symposium on Rockfill Dams with Upstream Membranes. ANCOLD Bull. No. 34.

FITZPATRICK, M.D., LIGGINS, T.B., LACK, L.J. and KNOOP, B.P. (1973). Instrumentation and Performance of Cethana Dam. Proc. Annual Engineering Conference of I.E. Aust., Perth.

JEFFRIES, P.J. (1972). Civil Engineering Investigations and Economic Studies for the Pieman River Power Development. Civil Eng. Trans. I.E. Aust. Vol. CE14, No. 2, October. pp. 119-125.

MARSAL, R.J. (1967). Large Scale Testing of Rockfill Materials. Proc. ASCE. Vol. 93, No. SM2, March. pp. 27-43.

MORONEY, M.J. (1956). Facts from Figures. 3rd edn. London, Penguin Books.

PATERSON, S.J., LIGGINS, T.B. and ALLEN, D.T.(1973) Mackintosh Concrete Face Rockfill Dam, Tasmania. Proc. Annual Engineering Conference of I.E. Aust., Perth.

RUSSELL, T. (1960). A Hydrostatic Settlement Gauge. Proc. Third ANZ Conf. on Soil Mech. and Foundation Engineering, Auckland.

TROLLOPE, D.H. (1968). The Mechanics of Discontinua or Clastic Mechanics in Rock Problems. Chapter 7 in Rock Mechanics in Engineering Practice ed. by K.G. Stagg and O.C. Zienkiewicz, 1st edition London, John Wiley.

WILKINS, J.K. (1968). Decked Rockfill Dams. Civil Eng. Trans. I.E. Aust. Vol. CE10, No. 1, April pp. 119-129.

WILKINS, J.K., MITCHELL, W.R., FITZPATRICK, M.D. and LIGGINS, T.B. (1973). The Design of Cethana Concrete Face Rockfill Dam. Proc. Annual Engineering Conference of I.E. Aust., Perth.

A Theoretical Investigation of the Constructional Behaviour of a Rockfill Dam

A. K. PARKIN
Senior Lecturer in Civil Engineering, Monash University, Australia
G. S. N. ADIKARI
Research Student, Department of Civil Engineering, Monash University, Australia

SUMMARY The increasing height of earth and rockfill dams now being built makes the evaluation of deformation behaviour considerably more critical. In the present study, a finite element analysis is made for Talbingo dam in Australia, a 162m high rockfill structure with a sloping silty clay core. Predictions are made using two dimensional elastic, non-linear inelastic and elasto-plastic constitutive assumptions, and results are compared with the observed constructional deformations and stresses in the maximum cross section of the dam. Whilst all the predictions have been quite satisfactory, the elastic model appears to have been the most successful, with no real advantages occurring from the more complex models.

NOTATION

c	cohesion (kNm^{-2})
d,F,G	Poisson's ratio parameters
E, E_t	modulus of elasticity (kNm^{-2})
K,K_{ur}	modulus number
n	modulus exponent
p_a	atmospheric pressure (kNm^{-2})
R_f	failure ratio
ν	Poisson's ratio
σ_1,σ_3	major and minor principal stresses (kNm^{-2})
γ	unit weight (kNm^{-3})

1 INTRODUCTION

Designers of earth and rockfill dams have available various procedures for stress-deformation analysis, involving different constitutive laws to represent material behaviour. Each has its own advantages and disadvantages, often linked to features of dam geometry.

To assist in the selection of appropriate analytical models, a study has been made of the various procedures in common usage, including two-dimensional elastic, non-linear inelastic and elasto-plastic models. The structure selected for this comparative study was Talbingo Dam in the Snowy Mountains of NSW, Australia, (Fig. 1) chosen because of its extensive instrumentation, together with its relatively simple cross section and a symmetrical valley profile. Its instrumentation is described by Hosking (1974).

Talbingo Dam is a 162m high structure with rockfill shells and a silty clay core, under the control of the Snowy Mountains Authority. Construction began in December 1968 and was completed in October 1970, with the storage reaching full supply level by January, 1972.

The dam has 6 zones in its cross section, divided into core (zone 1), filters and transition (zones 2A, 2B) and rockfill shoulders (zones 3A, 3B, 3C). The instrumentation and zoning of the maximum cross section are shown in Fig. 1. The core is an impervious clay of basaltic origin, compacted in 0.15m layers to a field dry density of 1.8 tm^{-3} at 15% moisture content, on the average 0.3% wet of optimum. The downstream filter 2A is processed fresh rhyolite, compacted in 0.5m layers to a density of 2.0 tm^{-3}. It is more rigid than the core. Transition zones are moderately weathered to fresh rhyolite compacted in 0.5m layers to a density of 2.0 tm^{-3}. The rockfill shoulders consist of slightly weathered to fresh rhyolite up to 1.0m size compacted in 1-2m layers to the same density as the transition zones.

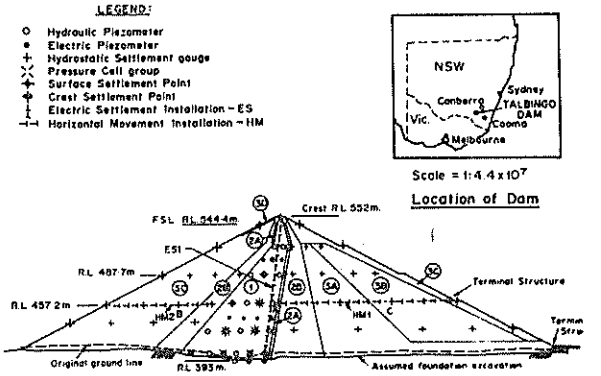

Fig. 1 Talbingo Dam - Instrumentation at maximum section.

The foundation bedrock is jointed rhyolite lava flows and tuff beds of varying permeability. Extensive foundation treatment was necessary prior to construction involving excavation and grouting (Wallace and Hilton, 1972).

2. CONSTRUCTION AND INSTRUMENTATION OF DAM

The embankment was built up in 10 lifts of approximately 15m each over a period of 22 months. Instruments placed in the dam enabled construction procedures to be controlled within safe limits and allowed the subsequent monitoring of performance. Readings taken on the maximum cross section, up to end of construction have been used in the theoretical analysis below.

3. CONSTITUTIVE MODELS

Incremental finite element analyses have been

performed on the maximum section using linear elastic elasto-plastic and non-linear inelastic constitutive models. Because valley slopes are less than 2:1, two dimensional plane strain conditions may be assumed. (Lefebvre et al, 1973). The finite element mesh used in the analysis is shown in fig. 2, the nodal points being chosen to coincide as closely as practicable with the instrument locations. For initial runs, 3 layers of foundation elements were included in the mesh to investigate the influence of the foundation on deformations. Although site investigations revealed that the bed-rock was highly jointed with random clay seams, foundation deformations proved to be negligible. Hence the foundation elements were removed from the mesh for subsequent runs.

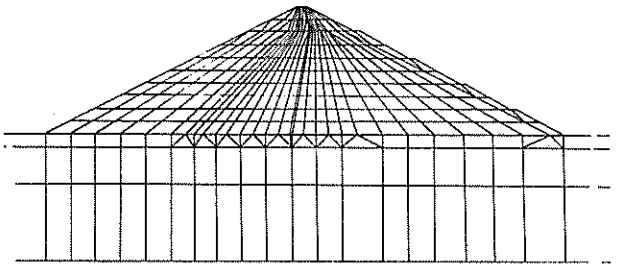

Fig. 2 Finite element mesh (full extent of mesh not shown)

Clough and Woodward (1967) demonstrated that the incremental method of analysis enabled actual embankment construction to be modelled, so that the deformations can be compared with theoretical predictions. Subsequently, several nonlinear constitutive models were developed for use in conjunction with incremental analysis, such as the hyperbolic model of Kulhawy, Duncan and Seed (1969). Other useful forms of variable modulus models are also available. (eg. Richards, 1978).

Constitutive models should be capable of describing the soil behaviour completely under any loading condition. This is often not so, and therefore each model should be evaluated carefully before use, in particular, with respect to the assumptions involved and the derivation of parameters.

The material models used here fall into two groups: constant modulus and variable modulus. In the former, the modulus of elasticity and Poisson's ratio are considered constant, and therefore the stress-strain behaviour approximates a straight line. In the latter, the modulus of elasticity and Poisson's ratio are stress dependent so that the stress-strain characteristics are not linear. The two types of variable moduli models used here are the elasto-plastic and nonlinear hyperbolic models. The Mohr-Coulomb failure criterion is used with all models.

Expressions for the determination of nonlinear modulus and Poissons ratio, and procedures for the derivation of parameters for the hyperbolic model have been given by Wong and Duncan (1974), whilst the elasto-plastic model has been described by Zienkiewicz et al.(1975). These equations will not be presented here.

4. LABORATORY TESTING

During the stages of design and construction, a large number of triaxial tests, grading analyses and compaction tests were carried out on both core and rockfill materials. On core material, consolidated undrained triaxial tests were performed on 0.15 m dia. saturated specimens, remolded at placement conditions and tested over confining pressures ranging up to 1035 kNm^{-2}. On rockfill material drained triaxial tests on 0.57m dia. specimens, compacted to field density, have been performed over a range of confining pressures from 276 kNm^{-2} to 1378 kNm^{-2}. In the field, the rockfill is well graded with maximum size ranging to 1m. For laboratory tests parallel scaling was used with a maximum size of 0.114m. A typical set of laboratory triaxial tests for rockfill are shown in Fig. 3. These tests, together with compaction and grading analyses formed the initial source of material parameters for the finite element analysis.

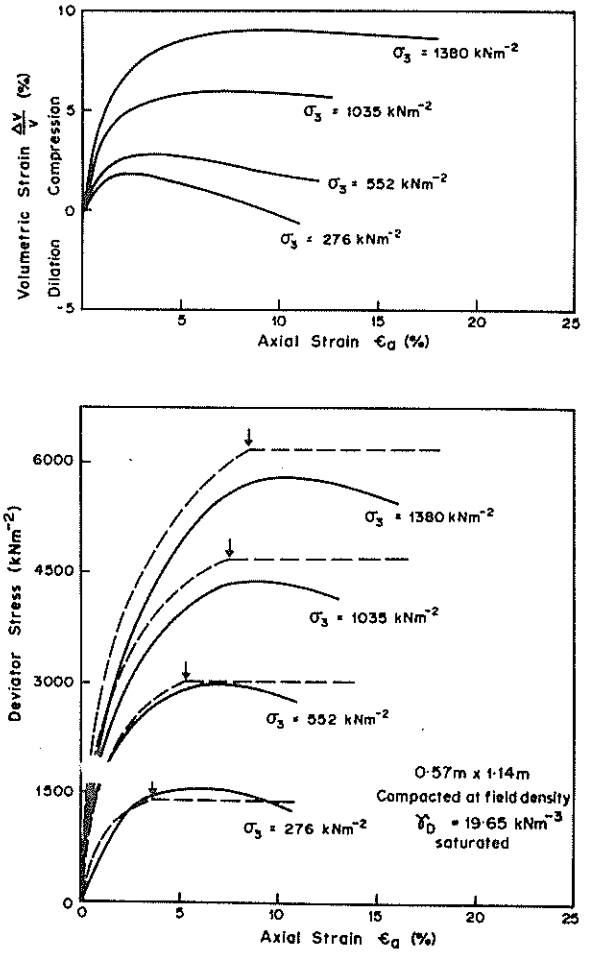

Fig. 3 Stress-Strain characteristics of rockfill material

5. MATERIAL PARAMETERS

Table 1 gives a summary of the material parameters used with each constitutive model. Analysis indicated that no elements yielded during any stage of construction. Therefore the elastic analysis produced results identical with the elasto-plastic analysis at this stage. For convenience both models will be subsequently referred to as elastic. A study of available test data on 6 different zones across the dam revealed that the material properties in zones 2A, 2B and in 3A, 3B 3C could be assumed similar. For nonlinear analysis, Poisson's ratio

parameters for the core were estimated from published data in the absence of triaxial tests with volume change measurements. These material parameters were then used to back-analyse the triaxial tests by the finite element method to confirm the values. A predicted stress-strain curve for zone 3 rockfill material is plotted in Fig. 3 from which it can be seen that hyperbolic model is in reasonable agreement with the actual rockfill behaviour.

Modulus and Poisson's ratio values for foundation rock were derived from triaxial tests on intact rock specimens, with a modulus reduction factor of 3. (Lama and Vutukuri, 1978).

Elastic analysis predicts a maximum of 1.23m at a slightly higher position. In the top third of the dam, nonlinear analysis predicts small downstream movements on the upstream side whereas these movements are upstream in the elastic case. On the downstream side, however, the movements are negligible in both cases. Elastic gravity turn-on analysis produces a set of horizontal movement contours nearly identical with elastic analysis, but with slight deviations in the top quarter of height. An explanation for this similarity has been given by Clough and Woodward (1967).

TABLE 1

TALBINGO DAM MATERIAL PARAMETERS

Relevant constitutive model	Parameter	Zone 1	Zones 2A,2B	Zones 3A,3B,3C	Foundation layers		
					Top	Middle	Bottom
linear elastic elasto-plastic	γ (kNm^{-3})	18.08	20.44	20.44	21.23	21.23	21.23
	E (MNm^{-2})	10.0	50.0	60.0	5000	10000	20000
	ν	0.44	0.32	0.31	0.15	0.10	0.05
	c (kNm^{-2})	70.0	0.0	0.0	-	-	-
	ϕ (Deg.)	25.0	45.0	45.0	-	-	-
non-linear inelastic	γ	18.08	20.44	20.44			
	K	250	850	675			
	K_{ur}	400	1200	1000			
	n	0.45	0.40	0.43			
	d	5.0	7.7	10.0			
	G	0.30	0.21	0.21			
	F	0.00	0.07	0.07			
	R_f	0.90	0.70	0.70			
	c (kNm^{-2})	70.0	0.0	0.0			
	ϕ (Deg.)	25.0	45.0	45.0			

6. PREDICTION OF DEFORMATIONS AND STRESSES

The results of the various analyses are shown in Figs. 4 to 9.

Contours of settlements predicted by non-linear inelastic analysis are similar in shape with maximum settlement occuring at the centre of the core. The magnitude of this maximum predicted by nonlinear analysis is 3.0m, as compared with 2.75m by elastic analysis, whereas the observed maximum at the end of construction was 2.6m. The broken lines on Figs. 4(a) and 4(b) show measured settlement contours, measurements being taken from hydrostatic settlement gauges and surface settlement points. Fig. 4(c) is the contour plot of predicted settlements by elastic theory, assuming the embankment is built in one step. The distribution of settlement does not follow the measurements but this analysis enables a very close prediction of the total cumulative settlement at any point in the section. Predicted settlement at the crest of embankment is 4.9m whereas the measured cumulative settlement is 5.2 m.

The corresponding horizontal movements are presented in Fig. 5. The location of the zero movement contour and the distribution of downstream movements are similar in both analyses but the magnitude of the upstream movement differs. Nonlinear analysis predicts a maximum upstream movement of 0.6m at a third height and in the upstream transition zone.

The distribution of maximum shear stress over the cross section is illustrated in Fig. 6. These contours are generally parallel with the slopes of the upstream and downstream rockfill shoulders. However, the core proves to be a region of low shear stress bounded by high shear stress gradients in the filter and transition zones. This supports field information indicating a near-fluid state in the core at this stage.

From the calculations of stresses and deformations by the elastic method, pore pressures have been calculated. These calculations have used undrained strength parameters for the core and drained parameters for the rockfill, ignoring dilation. The resulting pore pressures (Fig. 7) are the cumulative values generated during stage construction (Fig. 7a), and during two stage reservoir filling (Fig. 7b), and these are compared with measured values from electric and hydrostatic piezometers. Reasonable agreement has been obtained, at least near the centre of the core, but with greatest departure at the downstream filter.

7. DISCUSSION

It can be seen from the preceding results (Figs. 4 to 7) that predicted deformations and stresses are in good agreement with measured values.

The pattern of vertical and horizontal movements can

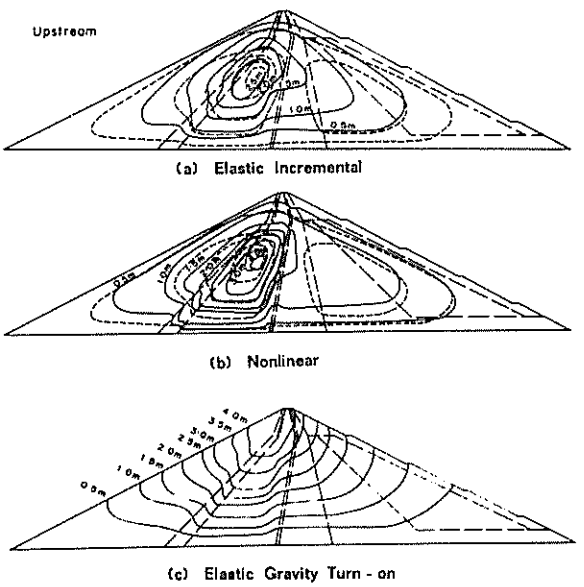

Fig. 4 Contours of predicted settlement at the end of construction

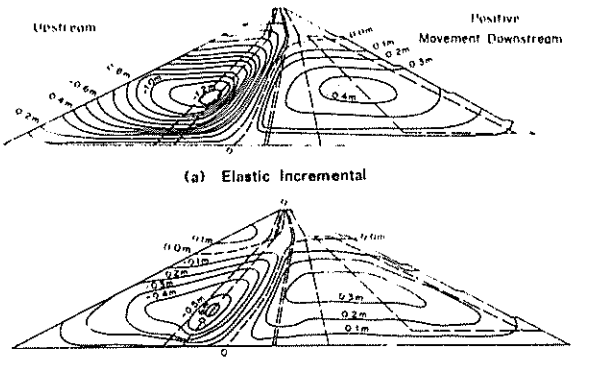

Fig. 5 Contours of predicted horizontal movement at the end of construction

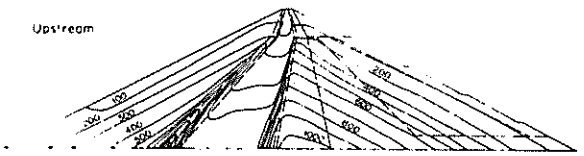

Fig. 6 Maximum shear stress contours (in kNm^{-2}) at the end of construction as predicted by non-linear analysis

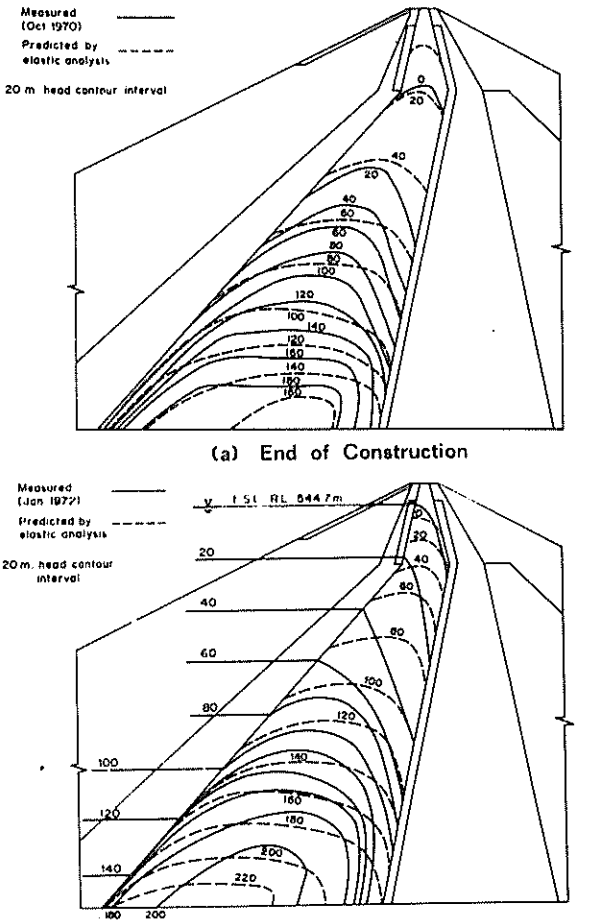

Fig. 7 Pore pressure contours

also be examined in terms of profiles at a particular elevation, as in Fig. 8. This shows that all models over-estimate core settlements and under-estimate surface settlements (by about 20%). Horizontal movements are best predicted by elastic analysis on the upstream side, whilst non-linear analysis is best on the downstream side.

From these results, it is clearly seen that the horizontal movement pattern is controlled by the geometry of the core. The magnitude of the upstream movement (Fig. 8) is approximately 3 times the downstream movement. The upstream rockfill shoulder at this level is compressed by about 0.35m. Compression of downstream shoulder is only about 0.2m, which represents a neglible strain since this shoulder is much thicker.

Elastic analysis has proved to give the best predictions at every stage of construction. Nonlinear analysis, on the other hand, was found to be rather unstable and stresses tended to fluctuate in the outermost elements of the core and rockfill zones as construction proceeded. This generates corresponding fluctuations in the non-linear modulus and Poisson's ratio values.

Poisson's ratio changes in the core have a considerable influence on the overall deformation pattern. Also, the friction angle of the rockfill has a

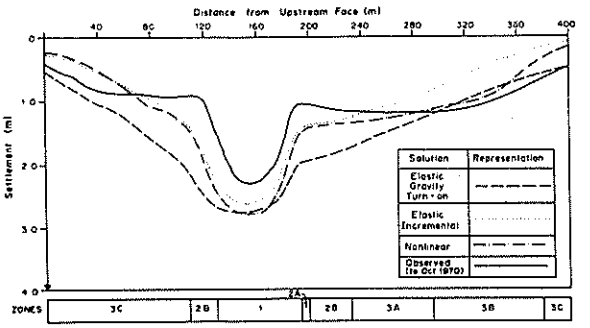

(a) Settlement

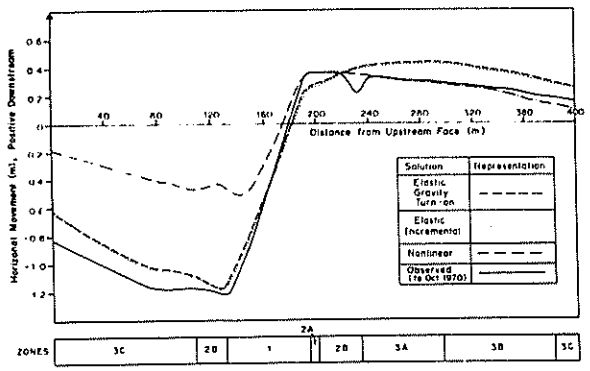

(b) Horizontal Movement

Fig. 8 Comparison of predicted and measured deformation at reduced level 457.2m

marked influence on the deformations of the rockfill zones, especially in zone 3A where stress levels at mid height were up to 70% of failure stress.

Measured pore pressures in Fig. 7 show high values at the bottom of the core. Construction moisture contents were kept within ±1 % of optimum, but tests later revealed that field optimum was 2% lower than the laboratory value. Earth pressure cells indicated that total stresses in the vertical and horizontal (2) directions were nearly equal, and equal to the overburden pressure, implying a hydrostatic stress state and near zero effective stress.

TABLE 11

CORE POISSON'S RATIO VALUES FOR SOLUTIONS SHOWN IN FIG. 9

Relevant constitutive model	Solution code	ν	E kNm^{-2}
linear elastic	L	0.44	10000 (TABLE 1)
elasto-plastic	L49	0.49	10000
	L49E	0.49	4000
non-linear	NL	TABLE 1	TABLE - 1
inelastic	NL44	0.44	TABLE - 1
	NL49	0.49	TABLE - 1

The results presented so far have used material parameters as listed in Table 1, derived from

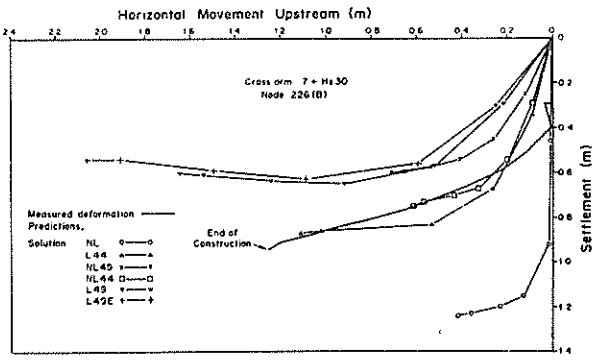

(a) Deformation at B

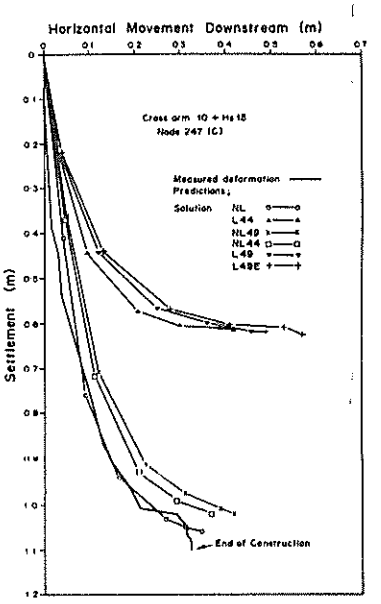

(b) Deformation at C

Fig. 9 Influence of the Poisson's ratio on the Prediction of deformations.

triaxial tests. It has often been found in the literature that saturated core materials of fill dams are modelled as a highly deformable medium with a high Poisson's ratio value. For the Talbingo core, a Poisson's ratio of 0.44 produced satisfactory results in the elastic analysis. In Fig. 9, the deformation vectors, as predicted by linear and non-linear analyses at nodal points 225 and 247 are compared in order to justify the chosen value of ν. Two Poisson's ratio values are assumed for each model. In addition to the non-linear Poisson's ratio, constant values of 0.44 and 0.49 are assumed for the non-linear model and 0.49 for the elastic model. The code given to each solution is shown in Table 11. Results of the six cases, presented in Fig. 9 show that the best overall prediction of deformations are found with Poisson's ratio values from Table 1.

8. CONCLUSIONS

Two dimensional elastic, non-linear inelastic and elasto-plastic finite element analyses were carried out to simulate the constructional behaviour of Talbingo Dam. Comparison of the predictions with observed deformations and stresses has made it possible to derive the following conclusions regarding the performance of different constitutive models.

The chosen constitutive models gave predictions of deformations and stresses in reasonable agreement with measurements. Elastic analysis provided the best agreement, probably due to the fact that Poisson's ratios are kept constant and that rotation of the principal stresses is negligible.

Modelling the dam as an elasto-plastic material, with a Mohr-Coulomb yield criterion and associated flow rule, did not improve the accuracy of the results. At the end of construction, no elements were found to have yielded, so that solution coincided with elastic analysis.

Non-linear analysis provided the best deformation prediction on the downstream side where stress fluctuations are minimal. However, changes in stress levels in the upstream transition and adjacent elements produced slightly unstable results during simulated construction.

The chosen constitutive models predicted settlements accurately in most areas of the cross section. At low elevations, core settlements were over-predicted whilst surface settlements were under-predicted by all models.

The deformation behaviour of Talbingo dam is mainly governed by the geometry and material properties of the core. The settlement of the core is three times larger than the rockfill shoulders and transitions, giving rise to high shear stress gradients across the transition and filter zones and high upstream horizontal movements. Further investigations into the behaviour of core material under partially saturated conditions are necessary .

High pore pressures were observed at low elevations in the core of the dam during construction and these pressures continue to exist even today. Dissipation during construction was negligible. Elastic analysis predicted the pore pressures in the middle of the core reasonably well. Hydrostatic stress conditions existed in the lower half of the core during construction, as measured by earth pressure cells.

Inaccuracies in predictions arise from two sources: the approximations made in respective constitutive models, and the difficulty in deriving representative material parameters. The stress paths followed in the dam are, in most elements, far from triaxial conditions. Anisotropy in material properties and variations in density also cause departures from the analytical model. Under these circumstances, complex and expensive analyses may not provide improvements over the simple elastic solution.

9. ACKNOWLEDGEMENTS

The authors are grateful to the Snowy Mountains Engineering Corporation and the Snowy Mountains Hydro-Electric Authority for making available extensive field observations and laboratory data for the Talbingo Project and also to the CSIRO Division of Applied Geomechanics for their financial support of this project. Much helpful discussion with Mr. B.G. Richards, of CSIRO is also acknowledged.

10. REFERENCES

CLOUGH, R.W. and WOODWARD, R.J. (1967). Analysis of embankment stresses and deformations. J. Soil Mech. Found. Div. ASCE, Vol. 93, SM 4, pp 529-549

HOSKING, A.D. (1974). Monitoring of earth-rock dams. Aust. Geomech. J., Vol. G4, pp 1-12.

KULHAWY, F.H. DUNCAN, J.M. and SEED, H.B. (1969). Finite element analysis of stresses and movements in embankments during construction. Report No. TE 69-4, University of California, Berkeley, U.S.A.

LAMA, R.D. and VUTUKURI, V.S. (1978). Handbook on Mechanical properties of rocks - testing techniques and results. Vol. II, Trans Tech Publications, Germany.

LEFEBVRE, G. DUNCAN, J.M. and WILSON, E.L. (1973). Three dimensionalfinite element analysis of dams. J. Soil Mech. Found Div. ASCE, Vol. 99, SM 7, pp 495-507.

RICHARDS, B.G. (1978). Application of an experimentally based nonlinear constitutive model of soils in laboratory and field tests. Aust. Geomech. J. Vol. G8, pp 20-30.

WALLACE, B.J. and HILTON, J.I. (1972). Foundation practices for Talbingo dam, Australia. J. Soil Mech Found Div. ASCE, Vol. 98, SM 10, pp 1081-1098.

WONG, K.S. and DUNCAN, J.M. (1974). Hyperbolic Stress-Strain parameters for nonlinear finite element analyses of stresses and movements in soil masses. Report No. TE 74-3, University of California, Berkeley, U.S.A.

ZIENKIEWICZ, O.C. HUMPHESON, C. and LEWIS, R.W. (1975). Associated and non-associated visco-plasticity and plasticity in soil mechanics. Geotechnique, Vol 25, No. 4, pp 671-689.

Prediction of the Behaviour of Rockfill Materials

T. RAMAMURTHY
Professor of Civil Engineering, Indian Institute of Technology, New Delhi
K. K. GUPTA
Lecturer, Department of Civil Engineering, Indian Institute of Technology, New Delhi

SUMMARY The paper presents an approach for predicting the behaviour of prototype rockfil materials by testing materials which have been reduced in size geometrically. Isotropic consolidation and consolidated drained triaxial tests were conducted on various fractions of Calcite and Quartz minerals under confining pressures varying up to 126 kg/cm^2. The ratio of d_{50} of coarsest to the finest material tested for these minerals was about 35. The experimental data of other investigators has been utilized in support of this approach. The approach presented seems to be promising in predicting the behaviour of prototype materials by testing at least two geometrically reduced smaller sized fractions at two different confining pressures.

1 INTRODUCTION

Coarse grain materials such as boulders, cobbles and coarse gravels are being extensively used in the construction of rockfill dams and such materials may exist in the foundations of civil engineering structures. To evaluate design parameters for these large size rockfill materials, testing requires equipment of formidable dimensions, particularly when their behaviour is to be evaluated under appropriate stress levels and stress combinations. As a consequence of this, the design parameters are sometimes assumed or obtained on the basis of tests conducted on smaller size fractions in the suitable sizes of test specimens.

To overcome these difficulties of testing large size materials under appropriate stress levels, namely, at low pressures (0 - 0.7 kg/cm^2), medium pressures (0.7 - 7 kg/cm^2), high pressures (7 - 70 kg/cm^2) or very high pressures (> 70 kg/cm^2),three different techniques, namely, scalping (Zeller and Wullimann, 1957), modelling (Lowe, 1964) and quadratic grain size distribution (Fumagalli, 1969)have been adopted. Of these, three techniques for evaluating the properties of the prototype materials, modelling by geometrically reducing the particle size has been found to stand to some theoretical justification (Gupta and Ramamurthy, 1978) for elastic bodies. Some experimental evidences is available in support of this technique, but no comprehensive study has been undertaken in predicting the behaviour of modelled rockfill materials on aspects such as stress-strain behaviour, strength, angle of shearing resistance, volume changes during consolidation and shear, extent of crushing and its influence on the behaviour of the material.

As a part of comprehensive programme of research undertaken at IIT Delhi during the last few years, these aspects are being studied in detail for Badarpur sand (locally available material), Calcite and Quartz minerals of different particle sizes.

In this paper the results of behaviour of different sizes of Quartz mineral are presented. The experimental data of Badarpur sand (Ramamurthy et al.1972, 1974), Calcite (Gupta and Ramamurthy, 1978),Pyramid dam material (Marachi et al.,1968) is also included to support the technique of prediction of the behaviour of large size material by testing small particle size material. These findings are applicable for confining pressures beyond 3 kg/cm^2.

2 PUBLISHED EXPERIMENTAL EVIDENCE

Chasil Bank coarse gravel and Ham river sand (Bishop, 1948) having parallel gradation have shown similar values of the angle of shearing resistance. Vallerga et al.,(1957), Ramamurthy et al.(1972) and Marachi et al.(1972) from their studies on different materials have shown that the angle of shearing resistance did not vary with the change of particle size of the material. Marachi et al.(1972) results suggest that volumetric strains during shear,axial strain at failure and initial tangent modulus are influenced with the increase of particle size to some extent.Leussink(1965),Huder & Fretz(1967)observed similar behaviour of angle of shearing resistance. Ramamurthy et al.(1972) have shown that the dilatancy rate $(1 + \delta v/\delta \epsilon_1)$, (where v and ϵ_1 are the volumetric strain and axial strain) did not change with the change of particle size. A unique relationship was observed between net energy observed and specific surface area at the end of shearing for four fractions of Badarpur sand.

On the contrary Lewis (1956) showed increasing angle of shearing resistance with the increase of particle size, while Leslie (1963), Kirkpatrick (1965) and Marsal (1967) observed decreasing values with increase of particle size. Rowe (1962) showed that the interparticle friction decreased with increasing particle size. Lee and Farhoomand (1967) and Fumagalli (1969) observed that compression increases with particle size. Ramamurthy et al. (1972,1974) observed that volumetric strain due to elastic compression, nonrecoverable compression due to slippage, degradation and rearrangement of particles increased with increasing size of particles and confining pressure. Membrane penetration during isotropic consolidation was also found increasing with particle size and confining pressure. Similar behaviour was observed for axial strain at failure and the volumetric strain during shear.

3 EXPERIMENTAL PROGRAMME

For a comprehensive understanding of the response of modelled material in predicting the behaviour of prototype material, isotropic consolidation and consolidated drained triaxial shear tests were conducted on three particle sizes ranging from fine sand to fine gravel of Calcite and Quartz at

confining pressures varying from 1.4 to about 127 kg/cm^2. At the end of each test grain size distribution of the material was determined. The physical properties of these materials are given in Table I.

TABLE I

PHYSICAL PROPERTIES OF CALCITE AND QUARTZ

100 percent passing mm	100 percent retained mm	Average size(d_{50}) mm	Porosity percent Min.	Porosity percent Max.	Cu
Calcite (Specific Gravity 2.73)					
0.124	0.075	0.096	43.4	57.4	1.28
1.18	0.853	1.0	42.5	55.4	1.15
4.75	2.36	3.4	43.5	56.1	1.44
Quartz (Specific Gravity 2.68)					
0.124	0.075	0.096	42.5	54.1	1.28
1.18	0.853	1.0	41.5	49.0	1.15
4.75	2.36	3.4	40.5	50.1	1.44

Isotropic consolidation and triaxial shear tests were conducted on cylindrical specimens with slender ratio 1:1 using enlarged friction free end platens. Fine and medium size materials were tested in 38 mm diameter specimen and coarse size material in 100 mm diameter specimen. Triaxial shear tests were conducted on smaller and larger size specimens at a constant rate of deformation of 0.096 mm/min. and 0.043 mm/min respectively. Sufficiently slow rate of deformation was selected in order to provide effective drainage even during degradation of the material at high confining pressures.

The smaller size specimens (38 mm diameter) were tested in a triaxial cell enabling to test specimen under confining pressures up to 140 kg/cm^2. A triaxial cell to test large specimens (100 mm diameter) was fabricated at IIT Delhi. This cell permits testing of the specimen under confining pressure up to 80 kg/cm^2. The confining pressure was applied through a self compensating pressure assembly.

The physical properties of sand used by Ramamurthy et al.(1972) and of Pyramid dam material used by Marachi et al.(1968) are presented in Table II.

TABLE II

PHYSICAL PROPERTIES OF BADARPUR SAND AND PYRAMID DAM MATERIAL

100 percent passing mm	100 percent retained mm	Average size(d_{50}) mm	Porosity percent Min.	Porosity percent Max.	Cu
Badarpur Sand (Specific Gravity 2.66)					
0.124	0.075	0.096	32	54	1.33
0.6	0.42	0.5	34.7	56	1.19
1.2	0.853	1.0	37.3	60	1.19
2.4	1.2	1.7	37.7	60	1.31
Pyramid Dam Material					
11.2	0.06	3.2	-	-	6.8
51	0.35	14.0	-	-	8.1
150	2.0	41.0	-	-	6.7

4 RESULTS

4.1 Compressibility

The variation of volumetric strains due to isotropic consolidation is presented as a function of confining pressure in Figure 1, for three fractions of Quartz mineral. A straight line relationship on log-log plot has been observed. Badarpur sand, Calcite and Pyramid dam material have also shown similar relationship. The volumetric strains increased with the increase of confining pressure and particle size. The specimens analysed for gradation analysis indicated increasing degradation of the material with confining pressure and particle size (Gupta and Ramamurthy, 1978).

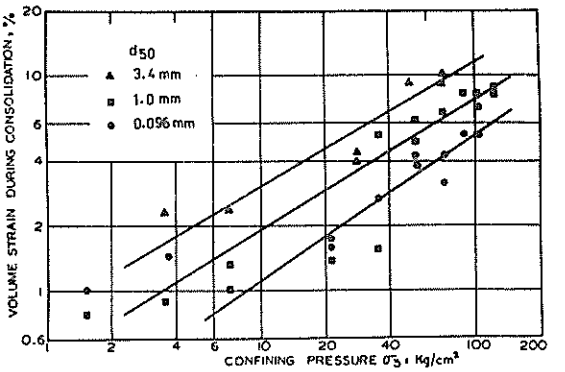

Figure 1 Influence of particle size and confining pressure on isotropic consolidation for Quartz fractions

4.2 Stress-Strain Characteristics

4.2.1 Axial strain at failure

Axial strain at failure increased from 8 to 18 per cent for the tests conducted at medium confining pressures(up to 7 kg/cm^2) for Calcite and Quartz. For tests conducted at higher confining pressures beyond 20 kg/cm^2 failure was not observed for most of the tests up to 20 percent axial strain. The deviator stresses continued to increase with the increase of axial strain. This is mainly due to continuous degradation of material and because of lubricated end platens which resulted in large axial strains. The particle degradation during shearing was more than the degradation during isotropic consolidation, it also increased with confining pressure and particle size. Badarpur sands and Pyramid dam materials were tested in triaxial with friction end platens and, therefore, have shown failure higher confining pressures.

4.2.2 Volumetric strains at failure

The variation of volumetric strain during shearing at failure or 20 percent axial strain whichever was earlier is shown as a function of confining pressure in Figure 2 for Quartz fractions. The specimens of fine and medium size fractions tested beyond medium confining pressures (i.e. 7 kg/cm^2) had shown volumetric contraction, whereas beyond 3 kg/cm^2 coarse fraction had shown contraction.

The volumetric contraction at failure increased with confining pressure for fine and medium size materials and the coarse materials has shown decrease in

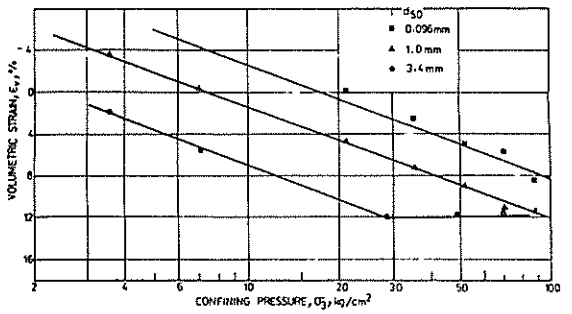

Figure 2 Influence of particle size and confining pressure on volumetric strain for Quartz fractions

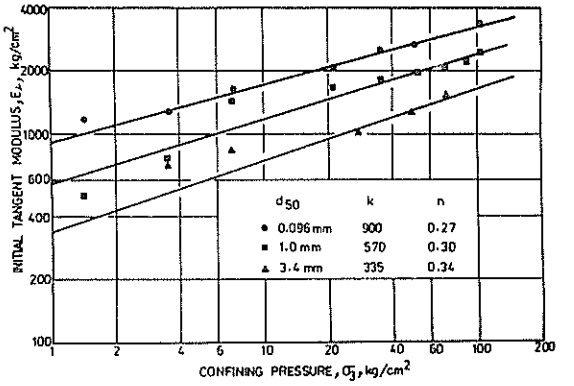

Figure 3 Influence of particle size and confining pressure on initial tangent modulus of Quartz fractions

volumetric contraction in the higher range of confining pressure. This may be because of increasing stiffness of the specimen due to continuous degradation.

4.2.3 Stress-strain curves

The stress strain curves for these materials follow the hyperbolic form (Kondner and Zelasko, 1963).

$$\frac{\epsilon_1}{\sigma_1 - \sigma_3} = a + b\epsilon_1 \qquad (1)$$

where

ϵ_1 = axial strain

$\sigma_1 - \sigma_3$ = deviator stress

a = constant (intercept corresponding to zero axial strain)

b = constant (tangent of the angle of slope of the straight line with axial strain axis)

The initial tangent modulus E_i, inverse of constant 'a' follows the relationship (Janbu, 1963).

$$E_i = K p_a \left(\frac{\sigma_3'}{p_a}\right)^n \qquad (2)$$

where

σ_3' = minor principal stress

p_a = atmospheric pressure in the same unit as σ_3'

K = modulus number

n = exponent determining the rate of variation of E_i with σ_3'

The variation of E_i with confining pressure for three fractions of Quartz is shown in Figure 3. It is observed that initial tangent modulus increases with confining pressure and decreases with particle size. The values of constant K and n are also indicated in this figure. Calcite mineral fractions also indicated similar behaviour having K values of (i) 364 (ii) 188 (iii) 92 and n values of (i) 0.35 (ii) 0.41 (iii) 0.55 for the three fractions in increasing size. The constant 'b' inverse of ultimate strength decreases rapidly with confinning pressure and is independent of particle size of the material. The variation of 'b' as a function of confining pressure for the three fractions of Quartz is shown in Figure 4, suggesting a unique relationship. The relationship for Badarpur sand and Calcite is also shown in this figure.

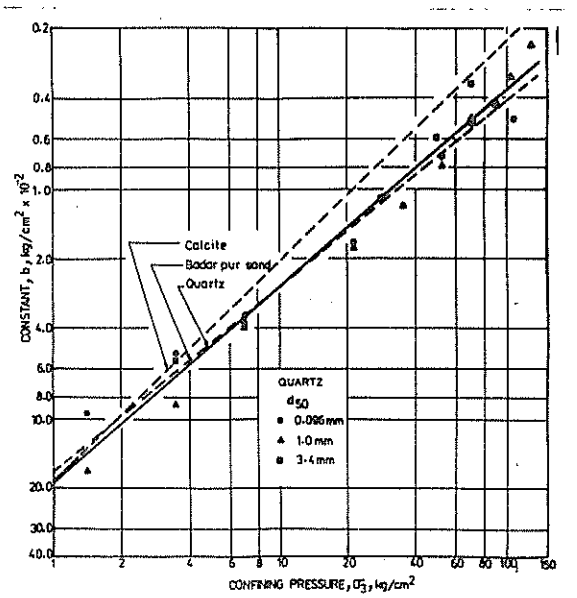

Figure 4 Influence of particle size and confining pressure on constant 'b'

4.2.4 Strength

The Mohr rupture envelopes are nonlinear for the three fractions of Quartz mineral. The effective angle of shearing resistance ϕ' at 20 percent axial strain or at failure whichever was earlier is presented as a function of confining pressure in

Figure 5. The variation in angle of shearing resistance with particle size is because of the variation of $R_f = (\sigma_1 - \sigma_3)_f / (\sigma_1 - \sigma_3)_{ult}$. The values of R_f corresponding to maximum confining pressure are indicated in this Figure. The Calcite mineral fractions have also shown similar variation in angle of shearing resistance. Badarpur sand and Pyramid dam materials have shown insignificant variation in angle of shearing resistance with respect to size. The tests on Badarpur sand and Pyramid dam material were conducted using standard end platens and failure was achieved in most of the tests.

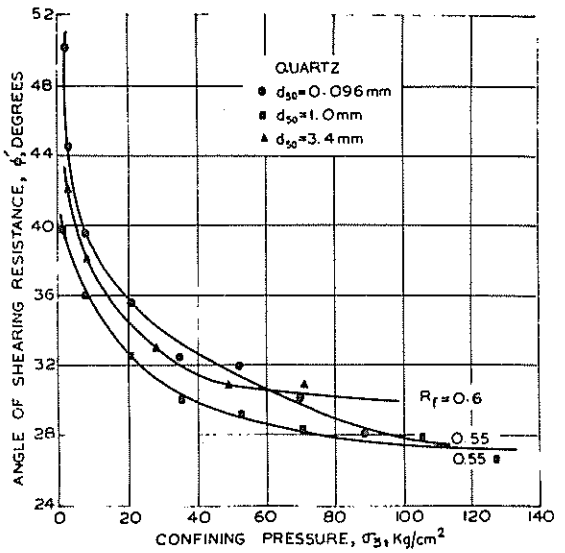

Figure 5 Influence of confining pressure on angle of shearing resistance of Quartz fractions

5 PREDICTION AND DISCUSSION

To predict the characteristics of a larger particle sized material from the test results of smaller sized fractions relative diameter is defined as the ratio of diameter of any larger sized material to the diameter of the smallest material tested. Similarly other parameters like volumetric strain due to isotropic consolidation, relative constants K and n are defined.

5.1 Compressibility

The relationship of the relative volumetric strain due to isotropic consolidation with respect to relative diameter is presented in Figure 6 for Badarpur, Calcite, Pyramid dam material and Quartz. This figure also shows the variation of relative volumetric strain over the range of confining pressures adopted in testing. The points for Calcite have not been shown to avoid overlap with Quartz data. It is observed from Figure 6 that by conducting isotropic consolidation tests on at least two different smaller sizes of the material one could predict the compressibility of the larger size material quite reasonably for a given confining pressure. Figure 1 suggests that one could also predict the behaviour under higher confining pressures by conducting tests at lower confining pressures.

5.2 Axial Strain at Failure

From the results of tests carried out on Quartz and

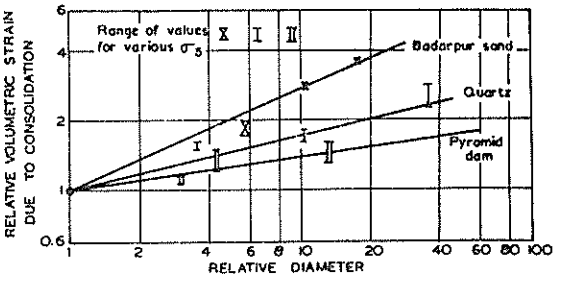

Figure 6 Relative volumetric strain due to isotropic consolidation versus relative diameter

Calcite using lubricated end platens it is observed that the failure is not achieved under high confining pressures even at 20 percent axial strain for large size material. Only fine and medium size materials have indicated failure below 20 percent axial strain up to medium confining pressures. Therefore, it appears that it is not possible to predict the failure axial strains but they are definitely higher than 20 percent for high confining pressures.

5.3 Volumetric Strains at Failure

Because of the changing behaviour of material from expansion to contraction with increasing confining pressure and also with increasing degradation of the material particulate structure becoming stiffer, the prediction seems to be not as good as in the case of other properties with the present available data.

5.4 Stress-Strain Curves

The stress-strain curves for large size material are predicted from the constitutive relationship of stress-strain curve given by the hyperbolic equation (1). To predict the stress-strain behaviour one requires to estimate the values of constant 'a' and 'b'. Constant 'b' has been found to be independent of size of the material and is a function of confining pressure as shown in Figure 4. So by testing atleast one fraction of the material at two different pressures one could evaluate 'b' for any size and confining pressure. The constants K and n of equation (2) are evaluated from Figures 7 and 8. Figure 7 shows a linear relationship between relative value of constant K and relative diameter of the minerals Calcite and Quartz on a semilog scale. Figure 8 shows a linear relationship between relative diameter and relative value of constant n for Calcite and Quartz minerals.

It appears that the relationship for constant K and n can be used for relative diameter as high as 50 to 100. For purpose of illustration, the stress-strain relationship were predicted for coarse fraction of Quartz and are shown along with the experimental curves in Figure 9. The predicted stress-strain curves agree reasonably well with the experimental data particularly for axial strains more than 4 percent. By testing minimum of two different sizes of material at atleast two confining pressures in the anticipated range. Constant 'a' and 'b'could be evaluated for larger size fractions subjected to desired confining pressure.

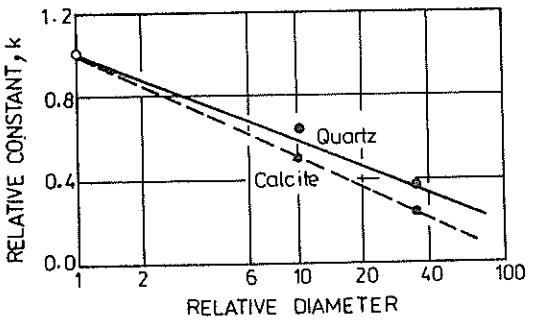

Figure 7 Relative constant K versus relative diameter

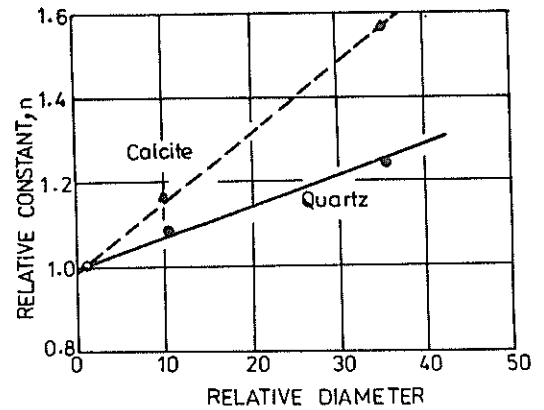

Figure 8 Relative constant n versus relative diameter

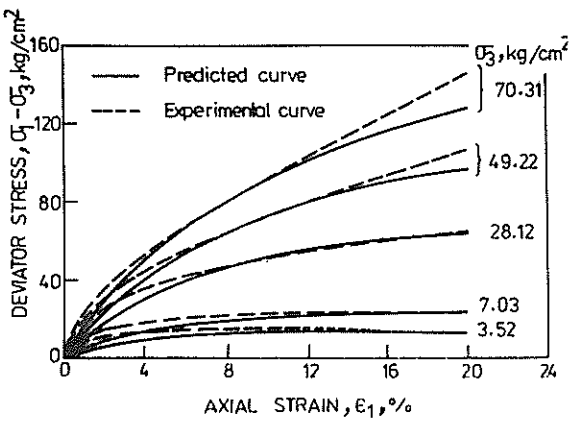

Figure 9 Predicted and experimental stress-strain curves for Quartz

6 CONCLUSIONS

On the basis of tests carried out in isotropic consolidation, and consolidated drained triaxial shear tests up to confining pressures of 126 kg/cm^2 on different fractions of Calcite and Quartz minerals and also on the basis of the tests results available from other investigators the following conclusions are drawn:

Volume compressibility increases with the increase of confining pressure and particle size. To predict the compressibility of prototype material tests have to be conducted on at least two different fractions of the material geometrically reduced in size. To predict the behaviour at higher confining pressures these tests have to be conducted at least at two lower confining pressures.

Failure axial strains were not reached for large size fractions under higher confining pressures, with lubricated end platens till the limit of tests (20 percent). Prediction was, therefore, not feasible for failure axial strains. In general, the volumetric contraction increased with confining pressure and particle size. It appears that the prediction of this behaviour is possible only to certain extent.

The initial tangent modulus E_i, increases with confining pressure and decreases with particle size. The constant 'b' inverse of $(\bar{\sigma_1} - \bar{\sigma_3})_{ult}$, decreases rapidly with confining pressure and is independent of particle size. It is possible to predict the stress-strain curves of the larger size fractions under higher confining pressures, by conducting tests on smaller size fractions and lower confining pressures and selecting the parameters in the desired stress-strain level. The modelling technique seems to be promising in predicting the behaviour of prototype materials such as rockfills. However, more experimental data is required to support this technique.

7 REFERENCES

BISHOP, A.W. (1948). A large shear box for testing sands and gravels. Proc. 2nd Int. Conf. Soil Mechanics and Foundation Engineering, Vol.1,pp.207-211.

FUMAGALLI, E. (1969). Testing on cohesionless materials for rockfill dams. Journal of the Soil Mechanics and Foundation Division, ASCE, Vol.95, No.SM 1, pp. 313-332.

GUPTA, K.K. and RAMAMURTHY, T. (1978). Prediction of the behaviour of rockfill materials. Proc. Geotechnical Conference, GEOCON-India, New Delhi, Vol.1, pp. 25-31.

HUDER, J. and FERTZ, L.B. (1967). Shear strength and density of Talus material used in the Goscheneralp Dam. Proc. Geotechnical Conference, Oslo, Vol.1, pp. 205-207.

JANBU, N. (1963). Soil compressibility as determined by Oedometer and triaxial tests. European Conference on Soil Mechanics and Foundation Engineering, Wiesbaden, Vol.1, pp. 19-25.

KIRKPATRIK, W.M. (1965). Effects of grain size and grading on the shearing behaviour of granular materials. Proc. 6th Int. Conf. Soil Mechanics and Foundation Engineering, Vol. 1, pp. 273-277.

KONDNER, R.L. and ZELASKO, J.S. (1963). A hyperbolic stress-strain formulation for sands. Proc. 2nd Pan Am. Conf. Soil Mechanics and Foundation Engineering, pp. 289-324.

LEE, K.L. and FARHOOMAND, I. (1967). Compressibility and crushing of granular soils in anisotropic compression. Canadian Geotechnical Journal, Vol. 4, No.1, pp. 68-86.

LESLIE, D.E. (1963). Large scale triaxial tests on gravelly soils. Proc. 2nd Pan Am. Conf. Soil Mechanics and Foundation Engineering, pp. 181-202.

LEUSSINK, H. (1965). Discussion. Proc. 6th Int. Conf. Soil Mechanics and Foundation Engineering, Vol.3, pp. 316-318.

LEWIS, J.C. (1956). Shear strength of rockfill. Proc. 2nd Australia-New Zealand Conf. Soil Mechanics and Foundation Engineering, pp. 50-52.

LOWE, J. (1964). Shear strength of coarse embankment dam materials. Proc. 8th Congress on large dams, Vol.3, pp. 745-761.

MARACHI, N.D. et al. (1968). Strength and deformation characteristics of rockfill materials. Report No. TE 69.5, Civil Engineering Department, Univ.of California.

MARACHI, N.D., CHAN, C.K. and SEED, H.B. (1972). Evaluation of properties of rockfill materials. Journal of Soil Mechanics and Foundation Division, ASCE, Vol. 98, No. SM 1, pp. 95-114.

MARSAL, R.J. (1967). Large scale testing of rock fill materials. Journal of Soil Mechanics and Foundation Division, ASCE, Vol.93, No. SM 2, pp. 27-43.

RAMAMURTHY, T. and KANITKAR, V.K. (1972). Elastic compression of sands under high isotropic consolidation stresses. Proc. Symp. Strength and Deformation Behaviour of Soils, Bangalore, India, Vol. 1, pp. 115-120.

RAMAMURTHY, T., KANITKAR, V.K. and PRAKASH, K. (1974). Behaviour of coarse-grained soils under high stresses. Indian Geotechnical Journal, Vol.4, No.1, pp. 39-63.

ROWE, P.W. (1962). The stress-dilatancy relation for static equilibrium of an assembly of particles in contact. Proc. Royal Society of London, Vol. A-269, pp. 500-527.

VALLERGA, B.A., SEED, H.B., MONISMITH, C.L. and COPPER, R.S. (1957). Effect of shape, size and surface roughness of aggregate particles on the strength of granular materials. ASTM, Special Technical Publication, No. 212.

ZELLER, J. and WULLIMANN, R. (1957). The shear strength of the shell materials for the Goschennalp Dam, Switzerland. Proc. 4th Int. Conf. Soil Mechanics and Foundation Engineering, Vol. 2, pp. 399-404.

Behaviour and Design of Post-Tensioned Residential Slabs on Expansive Clays

J. E. HOLLAND
Principal Lecturer, Swinburne College of Technology
D. J. CIMINO
Postgraduate Student, Swinburne College of Technology

SUMMARY. The design and construction of post-tensioned housing slabs on expansive clays in the southern states of the U.S.A. is outlined. The behaviour of a series of experimental post-tensioned slabs and housing slabs is then presented. The paper highlights the importance of accurately defining the mound shape under the slab and of not allowing runoff to pond against the edges of slabs.

INTRODUCTION

In the southern states of the U.S.A., slab-on-ground construction is used almost exclusively for housing foundations. In some of these states, (Texas especially) large surface seasonal heaves (up to 200 mm) occur in highly expansive clays found in most of the major cities. Post-tensioned steel slab reinforcing systems are used in approximately ninety percent of the housing slabs. Builders and engineers claim the following advantages of this reinforcement system over the conventional steel mesh and bars:

(1) Stronger for a common concrete cross section.

(2) Quicker, easier and more positive method of steel placement.

(3) Slightly cheaper if housing is built on a "tract" or production line basis at a limited number of large estates. For single homes, at individual sites over a large city, this system will be more expensive because of the additional travelling costs required to return and tension up the cables after the slab is poured.

The senior author has visited Texas on two occassions to study American performance, design and construction of post-tensioned housing slabs on highly expansive clays. As a consequence of these visits a research study into the design of post-tensioned housing slabs on Australian expansive clays was commenced in early 1977.

This paper will briefly outline the presently available design theories and American design and construction practices. The behaviour of three experimental slabs and three actual housing slabs (which have been instrumented and are being monitored as part of the research study) will be then discussed.

SLAB BEHAVIOUR

Clay soils in semi-arid climatic areas are subjected to seasonal soil moisture changes in their top few metres, which lead to cyclic volume changes and vertical movements. The vertical movement from a clay's seasonally driest to wettest states is defined as seasonal heave. The seasonal heave at a given clay soil site, and the depth to which it occurs, depends mainly on the clay type, the soil profile, the weather pattern and the site drainage.

When an impermeable surface cover, or slab, is placed on an expansive clay, the seasonal soil moisture change pattern will be altered, since surface evaporation from the clay will be terminated (Figure 1 (a)). If the site is very dry when a completely flexible slab is placed on it, edge wetting and heave of underlying clay will lead initially to the development of an edge heave or saucer type of slab distortion mode (Figure 1 (b)). With time the heave under the slab will slowly progress inwards (Figure 1 (c)), until ultimately a centre heave or mound distortion mode will form (Figure 1 (e)).

In the long term, the soil surface surrounding and under the edges of the slab will continue to move up and down with the seasons, so leading to flexing of the edges over a length which is commonly referred to as the edge distance, e (Figure 1 (e)). However, if the slab is sufficiently rigid it will not flex and distress of the superstructure will not occur. The economic design of an actual house slab

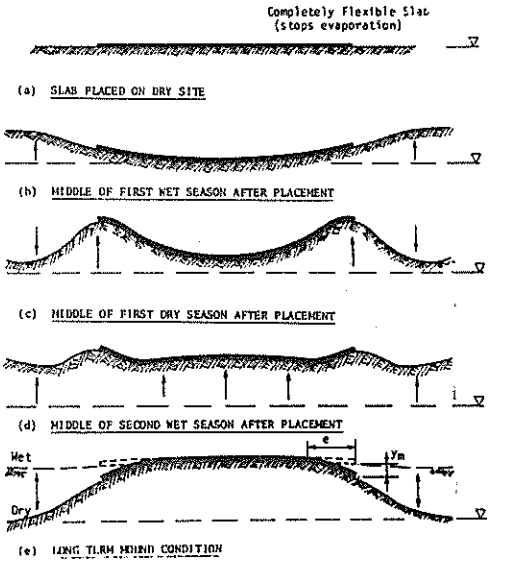

Figure 1 Idealized mound development

TABLE I

U.S.A. SLAB DESIGN SUMMARY

DESIGN METHOD	ASSUMED SLAB ACTION	SLAB LOADING & INITIAL MOUND SHAPE	DETERMINATION OF SLAB SUPPORT AREA COEFFICIENT	I-VALUE	LONG TERM E-VALUE	Fc (MPa.)	ALLOWABLE Ft (MPa.)	CURVATURE $\frac{\Delta}{L}$ (1 in.)	TOTAL POST-TENSIONING LOSSES (%)	SUBGRADE FRICTION LOSS	ρ (MPa.)	12.5mm Dia. CABLE SPACING (m)	MAXIMUM BEAM SPACING (m)	STEEL IN BOTTOM OF BEAMS	MINIMUM ULTIMATE MOMENT REQUIREMENT	CABLE TENSIONING
OLD P.T.I. (1975) OR MODIFIED B.R.A.B. (1968)	Dimensional	RIGID MOUND	From Empirical Relationship with clay type (P.I.) & Weather Pattern (Cw) $(c = \frac{L - 2y}{L})$	Using centre cross-section	E(Conc.) (28 days)	17.5	0.7	480	16	$\frac{1}{2}$ Slab Weight × μ where μ = 0.5 - 0.75 (μ = Coefficient of Friction)	0.35 Min.	1.2 to 2.8	P.T.I. & Reberts 4.5	Yes	Required	> 3-days < 7-days When F'_c=14MPa
NEW P.T.I. (1978)	Three	PARABOLIC	From Following Relationships: (1) e From Thornthwaite Moisture Index (2) y_m from: (a) % clay (b) Clay Mineral (c) Suction Profile (d) e (e) Velocity of Moisture Flow		of Soil	17.5	Centre Heave = 0.7 Edge Heave = 2.1	Centre Heave 480 Edge Heave 800	16		0.35 Min.	1.2 to 2.1	P.T.I. 4.5 to 6 Reberts 4.5	No	Not Required	> 3-days < 10-days When F'_c>14 MPa
LISSIAK (HOLLAND (1979))	Simplified	RIGID MOUND	From Empirical Expressions which Relate e & y_m to the Free & Confined Swell of Dried, Undisturbed samples of the Clay at Particular Site	Decreased	E (conc.) (28 days)	17.5	1.05	360	15	Nil	0.63 to 0.66	3.5 to 1.8	Approx. 4.5	No	Required	After F'_c >14MPa

consists of making it sufficiently stiff, so that any deflection of the slab due to mound development or due to seasonal wetting and drying under the slab edges will not lead to distortion of the house superstructure sufficient to cause cracking of brickwalls or jamming of doors or windows.

If a slab is placed on a very wet site, a mound will effectively already exist, so only seasonal wetting and drying of the clay under the slab edges will need to be accommodated by the slab.

U.S.A. DESIGN & CONSTRUCTION PRACTICES

In the areas of known high seasonal heave in the southern states of U.S.A. (Texas in particular) three methods are most commonly used to design housing slabs. Details of these three methods are presented in Table 1. The major points to note from this Table are as follows:

(1) It is of major importance in using these theories to accurately define the assumed, initial mound shape under the slab, if economical and realistic designs are sought. All the theories generally only consider the long-term, centre heave, or "doming" case, since it leads to significantly higher moments than the short-term, edge heave, or "dishing" mode, of slab distortion. The long-term mound shape is defined by the edge distance, e, and the differential mound heave y_m. Since both LISSIAK and OLD P.T.I. methods adopt vertical sided mounds, only the edge distance, e, is used to define the mound. In Figure 2, the design moment, M, and curvature deflection ratio, $\frac{\Delta}{L}$, obtained using these three methods for typical single single-storey housing are presented. This Figure clearly demonstrates the need to carefully estimate e and y_m at a particular site, if an economical housing slab design is required.

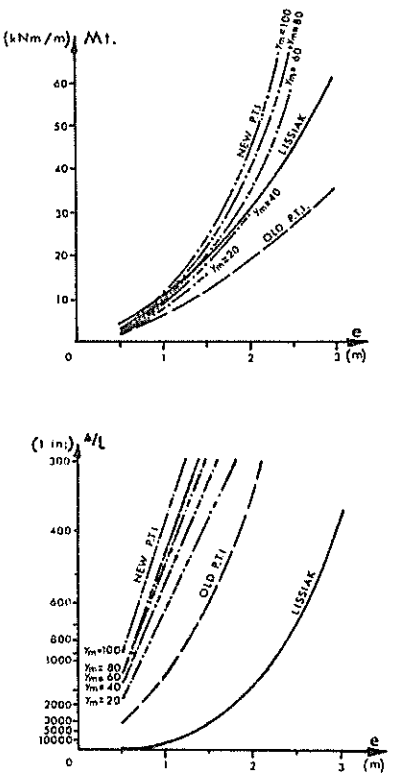

Figure 2 Moment and deflection versus edge distance

In the U.S.A., BRAB (1968) has attempted to relate edge distance empirically to the clay type (via P.I.) and the climatic pattern. This procedure cannot be used outside U.S.A. and is universally recognised by engineers designing housing slabs in expansive clays as being extremely conservative. However, this procedure is still widely used, but often in modified form to reduce its conservatism. The NEW P.T.I. (1979)

procedure,which was developed by R.LYTTON at the Texas A & M University, presents a more rigorous procedure to estimate e and y_m. The e estimation is done via an empirical correlation with the Thornthwaite Moisture Index. The correlation is extremely questionable in the authors' opinion and is not supported by the findings of this research study. A theoretical diffusion model was also used to develop a model to predict y_m. Unfortunately, this model requires the determination of far too many constants to be considered practical and economical for housing slab design. The values of ym obtained using this model appear to be excessively high for most clay types.

The Dallas, Texas empirical expressions relating e and y_m to the free and confined swell of dried undisturbed samples of clay from a particular site have been developed by engineers in this city. However, although the expressions are used widely in Dallas, they do not appear to be used greatly elsewhere. LISSIAK (Consultant) has used this procedure for over a decade. It commonly gives e values for Dallas clays of from 1 to 2.5 metres. The soil testing required is reasonably expensive and is considered to represent the slab-on-expansive clay-situation reasonably well. An unpublished current investigation of this procedure has indicated that it appears to be a most promising technique for estimating e & ym for Australian climatic conditions and clays.

(2) The accurate prediction of the mound shape is the most important factor in using these theories to produce the most economical slab design at a particular site. However, the assumption made in these three theories in relation to the allowable concrete tensile stress, the post-tensioning losses, the subgrade friction loss allowance and the allowable curvature deflection ratio, do significantly affect the resulting slab design.

The wide difference in opinion as to what allowable concrete tensile stress should be adopted is most apparent from Figure 3. Although post-tensioning losses due to elastic cable shortening, creep and shrinkage of concrete, and friction between cable and concrete may be estimated with some confidence, the question of the amount of subgrade-friction loss under a concrete housing slab is a very vexed one. The concept of subgrade-friction loss has been researched and developed mainly for constant thickness paving slabs which are only restrained laterally by the friction development between them and the soil subgrade. Housing slabs, however are restrained very significantly by the embedment of their beams into the subgrade. Obviously this subgrade friction loss must be greatly reduced by this lateral soil restraint on the slab beams. The coefficient of subgrade friction values suggested by both P.T.I. procedures do not appear to make any reasonable allowance for this embedment effect. LISSIAK considers that this loss will be negligible, if one considers the beam embedment restraint, and so ignores it.

(3) The use of the entire, uncracked cross-section and the common elimination of bottom steel beam reinforcement in American post-tensioned slabs, can lead to economy when compared to conventional steel reinforced slabs which do not generally assume these design conditions.

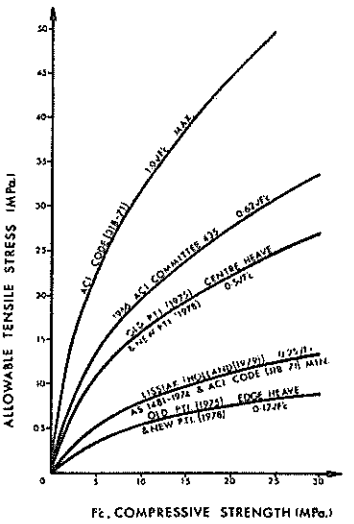

Figure 3 Allowable concrete tensile stress

It is also most common to increase the internal stiffening beam spacing to allow for the greater strength of the post-tensioned slab between the beams.

(4) The need for an ultimate moment check for housing slabs appears to be very questionable. This may be because this correction guards against a catastrophic failure resulting from extreme loading conditions (eg. abnormally high wind loading on a multi-storey building) which is much more likely to occur for an above ground structure than a housing slab. In fact, it is difficult for one to visualize any circumstances where extreme loading conditions will occur for housing slabs.

(5) The adoption of ultimate concrete compression strength, F'_c of only 17.5 MPa is significant in light of the Australian Prestressed Code (AS 1481-1974) setting a minimum value of 25 MPa. However, the use of post-tensioned housing slabs were probably not envisaged at the time of the formulation of this Code.

By Australian standards, the control generally exercised over housing slab designers and builders in the expansive soil areas, appears very lax. This, therefore, has lead to much lower construction standards. The use of very high slump concrete and very poor post-tensioning cable placement procedures is very common. Housing slab distress is commonly traced to lack of tensioning. The recommended time to conduct tensioning using the three design procedures is indicated in Table 1.

In the moderately expansive clay soils of California, the use of looped, post-tensioned cables is popular. This eliminates half the cable dead-end anchorages and saves about $100 for an average sized house. However, unless the loop is positively anchored to the inside face of the slab edge beams, it will be walked down during concrete placement and, following tensioning, it may shear through the beam and finish under the slab.

One aspect of the construction of housing slabs in U.S.A., that appears to be well controlled is that

of providing good drainage around them. (Figure 4). Obviously these requirements are more essential in U.S.A., since roof runoff drainage systems are not common, and at highly expansive clay sites the need to stop runoff ponding against slabs and leading to excessive localised clay heave under their edges is generally accepted. In fact, the Home Owner's Warranty Corporation, which offer the largest national warranty insurance plan for new homes in U.S.A., has a condition in its policy that will eliminate housing slab damage claims which can be shown to result from changes in the site drainage pattern after its construction. If it can be shown that the home owner changes this pattern, so that surface run-off water ponds against the house, and leads to high,localised clay heave and slab distress, then the claim will not be honoured.

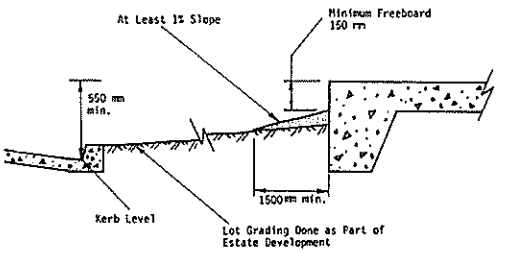

Figure 4 U.S.A. drainage requirements

BEHAVIOUR OF EXPERIMENTAL SLABS

Three 7.4 metre square experimental slabs were constructed at Sunshine, Melbourne, during 1977 and 1978. From previous extensive research studies (HOLLAND (1978)) at this site, significant seasonal soil movements in basaltic clays found there are known to occur. Details of the clays found at this site, together with the maximum seasonal heave and total soil water suction seasonal extremes observed over the last four years are presented in Figure 5. From the movement of a series of unloaded surface covers at this very poorly drained and very open, windy site (HOLLAND, PITT, WASHUSEN, CAMERON & JACKSON (1979)), a differential mound heave, y_m of 32 to 41 mm, coupled with an edge distance, e, of 2.1 to 2.5 metres, have been deducted.

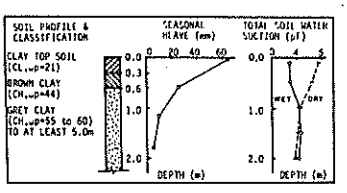

Figure 5 Sunshine soil properties

The three slabs have the same concrete cross-section and post-tension cable size and spacing (Figure 6). However, two of the slabs (S6 and S7) were lifted up on 200 mm of rock filling or sand so that their beams were sitting on the original ground surface. These two slabs were placed on initially wet sites in May, 1977. The other slab (S8) was not lifted out of the ground and was constructed on an initially,very dry site in March, 1978. None of the three slabs had any internal stiffening ribs. The designs of these three experimental slabs were based on the recorded behaviour of a series of conventionally reinforced slabs at this site (HOLLAND (1978)). The designs forthcoming from the theories outlined earlier required much stiffer slabs, and so were not used as a basis for sizing the slab. The slabs were loaded with pig-iron to simulate single-storey,brick veneer house construction. They were extensively instrumented with precision levelling points, pressure cells and strain gauges.

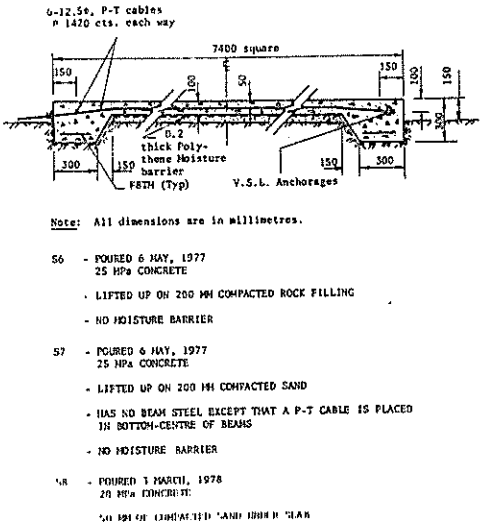

Figure 6 Sunshine experimental slab details

In Figure 7, the importance of the initial site soil moisture conditions in determining the future movement of slabs in areas of high,seasonal movements is demonstrated. In this Figure the centre and average edge movements with time for slabs S6 (placed on an initially wet site) and S8 (placed on an initially dry site) and the cyclic surface seasonal soil movement in the open are compared. The movements of S6 is negligible compared to S8. No significant flexing of the edges of S6 has been observed over the last two normally dry summer and early autumn periods (January to April). This same observation applies to S8. However, since the only drying cycle experienced by this slab was unseasonally short in 1979, it is expected some future significant edge flexing of this slab will occur. In a matter of a few months after it was placed on a very dry site,slab S8 changed from an edge to centre heave condition. In Figure 8 the most severe edge and centre heave distortion observed of this slab are presented. The behaviour of S6 and S8, even though they have no internal stiffening ribs and hence, the 100 mm slab spans 7.4 metres, has been quite satisfactory. The behaviour of S8 when exposed to more severe and longer seasonal clay drying conditions is uncertain.

BEHAVIOUR OF HOUSE SLABS

The site and drainage conditions at Sunshine are such that it floods regularly in the winter and spring and becomes extremely dry with clay fissures up to 75 mm wide being common in late summer and early autumn. Since these conditions were unrealistically severe from a soil movement viewpoint and unliveable for normal housing, it was decided to monitor three actual house slabs placed on dry clay sites where known moderate to high seasonal heaves occurred. The three house slab sites were located

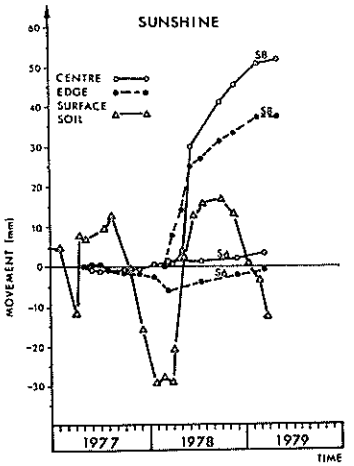

Figure 7 Movement of S6 and S8 slabs

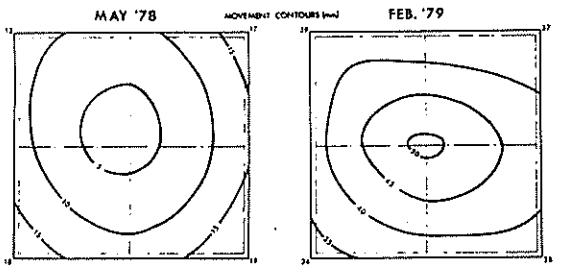

Figure 8 Distortion of S8 slab

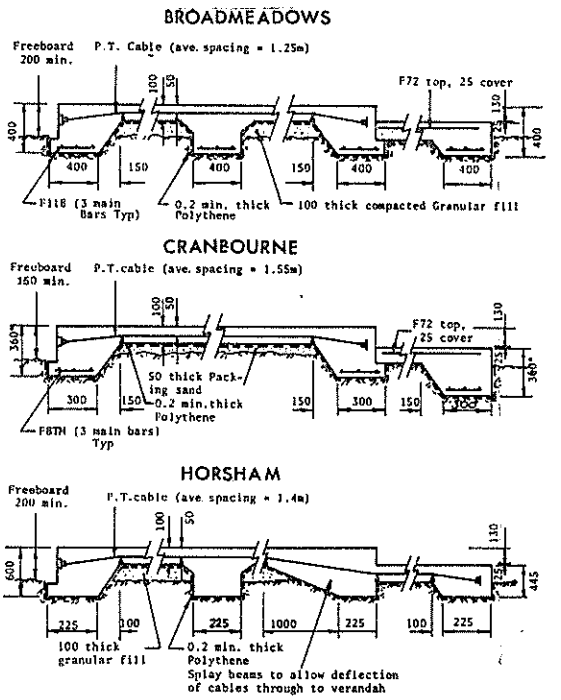

Figure 9 Details of house slabs

at Broadmeadows and Cranbourne (outer suburbs of Melbourne) and Horsham (a small provincial western district city in Victoria). The soil conditions at Broadmeadows are very similar to Sunshine, but the site is much better drained. Since highly expansive clays are known to exist to a depth of about six metres at the Horsham site, with a weather pattern more severe than in Melbourne, larger seasonal heaves of up to 80 mm at the surface are commonly observed in this flat, open, rural city. The brief design details of three actual housing slabs are presented in Figure 9. These designs were again mostly based on the known performance of actual slabs in these areas and the observed behaviour of a series of conventionally steel reinforced, experimental and actual house slabs established and monitored over a greater period as part of a separate but similar research study (HOLLAND (1979)). The design theories could not be used as the sole basis of the design selection because of lack of precise soil mound parameter input at these sites. The Horsham post-tensioned house slab design is interesting in that no bottom steel was used in the beams. The behaviour of this slab will not be discussed since it was only poured in April, 1979.

At the well-drained Broadmeadows site only limited edge heave of the housing slab has occurred. (Figure 10). It is of interest to note from this Figure that the wider stiffening rib spacing used has not had any noticeable detrimental affect on the slab performance. To date, one unusually short summer period in Melbourne, (1979), the observed surface seasonal heave at this site is only 21 mm. If one compares this heave with that at Sunshine (about 65 mm), accepting that the clay soils at both sites to at least a depth of two metres, have the same high potential for swell, then the importance of good site drainage is evident. If rain water is quickly removed from an expansive clay, then it will not be able to swell to the same degree as at poorly drained sites where regular and sustained flooding occurs. Clearly it is essential to stop water ponding against slabs by grading the surrounding surface away from them.

The housing slab at Cranbourne was constructed using no internal stiffening ribs. However, the existence of about 700 mm of filling and topsoil over the site required the edge beams to be increased in depth from 360 to about 850 mm so that they founded on the underlying (potentially highly expansive) slightly sandy clay. The movement of this slab after 12 months is presented in Figure 11. The slab has been in a fairly even edge heave condition since its placement, with no edge drying effects being observed to this stage. In the area of highest edge heave, surface water tends to pond against the slab. This behaviour further highlights the importance of grading the surface around the

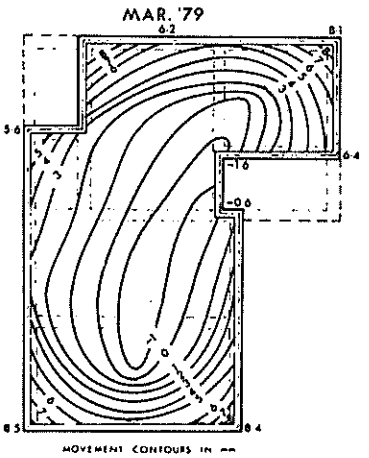

Figure 10 Distortion of Broadmeadows house slab

slab so this does not occur. The observed surface seasonal heave at this site, as measured in the open away from the influence of the slab is 26 mm. Since this heave is greater than at Broadmeadows, it follows that the stiffening ribs were unnecessary for both sites.

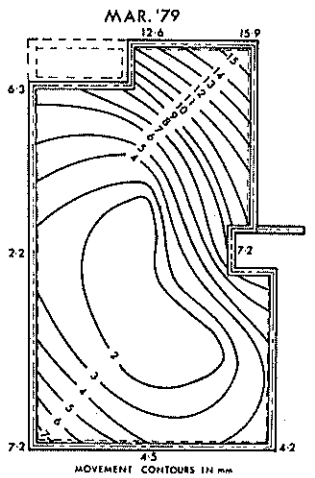

Figure 11 Distortion of Cranbourne house slab

Considering the behaviour of both housing slabs, one can conclude that the designs adopted were more than adequate and that stiffening ribs may be eliminated if only low to moderate levels of heave occur under slabs. It would appear that both slabs will remain in the less severe edge heave distortion mode for many years or possibly indefinitely. Unfortunately, because of a very short summer this year, no significant soil drying appears to have occurred under either of the slabs' edges. The importance of good site drainage away from the slabs is clearly evident.

CONCLUSIONS

Slabs placed on highly expansive clay sites, which are in their seasonally driest condition, are subjected to much greater underlying clay heave and therefore need to be significantly stiffer than those placed on wet sites.

For high seasonal heave clays, it is essential to grade the surface surrounding housing so as to ensure that surface runoff does not pond against foundation slabs. Ponding is likely to result in high localised slab heave.

The three slab design methods currently used in U.S.A., are all very dependent on precise definition of the mound shape that develops under the slab. The final designs derived from the theories are also dependent (to a lesser extent) on the assumptions made in relation to the amount of tensioning losses and the allowable concrete tensile stress value adopted.

Post-tensioned housing slabs appear to have strength and slight cost advantages over conventionally reinforced slabs at sites where high seasonal heaves are known to occur and large numbers of similar homes are to be constructed by only a few builders.

ACKNOWLEDGEMENTS

This research study would not have been possible without the generous financial support of the Australian Engineering and Building Industries Research Association Limited.

REFERENCES

ACI COMMITTEE 435 (1966), Chairman D.E.Branson, Deflections of Reinforced Concrete Flexural Members, ACI Journal, Proc. 63, 6, 637-674.

AMERICAN CONCRETE INSTITUTE (1971), ACI Standard 318-71, Building Code Requirements for Reinforced Concrete, Detroit.

B.R.A.B.(1968), Criteria for Selection and Design of Residential Slab-on-Ground, Publication Number 1571, Building Research Advisory Board, National Academy of Sciences - National Research Council, Washington D.C.

HOLLAND, J.E., PITT,W., WASHUSEN, J., CAMERON, D., JACKSON, J.(1979). Behaviour of Experimental Housing Slabs on Expansive Clays, 6th Asian Regional Conference on Soil Mechanics & Foundation Engineering, Singapore, Vol.1, pp. 289-292.

HOLLAND,J.E.(1978), Residential Slab Research-Recent Findings,Swinburne College Press, Swinburne College of Technology, Victoria, Australia.

HOLLAND,J.E.(1979), Report on Housing Slab Study Trip to U.S.A., Swinburne College Press, Swinburne College of Technology, Victoria, Australia.

NEW P.T.I.(1978),Design & Construction of Post-Tensioned Slabs-on-Ground, Post-Tensioning Institute, First Edition, Arizona.

OLD P.T.I.(1979), Tentative Recommendations for Prestressed Slabs-on-Ground used on Expansive or Compressible Soil, Post-Tensioning Committee, Prestressed Concrete Institute, U.S.A.

STANDARDS ASSOCIATION OF AUSTRALIA, (AS 1481-1974), S.A.A. Prestressed Concrete Code, North Sydney, Australia.

Behaviour and Design of Housing Slabs on Filling

J. E. HOLLAND
Principal Lecturer, Swinburne College of Technology
C. E. LAWRANCE
Postgraduate Student, Swinburne College of Technology

SUMMARY From a survey of the performance of housing slabs on filling and the behaviour of experimental rigid slabs at a variety of filled sites, a design method has been developed and is presented. An essential part of this method is a thorough site investigation by a competent soil engineer.

1. INTRODUCTION

An increasing number of housing allotments throughout the major Australian cities are having fill material deposited on them. This usually occurs during estate construction because of the expense of removing the excess cut soil from the road forming operation. Site spoil is placed on the lower blocks and, at least, track rolled in layers.Poorly and deeply filled lots are often found in the inner city areas. The use of old filled quarries and sand pits for housing in the established areas of the cities is now an attractive financial proposition as a result of escalating transport and housing costs.

In the past, at filled lots, the normal foundation system adopted has been to use piers to carry the house loading through the filling to the underlying natural soil. This is now a very expensive approach, especially for deeply filled lots. Recently, a limited number of rigid slabs placed directly on the filling have been used as a cheaper alternative. The cheaper cost of rigid slabs against the use of piers (Figure 1), however, must be weighed against the risk that unquestionably exists when placing foundations directly on filling. Obviously the more rigid the slab the less the risk at a particular filled site. But as the slab is made heavier its cost increases proportionally. It is therefore necessary to thoroughly investigate the filling and the underlying natural soil to determine the minimum slab rigidity which will give an acceptable level of risk at the most economical cost. It is essential to accurately define the filling depth and type and then estimate its future settlement behaviour over the area of the house. The predicted settlement behaviour can be expressed most simply for slab design purpose by the concept of the development of a soft spot. The greater the future uneven settlement of the filling the greater the soft spot and hence the more rigid the slab needs to be. For design purposes, the soft spot can be considered to occur anywhere under the slab. This design approach is obviously a simplistic model of the more complex and random support conditions likely to occur under a slab on filling. Great precision or refinement in the structural slab design using this concept is therefore unjustified.

As outlined later, the range of soft spot diameters likely to occur under housing slabs is from 0 to 5 metres. Unquestionably, in areas of mining subsidence or limestone sinkhole development, much larger diameters may occur. However, the behaviour

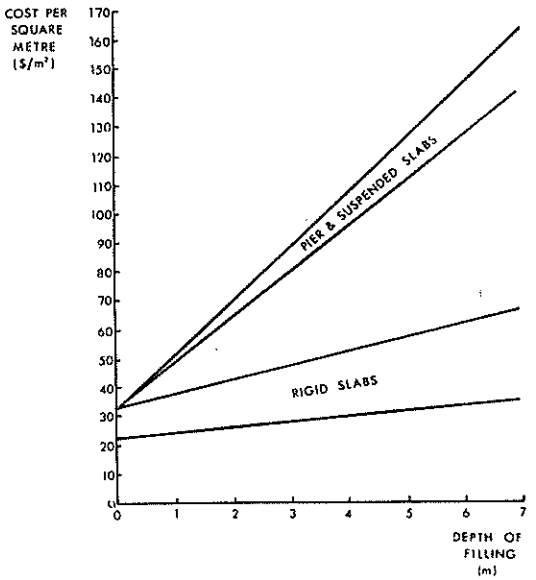

Figure 1 Relative foundation costs

of housing slabs when subjected to gross spot development from these two causes is outside the scope of this paper.

This paper will outline the details of housing slabs placed directly on filling throughout Melbourne, Victoria, Australia, over the last few years, and discuss briefly the failure of three of these slabs. A design approach for rigid slabs on filling will be suggested. Finally, the behaviour of seven experimental housing slabs on filling will be presented and discussed.

2. RIGID SLAB USAGE

Over the last ten years several thousand housing slabs have been placed directly on filled sites throughout Melbourne. The general details of the design of these slabs, together with the depth,age, type of filling, and the simplified natural soil profile are outlined briefly in Table 1. From this Table it can be seen that the soft spot diameter adopted can be related directly to the depth and

TABLE I

DETAILS OF RIGID SLABS USED IN MELBOURNE

FILLING						UNDERLYING SOIL	S S Ø	RIGID SLAB DESIGN				
DEPTH (m)	AGE (yrs)	STRENGTH LEVEL	AMT. OF GROSS ORGANIC MATTER	COMPACTION LEVEL	TYPE		(m)	ROCK FILL DEPTH (mm)	BEAM DEPTH (mm)	BEAM SPACING (m)	SLAB DEPTH (mm)	SLAB STEEL
0 to 2	0 to 1	High	Nil	High	Well Controlled, clean sandy clay placed in thin layers	Deep loose sand or a thin stiff clay layer over bedrock	about 1.5	Nil	300 to 400	4.5 to 6.0	100	F62 to F82
0 to 2.5	1 to 10	Medium	Low	Medium to High	Partly controlled, track rolled, sandy and clayey filling containing a little building rubble	Wet loose sand or soft deposits overlying stiffer clay and rock	1.5 to 2.5	Nil	300 to 500	4.5 to 6.0	100	F62 to F82
0 to 7	0 to 5	Medium	Low to Medium	Medium	Partly controlled, track rolled, silty clay or clay filling containing a little building rubble	Stiff clayey soil overlying bedrock	2.5 to 3.0	Nil	500 to 600	4.0 to 4.5	100	F82
0 to 7	0 to 5	Variable, Medium	Medium	Medium	Uncontrolled sand or sandy clay filling containing building rubble	Medium dense deep sand deposits or stiff clayey soil overlying bedrock	3.0 to 3.5	0 to 300	600 to 700	3.5 to 4.0	100	F82
0 to 8	0 to 3	Variable, Medium to Low	Medium to High	Medium to Low	Variable uncontrolled silty clay or clay filling containing building rubble	Soft topsoil layer overlying loose sands or stiff clayey soils overlying bedrock	3.5 to 4.5	300 to 600	700 to 800	3.5 to 4.0	125 to 150	2 Layers of F62 to F82
0 to 10	0 to 3	Very variable, Medium to Low	High	Medium to Low	Very variable, uncontrolled filling with possibly degradable material through	Soft topsoil layer overlying loose sands or stiff clayey soils overlying bedrock	4.5 to 5.5	600 to 1000	800 to 1000	3.5 to 4.0	150 to 200	2 Layers of F82

filling properties. In particular, the variability of the constitutents and depth of filling over the house area, the method of placement and compaction adopted, the age of the filling prior to slab construction and the amount of gross organic matter present all need to be considered.

To the authors' knowledge only three failures of these housing slabs on filling have occurred. In two of these cases, it was not realised that the sites were filled until superstructure distress was evident. At the third site, localized very highly organic filling caused excessive uneven distortion of the slab. Without indicating the locations, since legal action is in progress for two of the houses, these three failures will be discussed.

Case 1 : At this site an old gully has been filled with mainly grey silty clay and topsoil to a depth of between 1 and 4 metres. The filling is underlaid by a thin layer of topsoil and silty clay over siltstone. The filling was placed in 1973 under limited control, with possibly some track rolling of 500 to 1000 mm thick layers. In early 1975 the builder, unaware of the existence of the filling, placed a very light slab directly on it. Figure 2(a) & (b). Within months of completing the single-storey, solid brick house, excessive uneven dishing of the slab (Figure 2(c)) occurred and led to extensive damage of the superstructure. In fact, the slab has settled so far in the middle that it is just below the surrounding ground surface. This has resulted in internal flooding of the house following heavy rain.

A poor layout of internal stiffening ribs was used in this slab. Obviously it would have behaved in a more uniform and rigid manner if the ribs had been continuous from edge to edge and distributed more evenly over it. A recent set of levels on this slab indicated very little change in shape over the last nine months. This appears to indicate that the

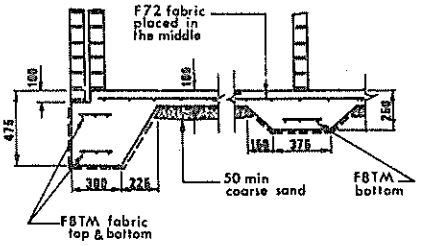

(a)

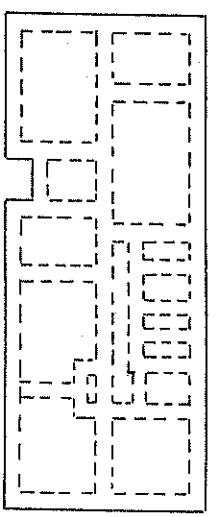

(b)

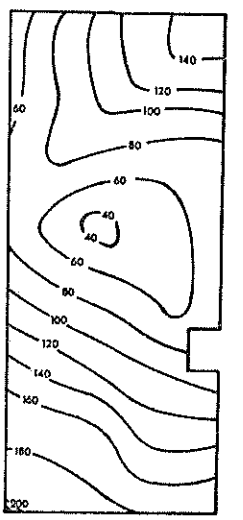

(c)

Figure 2 Case 1 details

filling has ceased to settle under both its self weight and that of the house weight.

Case 2 : In the northern and western suburbs of Melbourne relatively fresh basalt bedrock occurs at very shallow depths. This has led to numerous quarries being established throughout these suburbs- Some of these were used solely for exploration and were quite small (up to 5 to 10 metres across).

The second slab failure was in an area where a series of small exploratory quarries (up to about six metres deep) were very poorly filled with large basalt pieces and very soft, wet clay (Figure 3). Again, a builder completely unaware of the existence of these exploratory pits, placed a very light slab directly on one of them. Before the single-storey,solid brick house was completed the slab failed by dishing in the middle by an estimated 75 mm. Failure in this instance occurred immediately following a period of heavy rain. The house and slab were subsequently demolished.

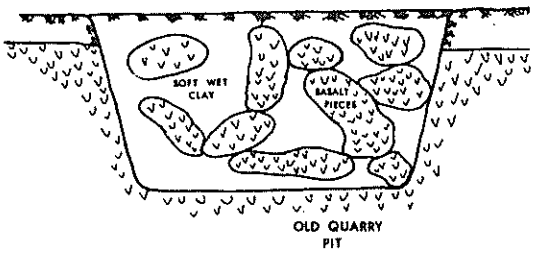

Figure 3 Case 2 subsoil details

Further, more extensive subsurface investigation of these filled pits was only possible using a large mechanical shovel. The test pits indicate that the basalt pieces are very variable in size and up to 900 mm across. The clay between the basalt pieces is kept wet and soft by the build-up of ground water in the pits.

Case 3 : In this case a limited initial site investigation indicated that between one and two metres of mainly stiff sandy clay filling exists over stiff to soft brown clay to at least a depth of seven metres. It was decided to remove the top two metres of filling and replace it in well compacted 300 mm thick layers. A modified suspended slab capable of spanning a soft spot of about two metres was then placed directly on the filling. About twelve to eighteen months after the slab was constructed, it began to settle substantially in the rear corner of the house (Figure 4). Unfortunately, the house sewerage lines were in this area and their design at the slab/soil interface was not capable of tolerating the large slab settlement and so sheared off. The leakage from these lines then aggravated the settlement problem by locally softening the filling and increasing the slab settlement. Recent subsoil investigation indicated the existence of a pocket of very poor, highly organic, filling under the corner of the slab that settled (Figure 5). It is the authors' opinion that this poor filling was created by the removal of the stump of a large tree and back filling the resulting hole with the surrounding topsoil and broken tree roots. Sandy clay filling was then placed over this extremely poor fill.

These three failed slabs form only a negligibly small percentage of the total number of rigid slabs

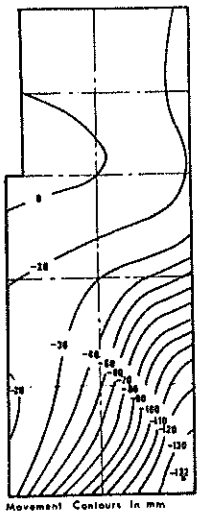

Figure 4 Case 3 slab settlement

that have been successfully placed on filling throughout Melbourne over the last decade. The extensive and successful use of about 1500 relatively light slabs on basically uncontrolled filling at Chelsea (a southern suburb of Melbourne) supports the view that the risk involved in using this foundation system on some filled sites is not excessive. The filling placed at Chelsea is generally an uncontrolled mixture of sands and sandy clays containing a little building rubble. It has been placed in a completely uncontrolled manner, then left for 5 to 7 years to settle under its own weight before the standard light Council designed slabs are constructed on it. This standard design is based on a 1.6 metre diameter soft spot and has been used for all forms of single and double-storey housing construction.

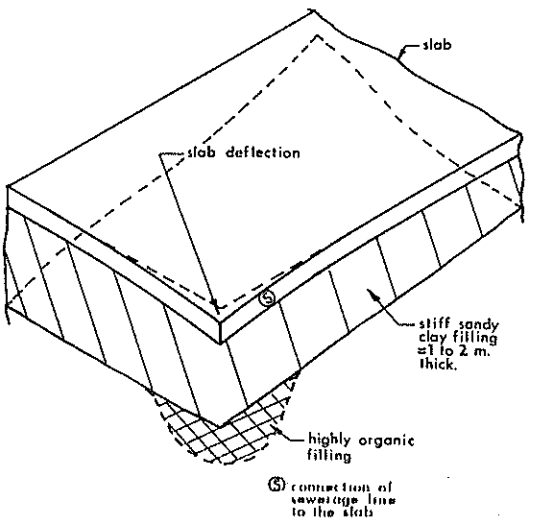

Figure 5 Case 3 filling details

Two further interesting rigid slab situations at Essendon and South Melbourne (suburbs of Melbourne), demonstrate the tremendous potential use and cost savings that can result from using this foundation system. At Essendon between 3 and 9 metres of uncontrolled mainly firm to soft, wet brown sandy to very sandy clay filling containing many large pieces of concrete, rock and steel (parts of car bodies), existed over thin layers of sandy topsoil and hard sandy clay underlaid by decomposed basalt. Initially an attempt was made to use a pier and suspended slab to support a large solid-brick, double-storey house. However, because of the numerous large pieces of concrete, rock and steel through the filling, it was not possible to drill pier holes through the filling using conventional equipment. It was then decided to place a very heavy rigid slab (Figure 6) directly on the very poor filling which had been placed about four years earlier. The use of the rigid slab foundation system saved the builder between $6,000 and $10,000 over the cost of a normally drilled pier and suspended slab system. As already stated, normally drilled piers were not possible, so if this system had been used much more expense would have been incurred using special pier drilling equipment, so increasing the rigid slab cost advantage by at least a few thousand dollars.

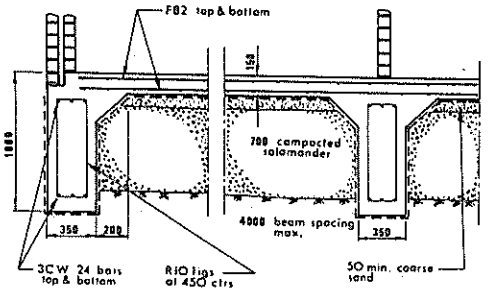

Figure 6 Essendon slab details

At South Melbourne, a light rigid slab (Figure 7) was placed about two years ago on about 1.5 to 2 metres of stiff sandy clay filling overlying about 5 metres of very soft and wet clayey silt. This is then underlain by stiff clay and siltstone. A single-storey, partly solid brick, office was constructed on the slab. Absolutely no signs of excessive uneven slab distortion exist in the superstructure of the office. However, the occupants claim the building shakes as trams pass by the front of the building. The excellent performance of this light rigid slab on a thin layer of filling over extremely soft natural deposits demonstrates again the load spreading ability and the

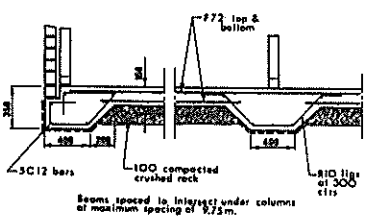

Figure 7 South Melbourne slab details

tremendous potential for the use of slabs at difficult sites. The more traditional driven piling foundation solution would be much more expensive. However, one must always be aware of the inherent risk in placing slabs directly on filling.

3 DESIGN GUIDELINES

Before attempting to design a rigid slab for a particular filled site it is essential that a competent soil engineer conduct a comprehensive site investigation. The investigation should include a series of boreholes carried through the filling and into the under lying natural soil. The number of boreholes depends on the type of filling encountered. The more variable the filling the greater the number of boreholes required so that the risk in using a rigid slab at a particular site can be minimized. The type of filling encountered in the boreholes must be carefully logged, particular note being taken of organic layers which could rot away and leave cavities. Estimates of strength and settlement characteristics of the filling should be obtained using appropriate soil testing techniques and experience. Because of the likelihood of gross variability in the filling properties, sophisticated and precise soil testing is unwarranted. Rather it is better to carry out many simple insitu or laboratory strength tests. Compaction testing in highly variable filling is of little value.

After the site investigation is completed, an estimate of the likely soft spot diameter that will effectively develop under the slab must be made. In making this estimation the following must be considered.

(i) The depth of filling and its variation over the house area.

(ii) The constituents of the filling. In particular the existence and amount of gross organic matter (i.e. timber pieces or large tree roots) must be considered as far as the possibility of it rotting away and producing sizeable cavities.

(iii) The strength, general degree of compaction and age of the filling is important in determining whether the filling is in fact still settling under its own weight.

(iv) The underlying natural soil profile. The likelihood of future uneven settlement of the natural soil under the filling self weight must be considered.

(v) The type of superstructure to be supported by the slab. Of particular importance is the amount of movement the walling will tolerate without distress and the evenness and level of loading applied to the slab.

(vi) The house size must also be considered, since the repair and likely associated legal costs resulting from excessive slab distortion will increase dramatically as the house cost increases.

(vii) The level of risk of excessive and uneven slab distortion and associated superstructure distress that the home owner is prepared to accept.

There is no question that the estimate of the soft spot diameter must be based on experience, however, the positioning of the soft spot under the slab controls the amount of steel reinforcing required

in it. The two critical positions of the soft spot are given in Figure 8 (a) & (b). Generally the corner soft spot gives the greatest amount of steel. The steel must be equal top and bottom in the beams

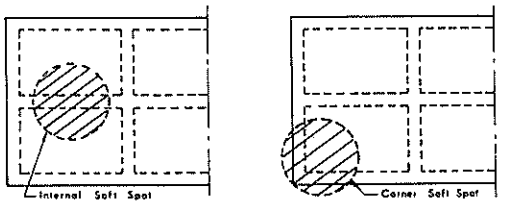

(a) (b)

Figure 8 Soft spot positioning

and based on the worst soft spot location under the slab. At poorly filled sites where large soft spot diameters must be assumed, the use of crushed rock under the slab is generally advisable. This rock should tend to reduce the size of soft spots or areas of localised settlement by flowing laterally. The slab panel between the beam grids must be designed so that it can span the design soft spot, which means the steel must be generally placed in the middle or near the bottom of the slab. For poorly filled sites, or where heave of clayey filling is likely, layers of steel in both the top and bottom of the slab panel must be used.

In light of the difficulty in accurately predicting the soft spot diameter and the resulting uncertainty thus inherent in the total design concept, the use of simple concrete design theory is suggested. The very conservative assumption that all house loading is taken by one beam over any particular design soft spot under the slab greatly simplifies the design calculations.

Since the design concept for slabs on filling is far from precise, house superstructure must be well articulated by floor to ceiling openings or frequent vertical expansion joints in unbroken lengths of brickwork. Extensive articulation is particularly important if solid brick house construction is to be placed on the slab and/or if brittle forms of brick and brickwork are to be used.

At poorly filled sites, the large uniform settlement of rigid housing slabs may lead to edge service piping failures. These failures could result in a sustained waste water leakage leading to the development of extremely large soft spot diameters. This potential problem can only be overcome by careful detailing of the sewerage lines, so that they can accommodate the likely level of rigid slab movement relative to the surroundings. Obviously this movement cannot be estimated with any degree of accuracy, but the two general sewerage line details outlined in Figure 9 should suffice in most situations.

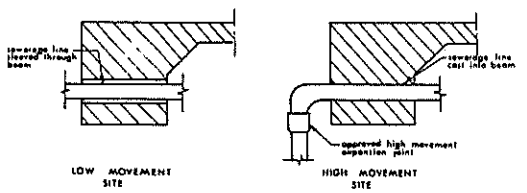

Figure 9 Suggested flexible plumbing joints

Based on experimental rigid housing slab behaviour and experience gained from a survey of the details and performance of a reasonably large number of existing housing using rigid slabs, a series of very tentative generalised designs for use on various types of filling have been outlined in Figure 10. A thorough site investigation is essential before even contemplating the use of a rigid slab. The generalised designs outlined in this Figure will not eliminate the need for this investigation or the use of an experienced engineer to design an appropriate rigid slab.

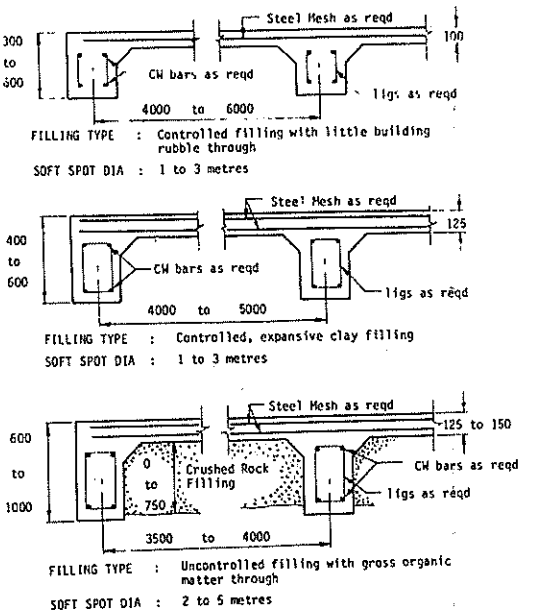

Figure 10 Generalised rigid slab details

4 EXPERIMENTAL RIGID SLABS

In an attempt to better understand the behaviour and design of rigid slabs on filling a series of seven actual housing slabs have been placed at a range of filled sites. The settlement of these slabs relative to deep bench marks is being monitored. The sites and slabs have been extensively investigated and designed according to the procedure outlined. General details of each slab design and the relevant site details are given in Table II.

At the Endeavour Hill site between 3 and 7 metres of track rolled sandy clay filling was placed about four years ago. The settlement of the rigid slab (placed in June 1978) has been relatively small (Figure 11); however, it is greatest where the filling is deepest. The movement also indicates that the filling had practically completely settled prior to placement of the slab. The major conclusion one could draw from this behaviour is that the slab was overdesigned, even though between 3 and 7 metres of only track rolled sandy clay filling existed under it.

The behaviour of the Chelsea slab in an old filled swamp area, where about 1500 houses have been constructed over the last decade using basically the same rigid slab design, is particularly interesting. The movement of the slab (Figure 12) indicates that a soft spot developed initially under the rear corner of the house. This caused a localised settlement

TABLE II

DETAILS OF EXPERIMENTAL RIGID SLABS

SITE	SLAB PLACED	FILLING			UNDERLYING SOIL	S.S ϕ (m)	SLAB DETAIL					COST SAVING (Figure 1) $
		DEPTH (m)	TYPE	AGE (Yrs)			BEAM DEPTH (mm)	SLAB THICK (mm)	SLAB STEEL	BEAM STEEL	BEAM SPACING (m)	
ENDEAVOUR HILLS (Melbourne)	June 1978	3 to 7	Track rolled, very stiff to stiff brown sandy clay to clay, with some building rubble through	4	Thin layers of grey sandy topsoil and stiff brown and grey sandy clay over granodiorite.	3	600	125	2 layers F62 top & btm	2CW 20 bars top & btm	4.0	11000
CHELSEA (Melbourne)	Aug 1978	1.2 to 1.5	Mainly stiff to very stiff brown and grey sandy to very sandy clay with minor amount of building rubble through	7 to 12	Stiff dark grey sandy clay to loose, wet grey clayey sand to at least 3 metres.	1.5	300	100	F72	F8TM btm	4.5	5000
WARRAGUL (Victoria)	Dec 1978	Up to 3	Very poor, wet. Sanitary filling overlaid by firm clay filling	5	Thin layer dark grey topsoil over stiff red brown clay to at least 3.5 metres.	3.5	750	150	F72 top & btm	2CW 24 bars top & btm	3.5	12000
WONGA PK (Melbourne)	Feb 1979	Up to 3	Well compacted very reefy clay	0.25	Thin layers of light brown and grey clayey silt overlying stiff brown and grey silt clay. This is underlaid by highly weathered siltstone.	3.0	600	100	F82	2CW 28 bars top & btm	4.0	3500
PATTERSONS LAKES (Melbourne)	June 1979	1.0 to 1.8	Mainly brown and grey silty and clayey sand	1.5 to 2	0 to 1.3m of organic silty clay overlying a very soft and compressible stratum of grey silty clay then sand to at least 7 metres.	2.0	450	100	F82	2 layers F11TN top & btm	4.0	3000
KILSYTH (Melbourne)	1979	Up to 1.3	Stiff to very stiff grey and brown silty clay with some building rubble through	5	Thin layer of topsoil overlying soft to firm grey and brown clayey silt overlying stiff to very stiff light grey and orange silty clay to at least 5 m.	1.5	300	100	F82	F8TM btm	6.0	3000
MODBURY (Adelaide)	1979	0.5	Well compacted red brown to brown silty clay	-	Stiff to very stiff red brown to brown silty clay to at least 0.8 metres.	1.5	500	100	12.5mm ø cables post^n.	Nil	No internal beams	2500

which was gradually redistributed by the stiffening beams to the rear portion of the slab. Since June, 1979, the settlement of the slab has practically ceased. The soft spot development appears to be due to the combination of a relatively more clayey natural underlying deposit and the close proximity of the edge of the general filling. The unfilled swamp is only about five metres from the rear of the slab.

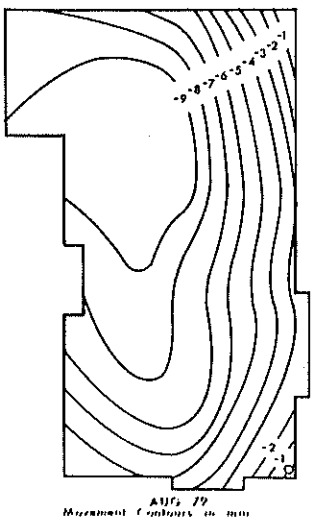

Figure 11 Endeavour Hills slab settlement

The Warragul site was used for sanitary land fill, so it represents the worst type of biodegradible filling likely to be encountered. The building is a single-storey, solid brick football pavilion. The settlement of the slab after nine months indicates that the slab has tilted towards the rear. (Figure 13). The greater settlement at the rear has resulted from the weight of the clay filling used to level the site. This clay filling was deeper under the rear of the slab. Obviously in light of the extremely poor type of filling, it is too early to draw conclusions as to the adequacy of the design used at this site. However, it has performed to date in a very rigid manner.

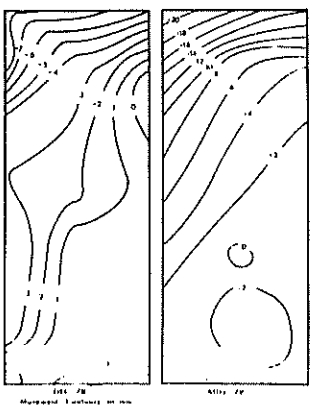

Figure 12 Chelsea slab settlement

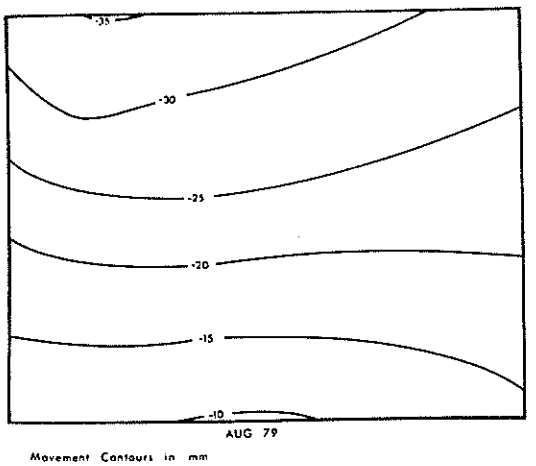

Figure 13 Warragul slab settlement

They type of filling placed at Wonga Park, in contrast to Warragul, represents possibly the best type of filling likely to be encountered. The filling consisted of basically clayey siltstone, carefully placed in thin layers with each layer being well compacted using a vibratory roller. No compaction testing was done, but the type of filling and its placement and compaction was visually monitored. The number of passes of the roller for each layer was set at a minimum of five. The filling depth varied from 0 to 3 metres, and, because of the fall over the house area, the top two corners of the slab required site cutting and are, in fact, sitting on the shallow underlying siltstone. The slab was placed about three months after the filling was completed and has not basically moved in the six months since. In light of the type of filling and the way it was placed, this behaviour is unlikely to change in the future. The slab obviously is overdesigned and a lighter design using a two metre diameter soft spot would have been more than adequate. However, the slab is supporting a large expensive house so the extra risk in using this lighter cheaper slab may not have been accepable to the owners. The excellent performance of this slab clearly demonstrates the ability of a rigid slab foundation system to perform with practically no risk, and at a much cheaper cost than the traditional pier and suspended slab system, at cut-fill sites where well controlled and suitably compacted cheap filling is available.

At the other two sites insufficient monitoring has been carried out to present any meaningful results. Monitoring of these slabs will continue until no further significant settlements occur, or until the end of 1982.

5 CONCLUSIONS

Based on the highly successful performance of thousands of rigid slabs on filling throughout Melbourne and the monitored behaviour of seven experimental housing slabs on a wide range of filled sites, a design procedure for rigid housing slabs on filling has been outlined. The procedure basically revolves around the determination of an effective soft spot diameter, which is then considered to occur anywhere under the slab, and allows the slab to be dimensioned using simple concrete theory. The critical soft spot diameter estimation requires a thorough site investigation by a competent soil engineer. In estimating the soft spot diameter at a particular site the following must be considered.

(i) The type, condition, depth and age of filling over the slab area.

(ii) The underlying natural soil deposits.

(iii) The size and type of superstructure of the house supported by the slab.

The design procedure suggested is not applicable to excessively large soft spot development due to mining subsidence and limestone sinkhole formation.The monitored behaviour of a series of rigid slabs at a wide range of filled sites is presented and shown to support the general design procedure outlined.

In closing, the complete lack of references accompaning this paper is significant. A very intensive search of the literature using manual and computer abstracting systems failed to produce one paper where the author was prepared to offer a design approach for rigid slabs on filling. Obviously this situation results partly from the fear of the legal consequences of failures and the past lack of use of this foundation system.

6 ACKNOWLEDGEMENT

The financial support of the Australian Engineering and Building Industries Research Association Limited made the monitoring of the experimental rigid slabs possible.

Settlement of Power Station Structures in the Latrobe Valley, Victoria

D. RAISBECK
Geotechnical Engineer, State Electricity Commission of Victoria, Australia

SUMMARY: A review is made of predicted and observed settlement at four power stations in the Latrobe Valley. The methods of settlement analysis are compared with those used to predict settlement at the new Loy Yang Power Station. Ground instrumentation installed to monitor both regional subsidence and net settlement of structures at Loy Yang is described. It is concluded that one-dimensional analysis is the most rational method of analysis for large structures underlain by a multi-layered soil profile.

1 INTRODUCTION

The Latrobe Valley contains one of the world's largest deposits of brown coal and forms the basis for power generation in the State of Victoria. There are at present four major power stations with a total generating capacity of some 3000 MW which is to be augmented in the 1980s by the Loy Yang Power Station of 4000 MW capacity.

The brown coal deposits occur in three major seams and have been recovered by open cut methods since the early 1920s. The location of the open cuts and their associated power stations is shown on Figure 1. The general stratigraphy and structural geology of the Latrobe Valley has been described by Gloe (1976).

The development of the Morwell Open Cut in the 1960s made it necessary to depressurise aquifers within and below the Morwell coal seams. This prevented hydrostatic pressures causing heave in the floor of the open cut. The dewatering of the extensive M1 and M2 aquifers has resulted in the regional subsidence shown on Figure 1. The effects of ground movements resulting from open cut development are discussed by Hutchings et al (1977).

In reviewing the settlement of large power station structures in the Latrobe Valley, previous methods of analysis will be compared with that adopted for Loy Yang A Power Station.

2 EFFECTS OF SETTLEMENT ON STRUCTURES

It is generally accepted by the Commission that differential settlements of 1.0 to 0.3% between structural columns can be absorbed without concern. There is greater concern for the effects of settlement on plant and machinery. Some notable exceptions are the central lift towers and the cooling towers. The lift towers are usually the

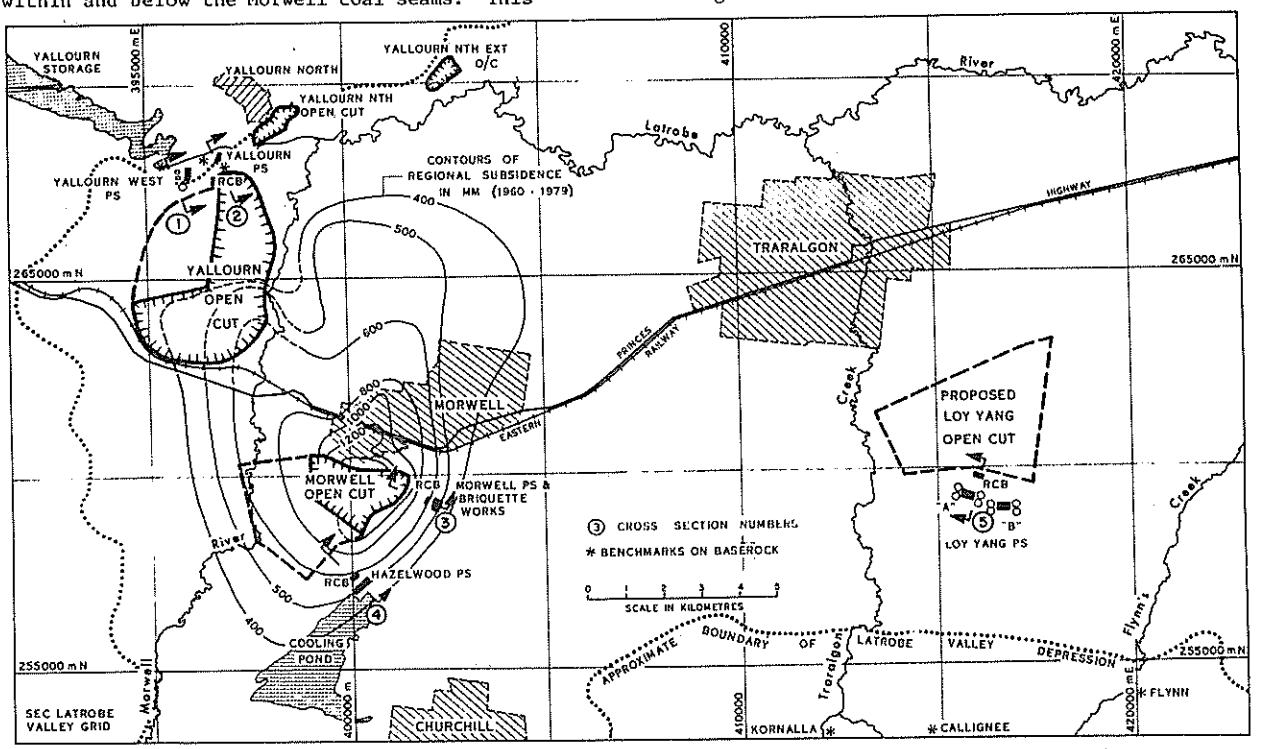

Figure 1 - Location of Power Stations and Open Cuts, Latrobe Valley, Victoria, Australia

TABLE I

Summary of Observed and Predicted Settlements for Power Station Structures

Power Stations & Structure	Date foundation completed	Foundation dimensions (metres)	Sustained Net. Press (kPa)	Predicted Net. Settlef (mm)	Observed Net. Settlef (mm)	Regional Settlement (mm)	Max. Tilt & direction (%)	Remarks on settlement analysis & soil conditions
YALLOURN (D) 470 MW								Elastic analysis based on plate load tests. E=275 MPa
–Boiler foundations	1954	55 × 15	188	6-20	25-30	38	0.05 SE	Turbine founds. all on CO.
–Boiler columns	,,	73 × 4.3	188	5-20	12-28	,,	,,	Remainder $\frac{1}{4}$ on CO, $\frac{3}{4}$ on
–Turbine foundations	,,	26 × 6	140	6-10	15	,,	,,	CLSA. Base rock at 300 m+
–Total Found. Area	,,	100 × 60*	35*	20	33 max.	,,	,,	GWL at 9 m (perched). See Section ①
							* * *	
YALLOURN WEST								I-D oedometer method using
STAGE 1 700MW								average m_v and μ=0.3.
–Boiler foundations	7/68-2/69	30 × 30*	160*	25-45	20	36	0.02 S	Elastic ignored.
–Boiler columns	7/68-2/69	8 × 8	170-255	20-40	20	36	,,	CLSI & CLSA with up to 3m
–Bunkerbay columns	2/68-6/69	7 × 8	200-240	30-40	10	36	,,	of compacted fill on E-side
–Turbine foundations	2/68-6/69	44 × 14	122	18-19	0-10	30	0 014 S	of boiler founds. Base rock
–Turbine columns	9/68-6/69	5 × 4	70-115	20	0-15	30	0.012 S	at 5-25m, GWL at 8m.
–Total Found. Area	1970	130 × 105*	72*	56	20	36	0.015 S	CT2 analysis based on plate
–Chimney No. 1	3/70	30 ø (168h)	100.	25	11	50	0.02 S	load tests. E=125MPa
–Cooling Tower 1	3/70	90 ø × 2.5 w	125	10	14	18	0.01 SE	CT1: Rock at 3-10m.GWL
–Cooling Tower 2	4/71	90 ø × 2.5 w	125	10	34	35	0.085 SSW	at 10m. CT2: $\frac{1}{2}$ on CO $\frac{1}{2}$ on
								CLSI. Rock at 10-25m.
Stage 2 750 MW								GWL 13-20m.
							* * *	
–Boiler foundations	6/76-6/77	50 ø*	150*	120	60+	20	0.01 SE	I-D oedometer method using
–Boiler columns	1976-77	8 × 5	220	120	60+	20	,,	m_v varying with applied
–Bunkerbay columns	4/76-12/76	33 × 12	260	130	70+	16	,,	press. and μ=0.3. Elastic
–Turbine foundations	4/76-3/77	42 × 14	131	81-95	28+	12	,,	component added. Based on
–Elect. Annexe cols.	3/77	8 × 6	200	125	25+	16	,,	E=80 MPa to 10m & E=150
–Total Found. Area	1976-79	130 × 110*	77*	130	70+	110 (p) 20	0.01 SE	MPa below. 5-10m of comp-
–Chimney No. 2	6/77	30 ø (168h)	130	85	21+	22	0.007 SE	acted fill. $\frac{3}{4}$ on site underlain
–Cooling Tower 3	8/76	103 ø × 3 w	100	16	23+	30	0.007 SE	by CO remainder CLSI &
Raw Coal Bunker (RCB)	11/75	120 × 45	180	120	67+	150 (p) 55	0.004 S	CLSA. Baserock at 60-120m.
								GWL at 9m (perched).
MORWELL (240 MW)								RCB Baserock 300mm
& BRIQUETTE WORKS							* * *	See Section ②
–Boiler foundations	6/55	100 × 92	115	NA	15	490	0.03 W	
–Turbine foundations	9/57	6 × 15.2	120	,,	9	480	0.04 W	German design predictions
–Turbine columns	9/57	3 × 5	115	,,	6	480	0.055 W	N.A. Mainly mat. foundations.
–Chimneys ×4	9/57	20 ø (94h)	115	,,	3	490	0.11 N	R.C.B. cellular raft.
Briquette Factories	1957-58	113 × 30	122-134	,,	6	480	0.01 W	Interbedded SACL & CLSA
Raw Coal Bunker	1957-58	70 × 23	128	,,	15	600	0.05 W	Baserock 300+m. GWL 12-15m (perched). See Section ③
							* * *	
HAZELWOOD 1600 MW								
–Boiler foundations	1962-68	30 × 14	188	12	15	380-400	0.02 N	
–Boiler columns	,,	7 × 7	260	18	15	,,	,,	I-D oedometer method using
–Bunkerbay columns	,,	3 × 3	260	5	15	,,	,,	average m_v. Elastic ignored.
–Turbine foundations	,,	28 × 10	160	0	18	,,	,,	Interbedded CLSA & SACL.
–Total Found. Area	1961-68	83 × 91 (×4)	83	18	25	,,	,,	Baserock at 300+m. GWL at
–Site Cut & Fill	1959-60	760 × 360	{-300 +150	{-245 +150	{-120** + 15	{425 350	0.03 E**	10m (perched). Site cut on East side. Fill on West side.
–Chimneys (×8)	1963-68	22 ø (137h)	140	0	0	390-410	0.02 N	See Section ④
Raw Coal Bunker	4/62-8/64	(116 × 10) × 4	160	160	140	425	0.09	
							* * *	
LOY YANG								
'A' Station 2000 MW								
–Boiler foundations	1979-82m	48 × 48*	153*	75-105	NA	85 (p)	0.10 N(p)	I-D oedometer method using
–Boiler columns	,,	10.5 × 10.5	163	80	,,	,,	,,	CR_1 for unload-reload & CR_2
–Turbine foundations	,,	42 × 20	85	70	,,	,,	,,	for net loading. Elastic
–Turbine columns	,,	4 × 6	50	25-35	,,	,,	,,	ignored. Post construction
–Total Found. Area	1979-83	140 × 150 (×2) *	70*	105	,,	,,	,,	assummed $\frac{1}{3}$ of oedometer.
–Boiler Excavation	1978	50 × 120	60	−20	−27	,,	,,	SACL underlain by inter-
–Chimneys (×2)	1979-80	40 ø (260h)	185	50	NA	100 (p)	,,	bedded SISA & CLSI
–Chimney Excavation	1979	50 ø	200	−40	−46	,,	,,	Baserock at 130-220m
–Cooling Towers (×4)	1979-83	103 ø × 3.2 w	100	25-30	NA	85 (p)	,,	GWL at 75m
Raw Coal Bunker	1979-80	166 × 68	190	150	,,	330 (p)	0.20 N (p)	See Section ⑤
–Bunker Excavation	1978	166 × 68	60	−20	−18	,,	,,	

NOTES: * Indicates foundation dimensions and net pressures are based upon averages.

** Measurements started 12 months after construction complete.

Soil Type; SA-sand SI-silt CL-clay CO-coal ie. SISA-silty sand.
NA-Not available (p) predicted w-width h-height ø-diameter

first structures erected in the centre of the power station block, usually between the boilers and adjacent to the bunker bay. Once erected these 100 m high concrete structures are subjected to tilt caused by subsequent construction. This produces connection problems with steelwork and floors at higher levels.

The thin shell hyperbolic cooling towers are constructed on a continuous strip footing at low bearing pressures to minimise differential settlements. To date, the maximum observed planar tilt has been 0.085% under Cooling Tower 2 at Yallourn West. It is noted that Ciesielski et al (1977) has reported values of planar tilt in the order of 0.10% and differential settlements between adjacent columns around the perimeter footing of 0.17%.

The major items of plant which are affected by settlements include the turbine house crane rail, the bunker bay shuttle rail, the boiler off-take ducts and turbo-generators. Provided that post-construction adjustments can be made to the supports for these items, the effects of settlement can be accommodated.

3 SETTLEMENT OF EXISTING STRUCTURES

The earliest power station for which survey records on settlements are available is located at Yallourn. The later "D" and "E" sections of this station were constructed after 1954. Morwell Power Station and Briquette Works were completed between 1955 and 1958, while Hazelwood and Yallourn West were constructed between 1962-68 and 1968-80 respectively. A summary of the observed settlements at these stations is presented in Table I. The stratigraphy beneath these stations is indicated on the cross-sections, Figure 2.

3.1 Yallourn D

Observed settlements at Yallourn D Power Station are approximately 50% higher than predicted. The difference may be attributed to the method of analysis which used the elastic modulus from plate load tests to determine an assumed elastic settlement. The method did not take into account the size of the loaded area or the time-dependent nature of settlement on coal. However, settlements have been relatively small and no structural distress has occurred.

3.2 Morwell

The Morwell Power Station and Briquette Works were designed in Germany in the early 1950s and no settlement estimates are available. The foundations are monolithic rafts on a site which had significant excavation prior to construction. Net settlements are small while regional settlements are the largest experienced in the Latrobe Valley. These settlements have not caused distress in the structures.

3.3 Hazelwood

Settlement predictions at Hazelwood were made using an average coefficient of compressibility m_v from laboratory oedometer tests and a large scale load test described by Green (1972). An allowance was made for site cut and fill in the choice of m_v values. No elastic settlement was considered.

3.4 Yallourn West

Stage 1 of Yallourn West Power Station was completed in 1971. Observations indicate that settlement of the structures is substantially complete with additional settlement due only to regional effects and construction of the Stage 2 structure. As shown in Figure 2, the base rock is much shallower under the Stage 1 structure and settlements are correspondingly lower than Stage 2 which is nearing completion. The method of analysis used in settlement prediction for Stage 1 adopted a one-dimensional (1-D) approach using average m_v values directly from laboratory consolidation curves. A correction factor $\mu = 0.3$ was then applied to the oedometer settlement ρ_{oed} thus calculated to obtain the estimated total settlement ρ_t ie $\rho_t = \mu\rho_{oed}$. This factor had its origin in the experience gained from settlement of structures at Hazelwood and was thought at the time to be related to Skempton and Bjerrum's correction factor μ quoted in Burland et

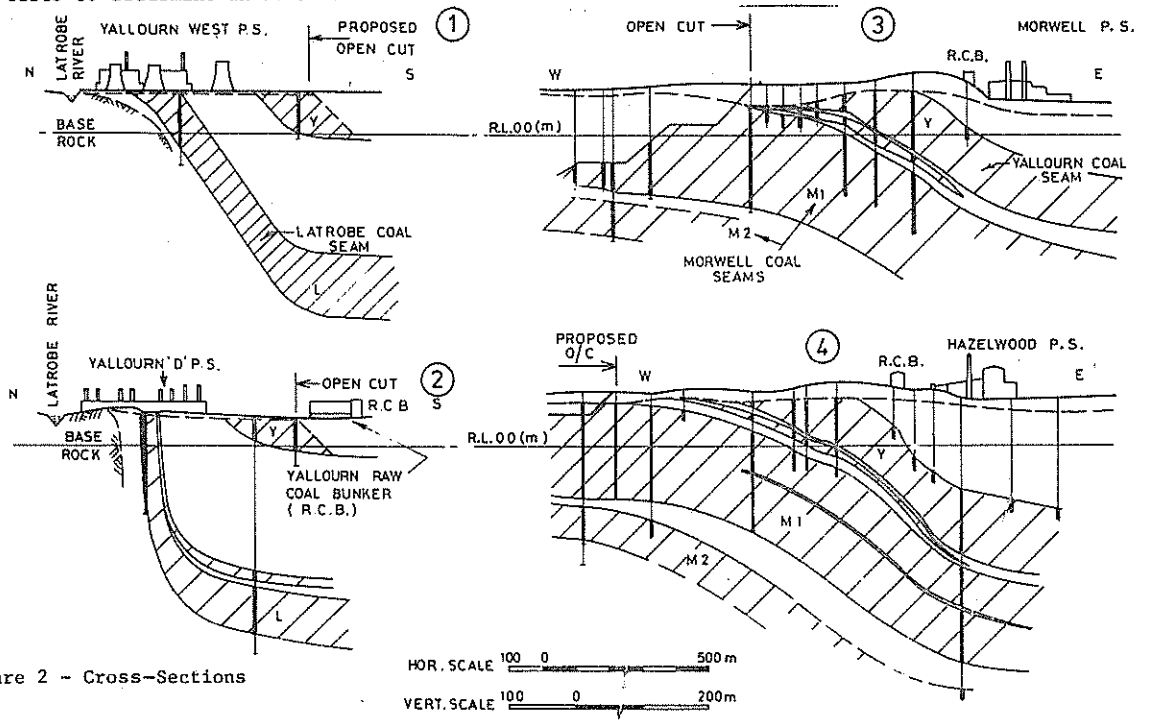

Figure 2 - Cross-Sections

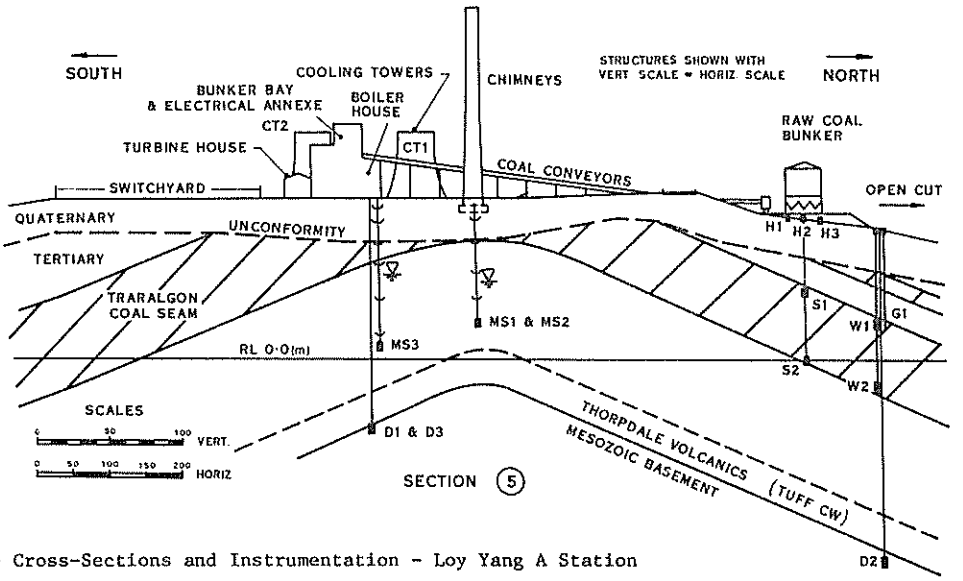

Figure 3 - Cross-Sections and Instrumentation - Loy Yang A Station

al (1977). No additional allowance was made for immediate elastic (lateral yield) settlement. Comparison of the predicted and measured settlement in Table I indicates a reasonable agreement in the Stage 1 power station block itself. The Stage 2 analysis used a variable m_v from laboratory curves and added an elastic component ρ_i after applying a factor $\mu = 0.3$ to the oedometer settlement $\rho_t = \rho_i + \mu\rho_{oed}$. The rate of settlement of Stage 2 foundations is being observed at present. Elastic settlement is predicted to be approximately 70% of total net settlement. By mid 1979 approximately 75% of the load had been applied resulting in some 50% of the predicted settlement occurring.

4 LOY YANG POWER STATION

The Loy Yang Power Station site lies across an anti-clinal dome structure on the southern flank of the proposed open cut. Two 2000 MW stations, A and B, are presently under construction on adjacent sites. The subsurface profile is shown in Section 5, Figure 3.

4.1 Soil Properties

At A Station a total of 28 distinct soil layers were identified in the upper 130 m of the soil profile. Study of the laboratory consolidation characteristics of these soils, shown idealised in Figure 4, indicates that the coefficient of compressibility m_v should not be used directly from the curve. Significant sample disturbance is shown to occur in the working range of P_o to P_c where the immediate strain component $\Delta\epsilon_i$ reaches its peak. This made it necessary to reconstruct the undisturbed consolidation curve by adopting a compression ratio CR_2 based on the rebound curve CR_2' or CR_2'' over a similar pressure ordinate range. A similar recycle from P_o gave a compression ratio CR_1 which was adopted for calculation of heave or reload. The virgin curve and preconsolidation pressure were determined by the Schmertmann method and the slope identified by the compression ratio CR_3. In general, the value of CR_2 was found to be about 10% of CR_3 and four times CR_1.

As the soil profile in Figure 5 shows, the apparent preconsolidation pressure decreases through the upper Quarternary materials due to desiccation of the upper clays. In the Tertiary materials there is an increase in the over-consolidation ratio which becomes more distinct in the coal seams. This additional apparent preconsolidation is the result of high secondary consolidation in the organic coal. This manifests itself in a high undrained strength compared with clays at a similar depth. Near the base of the Tertiary materials there is a formation known as the Thorpdale Volcanics consisting mainly of a completely weathered tuff. The deeper samples taken in this material showed a tendency to collapse at lower preconsolidation pressures. A rapid rise in preconsolidation results once the Mesozoic basement is encountered.

In the applied stress range these over-consolidated soils show little evidence of a Terzaghi type primary consolidation time curve. A typical curve tends to exhibit an initial immediate strain and

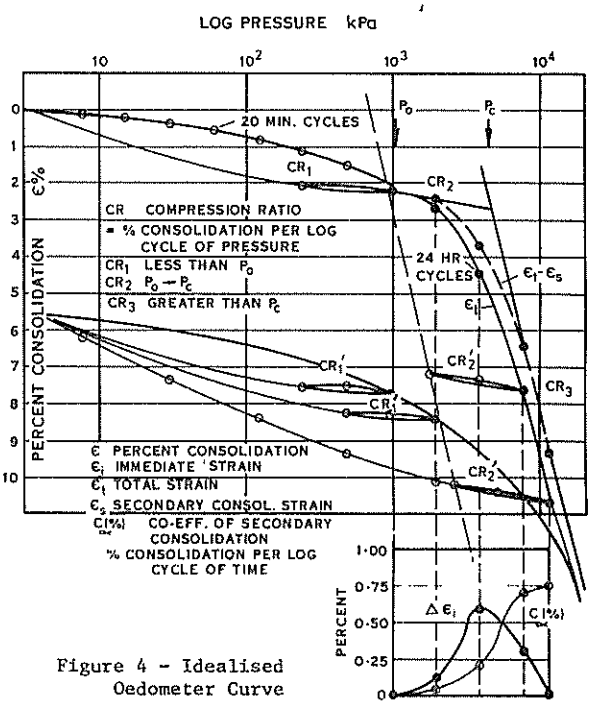

Figure 4 - Idealised Oedometer Curve

Heavy Structures Founded In Aeolian Soils

S. R. RONAN
Supervising Designing Engineer, Engineering and Water Supply Department, South Australia

SUMMARY Case histories relating to the foundations for three R.C. tanks are presented. Details of the site investigations are given. The design criteria, construction methods and the performance of the treated soil foundations are recorded.

1 INTRODUCTION

The treatment of the foundations for tanks at Waikerie, Woolpunda and Loveday provide the basis for these case histories. The tanks are all close to the River Murray in South Australia and are founded on "fossil" sand dunes. The locations of the tanks are shown in Fig. 1.

In the past the practice has been either to found at the surface or to use reinforced concrete piles to carry the structural loads through the aeolian soils. The former solution was not always successful, and the latter, although sound, was not necessarily the most economical.

In order to understand the behaviour of these soils, a study was made of the local geology and aeolian landforms.

2 RELEVANT GEOLOGY OF THE REGION

The aeolian soils of the Murray Basin of South Australia, are derived from sedimentary marine deposits laid down, during the Tertiary period. During this period limestones were formed, visible in river cliff formations downstream of Morgan.

Next an impervious layer of marl was laid down followed by the bright yellow Loxton Sand, typically 16 m thick. These unconsolidated sands were laid down in estuarine conditions.

More sands overlie the Loxton Sand. These occur as sandstones, sandy limestones and calcareous sands and were deposited in an estuary which more or less follows the present course of the Lower Murray. They are visible in cliff exposures at Waikerie and are found as partly consolidated sands in the river cliffs upstream of Loveday.

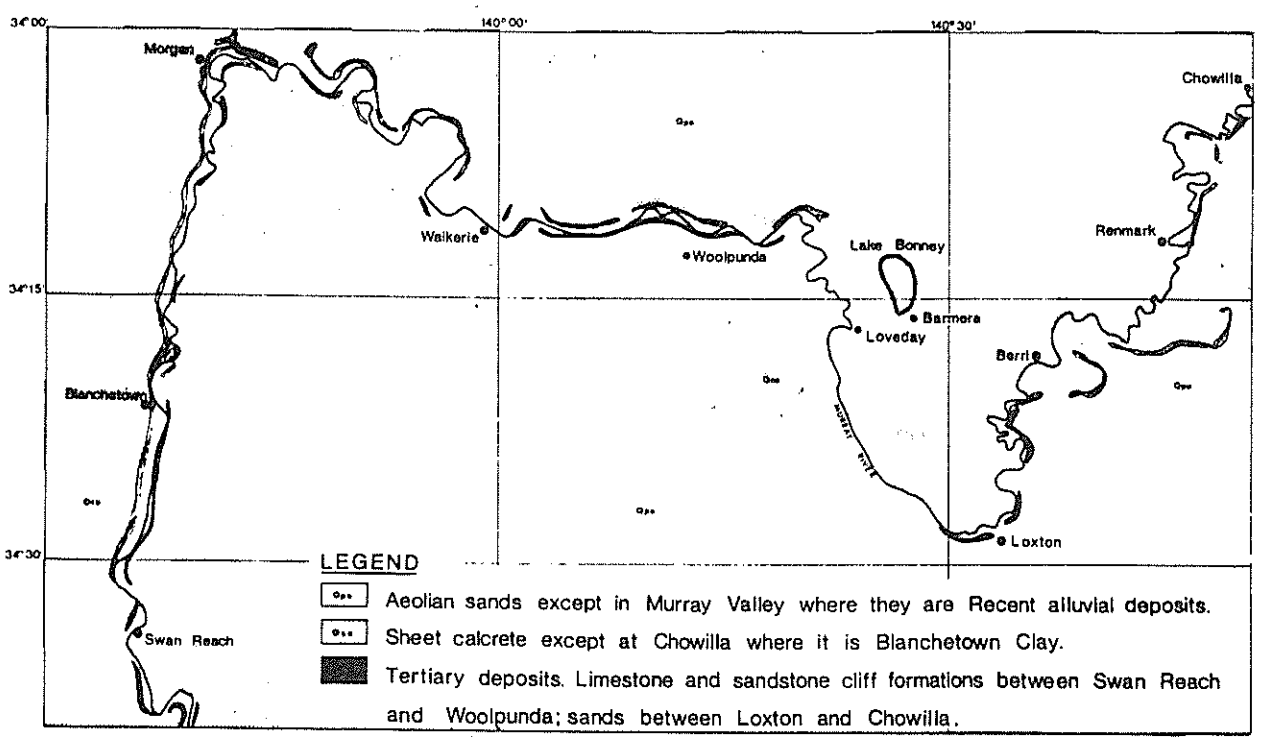

Figure 1 - Location plan and broad geology

Later, in the Quaternary, clays and limestones were formed as lake deposits. The eroded surface of these deposits is overlain by dune sands and pebble conglomerates derived from them and older rocks. This is the present-day blanket of loess and associated calcrete which forms the foundations for the Departmental tanks.

3 DESIGN TASK

3.1 The Structures

The dimensions of the 1.25 ML elevated tank at Waikerie and Woolpunda and of the surge tank at Loveday are shown in Fig. 2.

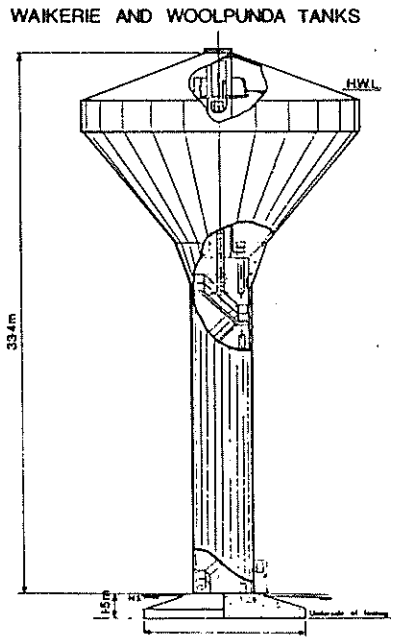

Figure 2 - Tank dimensions

3.2 Soil Loading

The load diagram for the Waikerie and Woolpunda Elevated Tanks is shown in Fig. 3.

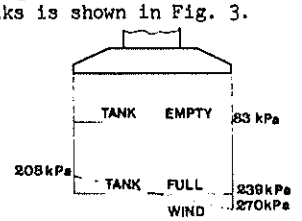

Figure 3 - Load diagram

3.3 The Foundation

It was realised that, should the foundation for any of the three structures become partly or completely wet then collapse of the open-structured soil would be inevitable. The foundation treatments considered were to:

Prevent the soil from becoming wet,
Excavate and recompact with fill for a selected depth,
Use concrete or steel piles,
Form sand or gravel piles,
Densify the soils by Vibroflotation,
Construct stone columns by Vibro-compaction,
Pre-load the site.

4 WAIKERIE ELEVATED TANK

4.1 Site Investigation

Typical soil profile and test results are given in Fig. 4.

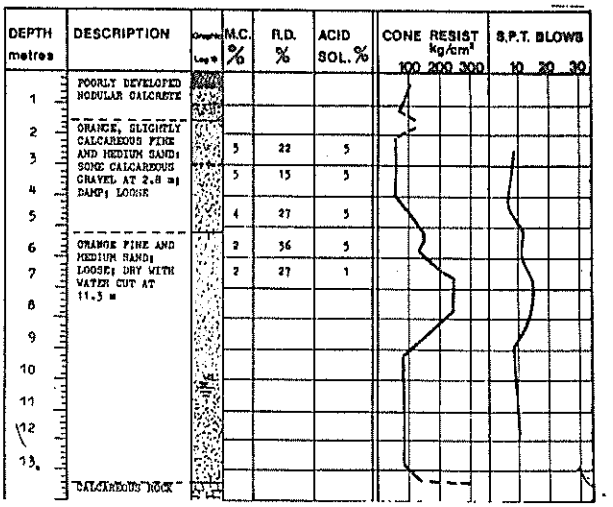

Figure 4 - Soil profile and test results

4.3 Design

Settlement predictions, based initially on the static cone soundings, gave 46 mm total settlement. The soundings showed the ground to be uniform. Hence, with the rigid tank base and small wind loading component, the differential settlement was expected to be small. Initially the natural soil foundation was therefore considered acceptable.

The inspection of the 1.5 m deep excavation for the foundation revealed aeolian deposits. A pit, then a shaft, were dug to obtain soil densities and determine the degree of cementation of the sand. This revealed how loose and also how weakly cemented the sand foundation was.

Plans to provide an adequate foundation by preventing the soil from wetting-up were therefore scrapped as the soil in its dry state was considered insufficiently cemented to prevent excessive settlement under the tank load.

Further deeper exploration was then done, the Standard Penetration Test being used to define the sands density. Low densities were found to 12 m with a small increase at 6.4 m. A rocky layer was found at 13.4 m.

Cost estimates for excavation and recompaction, cast-in-situ piles and sand piling came out in favour of sand piling and a design, based on this method, was prepared.

The design aim was to produce a mass of compacted sand, 15 m in diameter and 5 m thick beneath the footing. A triangular grid of piles, spacing 1.7 m, was used. The Contractor was required to displace 650 kg of sand per metre of pile into the ground. This "method" specification, was used as an alternative to requiring the Contractor to work to a performance specification.

The specification called for the first five piles to form a trial to ascertain whether the pile spacing or the amount of sand to be displaced should be altered.

The predicted settlement for the sand piled foundation was 50 mm. It was expected that this would be derived largely from the soil below 6.4 m.

4.4 Construction of Foundation

The sand piles were placed from a 380 mm tube which was driven percussively with a 3 tonne hammer to 6.4 m. The Contractor elected to backfill the excavation and form the piles from 1 m above foundation level, thereby ensuring the piles immediately below foundation level would be heavily compacted. The sand was hammered out of the tube as it was withdrawn, the Contractor being required to pull the tube in 250 mm increments. The first five piles, which formed the trial, indicated that the pile spacing and the amount of sand displaced were adequate to achieve the required sand density.

During the work a general tightening up of the sand occurred ahead of the piles being formed, particularly below a depth of 5.5 m. Piles became increasely hard to drive. Because of this the driving depth, for all except the perimeter piles, was reduced to 5.5 m.

The treated ground was extremely tight. Standard Penetration Test values in it ranged from 32 at 1.8 m to 100 at 6.5 m.

4.5 Performance of Structure

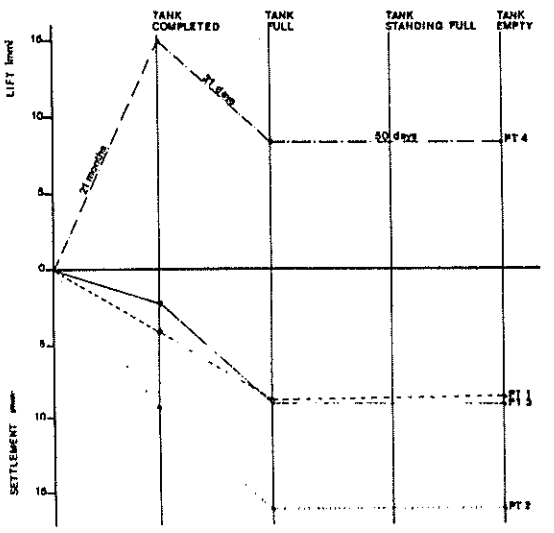

Figure 5 - Settlement data for Waikerie Tank

Settlement data for each loading stage is given in Figure 5. The measurement points are at the quarter points on the perimeter of the base and number consecutively around it.

These measured settlements imply a mean settlement of 5 mm with an overall tilt of 10 mm.

5 WOOLPUNDA TANK

5.1 Site Investigation

Typical soil profile and test results are given in Figure 6.

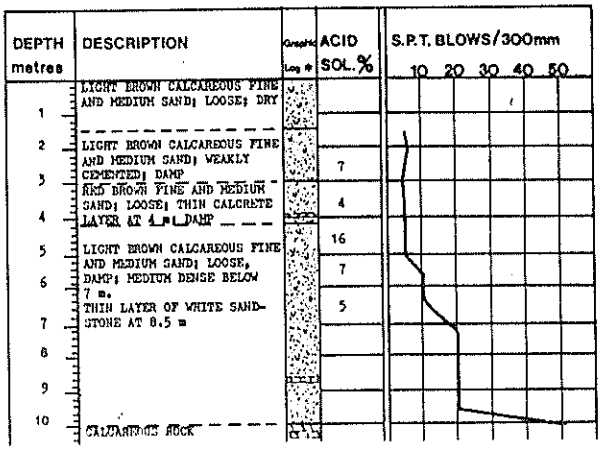

Figure 6 - Soil profile and test results

The soil investigation, confirmed the site as the crest of an aeolian dune. The sands were loose and weakly cemented. Sand densities started to improve at 7.5 m and a hard layer was hit at 9.5 m. Sand sizes to 6.5 m depth were typically 35% medium (200 to 600 microns) 50% fine (60 to 200 microns) and 15% less than 60 microns (with 8% less than 2 microns).

5.2 Design

Cost estimates based on foundations of concrete or steel piles, excavate and recompact and sand piling again came out in favour of sand piling. A treated volume of 15 m dia. by 4.7 m thick beneath the footing was selected.

An alternative tender based on vibro-compacted "stone columns" was submitted by one tenderer. This was cheaper than the lowest sand-piling tender. The "stone columns" were to extend from the surface to a depth of 6.5 m. Pile spacing varied between 2.35 m close to the centre of the foundation to 1.35 m at 4 m from the centre. The spacing then opened out until it became 2.08 m, 6 m from the centre.

The " stone column" design called for the removal of the top metre of the prepared foundation and its replacement with mat of compacted crushed rock. This was to ensure the adequate transfer of load into the "stone columns" and also to remove the less compact stone from the top of the columns.

It was assessed that the total settlement for the tank founded on the columns would not exceed 75 mm with a maximum differential settlement of 20 mm.

5.3 Construction of Foundation

The stone columns were selected both because they were cheaper and because the contractor had doubts whether sand piling would be completely successful in soil containing 15% less than 60 microns (silt size) and 8% less than 2 microns (clay size). It was accepted that total settlement would be greater with stone columns as the process does little to densify the natural soil between the piles. Pipework was therefore designed to allow for the settlement.

The stone columns were formed by the "Vibro-compaction" process, a 300 mm dia. x 5 m long vibro-flot being used to penetrate 6.5 m below ground surface. The vibro-flot was equipped with a 35 kVA electric motor and used up to 7 000 litres of water to form each column - which varied in diameter between 600 and 1 100 mm. An average of 6 cubic metres of 40 mm crushed rock was used to backfill each "vibro-flot crater". Density was confirmed by ensuring the vibro-flot's electric motor peaked at 75 amperes, there being an established correlation between the amperage and the density of the crushed rock forming the columns.

5.4 Performance of Structure

Settlement data for each loading stage is given in Figure 7.

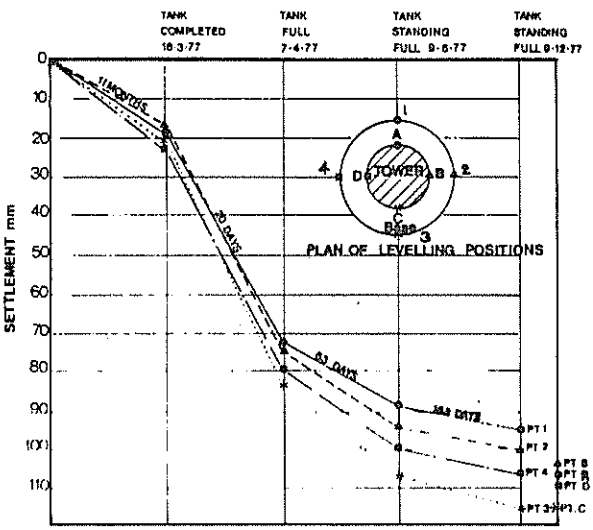

Figure 7 - Settlement data for Woolpunda Tank

6 LOVEDAY TANK

6.1 Site Investigation

Typical soil profile and test results are given in Figure 8.

The site investigation revealed very weak soils between depths of 3 and 7 m. The sands were calcareous and below 4 m and became increasingly clayey. This formation is compatible with certain aeolian landforms. A water table was intersected at 3 m, this being perched on the clay layer found at 5.5 m.

6.2 Design

A rough calculation of the settlement of the proposed tank, if founded on the natural soil, gave a figure of 250 mm under the uniformly distributed "tank-full" loading of 160 kPa. This was not acceptable, it being necessary to limit the settlement to 75 mm total and 25 mm differential.

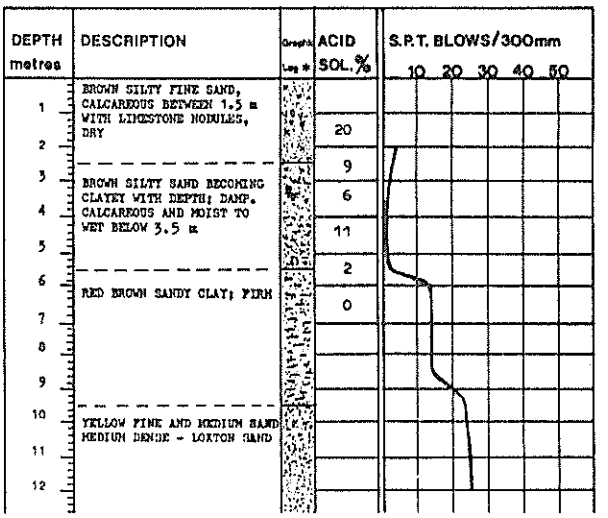

Figure 8 - Soil profile and test results

The various ground-treatment options were analysed and costed. Gravel piles constructed by the sand-piling process were initially shown to provide the most economical solution.

On receipt of tenders it was found that the number of gravel piles required had had to be doubled; also although the contractor expected the settlement criteria to be met he could not guarantee the differential settlement would be within the tolerance specified. Alternative foundation treatments were reconsidered. A causeway was to be constructed close to the tank site. It was found that a pre-load solution could be made economical by temporarily diverting the material destined for a causeway to the tank site. The pre-loading option was therefore selected.

To ensure total wetting of the foundation soils prior to pre-loading, the tank foundation was required to be flooded.

The shape of the rockfill pre-load is shown in Fig. 9. Also shown are the elevations and locations of the settlement measuring points.

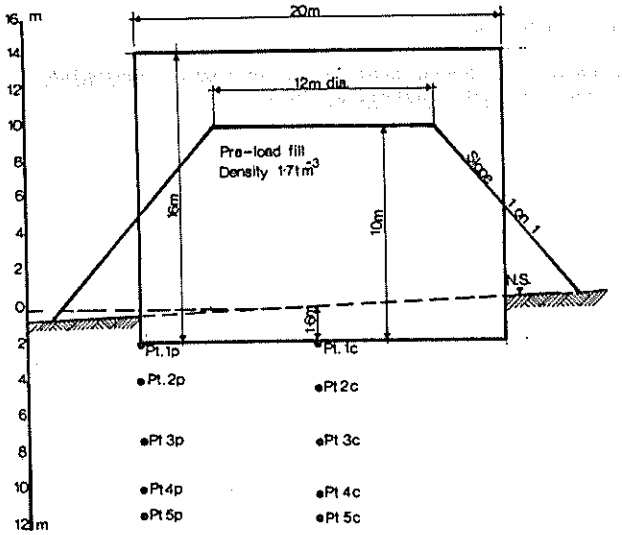

Figure 9 - Loveday pre-load and settlement points

6.3 Construction of Foundation

Construction started with the flooding of the shallow excavation. This lasted 14 days.

Sand drains were installed on a 5 m grid to accelerate the consolidation of the foundation soil under the pre-load. The complete saturation of the soil profile was confirmed during the drilling for the sand drains.

Settlement measuring points were established for three purposes.

1. To check when settlement under pre-load was effectively complete.

2. To measure ground movements at selected levels in the natural ground below the pre-load.

3. To monitor fill placement. This was done because a low safety factor had been used for the pre-load slope design and a failure of the pre-load foundation had to be guarded against.

Pre-load was placed within 3 weeks and remained for a further 6 weeks. No sign of any slope failure was observed despite using the 1 on 1 rock fill slope above the weak soils.

The surface settlements for points under the centre and the perimeter of the proposed tank are shown in Fig. 10, plotted against time and height of the preload. Ground movements below the surface are also shown.

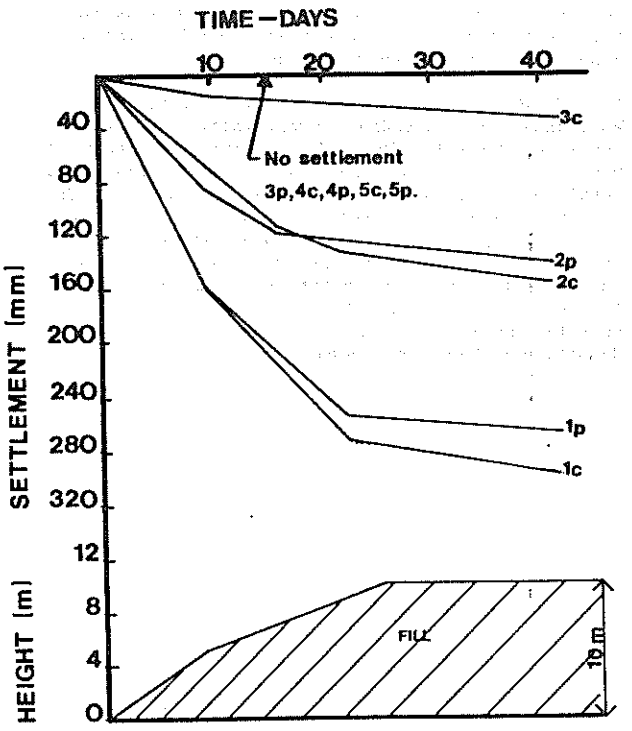

Figure 10 - Settlement data for Loveday preload

7 COSTS

The table below compares the actual costs of the treatments used with those for an equivalent reinforced concrete pile foundation (figures in brackets).

Tank	Date	Treated Area - m^2	Cost $ Actual	Cost $ 1979 Basis
Waikerie	1973	177	10 000 (17 000)	28 000 (47 600)
Woolpunda	1975	177	12 000 (14 000)	20 400 (23 800)
Loveday	1979	314	15 000 (48 000)	15 000 (48 000)

It is noted that the very favourable cost of the pre-loading is probably unique to this job. This is because the intensity of loading did not require a high fill to be placed; also because the filling was so readily available costs were reduced.

8 CONCLUSIONS

The flexible approach, which considered a wide range of engineering techniques, enabled a low cost foundation to be selected.

Technically, the foundation treatments achieved their purpose. The total settlement at Woolpunda was more than forecast but would in part have been derived from settlement of the untreated ground below the piles. Deepening of the treatment could therefore have reduced the settlement. The Loveday tank has still to be constructed but its settlement is not expected to exceed 10 mm.

The interpretation of the geology of the sites was valuable when evaluating the tank sites. The probable density of the soils, the degree of

cementation of the soil and the value of a potential soil (or rock) "basement" stratum could all be inferred. It was also a useful aid when planning the site investigations.

The Dutch deep sounder was not used in the Woolpunda and Loveday investigations. It was concluded from the Waikerie investigation that it was unreliable as a means of estimating settlements in these dry cemented soils. The Standard Penetration Test, although limited as a design tool, was a more reliable sounding device. The shaft at Waikerie provided valuable density information but was relatively expensive. In future work 75 mm dia. thin-walled push-tubes will probably be used to obtain an indication of soil density and degree of cementation.

9 ACKNOWLEDGEMENTS

The Director General and Engineer-in-Chief, Engineering and Water Supply Department has agreed to the publishing of the histories of these departmental structures. His permission to do this is gratefully acknowledged.

Mr. S.W. McLeod, The Manager of Ground Engineering (a division of Frankipile Ltd.), and Mr. K. Sissons, the Manager for Frankipile in South Australia provided much of the technical input for the ground treatments used. Their assistance was greatly appreciated.

10 REFERENCE

Handbook of South Australian Geology. Geological Survey of South Australia, 1969.

Vibroflotation of Calcareous Sands

D. C. ANDREWS
Partner, Dames & Moore, United Kingdom
D. B. McINNES
Ground Engineer, Public Works Department, Perth, Western Australia.

SUMMARY

This paper describes a vibroflotation field trial conducted in loose, calcareous sands. The results of the trial indicated that little ground improvement occurred in material which was expected to show substantial density increase following treatment. Probable reasons for the ineffectiveness of the vibroflotation technique are discussed. The effect of the ground vibrations induced on nearby structures and detailed operational data are also presented. The work reported is an example of a trial, conducted during the planning phase of a structure, intended to assess the feasibility and possible advantages of one form of ground treatment compared with other foundation systems.

1. INTRODUCTION

In late 1976 field trials were carried out at the site of proposed major additions to Fremantle Hospital in Western Australia to evaluate the effectiveness of vibroflotation for compacting loose, calcareous sands.

This paper describes the work undertaken and presents the results obtained and conclusions drawn from the study.

The 0.54 hectare site of the proposed additions to Fremantle Hospital is located in an area bounded by South Terrace, Alma Street and existing hospital facilities and is shown on Figure 1. The additions will comprise four adjoining structures, three eleven-storey buildings together with a five-storey building. The layout of these buildings is also shown on Figure 1.

The three high-level buildings will be constructed using post-tensioned primary beams and reinforced concrete columns and walls. The five-storey building will be constructed using reinforced concrete flat plate slabs supported on reinforced concrete columns.

Underside of basement floor level is RL-0.07 AHD (Australian Height Datum). This is approximately seven metres below the level of South Terrace with the lower two storeys of each building forming a double basement to the whole complex.

Foundation design studies by engineers of the Public Works Department of Western Australia, Architectural Division based on site investigation (Ref. 1) indicated that a piled foundation system would be the most satisfactory both technically and economically. However, since early 1973 when these studies were completed, construction costs have

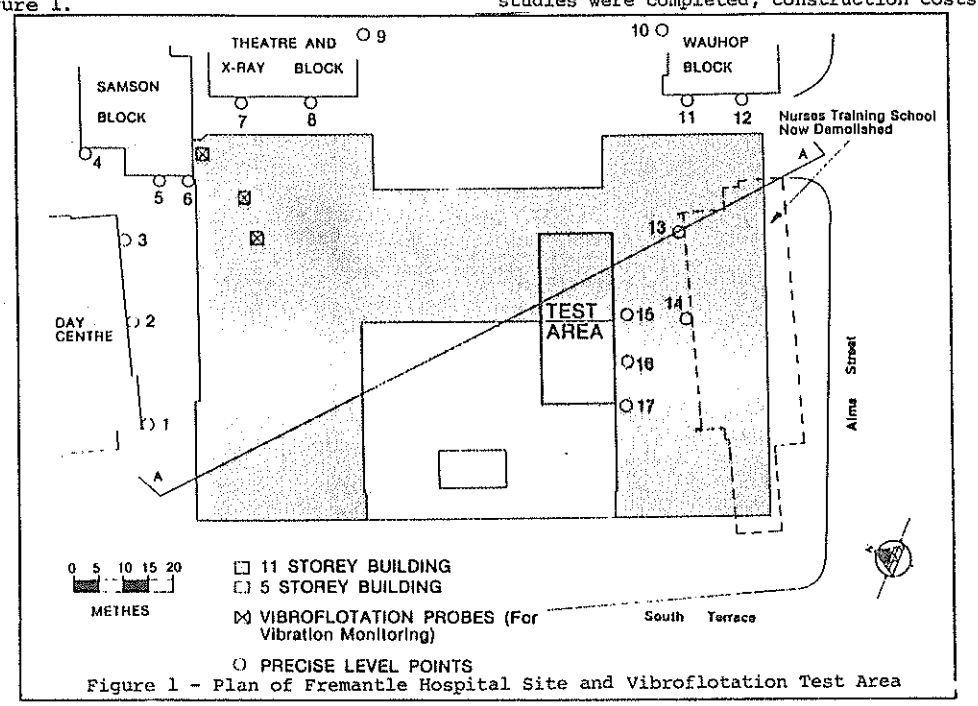

Figure 1 - Plan of Fremantle Hospital Site and Vibroflotation Test Area

risen significantly and differentially to the extent that, if technically sound, a shallow foundation system supported on ground compacted using vibroflotation could yield substantial time and cost savings.

The latter development prompted additional investigation into the use of vibroflotation and shallow foundations which culminated in the field trials described in this paper.

2. SITE CONDITIONS

Subsurface soil and rock conditions were initially examined by investigations conducted during the periods 1971 to 1973 (Ref. 1). Further investigation was conducted at the time of the vibroflotation trial (Ref. 2) and additional boreholes were drilled during the subsequent piling contract primarily to assess pile founding conditions within the sandstone beneath the site (Ref. 3).

Generalised subsurface profiles across the site are shown on Figure 2.

Material underlying the site to a depth of approximately 20 metres is believed to belong to the Safety Bay Sands of Recent age comprising aeolian and sedimentary deposits overlying calcareous sandstone. It is probable that material below this depth belongs to the Tamala Limestone Series (otherwise known as "Coastal Limestone") of Quaternary Age. (Ref. 4).

A generalised description of the various strata penetrated is given in Table 1.

The uppermost unit shown in Table 1 is dune sand and exists in a medium dense state with SPT values generally ranging between 12 and 60, the higher values probably indicating cemented zones.

The central unit contains a wide variety of material types, many of which are in a very loose condition. Typically, SPT values obtained were less than ten, many less than five and several times the SPT sampler fell up to two metres after one blow of the drop hammer. A gradation envelope constructed from gradings of a number of samples in this unit is presented in Figure 3 and illustrates the size range of material encountered.

TABLE 1

SUMMARY OF SUBSURFACE CONDITIONS

Reduced Level (metres)		Description	Density or Strength
Top	Bottom		
Up to +6.9	-1.0 to -5.0	SAND, calcareous, white, pale grey or pale brown, fine to coarse grained. Weakly cemented in part.	Medium dense to very dense.
-1.0 to -5.0	-6.1 to -16.8	SILTY SAND and SAND with discontinuous calcareous SANDSTONE bands. Very shelly. Contains decomposed organic matter.	Loose to very loose.
-6.1 to -16.8	-30.3*	Calcareous SANDSTONE, white to yellow, fine to coarse grained. Mainly moderately cemented, some calcreted surfaces. Cavernous in part.	Very weak to medium strong.

*Only one borehole penetrated the calcareous sandstone. This borehole intersected stiff black clayey silt of the Osborne Formation at RL-30.3.

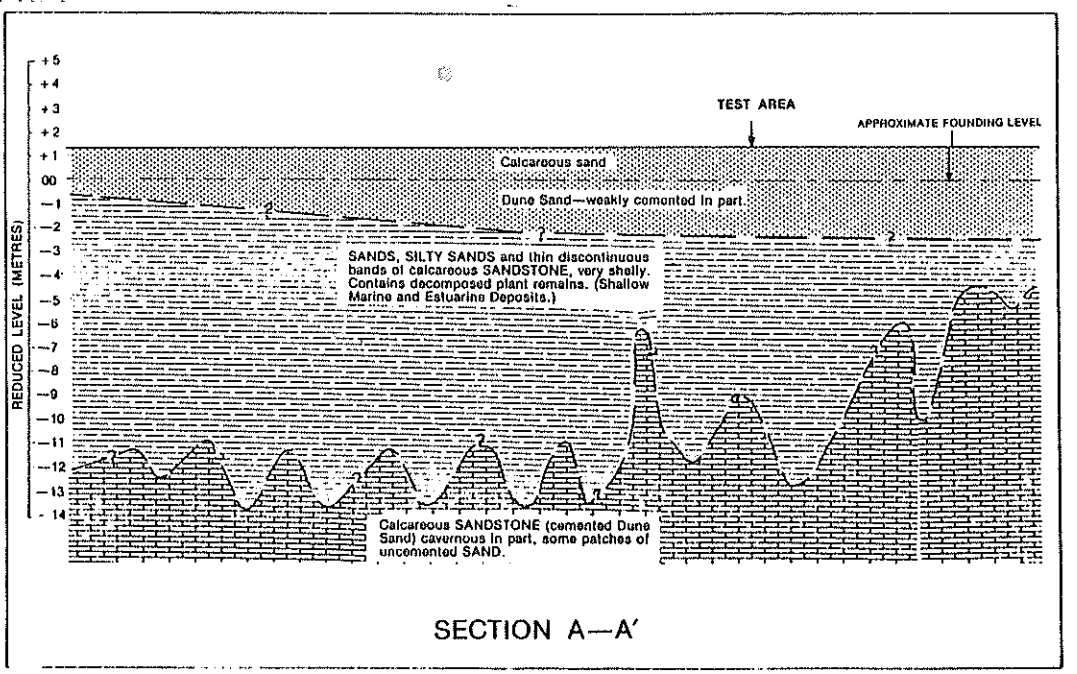

Figure 2 - Generalised Subsurface Profiles Across Site (Refer Figure 1 for Section A-A

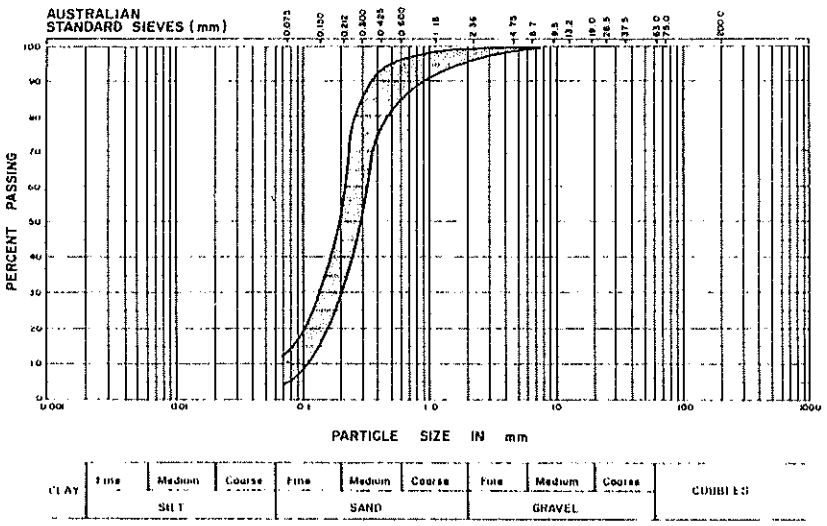

Figure 3 - Envelope of Particle Size Distribution Curves for Material from Central Unit, Table 1.

The lower unit is a calcarenite or calcareous sandstone formed of cemented dune sand. The upper surface is irregular. Closely spaced vibroflotation probes and boreholes indicated variations in levels of several metres, suggesting that the "surface" is in the form of a series of steep-sided pinnacles. There is evidence of cavities in this material and the degree of cementation varies widely.

Groundwater level was observed in a number of boreholes and occurs at approximately RL + 0.6.

3. TRIAL PROGRAMME

The vibroflotation trial had two main purposes. One was to evaluate the effectiveness of vibroflotation as a means of densifying the underlying loose silty sands and the other was to examine the impact of vibrations upon adjacent buildings during the operation of the vibroflot.

An area of the site was selected for the trial and is shown on Figure 1. The main basis for selection of this area was that it had been excavated to approximate founding level and was located clear of other work progressing on site.

Prior to the trial three boreholes were drilled in the trial area to investigate subsurface conditions in the zone above the calcareous sandstone. In addition five Dutch cone probes were performed within or close to the trial area. The results of this work are shown on Figures 4 and 5 respectively.

A suitable pattern of vibroflotation probes was then designed and agreed to by those involved in the trial. This pattern is shown on Figure 6. Further probes using the in situ sand and slag respectively as backfill, in place of the crushed rock used in the main trial, were installed after the main trial was completed. The locations of these probes are also shown on Figure 6.

The 75 kw vibroflot used in the trial is owned by the Vibroflotation Foundation Company and operated locally by Grouting and Foundations (W.A.) Pty Ltd.

Since some concern over the effect of the vibroflot operation on adjacent buildings was expressed, it was decided to monitor both vibrations and levels at a number of points around the site perimeter. To implement this a number of stainless steel precise level studs were installed in adjacent buildings and in concrete paving slabs on the floor of the excavation; these were then surveyed using precise levelling techniques. The locations of these precise level points are shown on Figure 1.

Before vibroflotation work commenced a photographic survey of all adjacent buildings was undertaken; this was augmented with notes concerning existing structural damage, cracks etc.

During the vibroflotation trial, ground vibrations were measured at several locations around the site using a Sprengnether seismograph. In addition noise levels were monitored during operation of the vibroflot.

Approximately 48 hours after the completion of the vibroflotation trial, three exploratory boreholes were drilled in the trial area at the locations shown on Figure 6. The borehole locations were selected to examine the soil density in the centre of four vibroflotation probes, in the centre of three probes and close (0.6 metres) to a probe centre. Dutch cone probing was also undertaken. The results of this works are shown on Figures 4 and 5 respectively.

At this stage a survey of all the precise level points was carried out.

The vibroflot was then moved to the northeast of the site and three probes were installed at locations progressively closer to the Samson Building (See Figure 1). The purpose of this work was solely to measure ground vibrations; again these were monitored using a Sprengnether seismograph. On completion of this work another survey of the precise level points was undertaken.

Following completion of the main vibroflotation trial the vibrflot was used to compact an area to the west of the trial area using in situ sand as backfill. The following day one borehole was drilled in the centre of three probes to measure the densification achieved. Later, an additional eight vibroflot probes were installed at a closer spacing than used in the main trial, utilising slag as backfill. The success of this operation was checked by drilling, testing and sampling at the centre of these probes. The locations of these probes and boreholes are shown on Figure 6 and the results of drilling and testing are shown on Figure 7.

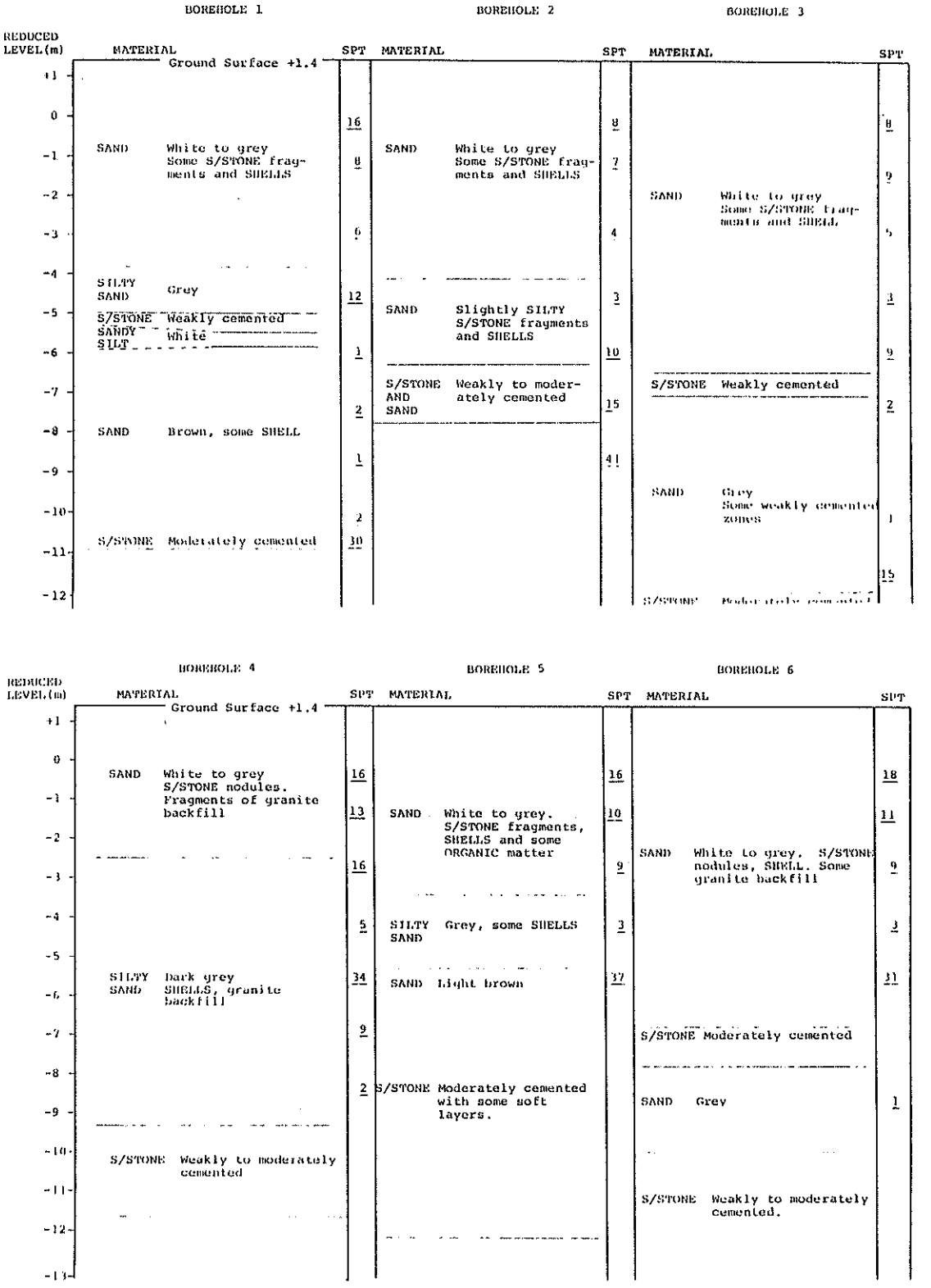

Figure 4 - Borehole Logs and SPT Results Prior to and Following Vibroflotation in Test Using Crushed Rock Backfill. (Refer Figure 6).

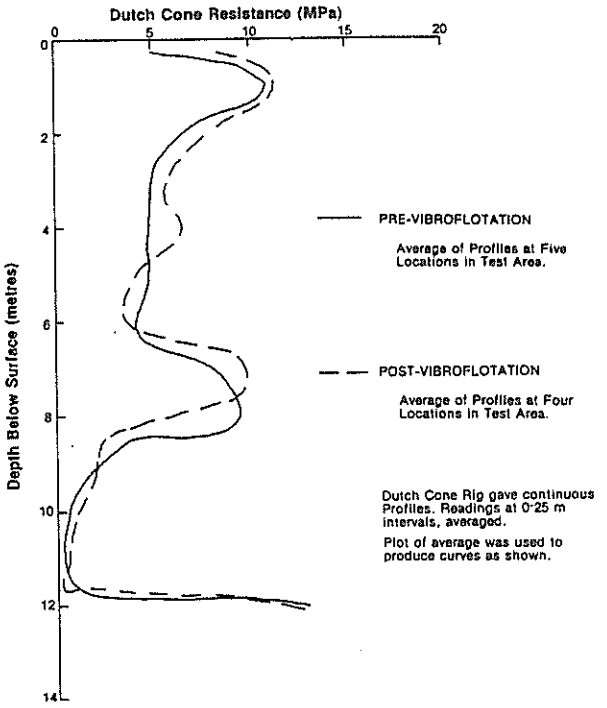

Figure 5 - Dutch Cone Resistance Prior to and Following Vibroflotation.

4. RESULTS OF TRIAL

4.1 Vibroflot Operation

During the vibroflotation trial the time taken to complete each probe, the depth of penetration of the vibroflot and the approximate volume of backfill used to form each stone column were recorded. These data are summarised in Table 2. These volumes were used to estimate the approximate diameter of the stone columns and this information is also presented in Table 2.

4.2 Evaluation of Compaction

Evaluation of the degree of densification achieved was based on a series of precompaction and post compaction Standard Penetration Tests and Dutch Cone probes. The locations of these tests are shown on Figure 6 and the results of the tests are shown on Figures 4, 5 and 7 respectively. Dutch Cone probing was only carried out in the area where crushed rock was used as backfill.

Examination of Figures 4 and 5 indicates that the vibroflotation achieved only slight increases in soil density. Figure 7 presents both results of SPT conducted in an area compacted using in situ sand as the backfill and in an area compacted using slag as backfill with stone columns more closely spaced than in the main trial. Again, perusal of these results also suggests that only slight soil density increases were achieved.

4.3 Precise Level Survey

Overall, the precise level data indicated that no measurable settlement of the buildings adjacent to the excavation occurred during the vibroflotation trial.

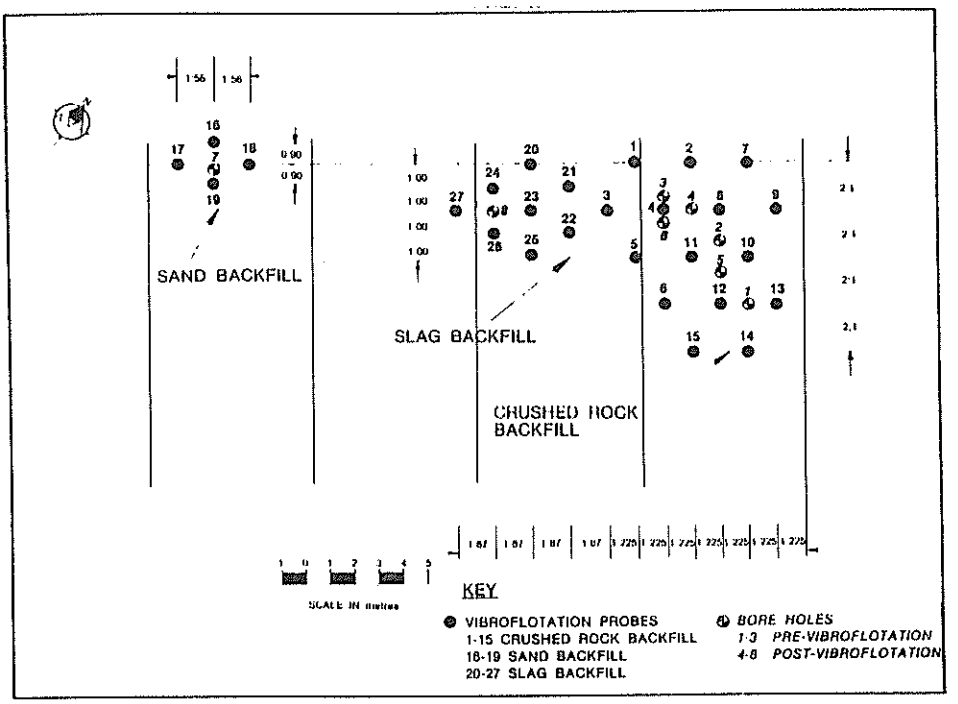

Figure 6 - Pattern of Vibroflotation Probing and Location of Boreholes in Test Area.

TABLE 2 DETAILS OF VIBROFLOTATION PROBES

Number*	Depth (metres)	Time Taken To Probe (minutes)	Time Taken To Backfill (minutes)	Backfill Used (cubic metres)	Estimated Diameter of Probe (metres)
a)	Crushed Rock Backfill Probes (In Order of Completion)				
1	11.89	3	16	10.8	1.07
2	11.89	2	16	10.8	1.07
3	7.93	2	13	7.7	1.11
4	8.24	2	16	9.2	1.19
5	14.34	2	14	12.3	1.05
6	13.27	3	17	15.4	1.22
7	10.37	3	14	12.3	1.23
8	8.85	4	11	10.0	1.02
9	10.37	2	13	10.8	1.15
10	10.06	2	12	7.7	0.99
11	13.57	4	12	13.8	1.14
12	9.61	4	12	9.2	1.10
13	7.02	3	-	-	-
14	7.02	-	-	6.2	1.06
15	9.46	3	11	7.7	1.02
Average Depth	10.26 m	Average Backfill Per Metre of Probe 1.0cu.m		Average Diameter 1.11 m	
b)	In-situ Sand Backfill Probes				
16	9.07	4	34	7.3	1.01
17	11.29	4	11	5.4	0.78
18	9.53	3	11	6.2	0.91
19	12.20	3	11	7.7	0.90
Average Depth	10.52 m	Average Backfill Per Metre of Probe 0.6cu.m		Average Diameter 0.90 m	
c)	Crushed Slag Backfill Probes				
20	7.63	2	20	13.8	1.52
21	7.63	2	17	13.8	1.52
22	7.63	2	12	9.2	1.24
23	7.63	3	14	10.0	1.29
24	7.63	3	11	6.9	1.07
25	7.63	2	14	9.2	1.24
26	7.63	3	10	8.5	1.19
27	7.63	3	11	10.0	1.29
Average Depth	7.63 m	Average Backfill Per Metre of Probe 1.3cu.m		Average Diameter 1.30 m	

* Refer to Figure 6 for probe location

4.4 Ground Vibration Monitoring

The vibroflot specification indicates that when in operation it has a free standing horizontal amplitude of approximately 10 mm at a frequency of 30Hz.

During installation of a vibroflotation probe two points of maximum vibration were observed. These were at the initial penetration of the vibroflot into the ground and at the start of backfilling to form the stone column. At most other points during vibroflotation the vibrations were approximately constant with the backfilling operation producing a slightly larger vibration than penetration.

Measurements taken approximately three metres from the vibroflot indicated predominantly horizontal vibrations, although the vertical component was quite large on initial penetration of the vibroflot. The maximum vibration amplitude was 0.13 mm at the start of backfilling and the average amplitude thereafter was approximately 0.08 mm. The major frequency recorded was 60Hz (although 30 Hz did occur in some cases) giving maximum peak accelerations of the order of 1.1 g both vertically and horizontally.

At a distance of 15 metres from the vibroflot, the average vibration amplitude was of the order of 0.02 mm with peaks of up to 0.04 mm. The influence of the vertical vibration was more evident in this case than at three metres from the vibroflot. The major frequency recorded was 30Hz in all cases - this being the frequency of vibration of the vibroflot - giving maximum peak accelerations of 0.04 g both vertically and horizontally.

4.5 Noise Levels

In general, the noise produced by the vibroflot could not be heard above the noise of the generator and the front end loader moving the stone backfill. The noise from the generator was measured at 86dB(A) at a distance of seven metres although this was located near a large earth embankment which would constitute a reflective surface. The noise level recorded could hence be reasonably reduced by approx-

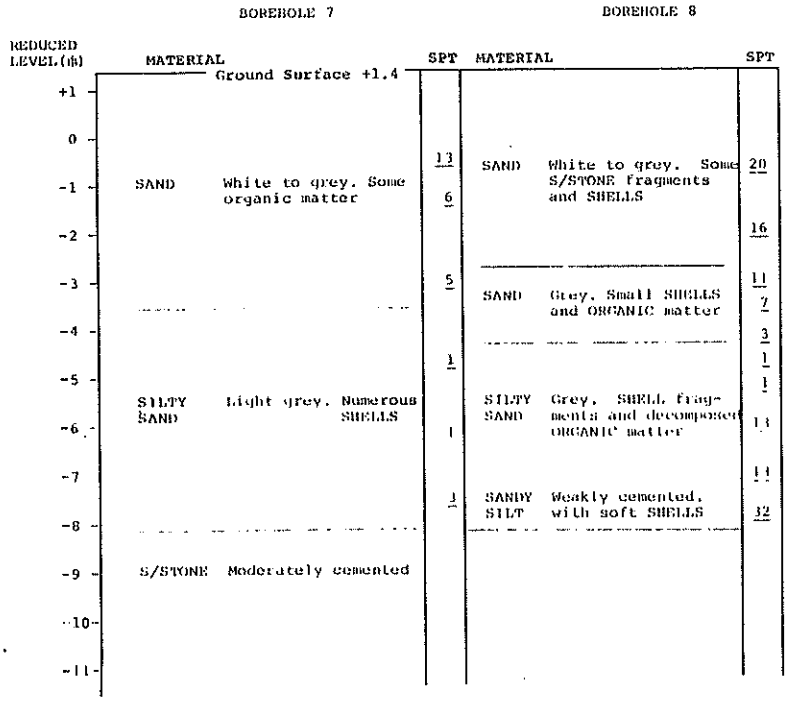

Figure 7 - Borehole Logs and SPT Results Following Vibroflotation in Test Using Sand and Slag Backfill (Refer Figure 6)

imately 3 to 4 dB (A) to a resultant level of 82 to 83 dB (A).

5. DISCUSSION AND EVALUATION OF RESULTS

Numerous accounts of successful vibroflotation projects, many at sites underlain by fine sands and silty sands, have been documented (e.g. References 5, 6 and 7) and it was generally assumed that vibroflotation would achieve compaction of the loose, saturated sands beneath this site.

Imported aggregate was used as fill material in preference to in situ sand because the latter was considered too fine to sink rapidly through the water surrounding the vibroflot. This was seen as an added advantage in the attempt to achieve good compaction.

Despite the apparent near ideal conditions for vibroflotation, evaluation of the results of testi indicates only marginal improvement. The question remaining to be answered is why the apparent lack of success at this site? Two possible explanations for the poor response of the fine calcareous sands to compaction by vibroflotation are offered. One relates to the formation of a zone of liquefied soil around the vibroflot inhibiting transmission of energy waves, while the other suggests weak cementation between sand grains could be the reason for lack of compaction.

5.1 Liquefaction of Soil around Vibroflot

Geological events related to the formation of the calcareous sands may have created a situation in which the present effective vertical stress between discrete grains is uniformly lower than theoretical overburden pressure calcualtions would suggest. Circumstances which could have resulted in low vertical stress conditions include large scale arching between cemented zones, leaching of calcareous material leaving only a skeletal structure and water table movements.

It is possible that liquefaction (wherein pore pressures under cyclic shear stress application build up to exceed effective stresses) in the zones close to the vibroflot reduced the shear modulus of the sands to almost zero. The development of such a liquefied state would be assisted by the low effective vertical stress situation. Transmission of energy from the vibroflot into the surrounding sand could therefore be greatly impaired or even negated through loss of effective shear strength in the sand.

A parallel to this loss of shear strain transmission capability has been reported in recent work relating to seismic induced ground movements of sand overlying rock. The estimation of ground surface accelerations under seismic influences, in terms of effective stress concepts, has been developed by Finn et al. (Ref. 8). In their approach the development of a zone of liquefaction in sand above the bedrock is deemed responsible for a reduction of surface accelerations to approximately zero shortly (6 to 10 seconds) after the onset of seismic induced shear stresses from the bedrock. As is pointed out by Finn et al the case histories of seismic activities for saturated sands on bedrock indicate the actual surface accelerations fall to relatively low values a certain time after seismic influences initiate ground movements.

5.2 Weak Cementation of Soil

Sands in the coastal fringe area of Perth generally have a high proportion of calcium carbonate; previous work (Ref. 9) has indicated that these sands often have a lime content of between 60 and 80 percent. Solution and redeposition of the lime as calcium bicarbonate has caused various degrees of leaching and cementation of the sands with depth. Evidence of this cementation was observed during the site investigations when a range of material from weakly cemented sand that could easily be broken in the hand to strongly cemented calcarenite core that could only be broken by a sharp hammer blow were intersected.

With a low density and weak cementation of the particles it is very probable that in a saturated condition the soil structure would break down under mechancial pressure (SPT sampler, Dutch Cone probe or vibroflot). This hypothesis is supported by the low penetration values recorded during the investigation and by the large volume of backfill consumed during the vibroflot operations.

It is believed the rapid attenuation in energy with increasing distance from the vibroflot that was measured during the trial resulted in insufficient disturbance to break the weakly cemented bonds between soil particles. Consequently, in areas relatively close to stone columns the loose sand remained unaffected. This hypothesis has been supported by engineers with considerable experience of vibroflotation who suggest that in the ground conditions occurring at the Fremantle Hospital site, more time should have been spent in forming the stone columns. It is considered that this additional time during the compaction phase would have broken the relatively weak inter-particle bonds in the sand outside the immediate area of the vibroflot, thereby increasing the amount of compaction achieved by the operation.

6. CONCLUSIONS

The information presented indicates that caution should be applied to the use of vibroflotation for improving the density of loose, calcareous sands outside the immediate area of the vibroflot. The accepted overall improvement does not appear to be achieved in these sands despite the consumption of large volumes of backfill. The reason for the poor performance of vibroflotation may be attributable to the weakly cemented bonds between soil particles and/or the development of liquefied sand zones adjacent to the probe significantly reducing transmission of energy from the vibroflot to the surrounding ground.

It seems the apparent lack of compaction achieved in this trial may well indicate that potential liquefaction of the sands beneath the site would not occur under seismic induced accelerations, which would reasonably be assumed to be lower than those produced by the vibroflot. If this were the case then it is feasible that the use of stone columns installed by vibroflotation deriving their lateral support from the weakly cemented sands could provide a foundation system with adequate bearing capacity and acceptable reductions in potential settlement. However, evaluation of such a foundation support system could only be achieved through large scale load tests.

6. ACKNOWLEDGEMENTS

The authors wish to acknowledge the permission granted by the Principal Architect and Director of Engineering, Public Works Department of Western Australia, to present the above information.

7. REFERENCES

1. SOILMECH PTY LIMITED,(January 1972) Job No. NW3C and(February 1973) Job No. PW33 . Reports on Site Investigations to Proposed Major Additions at Fremantle Hospital,Western Australia for Public Works Department.

2. DAMES & MOORE, (1976) Job No. 8076-010-71. Report Foundation Investigation - Proposed Major Additions Fremantle Hospital, Fremantle, Western Australia.

3. FRANKIPILE AUST PTY LIMITED. Diamond Drill Borehole Log Sheets - Fremantle Hospital.

4. GEOLOGICAL SURVEY OF WESTERN AUSTRALIA(1970) Perth and Environs Geological Map Sheet 3.

5. D'APPOLONIA, E., (1953) Loose Sands - Their Compaction by Vibroflotation,Symposium on Dynamic Testing of Soils Spec. Tech Publication No. 156, ASTM.

6. GRIMES A.S. & CANTLAY W.G. (1965). A Twenty-Storey Office Block in Nigeria Founded on Loose Sand. The Structural Engineer No. 2 Vol. 43 February, 1965.

7. FRANKIPILE AUSTRALIA PTY LIMITED (1974) C.B.H. Grain Terminal. Contracting & Construction Engineer, November 1974 pp 8-33

8. FINN, W.D.L., BYRNE, P.M. and MARTIN, G.R. (1976) Seismic Response and Liquefaction of Sands ASCE, Journal of the Geotech. Div. August 1976. p 841.

9. ANDREWS, D.C. (1970). Unpublished data on lime content of Perth sands.

A Study of Pipeline Stability with an Oscillating Water Table

P. J. MOORE
Reader in Civil Engineering, University of Melbourne
P. M. DIGHT
Department of Civil Engineering, Monash University

SUMMARY A study of the required depth of cover of a pipeline to prevent flotation when the pipeline is submerged below the ground water table in sandy soil has been carried out. This study includes consideration of the shear stresses that may be mobilized in the overburden soil. Comparisons between these calculated depths of cover at which pipeline flotation may occur and those observed experimentally were made. Reasonable agreement was obtained provided the calculation was carried out in a particular way. The phenomenon known as pipeline jacking was also examined experimentally. It was found that pipeline jacking did not occur unless large voids were purposely left beneath the pipe and the overburden material was loosely placed around the pipe.

NOTATION

B	radius of pipe
g	gravitational acceleration
F	factor of safety based on maximum uplift pressure
F_w	factor of safety based on overburden pressure
F_s	factor of safety based on angle of shearing resistance
K	earth pressure coefficient (= σ_h/σ_v)
U	uplift force per unit length of pipeline due to weight of displaced fluid
W_p	weight of pipe per unit length
z_B	depth of cover
γ	unit weight (= ρg)
ϕ	angle of shearing resistance of soil
ϕ_m	mobilized angle of shearing resistance
ρ	density of overburden soil
τ	shear stress
σ_v	uplift pressure
σ_{vmax}	uplift pressure required to cause pipeline flotation
σ_h	horizontal stress

1 INTRODUCTION

One of the geotechnical problems involved in the design and construction of large diameter gas pipe lines is to prevent the failure of the pipeline by upward heaving otherwise known as pipeline flotation when it is submerged beneath the ground-water table. A common procedure to overcome this problem in sandy soils is to provide a sufficient weight of overburden material to counteract the net uplift force (uplift force from buoyancy minus the weight of the pipe) with an appropriate factor of safety. If this cannot be economically done then it would be necessary to provide a coating around the pipe to increase its weight or the pipeline would have to be anchored by devices embedded deeper in the ground. These conservative procedures ignore the shear stresses that may be mobilized in the overburden.

The problems of pipeline flotation were discussed by the ASCE Task Committee (1961) and by the ASCE Pipeline Flotation Research Committee (1966) but there has been relatively little research carried out in recent years. The old conservative design procedures are apparently still being used. Bonar and Ghazzaly (1973) and Lim (1974) have examined the problems of pipelines buried in extremely soft clay soils. Begemann (1964) appears to be the only person who has directed attention to problems associated with sandy soils. One of these problems identified by Begemann, which is associated with an oscillating water table, is that known as pipeline jacking. This is a process where sand particles move into the voids left beneath a pipe when the pipeline is moved upward by a rising water table. This prevents the pipeline returning to its original position when the water table falls. A succession of these movements can result in the pipeline being jacked out of the ground.

In this study a theoretical analysis for the determination of the required depth of cover of a pipeline to prevent flotation, including consideration of shear stresses in the overburden, has been carried out. In addition an experimental program has been completed with the twofold aim of observing the cover at which pipe heaving takes place and examining the incidence of pipeline jacking under the effects of an oscillating water table.

2 CALCULATION OF COVER TO PREVENT PIPELINE FLOTATION

Pipeline flotation can occur when the net uplift pressure of the pipe is sufficiently large to overcome the vertical stress caused by the dead weight of the overburden plus any resisting shear stresses mobilized in the overburden as a result of the upward movement of the pipe. The relationship between the depth of cover of the pipeline, the uplift pressure to cause pipe heaving and the shear strength of the overburden may be obtained by adaptation of the simple model first proposed by Terzaghi (1943) in his discussion of arching. This model which is illustrated in Figure 1, assumes that the upward movement of the pipe will mobilize resisting downward acting shear stresses (τ) on two vertical planes a distance equal to the pipe diameter (2B) apart. The equation of vertical equilibrium for the element of width 2B and thickness dz is

$$\frac{d\sigma_v}{dz} = \frac{W}{2B.dz} + \frac{\tau}{B} \qquad (1)$$

$$= \gamma + \frac{K\,\sigma_v \tan\phi}{B} \qquad (2)$$

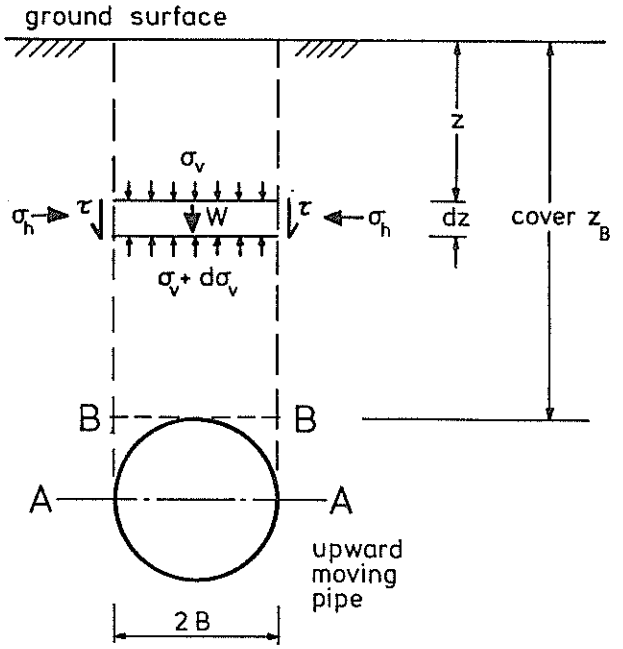

Figure 1 Identification of symbols

The solution to equation (2) is

$$\sigma_v = \frac{\gamma_B'}{K \tan \phi} \left(e^{K \tan \phi . z_B/B} - 1 \right) \qquad (3)$$

This equation can be interpreted in two ways. Firstly, the σ_v may be considered as the maximum uplift pressure (σ_{vmax}) acting at the depth of cover z_B (plane B-B in Figure 1) below the ground surface and which is just sufficient to counteract the overburden pressure plus the downward acting shear stresses in the overburden. The shear stresses are failure stresses and the angle of shearing resistance of the overburden material is considered to be fully mobilized. Under these conditions the factor of safety against a pipeline failure by upward heaving is defined as unity.

Secondly, the angle ϕ in equation (3) may be interpreted as a mobilized angle of shearing resistance (ϕ_m) which is smaller than the full angle of shearing resistance. This means that with the uplift pressure σ_v acting at a depth z_B (Figure 1) the pipeline is not on the point of failure by upward heave and the factor of safety is greater than unity. Both interpretations are used in this paper.

The uplift pressure, sometimes referred to as the net uplift pressure, operates when a pipeline becomes submerged, the value of σ_v being defined as

$$\sigma_v = \frac{U - W_p}{2B} \qquad (4)$$

where $U-W_p$ = net uplift force

In the case of permanently submerged pipelines it is usually recommended that a weight coating be applied to the pipeline to increase the weight of the pipe so that movements will be limited, as in the case of the SAA Submarine Pipeline Code (1976). In such cases W_p will be greater than U, there will be no uplift pressure, and movements of the type examined in this paper will not occur.

The resisting shear stresses in the overburden may be considered to act over a depth equal to the cover (Case A). Alternatively it may be argued that the overburden shear stresses should be considered to act over the greater distance between the ground surface and the pipe centreline (Case B). For Case B the uplift pressures required to cause pipeline failure are significantly greater than those for Case A. Instead of the arbitrarily chosen K values of 0.5 and 1.0, a more rational value may be derived from consideration of the failure Mohr stress circle from which it may be shown that

$$K = \frac{\sigma_h}{\sigma_v} = \frac{1}{(1 + 2 \tan^2 \phi)} \qquad (5)$$

An indication of the maximum uplift pressure for Case B compared with the maximum uplift pressure for Case A required to cause pipeline failure is given in Table I for the three values of K and for various angles of shearing resistance. The ratio of maximum uplift pressure for Case B to that for Case A is not unity and is seen to vary not only with angle of shearing resistance but also with the value of K used in the calculation. This indicates the desirability of checking whether Case A or Case B more accurately predicts experimental behaviour and whether the more rational value of K given by equation (5) is supported by the experimental data. This is discussed further in Section 5.

TABLE I

COMPARISON OF CALCULATED UPLIFT PRESSURES REQUIRED TO CAUSE PIPELINE FAILURE

Depth of Cover = Pipe Diameter

	Max. Uplift Pressure (Case B) / Max. Uplift Pressure (Case A)		
K Value	$\phi = 20^0$	$\phi = 30^0$	$\phi = 40^0$
0.5	1.33	1.48	1.66
1.0	1.58	1.94	2.47
$1/(1+2\tan^2\phi)$	1.47	1.56	1.56

3 FACTORS OF SAFETY

A commonly used factor of safety (F_W) that is used in the pipeline industry is one that is based on overburden pressure

$$F_W = \frac{\gamma z_B}{\sigma_v} \qquad (6)$$

where σ_v is as given in equation (4). If the overburden is completely submerged then γ is derived from the buoyant density of the overburden material. With this definition of the safety factor the contribution of the strength of the overburden in resisting the upward movement of the pipeline is ignored. It is to be noted that the factor of safety (F_W) in equation (6) bears no relation to the more traditional factor of safety with respect to strength (F_S), a measure of the degree of mobilization of soil strength that is used in soil engineering. For a cohesionless soil

$$F_S = \frac{\tan \phi}{\tan \phi_m} \qquad (7)$$

Since the overburden strength contributes in a minor way only to the resistance against the uplift pressure, F_S does not appear to be as convenient a measure of safety as F_W. F_W, however, provides a conservative indication of safety and it would be

TABLE III

. MINIMUM COVER REQUIREMENTS FOR GAS PIPELINES

cation Class	Minimum Cover (mm)	
	Division 1 Systems	
	Consolidated Rock	Other than Consolidated Rock
1	450	750
2	600	750
and 4	600	900
	Division 2 Systems	
	600	750

ding to the S.A.A. Gas Pipeline Code (1975) are minimum cover requirements for soil and ill overburden materials as detailed in Table The difference between Division 1 and Division tems relates to the maximum operating pressure he hoop stress level in the pipe. The location relates to the number of buildings in the liate vicinity of the pipeline. These cover rements are compared in Figure 3 with cover s calculated for various factors of safety. alculations are based on the equations des- d above and the factor of safety is defined in ion (8). The figure shows that for a par- ar cover requirement as specified by S.A.A. example 750 mm) the factor of safety against re by upward pipe heave decreases as the pipe ter increases. Figure 3 suggests that the t of cover should be related to pipe diameter.

LABORATORY OBSERVATIONS OF PIPELINE BEHAVIOUR

oratory based investigation into the stability natural gas pipeline buried in saturated sand and subjected to an oscillating water table was carried out by Dight (1977). The experimental arrangement consisted of a 3 m long 305 mm diameter pipe, sealed at the ends and surrounded by sand in a tank. The water table level was varied from below the pipe to the top of the sand overburden. Tests were carried out with three different sands, the properties of which are given in Table IV.

The pipe movements were monitored as the water table was oscillated and the depth of cover over the pipe was progressively decreased until failure of the pipe by upward heave was observed. The test data showed that no pipeline jacking was observed even for quite small depths of cover. This may be related to the fact that the amount of pipe movement per cycle of water table oscillation was significantly smaller than the grain size of the sand so that there was no opportunity for the sand particles to move beneath the pipe. For a cover depth of 230 mm, the pipe experienced settlement in all cases. This behaviour, similar to that described by Inckel (1972) for some field tests in the Netherlands, has been attributed to the compaction of the sand beneath the pipe. When the cover was reduced to 25 mm failure by upward heave occurred with all three sands.

During experimentation it was found possible to produce the pipeline jacking phenomenon referred to in the introduction, by purposely leaving large voids beneath the pipe at the installation stage and placing the overburden material loosely around the pipe. This would relfect poor construction practice in the field. Following water table oscillation the pipe commenced a steady upward movement as shown in Figure 4. At this rate the pipe would have failed ultimately by upward heave. After 340 cycles the pipe was subjected to vibration while the water level was at its lowest point.

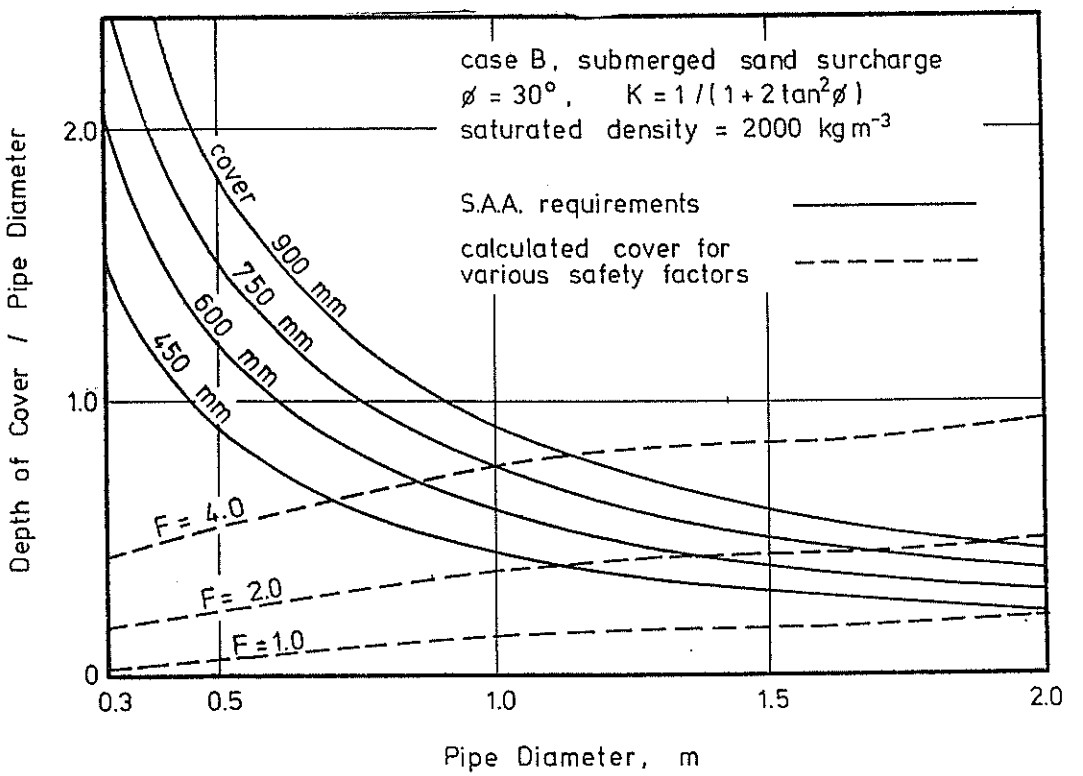

Figure 3 Comparison of cover requirements

TABLE II

COMPARISON OF FACTORS OF SAFETY F_w AND F

Depth of Cover = Pipe Diameter

Angle of Shearing Resistance $\phi = 30^o$

Uplift Pressure ($\sigma_v/\gamma B$)	F_w	F					
		Case A			Case B		
		K=0.5	K=1.0	K=1/(1+2tan²ϕ)	K=0.5	K=1.0	K=1/(1+2t
1.5	1.33	1.81	2.51	1.93	2.76	4.83	2.99
2.0	1.00	1.36	1.88	1.45	2.00	3.62	2.25
2.5	0.80	1.08	1.50	1.16	1.60	2.90	1.80
3.0	0.67	0.90	1.25	0.96	1.33	2.41	1.50
4.0	0.50	0.68	0.94	0.72	1.00	1.81	1.12
5.0	0.40	0.54	0.75	0.58	0.80	1.45	0.90
6.0	0.33	0.45	0.63	0.48	0.67	1.21	0.75

more appropriate to define a factor of safety (F) that incorporates both the weight and strength of the overburden. Such a factor of safety could be defined as

$$F = \frac{\sigma_{vmax}}{\sigma_v} \qquad (8)$$

where σ_v is given by equation (4) and σ_{vmax} is given by equation (3) (using the first interpretation as discussed in Section 2) for the case of the overburden on the point of failure by upward heave. Values of F_w and F are compared in Table II for a variety of arbitrarily chosen values of uplift pressure.

4 DEPTH OF COVER FOR COMMERCIALLY AVAILABLE PIPE

In order to apply the equations developed above for the determination of depth of cover for actual pipelines it is first necessary to evaluate the n lift force or the uplift pressure from equati For a particular pipe diameter, pipes with se wall thicknesses are normally manufactured. means that the net uplift force will be sprea a range of values for one particular diameter Using the uplift force corresponding to the m of the range for commercially available pipe, effect of the K coefficient on the depth of c examined in Figure 2 for various assumed angl shearing resistance. The line marked $\phi = 0^o$ Figure 2 is not affected by the K coefficient indicates that the dead weight only of the ov burden material is counteracting the net upli the pipeline. Figure 2 shows that for most overburden soils for which the angle of shear resistance is greater than 20^o and for K valu given by equation (5) the minimum depth of co not greatly influenced by the angle of sheari resistance.

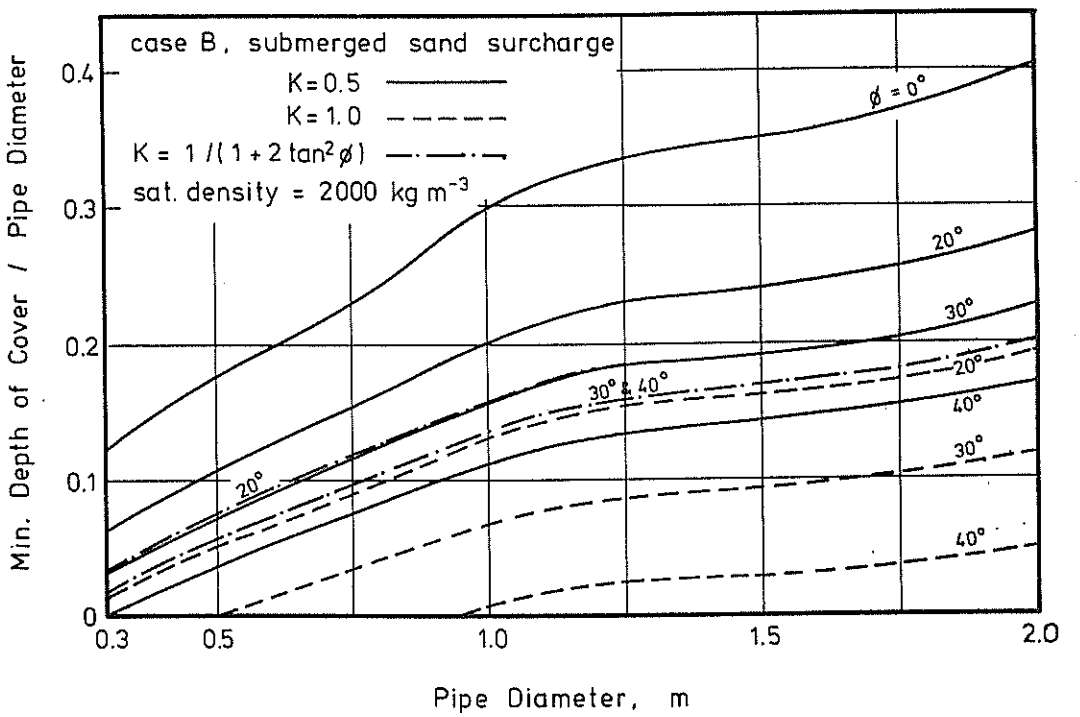

Figure 2 Influence of friction angle on minimum required depth of cover

TABLE IV

PHYSICAL PROPERTIES OF TEST SANDS

Sand	- 50 Sand	Gipps sand	30/60 sand
Description	Clean rounded sand with few fines	Silty subangular sand with some organic matter	Clean rounded sand, very few fines
D50 size (mm)	0.29	0.35	0.40
Saturated density ($kg\ m^{-3}$)	1950	1990	2060
Angle of shearing resistance (sat. samples)- degrees	31	39	28

Pipe settlement resulted but as the water table rose for the next cycle the pipe moved upward and failed by heaving.

In an associated series of tests to examine qualitatively the nature of the movement of the overburden material in response to upward movement of the pipe, the approximate boundary of the sand movement was identified and this suggested that the Case B assumption represents reality more closely than Case A for the analyses carried out above.

Regarding the depth of cover at which pipeline failure by upward heave took place, a comparison of observed and calculated values is given in Figure 5. This comparison confirms that the Case B assumption is clearly superior to the Case A assumption. Regarding the K coefficients it appears that the value of 0.5 and the value given by equation (5) are equally valid in predicting the depth of cover at which pipeline failure occurs.

6. CONCLUSIONS

Comparisons have been made between the calculated and observed depths of cover in sandy soils at which pipeline failure by upward heave takes place. These comparisons indicate good agreement provided it is assumed for calculation purposes that the shear stress is mobilized in the overburden down to a depth coinciding with the pipe centreline. The earth pressure coefficient (K) used in the calculation may be either 0.5 or $1/(1+2\tan^2\phi)$.

Pipeline jacking was found to occur in the experiments only when large voids were purposely left beneath the pipe and the overburden material loosely placed around the pipe.

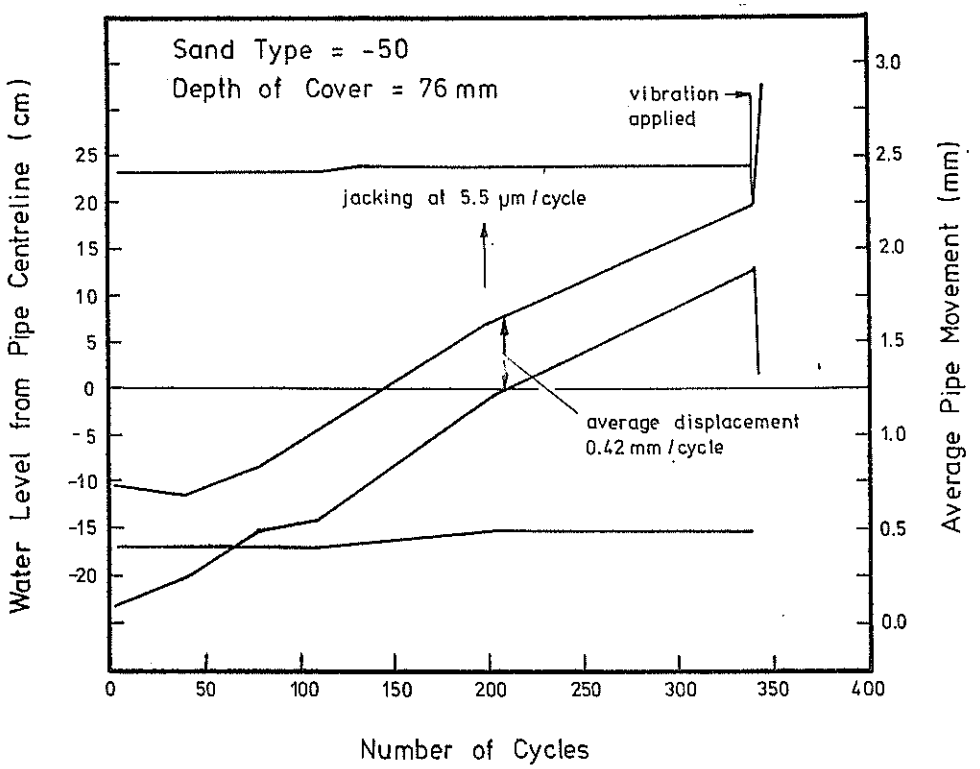

Figure 4 Observation of pipeline jacking

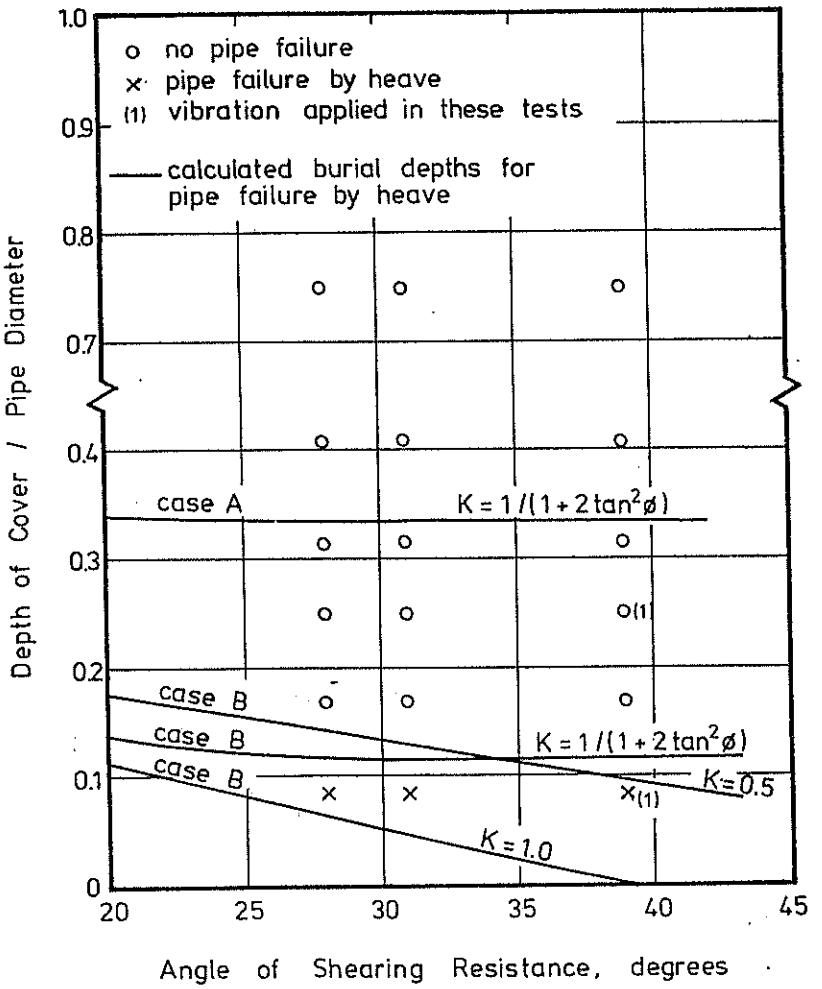

Figure 5 Comparison of calculated and observed incidence of pipe failure by heave

7. REFERENCES

A.S.C.E. Pipeline Flotation Research Committee, (1966), Preliminary Research on Pipeline Flotation, Journal of Pipeline Division Vol.92, PL1, pp.27-71.

A.S.C.E. Task Committee, (1961), Report on Rational Design for Pipelines across Inundated Areas, Journal of Pipeline Division, A.S.C.E., Vol.87, PL1, pp.31-58

Begemann, H.K.S. Ph. (1964), Natural Gas Pipelines in the Netherlands, Report to Bechtel International Company, Laboratorium voor Grondmechanica, Delft.

Bonar, A. and Ghazzaly, O. (1973), Research on Pipeline Flotation, Journal of Transportation Engineering, A.S.C.E., Vol.99, TE2, pp.211-233.

Dight, P.M. (1977), An Experimental Investigation into the Stability of Pipelines in Saturated Sands, M.Eng.Sc. thesis, Department of Civil Engineering, University of Melbourne.

Inckel, A.E. (1972), Postscript to the report by Begemann, Laboratorium voor Grondmechanica, Delft.

Lim, S.J. (1974), An experimental Investigation of Pipeline Stability in Very Soft Clay, Ph.D. thesis, University of Houston.

Standards Association of Australia, S.A.A. Gas Pipeline Code AS1697-1975.

Standards Association of Australia, S.A.A. Submarine Pipeline Code, AS1958-1976.

A STUDY OF PIPELINE STABILITY WITH AN OSCILLATING WATER TABLE

KEY WORDS: pipelines; water table; buoyancy; flotation; stability; stress analysis

ABSTRACT: A study of the required depth of cover of a pipeline to prevent flotation when the pipeline is submerged below the ground water table in sandy soil has been carried out. This study includes consideration of the shear stresses that may be mobilized in the overburden soil. Comparisons between these calculated depths of cover at which pipeline flotation may occur and those observed experimentally were made. Reasonable agreement was obtained provided the calculation was carried out in a particular way. The phenomenon known as pipeline jacking was also examined experimentally. It was found that pipeline jacking did not occur unless large voids were purposely left beneath the pipe and the overburden material was loosely placed around the pipe.

REFERENCE: MOORE, P.J. and DIGHT, P.M. (1980) A Study of Pipeline Stability with an Oscillating Water Table. 3rd Australia-New Zealand Conference on Geomechanics, Wellington, May 12-16. Preprints of Papers.

An Experimental Investigation of the Phenomenon of Pipe Jacking

P. J. YTTRUP
Lecturer in Civil Engineering Deakin University

SUMMARY The migration towards the ground surface of gas pipelines buried in sand and below the water table has been termed "pipe jacking" or "sand jacking". The mechanism leading to pipe jacking has been assumed to be fluctuations in the level of the ground water table. The mechanism of pipe jacking reported in this paper is internal pressure fluctuations which cause diametric deformations of the pipe leading to pipe jacking. It was found that pipe jacking will occur at a rate directly related to the magnitude of the pressure fluctuation and inversely related to the depth of burial of the pipe.

1 INTRODUCTION

The term "pipe jacking" was first used by the American Society of Civil Engineers Pipeline Flotation Research Council (1966). The Pipeline Floatation Research Council also suggested a possible mechanism causing pipelines to jack; the proposed mechanism is shown in Figure 1.

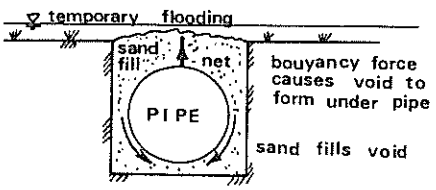

Figure 1 Pipe jacking mechanics

Buried gas pipelines with an average density less than that of the surrounding soil could potentially rise to the ground surface. Two modes of failure are usually recognised. Firstly the pipe may fail by floatation, a sudden failure where net bouyancy forces on the pipe exceeding the weight and strength of the overlying soil. Secondly, the pipe can "fail" by a slow migration towards the ground surface. In the case of pipes in sand, the migration is associated with movement of sand particles, that is, pipe jacking.

Pipeline floatation has been investigated by Bonar and Ghazzaly, 1973, for model pipelines buried in a slurry. The very low strength soil, or slurry, used by Bonar and Ghazzaly, was apparently intended to simulate a highly disturbed and very wet cohesive soil backfill. Their work is not relevant to cohesionless soils.

Inckel, 1972, conducted field tests on a prototype scale gas pipe buried in sand. The first experiments conducted by Inckel aimed at inducing liquifaction in the sand around the pipe and a floatation failure. In the second series of tests, the ground water table at the pipe was raised and lowered seven times, attempting to induce pipe jacking. Inckel did not detect any rise in the pipe, the pipe in fact settled slightly.

Large diameter natural gas pipelines are being built with relatively thin walls using high strength steels. Some sections of the proposed Sydney - Newcastle gas pipeline will have pipe of 864 mm O.D. and a wall thickness of 9.25 mm, that is, a wall thickness of only about 1% of the diameter, Telfer, 1979. The use of relatively thin walled pipelines subjected to fluctuating operating pressures can lead to distortion of the pipe sufficient to allow soil particles to migrate under the pipeline thus causing an upward migration of the pipeline, that is, pipe jacking. Fluctuating operating pressures in gas pipelines result from variations in the demand for gas by consumers.

The experimental investigation reported in this paper was conducted to evaluate the feasibility of the above pipe jacking mechanism. It was found that a model pipeline buried in rounded beach sand did "jack" when the pressure in the pipe was fluctuated. Further, the jacking rate increased as the pressure fluctuations increased in amplitude. The jacking rate decreased for greater depths of pipe burial and also for increased surface roughness of the pipe.

2 MODEL PIPELINE AND TEST PROCEDURE

2.1 The Model Pipeline

The model pipeline consisted of a 90 mm P.V.C. pipe, 1000 mm long. The pipe was connected to a pulsating pressure supply as shown in Figure 2. In order to reduce the volume of compressed air used for each pressure pulse, the pipe was filled with water, it was therefore necessary to counterweight the pipe via a pulley system to compensate for the weight of the water in the pipe. The counterweight used was equal to the weight of the water in the pipe. Hence the pipe was fully bouyant.

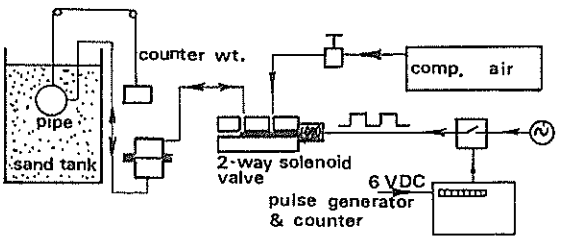

Figure 2 Model pipeline and pulse generation circuit

The diametric deformation of the model pipeline produced by internal static pressure is shown in Figure 3. The deformation of the pipe being "free" no soil interaction was present as would exist for a buried pipeline.

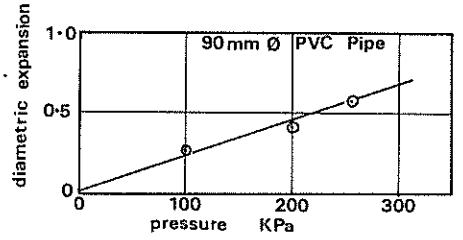

Figure 3 Model pipe deformation

The 90 mm diameter model pipeline was buried in a local beach sand from Thirteenth Beach near Barwon Heads, Victoria. The sand grading is shown in Figure 4 and sand particle shape can be seen in photograph Figure 5. The "characteristic" sand grain size adopted was 0.33 mm, that is, the diameter at 50% finer by weight.

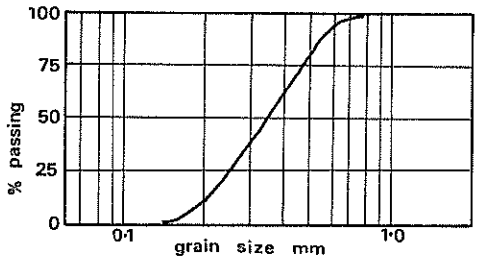

Figure 4 Sand grading

Figure 5 Sand particle shape

2.2 Model Pipeline Laying Procedure

The procedure used to lay the model pipeline was chosen to be approximately similar to a full scale pipeline construction. The sand in the tank, Figure 2, was first flooded by raising the water level in the tank from below and the sand was left flooded for several days. The sand was then "de-watered" by lowering the water in the tank to below the level of the pipeline. A parallel sided trench about 125 mm wide, was then excavated in the damp sand, the pipe placed in the trench and backfilled. The water table was then raised to the level of the sand surface and a further rest period of one or two days allowed. The above procedure was used primarily for reproducibility of the tests than for a simulation of an actual pipe laying operation.

2.3 Pressure Fluctuations

The pressure in the pipeline was fluctuated between zero and maximum pressures of 100 KPa, 200 KPa and 260 KPa. The pressure pulsing circuit is shown in Figure 2 and the resulting pressure pulse in the pipe is shown in Figure 6. The free diametric expansion of the pipe produced by the aforementioned pressures, was 0.28 mm, 0.41 mm and 0.57 mm respectively. The position of the pipe was monitored with dial gauges.

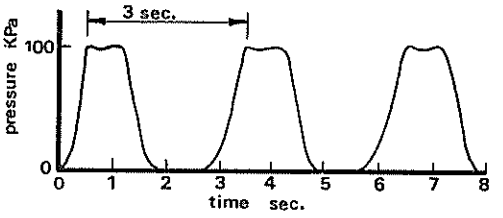

Figure 6 Pressure pulse forms

3 EXPERIMENTAL RESULTS

3.1 Pipe Jacking For Different Pressure Fluctuations

The rise, or jacking, of the model pipeline above its original position is shown in Figure 7, for the pipe buried to a depth of 1.5 pipe diameters. The trend in Figure 7 was also observed for depths of burial equal to 1 and 2 pipe diameters. However, for a depth of burial of 0.5 pipe diameters, the pipe jacking rate was continually accelerating, probably towards a floatation type failure.

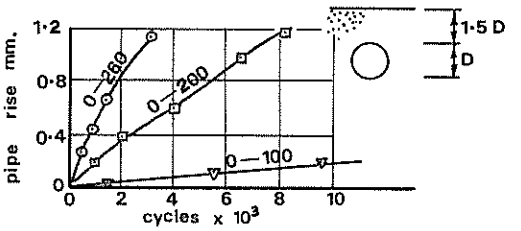

Figure 7 Pipe jacking at different pressure fluctuations

For several tests, the pipe was observed to settle before commencing to jack upwards as shown in Figure 8. The settlement of the experimental pipe used by Inckel, 1972, during the seven cycles of raising and lowering of the ground water table, may be only a transient response to be followed by pipe jacking.

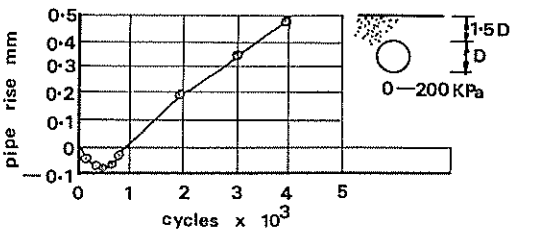

Figure 8 Pipe jacking with initial settlement

As the depth of burial of the pipe increased, the jacking rate decreased. The jacking rate of the pipe is shown in Figure 9 for different depths of burial but for the same pressure fluctuations.

The experimental results shown in Figure 9 are replotted in Figure 10. The vertical scale is free

pipe diametric deformation divided by characteristic sand grain size, and the horizontal scale is jacking "rate" in cycles of pressure fluctuations required to cause the pipe to rise by 1 mm.

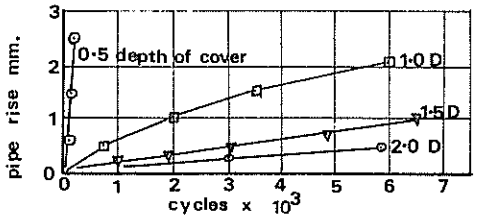

Figure 9 Pipe jacking at various depths

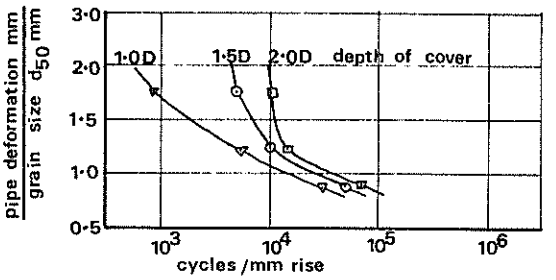

Figure 10 Pipe jacking results related to sand particle size

3.3 Influence of Pipe Surface Roughness on Jacking Rates

If the mechanism leading to pipe jacking is migration of sand particles at the surface of the pipe, then a smooth pipe could be expected to enhance jacking. Conversely, a pipe with a rough surface would retard jacking. The results in Figure 11 were obtained using the same pipe, the rough results for the pipe after coating with sand particles glued to the pipe.

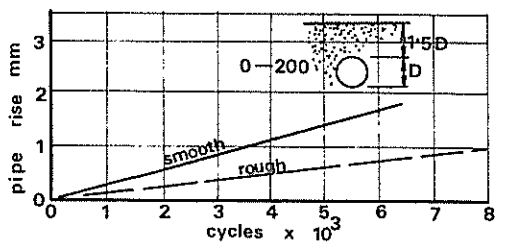

Figure 11 Pipe jacking rate for a rough pipe

4. Discussion Of The Results And Their Implication

From the model pipeline results it appears that internal pressure fluctuations can produce pipe jacking. The relevance of the model results to prototype pipelines is not known and will be studied in the future. However, for typical pressure fluctuations in actual pipelines, the rate of jacking would probably be very slow and of no consequence to the stability of the pipeline.

The jacking mechanism, that is, migration of soil particles in response to small deformations of the pipe, could modify the pipe-soil interaction.

For pipelines with discrete anchors, either swamp weights or helical anchors, the pipe jacking effect could lead to longitudinal bending stresses additional to those currently recognised by designers.

5 CONCLUSIONS

From the experimental results for the model pipeline the following conclusions can be drawn.

(i) Pipe jacking due to internal pressure fluctuations can occur for gas pipelines buried in sand and below the water table.

(ii) The pipe jacking rate is directly related to the magnitude of the pressure fluctuations within the pipe.

(iii) The pipe jacking rate decreases as the depth of burial of the pipeline increases.

6 ACKNOWLEDGMENTS

The assistance with experimental work given by Mr S. Maxwell, Mr R. Harrison and Mr B. Pitfield is greatfully acknowledged.

7 REFERENCES

American Society of Civil Engineers (1966). Report of the Pipeline Floatation Research Council. Journal of the Pipeline Division Proc. A.S.C.E. Vol. 92, No.PL1, pp 27-71.

BONAR, A.J. and GHAZZALY, O.I. (1973) Research on Pipeline Floatation. A.S.C.E. Journal of Transport Engineering, Vol. 99, TE2, May 1973, pp. 211 - 233.

INCKEL, A.E. (1972) Postscript to Design Notes by Begemann (1964) (Begemann (1964) Report to Bechtel International Company Laboratorium Voor Grondmechanica.

TELFER, J.M. (1979) Manager, Engineering, The Australian Gas Light Company. Personal Communication.

Model Studies on Anchors under Horizontal Pull in Clay

GOPAL RANJAN
Professor of Civil Engineering, University of Roorkee, India
MAJOR V. B. ARORA
Corps of Engineers (Indian Army), New Delhi, India

SUMMARY The behaviour of vertical anchor plates buried in clay and subjected to horizontal pull is studied through model tests in the laboratory. Five different size plates varying from 1.5 cm to 8.0 cm in height embedded at different depth have been tested in two dimensional condition. Development of failure surfaces during various stages of pull have been observed to study the failure mechanism of anchors. Test results have been analysed to study the influence of size of plate and depth of embedment on anchorage capacity and displacement at failure. The experimental results have also been compared with results of other investigators and theories.

1 INTRODUCTION

The design of Civil Engineering Structures like suspension bridges,antenna towers and anchored bulkheads require systems to resist the pull-out forces. These systems are referred to as 'anchors' or 'anchorage'.These anchorages could be in the form of a massive concrete block,a plate with shaft or a pile group etc. In some cases e.g.anchored bulkhead the anchorage system could be a vertical plate with a tie rod.The plate is thus mainly under a horizontal pull.

Behaviour of vertical plates under horizontal pull has not attracted much the attention of research workers. Also, the studies reported are limited in cohesionless soil e.g.Hueckel(1957),Neely et al.(1973),Meyerhof(1973),Ranjan and Kaushal(1977).In clays studies have been reported by Douglas (1964),Brinch Hansen(1953),Mackenzie(1955). Meyerhof(1973) also suggested uplift coefficients for computing the pull out capacity of anchor plates. However,uncertainties still exist as to how the anchor tends to move under load,the true pattern of the potential rupture surface that may develop in the surrounding soil,the factors that influence the anchor capacity. The present investigation was aimed to develop a better understanding of the load-deformation characteristics of vertical anchor plates under horizontal pull in clay medium. The test results have also been compared with the results reported by other investigators and theories.

2 EXPERIMENTATION

2.1 Anchor and soil

The experiments were carried out in box 8 cm wide,with wooden frame and perspex sides. The rigidity of the perspex sheet walls was maintained by using angle iron stiffners,suitably fixed with bolts and nuts. The model anchor plates were 8 cm wide made out of 3 mm thick steel plates. Plates of height, h of 1.5, 2.0, 1.25 and 4.00 and 8.00 cm deep (Fig.1) were used in the investigation.

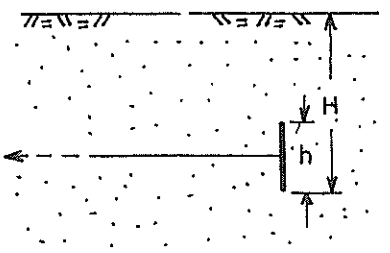

Figure 1 Geometric parameters of anchor

A locally available clay classified as CH as per Indian Standard (IS:1498-1968) was used in the investigation. Tests were performed in saturated clay at two different consistencies namely very soft (Average unconfined compressive strength,q_u of 0.122 kg/cm^2) and soft (Average unconfined compressive strength,q_u of 0.254 kg/cm^2).

The clay was prepared by mixing required quantity of water in the powdered soil and was filled in the box with anchor plate in position and by dropping small lumps of clay from a fixed height. The grid was then marked.(Arora,1976).

2.2 Load Application and Monitoring

The horizontal load was applied to the anchor through a wire with one end attached to the tie bar and the other attached to the hanger on which the weights could be placed. The wire passed over a smooth pulley.

A suitably mounted dial gauge of 0.01 mm least count resting against a plate mounted at the end of tie rod,was used to measure the displacement under the load. Figure 2 shows the experimental set up.

In each test the load displacement value under every increment of loading was recorded. Each increment was maintained for a

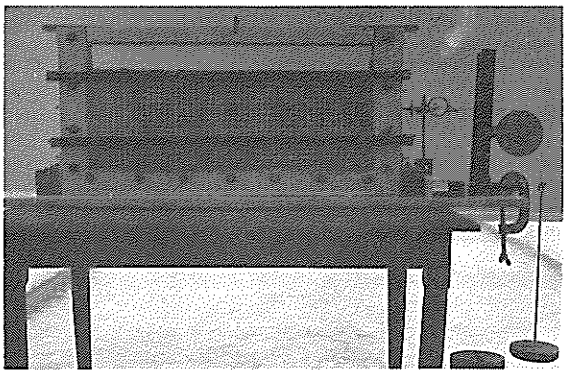

Figure 2 Experimental setup

period of 30 minutes. Figure 3 shows the typical results. Failure load is defined as the load at which the load displacement curve passes into a steep straight tangent. This failure load of the anchor is termed as anchorage capacity. Failure displacement corresponds to the displacement at the failure load. Table I shows the failure load and displacements at failure for the tests carried out.

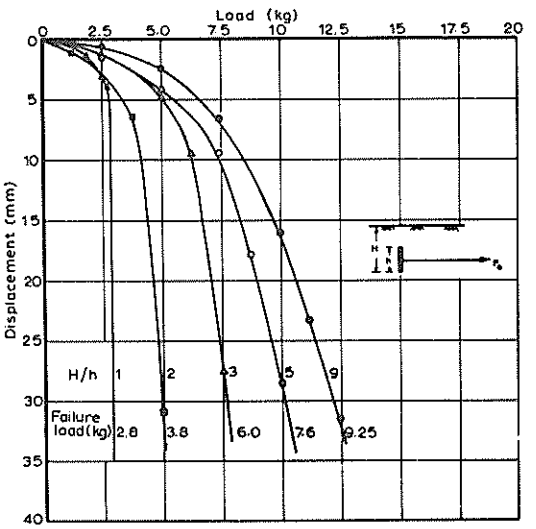

Figure 3 Load displacement curve (plate size 1.5 cm, very soft clay)

3 ANCHOR FAILURE PATTERN

Failure pattern in each test was carefully observed. Figure 4 shows a typical failure pattern. It was noted that at a small magnitude of the pull, the soil in front of the plate gets compressed resulting in a small movement of plate in the direction of the pull. As the plate starts moving active state develops on the rear side of the plate whereas passive state develops on the front side of the plate. With the further increase in pull, a crack on the active side starts developing from the upper edge of the plate progressing towards the soil surface. Upto this stage no crack was observed on the passive side. When the pull is further increased a clear cavity starts developing on the active side of the plate and the crack starting from top of the plate widens. At this stage a clear failure surface starts emerging on the passive side starting from the base of the anchor plate and moving towards the top of the soil surface. With further increase in pull failure surface on the passive side develops fully reaching the top surface of the soil. Heaving of the soil in passive side was observed. Cracking of the soil at the top surface on both the sides was also observed (Fig.4). The shape of the failure surface resembled a circle followed by its tangential straight line reaching the top surface. The centre of the circle was observed to be approximately located at the top edge of the plate. The extent of heaving in horizontal direction was about three times of the height of plate.

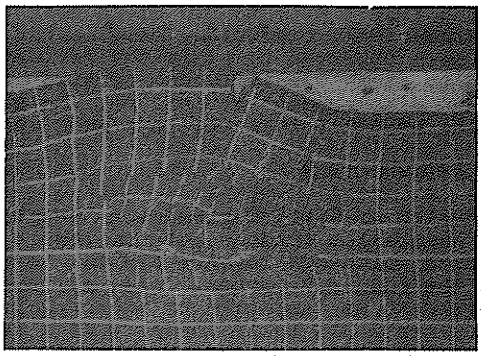

Figure 4 Rupture surface-shallow anchor in soft clay

The failure pattern was noted to change with the increase in depth of embedment. In case of deep anchors no distinct failure surface was observed to develop (Fig.5). The anchor appeared to fail by punching through the soil. A cavity of the size smaller than the plate size appeared to develop on the active side. Radial cracks also develop through. No clear rupture surface emerges. This probably is due to the fact that the overburden pressure is significant. Also no heaving of soil was observed.

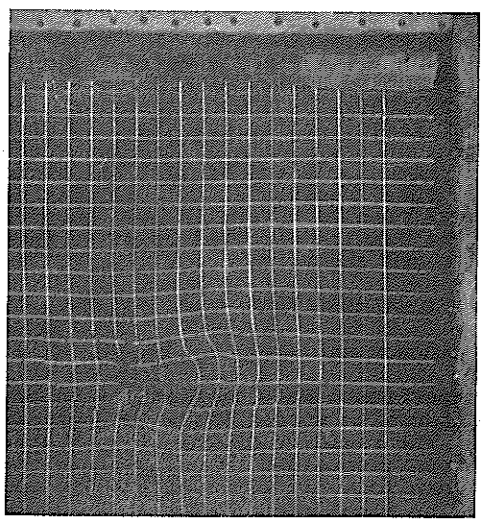

Figure 5 Rupture surface-deep anchor in very soft clay

For the depth of embedment in between shallow and deep cases the failure surface on passive side starts from base of the anchor plate but it does not reach the ground surface (Fig.6). On the active side a few cracks in the soil on the upper edge of the plate appear to develop.

Based on the rupture surfaces observed, two distinct trends of failure in soft and very soft clay can be identified. In the first category, the rupture surface reaches the ground surface and joins the surface cracks due to heaving of soil. These may be

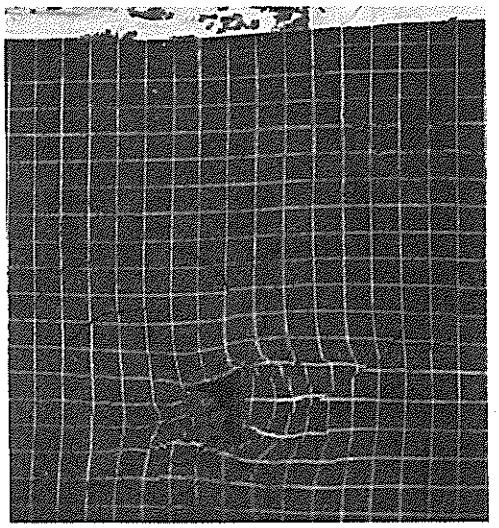

Figure 6 Rupture surface-anchor at intermediate depth in soft clay

termed as shallow anchors. The second category where the rupture surface does not clearly develop and the soil in passive zone fails in shear. These may be termed as deep anchors. In between these two extremes, the rupture surface does not reach the soil surface and appears to stop at an elevation slightly above the top edge of the plate.

The test results thus indicate that

	Very soft clay	Soft clay
shallow anchor	$H/h < 2$	$H/h < 2$
deep anchor	$H/h > 5$	$H/h > 10$

For shallow anchors, the rupture pattern can be approximated to a part of circle followed by its tangential straight line meeting the ground surface.

4 ANCHOR CAPACITY

The plot between the embedment ratios, H/h and anchorage capacity for different size plate in very soft clay is depicted in Fig.7. It shows that the anchorage capacity increases almost at a uniform rate upto a certain embedment ratio beyond which it practically attains a constant value. This probably is due to the fact that the overburden pressure influences the anchorage capacity upto certain depth only beyond which it tends to behave as a deep anchor. Similar trend was observed in case of anchors in soft clay.

5 DISPLACEMENT AT PULLOUT LOAD

Figure 8 shows the plot between the displacement at failure of anchors versus plate size for different embedment ratios in case of soft clay. The results indicate that for the same embedment ratio the failure displacement increases with the size of the plate. The increase in displacement appears to be due to the fact that the zone of the soil which gets appreciably stressed increases with the increase in

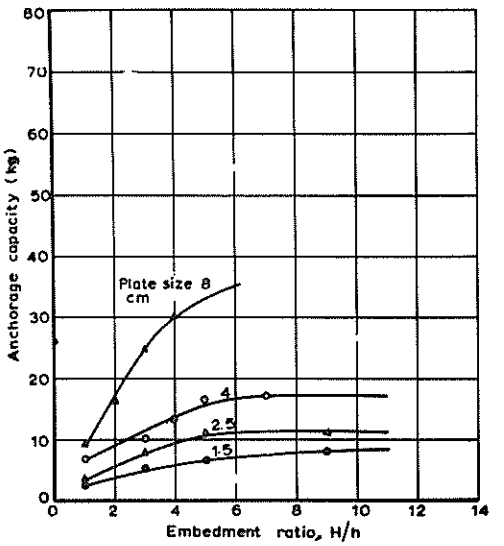

Figure 7 Anchorage capacity vs embedment ratio for anchors in very soft clay

size of the plate.

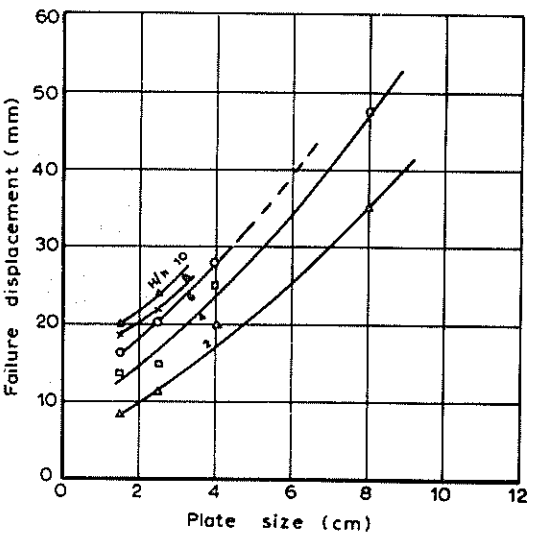

Figure 8 Failure displacement vs plate size for anchors in soft clay

Similar trend was observed in case of anchors in very soft clay.

6 NON-DIMENSIONAL PLOT

The test results in terms of dimensionless force coefficient, M_{cq} (Equation 1) and embedment ratio are plotted in Fig.9. The plot shows an increasing trend of the force coefficients with increase in embedment ratio. Though the rate of increase for initial embedment ratios is relatively rapid yet as the embedment ratio increases the rate of increase of force coefficient decreases. This may be due to the change in behaviour of anchors at deeper depths.

$$M_{cq} = \frac{p}{ch} \qquad \ldots (1)$$

where p = anchorage capacity per unit width of plate

c = cohesion

h = height of plate

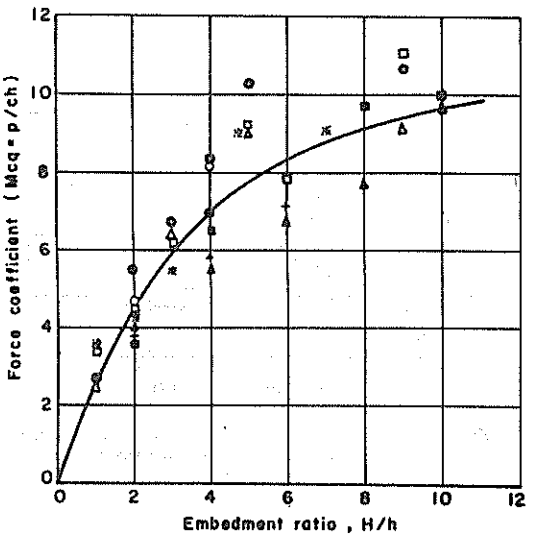

Figure 9 Force coefficient vs embedment ratio

The load displacement diagrams is normalized comparing the load, P at a particular instant with the anchorage capacity, Pu and displacement at a particular instant, Δ with the failure displacement Δu (Fig.10). It is interesting to observe that plotting all the test results a clear pattern emerges. An average curve is drawn. The average curve can be approximated by a rectangular hyperbola expressed in the form.

$$\bar{P} = \frac{\bar{\Delta}}{a + b\bar{\Delta}} \qquad \ldots (2)$$

where $\bar{P} = P/Pu$

$\bar{\Delta} = \Delta/\Delta u$

a and b = constants

If the variation of 'a' and 'b' parameters for the soil type is known the displacement at load can be estimated.

7 COMPARISON OF RESULTS

Figure 11 shows the comparison of results with other investigators. It is interesting to note that the experimental value of anchorage capacity per unit width of plate is quite comparable and lies between the values reported by Brinch Hansen(1953) and

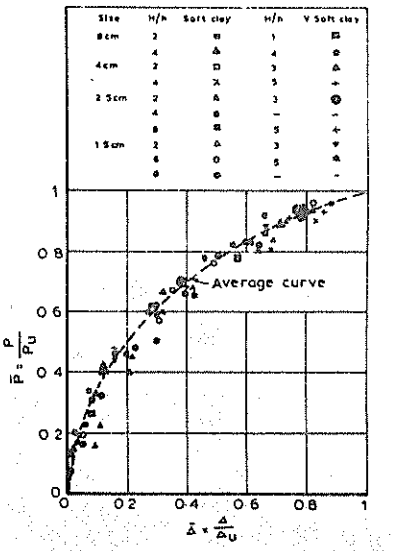

Figure 10 Plot of $\bar{P}$ vs $\bar{\Delta}$ for all model anchors

Mackenzie(1955).

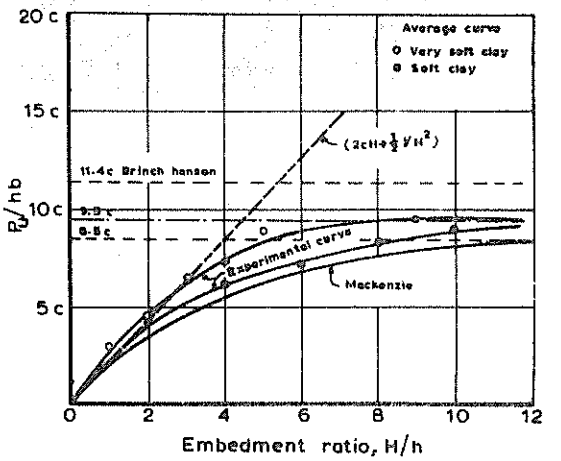

Figure 11 Comparison of results

Theoretical ultimate capacity based on conventional method is also shown by dotted line in Fig.11. The theoretical estimate by conventional method and experimental values for soft clay are same upto embedment ratio of about 1.0 i.e. when the anchor plate reached the ground surface but for larger embedment ratios the experimental anchorage capacity gradually becomes smaller than the values obtained on the basis of conventional earth pressure theory.

The experimental results have been compared with Meyerhof's theory(1973) assuming uplift coefficient K_o as 2 (Table II). In case of very soft clay, the results are quite comparable upto embedment ratio, H/h of 3, beyond which Meyerhof's theory gives higher values. This may be reasoned that the failure surface does not reach the ground surface and the expression for shallow anchors may not be valid. In case of soft clay the

TABLE I

TEST RESULTS

h(cm)	1.5		2.0		2.5		4.0		8.0	
H/h	P(kg)	Δu(mm)	P (kg)	Δu(mm)	P(kg)	Δu(mm)	P (kg)	Δu(mm)	P(kg)	Δu(mm)
Very soft clay										
1	2.55	4.50	2.60	5.50	3.00	6.00	6.90	6.50	9.32	8.7
2	3.36	7.00	-	-	5.43	7.60	8.48	10.00	16.85	15.0
3	5.45	8.75	7.63	8.75	7.87	9.00	10.11	12.25	24.88	19.0
4	-	-	8.48	11.00	-	-	13.25	12.50	31.30	24.5
5	6.84	10.00	10.15	11.25	11.06	11.80	16.67	15.00	-	-
6	8.28	12.50	10.44	13.00	11.07	12.00	-	-	-	-
Soft clay										
2	5.42	8.25	-	-	10.27	11.25	13.25	20.00	44.75	35.0
4	9.91	13.70	-	-	13.94	14.75	22.32	25.00	57.48	47.5
6	12.00	16.75	-	-	17.24	20.00	28.55	28.00	-	-
8	14.85	18.75	-	-	19.59	22.00	-	-	-	-
10	15.55	20.00	-	-	21.01	24.00	-	-	-	-

P = ultimate pull out load (anchorage capacity) of 8 cm wide plate after deducting the tie rod resistance.

Δu = displacement corresponding to anchorage capacity.

TABLE II

COMPARISON WITH MEYERHOF'S THEORY

S. No.	h(cm) H/h	1.5 P_{exp} (kg/cm)	1.5 P_t (kg/cm)	2.5 P_{exp} (kg/cm)	2.5 P_t (kg/cm)	4.0 P_{exp} (kg/cm)	4.0 P_t (kg/cm)	8.0 P_{exp} (kg/cm)	8.0 P_t (kg/cm)
Very soft clay									
1.	1	0.32	0.183	0.380	0.305	0.86	0.488	1.160	0.966
2.	3	0.68	0.549	0.980	0.915	1.28	1.464	3.110	2.900
3.	5	0.83	0.915	1.380	1.525	2.08	2.440	-	-
4.	9	1.01	-	1.380	-	-	-	-	-
Soft clay									
1.	2	0.68	0.762	1.280	1.270	1.66	2.03	5.570	4.060
2.	4	1.24	1.524	1.745	2.540	2.79	4.06	7.185	8.120
3.	6	1.50	2.280	2.150	3.810	3.57	6.18	-	-
4.	8	1.85	2.360	2.450	5.080	-	-	-	-
5.	10	1.94	-	2.630	-	-	-	-	-

P_{exp} = experimental value of anchorage capacity/unit width of anchor plate,
P_t = theoretical value of anchorage capacity/unit width of anchor plate.

values are comparable only upto H/h = 2.0 beyond which Meyerhof's theory gives higher results.

Meyerhof suggested that critical depth is at embedment ratio, H/h of 8 in case of strip anchors. The test results show that the depth at which the anchor starts behaving as deep varies with the stiffness of the soil. The anchors could be considered as deep for

H/h = 5 in very soft clay

and H/h = 10 in soft clay.

8 CONCLUSIONS

On the basis of the present study the following conclusions are drawn:

Anchor failure phenomenon seems to be a progressive phenomenon with failure surface originating in the passive zone from the bottom edge of the anchor plate. At shallower depths, the failure surface reaches the ground surface but as the embedment depth increases the failure surface does not reach the ground surface. At deeper depths the failure pattern altogether changes and the anchor seems to fail by punching through the soil.

The capacity of an anchor plate keeps on increasing with the embedment ratio upto certain depth beyond which there is practically no increase in the anchor capacity and the anchors exhibit a definite change in their behaviour. The critical depth increases with the consistency of the soil. Based on the failure surface the anchors may be classified as follows:

	Very soft clay		Soft clay	
Shallow anchors	H/h	2	H/h	2
Deep anchors	H/h	5	H/h	10

The anchorage capacity increases with size of the plate. The rate of increase is less for small size plates but the capacity increases at a faster rate for large size plates. For the same size plate the capacity increases with embedment ratio upto the critical depth beyond which it approaches a constant value.

The failure displacement increases with the size of the plate, for a particular H/h.The failure displacement also increases with the embedment ratio and approximately become constant at critical depths.

Experimental results show a reasonable agreement with Meyerhof's theory, in shallow and deep anchors in very shoft clay,and also for shallow anchors in soft clay. However for deep anchors in soft clay Meyerhof's theory gives higher values.

9 ACKNOWLEDGEMENTS

The authors wish to express their sincere thanks to Mr. Chandra Prakash, Scientist, Central Building Research Institute,Roorkee for reviewing the manuscript and offering the comments. Thanks are also due to the staff of Geotechnical Engineering Laboratory,Civil Engineering Department,University of Roorkee for assistance during the testing.

10 REFERENCES

ARORA, V.B.,(1976). Behaviour of anchors under horizontal pull in clay medium,M.E. Thesis,Civil Engineering Department,University of Roorkee,Roorkee.

BRINCH HANSEN,J., (1953). Stabilizing effects of piles in clay,Christiani and Nielson Post,1953.

DOUGLAS(1964), 'The movements of burried footings due to moment and horizontal load and the movement of anchor plates',Geotechnique,London,Vol.14,p.115.

HUECKEL,S.,(1957). Model tests on anchoring capacity of vertical and inclined plates, Proc.4th International Conf.on Soil Mech. and Found.Engg., London,Vol.11,p.203.

MACKENIZIE, Thomas,R.,(1955),Strength of Deadmen anchors in clay, Master's Thesis, Princeton University.

MEYERHOF,G.G.(1973), Uplift resistance of inclined anchors and piles, Proceedings, Eighth International Conference on Soil Mechanics and Foundation Engg.,Vol.2, Moscow,pp.167-172.

NEELY,W.J., STUART,J.C., and GRAHAM, J., (1973). Failure loads of vertical anchor plates in sand, Jour.of Soil Mech. and Found.Div., ASCE,Vol.99,No.9,pp.669-685.

RANJAN,G., and Y.P.KAUSHAL(1977). Load deformation characteristics of model anchors under horizontal pull in sand,Geotechnical Engineering,Bangkok,Dec.1977, p.68.

TSCHEBOTARIOFF,G.D.(1973), Foundations, retaining and earth structures, Second Edition, New York, McGraw-Hill.

The Relief of Negative Skin Friction on Piles by Electro-Osmosis

E. H. DAVIS
Professor of Civil Engineering, University of Sydney
H. G. POULOS
Reader in Civil Engineering, University of Sydney

SUMMARY The paper describes a method of analysing the magnitude and rate of reduction of negative skin friction on piles. The method combines a pile-soil interaction analysis (based on elastic theory) with a diffusion analysis for pore water flow under an electrical gradient. The method has been applied to predict the behaviour of a pile subjected to electro-osmosis in two cases.

(i) a full-scale field trial carried out in Boston some years ago in which one pile in a group supporting a bridge abutment was cut, released from the pile cap and then subjected to electro-osmosis. "Class A" predictions were made of the pile deflection at various stages in the trial, and comparisons are described between the predictions and the measurements.

(ii) a laboratory model test, in which negative friction has been induced in a pile by consolidation of the surrounding soil and then brief periods of electro-osmotic treatment have been applied to the pile. Predictions of the downdrag load versus time relationship are compared with the observed relationships.

1 INTRODUCTION

Consolidation and settlement of soil surrounding a pile may cause large downdrag forces to be developed in the pile due to negative friction (Johanessen and Bjerrum, 1965, Bjerrum et al, 1969; Walker and Darvall, 1973). One of a number of methods that have been suggested to relieve or reduce these downdrag forces is the application of electro-osmosis to the pile. In this method, an electric current is passed through the soil between the pile (which is made the cathode) and an anode. The passage of the current causes positive excess pore pressures to be generated near the cathode and negative values near the anode. Since the total stresses are unaffected, the increase in pore pressure near the treated pile causes a decrease in the effective stresses and consequently, a reduction in the pile-soil shear strength and the downdrag forces in the pile. As well as reducing negative friction, electro-osmosis can be used to reduce the penetration resistance of a pile during installation (Johnston, 1978) or, by making the pile the anode, to increase its ultimate load capacity (Soderman and Milligan, 1961).

Although some applications of electro-osmosis to piles have been reported in the literature, there appears to be little attempt to predict theoretically the effect of this treatment on the downdrag force. This paper therefore summarizes an approach for

(a) the prediction of the magnitude and rate of development of downdrag force in a pile, and

(b) the effect of electro-osmotic treatment on the downdrag force.

Two applications of this approach are then described, the first for a field trial in Boston in which " "Class A" predictions of the pile behaviour before and after electro-osmotic treatment, and the second a laboratory test on a model pile subjected to a sequence of consolidation and electro-osmotic treatment.

2 THEORETICAL ANALYSIS

2.1 Downdrag Force in Pile

The analysis is a simplified form of the boundary element method and is based on the use of elastic theory. The problem of an end-bearing pile is illustrated in Fig. 1. As previously described by the authors (1972, 1975), the pile is divided into a number of cylindrical elements, each acted upon a uniformly-distributed vertical interaction stress. Vertical movement of the soil at each element arises from two sources:

(i) settlement of the soil (e.g. due to consolidation), the distribution of which has to be specified in the analysis - these settlements will be referred to as "free-field" settlements.

(ii) the effect of the pile-soil interaction stresses; an expression for this component can be derived by use of Mindlin's equations for subsurface loading in an elastic mass.

By assuming the pile to deform as an elastic column, the movement of each element of the pile can be expressed in terms of the interaction stresses, the elastic properties of the pile and the applied load

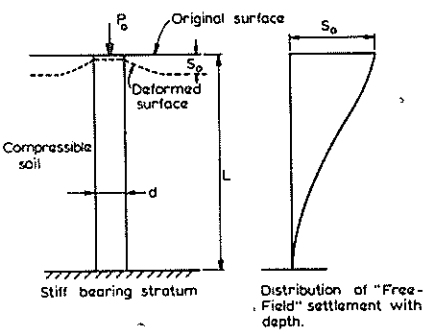

Figure 1 End-bearing pile subjected to negative friction

at the pile head. While conditions at the pile-soil interface remain elastic, the soil and pile displacements are equal, and hence by equating the expressions derived for these displacements, a solution may be obtained for the interaction stresses; the distribution of displacements and downdrag force in the pile may then be obtained.

However, because only small relative movements between the pile and soil are needed to cause pile-soil slip, it is important to incorporate the effects of such slip into the analysis. This may readily be done by checking the elastic interaction stresses against the available pile-soil shearing resistance; at elements where the available resistance, slip will occur and the displacement compatibility equation is replaced by an equation setting the interaction stress equal to the available resistance. The solution is then recycled until the interaction stresses on all elements do not exceed the limiting values.

The limiting pile-soil shear resistance τ_a' is generally calculated from the Coulomb expression, in terms of effective stresses, as

$$\tau_a' = c_a' + K_s \tan\phi_a' . \sigma_v' \qquad (1)$$

where c_a' = pile-soil adhesion
ϕ_a' = effective pile-soil friction angle
K_s = lateral pressure coefficient
σ_v' = vertical effective stress

Poulos and Davis (1975) present a series of solutions which indicate conditions under which full pile-soil slip along the pile shaft is likely to occur, and the range of pile-soil parameters for which a transition from full slip to purely elastic conditions occurs.

2.2 Time Effects

If the soil movements arise from consolidation (e.g. due to surcharging or dewatering), the development of downdrag force and displacement in the pile may be analysed by performing the above analysis for a number of times. At each time, the distribution of excess pore pressure and free-field settlement with depth can be determined from consolidation theory. The soil settlement distribution is input into the analysis while the excess pore pressures are used to calculate σ_v', and hence τ_a', in Eq. 1.

A series of solutions for the rate of development of downdrag force and displacement in an end-bearing pile are presented by Poulos and Davis (1975).

2.3 Effects of Electro-Osmosis

Consideration of electro-osmotic flow through a soil leads to the following equation for a homogeneous isotropic soil (Esrig, 1971):

$$\nabla\xi^2 = \frac{1}{c_v}\frac{\partial\xi}{\partial t} \qquad (2)$$

where ξ = u+MV
u = excess pore pressure
$M = \frac{k_e}{k} \cdot \gamma_w$
k_e = electro-osmotic permeability
k = hydraulic permeability
γ_w = unit weight of water
V = applied potential difference between electrodes
c_v = coefficient of consolidation

Fig. 2 is of identical form to the consolidation equation from diffusion theory and can be solved analytically for simple boundary conditions, or by numerical methods (such as finite differences) for more complicated cases. The variation with time of excess pore pressure u within the soil, and in particular, at the cathode, can thus be determined, and the change $\Delta\tau_a'$ in the pile-soil shear resistance τ_a' can be calculated as:

$$\Delta\tau_a' = u . K_s \tan\phi_a' \qquad (3)$$

Consequently, it is then possible to calculate the shape in downdrag load in the pile with time (or correspondingly, increase in load capacity at the anode).

If a full analysis of pile-soil interaction is to be carried out, the effect of the excess pore pressure u on the free-field settlement near the pile can be calculated from conventional settlement theory; the use of an unloading Young's modulus for the soil would be appropriate in this case.

3 PREDICTIONS FOR CUTLER CIRCLE BRIDGE PILE

3.1 Prediction Symposium

As part of a research program at MIT (Boston, U.S.A.) into negative friction, a Symposium was held in 1973 in which a number of geotechnical engineers, including the authors, were invited to predict the downdrag force on a pile at the Cutler Circle Bridge near Boston, and the subsequent effects of electro-osmotic treatment of this pile. These predictions were then compared with the results of a field testing program. The Cutler Circle Bridge was built in 1956 as part of the Interstate Highway System but was not put into use as the section of highway adjacent to the bridge was not completed. There was evidence that the piles supporting the bridge abutment had been subjected to downdrag; this evidence included a 450 mm differential settlement of the approach slab, settlement and cracking of the slope protection beneath the bridge, and a backward tilting of the abutment.

A full description of the Symposium is given by Garlanger and Lambe (1973). Fig. 2 illustrates the soil profile and the abutment pile group. Because the research pile was not instrumented before driving, the actual load in the pile was not known, and had to be deduced indirectly. The field testing program consisted of the following five steps:

(a) a 1.5 m by 2.1 m shaft was excavated and braced behind the abutment, thus exposing the centre - pile (the research pile).

(b) a small section was cut out of the pile, and measurements were made of the strain and movement at a point (A) near the top of the pile.

(c) the fill and sand immediately surrounding the pile were excavated to the elevation of the clay layer, and the movement of point A measured.

(d) the pile was subjected to electro-osmosis by passing a direct current between the test pile (cathode) and the neighbouring pile (anode), and the movement of point A was measured.

(e) with the electro-osmosis still applied, the pile was jacked back to its original position, and the required load at the top of the pile was measured.

Working independently, each participant made a prediction of the behaviour of the test pile,

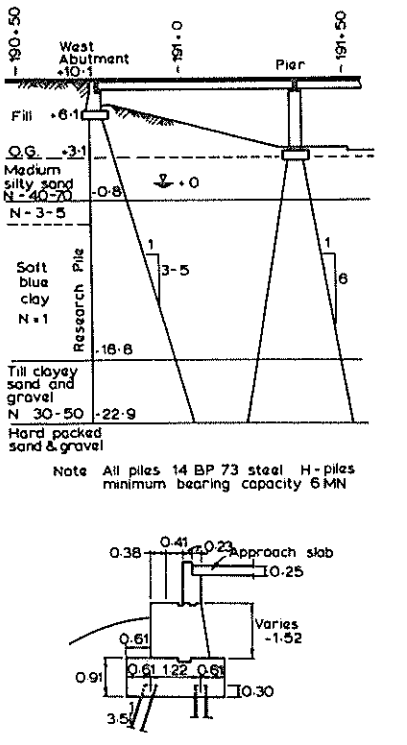

Figure 2 Details of Cutler Circle bridge abutment

including the pile movements in Steps (b) to (d) above, and the load in Step (e). The results of a field and laboratory sampling and testing program were made available to the predictions, and this data is summarized in Fig. 3.

3.2 Prediction Procedure

The first step in the Authors' predictions was to estimate the existing load at the pile head due to dead loading. In the absence of other data, this load was taken as two-thirds of the design load of

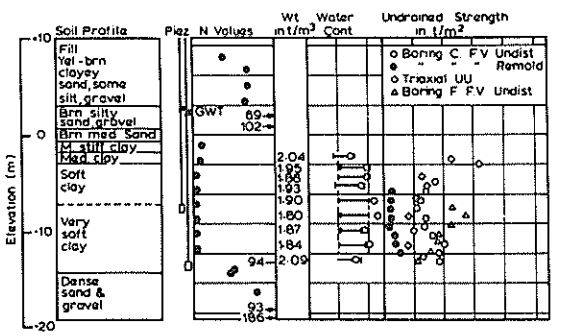

Figure 3 Summary of geotechnical data - Cutler Circle bridge

570 kN. The axial load distribution due to dead loading and negative friction was then calculated from the analysis described previously. In this analysis, the soil modulus was taken as 8.3 MPa and that of the underlying sand and gravel layer was assumed to be 345 MPa. The factor $K_s \tan\phi_a'$ was taken as 0.30 for the fill, the sand and the clay and the distribution of effective vertical stress σ_v' was calculated as the sum of the overburden pressure and the vertical stress due to the embankment (the latter being calculated from elastic theory). One - dimensional consolidation theory was used to estimate the free - field soil settlements in the 17 years since placement of the fill. The analysis showed that the relative movements between the pile and soil were sufficiently large to cause full slip along almost the entire length of the pile shaft.

Having thus established the conditions along the pile prior to the field test program, the predictions for Steps (b) to (e) were made as follows:

Step (b): the cutting of the pile was simulated by removing the estimated axial dead loading of 380 kN. The strain and movement at point A of the pile were thus calculated.

Step (c): the effect of excavation of the fill and sand was considered by reducing the value of τ_a' for these layers to zero, and calculating the corresponding movement of point A.

Step (d): the effects of electro-osmosis were predicted by carrying out a finite difference solution of Eq. 2 using a two-dimensional analysis in the horizontal plane. This prediction presented some difficulty as the voltage and the treatment period was not known; a voltage of 32 V and a continuous treatment period of 48 hours were arbitrarily chosen. Other parameters used in the analysis were c_v = 32 mm²/sec, $k = 1.5 \times 10^{-6}$ mm/sec and k_e = 0.2 mm²/sec volt. From the excess pore pressures thus calculated, the change in τ_a' (Eq. 3), and hence the change in downdrag load, with time, was calculated. The consequent movement of the pile with time was calculated by integrating the strains in the pile developed as a result of the downdrag load changes.

Step (e): the load required to jack the pile back to its original position was calculated by finding the load necessary to cause a pile head movement equal to the sum of the movements in Steps (b) to (d). Full slip was assumed to exist along the length of the pile.

For the above predictions, no account was taken of the possible effects of horizontal movements, or of interaction between the research pile and the adjacent piles.

The Authors' predictions are summarized in Table I.

3.3 Other Predictions

All six predictors used much the same basic aproach. The load distribution in the pile was calculated for assumed conditions prior to cutting, after cutting, after excavation of the fill and sand, and after electro-osmosis. Differences between predictions arose in their estimates of the initial structural load, the factor $K_s \tan\phi_a'$, the vertical effective stress distribution, and the behaviour of the bearing layer. None of the other five predictors considered the time effects associated with electro-osmosis, all assuming that the treatment would be totally effective in reducing downdrag. Also, all the other predictors assumed full pile-soil slip along the shaft.

The range of predictions made by the other participants is shown in Table I. A more detailed description of their predictive procedures is given by Garlanger and Lambe (1973).

TABLE I

SUMMARY OF PREDICTIONS AND MEASUREMENTS FOR CUTLER CIRCLE BRIDGE TEST PILE

Quantity	Authors' Predictions	Range of Participants' Predictions	Measured Value
Strain at A after cutting of pile ($x10^{-6}$)	150	100 - 190	365
Movement of A after cutting of pile mm	3.0	1.5 - 19.2	10.2
Movement of A after excavating sand and fill mm	1.7	1.2 - 6.1	2.5
Movement of A after electro-osmosis mm	3.6	2.0 - 4.6	4.0
Load to return pile to pre-test position kN	1183	766 - 1677	≈ 1920

3.4 Comparison Between Predicted and Measured Values

The measured values in the field test are shown in Table I, together with the predicted values. It is immediately apparent that the largest discrepancy between prediction and measurement is in the strain and movement of point A after cutting, and this reflects an erroneously predicted initial load at the top of the pile. The load required to return the pile to its original position was also underestimated because of the underestimate in the initial load. It was determined from the measured deflections that this initial load must have been about 1090 kN i.e. two to three times the values assessed by the predictors. This difference suggests considerable nonuniformity of the load distribution within the group, and even the possibility of some piles carrying tension. This suggestion was confirmed by the subsequent finding that two of the batter piles had pulled out of the pile cap. This in turn indicates that the effects of negative friction on battered piles are much more severe than on vertical piles, as they are subjected to both normal and axial components of soil movement.

The predictions of the pile behaviour subsequent to the initial cutting (Steps (c) and (d) are in reasonable agreement with the measurements, thus demonstrating that the assessments of the negative friction and electro-osmosis treatment were satisfactory. An evaluation of the measured pile deformations indicated that the maximum downdrag force in the pile, prior to excavation, was about 1100 kN, as compared with the authors' prediction of 1375 kN.

The predicted and measured effects of electro-osmosis cannot be compared in detail because the field test procedure differed from that assumed in the prediction. In the field test, an initial test was performed using a 12 volt car battery, and then a second test was carried out using a welding generator at outputs of 30, 45 and 60 amps. The second test was continued until the pile movement ceased; however, it was found that 70% of the total movement was realized in the first 1.5 hours. This rate of movement, and hence downdrag load relief, is much more rapid than predicted. Fig. 4 shows the result of the electro-osmotic treatment and indicates complete relief of downdrag after only about 120 minutes whereas the predicted time was about 2 days. This discrepancy may be attributable to the assumed values of k and c_v being too low, or the assumed value of k_e being too large.

Despite the differences between predicted and measured behaviour, three clear points emerge from the Cutler Bridge Pile Test:

(i) large downdrag forces can be developed in piles due to negative friction

(ii) the effects of negative friction on battered piles are much more severe than on vertical piles

(iii) electro-osmosis can be effectively used to reduce downdrag forces in piles in a very short time and with a relatively small expenditure of electrical power.

4 MODEL PILE TEST

4.1 Apparatus

To obtain further data on the development of negative friction and its relief with electro-osmosis, a test was carried out on a model pile under controlled laboratory conditions. The apparatus was similar to that previously used for model pile tests by Mattes and Poulos (1971). The pile was situated in a cylindrical pressure vessel consisting of three sections, a base section through which drainage could be provided and into which the pile was screwed, a centre section approximately 400 mm long which was filled with soil, and an upper section which was separated from the centre section by a rubber membrane and which contained water under a controlled pressure. The pile itself consisted of a 25.4 mm diameter aluminium tube, 400 mm long, and had four strain gauges installed near the pile base in order to determine the axial load. To remove the possible effects of pile bending the mean of the four strain gauge readings was calibrated against axial load.

After the pile was screwed into the base, remoulded Kaolin (LL = 55, PL = 33) was placed around the pile, at about the liquid limit. By applying a pressure to the surface of the soil and allowing drainage at the base and top, the clay could be consolidated, thus inducing negative friction and downdrag

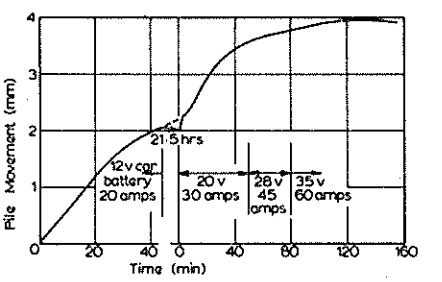

Figure 4 Pile movement vs. time during electro-osmosis-cutler circle bridge

into the pile. The axial load at the pile base could be determined from the strain gauge readings.

To enable application of electro-osmosis to the pile, a single 2 volt cell of a heavy duty battery was used as a voltage source, the potential difference being applied between the pile base (cathode) and the outer wall of the pressure vessel (anode).

4.2 Test Sequence

The test pile was subjected to the following sequence of events:

(a) an initial effective consolidation pressure of 34.5 kPa was applied to the soil as a "seating" pressure (a back pressure of 69 kPa was used for the pore water).

(b) the consolidation pressure was increased by 34.5 kPa and readings of axial load versus time taken over a period of about 2 days

(c) electro-osmotic treatment was applied to the pile by imposing a 2 volt potential difference between the pile and the vessel wall for 30 minutes. The voltage was then removed and a rest period of approximately 6 days was allowed, during which the consolidation pressure remained unchanged

(d) a further 34.5 kPa pressure increment was applied for a one-day period, with readings of axial load versus time being taken

(e) electro-osmotic treatment was applied (2 volts for 30 minutes), followed by a rest period of approximately 6 days during which the consolidation pressure remained unchanged

(f) a final pressure increment of 34.5 kPa was applied for a period of about 2 days.

4.3 Measured Behaviour

Fig. 5 shows the axial load versus time relationship for the pile, for the whole test sequence subsequent to the initial consolidation stage. The following observations may be made:

(i) the first application of electro-osmosis causes a significant and rapid reduction in downdrag load, and there is little recovery of this load in the 6 days following the treatment

(ii) the second electro-osmotic treatment has a similar short-term effect on the downdrag load; however, a complete recovery of the downdrag load occurs in the first 12 hours or so following cessation of the treatment.

The reason for the re-development of downdrag after the second treatment is probably that the treatment was applied at a much earlier stage of consolidation. The remaining consolidation settlements which occurred after cessation of the second treatment were sufficient to again cause full pile-sand slip and cause a build-up of downdrag load to the level it would have achieved if no treatment had been applied. In contrast, the first treatment was applied when the consolidation of the clay was nearly complete, and consequently, there was little further settlement and little recovery of downdrag load.

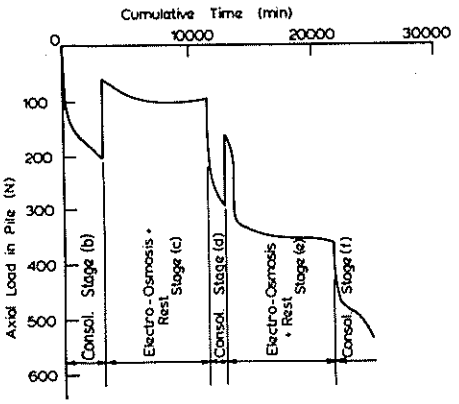

Figure 5 Time-load history of model pile

The implication of these results is that, in field situations, the reduction of negative friction by a short period of electro-osmosis may only be temporary if significant consolidation settlements can occur after the treatment ceases. In such cases, it may be necessary to apply frequent short periods of electro-osmotic treatment in order to prevent a long-term build-up of downdrag load.

4.4 Comparison With Theory

4.4.1 Downdrag force versus time

The solutions presented by Poulos and Davis (1975) were used to predict the magnitude and rate of development of downdrag load in Stages (b), (d) and (f) of the test. On the basis of previous tests, $K_s \tan\phi_a'$ was taken as 0.15 while, from oedometer tests, c_v was taken to be 0.38 mm^2/min. The theory indicated that, for all three Stages, pile-soil slip should occur along the pile during consolidation, and thus estimates of the elastic parameters of the soil were not necessary.

Fig. 6 compares the theoretical and measured load-time relationships. The load is the sum of the downdrag load at the pile base and the immediate axial load increase on the pile head caused by the increase in consolidation pressure. Because the same increase in pressure occurred in all three stages and the pile and soil parameters were assumed to remain constant, a single theoretical curve applies to the three cases. There is some variability between the three measurement curves, and the loads near the end of consolidation vary rather erratically, possibly due to drift of the strain gauges. Nevertheless, the overall agreement is quite reasonable and the theory appears to be capable of giving a satisfactory prediction of the magnitude and rate of development of downdrag force in a pile.

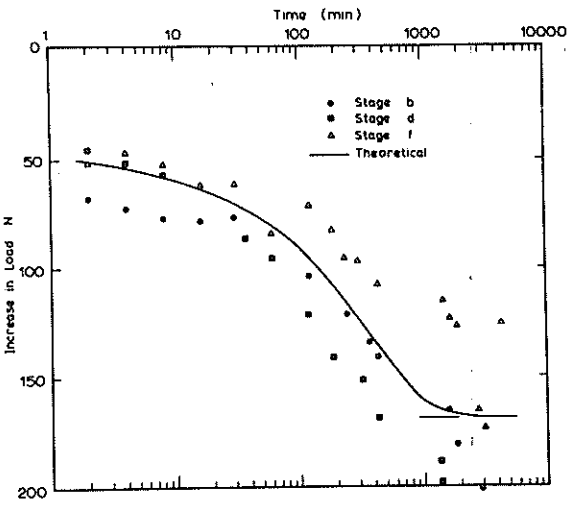

Figure 6 Measured and predicted load vs. time

4.4.2 Downdrag reduction due to electro-osmosis

The reduction in downdrag load due to electro-osmosis was determined by integration the change $\Delta\tau_a'$ in pile-soil resistance (Eq. 3) over the pile surface. The excess pore pressure u at various times was obtained by numerical solution of Eq. 2. For this model test, the boundary conditions differed from those of the Cutler Circle pile test in that the anode in the model test was the circular wall of the pressure vessel, rather than an adjacent pile. A solution to the model test problem was obtained by Townley and Lo (1975) and is shown in Fig. 7.

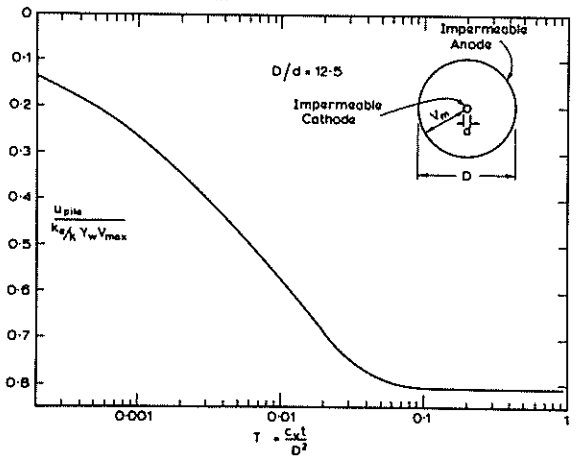

Figure 7 Theoretical solution for model pile

The magnitude of the final maximum excess pore pressure developed at the pile is given by

$$u_{max} = \left(\frac{R^2}{R^2-1} - \frac{1}{2\ell nR}\right) MV \qquad (4)$$

where R = r_e/r_p (here R = 12.5)

V = applied potential difference between electrodes

M = is defined in Eq. 2 and r_e and r_p are defined in Fig. 8.

Tests were not carried out to determine the value of M for the kaolin and therefore various values were assumed within the range of previously - experienced values of 5 to 30 kPa/volt.

Fig. 8 shows the observed relationships between downdrag reduction and load obtained from Stages (c) and (e), together with the theoretical curves for three values of M. The two experimental curves are similar and are in quite good agreement with the theoretical curve for M = 24 kPa/volt. When the electro-osmosis was halted after 30 minutes, the theory suggests that only 75% of the final excess pore pressure had been developed. Consequently, for M = 24 kPa/volt, a further reduction of about 43 kN in the downdrag load could have been achieved if the electro-osmosis had been continued.

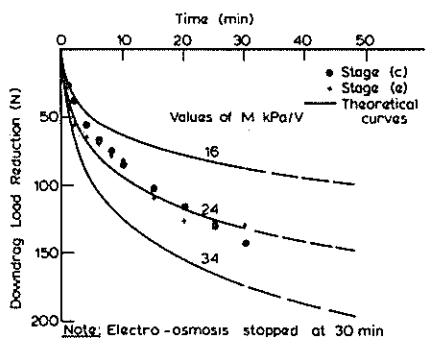

Figure 8 Comparison between measured and theoretical downdrag reduction due to electro-osmosis

5 CONCLUSIONS

The results of the field and model tests described herein clearly demonstrate that electro-osmosis can be effectively used to rapidly reduce downdrag forces in piles subjected to negative friction. The permanence of this reduction depends of the amount of soil movement which will occur following the cessation of electro-osmotic treatment. If this treatment is applied at a late stage of consolidation, there may be only small further downdrag forces developed, whereas, if the treatment is applied at a relatively early stage of consolidation, almost complete recovery of the downdrag force may occur.

The comparisons between theory and measurement, although limited, indicate that the theoretical approach used can predict, with fair accuracy, the downdrag force in the pile, its rate of development and the reduction of electro-osmosis to the pile. The main problem in applying this theory is (as is usually the case in geomechanics) the selection of the appropriate soil parameters, including here the electro-osmotic parameter M.

6 ACKNOWLEDGEMENTS

The work described in this paper forms part of a general research program on the behaviour of foundations being carried out in the Department of Civil Engineering, University of Sydney, and supported by a grant from the Australian Research Grants Committee. The authors are indebted to Mr. K. L. Larymore for his assistance with the experimental work and to Professor T. William Lambe of M.I.T. who organized the downdrag prediction Symposium.

7 REFERENCES

BJERRUM, L., JOHANESSEN, I.J. and EIDE, O. (1969). "Reduction of negative skin friction on steel piles to rock". Proc. 7th Int. Conf. Soil Mechs. Fndn. Eng., Mexico, Vol. 2, p. 27.

ESRIG, M.I. (1971). "Electrokineties in soil mechanics and foundation engineering". Trans. New York Acad. of Sciences, Series II, Vol. 33, No. 2, p. 234.

GARLANGER, J.E. and LAMBE, T.W. (1973). "Proceedings of a symposium on downdrag of piles". MIT Soils Pub. No. 331.

JOHANESSEN, I.J. and BJERRUM, L. (1965). "Measurement of the compression of a steel pile to rock due to settlement of the surrounding clay". Proc. 6th Int. Conf. Soil Mechs. Fndn. Eng., Montreal, Vol. 2, p. 261.

JOHNSTON, I.W. (1978). "Electro-osmosis and its application to soil and foundation stabilization". Symp. on Soil Reinforcing and Stabilizing Techniques, N.S.W. Inst. Tech., Sydney, p. 459.

MATTES, N.S. and POULOS, H.G. (1971). "Model tests on piles in clay". Proc. 1st Aust.-New Zealand Conf. Geomechanics, Melbourne, Vol. 1, p. 254.

POULOS, H.G. and DAVIS, E.H. (1972). "The development of negative friction with time in end-bearing piles". Aust. Geomechs. Jnl. Vol. G 2, No. 1, p. 11.

POULOS, H.G. and DAVIS, E.H. (1975). "Prediction of downdrag forces in end-bearing piles". Jnl. Geot. Eng. Divn., ASCE, Vol. 101, No. GT 2, p. 189.

SODERMAN, L.G. and MILLIGAN, V. (1961). "Capacity of friction piles in varved clay increased by electro-osmosis". Proc. 5th Int. Conf. Soil Mechs. Fndn. Eng., Paris, Vol. 2, p. 143.

TOWNLEY, L.R. and LO, F.S. (1975). "The reduction of negative friction on piles by electro-osmosis". B.E. Thesis, Dept. Civil Eng., Univ. of Sydney.

WALKER, L.K. and DARVALL, P. Le P. (1973). "Drag-down on coated and uncoated piles". Proc. 8th Int. Conf. Soil Mechs. Fndn. Eng., Moscow, Vol. 2, No. 1, p. 257.

Model Pile Groups Subject to Lateral Loading

J. M. O. HUGHES
Director of Situ Technology Inc, Vancouver, (formerly University of Auckland)
H. D. W. FENDALL
Research Student, University of Auckland
P. R. GOLDSMITH
Research Student, University of Auckland

1 INTRODUCTION

It is generally recognised today that the lateral load carrying capacity of a vertical pile is significant in resisting horizontal loads.

Unfortunately the understanding of the mechanism of soil resistance to laterally load piles and particularly pile groups is far from complete. The ability of designers to predict the load-deflection characteristics of even a single pile has not been resolved to within acceptable measures of certainty.

In this paper the authors attempt to indicate some of the uncertainties that exist in our fundamental understanding of pile-soil interaction.

The results reported herein are concerned mainly with the interaction of two piles. The results indicate that the combined action of two piles can be substantially less than the contribution of two individual single piles.

The authors believe that the state-of-the-art on laterally loaded piles and pile groups is well served by analytical techniques (Hughes, Goldsmith and Fendall, 1978). The problem facing designers today is not the lack of mathematical models but the uncertainties involved in choosing suitable soil parameters to use in the analysis, and a lack of understanding of the process of soil-structure interaction.

Many variables which are known to affect the response of a pile group to lateral loading have yet to be understood fully, and at present are not able to be quantified with any degree of confidence. These variables include:

(a) Method of pile installation.
(b) Rate of load application, i.e. static, repeated or cyclic.
(c) Effect of pile cap in providing additional restraint.
(d) Interaction of piles through the soil.

Although the literature reports the results of many lateral load tests on full scale piles and pile groups these are often of little help in determining the influence of the above variables. Full scale tests are generally constrained to very restricted testing programmes, possibly due to financial and/or time considerations, hence the parameters modelling the above effects are not easily determined with any degree of certainty.

Analytical studies can make allowance for most of these points but the accuracy and therefore usefulness of these models is dependent upon the suitability of the soil model used.

Model testing has therefore become a common and widely accepted method of studying the response of piled foundations to both vertical and horizontal loads.

Since model tests are easy to perform the literature abounds with the results and conclusions of such test programmes. Unfortunately the results are often open to considerable interpretation and are only applicable to the situation in which they were obtained. (e.g. placing of sand around pre-positioned piles - a situation that occurs seldom in practice).

2 EXPERIMENTAL PROGRAMME

The experimental apparatus used in this study has been developed with the aim of being as simple as possible and able to produce accurate and repeatable results under controlled conditions. The effect of varying a single parameter, can therefore be studied more precisely. In this paper only the effects of varying pile spacing on rigid, pinned head piles have been considered.

Dry sand has been utilised as the soil medium since it is relatively easy to place uniformly at a known density. The strength of uniform sand increases with depth (due to linearly increasing overburden pressure) thus modelling most naturally occurring soils which increase in strength with depth. Further the response of sand to load is essentially time independent.

The experimental programme has included both rigid and flexible piles, in dense and loose sand. The pile heads have been either pinned, fully fixed (no rotation) or capped.

The results and conclusions presented in this paper are, however, restricted to the influence of spacing on pin-headed, rigid smooth piles in dense sand.

2.1 Pile Installation

A large proportion of the piles used in cohesionless soils today are driven and the effect this has on the subsequent lateral response is not well understood and can only be allowed for on an empirical basis, if at all (e.g. Tomlinson 1977).

Almost all piles used in this study have been driven. This is in contrast to the majority of other researchers who generally place the sand around the pre-positioned piles - a situation that occurs seldom in practice (for example Prakash 1962, Davisson and Salley 1970, Singh 1969).

In order to obtain qualitative information about the effects of pile driving, both photogrammetric

and radiographic techniques have been utilised to determine the sand movement which occurs around a driven pile or piles.

In the photogrammetric technique a model 'half' pile is driven against the glass side of a sand filled box. Photos taken before and after driving can then be compared stereoscopically to determine the movement of the sand particles. The technique for measuring displacements was developed by Butterfield, Harkness and Andrawes (1970). Figure 1 is a schematic view of the apparatus.

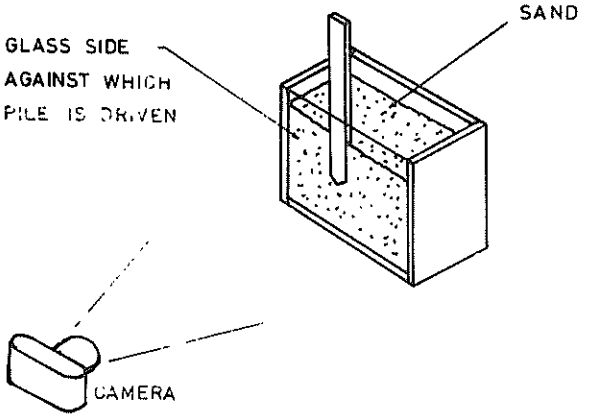

FIGURE 1 - Schematic View of Apparatus for Photogrammetric Technique

It is clear that sand grains up to 6 diameters from the centreline of the pile have moved.

(Figure 2b indicates the influence of driving 2 piles spaced at 4 diameters.)

Radiographs of lead shot embedded at 12 mm centres in the sand have indicated that the effects of friction on the glass plate in modifying the observed displacement patterns are slight. A schematic view of the radiograph apparatus is shown in Figure 3.

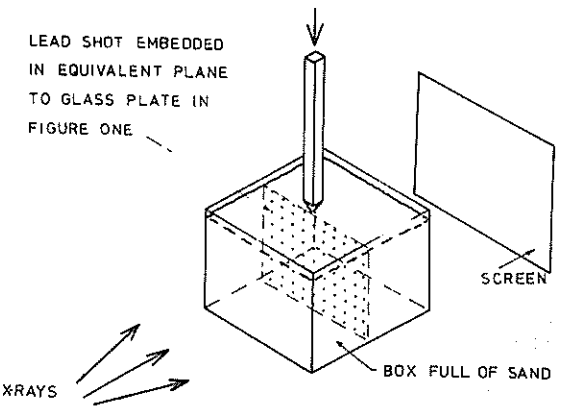

FIGURE 3 - Schematic View of Radiograph Apparatus

Pictorial impressions of the effects of driving are shown in Figures 2a and b. They are superpositions of photos taken before and after driving piles into dense vibrated sand. The single pile effect is shown in Figure 2a.

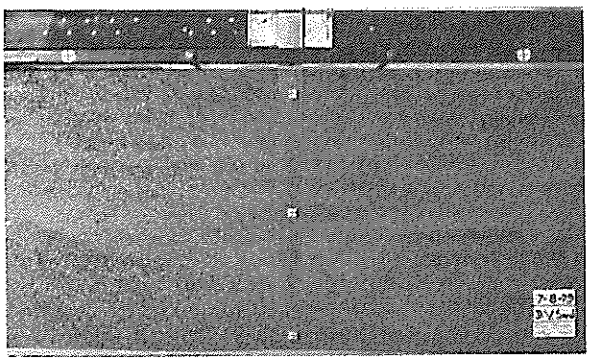

Driving also causes changes to the insitu stresses within the soil. In order to study this effect a model pile was constructed with which it is possible to measure the horizontal stress acting against the pile, at 5 different positions. Figure 4 shows

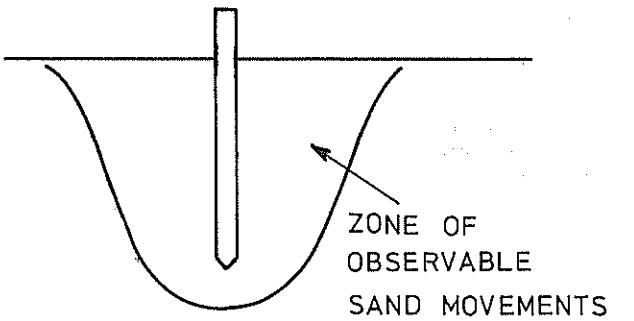

Figure 2a - Sand Movements Caused by Driving a Single Pile

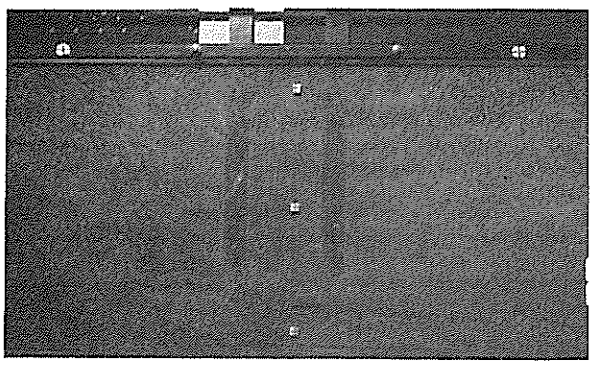

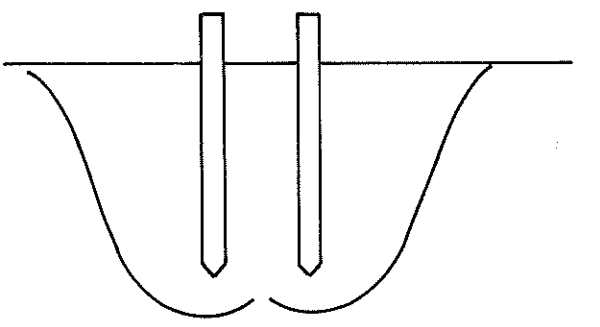

FIGURE 2b - Sand Movements Caused by Driving Two Piles Spaced at 4 Diameters

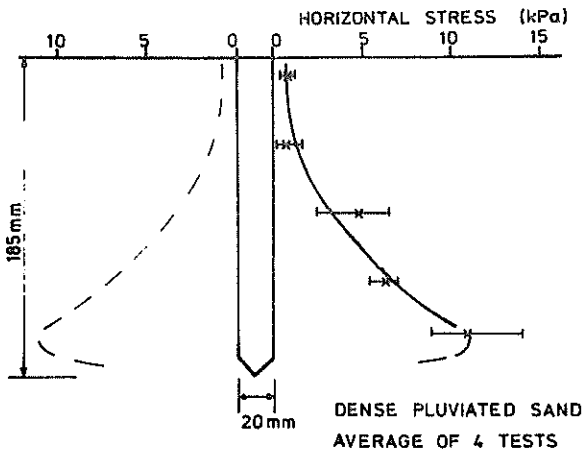

FIGURE 4 - Horizontal Pressures after Driving into Dense Pluviated Sand

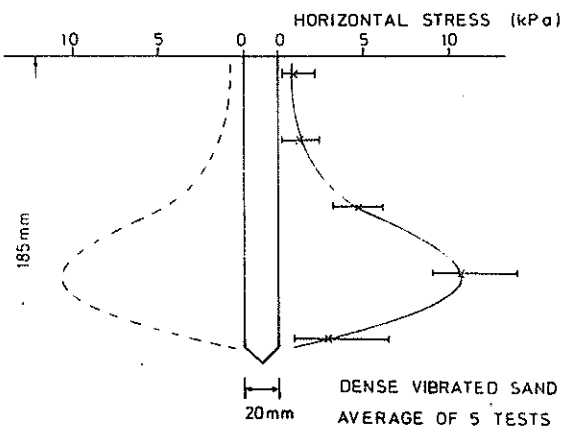

FIGURE 5a - Horizontal Pressures after Driving into Dense Vibrated Sand

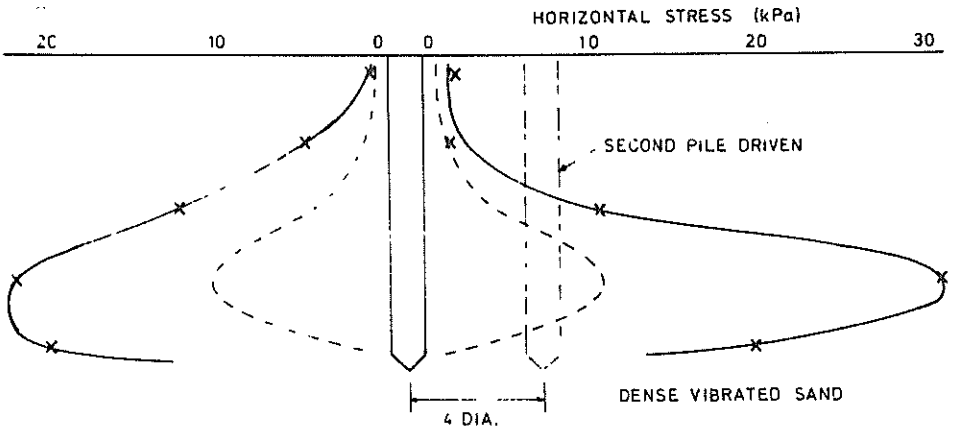

FIGURE 5b - Stress Changes caused by Driving a Second Pile at a 4 Diameter Spacing

the horizontal pressure distribution measured after driving the pile into dense sand which was placed by pluviation through air. In comparison, Figure 5a shows the horizontal stress distribution against the pile after it has been driven into dense sand which had been compacted by vibration. It is interesting to note that the maximum horizontal stress is approximately the same in both cases although the position of this maximum pressure has changed. The stress changes (on the initially installed pile) caused by driving a second pile four diameters away are shown in Figure 5b.

The main conclusion that can be drawn from these diagrams is that the effects of driving are considerable and greatly alter the distribution of horizontal stresses within the soil. As Figure 5b shows the changes in horizontal stress caused by driving a second pile four diameters away from the first are of the same order of magnitude as the original stress changes. These stress changes are likely to be very important in modifying the subsequent response to lateral load.

2.2 Lateral Loading

2.2.1 Sand Movement

The photogrammetric technique mentioned earlier has also been applied to the lateral loading situation. Displacement fields of sand particle movement obtained for lateral loading of rigid piles in

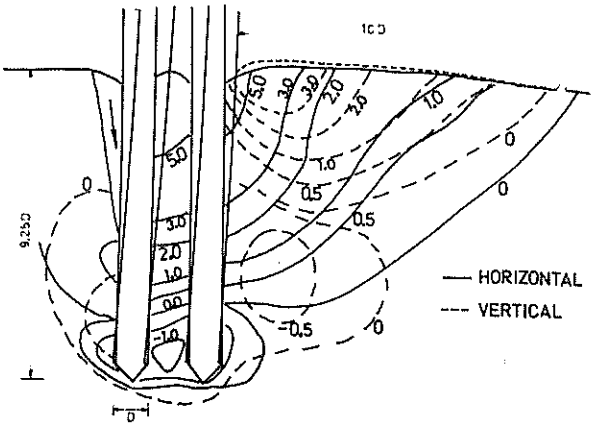

FIGURE 6 - Displacement Field for Laterally Loaded Piles at 2 Diameter Spacing

dense dry sand at 2, 6 and 10 diameter spacings are shown in Figures 6, 7 and 8. Clearly, as the pile spacing increases, the distance from the front pile to the limit of observable displacements (represented by the zero displacement contour) remains essentially constant at 9 to 10 diameters. It is significant that the proximity of the rear pile does not influence the sand displacement patterns in front of the front pile. In contrast, the displacement patterns occurring in the sand in front of the rear pile are greatly influenced by the pile spacing. The sand displacement

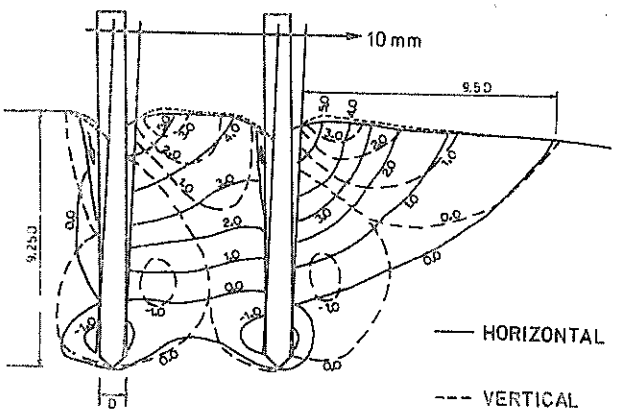

FIGURE 7 - Displacement Field for Laterally Loaded Piles at 6 Diameter Spacing

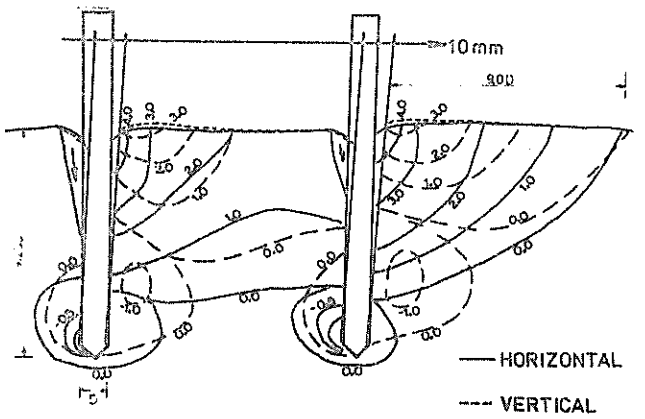

FIGURE 8 - Displacement Field for Laterally Loaded Piles at 10 Diameter Spacing

contours obtained for a 10 diameter pile spacing indicate that significant interaction is still occurring. Hence it can be assumed that a spacing greater than this will be required for piles to act independently.

2.2.2 Load Tests on Model Piles

Another aim of the two pile research programme has been to obtain a measure of the actual distribution of load between the piles in a group. A schematic outline of the experimental apparatus is shown in Figure 9. The important aspect of the loading system is that each pile is forced to displace precisely the same amount (Fendall 1980). This is similar to the field situation since piles in a group are generally capped with concrete, hence the pile heads are forced to displace laterally the same amount. The horizontal loads have been applied approximately three diameters above the surface hence the groundline loading consists of moments as well as horizontal shear.

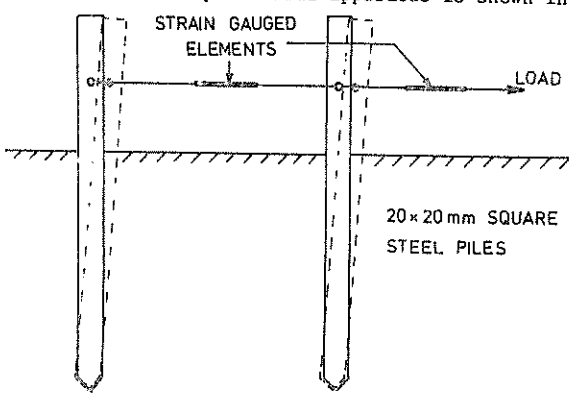

FIGURE 9 - Experimental Apparatus for Pile Load-Sharing Tests

Typical load-deflection curves obtained from a single pile test are shown in Figure 10. It is clear that these curves are far from linear. It is also interesting to note that the method of placing the sand has a substantial effect on the stiffness even though the densities are exactly the same. For example for an applied load of 70N the difference in the resulting lateral deflections is approximately 30%.

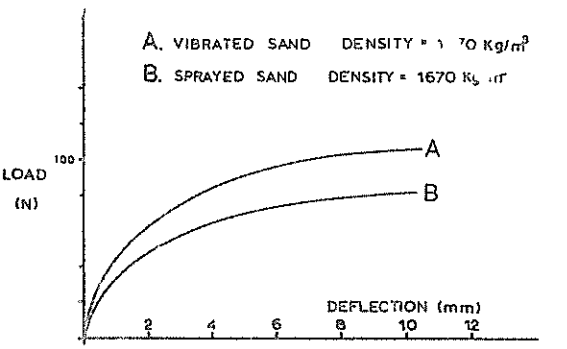

FIGURE 10 - Load Deflection Curves for Single Pile Tests

A typical load-deflection curve obtained using rigid piles spaced at four diameters centre to centre is shown in Figure 11. The front pile clearly takes more load than the rear pile. This is in agreement with the results obtained by other

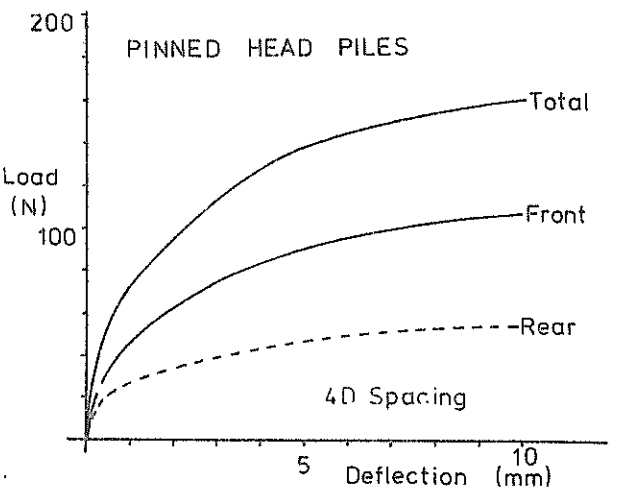

FIGURE 11 - Typical Load Deflection Curves for 2 Pile Case

researchers who have performed model tests and can be contrasted with the results obtained from an elastic continuum analysis, such as that shown in Figure 12 (after Poulos 1971), which suggests equal distribution of load between the front and rear piles.

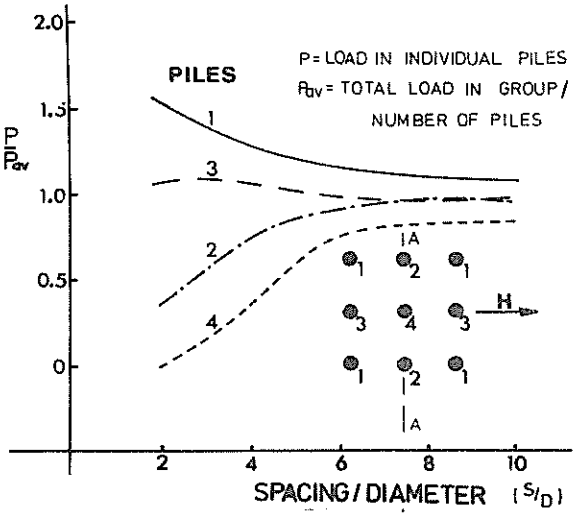

FIGURE 12 - Horizontal Load Distribution in Fixed Head Pile Group (after Poulos 1971)

Figure 13 presents the ratio of front pile load to rear pile load, plotted against pile deflection for the results shown in Figure 11. The ratio stabilises quickly to a near constant value.

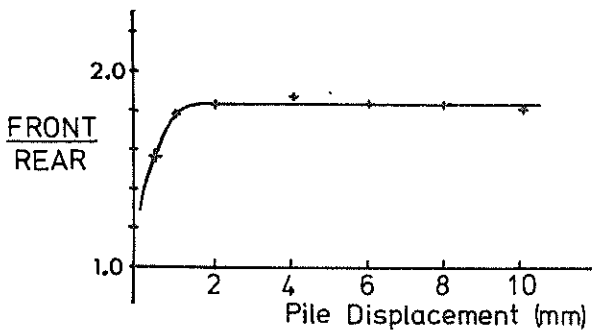

FIGURE 13 - Variation of Pile Load Ratio throughout Loading

Similar tests performed over a wide range of pile spacings give rise to the results indicated in Figure 14. Clearly as the spacing increases the interaction effect becomes less.

Intuitively, this is what would be expected and the results obtained by Prakash (1962) and Tamaki et al (1971) tend to support this view.

Figure 15 is a plot of the total, front pile and rear pile loads acting of the two pile group against pile spacing. It is possible to see how the individual pile load varies with pile spacing. The loads in Figure 15 are those required to move the piles 0.5 diameter at the load line.

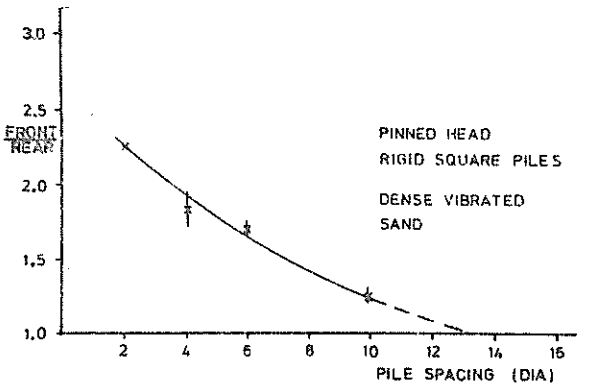

FIGURE 14 - Pile Load Ratio versus Pile Spacing

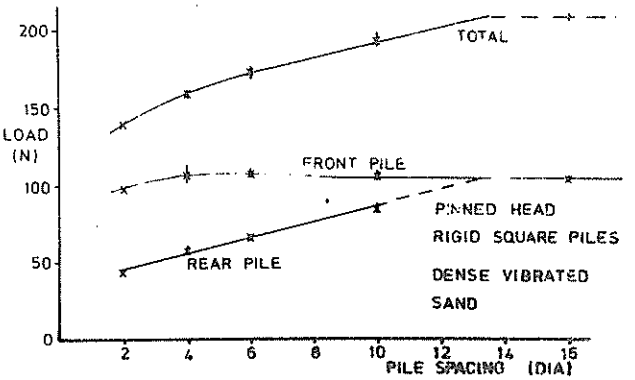

FIGURE 15 - Distribution of Load between Front and Rear Piles at a Load Line Displacement of 0.5 Diameter for Various Pile Spacings

Clearly, from both Figure 14 and Figure 15 the pile spacing required for no interaction effect is approximately 13 diameters. This is significantly higher than that reported by other authors (e.g. Prakash 1962 and Tamaki et al 1971). It is interesting to note that the load on the front pile is not influenced at all by the rear pile except for pile spacings of less than 4 diameters. This is consistent with the sand displacement patterns reported earlier and is due to the fact that the greater part of the pile's resistance to load comes from the strength mobilised in the soil in front of the pile and is independent of influence from the rear pile.

In contrast the load on the rear pile increases linearly to the equivalent single pile load as the pile spacing increases.

The 'pressure sensitive' pile previously discussed has also been used to study the laterally loaded pile problem. Figure 16 shows the pressure distribution against two piles spaced 4 diameters apart. The pressure distribution contours have been plotted for three different load line displacements - namely 1, 5 and 10 mm. The piles are square with a width of 20 mm.

It is noticeable that the sand pressures acting on the rear pile are substantially less than those on the front pile. The centroid of the pressure curves on the rear pile are also significantly deeper than those on the front pile.

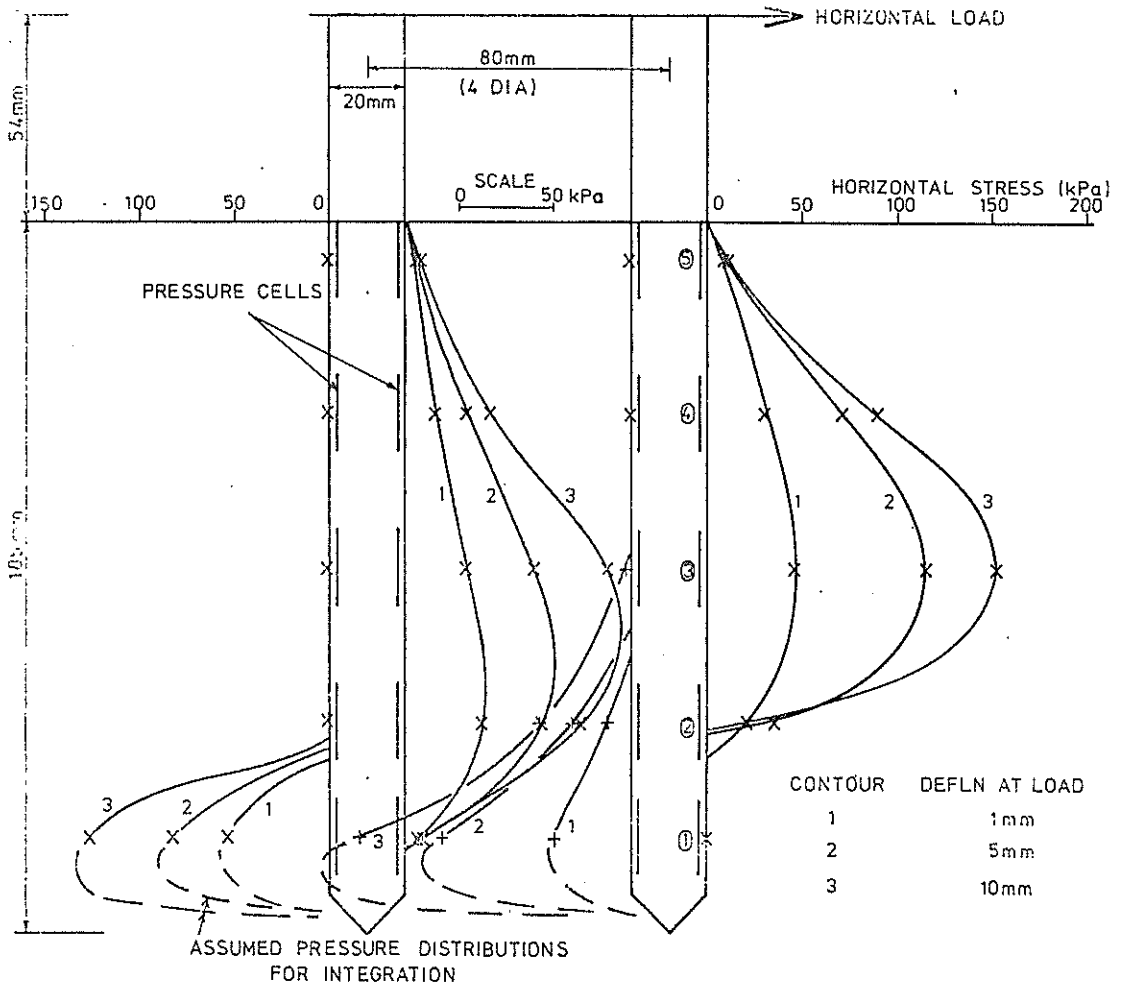

FIGURE 16 - Pressure Distributions against Laterally Loaded Piles at 4 Diameter Spacing

The sand pressure near the surface quickly reaches a limiting value (number 5 gauge) as the deflection is increased while the pressures deeper in the sand (gauges 1 and 3) rise to maximum values of between 150 and 200 kPa. The ratio of these horizontal stresses to overburden pressure exceeds 100 and is approximately 5 to 10 times in excess of the values proposed by Broms (1964) and Brinch Hansen (1961) for these gauge depths.

In order to confirm the quantitative form of the pressure contours, the curves shown in Figure 20, have been integrated over the pile width and length and the resulting forces and moments compared with the actual applied load. In the analysis the effect of friction on the pile sides has been considered to be negligible. Further, if the pressure distribution between the lowest gauge and the pile tip is assumed to be that shown in Figure 16, then the agreement between the measured and predicted loads is generally within 10%.

3 CONCLUSION

In this paper some of the research currently being conducted at Auckland University on the understanding of laterally loaded piles has been reviewed and some of the major results discussed.

The ultimate aim of the research will eventually be to apply the results to the full size situation, however, the model studies reported herein have been performed only with the aim of gaining an understanding of the soil behaviour surrounding a laterally loaded pile, and at this stage, care must be exercised if the results are applied to the field situation.

4 ACKNOWLEDGMENTS

Financial support for this project has been generously provided by the National Roads Board (N.Z.) for which the authors are grateful. The use of equipment and assistance provided by the Otago University School of Surveying is acknowledged. The assistance of the members of the Geomechanics Group at Auckland University is also appreciated.

5 REFERENCES

BRINCH-HANSEN, J. (1961). The Ultimate Resistance of Rigid Piles Against Transversal Forces; The Danish Geotechnical Institute, Copehagen, Bulletin No. 12

BROMS, B.B. (1964). Lateral Resistance of Piles in Cohesionless Soils; Journal of the Soil Mechanics and Foundation Division, ASCE, Vol. 90, May, SM3

BUTTERFIELD, R., HARKNESS, R.M. and ANDRAWES, K.Z. (1970). A Stereo-photogrammetric Method for Measuring Displacement Fields; Geotechnique, Vol. 20

FENDALL, H.D.W. (1980). Lateral Loading of Pile Groups; Ph.D Thesis presented to University of Auckland (in preparation)

HUGHES, J.M.O., GOLDSMITH, P.R. and FENDALL, H.D.W. (1978). The Behaviour of Piles Subject to Lateral Loads; School of Engineering Report No. 178, University of Auckland

MEYERHOF, G.G. (1959). Compaction of Sand and Bearing Capacity of Piles; Journal of the Soil Mechanics and Foundation Engineering Division, ASCE, December, SM6

OTEO, C.S. (1972). Lateral Bearing Capacity of a Pile Group; 5th European Conference on Soil Mechanics and Foundation Engineering, Madrid, Vol. 2

POULOS, H.G. (1971). Behaviour of Laterally Loaded Piles: II - Pile Groups; Journal of the Soil Mechanics and Foundation Engineering Division, ASCE, May, SM5

PRAKASH, S. (1962). Behaviour of Pile Groups Subjected to Lateral Loads; Ph.D Thesis presented to University of Illinois, U.S.A.

SINGH, A. (1967). Investigations of Pile Groups under Lateral and Vertical Loads; Ph.D Thesis presented to University of Jodhpur, India

TAMAKI, O., MITSUHASHI, K. and IMAI, T. (1971). Horizontal Resistance of a Pile Group Subjected to Lateral Load; Proc. 4th Asian Regional Conf. on Geomechanics, Bangkok, Thailand, Vol. 1

TOMLINSON, M.J. (1977). Pile Design and Construction Practice; Cement and Concrete Association, A Viewpoint Publication

Principles of Side Resistance Development in Rock Socketed Piles

A. F. WILLIAMS
Graduate Student, Monash University

SUMMARY An understanding of the principles associated with the side resistance of rock socketed piles has been developed by considering the pile-rock interface as a confined joint. The approach indicates that relative displacement between the pile and rock will occur by either sliding of one surface on the other or by shearing through the concrete or rock asperities. In either case, a dilation has been shown to occur across the interface which has given rise to significant stresses normal to the pile. The side resistance has been found to be a function of the normal stresses and the strength properties of the concrete and rock.

The validity of the concepts developed has been investigated by field testing several piles 1 to 1.2 m diameter and 2 to 2.5 m long in highly to moderately weathered mudstone. The stresses acting normal to each pile have been calculated from measurements of strain in the pile segments, and the socket dilations have been measured by displacement transducers installed in the rock mass. These measurements showed agreement with the postulated principles and have allowed investigation and design procedures to be rationally developed. Further, the developed principles simply explain the work strengthening or work weakening observed during field testing of side resistance piles.

1 NOTATION

A area

c_i cohesion (bond) of the concrete-rock interface

c_o apparent cohesion of the joint

c_s cohesion of the rock substance

E_i Young's modulus of intact rock

E_m Young's modulus of a rock mass

f_{su} peak side resistance

f_{sr} residual side resistance

i asperity angle relative to the overall shear direction

j mass factor $= E_m/E_i$

N normal force

q_a unconfined compressive strength of rock

R radius of a rock socket

S shear force

S_H standard deviation of asperity height above a line running through the roots of the asperities

S_i standard deviation of the asperity angle

α side resistance reduction factor reflecting changes in the strength of intact rock

$$= \frac{f_{su} \text{ (for intact rock)}}{q_a}$$

β side resistance reduction factor reflecting changes in the mass modulus

$$= \frac{f_{su} \text{ (for jointed rock)}}{\alpha q_a}$$

δ_n normal displacement (dilation)

ΔR change in the radius of a rock socket

ϕ_i friction angle of the concrete-rock interface

ϕ_o apparent friction angle of the joint

ϕ_r residual friction angle of the rock resistance

ϕ_s peak friction angle of the rock substance

σ normal stress

τ shear stress

ν Poisson's ratio of a rock mass.

INTRODUCTION

The foundations for high and concentrated loads frequently consist of large diameter piles socketed into rock. Such piles may be designed to carry their load in side resistance only, in base resistance only or in both side and base resistance, according to the construction methods and local practice. The allowable values of side or base resistance are often determined on the basis of guidelines contained in Codes of Practice, previous experience or special investigations designed to suit the need of the particular project.

Investigations concerning the side resistance of rock socketed piles have usually involved the construction and load testing of small or full size test piles. Typical investigations, e.g. Rosenberg and Journeaux (1976), Hvorath (1978) and Williams *et al.* (1980a) have measured the peak side resistance f_{su}, and the residual side resistance f_{sr}, and related these capacities to the unconfined compressive strength, q_a, of the rock. As a result, useful empirical correlations now exist between side resistance and rock strength. Unfortunately, investigators reporting the results of load tests have not proceeded with their various analyses to obtain an understanding of the principles associated with the development of side resistance, which makes it difficult to apply data obtained from one set of conditions to a different situation. For example, the importance of socket roughness does not appear to have been fully considered, and no attention appears to have been given to the effects of jointing or the rock mass compressibility. These and

other factors need to be considered if a proper understanding of side resistance is to be achieved and sensible pile designs are to be produced.

This paper develops the principles governing the development of side resistance by considering the pile-rock interface as a joint and by applying the technology established for rock-rock joints to the pile-rock joint. The concepts developed have been supported by laboratory tests designed to simulate the action of side resistance and by small and large size field pile tests, with particular attention being given to the effects of the following:

(i) roughness of socket walls

(ii) construction under bentonite

(iii) the modulus of the rock mass including the effects of jointing.

3 PILE-ROCK INTERFACE AS A JOINT

3.1 Shear Strength of Joints

The shear characteristics of rough joints which are applicable to the present discussion may be considered initially in terms of the bilinear joint model (Patton, 1966) and the semi-empirical strength criteria of Barton (1976). The bilinear model used by Patton (1966) to describe the behaviour of the regular joint shown in Figure 1 indicates that sliding will occur along the asperities according to Equation 1 and that shear will then occur through the asperities according to Equation 2.

$$\tau = \sigma \tan(\phi_i + i) \qquad (1)$$

$$\tau = c_o + \sigma \tan \phi_o \qquad (2)$$

Equation (1) indicates that sliding on the interface will not occur if $\phi_i + i \geq 90^o$, which, for typical values of $\phi_i = 30^o$ to 40^o, implies that sliding will not occur if the asperity angle, i, is greater than about 50^o to 60^o. Asperity angles of this order seldom occur in natural joints, however, they may be common in the case of rock socketed piles, particularly if the socket has been hand excavated or if the socket has been specially grooved. Further, it may be seen from Equations (1) and (2) that if $\phi_i + i$ is greater than about 75^o to 80^o, i.e. if i is greater than about 35^o to 50^o, only a small normal stress will preclude failure according to Equation (1), and failure will therefore occur by shearing through the roots of the asperities according to Equation (2).

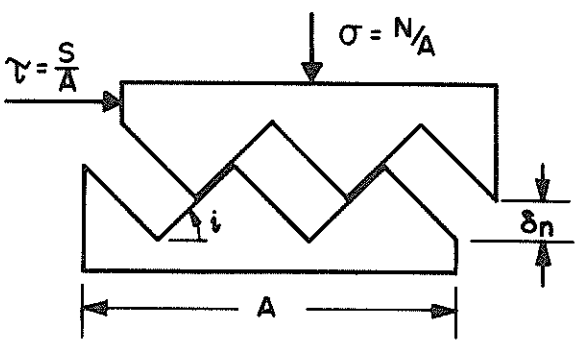

Figure 1. Model of a joint with regular asperities (after Patton, 1966)

Patton's model has treated the interface as a friction surface; however, if the concrete is cast against a clean socket wall, a significant bond will develop. The presence of such a bond, or cohesion, will influence the initial mode of failure only, because it will be destroyed if any sliding on the interface occurs. It is therefore appropriate to modify Equation (1) to include the interface cohesion, using a static analysis, as shown in Equation (3) for the condition before shear displacement has occurred.

$$\tau = \frac{c_i}{2 \cos i \, (\cos i - \sin i \tan \phi_i)} + \sigma \tan(\phi_i + i) \qquad (3)$$

In order to determine whether failure will occur initially along the interface or through the roots of the asperities, Equations (2) and (3) may be combined, then if the normal stresses are considered to be negligible before the initial failure, the criterion for initial failure by sliding is given by Equation (4).

$$2 \frac{c_o}{c_i} \cos i(\cos i - \sin i \tan \phi_i) > 1 \qquad (4)$$

In the case of a rock socketed pile observations indicate that it may be assumed that $c_o = c_i$, and Equation (4) then indicates that failure will occur by sliding only if $(\phi_i + i) < 60^\circ$ to 65°. The effect of a concrete-rock bond therefore has the effect of reducing the value of i, below which sliding may occur, to about 20° to 35°.

The foregoing analysis is simplistic and it has been included to simply illustrate the commonly accepted failure mechanism for rock joints and the importance of the interface bond and asperity angle. It is more practical and realistic to consider the shear characteristics of an irregular joint in terms of Barton's (1976) strength criteria, viz.:

$$\frac{\tau}{\sigma} = \tan \left[JRC \log_{10} \left(\frac{q_a}{\sigma} \right) + \phi_r \right] \qquad (5)$$

where JRC is an empirical joint roughness coefficient.

The ratio q_a/σ effectively provides for a sliding type of failure when the normal stress is low compared with the compressive strength of the rock, and for a progressive increase in shearing through the asperities as the normal stress increases.

The joint roughness coefficient, JRC, has been determined empirically by analysing the strength of various joints with different roughness profiles. In order to use Barton's equation, the JRC must be estimated, and this is often done by comparing typical standard roughness profiles with the profile in question. This method of determining the JRC is rather subjective and often difficult in practice. It has been found practicable to describe the roughness of rock sockets in terms of the statistical shape of the asperities. The statistical shape parameters found to reflect shear characteristics by Meyers (1962) for metal surfaces and by Krahn and Morgenstern (1979) for rock surfaces may be translated to the standard deviation of asperity height above the root line of the asperities, S_H, and the standard deviation of the asperity angle, S_i, although both Meyers (1962) and Krahn and Morgenstern (1979) found that S_i alone adequately represented the roughness from the shear strength viewpoint. A statistical analysis of the typical roughness profiles considered by Barton (1976) has produced the correlation between the JRC and the

asperity angle S_i as shown in Figure 2, which tends to confirm the ability of S_i to adequately represent the roughness of joints subjected to a constant normal force.

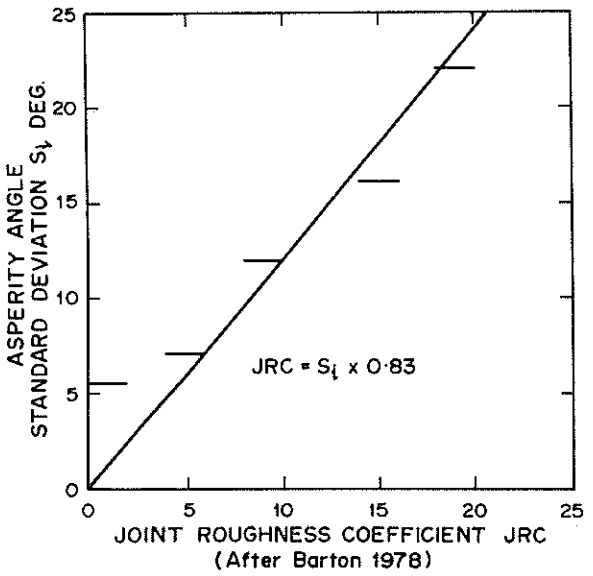

Figure 2 The correlation between Barton's (1978) joint roughness coefficient and the asperity angle standard deviation.

3.2 Application of Joint Analysis to Rock Sockets

The discussion above has been based on the concept of the common direct shear test in which the normal stress (or force) is maintained at a constant value until a peak, and sometimes residual, strength is indicated. Such test results are obviously applicable to the analysis of slope stability problems for example, where the normal force is reasonably constant.

In cases where the joints are confined, as in rock sockets and in many other underground situations, the normal stress develops as a result of dilation normal to the joint as sliding or shearing occurs and as a result of elastic effects, and as such it is not constant. The dilation normal to the joint is usually small enough to allow elastic theory to be used to relate joint dilation to normal stress. In the case of a rock socket the normal stress caused by joint dilation may be estimated according to the expanding infinite cylinder theory, e.g. Boresi (1965), as indicated by Equation (6)

$$\sigma = \frac{\Delta R}{R} \frac{E_m}{1 + \nu} \qquad (6)$$

The normal stress which results from Poisson's ratio effects in the pile and surrounding rock mass, and which should be added to that given by Equation (6), may be estimated from elastic finite element analysis, however, preliminary work by Williams *et al.* (1980b) has found this to be small compared with the normal stresses discussed in Section 5.

4 LABORATORY DATA

It is possible to determine the shear characteristics of a confined joint by carrying out a direct shear test in which the normal stress is determined automatically according to the normal stress-dilation relationship. Such a test may be termed a "constant normal stiffness direct shear test", (CNS direct shear test), because the ratio of normal stress to dilation, σ/δ_n, is constant. In the case of a rock socketed pile the normal stiffness may be determined according to Equation (6) for the particular socket size being considered.

A direct shear machine has been designed by the author and built at Monash University to enable tests to be made with a constant N/δ_n, which provided a practical approximation to the constant σ/δ_n concept. The CNS machine was designed to test specimens nominally 150 mm wide x 200 mm long.

Initial laboratory tests were made on plaster-concrete samples with regular 12° and 45° asperities to provide simple models on which to develop an understanding of the CNS direct shear test. A typical result from a test on 45° asperities made with a normal stiffness of 1017 kPa/mm is shown in Figure 3.

The initial dilation angle of 45° shown in Figure 3(b) corresponds to the asperity angle which indicates that the initial linear portion of the curves corresponds to sliding along the plaster-concrete interfaces. An abrupt decrease in shear resistance is apparent at a displacement of 3 mm when failure occurred through the asperities, however, the normal stress was apparently unaffected by the asperity failure. The abrupt decrease in shear resistance may therefore be attributed to the loss of cohesion of the asperity, with the subsequent behaviour becoming largely frictional as the remaining roughness was worn away. The results of several tests on plaster-concrete joints with 12° and 45° asperities are summarized in Figure 4.

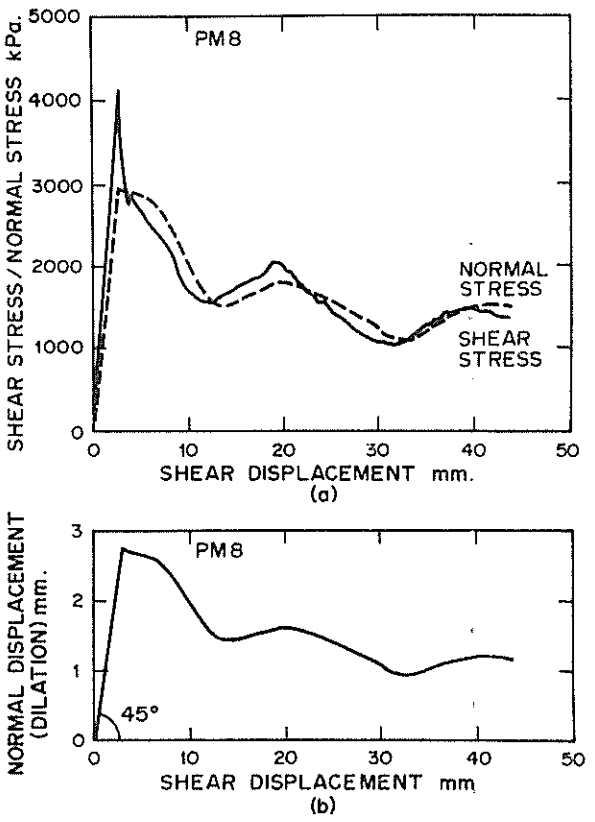

Figure 3 The result of a typical constant normal stiffness direct shear test on a plaster-concrete joint with regular 45° asperities.

Figures 4(a) and (b) indicate a significantly greater shear displacement and a greater dilation at the overall peak shear stress for the 12° asperities, however, Figure 4(c) suggests that the overall peak shear stress is the same for the 12° and 45° asperities.

The shear tests on plaster-concrete joints were followed by similar tests on mudstone-concrete joints. The mudstone samples were obtained from the sides of 1 m to 1.2 m diameter sockets drilled in mudstone adjacent to the test piles discussed in Section 5. The CNS direct shear tests were therefore designed to model the behaviour of the test piles.

In the first series of tests samples were obtained from 1 m diameter sockets drilled in highly weathered mudstone. One socket had been drilled normally without any special regard being given to the socket roughness, while a second socket was drilled normally and then specially roughened by adding an extra tooth to the auger. The roughness parameters obtained are represented by the parameters quoted for the test piles S3 (roughened) and S5 (normal) in Table II. The result of a CNS direct shear test on a specimen from a normally drilled rock socket is shown in Figure 5. Similar results were obtained for specimens from roughened sockets. Figure 5(a) indicates that an abrupt loss of shear resistance does not occur as progressive shearing of the asperities occurs. This is presumably because of the dilation which occurs and the normal stress which develops during the shearing of a confined, irregular, rough joint. The normal stress and normal displacement are seen to remain reasonably constant after the main asperity shearing, while the shear resistance is seen to decrease gradually to a residual value. The results of the tests on specimens from normally drilled and roughened sockets in highly weathered mudstone are summarized in Figure 6.

A second series of CNS direct shear tests was made on specimens obtained from a 1 m diameter socket drilled normally into moderately weathered mudstone. The roughness parameters pertaining to these specimens were similar to those for test piles M1 and M3 as listed in Table II. The results of the tests were similar to those for the highly weathered mudstone, and are summarized in Figure 7.

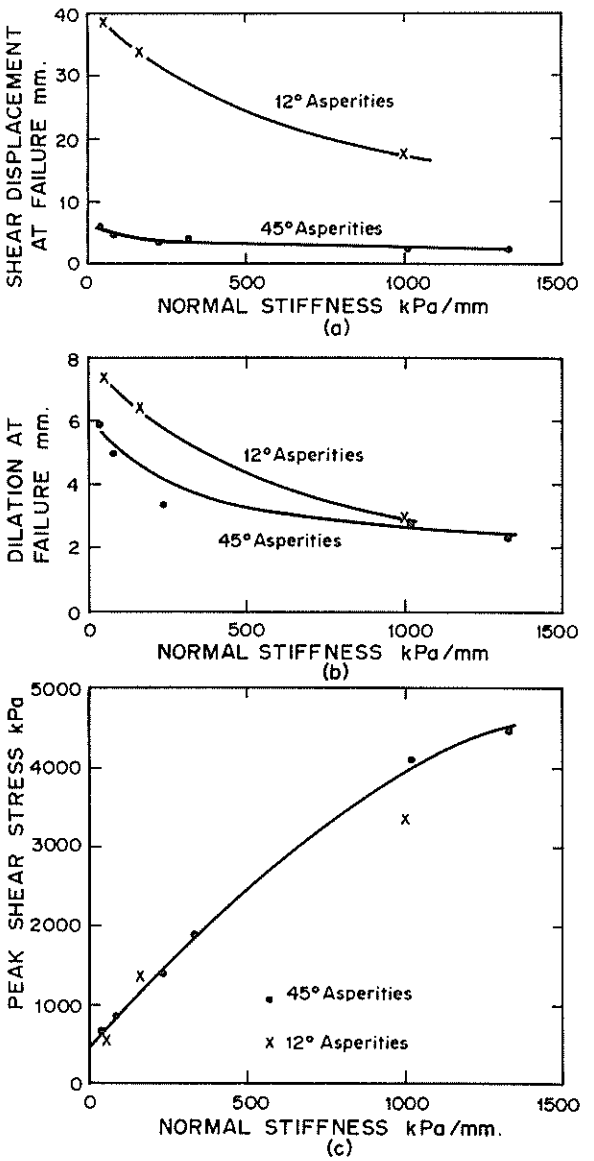

Figure 4 Summary of constant normal stiffness direct shear tests on plaster-concrete joints with regular 12° and 45° asperities.

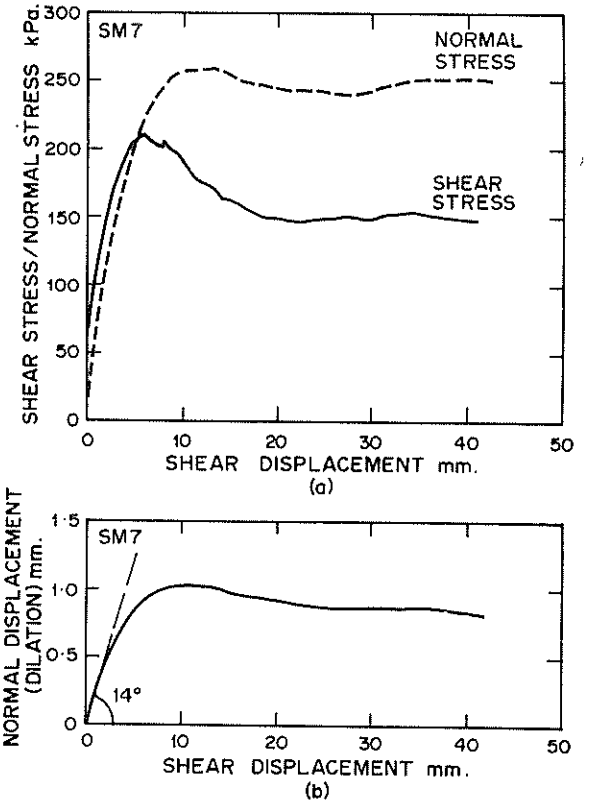

Figure 5 The result of a typical constant normal stiffness direct shear test on a mudstone-concrete joint. The mudstone was obtained from a normally drilled socket in highly weathered mudstone.

Figures 6(c) and 7(c) indicate the effect of normal stiffness, i.e. rock mass modulus, on the peak side resistance. This effect is particularly relevant to the design of piles socketed into a jointed rock mass in which the mass modulus has been significantly reduced by jointing (e.g. Deere *et al.*, 1966). In order to quantify the effect of modulus changes in a general form, it is necessary to normalize the curves contained in Figures 6(c) and 7(c) in terms of the side resistance factor β, which represents the decrease in side resistance relative to that in an intact rock, and the mass factor j, which represents the decrease in mass modulus relative to that of an intact rock. The result of normalizing the curves is shown in Figure 8, which indicates that the peak side resistance decreases at a much slower rate than the rock mass modulus.

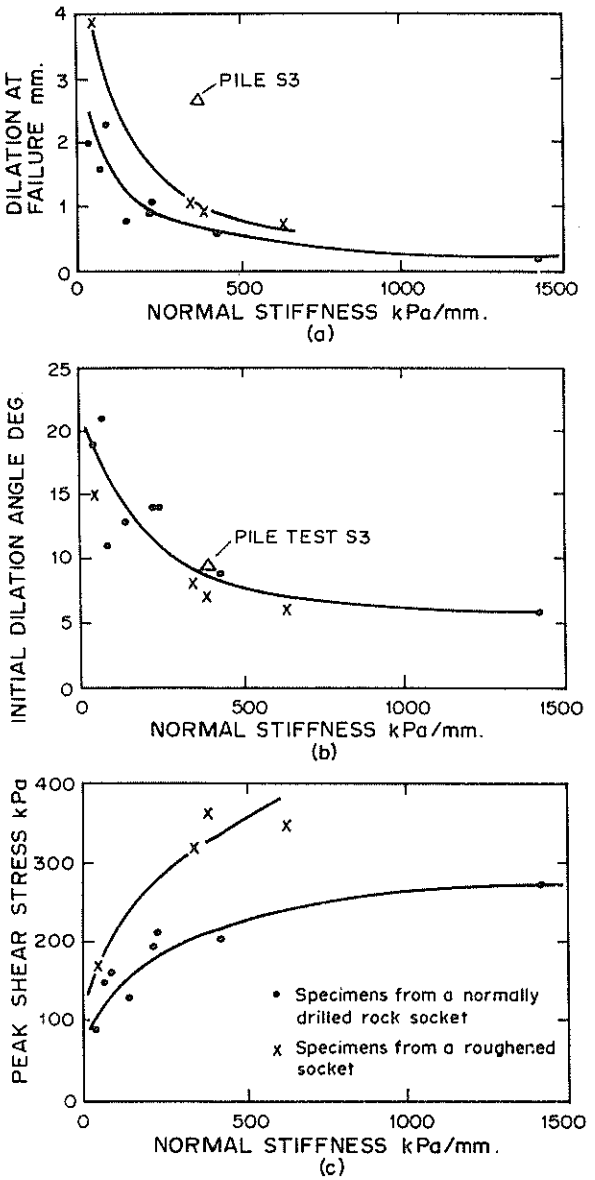

Figure 6 Summary of constant normal stiffness direct shear tests on mudstone-concrete joints. The mudstone was obtained from normally drilled and roughened rock sockets in highly weathered mudstone. The results of pile test S3 are also shown.

5 FIELD DATA

A series of pile tests was made on 660 mm to 1300 mm diameter piles constructed in highly and moderately weathered mudstone. The tests were designed primarily to measure the peak and residual side resistances, however, the opportunity was taken to obtain field data concerning the dilation of pile-rock interfaces and the development of normal stresses during shearing.

The dilation of the pile-rock interface was assessed from the results of displacement transducers installed in the rock to measure the radial diplacement of the rock between a point near the interface and a point 1 m from the interface. The displacement measured over the gauge length was adjusted to provide an estimate of the interface dilation relative to an infinite boundary (Boresi, 1965). A typical result is shown with the load-settlement curve for pile S3 in Figure 9, where it is seen that the

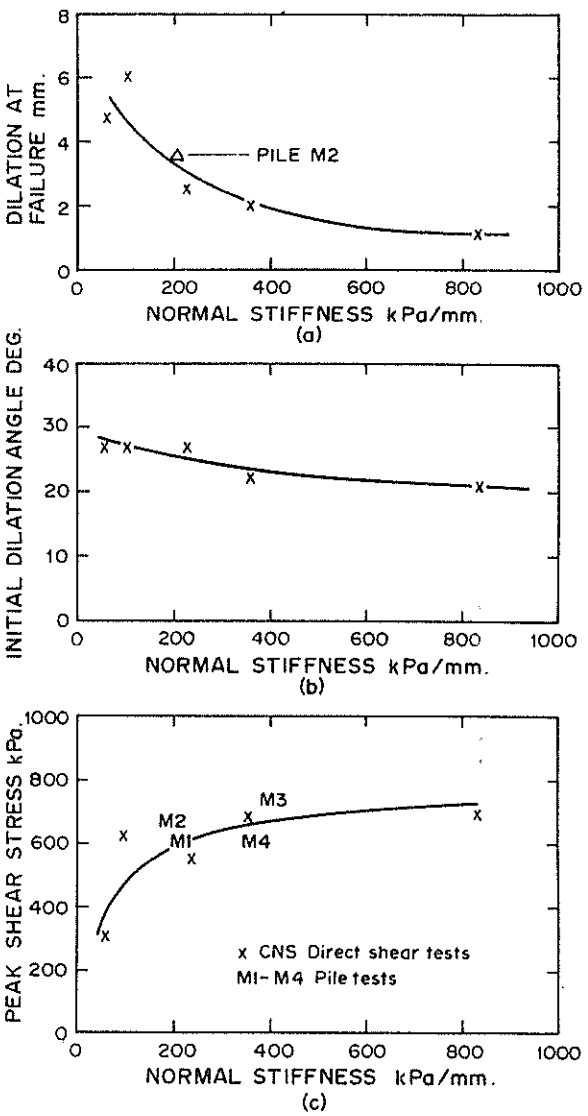

Figure 7 Summary of constant normal stiffness direct shear tests on mudstone-concrete joints. The mudstone was obtained from normally drilled sockets in moderately weathered mudstone. The results from pile tests in the same mudstone are also shown.

TABLE I

	TEST PILE			
	S3	S5	M2	M8
Pile dimensions mm				
diameter	1170	1120	1300	660
length	2510	2590	2000	1800
Socket roughness S_H mm	8.3	2.3	10.2	-
S_i deg	18	11	25	-
Rock unconfined compressive strength kPa	570	620	2300	2000
Residual interface dilation from transducers in rock mm	2.6	2.5	3.3	-
Residual normal stress from strain gauges kPa	1190	990	-	1570
Residual side resistance from load test	505	479	632	804
Residual side resistance from dilation gauges[1]	760	670	740	-
Residual side resistance from strain gauges[2]	460	380	-	770
Residual side resistance from laboratory tests[3]	340	220	600	-

Notes:

1 The normal stress has been calculated according to Equation (6) and residual side resistance has been calculated from $f_{sr} = \sigma \tan \phi_r$ with $\phi_r = 21^o$ for piles S3 and S5, 25^o for pile M2 and 26^o for pile M8 as indicated from residual direct shear tests.

2 The residual side resistance was calculated according to $f_{sr} = \sigma \tan \phi_r$ with ϕ_r as above.

3 Values selected from Figure 6(c) for piles S3 and S5 and from Figure 7(c) for pile M2 according to the rock modulus indicated by the pile tests.

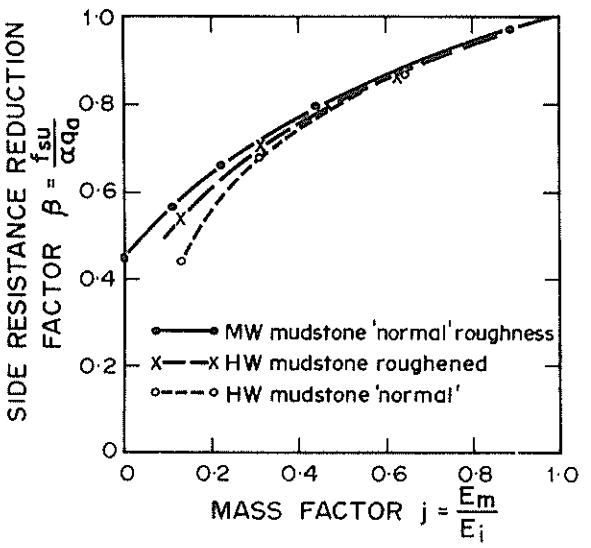

Figure 8 The effect of a reduction in the modulus of a rock mass on the peak side resistance, for sockets drilled in highly or moderately weathered mudstone.

dilation increases quickly as the pile load increases and then the dilation angle decreases to a very small value as the pile apparently reaches a residual condition.

The development of normal stress was determined for the test piles from the results of resistance wire strain gauges embedded into microconcrete briquettes and cast into the test piles. The strain gauges were placed to measure vertical and radial strain at various locations within the piles. The vertical and radial stresses in the pile were calculated on the basis of elasticity, e.g. Zienkiewicz (1971), to provide the distribution of vertical stress and radial (normal) stress with depth.

The results obtained from the test piles have been analysed with respect to the residual side resistance and summarized in Table I.

Although there is some scatter in the estimation of the residual side resistance according to the various measurements, the estimates are all of the same order and thus support the suggestion that the residual resistance depends largely on the development of normal stresses due to dilation of the pile rock interface.

6 DISCUSSION

The preceding paragraphs have demonstrated that the behaviour of the pile-rock interface of a side resistance pile is similar to that of a natural

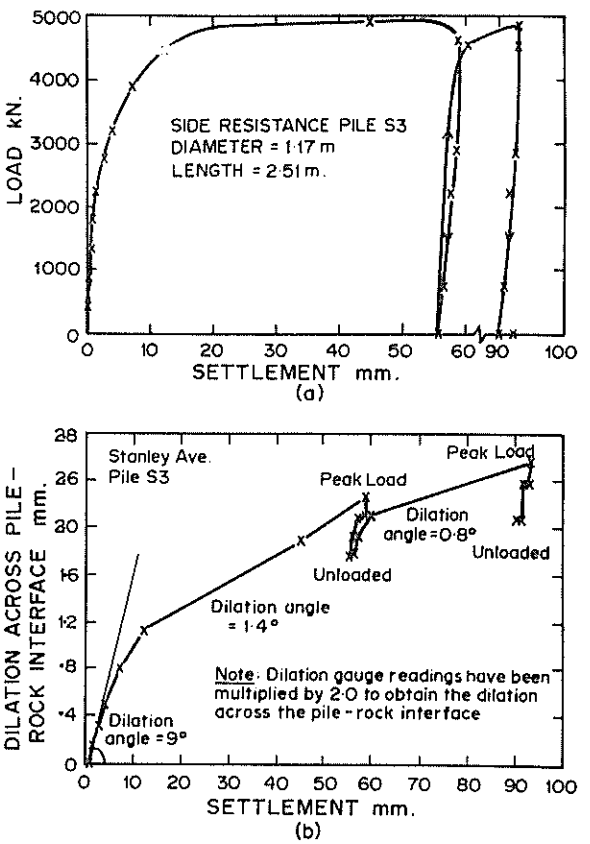

Figure 9 The load-settlement curve for a side resistance test in a roughened mudstone socket and the corresponding measured socket dilation.

TABLE II

THE IMPORTANCE OF ROUGHNESS TO SIDE RESISTANCE

Pile No.	Rock Description	Socket Size mm	Socket Roughness S_H mm	Socket Roughness S_i deg	q_a kPa	f_{su} kPa	f_{sr} kPa	$\frac{f_{su}}{q_a} = \alpha$	$\frac{f_{sr}}{f_{su}}$
S3	HW Siltstone (Melbourne mudstone)	1170 dia. x 2150	6.4	18	570	505	505	0.89	1.0
S5	" "	1120 dia. x 2590	3.3	13	620	485	479	0.78	0.98
S12	" "	335 dia. x 900	< 1 mm	-	620	412	275	0.44	0.67
M2	MW Siltstone (Melbourne mudstone)	1300 dia. x 2000	10.2	25	2300	640	632	0.28	0.99
M3	" "	1230 dia. x 2000	3.1	14	2300	710	710	0.31	1.0
M1	MW Siltstone (Melbourne mudstone)	1220 dia. x 2000 (bentonite)	2.3	13	2460	609	609	0.25	1.0
M4	" "	1350 dia. x 2000 (bentonite)	12	27	2340	617	590	0.26	0.96
Pells (1979) 6 tests	Sydney sandstone	160 to 710 dia.	smooth		6000	1000	640	0.17	0.64
Pells (1979) 2 tests	" "	210 dia.	2 mm grooves at 10 mm pitch		6000	1030	920	0.17	0.89
Pells (1979) 3 tests	" "	210 to 315 dia.	7.5 mm deep grooves at 10 mm pitch		6000	1240	1160	0.21	0.94

rock joint. There appears to be an initial phase during which dilation and normal stress increase rapidly in a manner similar to the sliding phase of the bilinear model. The rate of dilation appears to diminish to a negligible value as major shear planes develop approximately parallel to the direction of shear, and the behaviour enters a second phase which is similar in effect to the shearing of the asperities of the bilinear model. There appears to be a gradual transition from the first phase to the second as observed for natural rough joints by Barton (1976) and Ladanyi and Archambault (1970).

The peak side resistance may be regarded as a function of the normal stress, the bond between the concrete and rock, the strength of the intact rock, and the shape of the asperities. However, the residual side resistance will depend only on the normal stress and the residual friction angle of the rock, with the normal stress being determined primarily by the dilation due to shearing and elastic effects. The implications of this are apparent when the results of tests on smooth and rough sockets are compared for the results of pile tests shown in Figure 10.

The peak side resistance of a pile cast into a smooth sided socket will depend on the interface cohesion, or bond, plus a small normal stress due to Poisson's ratio effects. Such a pile will experience an abrupt loss of capacity when the bond is broken and will have a residual capacity which is significantly lower than the peak capacity. Pile behaviour of this type is illustrated in Figure 10 for pile C2 in a smooth sandstone socket and for pile S12 in a relatively smooth mudstone socket. Because the peak side resistance of a smooth socket depends largely on the concrete-rock bond, any smearing of remoulded rock or bentonite which may reduce the bond will also affect the peak side resistance. This effect was noted by Pells (1979), who found that failure to remove a thin coating of remoulded sandstone reduced the peak resistance by 60%, and that the casting of a pile under bentonite reduced the peak resistance by 76%.

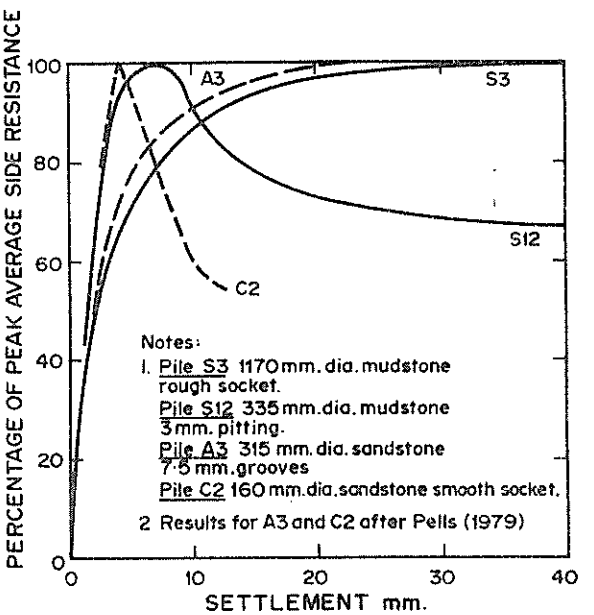

Figure 10 The effect of socket roughness on sockets in sandstone and mudstone

The behaviour of piles constructed in sockets with some degree of roughness has been found to be distinctly different to the smooth socket piles, as indicated in Table II and illustrated in Figure 10 for the relatively smooth socket tests C2 and S12 and the rougher socket tests A3 and S3. The provision of 7.5 mm deep grooves in 210 to 315 mm diameter sandstone sockets (Pells, 1979) and S_H of more than about 3mm in 1.1 to 1.2 m diameter mudstone sockets was found to increase the peak side resistance by 60% to 80%. The provision of roughness was also found to increase the residual side resistance to at least 90% of the peak value, as indicated in Table II. Further, the construction of piles under bentonite was found to reduce the capacity of rough sockets by less than 10%.

7 CONCLUSIONS

The mechanism of side resistance in rock socketed piles has been shown to be consistent with the concepts developed for the shear strength of rock joints.

In the case of smooth sockets, the failure mechanism has been found to consist initially of breaking the concrete-rock bond which results in a sharp loss of side resistance, followed by the development of a small normal stress due to minor interface dilation and Poisson's ratio effects. The peak side resistance of such sockets has been shown to be sensitive to the presence of any smear on the socket surface which could reduce the concrete-rock bond. The residual side resistance of smooth sockets has been shown to be much lower than the peak side resistance.

In the case of rough sockets, the failure mechanism has been found to consist of a sliding and progressive shearing of asperities, which produces a significant dilation across the pile-rock interface. The side resistance has been shown to approach the residual condition slowly, generally with little loss of side resistance because the interface dilation and associated normal stress are maintained naturally at a relatively high level. Although the provision of roughness on a rock socket has been shown to increase the peak side resistance, it appears that the peak side resistance does not increase significantly further for asperities rougher than about S_H = 3 mm and $S_i = 12^o$ (JRC = 10). The peak side resistance has also been shown to depend on the modulus of the rock mass, which follows from the relation between the interface dilation and the resulting normal stress.

8 AKCNOWLEDGEMENTS

The work described in the paper was carried out at Monash University as part of a research project sponsored by the Country Roads Board of Victoria. It also forms part of a continuing programme of research at Monash University, under the direction of Associate Professor I.B. Donald and Dr. I.W. Johnston, into the performance of foundations on Melbourne mudstone with special reference to rock socketed piles. The paper is published with the permission of the Chairman of the Country Roads Board of Victoria, Mr. T.H. Russell.

9 REFERENCES

BARTON, N. (1973) Review of a new shear stress criterion for rock joints. Engineering Geology, Vol. 7, pp. 287-882.

BORESI, A.P. (1965) Elasticity in Engineering Mechanics. Prentice Hall Inc., New Jersey. p.157.

DEERE, D.U., HENDRON, A.J., PATTON, F.D. and CORDING, E.J. (1966) Design of surface and near surface construction in rock. Failure and Breakage of Rock. 8th Symp. on Rock Mech., Univ. of Minnesota, p. 237-302.

HVORATH, R.G. (1978) Field load test data on concrete-to-rock 'bond' strength for drilled pier foundations. Univ. of Toronto, Dept. of Civ. Eng. Publ. No. 78-07.

KRAHN, J. and MORGENSTERN, N.R. (1979) The ultimate resistance of rock discontinuities. Int. Jnl. Rock Mech. Min. Sci., Vol. 16, No. 2 pp. 127-133.

LADANYI, B. and ARCHAMBAULT, G. (1970) Simulation of shear behaviour of a jointed rock mass. Proc. 11th Symp. on Rock Mech. Amer. Inst. Min. and Metallurgy. pp. 105-125.

MEYERS, N.D. (1962) Characterization of surface roughness. Wear. pp. 182-189.

NEVILLE, A.M. (1973) Properties of Concrete John Wiley and Sons. New York. p. 332.

PATTON, (1966) Multiple modes of shear failure in rock. Proc. 1st Inst. Congr. ISRM, Lisbon, p. 509.

PELLS, P.J.N. (1979) Investigation into the allowable loadings for bored piles founded on Hawkesbury Sandstone. Prog. Report No. 3. Univ. of Sydney, Dept. Civ. Eng. Investigation Report No. S243.

ROSENBERG, P. and JOURNEAUX, N.L. (1976) Friction and end bearing tests on bedrock for high capacity socket design. Can. Geotech. Jnl. Vol. 13, pp. 324-333.

WILLIAMS, A.F., JOHNSTON, I.W. and DONALD, I.B. (1980a) The design of piles socketed into weak rock. Proc. Int. Conf. on Structural Foundations on Rock, Sydney. Balkema, Netherlands.

WILLIAMS, A.F., DONALD, I.B. and CHIU, H.K. ((1980b) Stress distributions in rock socketed piles. Proc. Int. Conf. on Structural Foundations on Rock, Sydney. Balkema, Netherlands.

ZIENKIEWICZ, O.C.(1971) The finite element method in engineering science. McGraw-Hill, London. Chapter 5.

Comparisons between Theoretical and Observed Behaviour of Pile Foundations

H. G. POULOS
Reader in Civil Engineering, University of Sydney

SUMMARY The paper describes a number of case studies in which the deformation behaviour of single piles or pile groups has been calculated theoretically and compared with the observed behaviour. The cases include: (a) the settlement of two grout-injected test piles in sand, for which "Class A" (before the event) predictions were made, (b) the settlement of steel pipe piles and step-taper piles in a soil profile consisting of clay overlying dense sand, (c) the lateral response of two test piles, the predictions being based on pressuremeter data, (d) the lateral load-deflection behaviour of pile groups tested in Rumania, (e) the settlement of a large office block founded on rock-socketted piles. In the last two cases, the results of tests on single piles have been used to predict group behaviour. The theoretical approach used for the calculations is based on elastic theory and is outlined briefly in the paper. The selection of the required soil parameters is also discussed. It is concluded that the theory used can give quite acceptable estimates of pile performance, particularly if used in conjunction with test pile data.

1 INTRODUCTION

The past decade has seen considerable advances in the development of theoretical methods for predicting the behaviour of single piles and pile groups subjected to axial and lateral loads. Several techniques have been employed, ranging from simplified closed form solutions (Randolph and Wroth, 1978) and boundary element methods of varying degrees of complexity (e.g. Poulos and Davis, 1968); Mattes and Poulos, 1969; Butterfield and Banerjee, 1971; Poulos, 1971; Banerjee, 1978) to finite element analyses (e. g. Ellison et al, 1971; Desai, 1974; Valliappan et al, 1974; Balaam et al, 1975). A number of comparisons have been made between the theoretical and observed behaviour of piles (Poulos, 1974; Butterfield and Ghosh, 1977; Banerjee and Davies, 1979) and these have generally demonstrated the applicability of the theory to both model and full-scale piles. Nevertheless, further comparisons are desirable in order to gain a better appreciation of the capabilities and limitations of the theoretical approaches, and also to gain further experience in selecting soil parameters to use with the theory.

The present paper describes six case studies of comparisons between theoretical and observed behaviour of single piles and pile groups. In all cases, the theoretical behaviour has been derived from an analysis which employs elastic theory but allows for non-linear behaviour at the pile-soil interface. A brief review of the theory is given and then each case is described in detail, with particular attention being paid to the method of selection of the requisite soil parameters. Two of the cases involve "Class A" predictions, in the terminology of Lambe (1973) i.e. made before the measurements were taken, while the remainder involve "Class C" predictions, made after the test results were known.

2 BRIEF REVIEW OF THEORY

2.1 Single Piles

The analyses used in this paper are all derived from the theory of elasticity, using a simplified form of the boundary element method. The analysis of a single axially loaded pile using this approach has been described by Poulos (1977) and involves the discretization of the pile into a series of shaft and base elements, each acted upon by an unknown pile-soil interaction stress. An expression for the axial deflection of each element of the pile can be written in terms of these interaction stresses by assuming the pile to deform as an axially loaded cylinder. A corresponding expression for the axial deflection of the soil adjacent to each element can be obtained by integration of the appropriate Mindlin elastic equation for vertical subsurface loading. The expressions for soil and pile deflections can be equated and solved to give the distribution of interaction stress, and hence deflection, along the pile. To allow for the possibility of pile-soil slip, limiting values of the interaction stress can be specified at each element. An interative analysis may then be performed to evaluate the load-settlement behaviour of the pile to failure. By introducing simplifying assumptions, it is also possible to consider, with reasonable accuracy, piles in non-homogeneous soils (Poulos, 1979a).

Single laterally loaded piles may be treated in a similar fashion. The pile is idealized as a thin beam, with the horizontal pile deflections being evaluated from beam bending theory and the soil deflections from integration of the Mindlin elastic equation for horizontal subsurface loading (Poulos, 1971). Again, by specifying limiting values of lateral pile-soil interaction stresses at each element, non-linearity of the lateral response of the pile can be reproduced.

For hand calculations, parametric solutions have been presented for the settlement and lateral deflection of a single pile (Poulos and Davis, 1980). For more detailed computations and cases not readily covered by these parametric solutions, computer programs have been developed (TAPILE for axial analysis, PULL for lateral analysis).

2.2 Pile Groups

For pile groups subjected to axial loading, a simplified analysis has been developed which involves the superposition of "interaction factors" for two piles (Poulos, 1968). These interaction factors

represent the relative increase in displacement of a pile due to an identical loaded pile, and depend on pile spacing, geometry and stiffness relative to the soil. This analysis enables a solution to be obtained for the distribution of load and settlement within a group of piles and provides a theoretical relationship between the group settlement and the settlement of an isolated single pile. Such an approach is very useful from a practical point of view in that it enables the results of a load test on a single pile to be used to predict the behaviour of a pile group.

A similar approach has been developed for laterally loaded pile groups except that consideration needs to be given to interaction factors for both pile head deflection and rotation due to lateral load and moment. Furthermore, depending on the head conditions imposed by the pile cap, it may be necessary to consider both the lateral and axial response of the piles.

While it is possible to obtain parametric solutions for the axial and lateral behaviour of pile groups, the range of variables which can be covered is necessarily limited, and hence more frequent resort must be made to a computer analysis than is the case for single piles. A program called DEFPIG has been developed for this purpose.

2.3 Soil Parameters

The major problem in the application of the above theories (or indeed any theory) to practice, is the selection of appropriate soil parameters. It has been found that conventional laboratory tests are of little direct value for predicting pile performance. While in-situ tests may provide a more reasonable basis for parameter selection, their utility still remains to be fully investigated. The most reliable means of making predictions is considered to be to interpret the results of a load test on a single pile in terms of the theory, and then to use the values of soil modulus and limiting pile-soil stress so derived to predict the behaviour of the prototype piles or pile groups. In the absence of pile test results, a number of empirical correlations have been developed for preliminary estimates of piles in clay or sand. For clay, these correlations relate the soil modulus to undrained cohesion while for sand, the soil modulus is related approximately to the relative density of the soil (Poulos, 1974). Values of limiting skin adhesion and lateral pile-soil pressure can be estimated from conventional theories of ultimate pile resistance.

3 SETTLEMENT OF GROUT-INJECTED PILE AT SURFERS PARADISE, QUEENSLAND

In 1977, a load test was performed on a grout-injected pile in Surfer's Paradise, Queensland, at the site of a new residential development. The details of the pile and the subsoil profile are summarized in Fig.1. Prior to the load rest results being revealed, a "Class A" prediction was made of the load-settlement behaviour of the pile. The only quantitative information on the subsoil properties consisted of SPT values, and on the basis of these values, the soil profile was classified as being very dense sand. Based on the suggestions of the SAA Piling Code (1978), a constant soil modulus of 100 MPa was assumed, while the corresponding distribution of ultimate skin friction is shown in Fig.1. The ultimate base resistance was calculated using a value of the bearing capacity factor, N_q, of 180. The load-settlement prediction was made using the program TAPILE.

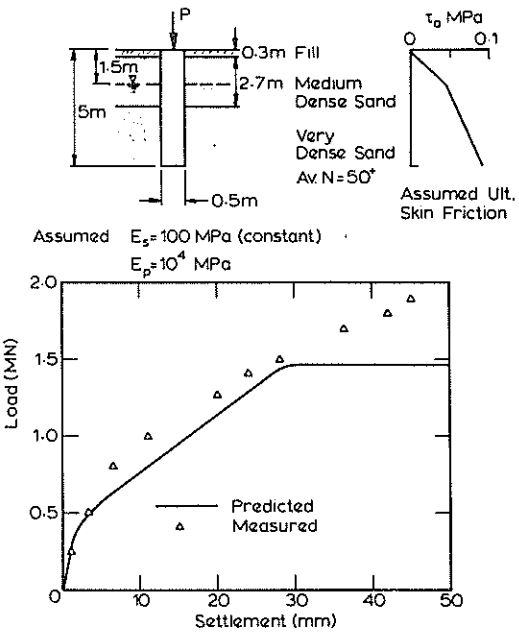

Figure 1 Predicted and measured settlements of grouted pile-Surfer's Paradise

The predicted load-settlement curve is shown in Fig. 1 together with the measured curve. The agreement is good up to a load of about 500 kN (the working load on the pile was to be about 550 kN). Beyond 500 kN load, the theory overestimates the settlement somewhat and predicts that full shaft slip occurs and that any additional load is carried by the base. The predicted ultimate load was 1460 kN whereas the actual pile carried a load of 2300 kN with a settlement in excess of 80 mm. Even if the failure load is defined as that to cause a settlement of 10% of the base diameter, it would be found to be about 2000 kN, still considerably in excess of the predicted value. The difference is believed to result primarily from an underestimate of the base bearing capacity, as the average soil modulus and ultimate skin friction values appear to have been chosen with reasonable (if fortuitous) accuracy.

Nevertheless, it may be said that, for a "Class A" prediction, based on very limited soil data, the theory provided excellent agreement with the measured behaviour up to and beyond the proposed working load.

4 SETTLEMENT OF TEST PILE IN HAMILTON, N.S.W.

In November, 1978, a load test was carried out on an instrumented grout-injected test pile in Hamilton, N.S.W. The soil profile consisted of layers of clay and sand to 6 m depth overlying an 8 m thick sandy clay layer which was in turn underlain by very stiff shaley clay (see Fig.2). The pile was 12 m long, 0.45 m diameter, and was reinforced with a helical spiral steel cage 11.8 m long. It also contained a central pipe to which resistance wire strain gauges were cemented at nine locations in order to deduce the load distribution along the shaft.

Prior to the load test, a "Class A" prediction was made of the load-settlement curve to failure and the load distribution in the pile at various load levels. Load-settlement predictions were made both by using a hand calculation procedure proposed by Poulos (1972), and also by use of the program

TAPILE. The latter program also produced the load distribution along the pile shaft. From the average value of undrained cohesion deduced from the cone

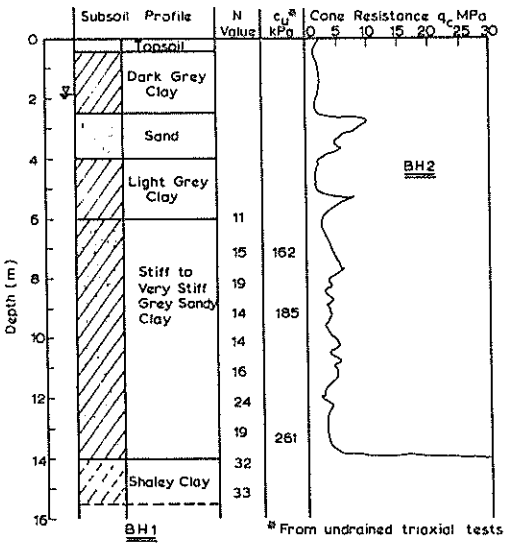

Figure 2 Geotechnical data for Hamilton site

resistance data (taking c_u=cone resistance/15), a constant soil modulus E_s of 70 MPa was selected for the hand calculations, based on the correlations of Poulos (1972). For the computer predictions, a value of E_s varying linearly with depth along the shaft from 40 MPa to 80 MPa was chosen. The ultimate skin friction τ_a was estimated on a total stress basis from the deduced c_u values, and was taken to be 40 kPa to a depth of 6 m, increasing linearly to 65 kPa at pile tip level. For the ultimate base resistance, a value of 9 c_u(=1660 kPa) was taken. The pile itself was assumed to have a Young's modulus of 21 GPa.

Fig.3a compares the predicted and measured load-settlement curves. The latter were corrected to exclude time-dependent movements during a period of maintained loading and load removal at a load of 380 kN. The measured settlements are in remarkably good agreement with both the hand and computer predictions up to a load of about 600 kN (the design working load for this pile was 390 kN). At larger loads, the measured settlements significantly exceed the predicted values, and it is obvious that the actual failure load was significantly less than the predicted value of 1055 kN. Both the ultimate skin and base resistances appear to have been overestimated in this case.

Fig.3b compares the measured and predicted axial load distributions at loads of 300 kN and 800 kN. The agreement is quite good for both cases, except that the actual load in the pile near the lower part of the pile is greater than predicted, suggesting that perhaps the soil beneath the pile tip may have been somewhat stiffer than assumed. It is interesting to note that, prior to the application of the test loads, the strain gauge readings indicated considerable tensile strains in the pile, due possibly to the swell of the grout during curing or the expansion of the grout due to the development of high temperatures during initial curing.

In summary, the settlement behaviour up to working load has been quite well-predicted, as in the case of the Surfer's Paradise pile. However, the ultimate load prediction has again been far from accurate; this finding is rather surprising, as it is often considered that ultimate pile loads can be more accurately predicted than pile settlement.

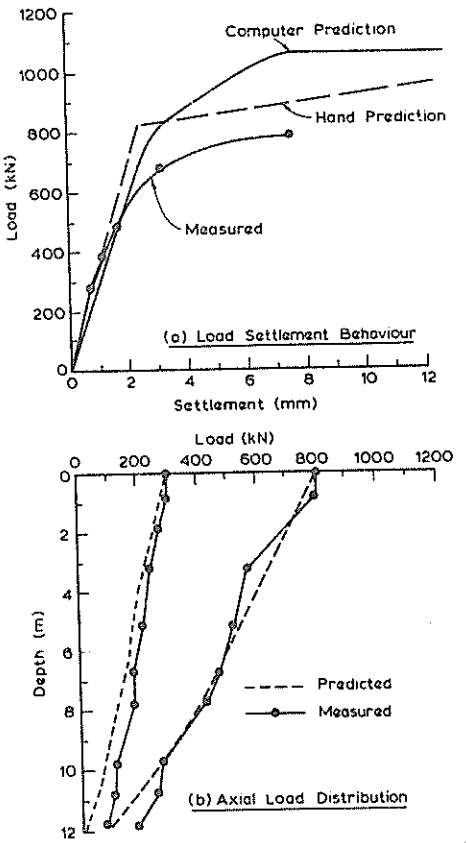

Figure 3 Measurement vs prediction-Hamilton test pile

5 TESTS OF SULLIVAN (1973)

Sullivan (1973) reported the results of load tests on four piles, (two steel pipe piles and two step-taper piles) in a soil profile consisting of stiff clays and silty clays overlying dense fine sand overlying further stiff clay. Fig.4 shows the profile and the available geotechnical data. "Class C" (after the event) predictions of the load-settlement behaviour of the four piles during maintained loading tests were made in two ways:

(i) using soil parameters selected on the basis of available soil information at this side and previously-developed empirical correlations;

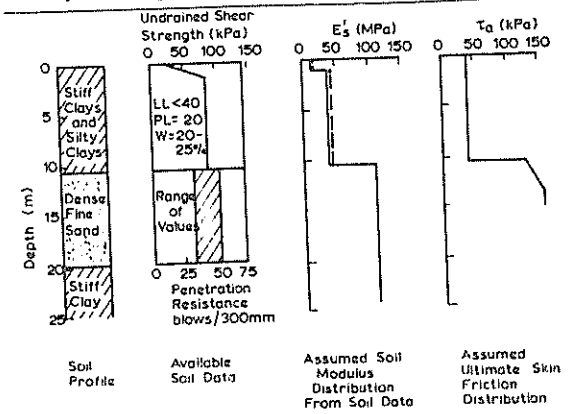

Figure 4 Soil conditions and parameters for tests of Sullivan (1973)

(ii) using soil parameters backfigured from the results of the load tests on one of the steel pipe piles (Pile 1).

For method (i), empirical relationships between drained soil modulus E'_s and c_u were used for the clay while E'_s for the sand was taken as 110 MPa. For both soils, the drained Poisson's ratio ν'_s was taken as 0.35. In the clay, the ultimate skin friction was taken as 43 kPa, and in the sand, τ_a was calculated on an effective stress basis as $F\sigma_v'$, where σ_v'=vertical effective stress and F was taken as 1.0 because of the dense nature of the sand. Based on the SAA Piling Code (1978), τ_a was assumed to reach a limiting value at a penetration of 8 diameters into the sand. Fig.4 shows the distributions of E'_s and τ_a thus determined. The ultimate base resistance P_{bu} was also calculated on an effecitve stress basis as $N_q.\sigma_v'$, with N_q=100, and σ_v' assumed to reach a limiting value at a penetration of 8 diameters in the sand.

For method (ii), the measured settlement of Pile 1 was fitted to elastic theory at a load of 670 kN to determine an equivalent average drained modulus of the soil profile. The resulting value of E'_s was 61 MPa.

Having derived the required input parameters, the program TAPILE was then used to predict the load-settlement behaviour of the four test piles. Fig.5 shows the curves thus obtained, together with the measured curves. The following observations may be made: (i) The predicted load-settlement curves from both methods are in reasonably close agreement. (ii) The predicted settlements are in fair agreement with the measured values for Piles 1 and 3, but are more than the measured values for Piles 2 and 4. The reason for the somewhat stiffer measured behaviour of Piles 2 and 4 is not clear, as quick-loading tests carried out on the piles after completion of the maintained loading tests indicated that the settlement of all four piles at working loads was quite similar. This finding is in agreement with the theoretical predictions.

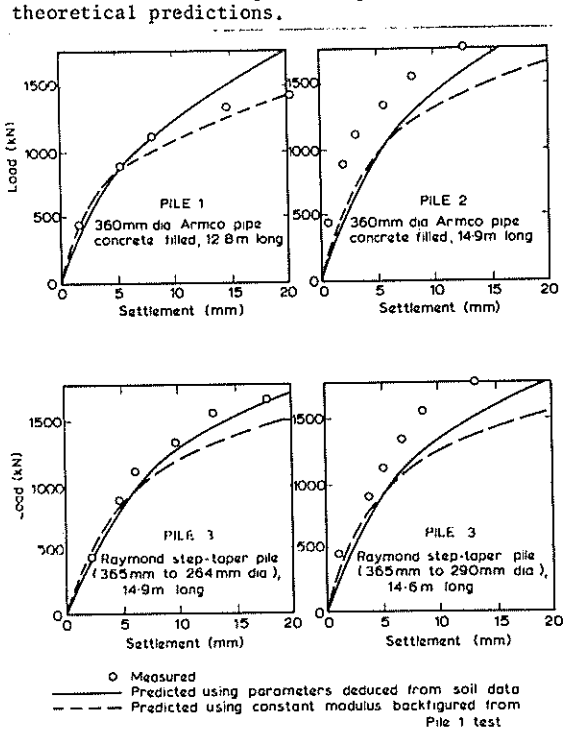

Figure 5 Comparison between measured and predicted load-settlement curves tests of Sullivan (1973)

(iii) The calculated ultimate load capacities are in generally good agreement with the values indicated from the load tests.

Piles 1 and 3 were each instrumented with "tell-tales", thus enabling the axial load distribution to be determined. Fig.6 shows comparisons between these measured distributions and those calculated from the TAPILE analysis, for a working load level of 530 kN. Bearing in mind the limited accuracy of the measured distributions because of the small number of tell-tales, the agreement with the theoretical load distributions is reasonable.

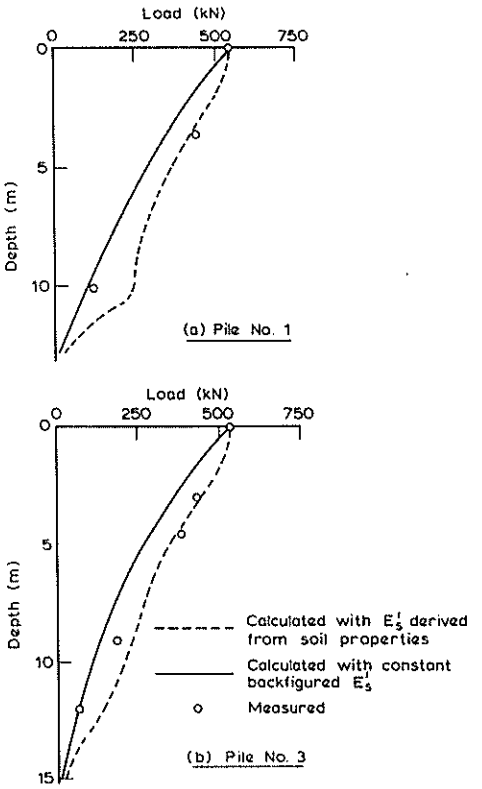

Figure 6 Measured vs predicted load distributions tests of Sullivan (1973)

This case study indicates that the theory can give reasonable, if somewhat conservative, predictions of load-settlement behaviour of both uniform diameter and step-taper piles, using a common set of soil data. The usefulness of the previously-derived empirical correlations of soil modulus is again demonstrated. As with the two previous case studies, the predicted settlements at loads well towards the ultimate become inaccurate, but from a practical viewpoint, such a deficiency in the theory is not significant.

6 TESTS OF FRYDMAN ET AL (1975)

Frydman et al (1975) have reported the results of lateral load tests on two prestressed concrete piles driven through highly plastic clay into fine dense sand in the Haifa Bay area of Israel. Fig.7 shows the soil profile, together with geotechnical data obtained from SPT, vane and Menard pressuremeter tests. One of the piles (Pile A) was instrumented with a slope indicator casing along its length, and in order to minimize its head rotation, had its upper part encased in a rigid concrete block supported on knife edge supports resting on the ground

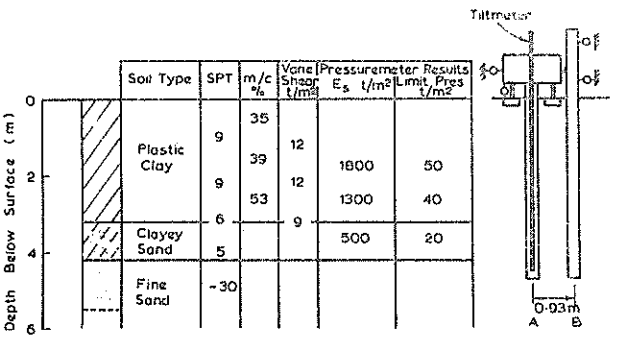

Figure 7 Soil profile and test pile arrangement (Frydman et al, 1975)

surface. The other pile (Pile B) was free-standing and had dial gauges at two points above the ground surface in order to measure both deflection and rotation (see Fig.7). Loading was applied by means of a jack acting between the piles.

In calculating the theoretical behaviour of the piles, it was decided to attempt to use the Menard pressuremeter tests directly to obtain the soil modulus E_s and the lateral pile-soil yield pressure P_y. E_s was taken to be the value determined directly from the pressuremeter results and reported in the paper. P_y was taken to be $c_u.N_c$, where c_u was determined as the pressuremeter limit pressure divided by 5.5, and N_c varied between 2 at the ground surface to 9 at a depth greater than or equal to 4 diameters. For Pile A, the presence of the concrete block caused some difficulty in the choice of an appropriate head condition in the analysis. It was felt that the concrete block, while reducing head rotation, would not compietely eliminate it, and it was therefore decided to assume that the block carried the moment load, while the shear was taken by the pile itself.

Two sets of calculations were carried out: (i) assuming Piles A and B are isolated and do not influence each other; the program PULL was used for this calculation, (ii) assuming Piles A and B interact; the program DEPPIG was used and the piles analyzed as a two-pile group, Pile A being subjected to shear only and Pile B to both shear and moment.

Fig.8 compares the theoretical and measured load-deflection curves for Pile A at the ground line. As would be expected, the theoretical curve allowing for interaction gives smaller deflections and rotations than if the piles are assumed isolated. The effect of interaction on rotation is less than on deflection. For loads up to about 60 kN, the agreement between both the theoretical curves and the measurements is quite good, but at larger loads, the measured values are larger than the theoretical values. Fig.9 compares theoretical and measured deflection profiles along Pile A at two different load levels. At the lower load of 43 kN, excellent agreement is found between the measurements and the theoretical curve including interaction effects. However at the higher load, the agreement is not as good, particularly near the surface. Whether this discrepancy is due to the assumed parameters or the pile head condition changing as the load increases, cannot be stated with certainty, although the latter appears to be more likely in view of the good agreement at lower load levels.

Detailed measurements were not reported for Pile B, but at a load of 43 kN, the measured deflection of Pile B 470 mm above the groundline was 4.1 mm. The

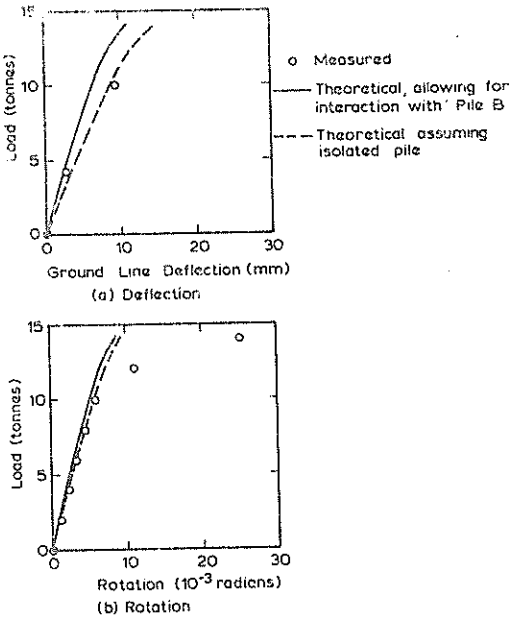

Figure 8 Comparison between theoretical and observed behaviour of Pile A (Frydman et al, 1975)

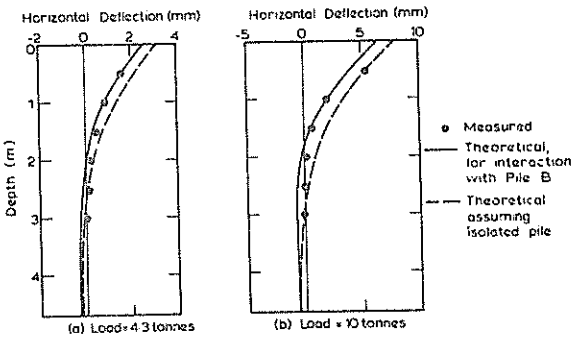

Figure 9 Comparison between theoretical and observed deflection profiles for Pile A (Frydman et al; 1975)

calculated deflection, assuming Pile B to be an isolated pile, was 6.3 mm; taking interaction into account gave a deflection of 5.8 mm, which is in slightly better agreement with the measurements.

This case study therefore suggests that the results of pressuremeter tests may be applicable to the prediction of lateral pile performance, although more case studies would be required in order to gain confidence in this application. In addition, it illustrates the importance of considering the interaction between two test piles jacked apart.

7 PILE TESTS IN RUMANIA (Manoliu et al, 1977)

Manoliu et al (1977) have presented the results of a program of field tests in Rumania on single piles and pile groups subjected to both axial and lateral loading. The subsoil profile at the site is shown in Fig.10a. Six single piles were tested, two under axial load, and four under lateral loading. The piles were of reinforced concrete, 17 m long (embedded length 16 m), and generally of 0.4 m square cross-section, although some were of rectangular section (0.35 m by 0.45 m). Five different groups were subjected to lateral loading, three groups of two vertical piles, one group of two battered piles, and

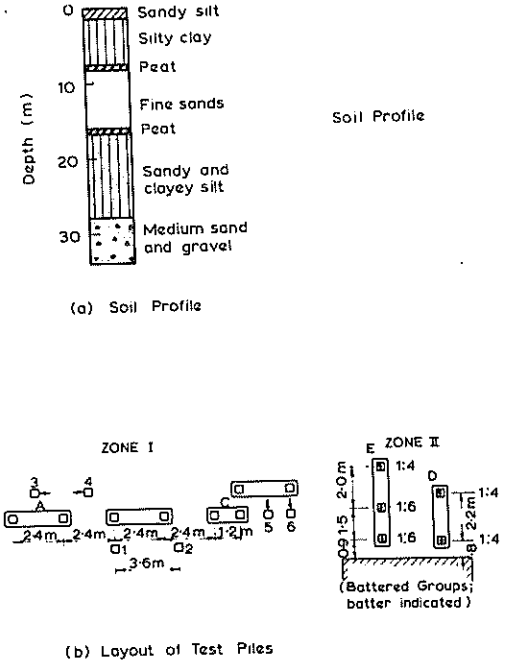

Figure 10 Tests of Manoliu et al (1977)

one group of three battered piles, as shown in Fig. 10b. The published data thus provided a good opportunity for the "Class C" prediction of the load-deflection behaviour of the pile groups, using the single pile behaviour in conjunction with the theoretical analysis of pile group response.

The first step in the prediction process was to attempt to backfigure the average soil modulus and limiting pile-soil stress values for axial loading by fitting the theoretical solutions to the measured load-settlement curves. This involved a trial and error process using the program TAPILE. Fig.11a compares the best-fit theoretical load-settlement curve and the two measured curves, and indicates the parameters used for the fit. Both the soil modulus, E_{sv}, and limiting skin friction τ_a, were assumed constant with depth. While a reasonable fit is obtained at relatively low load levels, the theoretical curve shows too stiff a response at higher loads. This is a previously-observed characteristic of analyses with constant E_{sv} and τ_a, and a better fit could have been obtained by altering the distributions of these parameters. However, the discrepancy should not lead to serious inaccuracy in group deflection response predictions until relatively high load levels are reached.

The second step was to backfigure the average lateral soil modulus, E_{sh}, and limiting lateral pile-soil pressure p_y by a similar process of trial and error, using the program PULL 2B to generate the theoretical curves. Figs.11b and c show the fit obtained between the theory and the four measured curves, using constant values of E_{sh} of 35 MPa and p_y of 0.2 MPa. In the light of the variability of the measured results, the fit obtained is quite reasonable. It is interesting to note that the backfigured modulus value for lateral loading, E_{sh}, is one-half of the value for axial loading, E_{sv}. This difference is probably attributable largely to the effects of pile-soil separation at the back of the laterally loaded pile.

The first step in the prediction procedure was to use the backfigured parameters from the single pile tests to predict the entire lateral load versus

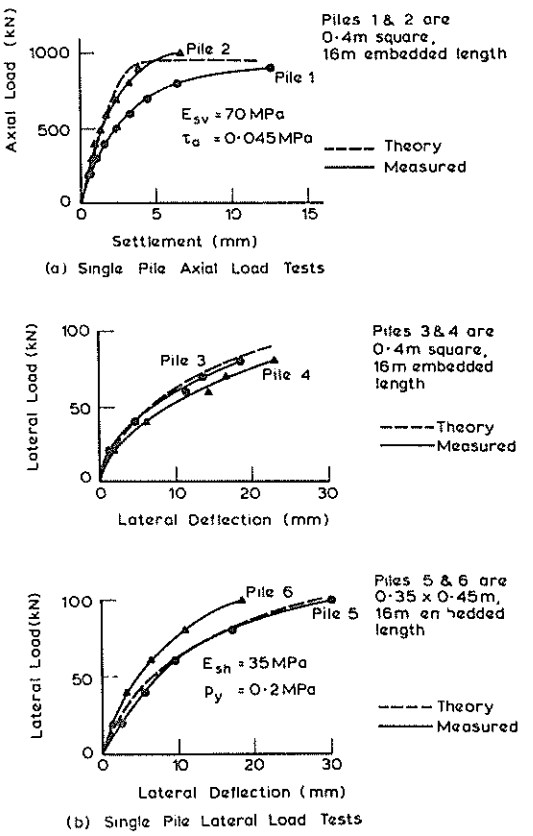

Figure 11 Single pile tests

deflection behaviour of the pile groups, using the program DEPPIG. This necessitated the estimation of the lateral efficiency factor η_L by which the value of p_y was reduced to allow fro group effects. Based on a small amount of previous data and experience, values of 0.85, 0.6, 0.9 and 0.7 were chosen for Groups A, C, D and E respectively.

Fig.12 shows the predicted and measured load-deflection curves for the above four groups. The agreement for the two groups with vertical piles (Groups A and C) is very good over the entire load range. For the groups containing battered piles (Groups D and E), the agreement is less satisfactory; the theory overpredicts deflections at lower load levels and underpredicts at higher load levels. Nevertheless, the agreement is not unreasonable, bearing in mind the possibility of some variation in soil conditions from Zone II, where these groups are located, to Zone I, where the single test piles were located.

In summary, this case suggests that the philosophy of using the single pile tests to evaluate the pile-soil parameters and then using the theory to predict group response, is basically sound.

8 COVENTRY POINT OFFICE BLOCK (Cole and Stroud, 1977)

Cole and Stroud (1977) have described some aspects of the foundation design of a medium rise office development, Coventry Point, in the city of Coventry, U.K. The development consists of two inter-linked office blocks of fifteen storeys (Block A) and sixteen storeys (Block B) which have been supported on groups of rock-socketted piles. The subsoil profile consists of up to 5 m of fill and firm silty sandy clay overlying siltstones and sandstones of varying strength, interbedded with extensively-weathered

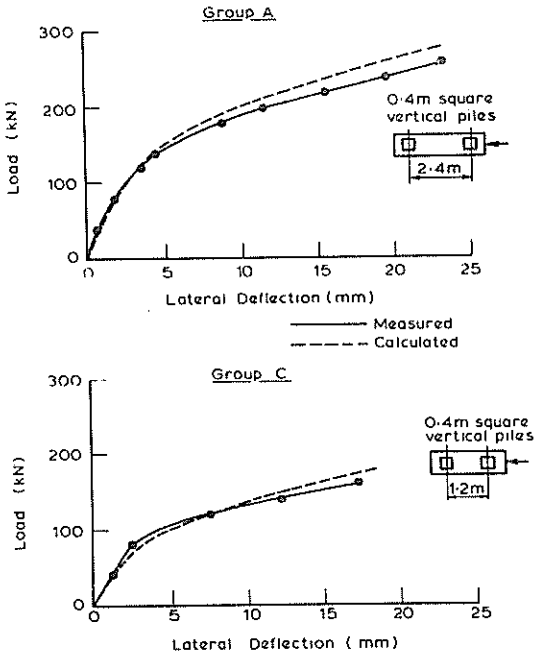

Figure 12 Comparisons between measured and theoretical group behaviour

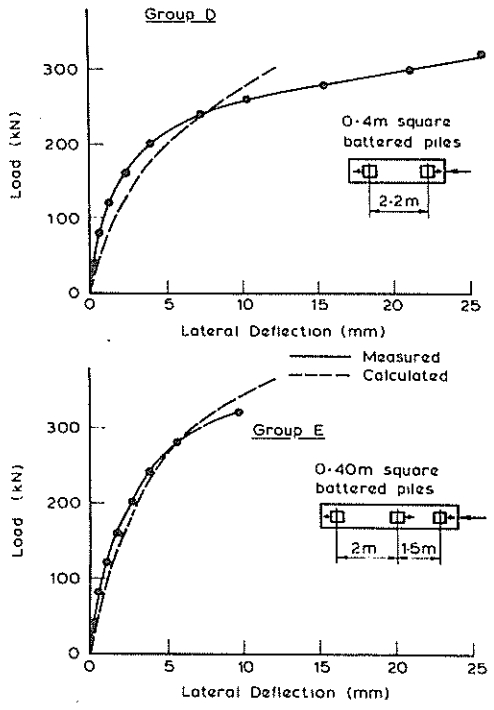

Figure 12cont'd. Comparisons between measured and theoretical group behaviour

bands of mudstone (Fig.13a). Typically, SPT values in the upper layer ranged between 10 and 50, whereas below 5 m, values between 100 and 400 (with occasional larger values) were experienced. To aid the foundation design, a contract pile, 1.06 m diameter and approximately 8.5 m long, was test loaded. This pile settled 12 mm under the design load of 4.5 kN.

In order to assess the applicability of pile settlement theory to this case, the above test pile data was interpreted to obtain modulus values for the

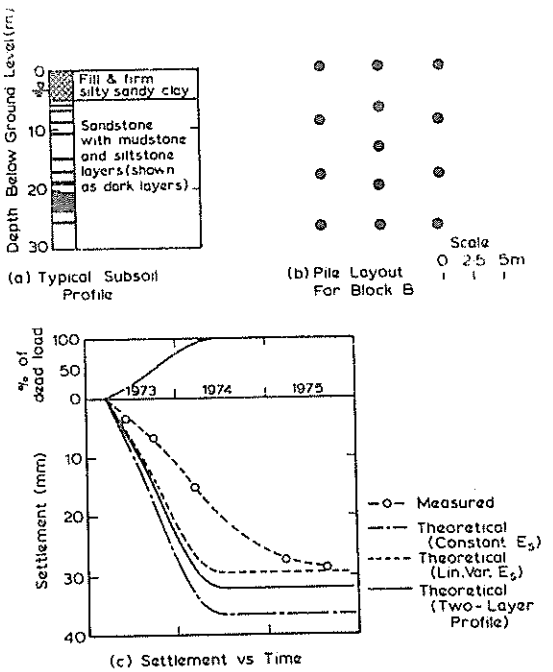

Figure 13 Comparison between observed and theoretical settlement - Coventry Point Block B (Cole & Stroud, 1977)

subsoil profile, and a group settlement analysis was then performed for Block B. Three different assumptions were used in interpreting the test pile results: (a) a constant modulus E_s with depth, (b) a linearly increasing modulus with depth, (c) a two-layer profile, with the upper 5 m having a modulus one-fifth of the value for the underlying material (this assumptions was based on the SPT results).

In each case, the program TAPILE was used to develop relationships between the pile head settlement and modulus, from which the modulus to give a 12 mm settlement was determined. The following values were obtained for the three assumptions listed:

(a) E_s = 51.3 MPa
(b) E_s at 8.5 m depth = 78.1 MPa
(c) E_s (0-5 m) = 12.6 MPa
E_s (5 m$^+$) = 63 MPa.

The program DEPPIG was then used to compute the settlement of Block B, which was founded primarily on 13 piles, 1.22 m diameter, and penetrating to 8 m below the ground surface (Fig.13b). A rigid pile cap was assumed, and based on the available information, a dead load of 65.5 MN was assumed to act on the foundation. Table 1 compares the three predicted settlements with the measured settlement approximately 18 months after completion of construction. Good agreement is found with the values from assumptions (b) and (c). The settlement predicted on the assumption (a) of a constant modulus is too large, as a result of the larger settlement interaction factors which occur in this case (Fig.14).

A closer examination of the rate of settlement during and after construction reveals that the actual settlement developed more slowly than given by the theory if the settlements are assumed to occur instantaneously upon application of the load (Fig. 13c). This slower development of settlement and the continued increase after completion of construction are probably a consequence of consolidation of the

interbedded mudstone and siltstone layer beneath the pile tips.

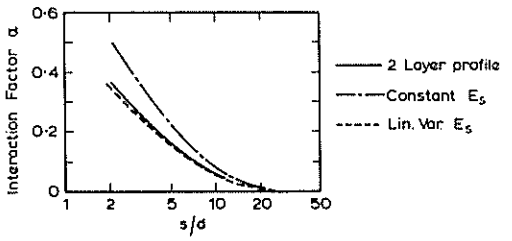

Figure 14 Comparison between theoretical interaction factors from various assumptions

Two interesting points thus emerge from this case study: (a) the theory appears to provide a useful link between the settlement of a single pile and a pile group, provided that a judicious assumption is made regarding the distribution of modulus with depth, (b) the time-dependence of settlement is more pronounced with pile groups than with single piles, as predicted theoretically by Poulos (1968). However, practical solutions for the rate of settlement of pile groups have not yet been published; moreover, in this case, the interbedded nature of the soil profile would make accurate prediction of time-settlement behaviour difficult.

TABLE 1

COMPARISON BETWEEN MEASURED AND THEORETICAL SETTLEMENTS. COVENTRY CENTRE - BLOCK B

Method	Settlement mm
Calculated for Constant E_s	36.5
Calculated for Linearly Increasing E_s	29.3
Calculated for 2-Layer Profile E_s (0-5m) = 1/5 E_s ($5m^+$)	32.0
Measured, 1½ years After Completion of Construction	28.6

9 CONCLUSIONS

The case histories examined in this paper have involved single piles and pile groups subjected to axial or lateral loading, and a common theoretical approach has been applied to the prediction of the load-deflection behaviour in all cases. The requisite soil parameters have been estimated in a variety of ways, including empirical correlations based on previous experience, the interpretation of load test results, and the application of pressuremeter data. The agreement between the measured and theoretical behaviour has been found to be generally satisfactory, even for the two "Class A" predictions where the soil parameters were based on empirical correlations. For the pile groups, successful predictions of load-deflection behaviour have been made by using soil parameters backfigured from single pile load tests.

However, the predictions for battered pile groups appear to be less satisfactory than for groups of vertical piles, and there may be some scope for improving the theory for battered pile groups. In addition, it is desirable, when predicting group behaviour, to assume a reasonable distribution of soil modulus with depth, as the interaction factors may be overestimated if a homogeneous soil mass is assumed.

Provided that an appropriate measure of engineering judgment is employed, the elastic-based theory appears to provide a reasonable practical basis for predicting the performance of pile foundations subjected to axial or lateral loading.

10 ACKNOWLDEGMENTS

The work described in this paper forms part of a general programme of research into deformation of all types of foundation, under the general direction of E.H. Davis, Challis Professor and Head of the Department of Civil Engineering at the University of Sydney. This research is supported by a grant from the Australian Research Grants Committee. The author gratefully acknowledges the value of discussions with Mr. P.J.N. Pells, Senior Lecturer in Civil Engineering, who supervised the instrumentation of the tests on grout-injected piles, and the permission given by Mr. D.J. Douglas, Managing Director of Ground Test Australia Pty Ltd, to present the results of these load tests.

11 REFERENCES

BALAAM, N.P., POULOS, H.G. and BOOKER, J.R. (1975). "Finite element analysis of the effects of installation on pile load-settlement behaviour". Geot.Eng. Vol.6, No.1, pp.33-48.

BANERJEE, P.K. (1978). "Analysis of axially and laterally loaded pile groups". Ch.9 of Developments in Soil Mechanics, Ed. C.R. Scott, Appl. Science, U.K.

BANERJEE, P.K. and DAVIES, T.G. (1979). "Analysis of some reported case histories of laterally loaded pile groups". Proc. Conf. on Num. Methods in Offshore Piling, I.C.E. London, pp.83-90.

BUTTERFIELD, R. and BANERJEE, P.K. (1971). "Elastic analysis of compressible piles and pile groups". Geotechnique, Vol.21, No.1, pp.43-60.

BUTTERFIELD, R. and GHOSH, N. (1979). "The use of a numerical analysis to correlate soil shear moduli determined from model tests on single piles and groups of piles in clay". Proc. Conf. on Num. Methods in Offshore Piling, I.C.E. London.

COLE, K.W. and STROUD, M.A. (1977). "Rock socket piles at Coventry Point, Market Way, Coventry". Piles in Weak Rock, I.C.E., London, pp.47-62.

DESAI, C.S. (1974). "Numerical design-analysis for piles in sands". Jnl. Geot. Eng. Divn. ASCE, Vol. 100, No.GT6, pp.613-635.

ELLISON, R.D., D'APPOLONIA, E. and THIERS, G.R. (1971). "Load-deformation mechanism for bored piles". Jnl. Soil Mechs. Fndns Divn, ASCE, Vol.97, No.SM4, pp.661-678.

FRYDMAN, S., SHA'AL, B. and MAZURIK, A. (1975). "Analysis of an instrumented laterally loaded pile". Proc. 5th Asian Reg. Conf. Soil Mechs. Fndn. Eng., Bangalore.

LAMBE, T.W. (1973). "Predictions in soil engineering". Geotechnique, Vol.23, pp.151-202.

MANOLIU, I., BOTEA, E. and CONSTANTINESCU, A. (1977). "Behaviour of pile foundations submitted to lateral loads". Proc. 9th Int. Conf. Soil Mechs. Foundn. Eng., Tokyo, Vol.1, pp.637-640.

MATTES, N.S. and POULOS, H.G. (1969). "Settlement of single compressible pile". Jnl. Soil Mechs. Divn., ASCE, Vol.95, No.SM1, pp.189-207.

POULOS, H.G. (1968). "Analysis of the settlement of pile groups". Geotechnique, Vol.18, No.4, pp.449-471.

POULOS, H.G. (1971). "Behaviour of laterally loaded piles: I - single piles". Jnl. Soil Mechs. Fndns. Divn., ASCE, Vol.97, No.SM5, pp.711-731.

POULOS, H.G. (1972). "Load-settlement prediction for piles and pier". Jnl. Soil Mechs. Fndns. Divn., ASCE, Vol.98, No.SM9, pp.879-897.

POULOS, H.G. (1974). "Some recent development in the theoretical analysis of pile behaviour". Ch.7 of Soil Mechanics - New Horizons, Ed. I.K. Lee, Newnes-Butterworths, London, pp.237-279.

POULOS, H.G. (1977). "Settlement of pile foundations". Ch.10 of Numerical Methods in Geotechnical Engineering, Ed. C.S. Desai and J.T. Christian, McGraw-Hill, New York.

POULOS, H.G. (1979a). "Settlement of single piles in non-homogeneous soil". Jnl. Geot. Eng. Divn., ASCE, Vol.105, No.GT5, pp.627-641.

POULOS, H.G. (1979b). "An approach for the analysis of offshore pile groups". Proc. Conf. on Num. Methods in Offshore Piling, I.C.E., London, pp.91-98.

POULOS, H.G. and DAVIS, E.H. (1968). "The settlement behaviour of single axially loaded incompressible piles and piers". Geotechnique, Vol.18, No.3, pp.351-371.

POULOS, H.G. and DAVIS, E.H. (1980). Pile foundation analysis and design. John Wiley and Sons, New York.

RANDOLPH, M.F. and WROTH, C.P. (1978). "Analysis of deformation of vertically loaded piles". Jnl. Geot. Eng. Divn., ASCE, Vol.104, No.GT12, pp.1465-1488.

SAA (1978). "SAA piling code AS2159-1978". Standards Association of Australia.

SULLIVAN, R.A. (1973). "Load tests of pipe and step-taper piles". Paper presented to ASCE, Texas Section Spring Meeting, Austin, Texas, April 5-7, 1973.

VALLIAPPAN, S., LEE, I.K. and BOONLUALOHR, P. (1974). "Settlement analysis of pile in layered soil". Proc. 7th Bien. Conf. Aust. Road Res. Bd., Adelaide, Vol.7, Pt.7, pp.144-153.

The Testing of Large Diameter Pile Rock Sockets with a Retrievable Test Rig

I. W. JOHNSTON
Lecturer, Department of Civil Engineering, Monash University
I. B. DONALD
Associate Professor, Department of Civil Engineering, Monash University
A. G. BENNET
Associate and Senior Geomechanics Engineer, John Connell-Mott, Hay & Anderson, Hatch, Jacobs
J. W. EDWARDS
Associate and Project Engineer, John Connell-Mott, Hay & Anderson, Hatch, Jacobs

SUMMARY This paper describes the design, construction and use of a retrievable test rig for evaluating the performance characteristics of large diameter pile rock sockets. The test rig is prefabricated at ground level, lowered into a contract socket, and concreted into position. Large flat jacks react against the base of the socket to force a concrete annulus, representing a section of the pile shaft, upwards eventually to failure. The side shear resistance characteristics to failure and the base resistance characteristics well in excess of design load may be determined. After testing, by use of special design features, the rig and concrete may be rapidly removed from the socket to allow the contract pile to be completed. The results of two such tests conducted in a contract socket of a major construction project in Melbourne are reported to demonstrate the effectiveness of the technique.

1 INTRODUCTION

The Rail Overpass from Flinders Street Station to Spencer Street Station of the Melbourne Underground Rail Loop Project included the construction of 105 bored piles of which 85 were to be socketed into the Silurian Mudstone underlying the poor quality near surface soils. These piles were generally of 1000 mm and 1250 mm nominal diameter to carry working loads of between about 3.5 MN and 6.0 MN. The depths to the upper surface of the mudstone varied from about 2 metres to 35 metres from ground level with socket lengths of between about 5 and 15 metres.

During December 1975, the Department of Civil Engineering at Monash University was approached by John Connell-Mott, Hay & Anderson, Hatch, Jacobs, Principal Consultants for the project and entered into discussions concerning the possibility of developing and conducting a limited test programme to verify the design adequacy of, and to provide further performance information on the pile sockets to be formed the following year.

However, from the inception of the test programme, it was recognised that a number of constraints had to be imposed on the development of the programme, the most important of which follow :-

(a) The tests should take place in one of the contract sockets at a considerable depth below ground level.

(b) The tests were to take place during the execution of the piling for the contract and therefore had to be designed to cause a minimum of interference to the contract.

(c) On completion of the test programme, the pile socket was to be restored and handed back to the contractor for completion as a contract pile.

(d) It was desirable to conduct the tests to well in excess of working loads, preferably to failure.

(e) Although a number of fully instrumented pile loading tests have been reported in the literature, it was the authors' opinion that information from such tests was subject to a variety of problems including interpretation, time delays, and instrument reliability. Therefore it was considered that the tests should be as definitive as possible.

2 PRINCIPLE OF TESTING TECHNIQUE

During the development stages, a great number of possible solutions were examined but the overriding constraint concerned the need to minimise delays to the contract. It became evident that the technique should involve the minimum possible operations in the socket to set up the test. This could be best achieved by prefabricating the test rig, including all loading devices away from the contract area. When the socket became available, the test rig could be located in the socket, the test conducted and the test rig immediately removed. The general principle of testing is illustrated in Figure 1.

A base plate was located immediately beneath three 920 mm diameter flat jacks, each of about 8600 kN capacity. The reaction frame, resting on top of the flat jacks had two purposes. Firstly it provided a space between the base of the socket and the socket wall test section so as to remove the likelihood of significant interaction effects. Secondly it provided a location for a large water pump which was considered necessary to remove the quantities of ground water likely to seep into the socket. Located on top of the reaction frame was the section of the test which was to be concreted against the socket wall to represent a section of pile shaft. However, had this cylinder of about 1250 mm diameter consisted of in-situ concrete, considerable difficulties in both time and effort would have been experienced in its removal after testing. Therefore, the technique adopted was to centrally locate an inverted truncated cone, or bucket, on top of the reaction frame. The bucket was made of thin steel plate into which concrete was cast with sufficient ducts to allow the passage of various hydraulic and pump connections.

At the base of the bucket was a 220 mm diameter flat jack of 400 kN capacity. The purpose of this flat jack was to release the bucket after testing from the thin concrete annulus cast around the bucket to form the side shear resistance section. Once the bucket was released, the thin concrete annulus

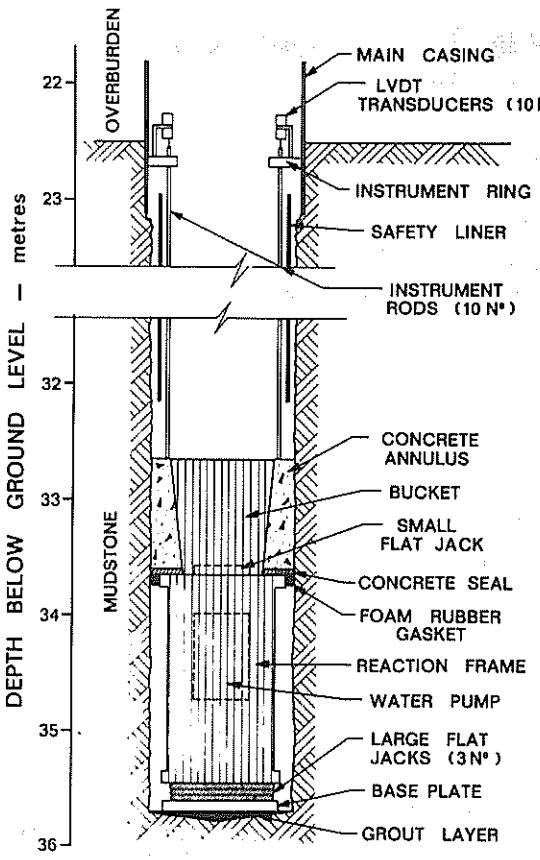

Figure 1 Diagrammatic principle of testing technique

could be easily broken out and removed to allow the remainder of the test rig to be lifted from the socket.

Since on inflating the large flat jacks it was difficult to ensure that both base and side shear resistance became fully mobilised, the dimensions of the side shear section were fixed at one metre length so that this section could be failed with the base pressure reaching about three times the design stress.

The vertical deflections at the base of the socket were to be measured at two diametral points. The deflections of the side shear section were measured at four points each at the bottom and top surfaces. It was considered that LVDT transducers suitably waterproofed could relay the measurements to the surface, but if they were attached to the rig itself, the socket wall or the safety liner, they would be susceptible to movement. The nearest rigid object was considered to be the main pile casing which was sealed into the top of the rock socket several metres above the test location. Therefore, the solution adopted consisted of transmitting the deflections from the ten points of measurement to the level of the bottom end of the pile casing by means of steel rods. These ten rods extended through the instrument ring which was rigidly bolted onto the pile casing. The transducers were mounted on the instrument ring. The instrument ring had a 800 mm internal diameter to allow the passage of a mancage for operations required in the socket itself.

Two tests were conducted in one socket; the first with the test rig located at the base of the socket and the second some four metres above the first location by making use of a four metre long concrete spacing column placed at the base of the socket.

Full details of the design and construction of the rig may be found in Johnston and Donald (1979).

3 TEST PROCEDURE

Site operations commenced with a "windowed" safety liner in the socket for a detailed inspection and sampling of the rock socket surface. A water pump was then removed to allow the placement of a thin bedding layer of grout at the base of the socket. The safety liner was removed and the test rig lowered to the base of the socket (Figure 2). This was followed by the lowering of a second shorter safety liner so that its lower end was about 0.5 metre above the test rig and was secured by slings to the top of the pile casing. Although there were no rock falls from the sides of the socket, the safety liners were used at all times.

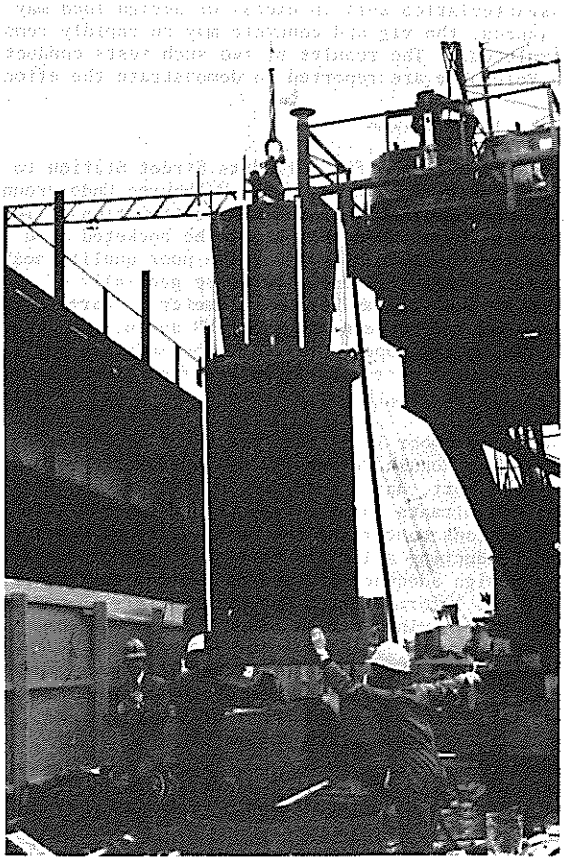

Figure 2 Lowering of test rig into the socket.

The top plate of the reaction frame was 1100 mm diameter and the socket was nominally 1250 mm diameter. This left a gap of approximately 75 mm which was plugged with strips of high density foam rubber. Immediately after placing this gasket, a 50 mm layer of rapid setting concrete was placed over the visible portion of the top plate of the reaction frame to complete the seal. Once set, the remainder of the concrete annulus was placed and vibrated. The instrument ring was then positioned, the instrument rods placed, the hydraulic connections made, and finally the transducers were installed and adjusted.

Once all these operations were completed, the mancage

and "down-hole" operator were lifted from the pile casing and the test loading was ready to commence. The pressurising equipment of electric and manual pumps, and the recording equipment consisting of digital data logger, chart recorders and pressure gauges were all located at the ground surface.

The test itself was conducted by pressurising the large flat jacks and recording the transducer outputs. The load was applied in increments, with some load cycling, until excessive creep movement in the side shear section occurred, making it impossible to maintain a constant pressure in the flat jacks.

Immediately after the test, the rig was removed from the socket by a reverse procedure to installation. The main variation concerned the removal of the concrete annulus. Once the instrumentation was removed, the small flat jack at the base of the bucket was inflated to release the bucket which was then lifted clear. The concrete annulus could then be broken out before lifting the rest of the rig from the socket.

The total duration of each test from initial inspection to final removal of the rig was 11 and 8 working days respectively for tests 1 and 2.

4 TEST RESULTS

Two tests were conducted in the socket of pile No. 7A, immediately south-east of the Flinders St - Spencer St. intersection. A much simplified geological profile at that location consisted of some fill, soft clays and silts overlying stiff and very stiff clays and silts to a depth of about 22.5 metres below ground level. Below this depth, the Silurian Mudstone was encountered and was generally found to be moderately weathered with clean tight jointing of about 60 mm spacing and a dip of approximately 80°.

Based on borehole data and on socket inspections, a general description of the test locations, classified according to the zone gradings defined by Neilson (1970) is as follows :-

(a) Base of the socket.
This was located at a depth of 35.7 metres and was immediately underlain by medium grey mudstone of Zone 3 weathering. At a depth of about 36.0 metres, the mudstone appeared to become more fractured increasing its weathering designation to Zone 2. At about 36.4 metres the mudstone appeared to be of Zone 1 until about 36.7 metres. At this depth the mudstone quality improved to Zone 3, becoming Zone 3-4 at about 36.9 metres to at least about 39.0 metres.

(b) Socket wall - Test 1.
The concrete test section was cast against the socket wall between depths of 32.7 and 33.7 metres. The rock at this location was generally a medium grey mudstone of Zone 4 weathering. There appeared to be insignificant softening of the socket wall during the period between the drilling process and immediately prior to casting the test annulus.

Samples recovered from this location yielded an average moisture content of 9.3%, which corresponded to a compressive strength (σ_1-σ_3) of about 5600 kPa for cores tested under a confining pressure of 690 kPa. Measurements of the roughness of the socket wall at this location indicated that the surface was undulating with asperity heights of between about 5 and 10 mm at wavelengths of about 100 mm.

(c) Socket wall - Test 2
The second test location was between 28.7 and 29.7 metres depth. The mudstone was generally dark grey and pyritic. Weathering was such that at 28.7 metres, the mudstone was of Zone 2, with a clay Zone 1 fault between 28.73 and 28.83 metres. Below this level, the mudstone was generally Zone 3 to 29.7 metres with a thin layer of Zone 2 mudstone between 29.31 and 29.56 metres. Samples recovered indicated an average moisture content of about 11.7% which corresponded to a confined compressive strength (σ_1-σ_3) of about 3600 kPa. The roughness of the socket at this location was similar to the location of test 1.

The average load-displacement curves for side shear resistance and for base resistance are shown in Figures 3 and 4 respectively.

5 DISCUSSION OF TEST RESULTS

5.1 Side shear resistance - Test 1.

Figure 3 shows that the initial portion of the load-displacement curve is very steep with negligible displacement at loads up to about 500 kN. The average displacement of the annulus at the design load of 785 kN (200 kPa) was about 0.3 mm, and at three times design load, it was about 2 mm. The socket section exhibited work strengthening behaviour without actually reaching a peak load at an average displacement of 12.5 mm. However the curve is relatively flat at displacements beyond about 10 mm, at which the load, 4144 kN, may be taken as the failure load. This load corresponds to a maximum side shear resistance of about 1050 kPa.

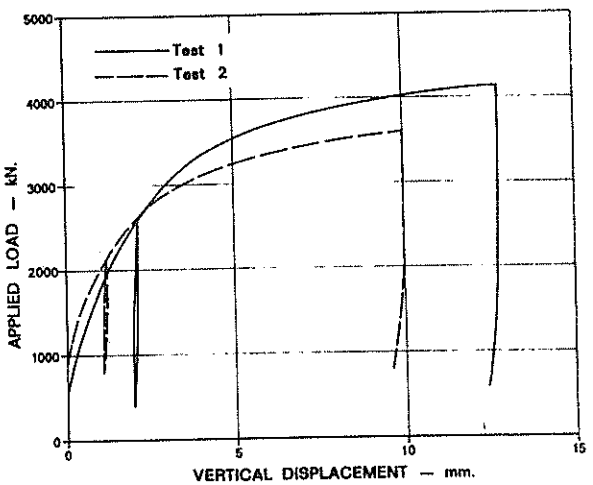

Figure 3 Side shear resistance load-displacement curves.

In conventional design, the saturated mudstone is treated as a $\phi = 0$ material giving an undrained "cohesion" of 2800 kPa. Therefore, the side shear resistance reduction factor, α_c, is given by:

$$\alpha_c = \frac{\text{shear stress at failure}}{\text{undrained "cohesion"}} = \frac{1050}{2800} = 0.37$$

5.2 Side shear resistance - Test 2

Figure 3 also shows that the average load-displacement curve for Test 2 is similar to Test 1, except that the initial behaviour is slightly stiffer. The displacement at the design load of 393 kN (100 kPa) was too small to be measured, and even at three times design load, it was only 0.4 mm. Using 10 mm

displacement as a criterion, the failure load for Test 2 was 3600 kN, equivalent to a side shear stress of 943 kPa. As before, the estimated undrained "cohesion" of the rock would be on average about 1800 kPa.

$$\therefore \quad \alpha_c = \frac{943}{1800} = 0.52$$

The unload-reload curves for both tests show very stiff behaviour and little hysteresis, and creep behaviour was insignificant at stress levels below failure. It can be concluded that a socket in this material would not exhibit work softening behaviour at acceptable levels of deformation, and that the component of deformation due to live load would decrease markedly after the first full loading.

5.3 Base resistance - Test 1

Figure 4 shows the average load-displacement curves for the base. However, for this component of the test the grout layer at the base of the socket did not achieve the desired rigidity. Consequently, this layer was relatively compressible and its decrease in thickness under load represented at least 70% of the total measured base displacement of 19.9 mm. The value of 70% was estimated from the indentation on a thin base tray (Figure 2), originally incorporated in the design as a protection against grout penetration of the flat jacks when the rig was to be seated initially on wet grout.

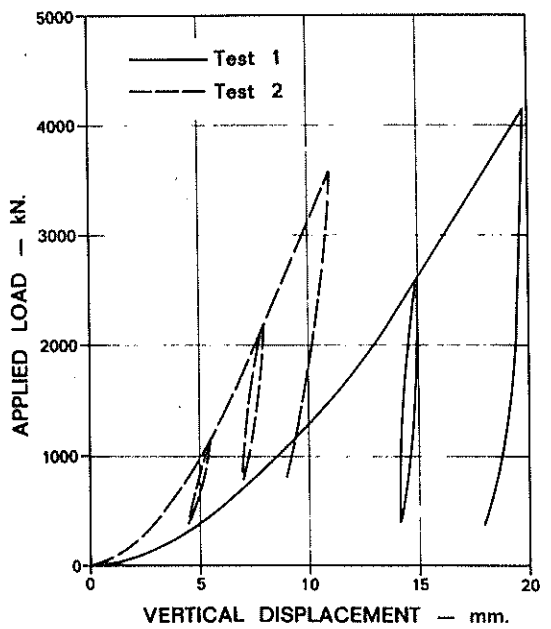

Figure 4 Base resistance load-displacement curves.

The average maximum normal stress beneath the base plate was 4360 kPa, which was 2.73 times the design stress of 1600 kPa. The load-displacement curve is quite linear over its final section, and the base behaviour was still within the elastic range. It is impossible to predict from this curve what the ultimate base failure load would have been, but it can be stated with confidence that the factor of safety against end bearing failure would be significantly higher than 2.73.

5.4 Base resistance - Test 2

The reinforced concrete spacer column used for this test was placed in the depression in the grout caused during Test 1. The load displacement curve shown in Figure 4 does not show the large irrecoverable grout compressions of Test 1. However, based on the shape of this curve it is likely that some bedding compression was still present. The average stress under the base plate, at maximum load, was 3750 kPa at 11 mm total displacement. This was equivalent to a safety factor of 2.34 on the design stress. As before, the base behaviour is still essentially elastic and there is no indication of incipient failure.

6 CONCLUSIONS

In this paper, the design, construction and use of a retrievable test rig for the determination of the performance characteristics of large diameter rock socketed piles has been described.

The test rig may be used to evaluate load-displacement curves for side shear resistance to failure and for base resistance to at least twice the design load. The test rig has the advantages of allowing a complete test to be made in a matter of days, without significant delay to a contact, at minimal disturbance to contractors, in a contract socket and without the need for costly external loading systems.

The results obtained from the two tests showed that the design of the rock socketed piles was adequate with side shear resistance reduction factors, α_c, of 0.37 and 0.52 for failure of the mudstone of confined triaxial shear strengths (σ_1-σ_3 at σ_3 = 690 kPa) of 5600 kPa and 3600 kPa respectively.

7 ACKNOWLEDGEMENTS

The authors express their appreciation to the organisations and individuals who afforded invaluable assistance during this test programme. In particular the Melbourne Underground Rail Loop Authority (MURLA) for their financial support, provision of access to a contract pile socket and permission to publish the findings, and John Holland (Constructions) Pty. Ltd., as MURLA contractor for providing services to the tests.

The work described in this paper forms part of a general programme of research into the performance of rock socketed piles under the direction of the first two authors.

8 REFERENCES

JOHNSTON, I.W. and DONALD, I.B. (1979). Final report on rock socket pile tests, Contract 703, Flinders St.-Spencer St. Overpass, Melbourne Underground Rail Loop Project. Report No. 79/1/C, Dept. of Civil Engineering, Monash University.

NEILSON, J.L. (1970). Notes on the weathering of the Silurian rocks of the Melbourne district. J. Inst. Eng. Aust., 42:1-2, pp 9-12.

The Uplift Capacity of Steel Piles Driven Into Hawkesbury Sandstone

R. L. RODWAY
Principal Investigations Engineer, Australian Commonwealth Department of Housing and Construction (N.S.W. Region)
R. K. ROWE
Assistant Professor, University of Western Ontario, Formerly Investigations Engineer, Australian Commonwealth Department of Housing and Construction

SUMMARY An investigation is described in which two steel H-piles were driven in Sydney Harbour through harbour sediment into the sandstone bedrock and the uplift capacity of the "rock sockets" measured as the piles were withdrawn. An on-land driving test designed to confirm that steel piles can be driven significant distances into medium-strength (10-15 MPa unconfined compressive strength) Hawkesbury Sandstone is also reported.

The results indicate that, at the Sydney Harbour site, a substantial contribution to uplift resistance can be reliably obtained from the bedrock using heavy-driven solid section steel piles.

1 INTRODUCTION

When a piled wharf structure is not braceable against the shore, berthing and mooring forces are resisted by the weight of the structure, by raker piles if these are used, and possibly by the uplift resistance of vertical piles provided by soil and perhaps bedrock. In cases where large deck widths and deck weights are fixed by factors other than berthing and mooring forces, the piles may not be required to provide any uplift resistance at all. In general, however, all potential ways of providing such resistance need to be considered in optimising a design.

The contribution of soil strata to resisting upward and downward loading can be calculated by standard soil mechanics methods using site investigation data. If bedrock is overlaid by only several metres of soil the contribution of the soil in supporting downward loads is often small by comparison to that offered by the rock, and detailed soil investigation and analysis is seldom warranted. If uplift is involved, however, the soil is more important because only its contribution is relied upon; there is rarely any reliance placed upon the possible contribution from the rock. Where uplift resistance is demanded from the rock this may be achieved by driving large diameter steel tubes, chopping an inspectable socket, and concreting. Some socketting is, in any case, usually undertaken to seal the tube into rock so that the founding material can be inspected to establish its adequacy to support the downward load. Installation of this type of pile is slow and expensive relative to solid section steel piles driven to practical refusal in rock. The cost differential is due largely to the difference in design bearing pressures adopted for the two systems; 85 MPa for the solid driven pile, and a typical maximum of 3 MPa for the concrete pile. The rationale for the higher stress depends essentially on the driving being regarded as an effective proving test of each pile position. From experience and load tests it has been found that significant movement under a working stress of 85 MPa rarely occurs provided the pile has been driven to practical refusal in rock.

But when steel piles are driven through soils which overlie medium-strength rock (10-15 MPa unconfined compressive strength) it is generally assumed that they will stop at the rock surface rather than penetrate it by any significant amount. Consequently no uplift resistance is expected. If piles penetrate deeper than site investigation data predicts it is usually assumed that the medium-strength rock stratum is at a lower level than expected or that the pile is deflecting or damaged. The latter explanation is prompted by instances of damaged piles having been extracted. In extreme cases, heavy-driven H-piles have split along the web and the flanges have been bent back through one hundred and eighty degrees into a double hook configuration.

The pile tests described in this paper form part of a site investigation of the near offshore area of Garden Island, the site of a Naval establishment in Sydney Harbour. The Island was joined to the harbour shore by reclamation works carried out in 1945. The purpose of this investigation was to obtain sediment and bedrock data to assist in evaluating various options being considered in developing an overall modernisation plan for the Island. Wharf structures costing up to 25 million dollars were included amongst the options and piling work accounted for 6 million dollars of this amount. The estimate was based on the driven steel liner, rock socketted, concrete filled piles described above. An estimated saving of 0.8 million dollars was considered possible provided the site investigation could establish the suitability of solid-section driven steel piles for the site. This paper limits itself to considering the driving of steel piles into sandstone bedrock and the resistance to pile extraction provided by the rock; the investigation of the overlying several metres of sediment is not reported.

2 HAWKESBURY SANDSTONE

Cores were recovered from the bedrock at nine locations. Figure 1 shows the positions of all boreholes and the two overwater pile tests. The results of unconfined compressive strength tests on the cores are listed in Table 1. The average result for cores taken from the top 0.5m was 9.6 MPa. This figure overestimates the average rock strength however because acceptable test specimens could not be obtained from much of the weaker rock in this zone. The average results from 0.5-1.0 m,

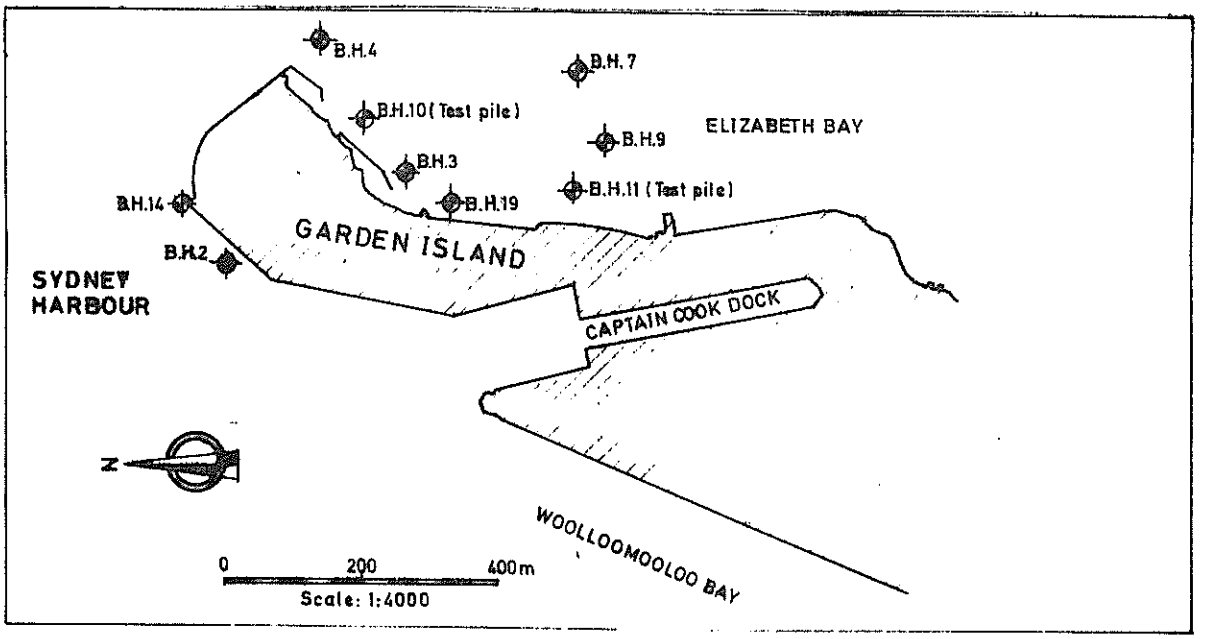

Fig. 1 Locations of boreholes and pile tests

from 1.0-2.0 m and from 2.0-3.0 m into the rock were 10.1, 13.8 and 14.3 MPa respectively. The few tests on deeper cores all gave results in excess of 20 MPa. A picture of the bedrock for the site was developed from these results together with records of past drilling within the subject area, a close-spaced seismic reflection survey, and the well established general characteristics of the Hawkesbury Sandstone geological formation.

The bedrock over the entire site is Triassic Hawkesbury Sandstone which extends for more than 200 metres below Garden Island. The formation consists of 95% lenticular sandstone but significant amounts of shale, shale breccia, clay and sandy claystone occur in the top 60 metres of the formation. The shale may occur finely laminated with fine sandstone in thin lenses but layers up to 30 metres thick have been encountered. Primary bedding within the formation is near horizontal but cross or current bedding and cut and fill structures are common and locally result in rapid vertical and lateral variations in rock type.

Present surface weathering is restricted to outcrops above sea level which are subjected to wetting, drying and oxidation. However, the bedrock adjacent to Garden Island was completely exposed during periods of lower sea level in the late Quaternary so relict weathering profiles are

TABLE 1

UNCONFINED COMPRESSIVE TEST RESULTS ON BEDROCK CORES - MEGAPASCALS

Borehole number	2	3	4	7	9	10	11	14	19
Distance into rock in m									
0		10.1			6.9		14.9	7.2	
	4.9	11.4					13.7		4.4
						5.4			17.1
	11.5	12.6		5.4		10.7	9.3	8.3	
1.0				7.3					14.6
	22.5					5.1	16.3		
				6.4					15.2
		14.2	12.4		4.0		17.6	18.2	
	11.9		17.7						11.0
				6.2		8.1		17.6	
	15.5				12.7				
2.0		18.8			22.6		14.4		22.1
				10.7				13.4	
			11.4		19.8				
					11.8				
				16.0		9.4	20.9		
									23.5
3.0		15.3				6.2			

expected below the present sea level. Weathering within sandstone is not usually extensive and is typically limited to one metre, but shale lenses at or very near the bedrock surface may be completely weathered for 6 to 10 metres. Within the sandstone, joints are usually near vertical. Tertiary basaltic dykes have intruded the sandstone, typically through joints,and may be locally weathered to depths in excess of 30 metres.

The results from the drilling carried out for this investigation were in accord with the general features of the Hawkesbury Sandstone formation given above. The drilling indicated that the rock surface was weathered to depths of up to one metre throughout most of the area. Shale was intersected near the bedrock surface in only one location. In this borehole, 6 metres of weathered sandstone and shale were found to overlie solid shale.

Thus the situation was one of a generally very sound bedrock persisting to great depths but possibly containing serious localised weaknesses which occurred randomly at or near the bedrock surface. The implications of this situation for selection of pile type and investigation strategy will be discussed later.

3 OVERWATER PILE TESTS

The two tests were conducted at the positions of boreholes 10 and 11. At borehole 10 the sandstone was weathered, with no parts of the upper 0.5 metre of core testable. Unconfined compressive strength test results on the next metre of core were 5.4, 10.7, 5.1 and 8.1 MPa. Penetration of a driven pile into at least the upper half metre of the rock would normally be expected.

At borehole 11 there appeared to be no significant weathered rock transition. The unconfined compressive strength result at the bedrock surface was 14.9 MPa and test results for the next metre of core were 13.7, 9.3, 16.3 and 17.6. In this situation no significant penetration of a driven pile into the rock would usually be expected; the total uplift resistance of the pile would be attributed to the overlying soil.

Initially a 20 metre long 310 UC 158 steel H-pile was driven into the sediment to a point just short of the underlying bedrock surface at each location. A 3.3 tonne drop hammer falling through one metre was used. The mass of each pile was 3.2 tonnes. Soil profiles consisted of layers of sands and clayey sands of variable density and plasticity. After two days each pile was extracted, recording the forces required. The pile at Borehole 10, which was embedded to a depth of 5.2 metres, sustained a peak pullout load of 320 kN while the pile at Borehole 11, which was embedded to a depth of 7.7 metres, sustained a peak load of 290 kN. The difference between the average shear resistance measured in the two tests was consistent with the differences in soil profile at the two locations.

Each pile was then redriven at its same position and driving was continued to practical refusal using a hammer drop of 2 metres. For the pile at Borehole 10 this involved a penetration of approximately 1.4 metres beyond the point reached in the initial drive. From the borehole information and subsequent inspection of material adhering to the recovered pile it appeared that the upper half of the 1.4 metres was dense sand or highly weathered sandstone and the lower half was soft sandstone of approximate compressive strengh 5 MPa. The pile at Borehole 11 penetrated through a further metre of material on redriving and from the borehole information and subsequent inspection of material adhering to the recovered pile,it appeared to be 0.4 metres of sand overlying 0.6 metres of sandstone of approximate compressive strength 10 - 15 MPa. Redriving data together with borehole information and test results is given in Table II.

Neither pile could be extracted by a dynamometer - measured pulling force of 600 kN or by a force of 750 kN (calculated from submergence measurements of the ballasted pulling barge) even though jetting was used to lessen soil resistance. At this stage of the operation it was confidently expected that the high resistances would be seen, on extraction, to be due to severe distortion of the piles. The pile at Borehole 11 was finally removed using a heavy extracting vibrator in conjunction with a 750 kN pulling force. The remaining pile was removed by a 750 kN pull only after explosives had been used to loosen rock near the toe of the pile. Both piles were straight and completely undamaged apart from the distortion clearly attributable to the explosives.

Due to the methods necessary to finally extract the piles, the actual ultimate uplift resistance provided to each by the sandstone could not be calculated but a value in excess of 1000 kN is considered probable.

Although the material impacted between the flanges of the extracted piles appeared to be consistent with the investigation drill cores and the driving records, there remained some doubt as to the quality of the rock penetrated. The impacted rock had been altered by the pile driving so tests upon it could not confirm its in-situ compressive strength. Limitations on the accuracy with which the site investigation drilling barge and the pile driving barge could be positioned further compounded the uncertainty as to the strength of the penetrated rock. Consequently an on-land driving test was conducted at Balmain in similar rock using the same pile section, hammer and driving frame.

4 ON-LAND PILE TEST

A 3.4 metre long section of 310 UC 158 piling was driven through 1.2 metres of fill and a further 0.92 metres into bedrock. The rock was observable in cross-section in outcrop approximately 3 metres from the test position and appeared to be sound, uniform, seam-free sandstone of medium strength. Four cores were drilled immediately adjacent to and surrounding the test position. These were tested in unconfined compression. The test results for the upper one metre of sandstone ranged between 9.9 MPa and 16.3 MPa with an average value, from 15 tests, of 13 MPa. The test results together with driving resistances are presented in Table III. The pile was driven to practical refusal with an average set over the last 50 blows of 0.4 mm per 2 m hammer drop. Details of pile penetration over the final 75 mm are given in Table IV for both the on-land and offshore tests.

Excavation of the overlying fill revealed that the surface of the sandstone around the pile was free of any joint or defect that could have affected the test. Only two cracks emanated from the pile and both terminated within 200 mm of the pile. The apparent zone of influence of the pile upon the sandstone was very limited: the rock within approximately 10 mm of the pile had been pulverized but was very compact and there was no indica-

TABLE II

OVERWATER PILE DRIVING TESTS - GARDEN ISLAND

Depth below harbour floor in m	BOREHOLE 10		BOREHOLE 11	
	Driving resist. Blows x Drop (m) per 333mm set	Notes	Driving resist. Blows x Drop (m) per 333mm set	Notes
0		Loose sand Sand % 88		Loose sand Sand % 88
1		Soft clayey sand Sand % 65, P.I. 17		Stiff clayey sand Sand % 75, P.I. 23
	5 x 0.3			
2	4 x 1			S.P.T. 10
	6 x 1	S.P.T. 10 Clayey sand		Medium density sand
	6 x 1	S.P.T. 8	2 x 0.3	
3	8 x 1		4 x 1	
	8 x 1	Clayey sand Sand % 65, P.I. 20	5 x 1	Medium density sand Sand % 85
	11 x 1	S.P.T. 12	7 x 1	
4	10 x 1		7 x 1	S.P.T. 27
	15 x 1	Dense sand Sand % 70, P.I. 20	16 x 1	Dense clayey sand
	15 x 1	S.P.T. 15	15 x 1	
5	15 x 1	Limit of initial drive	15 x 1	
	50 x 1	Dense sand Sand % 70 S.P.T. 40	10 x 1	
	50 x 1 + 32 x 2		10 x 1	Sand % 65 S.P.T. 8
6	60 x 2	Auger refusal-sandstone	15 x 1	
	130 x 2	Driving Refusal U.C.S. 5.4 MPa	15 x 1	Medium density clayey sand
		U.C.S. 10.7 MPa	15 x 1	
7		U.C.S. 5.1 MPa	15 x 1	Sand % 75, P.I. 16 Dense sand
			15 x 1	
				Limit of initial drive
8		U.C.S. 8.1 MPa	20 x 1	Auger refusal-sandstone U.C.S. 14.9 MPa
			20 x 1	U.C.S. 13.7 MPa
			35 x 1 + 60 x 2	U.C.S. 9.3 MPa
		U.C.S. 9.4 MPa	180 x 2 for 100mm	U.C.S. 16.3 MPa Driving refusal U.C.S. 17.6 MPa
9				

tion of rock distortion beyond this zone. Heavy pulling gear was not available so rock had to be excavated from around the pile before it could be extracted. The pile was essentially undamaged with one leaf of one flange bent slightly from its plane at the pile toe.

5 DISCUSSION

Hawkesbury sandstone presents the foundation designer with a frustrating problem in that it has a very high load capacity almost generally but the presence of some localised weaknesses may preclude him from depending upon the high capacity at any particular position. A similar situation exists with respect to the uplift capacity of driven piles. Even when a site investigation indicates that a penetrable rock zone is present over most of the area, the possibility of the bedrock surface being harder and impenetrable at some spots may preclude the designer from depending upon uplift resistance at all.

ON-LAND PILE DRIVING TEST-BALMAIN

Depth Below Ground Level in m	Test Results Unconfined Comp. Strength in MPa	Driving Resistance Number of Blows x Hammer drop (m) per 100 mm Set	Notes
		15 x 0.3 total	Loose fill
1.2	15.7	12 x 1	Top of sandstone
		20 x 1	
1.4	15.5		
	15.1 11.7	31 x 1	
	10.4		
		31 x 1	
1.6	13.7		
	16.3	5 x 1 + 20 x 2	
	10.0		
	12.4	40 x 2	
1.8	15.4		
	14.2	40 x 2	
		50 x 2	
2.0	11.0 11.1		
	9.9	100 x 2	
	13.3	55 x 2 for 20 mm	2.12 m Refusal
2.2	15.3		

TABLE IV

TERMINAL DRIVING RESISTANCES OF TEST PILES

	Pile		
	On-Land Balmain	BH 10 Garden Island	BH 11 Garden Island
No. of blows* per 25 mm set over the last 75 mm	23, 35, 55	7, 13, 50	20, 25, 35
Distance driven beyond nominal refusal**	162 mm	15 mm	195 mm
No. of blows after nominal refusal	170	40	180
Average set over last 50 blows	0.4 mm	0.5 mm	0.9 mm

* A blow = a 3.3 tonne hammer falling through 2 m

** "Nominal Refusal" is assumed to correspond to a set of less than 25 mm per 10 blows over 20 blows

This problem of variation across the site has been compounded in wharf construction by the increasing use of single high capacity piles because the associated increased pile spacings reduce the extent to which loads can be redistributed from a defective pile through the deck structure to adjacent piles. Consequently it becomes more important to ensure that each and every pile is capable of resisting the forces for which it has been designed. However, the uplift resistance of individual piles is less critical than their performance under downward loading. This is because the capacity of deck structures to redistribute load differs significantly for upward and downward loading: mooring and berthing forces are sub-horizontal. The deck, too, is horizontal and consequently stiff in this plane so considerable spreading of the uplift-producing forces occurs. This is not the case with the large concentrated forces which result from cranes and other live loads.

For the Garden Island site, and for others where localised variations in rock quality are expected, the selection of a piling system is strongly influenced by the extent to which the installation process supplements the site investigation by proving the founding material at each pile position. Large diameter driven steel tubes socketted into the rock and filled with concrete fulfill this function well but installation is slow and expensive. In addition there are significant practical problems associated with arranging down-the-hole inspections and drilling of proving holes ahead of the founding depth for every socket, especially when there is persistent water ingress into the socket. Delays to the construction programme are not infrequent.

The driving tests showed the heavy section steel piles can be driven into 10 - 15 MPa Hawkesbury sandstone. This information, taken together with the bedrock picture built up by the site investigation, indicates that a driven pile system would provide the designer with an assurance of the capability of individual piles to support downward loads that is comparable to that provided by the dearer, slower system described above.

The uplift tests are open to some interpretation. The ultimate loads sustained by the piles can be only estimated because of the methods finally needed to extract them. Also some assumption needs to be made of the effectiveness of jetting in reducing the soil restraint. However, the most conservative interpretation suggests an ultimate average skin friction in the rock of at least 230 kPa. It appeared that the piles could be driven at least 0.5 metres into the sandstone over the subject area. Based on these figures the uplift resistance of the rock would add 50% to that contributed by the average 7 metres of sand and clayey sand sediments which overlie the rock. Final design figures would need to be chosen having regard to the capacity of the particular wharf structure to distribute berthing and mooring forces amongst the piles. The amount of the soil's contribution would also be an influencing factor.

For the 310 UC 158 piles used in the tests it is considered that the rock uplift resistances would be realized with acceptable reliability when the piles are driven to practical refusal using a hammer of similar mass to the pile and a hammer drop of 2m. In this context practical refusal is considered to correspond to either:

(i) a set of less than 10 mm per ten blows over the last thirty blows;
OR
(ii) a penetration of 150 mm beyond nominal refusal where nominal refusal is defined as a set of less than 25 mm per ten blows over the last twenty blows.

Consideration would need to be given to the driving energy required to achieve adequate penetration of other pile sections and to the possibility that the required energy may be such as to cause damage to the piles.

Little generality should be assumed for the above conclusions. Extrapolation of the results beyond the investigated site and to other rock types could not be undertaken without specific corroborative investigations.

6 CONCLUSIONS

The investigation showed that heavy section steel H-piles could be driven up to 1 metre into medium strength (10 - 15 MPa unconfined compressiv strength) Hawkesbury sandstone and that, at the Sydney Harbour site, substantial uplift resistance could be achieved with an acceptable degree of reliability by driving piles to practical refusal in the bedrock.

With respect to downward loading it is considered that, for this particular site, where the major risk is the presence of localised weaknesses in an otherwise strong rock, heavy driven solid section piles provide an assurance of individual pile performance comparable to that produced by the slower, far more expensive system of driving steel casings to rock, chopping an inspectable socket, drilling an inspection hole ahead of the founding depth, then concreting.

7 ACKNOWLEDGMENT

The author wishes to thank the Secretary of the Australian Commonwealth Department of Housing and Construction for permission to present this paper. The views put forward in the paper are the author's own and do not necessarily represent those of the Department.

The Design and Performance of Cast In Situ Piles in Extensively Jointed Silurian Mudstone

A. F. WILLIAMS
Engineer, Country Roads Board of Victoria
M. C. ERVIN
Senior Engineer, Coffey & Partners Pty Ltd, formerly Engineer, Country Roads Board of Victoria

SUMMARY Reasonable methods exist for the design of piles socketed into rock which is massive or which has only a few tight joints, however, difficulties arise when the rock is extensively jointed. Such difficulties were experienced during the construction of Melbourne's Eastern Freeway, which required twin bridges to be constructed over the Yarra River in an area known as the "Studley Park Fault Zone", where the Silurian sedimentary rocks have undergone severe folding, faulting and fracturing. The joints in the area were found to be slickensided, generally with thin clay coatings and with joint frequencies of 10 to 100 joints/m.

In order to confirm the practicability of economically constructing sockets in the faulted rock and in order to develop a design method, two test sockets were constructed. An end-bearing test was carried out in one and a side-resistance test was carried out in the other. During the subsequent bridge construction, eight of the service piles were proof loaded to reduce the expected high first-loading settlements. The work was supported by detailed geological logging of N size core and the rock sockets, triaxial tests on intact samples of rock, and pressuremeter tests. The results of the pile tests and the pressuremeter tests have been related usefully to joint frequency.

1 NOTATION

D	pile diameter
f_b	base resistance
f_{be}	base resistance according to linear elastic analysis
f_{bl}	base resistance at $\rho/D = 1\%$
f_s	side resistance
f_{se}	side resistance according to linear elastic analysis
f_{su}	peak side resistance
J_f	joint frequency in joints/m
q_a	unconfined compressive strength
α	side resistance reduction factor $= \frac{f_{su}}{q_a}$
ρ	pile settlement.

2 INTRODUCTION

The construction of Melbourne's Eastern Freeway required twin bridges to be constructed over the Yarra River in an area known locally as the "Studley Park Fault Zone", where the Silurian sedimentary rocks have undergone severe folding, faulting and fracturing. The joints in the area were found to be slickensided, generally with thin clay coatings and with joint frequencies of 10 to 100 joints/m.

Initial investigations indicated that it was desirable from economic and fixity considerations to found those bridge piers which were adjacent to the river on piles socketed into the mudstone. The design of piles socketed into rock has usually been based on allowable side and base resistance stresses which have been determined from a consideration of data pertaining to relatively intact rock. The Eastern Freeway piles were designed in 1975 and at that time rational methods of designing piles in extensively jointed rock did not exist, and it was therefore necessary to carry out the work described in this paper. In order to confirm the practicability of economically constructing sockets in the faulted rock and in order to provide a basis for designing the service piles, two test piles were constructed and loaded to failure.

This paper describes the test pile work and the analysis made of the properties of the jointed rock mass as a case history, and relates the results of the pile tests to the pile design method proposed by Williams *et al.* (1980).

3 SITE INVESTIGATION

The Eastern Freeway site was located east of Melbourne as shown in Figure 1, in an area where the Silurian mudstone was overlain by up to 3 m of Recent Alluvium. The mudstone was typical of that existing around Melbourne in that it consisted predominantly of siltstone with minor sandstone and a negligible amount of claystone. The bedding thickness varied from 1 to 100 mm with occasional beds up to 300 mm thick. The bedding dipped generally at 50° to 70° towards the north-west. It was usually possible to identify three sets of approximately orthogonal joints, with the two dominant sets being parallel to the bedding and normal to the bedding. A more detailed description of the joints is included with the description of the rock sockets in Section 4.

The weathering of the mudstone has occurred under a reducing environment which has resulted in the colour of the claystone and siltstone being blue-grey and the sandstone being a paler grey. The mudstone is similar in this respect to that encountered by Parry (1970) for the King Street Bridge and by Parkin and Donald (1975) for the Johnson Street Bridge.

Site investigation drilling consisted of one N size bore drilled at each pile position. The cores were described according to the weathering classification of Neilson (1970) and particular attention was paid

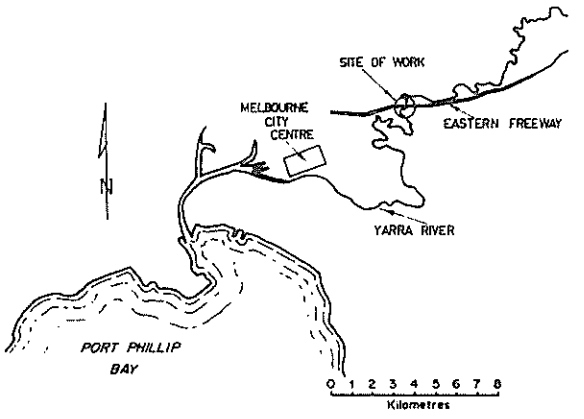

Figure 1 Locality Plan

to the condition and frequency of the joints. The frequency of the relatively blocky joint system was determined simply by counting the number of joints seen in the core for joint frequencies of less than 50 joints/m or by visually assessing the representative fragment size for greater joint frequencies. It was not considered worthwhile or practicable in this situation to endeavour to determine the frequencies of each joint set or to allow for the orientation of the bore with respect to the joint sets.

The intact fragments of rock were generally moderately or slightly weathered with a significant proportion being fresh fragments. The joint frequencies of commonly 10 to 100 joints/m indicated that the properties of the rock mass were likely to be very different from those of the intact fragments. It was therefore appropriate to carry out a series of Ménard pressuremeter tests to measure the strength and compressibility of the rock mass. Such tests have since been found particularly suited to the measurement of the in situ properties of the Silurian mudstone, e.g. Walker *et al.* (1975) and Walker (1978).

In order to provide the basis for a design method, the modulus of the rock mass as measured by the pressuremeter has been correlated with joint frequency as shown in Figure 2. The mass modulus is seen to decrease rapidly at relatively low joint frequencies in a manner similar to that observed by Deere *et al.* (1966), Manev and Avramova-Tacheva (1970) and Hobbs (1974). In a similar manner, the in situ shear strength from the pressuremeter results, calculated according to Gibson and Anderson(1961), has been correlated with joint frequency in Figure 3. The correlation shown in Figure 3 may be regarded as the lower bound of the shear strength-joint frequency correlation, because only pressuremeter tests which clearly indicated a limit pressure have been plotted. Other pressuremeter tests were made but did not indicate a limit pressure, however, such tests indicated a relatively high modulus which indicated a tighter joint system and a higher in situ strength.

The shape of the strength correlation is similar to that obtained for model rock by Lama (1974), and it is also similar to that of the modulus correlation, although the effect of joint frequency on strength does not appear to be as great as it is on modulus. The in situ modulus and strength have been combined in Figure 4 where it is seen that the modulus to strength ratio increases with modulus. The correla-

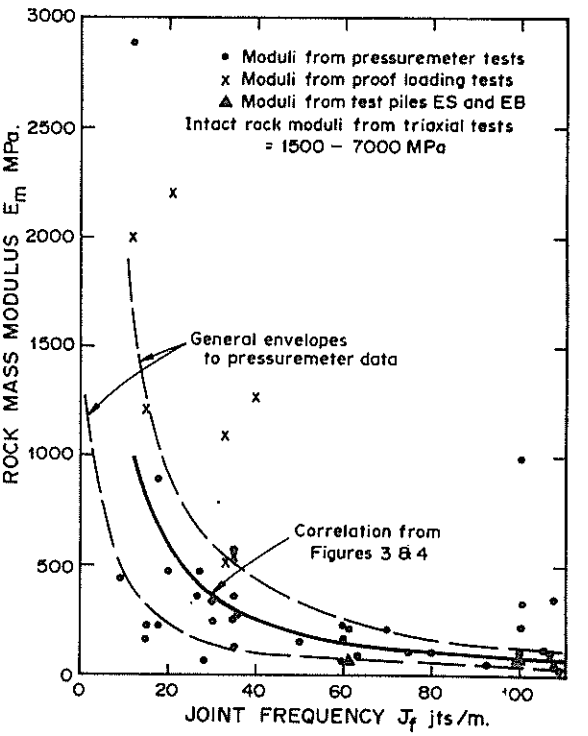

Figure 2 Correlation between joint frequency and the modulus of the rock mass.

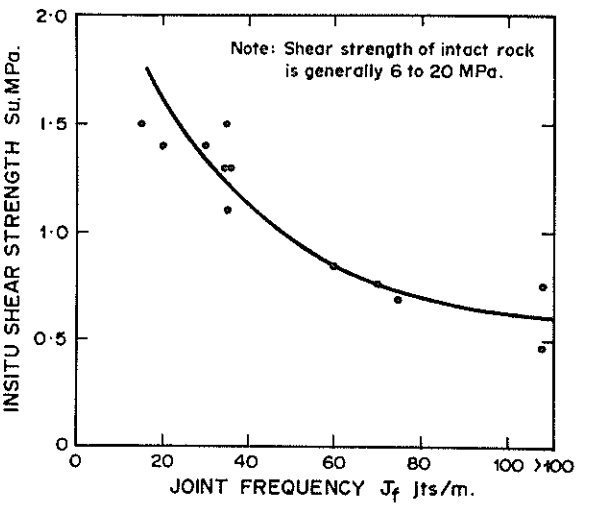

Figure 3 Correlation between joint frequency and shear strength of the rock mass.

tions in Figures 3 and 4 are reasonably well defined and they have been used to construct the correlation adopted between the mass modulus and joint frequency shown in Figure 2. An attempt was made to identify the dominant dip of the joints at each pressuremeter test position in an effort to make some allowance for any anisotropy, however, the blocky structure produced by the three joint sets made such an assessment very uncertain and the question of anisotropy was not pursued.

Moisture content samples were taken from the cores approximately every 300 mm and samples were selected where possible for triaxial testing to assist in estimating the strength of intact rock on the basis of moisture content. Triaxial tests were made on samples under unconsolidated undrained conditions with a confining pressure of 0.7 MPa, thus following the procedure established by Parry (1970) and continued by Parkin and Donald (1975).

The results of the triaxial tests have been plotted against moisture content in Figure 5, where the correlation found by Parkin and Donald (1975) is also shown for comparison. The triaxial shear strength of the intact rock is generally in the range of 6 to 20 MPa, which is much greater than the shear strength of the highly jointed rock mass indicated in Figure 3.

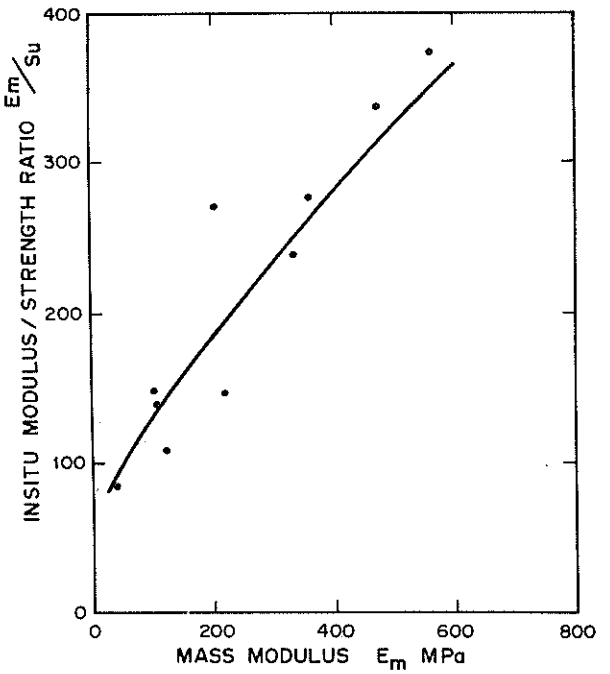

Figure 4 Relation between the modulus of the rock mass and the modulus/strength ratio

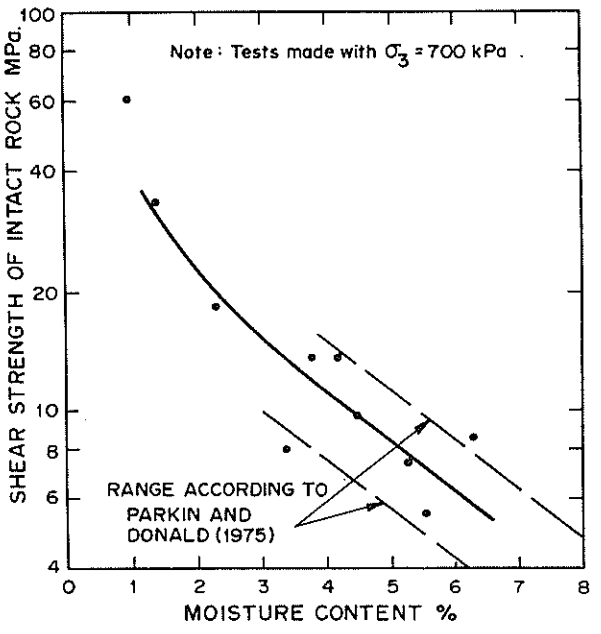

Figure 5 Correlation between triaxial shear strength and moisture content

4 TEST PILES

4.1 Pile Construction

The decision to construct and load to failure one end bearing only test pile and one side resistance only test pile was based on the need to:

(a) determine the feasibility of constructing stable sockets in the intensely fractured rock

(b) determine the allowable side resistance and base resistance components of pile capacity, and,

(c) assess the need to proof load the service piles in order to tighten the jointed rock and to thus reduce pile settlement during service loading. The advantages of cycling such proof loads were also to be considered.

A test site close to the service piles was selected where investigation drilling had shown that the rock was most intensively jointed and therefore likely to cause the greatest difficulty.

The sockets for the two test piles were drilled by a Caldwell 250B rig using a bucket auger, according to the depths shown in Figure 6. After the outer steel casings had been placed, the sockets were dewatered and inspected. An engineering geologist provided the following socket descriptions:

Side Resistance Socket: The exposed rock comprised predominantly blue-grey moderately weathered (Zone 3) mudstone. More highly weathered rock was brownish yellow. The mudstone was generally highly fractured and included frequent thin clay seams and

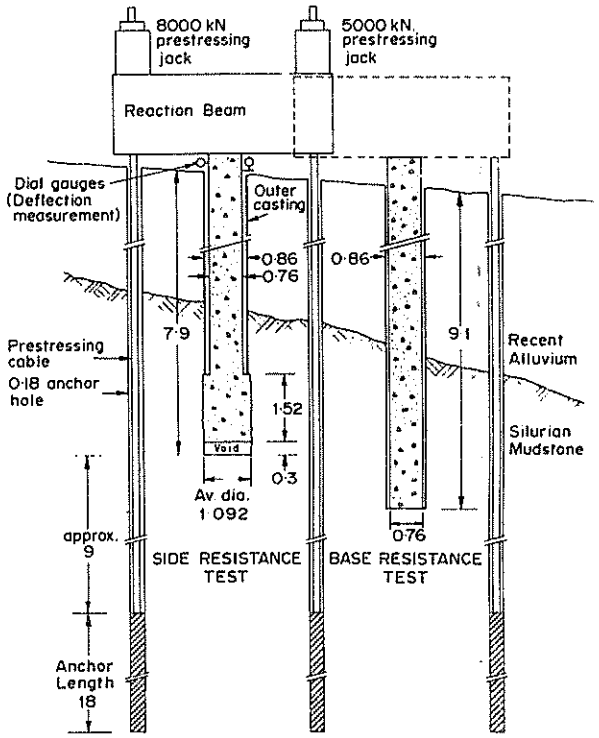

All dimensions are in metres

Figure 6 General arrangement of the test piles

thin irregular patches of more highly fractured and weathered rock. Three roughly orthogonal sets of joints resulted in a generally blocky structure in many parts. The two dominant joint sets were steeply dipping: one being parallel to the bedding at 50° to 70° and the other dipping at 70°. The third, less dominant joint set had a shallow dip and was often indistinct. The joints included thin clay films, or in the more fractured and lightly weathered areas, free clay. The joints were mostly planar and smooth, although some were slightly ridged and slickensided. The jointing appeared to be tight except for moderately tight areas of intense fracturing. The general joint frequency appeared to range from 40 to 120 joints/m with most of the socket exhibiting 40 to 80 joints/m. The appearance of the socket walls is sketched in Figure 7.

Base Resistance Socket: The rock mass was similar to that exposed for the side resistance test. The appearance of the socket base has been sketched in Figure 8.

The test piles were constructed and loaded according to the arrangement shown in Figure 6. The 9 m of free anchor length below the test piles was selected to minimize settlement interaction effects (Poulos and Mattes, 1975). Two precision spirit levels were attached to the reaction beam so that it could be maintained horizontal during simultaneous stressing of both rock anchors. Pile settlement was measured with dial gauges fixed to 5 m long insulated reference frames and with a precision level fixed to a rigid pedestal. The stability of the precision level was checked by sighting to a remote benchmark, and the stability of the reference frames was checked by the precision level. No movement of the level or of the reference frames was detected outside ±0.2 mm accuracy of the precision level. The pile settlements indicated by the dial gauges and by the precision level thus agreed to within ±0.2 mm.

4.2 Side Resistance Test

The socket for the side resistance test pile was drilled to a nominal diameter of 915 mm, however, overbreak increased the average diameter to 1090 mm. The test pile was constructed with a 300 mm thick polystyrene foam compressible base as shown in Figure 6. A one-dimensional oedometer test was made on a sample of polystyrene to model its behaviour under the test pile and to indicate the load carried by the polystyrene base. The oedometer test indicated that the load carried by the polystyrene would not have exceeded 50 kN and the effect was therefore neglected.

The pile was loaded in increments of 500 kN by simultaneously stressing the two cable anchors. The load was measured according to a calibration between the load and pressure of the two stressing jacks. Each load increment was held for at least one hour, during which settlement and time readings were taken to provide the basis for the load-settlement curve shown in Figure 9 and the creep rate curve shown in Figure 10. The load-settlement curve indicates a "yield" point at a load of about 2000 kN (380 kPa) which corresponds to the beginning of a sharp increase in creep rate.

Although the creep rate increases sharply, the load-settlement curve shows a significant increase in side resistance as displacement increases and at a displacement of 175 mm the load was 4400 kN (840 kPa). The load-settlement curve gives no suggestion of an abrupt failure commonly observed for smooth sockets, and it has not developed a peak value which is approximately maintained at large displacements as commonly observed for rough sockets (Williams and Pells, 1979).

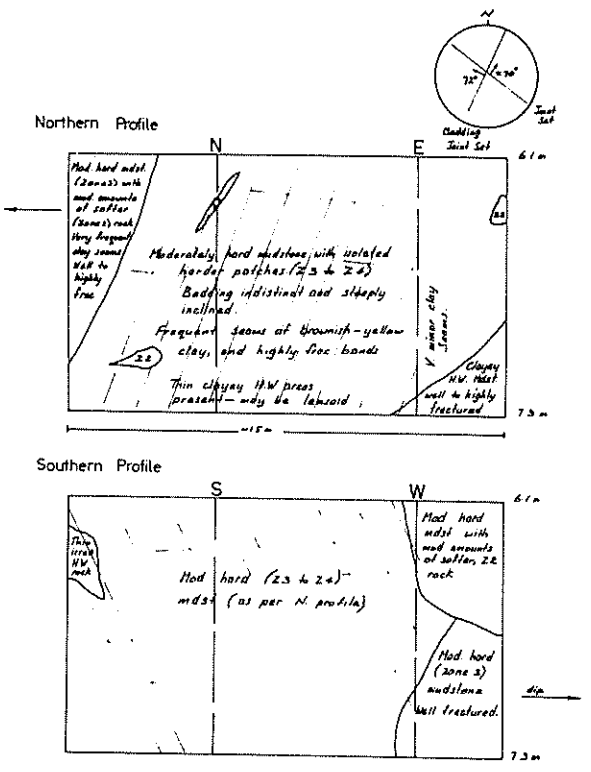

Figure 7 Geological structure of the rock exposed on the walls of the side resistance socket

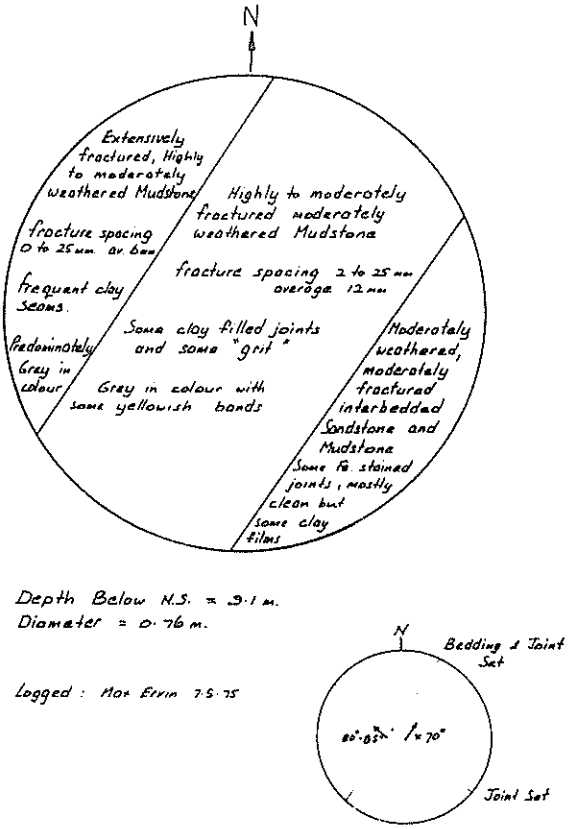

Figure 8 Geological structure of the rock exposed on the base of the end bearing socket

The peak side resistance is commonly related to the unconfined strength of the intact rock, e.g. Rosenberg and Journeaux (1976), Hvorath (1978), Pells *et al.* (1978) and Williams and Pells (1979). The unconfined strength of the intact rock in this case was between 6.0 and 8.5 MPa for mudstone with a moisture content of 3 to 5%. The side resistance factor, α, is then given by:

$$\alpha = \frac{\text{peak side resistance, } f_{su}}{\text{unconfined compressive strength, } q_a}$$

$$= \frac{.840}{6.0 \text{ to } 8.5}$$

$$= 0.10 \text{ to } 0.14$$

The value of α = 0.10 to 0.14 is towards the low side of the general scatter of results which form the basis for a relation between α and q_a suggested by Williams *et al.* (1980), however, it lies on the generally lower bound curve recommended as a design basis.

The results of the pile test were used to calculate the modulus of the rock mass according to the method suggested by Pells and Turner (1978). The first loading modulus indicated by the initial tangent to the load-settlement curve was 70 MPa. This modulus has been plotted at the average joint frequency of 60 joints/m on Figure 2, where it is seen to be below the adopted correlation although it is well within the general scatter of results. The slopes of the unloading and reloading parts of the load-settlement curve were similar and indicated a reloading modulus of 350 MPa, which is about six times the first loading modulus. The significant increase in modulus indicates a significant tightening of the joints during the initial loading and it therefore indicates the advantage of proof loading the service piles.

4.3 Base Resistance Test

The base resistance test was made on a 760 mm diameter pile as shown on Figure 6. The load was applied and the settlement was measured in the same manner as already described for the side resistance test.

The load-settlement curve shown in Figure 11 indicates a "yielding" at a load of about 1500 kN (3300 kPa), which is approximate to the increase in the rate of creep settlement shown in Figure 10. The load-settlement curve does not indicate a peak or residual capacity but shows a continuing increase of capacity with settlement, even at the maximum settlement of 150 mm. The result is similar in this respect to the base resistance tests carried out at depths of more than three pile diameters by Williams (1980), in which the base resistance continued to increase with settlement without exhibiting a well defined peak capacity. In the absence of a well defined peak capacity, Williams *et al.* (1980) have found it convenient to normalize the load-settlement curves from base resistance tests on the basis of f_{b1}, the resistance corresponding to a settlement ratio ρ/D of 1%. In the case of the test described, f_{b1} = 1760 kPa.

The initial tangent modulus of 80 MPa, calculated according to Pells and Turner (1978), has been plotted at 100 joints/m in Figure 2 where it is seen to correspond with the adopted correlation. The pile was subjected to six cycles of loading between 500 kN and 1500 kN which indicated a significant stiffening of the rock mass and a reloading modulus of 425 MPa. The increase in modulus of about 5 times was similar to the increase observed from the side resistance test.

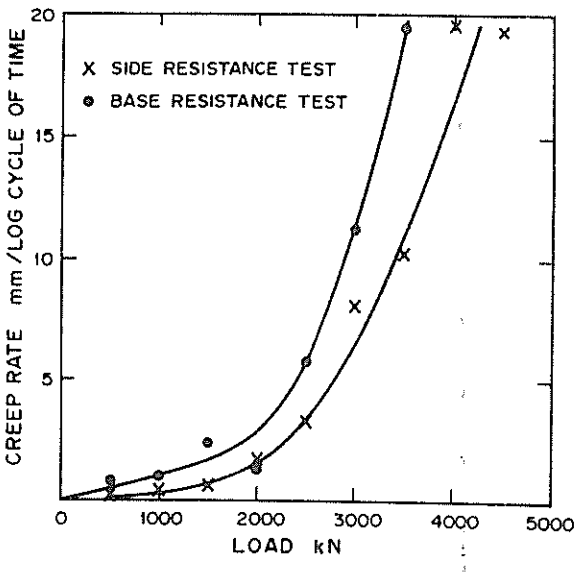

Figure 10 Creep rate at each load level for the side resistance test and base resistance test.

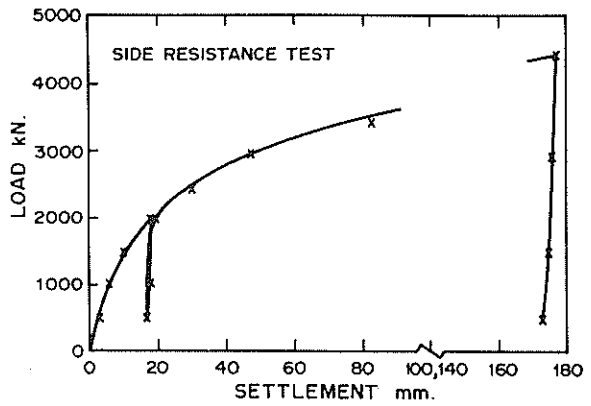

Figure 9 Load-settlement curve for the side resistance test

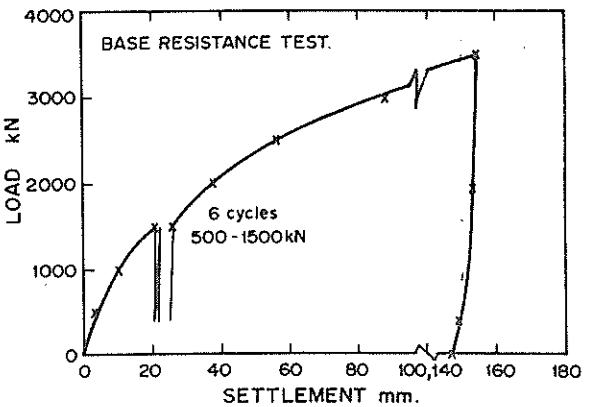

Figure 11 Load-settlement curve for the end bearing test

5 CONSTRUCTION AND PROOF LOADING OF SERVICE PILES

The test pile programme indicated that it was practicable to proceed with the installation of the proposed rock socketed piles, and that proof loading was necessary for the eight piles socketed into the most fractured rock to ensure that unacceptably large settlements did not occur under service conditions. The piles were proof loaded to 1.5 times their design load.

The sockets were constructed using rotary drilling techniques under a positive head of water, and the piles were cast under water with a tremie pipe. A single cable anchor was installed through the centre of the piles to be proof loaded and proof loading was then carried out using two prestressing jacks mounted in series.

The results obtained from the proof loading tests are presented in Table 1 where the rock mass moduli which have been calculated from the pile tests are seen to be higher than the moduli suggested by the pressuremeter tests. The reasons for the difference in moduli are not certain, however, the following three effects may have contributed to the difference. Firstly, lateral loosening of the rock round the site investigation bores may have reduced the essentially horizontal modulus measured by the pressuremeter, whereas similar loosening in the case of a rock socketed pile may not have seriously affected the essentially vertical modulus measured by the pile tests. Secondly, the jointing of the

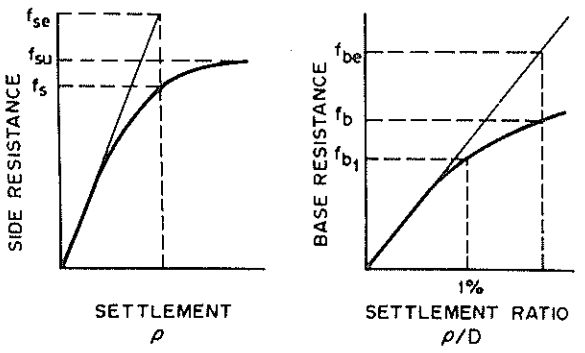

Figure 12 Definition of terms used to normalize the load-settlement curves

TABLE 1

SUMMARY OF PROOF LOADING TEST RESULTS

Pile No.	Average Joint Frequency J_f	Maximum Settlement mm	Estimated Rock Mass Moduli MPa	Measured Rock Mass Moduli	
				1st Loading MPa	Re-loading MPa
EB	100	-	55	80	425
ES	60	-	105	70	354
E1	21	1.5	470	2400	6860
E2	12	1.6	810	2010	9630
E3	33	4.1	270	515	1790
E5	35	2.2	250	550	995
E6		1.1		1270	2210
E7	15	1.5	710	1220	3100
E8	33	1.5	280	1090	2350

Notes: (1) The average joint frequency is a weighted average determined over the length of the socket plus one diameter below the socket.
(2) The maximum settlement is the settlement at a load of 6700 kN after one previous load-unload cycle.
(3) The estimated rock modulus has been determined from Figure 2.
(4) The measured rock moduli have been determined from the pile tests as the secant moduli between 0 and 6700 kN.

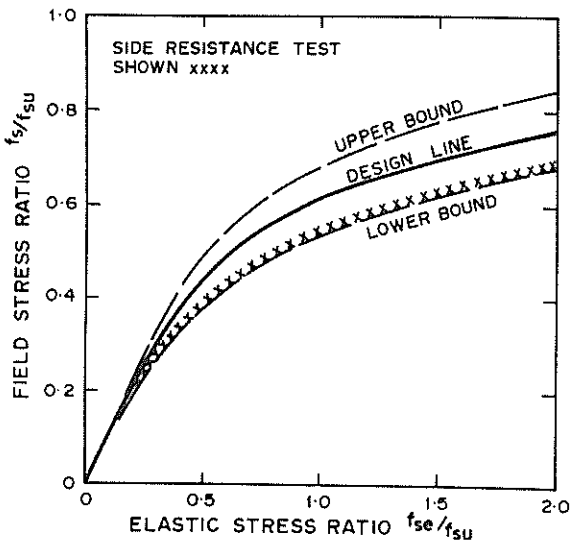

Figure 13 A comparison of the side resistance test with the normalized design curve proposed by Williams *et al.* (1980)

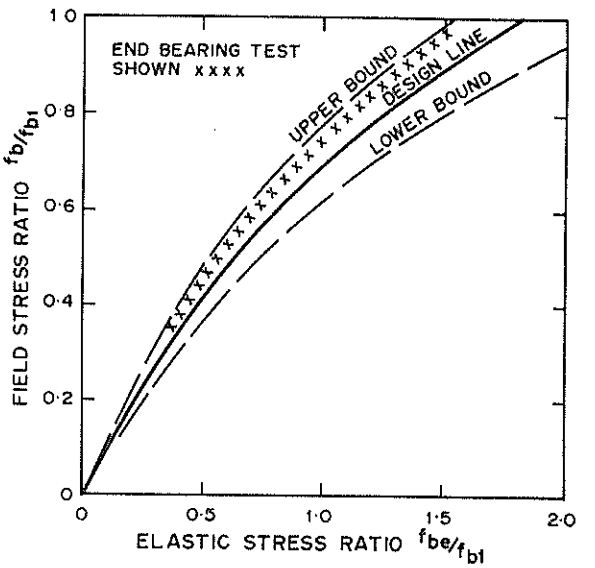

Figure 14 A comparison of the base resistance test with the normalized design curve proposed by Williams *et al.* (1980)

rock may have caused a modulus anisotropy which has been identified only with the comparison of the horizontal pressuremeter modulus and vertical pile modulus. Thirdly, the pressuremeter moduli were measured over large strains whereas the pile moduli have been determined from very small displacements. However, although there is a difference in magnitude between the pressuremeter and pile moduli, the variations in pile moduli do appear to reflect the variations in the joint frequency of the rock.

6 PILE DESIGN METHOD

The 1.52 m diameter service piles for the Eastern Freeway were designed on the basis of the results of the test piles and an assessment of the effects of jointing as indicated by Figures 2 and 3. However, rather than review the design of the Eastern Freeway piles, it is intended to assess the applicability of the pile design method proposed by Williams *et al.* (1980) to the extreme case of the extensively jointed rock encountered at the Eastern Freeway site.

The load-settlement curves obtained from the test piles have been normalized according to the elastic and plastic stress ratios, as defined in Figure 12 and plotted in Figures 13 and 14. The normalized load-settlement curves have been determined on the basis of the actual values of initial tangent moduli, maximum side resistance, f_{su}, and the base resistance at a settlement ratio of 1%, f_{b1}, as calculated in Section 4. A comparison of the normalized curves obtained from the test piles and the general envelopes suggested by Williams *et al.* (1980) indicate that the side resistance curve lies along the lower bound of the suggested envelope and that the base resistance curve lies slightly above the suggested envelope although in both cases the variation from the mean design basis is not large.

7 CONCLUSIONS

The construction and subsequent loading to failure of two test piles in extremely jointed rock has demonstrated that it is practicable and economic to use rock socketed piles in such conditions, provided that the investigation, design and construction stages are carefully matched to the rock conditions. In order to provide the basis for a sound design, it was found useful to relate the strength and modulus properties of the rock mass to the joint frequency, and it was found that the pressuremeter test was an appropriate means of achieving this.

The results of the test piles and the proof loading of the service piles indicated that proof loading the piles caused a marked increase in the rock modulus and a corresponding decrease in subsequent pile settlement, thus demonstrating the usefulness of proof loading foundations in extremely jointed rock to ensure that settlements under service conditions do not exceed the settlement criteria.

Although the two test piles were constructed in extremely jointed rock, the load-settlement curves were found to agree well with the normalized design curves suggested by Williams *et al.* (1980).

8 ACKNOWLEDGEMENT

This paper is presented with the kind permission of the Chairman of the Country Roads Board of Victoria, Mr. T.H. Russell.

9 REFERENCES

DEERE, D.U., HENDRON, A.J., PATTON, F.D. and CORDING, E.J. (1966). Design of surface and near surface construction in rock. Failure and Breakage of Rock. 8th Symp. on Rock Mech. Univ. of Minnesota.

GIBSON, R.E. and ANDERSON, W.F. (1961). In situ measurements of soil properties with the pressuremeter. Civ. Eng. and Pub. Works Review. V56. pp. 615-618.

HOBBS, N.B. (1974). Factors affecting the prediction of settlement of structures on rock with particular reference to the Chalk and Triass. Settlement of Structures. Pentech Press, London, p. 579-610.

HVORATH, R.G. (1978). Field load test data on concrete-to-rock bond strength for drilled pier foundations. Univ. of Toronto Dept. of Civ. Eng. Pub. No. 78-07.

LAMA, R.D. (1974). The uniaxial compressive strength of jointed rock. Inst. of Soil Mech. and Rock Mech. Univ. of Karlsruhe.

MANEV, G. and AVRAMOVA-TACHEVA, E. (1970). On the evaluation of strength and resistance condition of the rocks in natural rock massif. Proc. 2nd Congr. Int. Soc. Rock Mech. Belgrade. Vol. 1, pp. 59-65.

NEILSON, J.L. (1970). Notes on weathering of Silurian rocks of the Melbourne District. Jnl. I.E. Aust. Vol. 42, pp. 9-12.

PARKIN, A.K. and DONALD, I.B. (1975). Investigations for rock socketed piles in Melbourne mudstone. Proc. 2nd Aust.-N.Z. Conf. on Geomechanics, Brisbane, I.E. Aust. Pub. No. 75/4, pp. 195-200.

PARRY, R.G.H. (1970). Triaxial tests on Melbourne mudstone. Jnl. I.E. Aust. Vol. 42, pp. 5-8.

PELLS, P.J.N., DOUGLAS, D.J., RODWAY, B., THORNE, C. and McMAHON, B.K. (1978). Design loadings for foundations on shale and sandstone in the Sydney Region. Aust. Geomech. Jnl. Vol. G8, pp. 31-39.

PELLS, P.J. and TURNER, R.M. (1978). Theoretical and model studies related to piles and footings on rock. Univ. of Sydney, School of Civ. Eng. Research Report No. R314.

POULOS, H.G. and MATTES, N.S. (1975). A theoretical examination of errors in measured settlements of test piles. Proc. 2nd Aust.-N.Z. Conf. on Geomechanics, Brisbane. I.E. Aust. Pub. No. 75/4, pp. 174-178.

ROSENBERG, P. and JOURNEAUX, N.L. (1976). Friction and end bearing tests on bedrock for high capacity socket design. Can. Geotech. Jnl., Vol. 13.

WALKER, L.K., PECK, W.A. and BAIN, N.D. (1975). Application of pressuremeter testing to weathered rock profiles. Proc. 2nd Aust.-N.Z. Conf. on Geomechanics. Brisbane. I.E. Aust. Pub. No. 75/4, pp. 287-291.

WALKER, L.K. (1978). Analysis of some pressuremeter results obtained in Melbourne's Silurian mudstones. Symp. Engineering Properties of Melbourne Mudstone. Aust. Geomech. Soc. Vic. Group. Contribution No. 5.

WILLIAMS, A.F. and PELLS, P.J.N. (1979). The design of side resistance rock sockets in sedimentary rock. Proc. Concrete 79. Concrete Inst. of Australia.

WILLIAMS, A.F., JOHNSTON, I.W. and DONALD, I.B. (1980) The design of piles socketed into weak rock. Int. Conf. on Structural Foundations on Weak Rock. Sydney. A.A. Balkema, Netherlands.

WILLIAMS, A.F. (1980). The design and performance of piles socketed into weak rock. Ph.D. Thesis. Dept. Civ. Eng., Monash University.

Investigation of Soft Foundations with Surface Reinforcement

H. OHTA
Associated Professor, Dept of Civil Engineering, Kyoto University
R. MOCHINAGA
Manager, Engineering Dept, Sapporo Construction Bureau, Japan Highway Public Cooperation
N. KURIHARA
Senior Engineer, Sapporo Construction Bureau, Japan Highway Public Cooperation

SUMMARY Transverse surface reinforcements at the bottom of embankments placed on very soft foundations are found to reduce the amount of deformation of the foundations and improve the bearing capacities through the elastic-plastic finite element analysis on an idealized model of soft foundation as well as on a field trial embankment.

1 INTRODUCTION

It is being found, through field tests to improve bearing capacities and rigidities of soft foundations loaded by embankments, that restrictions on lateral movements of the ground surface beneath the load (such restrictions caused by steel reinforcements at the bottom of the embankments or at the surface of the soft ground) can be effective in increasing the bearing capacity and decreasing the undrained settlement (due mainly to lateral flow of soft material beneath the load). This lateral reinforcement has been achieved by using either strips, nets, bars or beams of steel or chemical or natural materials such as nylon or glass fibers or bamboo-fascines; Kawakami et. al. (1967), Eide and Holmberg (1972).

The effect of this sort of transverse reinforcement at the bottom of an embankment will depend not only on the material properties of the soft foundation but also on the geometry of the cross section of the fill and the stratification of the soft materials, especially on the ratio of the width of the embankment to the thickness of soft soil layer. This paper presents an investigation of the effectiveness of surface reinforcements, by the use of finite element computations on undrained behaviour and subsequent two dimensional consolidation deformation of loaded soft foundations with and without surface reinforcements, focusing on the width/thickness ratio while material properties are held constant throughout the investigation.

The constitutive equation employed in the finite element computations is an infinitesimal elastic-plastic stress-strain relation which is reduced to the Original Cam Clay model (Roscoe, Schofield and Thurairajah 1963) under conditions of isotropic initial stress state and which is able to describe the anisotropic behaviour of clay including the complicated responses to the rotation of principal stress directions as discussed by Sekiguchi and Ohta (1977) and by Ohta and Sekiguchi (1979).

2 CONSTITUTIVE EQUATION

2.1 Stress Parameters

It is convenient to introduce the stress parameters to appear in the following sections before discussing the details of the constitutive equation employed in the computations. The effective stress tensor σ'_{ij} is divided into two components; hydrostatic component p and deviatoric component s_{ij} where ij denotes (i,j) component of a tensor,

$$p=\frac{1}{3}\sigma'_{ij}\delta_{ij} \qquad (1) \qquad\qquad s_{ij}=\sigma'_{ij}-p\delta_{ij} \qquad (2)$$

δ_{ij} in Eqs.(1) and (2) is Kronecker's delta. In the Sekiguchi-Ohta model a new parameter "pressure-normalized deviatoric stress tensor η_{ij} is employed,

$$\eta_{ij}=\frac{s_{ij}}{p} \qquad (3)$$

The pressure-normalized deviatotric stress tensor at the end of Ko-consolidation is defined as

$$\eta_{ij0}=\frac{s_{ij0}}{p_0} \qquad (4)$$

where s_{ijo} and p_o are deviatoric stress and hydrostatic effective stress at the end of consolidation. The ratio of shear stress to hydrostatic effective stress can be defined in terms of pressure-normalized deviatoric stress tensor as

$$\eta^*=\sqrt{\frac{3}{2}(\eta_{ij}-\eta_{ij0})(\eta_{ij}-\eta_{ij0})} \qquad (5)$$

2.2 Material Constants

The material constants used in the Sekiguchi-Ohta model are introduced here,

1. λ and κ: parameters representing compressibility of soil respectively defined as 0.434Cc and 0.434Cs where Cc and Cs are compression and swelling indices,
2. D: parameter representing dilatancy of soil defined by Shibata (1963). In the Original Cam Clay model a parameter M is used (instead of D) which is related to D through

$$M=\frac{\lambda-\kappa}{D(1+e_0)} \qquad (6)$$

3. e_o: void ratio of soil isotropically or anisotropically consolidated with pressure of p_o. In the Original Cam Clay model p_o is taken as a unit value of pressure. However this discrepancy in the definition of p_o and hence of e_o is not essential.

2.3 Plastic Potential Function

The plastic potential function f assumed in the Sekiguchi-Ohta model is defined as

$$f=\frac{\lambda-\kappa}{1+e_0}\ln\frac{p}{p_0}+D\eta^*-v^p \qquad (7)$$

where hardening parameter v^p is the plastic volumetric strain. It may be appropriate to note that the yielding should occur when the principal stress directions rotate while both the effective hydro-

static pressure and the octahedral shear stress are kept fixed at the values of those at the end of Ko-consolidation, according to the Sekiguchi-Ohta model, because the value of stress ratio parameter η^* can increase by the rotation of principal stress directions. This does not mean that the model has lack of frame indifference, however, since the stress ratio parameter η^* is a scalar.

2.4 Stress-Strain Matrix (General)

The stress-strain matrix used in solving elastic-plastic problems by means of finite element method is derived here employing a technique proposed by Yamada, Yoshimura and Sakurai (1968). The elastic part of the stress-strain relation can be written in an incremental form as

$$d\sigma'_{ij} = D^e_{ijkl}(d\epsilon_{kl} - d\epsilon^p_{kl}) \tag{8}$$

where D^e_{ijkl} is the elastic stress-strain matrix and ϵ_{kl}, ϵ^p_{kl} are the total strain tensor and its plastic component respectively. The plastic component of strain increment is given as

$$d\epsilon^p_{ij} = \Lambda \frac{\partial f}{\partial \sigma'_{ij}} \tag{9}$$

where plastic potential function f is a function of the effective stress tensor and of hardening parameter L, i.e.

$$df = \frac{\partial f}{\partial \sigma'_{ij}} d\sigma'_{ij} + \frac{\partial f}{\partial L}\frac{\partial L}{\partial \epsilon^p_{ij}} d\epsilon^p_{ij} \tag{10}$$

A proportional function Λ is given by substituting Eqs.(8) and (9) into Eq.(10) as follows,

$$\Lambda = \frac{f_{ij} D^e_{ijkl} d\epsilon_{kl}}{\left(f_{ij} D^e_{ijkl} - \frac{\partial f}{\partial L}\frac{\partial L}{\partial \epsilon^p_{kl}}\right) f_{kl}} \tag{11}$$

where

$$f_{ij} = \frac{\partial f}{\partial \sigma'_{ij}}$$

Substituting Eqs.(9) and (11) into Eq.(8), we get a general form of the elastic-plastic stress-strain matrix as

$$d\sigma'_{ij} = (D^e_{ijop} - D^p_{ijop}) d\epsilon_{op} \tag{12}$$

where

$$D^p_{ijop} = D^e_{ijop} \frac{f_{mn} D^e_{mnop} f_{kl}}{\left(f_{mn} D^e_{mnqr} - \frac{\partial f}{\partial L}\frac{\partial L}{\partial \epsilon^p_{qr}}\right) f_{qr}} \tag{13}$$

If we adopt an incrementally linear isotropic elasticity in the elastic stress-strain matrix, we get

$$D^e_{ijop} = \bar{\lambda}\delta_{ij}\delta_{op} + \bar{\mu}(\delta_{io}\delta_{jp} + \delta_{ip}\delta_{jo}) \tag{14}$$

where $\bar{\lambda}$ and $\bar{\mu}$ are Lame's constants. Substituting the thus obtained Eq.(14) into Eq.(13), the plastic stress-strain matrix is reduced to

$$D^p_{ijop} = \frac{A_{ijop}}{B - C} \tag{15}$$

where

$$A_{ijop} = \bar{\lambda}^2 f_{kk}^2 \delta_{ij}\delta_{op} + 2\bar{\lambda}\bar{\mu} f_{kk}(f_{ij}\delta_{op} + f_{op}\delta_{ij}) + 4\bar{\mu}^2 f_{ij} f_{op} \tag{16}$$

$$B = \bar{\lambda} f_{mm} f_{qq} + 2\bar{\mu} f_{qr} f_{qr} \tag{17}$$

$$C = \frac{\partial f}{\partial L}\frac{\partial L}{\partial \epsilon^p_{qr}} f_{qr} \tag{18}$$

2.5 Stress-Strain Matrix (Sekiguchi-Ohta model)

The plastic stress-strain matrix can be specified through Eqs.(15)-(18) by calculating both f_{ij} which appears in these equations and C in Eq.(18). Differentiating the plastic potential function given by Eq.(7), we get

$$f_{ij} = \frac{D}{3p}\left(\frac{\lambda - K}{(1+e_o)D} - \frac{3}{2\eta^*}\frac{S_{kl}}{p}(\eta_{kl} - \eta_{klo})\right)\delta_{ij} + \frac{3D}{2\eta^* p}(\eta_{ij} - \eta_{ijo}) \tag{19}$$

$$C = -f_{qq} \tag{20}$$

By the use of Eqs.(19) and (20) we can specify all the components of the plastic stress-strain matrix.

3 FINITE ELEMENT COMPUTATIONS

3.1 Computer Programme

The computer programme employed in this investigation is the one originally written by Akai and Tamura (1976) for the model proposed by Ohta (1971) and Ohta, Yoshitani and Hata (1975) and afterwards modified by Tamura for the Sekiguchi-Ohta model which is employed in this investigation. Finite element formulation used in the Akai-Tamura programme is developed by adopting the technique proposed by Christian (1968) and Christian and Boehmer (1970). Although Christian used the forward finite difference scheme in his analysis of consolidation processes, the Akai-Tamura programme emp'oys the backward finite difference scheme so as t ensure better stability in computations.

3.2 Models Analysed

Imaginary embankments with and without the t ansverse reinforcement at the bottom of the fill placed on an imaginary uniform soft clay layer underlain by a very hard sand are analysed in order to estimate the effect of surface reinforcement on the deformability and the bearing capacity of soft clay foundation. The dimensions of the embankment are 20m in shoulder to shoulder distance and 40m in toe to toe distance. The weight of the embankment is chosen to be $100kN/m^2$. The soft clay layer is assumed to be a slightly overconsolidated one which was consolidated under conditions of no lateral deformation with the vertical effective preconsolidation pressure σ'_{vo} of $90kN/m^2$. The current effective overburden pressure σ'_{vi} is $75kN/m^2$, i.e. the overconsolidation ratio is 1.2.

Analyses were carried out for 8 cases which are classified into two groups, one of which is without surface reinforcement and the other of which is the cases with reinforcement. Each group consists of 4 cases distinguished by the thickness H of the clay layer (H=5m, 10m, 15m, 20m) so that the effect of the ratio of the fill width and the thickness of soft layer is studied. It is generally estimated that the Young's modulus E of well compacted fill is between $E=20,000kN/m^2$-$30,000kN/m^2$. However in this investigation the rigidity of the fill itself is ignored for simplicity, i.e. the fill is substituted by a vertical load. The transverse reinforcement at the bottom of the embankment is replaced by an elastic band of 0.5m thickness, the elastic parameters of which are assumed to be $E=1,000,000kN/m^2$ and Poisson's ratio=0.3. Loading is incremental (20 steps) under fully undrained conditions and subsequent consolidation processes are computed stepwise through 40 steps.

The clay layer is assumed to be uniform, i.e., a particular set of material parameters and effective stress states both at the end of pre-consolidation and at the moment just before loading is assigned to the clay regardless of the depth. Although this assumption is not very realistic, it provides a simpler and clearer comparison between the performance

of reinforced fill and unreinforced fill placed on a thin clay layer as well as on a thick clay layer. The clay layer is assumed in this investigation to have been anisotropically (Ko=0.5) preconsolidated with the effective vertical stress of 90kN/m^2 (e_o= 1.5) and then have been brought to a slightly over-consolidated state with the current effective overburden pressure of 75kN/m^2 (coefficient of earth pressure at rest is assumed to remain at 0.5). The material parameters are λ=0.231, κ=0.042, D=0.053, permeability=5x10^{-5} m/day. During the consolidation process, the pore water is allowed to drain either from the surface or from the bottom of the soft clay layer.

3.3 Computed Results

Figs.1 (a) and (b) show the settlement of the surface of the clay layer beneath the centre of the embankment during undrained loading and the subsequent consolidation process for the case of unreinforced fill and of reinforced fill, respectively.

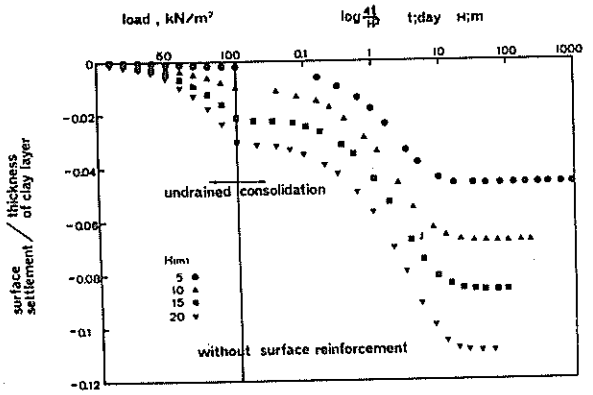

(a) Unreinforced fill

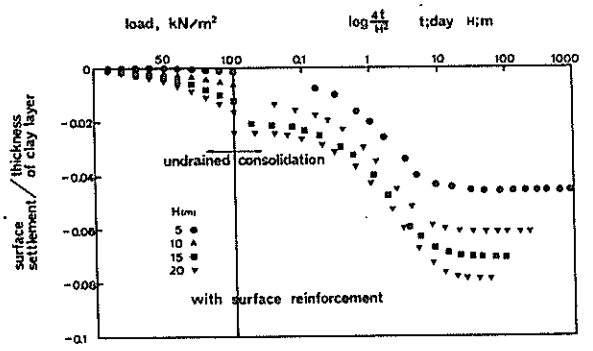

(b) Reinforced fill

Figure 1 Settlement at the centre of fill

From the above model and computations, it is found that the surface reinforcement reduces the settlement both for undrained and drained consolidation processes.

Figs.2 (a) and (b) show the overall patterns of surface settlement for both cases. It is also clear that the surface reinforcement reduces the settlement of the embankment and the heave of the ground surface adjacent to the embankment. It may be noteworthy that the settlement of the centre of the fill is much less than the settlement of the shoulder of the fill in the case of thin soft clay layer, especially for unreinforced fill.

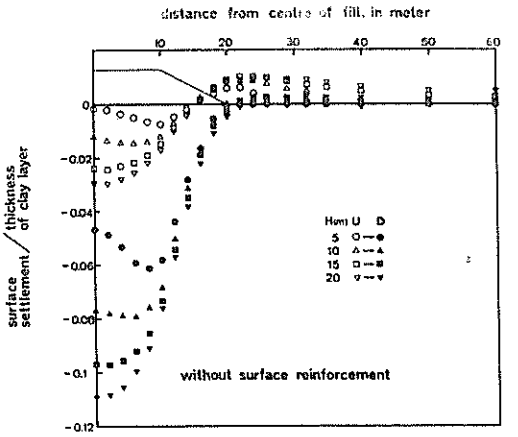

(a) Unreinforced fill

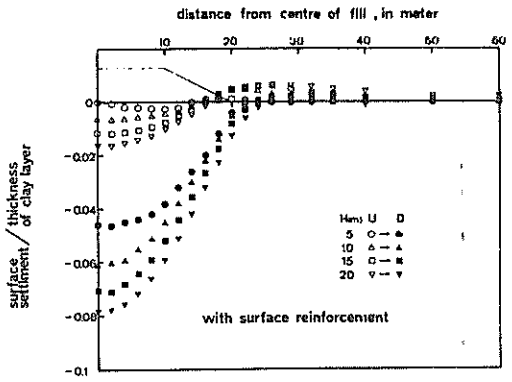

(b) Reinforced fill

Figure 2 Patterns of surface settlement at the end of undrained loading (U) and consolidation (D)

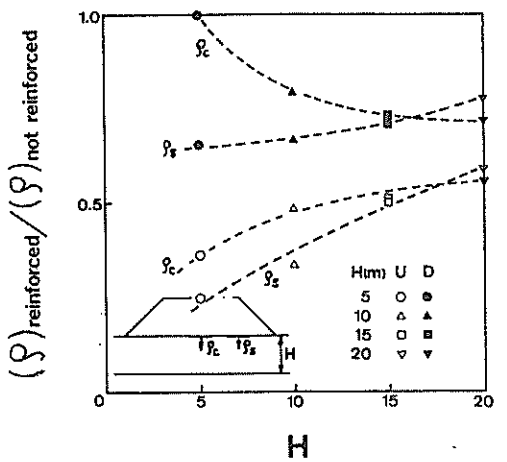

Figure 3 Settlement reduction effect of surface reinforcement

Summarizing the results shown in Figs.1 and 2, the settlement reduction effect of surface reinforcement can be roughly estimated through Fig.3 where the settlement reduction ratio is defined by the settlement of reinforced fill divided by the settlement of unreinforced fill. The surface settlements beneath the centre and beneath the shoulder of the fill are denoted by ρ_c and ρ_s respectively. Generally speaking, the surface reinforcement is more effective in reducing the undrained settlement, shown by white

marks plotted in Fig.3, below drained settlement (black marks). Fig.3 also shows the better performance of surface reinforcement in the case of thinner clay layer rather than in the case of thicker clay layer, both for undrained and drained settlement in general. The reduction of drained settlement caused by the surface reinforcement can be explained as the consequence of a smaller amount of volume decrease due to the dilatancy characteristics accompanied by distortional deformation of clay.

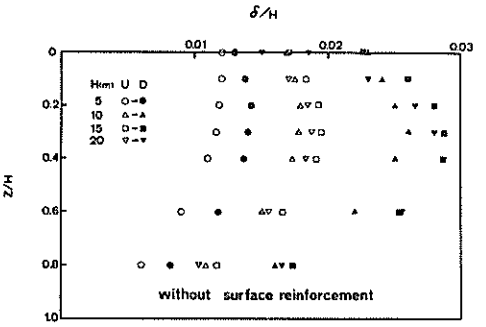

(a) Unreinforced fill

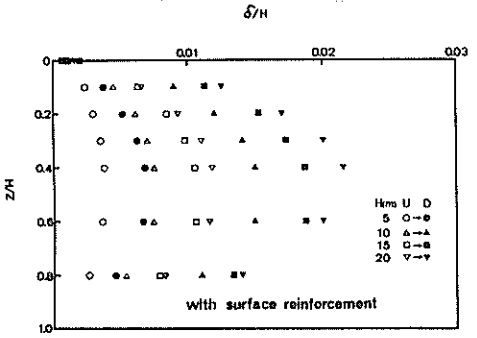

(b) Reinforced fill

Figure 4 Horizontal displacement beneath the toe of the embankment

The horizontal displacement of the points initially located on a vertical line beneath the toe of the fill are plotted in Figs.4 (a) and (b) showing that the surface reinforcement reduces the horizontal displacement not only at the surface of soft clay but also at any depth, both in the case of undrained loading and of fully drained.

All the Figs.1-4 suggest that the surface reinforcement is effective in reducing the amount of deformation of soft clay layer loaded by an embankment. However we are interested in estimating the effect of surface reinforcement on the bearing capacity of the soft foundation as well as its deformability. Unfortunately, the ultimate bearing capacity of a soft clay layer can hardly be estimated by finite element computations. In this investigation an indirect method of estimating the bearing capacity proposed by Matsuo and Kawamura (1974) is employed. Based on a great deal of data obtained from a number of trial embankments placed on various type of soft foundations, they found the existence of a very narrow band which they called the "failure criterion curve" on a diagram the ordinate of which was the settlement ρ of the ground surface at the centre of the fill and the abscissa of which was the horizontal displacement δ of the ground surface at the toe of the fill divided by ρ. According to them, it is a serious warning when ρ-δ/ρ plot measured during construction of a fill comes very near to the failure criterion curve. This warning may be only a crude guidance for possible failure of foundations, and the theoretical background of their proposal is still open to question. However, additional case studies carried by Matsuo and Kawamura (1977) and Matsuo, Kuroda, Asaoka and Kawamura (1977) show that their failure criterion curve gives a reasonable prediction of failure of an embankment for either rapid or very slow loading process.

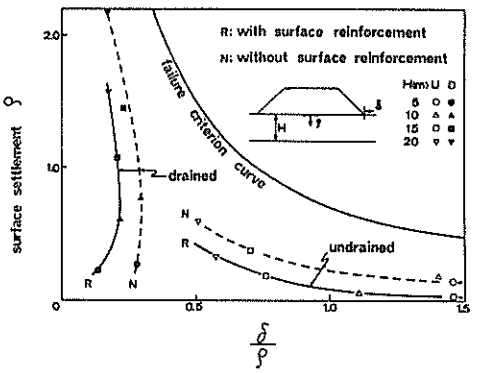

Figure 5 Foundation stabilizing effect of surface reinforcement

Fig.5 shows the stability estimations of the fill with and without surface reinforcement for either the undrained loading process or the fully drained state. In each case the plots for the reinforced embankment are located farther from the failure criterion curve in Fig.5 showing that the reinforced embankments are safer than the embankments without the reinforcement. The computed horizontal displacements at the toes of the reinforced embankments are very small as shown in Fig.4 (b) and consequently give very small values of δ/ρ. Plotting Fig.5, the horizontal displacement δ of the reinforced fill is calculated by multiplying the maximum value of horizontal displacement among those points located on the vertical line beneath the toe of the reinforced embankment by the ratio of the horizontal displacement at the surface of the ground to that at a depth where the largest horizontal displacement is induced for the unreinforced embankment. Thus obtained equivalent horizontal displacements at the toe of the embankment are plotted in Fig.5 showing a conservative estimate of the effect of the reinforcement on the increase in stability. Fig.5 does not give a quantitative increase in the factor of safety due to the surface reinforcement. However we see in Fig.5 a general tendency of the effectiveness of surface reinforcement.

Although the results discussed above are only computational results of an idealised model and not reality, we can still conclude that surface reinforcement is effective in reducing the deformation of soft foundation and in stabilising the embankment as well.

4 FIELD TRIAL EMBANKMENT

4.1 Trial Embankment at Ebetsu

A trial embankment was placed on a very soft layer of peat and clay at Ebetsu, Hokkaido in order to obtain data of settlement and of stability of a newly proposed motorway from Sapporo to Iwamizawa (32 km) about 85% of which was to be high embankment (5 -8m) on very soft layer of peat and clay (20-35m thick). The trial embankment, 386.3m long, was divided into 4 sections; natural ground section, surface reinforcement section with sand drain treatment, sand compaction pile section and chemical pile section, each of which was about 50m.

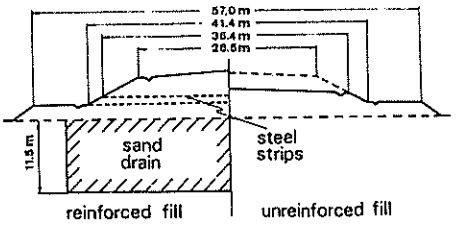

Figure 6 Cross sectional views of trial embankment

The cross sectional views of natural ground section and surface reinforcement section are shown in Fig. 6 where we see the sand drain treatment under the surface reinforcement section. These sections were to be loaded up to the fill height of about 8.5m above the original ground surface. The reinforced section was raised to the proposed height without having any cracks, but the natural ground section had a major crack (0.1m wide, 10m long) along the centre line of the fill accompanied by two minor cracks along the line joining the main body of the fill with the berm on both sides of the embankment when the fill height was about 3.5m above the original ground surface. After finding these cracks, the natural ground section was left without any additional loading while the other three sections underwent further loading.

Table I Parameters used in computation

type of soil	peat	clay with peat	sand	silty clay	sand	silty clay	sand	silty clay
depth m	0 - 3 0 - 4	3 - 6 4 - 6	6 - 7 6 - 8	7 - 9 8 -10	9 - 11 10-11	11 - 18	18-19	19 -30
λ	1.73	0.35	0.06	0.22	0.06	0.17	0.06	0.17
κ	0.17	0.13	0.02	0.12	0.02	0.06	0.01	0.06
D	0.11	0.08	0.02	0.06	0.02	0.05	0.02	0.05
σ'_{vo} kN/m²	20	50	200	70	200 450	180	1170	180
e_o	7	1.6	0.8	1.2	0.8	1.1	0.7	1.1
K_o	0.6	0.6	0.6	0.6	0.6	0.6	0.6	0.6
σ'_{vi} kN/m²	1	9 7	20	31 35	20 46	85 80	120 115	172 167
K_I	1.4	1.1	0.6	0.75	0.6	0.76	0.6	0.6
permeability k_{v} m/day	6×10^{-3} 10^{-3}	4.2×10^{-3} 7×10^{-4}	21 3.5	6×10^{-3} 10^{-3}	21 3.5	7×10^{-4}	3.5	7×10^{-4}

upper column for reinforced fill; lower column for unreinforced fill

Because this example was considered somewhat extreme and perhaps unpresentative, it was decided to carry out an analysis employing the computer programme introduced in the previous section. The material parameters for peat and clay were determined as follows: (1) λ from Cc value obtained from oedometer tests, (2) M in Eq.(6), which is related to ϕ' value , is calculated from c_u/p value estimated in laboratory tests, (3) Cs/Cc is calculated from an empirical equation 1-Cs/Cc=M/1.75 proposed by Karube (1975). For sand we determined ϕ value from which M is obtained leading to the value of Cs/Cc through Karube's equation. Although the value of Cc or Cs was not obtained in the laboratory tests for sand, the value of λ was determined in a way the authors thought reasonable without having any objective justification. The sand layers were treated as if they were overconsolidated with an overconsolidation ratio of 10. The permeabilities of peat, clay and sand were assumed to be 10 times those obtained from oedometer tests or from permeability tests for natural ground and 60 times for the ground with sand drain treatment. All the parameters used in the computations are listed in Table I. The surface reinforcement was replaced by a 1.2m thick elastic band ($E=2.2\times10^5$ kN/m^2, Poisson's ratio=0.3).

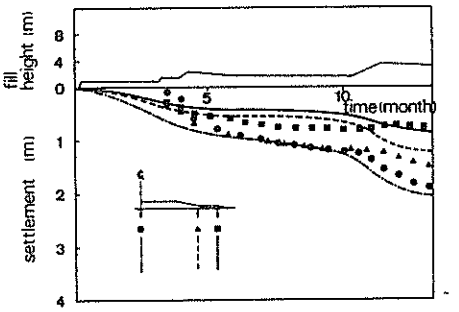

(a) Unreinforced section

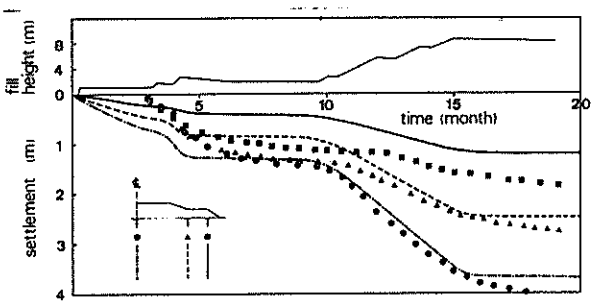

(b) Reinforced section

Figure 7 Settlement-time relations

Fig.7 shows the general tendency of the settlement-time relations both for the natural ground section and the surface reinforcement section. The computed curves roughly agree with measured settlements shown by the plots in Fig.7.

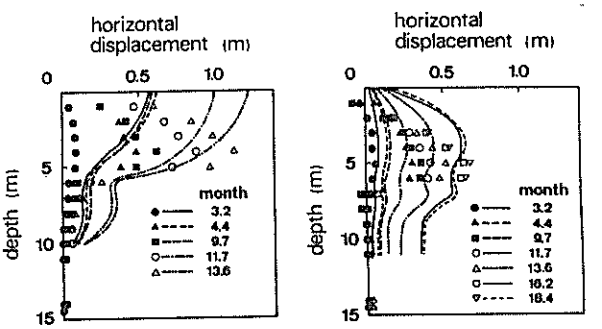

(a) Unreinforced section (b) Reinforced section

Figure 8 Horizontal displacement at the toe of embankment

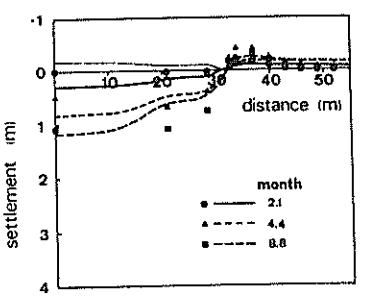

(a) Unreinforced section

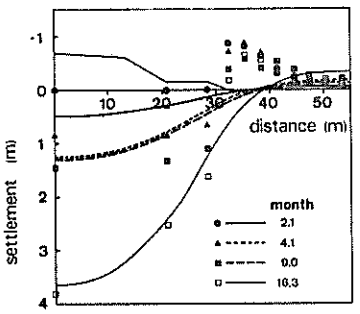

(b) Reinforced section
Figure 9 Surface settlement

Figs.8 and 9 show the general patterns of horizontal displacement of the points initially located on a vertical line beneath the toe of the fill and of the settlement of the ground surface (plots for measured and curves for computed). Because the fills are replaced by vertical loads in the computation the horizontal displacement near the surface of the ground in the case of unreinforced fill is computed to be larger than measured displacement. However it seems to the authors that the computed results are acceptable and that this acceptable performance of the computation gives some support to the discussions in the previous section derived from the same computer programme employed in the analysis presented in this section.

5 CONCLUSIONS

A finite element analysis of an idealized model suggests that the transverse surface reinforcement at the bottom of an embankment placed on a very soft foundation can considerably reduce the amount of deformation of the foundation and improve the bearing capacity. The performance of a field trial embankment demonstrating the effectiveness of surface reinforcement is introduced and back-analysed, with reasonable agreement, by means of a finite element technique exactly the same as the one employed in the analysis of the idealized model. As the result of these investigations, it is concluded that the transverse surface reinforcement is one possible technique to improve the undesirable characteristics of soft foundations.

6 ACKNOWLEDGEMENTS

It is acknowledged that the finite element computations reported in this paper were carried out using the FACOM M200 digital computer of the Computer centre, Kyoto University. Some of the studies described in this paper were supported by a grant (No. 3851 43, 1978-1979) from the Ministry of Education.

7 REFERENCES

AKAI, K. and TAMURA, T. (1976). An application of nonlinear stress-strain relations to multi-dimensional consolidation problems. Annuals, Disaster Prevention Research Institute, Kyoto Univ., No.19, B-2, pp 15-29, (in Japanese).

Christian, J.T. (1968). Undrained stress distribution by numerical method. Proc.A.S.C.E., SM 6, pp 1333-1345.

CHRISTIAN, J.T. and BOEHMER, J.W. (1970). Plane strain consolidation by finite elements. Proc.A.S.C.E., SM 4, pp 1435-1457.

EIDE, O. and HOLMBERG, S. (1972). Test fills to failure on the soft Bangkok clay. Proc. Specialty Conf. on Performance of Earth and Earth-Supported Structures, Vol.1, Part 1, pp 159-180.

KARUBE, D. (1975). Unstandardized triaxial testing procedures and related subjects for inquiry. Proc. 20th Symp. on Geotechnical Engineering, pp 45-60, (in Japanese).

KAWAKAMI, F., SATAKE, M., OGAWA, S., ITOH, T. and SATO, S. (1967). Stress measurement and analysis of H-shaped steel beam placed beneath a breakwater embankment in Ishinomaki Industrial Harbour. Journal of Japan Society for Soil MEch. and Found. Engrg, Vol.15, No.9, pp 15-19, (in Japanese).

MATSUO, M. and KAWAMURA, K. (1975). Study on modified method of design of embankment by observation during construction. Proc.J.S.C.E., No.240, pp 113-123, (in Japanese).

MATSUO, M. and KAWAMURA, K. (1977). Diagram for construction control of embankment on soft ground. Soils and Foundations, Vol.17, No.3, pp 37-52.

MATSUO, M., KURODA, K., ASAOKA, A. and KAWAMURA, K. (1977). Dynamic decision procedure of embankment construction. Proc. 9th Int. Conf. on S 'l Mech. Found. Engrg, Vol.2, pp 117-120.

OHTA, H. (1971). Analysis of deformations of soils based on the theory of plasticity and its application to settlement of embankments. Dr.Eng. Thesis submitted to Kyoto Univ.

OHTA, H., YOSHITANI, S. and HATA, S. (1975). Anisotropic stress-strain relationship of clay and its application to finite element analysis. Soils and Foundations, Vol. 15, No.4, pp 62-79.

OHTA, H. and SEKIGUCHI, H. (1979). Constitutive equations considering anisotropy and stress reorientation in clay. Proc. 3rd Int. Conf. on Numerical Methods in Geomechanics, Aachen, A.A.Balkema, Rotterdam, pp 475-484.

ROSCOE, K.H., SCHOFIELD, A.N. and THURAIRAJAH, A. (1963). Yielding of clays in states wetter than critical. Geotechnique, Vol.13, pp 211-240.

SEKIGUCHI, H. and OHTA, H. (1977). Induced anisotropy and time dependency in clays. Constitutive Equations of Soils, Proc. Specialty Session 9, Ninth Int. Conf. Soil Mech. Found. Engrg, Tokyo, pp 229-238.

SHIBATA, T. (1963). On the volume changes of normally-consolidated clays. Annuals, Disaster Prevention Research Institute, Kyoto Univ., No.6, pp 128-134, (in Japanese).

YAMADA, Y., YOSHIMURA, N. and SAKURAI, T. (1968). Plastic stress-strain matrix and its application for the solution of elastic-plastic problems by the finite element method. Int. J. Mech. Sci., Vol.10, pp 343-354.

The Use of Trial Embankment Observations in the Construction Control of Roadway Embankments on Soft Soil

N. F. ROBERTSON
Engineer, Main Roads Department, Queensland
I. N. REEVES
Engineer, Main Roads Department, Queensland

SUMMARY Measurements from an instrumented trial embankment were used to develop calibrated stability and settlement analysis models, for the behaviour prediction of high roadway embankments on soft soil. The analysis models were based on the relatively unsophisticated classical theories. The effective stress stability model was used to prepare a Stability Monitoring Diagram, which, in conjunction with very simple pore pressure and settlement measurements, was used to control the rate of filling the roadway embankments. The settlement model provided realistic estimates of settlement behaviour, and showed that surcharging was required to bring consolidation times within the available construction period. The embankments were successfully constructed under stability control without need of stabilisation measures, and primary consolidation effectively completed within the available construction period.

1 INTRODUCTION

The approaches to a new high level bridge over the Pioneer River at Mackay, Queensland included embankments up to 7 m high located over tidal river mudflats. The embankment foundations included varying depths of very soft organic silty clay alluvium overlying loose to dense sandy alluvium and stiff silty clay above bedrock.

The initial site investigation incorporated total stress stability analyses using peak undrained shear strengths, which showed that extensive toe berms, at least 2 m high, would be required to maintain stability of the high embankments during construction. Settlement analyses indicated that settlements in excess of 1 m would occur over 2 to 12 years. In order to more reliably define the expected behaviour of the proposed embankments, an instrumented trial embankment was constructed with the following general aims.

(i) Determine reliable insitu strength and consolidation data for use in prediction analyses.

(ii) Assess changes in the state of stability during and after construction and, if necessary, devise corrective or control measures for use with the roadway embankments.

(iii) Assess the settlement behaviour with a view to the reliable prediction of settlement behaviour for the roadway embankments.

This paper describes the development of stability and settlement analysis models, based on the trial embankment observations, and the application of these to the construction control of the roadway embankments.

Stability monitoring of daily construction, using Stability Monitoring Diagrams, has been described by a number of authors (e.g. Margason and Symons, 1969; Cook and Ingold, 1974; Cole, 1974; Symons, 1976), in which the most popularly used method of control is based on effective stress stability analyses relying, as input data, on excess pore pressure observations. The relevance of this technique to the control of the roadway embankment construction was recognised. However, practical necessity dictated that the aims of reliable prediction and control would have to be achieved by largely relying on the commonly available, relatively unsophisticated computer-based settlement and stability analytical tools, and on simple, limited scope but reliable instrumentation for the roadway embankments. Consequently, reliance was placed on calibration of the settlement and stability analytical models for the local situation, based on back-analysis of the trial embankment observations.

2 SITE DESCRIPTION

The soft compressible surface alluvium consisted predominantly of silty clay, and varied in thickness from 2 m to 9 m across the site. A continuous silty sand layer, between 0.2 m and 1.8 m thick, existed over the site within the silty clay below a depth of 1.5 m to 3.0 m, and numerous other thin sandy lenses of unknown continuity were observed within the silty clay. A typical profile is shown in Figure 1 together with moisture content data and undrained shear strengths from field shear vane tests. The silty clay is highly sensitive (sensitivity range 4-34), with mean sensitivity of 15. The sensitivity is reflected in the apparent high state of liquidity shown by the moisture content and plasticity results. Extensive consolidated undrained triaxial testing was carried out from which representative (c', ϕ') values were selected (Figure 1) for effective stress stability analyses.

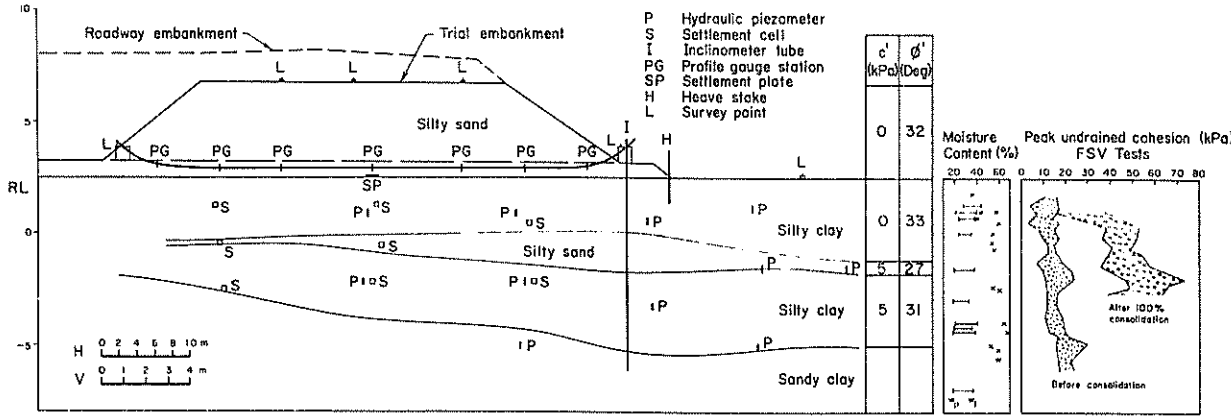

Figure 1 Typical subsurface details and trial embankment instrumentation

Insitu undrained shear strengths were remeasured by field shear vane after completion of consolidation of the trial embankment. Strength increases of 3 to 5 times were recorded, and the sensitivity reduced to a mean of 8, and range of 2 to 16.

Laboratory consolidation tests were performed on 23 specimens (76 mm diameter) of silty clay, and the consolidation parameters (Coefficient of volume change m_v, and Coefficient of consolidation C_v) were statistically reduced, assuming log normal distributions (Lumb, 1968) at constant effective stress. The laboratory mean relationships with effective stress, and confidence limits are shown later in Figure 6, compared with insitu relationships derived from back-analysis of the trial embankment settlement.

3 EMBANKMENT DETAILS

The roadway embankments included approximately 700 m of 2 and 4 lane embankment over the soft soil foundation, incorporating a large intersection area, and with heights of 5-7 m. They were constructed between October, 1978 and June, 1979, using the stability and settlement control methods described in this paper.

The trial embankment consisted of a rectangular embankment, 100 m by 60 m at the base, with maximum 1 on 3 batters, which was located wholly within the limits of the final roadway embankments. The trial and final embankments had a common batter under which the instrumentation for stability and settlement monitoring was concentrated on three cross-sections. The instrumentation included hydraulic and pneumatic piezometers, horizontal profile settlement gauges under the embankment at ground surface, pneumatic settlement cells within the silty clay, vertical borehole inclinometers, settlement plates, heave stakes and survey stations. The instruments were selected with a view to portability of readout equipment and minimising obstructions to construction activities, and were mainly commercially available items from the United Kingdom. Monitoring positions for one cross-section are shown in Figure 1. The instrumentation and monitoring for the trial construction constituted a net additional cost to the project of approximately A$51,000.

The trial embankment was constructed during August-November, 1977. After raising to an initial 4.1 m height in 4 weeks, construction was halted because of instability indications, discussed later. A further 0.4 m was added after a 6 week break to allow some dissipation of pore pressure. Complete dissipation of excess pore pressures had occurred by November, 1978, i.e. approximately 12 months after the end of construction.

4 TRIAL EMBANKMENT STABILITY

The trial embankment instrumentation was designed to allow stability monitoring of construction on a daily basis, as well as to provide data for the detailed stability analysis of the roadway embankments. As the embankment was to be

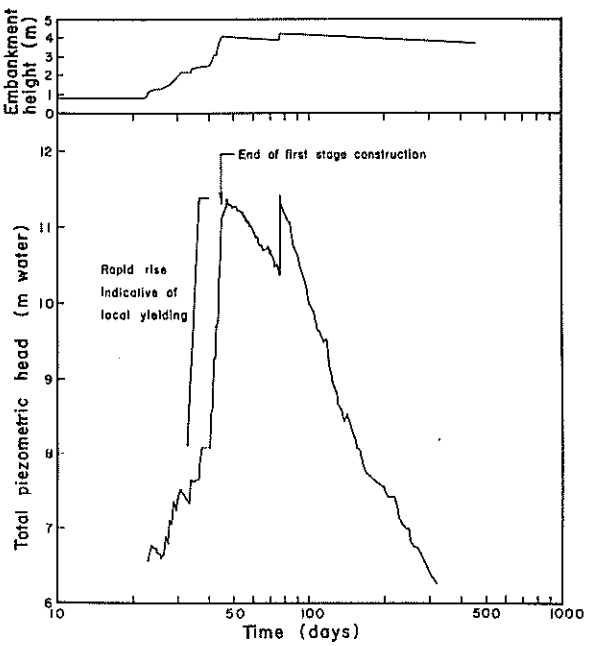

Figure 2 Example trial embankment piezometer response

incorporated within the final works, prevention of failure was of paramount importance. However, no specific failure criteria were defined for the trial. Reliance was placed on daily computer reduction, plotting and interpretation of a large volume of data covering pore pressures, inclinometer deflections, and vertical and horizontal surface survey in the vicinity of the toe, to detect significant trends.

An example of piezometric response under the centre of the embankment, related to loading history, is shown in Figure 2. All piezometers under the embankment showed a marked increase in rate of pore pressure rise above an embankment height of 2.5 m, indicative of local yielding

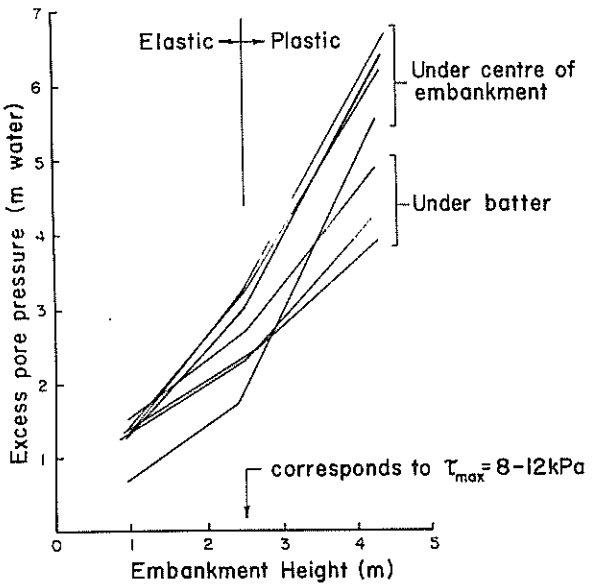

Figure 3 Excess pore pressure response with increasing embankment height

occurring within the silty clay. Pore pressures continued to rise during overnight breaks, and after construction was halted. The change in rate is also apparent in Figure 3, relating excess pore pressure to embankment height for piezometers under the centre of the embankment, and under the batter. Pore pressure changes within the pre-failure "elastic" region tend to be masked by concurrent dissipation. Within the plastic region, pore pressure changes are related to the major principal stress (Hoeg et al, 1969; D'Appolonia et al, 1971; Symons, 1976) by

$$\Delta u = \Delta \sigma_1 \quad (1)$$

The observed relationships are, under the centre of the embankment

$$\Delta u = (0.8 \text{ to } 1.0) \quad \Delta \sigma_1 \quad (2)$$

and under the batter (where the effects of dissipation are greater)

$$\Delta u = (0.6 \text{ to } 0.9) \quad \Delta \sigma_1 \quad (3)$$

Under the 2.5 m high embankment, the maximum shear stresses lie approximately in the range 8 to 12 kPa, which is within the observed range of insitu undrained shear strengths.

Stability analyses based on peak undrained shear strengths indicated on allowable initial height of 4.4 m for a factor of safety of 1.5. The first stage construction was halted at 4.1 m height, as a result of the observed pore pressure behaviour. At this stage, effective stress analyses using the measured excess pore pressures gave safety factors in the range 1.1 to 1.4. Shallow seated failure circles, within 2.5 m below ground surface, were indicated. This was supported by horizontal deformation measurements, showing maximum deformation occurring approximately at ground surface, and major shear deformation within a zone to 2.5 to 3.0 m below ground surface.

Other methods of instability detection, by interpretation of deformation measurements, were attempted and shown to be inconclusive. Interpretation of inclinometer data by the method of Wilkes (1974) showed that rates of change of maximum horizontal deformation with increasing embankment height appeared to decrease (rather than an expected increase) for the higher fill heights. A non-uniform rate of filling has affected the interpretation method, as there was evidence of a time lag between placing a fill layer, and detecting consequent horizontal deformation. Surface survey measurements in the vicinity of the toe were also inconclusive indicators, as any significant movements were completely masked by tidal movements.

5 ROADWAY EMBANKMENT STABILITY CONTROL

5.1 Monitoring Details

Roadway embankment construction above 3.5 m height was controlled using a stability monitoring diagram (SMD), prepared using effective stress analysis (with circular failure arcs) of stability models based on the trial embankment strength and excess pore pressure observations. Monitoring was performed at 10 locations under the embankment batters. At each location, measurements consisted of embankment height, pore

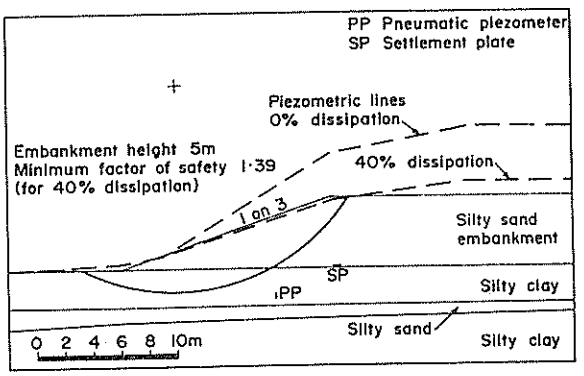

Figure 4 Typical monitoring section used for SMD preparation

pressure (using only 1 suitably located pneumatic piezometer), and settlement of ground surface above the piezometer. A typical arrangement is shown in Figure 4. The shallow nature of predicted failures, and the uniformity in depth of the upper silty clay layer, allowed the use of one SMD, shown in Figure 5, to cover all positions.

5.2 Construction of Stability Monitoring Diagram

The SMD relates embankment height, measured excess pore pressure at a point, and factor of safety. The essential points in derivation of the relationships for different embankment heights are as follows.

(a) The theoretical lateral distribution of undrained excess pore pressure was obtained for the mid-depth of the upper silty clay layer, using the classical Skempton theory with pore pressure parameters A = 0.7, B = 1.0, obtained from laboratory tests. This tended to over estimate the observed lateral distribution under the batters, a feature noted by Symons (1976). The observed undrained excess pore pressures were approximately constant with depth under the trial embankment.

(b) A "zero dissipation" piezometric line was obtained by subjectively adjusting the theoretical distribution line to account for lower excess pressure under the batter region.

(c) Piezometric lines representing other degrees of dissipation were obtained largely by proportion, but modified to account for observed lower rates of dissipation under the centre of the bank.

(d) Minimum factors of safety for combinations of embankment height and degree of dissipation were obtained and used to construct Diagram 2 of the SMD.

(e) The measured excess pore pressure at the piezometer was assumed to be equal to the single ordinate of the excess head piezometric line above the piezometer tip. The measured excess pore pressure was related to degree of dissipation and embankment height by constructing Diagram 1 of the SMD.

An allowable minimum factor of safety of 1.5 from the SMD was adopted for the following reasons.

(i) Factors of safety in the range 1.1 to 1.4 were obtained for the trial embankment, using the same calibrated stability model. Allowing the same degree of local yielding over the whole site was considered to be too high a risk.

(ii) Limited analyses with non-circular failure surfaces indicated factors of safety approximately 0.2 lower than those from the circular analysis. Shallow non-circular failures were considered more likely, but more difficult to analyse for the SMD development.

(iii) The silty clay was highly sensitive.

5.3 Observed Stability Behaviour

Factors of safety at all positions were in the range 1.5 to 2.0 throughout construction and no failures occurred. At most locations dissipation was relatively rapid, and only at one location did the stability control impede construction progress. At this location the SMD factor of safety was

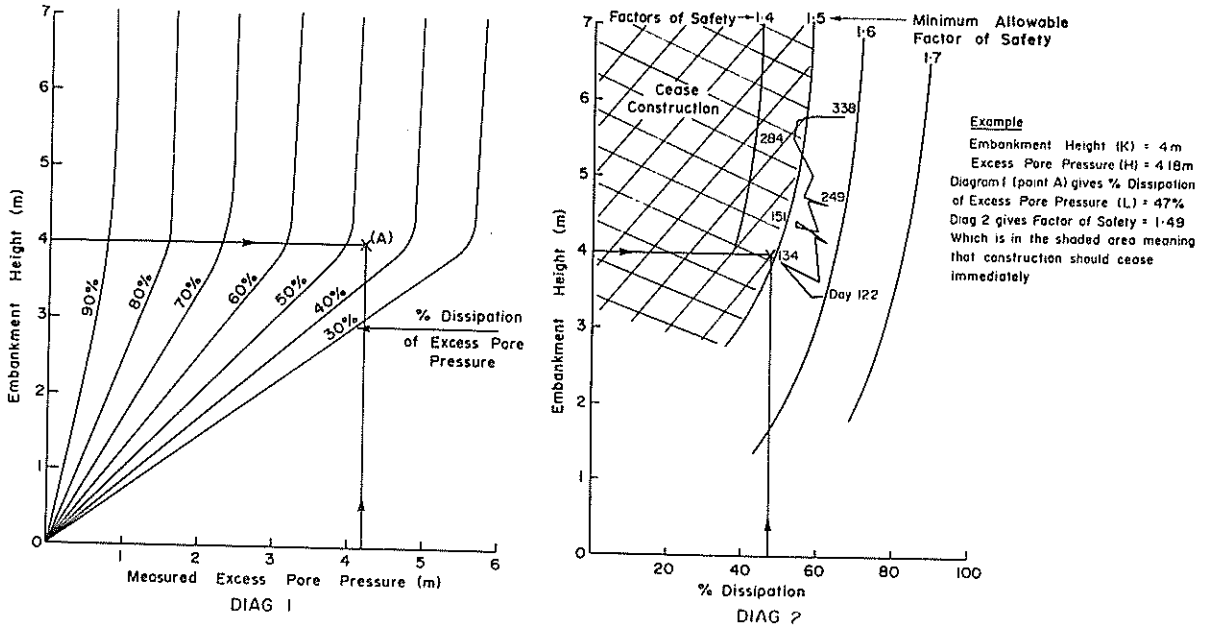

Figure 5 Stability Monitoring Diagram

consistently between 1.5 and 1.6 through most of the loading history (see Figure 5) and dissipation was slow. Detailed check calculations at Day 284, incorporating additional data from a second piezometer close to the monitored cross-section, showed a minimum factor of safety in the range of 1.47 to 1.74, depending on the assumed pore pressure distribution within a feasible range. The corresponding SMD result was 1.48 and was therefore conservative.

Major factors influencing the success of the adopted control method are the assumptions concerning excess head piezometric lines, with respect to lateral and depth pore pressure distributions, and the ability of a single piezometer to reliably characterise the whole excess pore pressure distribution. Local drainage effects at the piezometer tip would also have an important influence on results. For this reason, locations of piezometer tips free of the influence of sandy lenses were selected by use of static friction cone penetrometer soundings at each piezometer position.

While the control method has been successful in this case, universal application must be considered with caution, because of the abovementioned factors.

6 TRIAL EMBANKMENT SETTLEMENT BACK-ANALYSIS

6.1 The Settlement Analysis Model

All settlement analyses were to be carried out using a computer program based on the Terzaghi one-dimensional consolidation theory, in which variation in the consolidation parameters (m_v and C_v) with changes in effective stress are taken into account. Thus voids ratio vs effective stress p' (and therefore m_v vs p') and C_v vs p' relationships form part of the input data, together with soil profile and loading details. The aim of the trial embankment back-analysis was, therefore, to obtain "insitu" consolidation parameter relationships which, when used with the one-dimensional consolidation program, constituted a calibrated settlement model. This could then be applied to all parts of the roadway embankments, with differing soil depth profiles and differing embankment loading magnitudes and histories.

6.2 Consolidation Parameter Modelling

Back analysis of the trial embankment settlement behaviour was carried out using the measured time/settlement data for five profile gauge positions located within the embankment shoulders on one cross section, shown in Figure 1. Using the measured data, it was possible to model soil consolidation characteristics at each position (using the known soil profile and load history at the position) to give similar time/settlement behaviour. The aim was to obtain statistical mean consolidation parameter relationships representative of the five PG positions. These are here referred to as the insitu consolidation parameters, to be distinguished from the laboratory consolidation parameters.

The m_v vs p' relationship determines the predicted magnitude of settlement, while the C_v vs p' relationship determines the predicted time performance. In the back analysis for each PG position, assumed relationships were adjusted, firstly to achieve equality between predicted and measured final settlement, and secondly to achieve, as closely as possible, agreement throughout the time/settlement history. Equality in the final settlement was considered reasonable as primary consolidation was effectively completed (i.e. better than 95% dissipation of excess pore pressure). No allowance was made for possible secondary consolidation occurring in conjunction with primary consolidation.

It was found that, while different m_v vs p' relationships were obtained for each PG position, the same C_v vs p' relationship suitably predicted the time performance at all positions. The five m_v vs p' relationships were statistically reduced, using the log-normal distribution model, to yield an insitu mean relationship, which is shown in Figure 6, together with the 95% confidence interval. The adopted insitu C_v vs p' relationship is also shown. These relationships are compared with laboratory determined data.

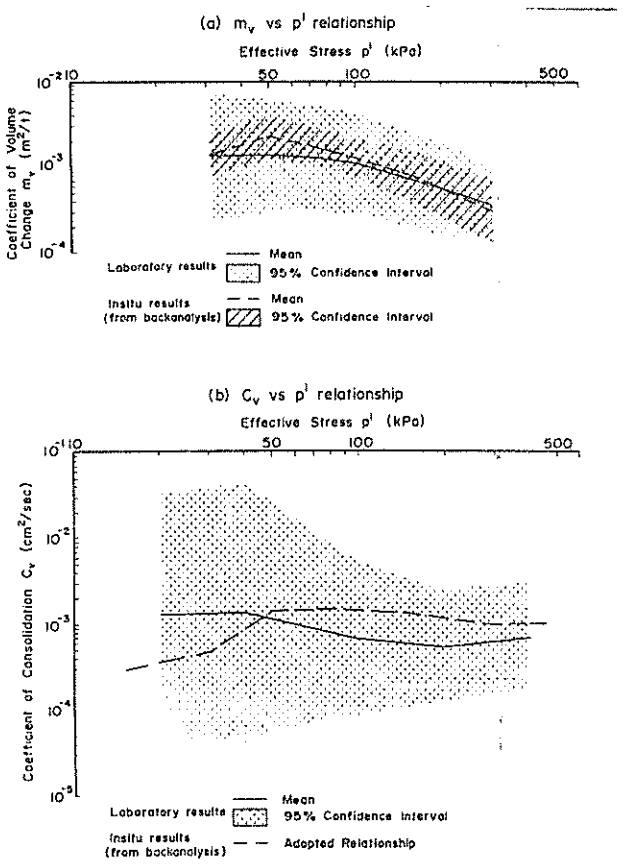

Figure 6 Consolidation parameter relationships

6.3 Comparison of Laboratory and Insitu Data

The confidence intervals obtained for the laboratory data are wide, particularly so in the case of the C_v relationship. This largely unavoidable factor is one of the principal sources of inaccuracy in predictions of settlement time and magnitude, when based on laboratory data.

Comparison of the laboratory and insitu m_v vs p' relationships in Figure 6 shows that the insitu mean values are slightly higher than the corresponding laboratory mean values, and that the 95% confidence interval is considerably narrower for the insitu results.

Both features of the insitu property result from the elimination of the sample disturbance factor present in the laboratory results, and the effect of inbuilt "vertical averaging" present in the insitu results, which are obtained from a surface settlement measurement over a considerable depth of compressible soil whose compressibility varies from point to point with depth.

The adopted insitu C_v vs p' relationship shown in Figure 6 is considerably higher than the laboratory mean relationship over the effective stress range (i.e. greater than 50 kPa) applicable to most of the loaded foundation. The laboratory C_v results are very sensitive to sample disturbance (causing reduction in apparent permeability) and are usually not representative of the apparent macro-permeability of the non-homogeneous soil mass. For this reason, settlement predictions based on laboratory C_v values commonly seriously over-estimate consolidation times.

Use of the insitu mean parameter relationships in an after-the-event prediction (Type C1, Lambe, 1973) of the behaviour of the PG positions results in predictive errors in final settlement, when compared with measurements, in the range 3 to 10% (mean 7%) for points between the embankment shoulders. The error becomes considerably larger for points under the batters, where the measured settlement was considerably less than the prediction. This is indicative of the limitations in the use of the one-dimensional consolidation theory under the batter regions of an embankment. However, generally, the settlements of consequence under a road embankment are those under the pavement, except, perhaps, when considering the deformed profile of a cross drainage pipe.

7 ROADWAY EMBANKMENT SETTLEMENT CONTROL

Settlement control was necessary to the extent that all significant primary consolidation was required to be complete by the end of 1979, so that paving and other finishing works could proceed early in 1980. There was thus a total available consolidation period, including a 6 month construction period, of 15 months. For comparison, the trial embankment primary consolidation was complete in 15 months, including a 3 month construction period.

Settlement predictions, using the calibrated analysis model, were made for all proposed roadway embankment monitoring positions, established for stability control. The insitu mean consolidation parameter relationships were used in the models. The calculations established that embankment surcharges of 1.0 m and 1.5 m (for the worst case) were required to achieve the timing objectives.

The measured behaviour has shown that the predictions have tended to overestimate both settlement rate and magnitude - i.e. the actual settlements have been smaller, and have occurred more slowly. An example of measured settlement/time curves, compared with the predictions, is shown in Figure 7. Settlement is not complete at the end of the measurements shown. In spite of the slower rate, the timing and settlement objectives will have been satisfied, and in some parts of the embankments, an earlier start on the finishing works has been possible. The surcharge requirement has been proven.

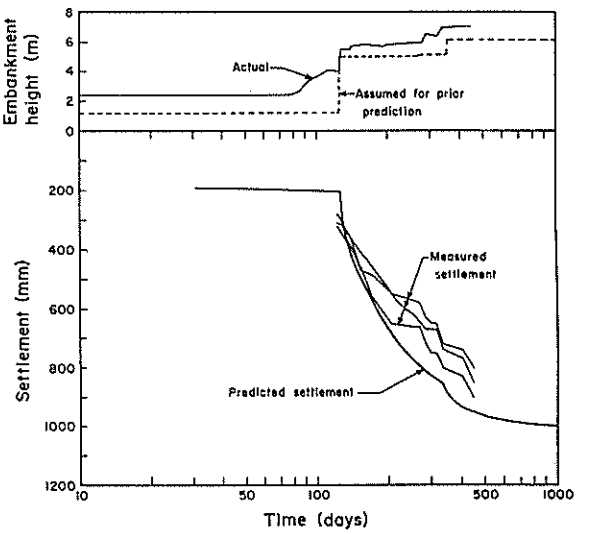

Figure 7 Example settlement behaviour of roadway embankment

Major sources of error having an influence on the accuracy of the settlement predictions should be noted. These have firstly influenced the predictive processes in the trial behaviour back-analysis, and some then have had a further, potentially greater influence on the roadway embankment predictions.

(i) Soil profiles are based on interpolations between borehole and penetrometer data, so that the adoption of layer arrangements, thicknesses and most particularly, drainage characteristics usually required important simplifying assumptions.

(ii) The consolidation parameters, which exhibit a proven natural variability, are approximated by the insitu mean parameters in the analysis. The true variability is offset somewhat by the

"vertical averaging" which results from the back-analysis process.

(iii) The actual, irregular loading history is not entirely consistent with the prior analysis assumptions of a series of instantaneously applied load increments at different times. This does not greatly affect the final settlement outcome, but is a partial explanation for discrepancies between prediction and measurement in the early consolidation stages.

(iv) The analysis method assumes one-dimensional vertical compression and drainage only, whereas these phenomena exhibit significant two-dimensional components under the outer regions of embankment.

(v) The stress and pore pressure distribution from the embankment and within the deforming foundation can only be approximated by the elastic stress distribution necessarily assumed in the analyses.

8 CONCLUSIONS

A large-scale instrumented trial construction project has been used to facilitate reliable prediction of stability and settlement behaviour of high road embankments built on a soft soil foundation. The data obtained from the trial has been used in conjunction with the classical methods for analysis of stability and settlement to produce, by back-analysis, calibrated stability and settlement models. Reliable behaviour predictions for the roadway embankments were obtained by the use of these models, giving effective means of control of both stability and settlement during the construction period.

A condition of local contained yield in the very soft, highly sensitive silty clay was detected under the trial embankment at a height approximately 0.6 of the final height at which construction was terminated on stability grounds. This condition was readily identified on graphical plots of excess pore pressure against embankment height, for virtually all piezometers located under the embankment. Attempts at alternative instability detection methods, based on inclinometer and surface survey measurements, gave inconclusive results.

The first onset of local yield was not taken as sufficient loss of stability to halt construction. The trial construction was terminated when effective stress stability analyses, incorporating the measured excess pore pressures, yielded minimum factors of safety in the range 1.1 to 1.4.

Stability control was applied to the roadway embankments using a Stability Monitoring Diagram (developed using the calibrated stability model) and very simple instrumentation installed at 10 monitoring sections within the embankments. At each section, the pore pressure measured by only one piezometer was used together with settlement and embankment height measurements, to establish the degree of dissipation, and predict factor of safety using a simple rapid pro forma and graphical procedure on a daily basis. The minimum allowable factor of safety below which construction should be terminated was set at 1.5.

The success of the control method depended on analysis assumptions of the excess pore pressure distribution, and on the ability of the piezometer to adequately characterise the whole pore pressure distribution under the embankment. All sections of the embankments were successfully constructed using this method, without the need of "safe" but expensive toe berms, which were considered to be necessary in the early stages of the project investigation. The method of control, therefore, was apparently successful in this case, with an important benefit being the timely availability to construction personnel of a reliable result. However, the simplicity of the method can not be considered universally applicable at this stage.

The settlement model showed that for the roadway embankment some control of settlement rate was necessary to achieve the project timing constraints. Embankment surcharges of 1 m and 1.5 m height were employed. The observed behaviour has shown no major unexpected departure from prediction at all monitoring positions. However, some tendency is evident that smaller settlements are occurring slightly slower than the predictions indicated. The method of settlement control (through more reliable prediction) has successfully met the timing requirements, to a satisfactory level of accuracy.

The benefits to the construction project, in terms of achieving full embankment heights without stabilisation, and in terms of satisfying critical path project timing, have fully justified the net cost of the trial.

9 ACKNOWLEDGEMENT

The permission of the Commissioner, Main Roads Department, Queensland, for publication of the data presented in this paper is gratefully acknowledged. Appreciation is due to all departmental officers involved in the project in recognition of their contribution to the final outcome.

10 REFERENCES

COLE, K.W. (1974). Discussion to Session 3 : Application. Proc. Symp. on Field Instrumentation in Geotechnical Engineering. London, Butterworths. pp. 623-632.

COOK, D.A. and INGOLD, T.S. (1974). A practical method for field control of loading. Proc. Symp. on Field Instrumentation in Geotechnical Engineering. London, Butterworths. pp. 100-111.

D'APPOLONIA, D.J., LAMBE, T.W. and POULOS, H.G. (1971). Evaluation of pore pressures beneath an embankment. Proc. ASCE Jnl. of Soil Mechanics and Foundations Division, Vol. 97, No. SM6, pp. 881-898.

HOEG, K., ANDERSLAND, O.B. and ROLFSEN, E.N. (1969). Undrained behaviour of quick clay under load test at Asrum. Geotechnique, Vol. 19, No. 1, pp. 101-115.

LAMBE, T.W. (1973). Predictions in soil engineering. 13th Rankins Lecture. Geotechnique Vol. 23, No. 2, pp. 149-202.

LUMB, P. (1968). Statistical aspects of field measurements. Proc. 4th Australian Road Research Board Conf., Melbourne, Vol. 4, Part 2, pp. 1761-1770.

MARGASON, G. and SYMONS, I.F. (1969). Use of pore pressure measurements to control embankment construction. Proc. 7th Int. Conf. on Soil Mechanics and Foundation Engineering, Mexico, Vol. 2, pp. 307-315.

SYMONS, I.F. (1976). Assessment and control of stability for road embankments constructed on soft subsoils. Transport and Road Research Laboratory, Report LR 711.

WILKES, P.F. (1974). Instrumentation for the King's Lynn Southern Bypass. Proc. Symp. on Field Instrumentation in Geotechnical Engineering. London, Butterworths. pp. 448-461.

Design and Performance of an Embankment on Soft Ground Retained by a Flexible Wall

I. H. WONG
Consulting Engineer, Ebasco Services Incorporated, New York
T. A. GLEASON
Senior Vice President, Converse Ward Davis Dixon, Cincinnati, Ohio

SUMMARY: This paper describes a case history involving the design of a high embankment on soft ground retained by a flexible wall. Analyses using limiting equilibrium method, and the finite element method were performed to assess the stability of the embankment. This paper discusses the results of the analyses, and compared them with measured field performances. It also discusses the selection of relevant soil parameters for use in the analyses.

1 INTRODUCTION

This paper describes a case history involving the design and performance of a high embankment on soft ground retained by a flexible wall. It discusses the design analyses performed to evaluate the stability of the embankment, within the framework of a consulting engineering project.

2 CONSTRUCTED FACILITY

The constructed facility is a coal transfer terminal located at Wilder, Kentucky, along the Licking River, which is a tributary of the Ohio River.

The constructed facility includes a tied-back sheet pile retaining wall system. An embankment is located behind the retaining wall. This embankment rises at a slope of 3 horizontal to 1 vertical from Elevation +142.7 m (+468 ft) to Elevation +151.3 m (+496 ft). The toe of the embankment is located 9.1 m (30 ft) from the top of the retaining wall. Five railroad tracks are located at the top of the embankment imposing a load of 22 kN (5 kips) per track. The river bed in front of the retaining wall is dredged to Elevation +135 m (+443 ft). The normal water pool in the river is Elevation +138.8 m (+455 ft). A picture of the completed facility is shown in Figure 1.

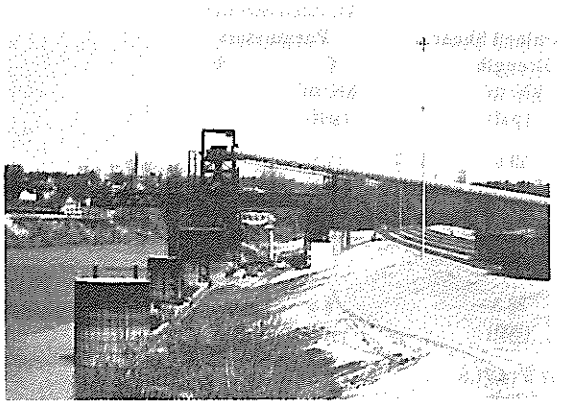

Figure 1 Completed Coal Transfer Facility

A typical section of the embankment and the retaining wall is shown in Figure 2. The retaining wall consists of interlocking steel sheeting, ZP 27; the tie rods are located at 2.4 m (8 ft) on centers and are anchored to a deadman consisting of an interlocking steel sheet piling.

3 SUBSURFACE CONDITIONS

Prior to the construction of the facility, several test borings were drilled on land and in the river. The subsurface conditions revealed by these borings are presented in the generalized subsurface profile shown in Figure 2.

As shown in Figure 2 the soil layer immediately below the original ground surface consists of a soft, normally consolidated clay with an average undrained shear strength on the order of 24 kN/m² (500 psf). This is underlain by a medium stiff clay with an undrained shear strength of about 38 kN/m² (800 psf). The medium stiff clay is in turn underlain by a stiff clay with an undrained shear strength ranging from about 57 kN/m² (1200 psf) to 72 kN/m² (1500 psf). The shear strength values were based on unconsolidated undrained triaxial tests.

The interface between the three clay layers are gradual rather than distinct. All three layers have similar index properties, with a liquid limit ranging from 40 to 50 percent, and a plasticity index ranging from 15 to 25 percent.

4 CONSTRUCTION CONSIDERATIONS

The construction schedule required that embankment placement and dredging in front of the retaining wall be completed within 18 months. The overall schedule also dictated that embankment construction precede dredging. In view of the relatively large combined thicknesses of the clay layers at the site, and the relatively low permeability of the clay materials, it was recognized that the behavior of the clay formations during construction of the embankment would be controlled by the undrained shear strengths of the clays. Relatively little pore pressure dissipation, and strength gain were expected to occur within this 18-month construction period.

The overall computed factor of safety of the embankment and retaining wall system was low and was on the order of 1.2. Because of this low factor of safety, a field instrumentation program was implemented as a means of construction control. This program involved inclinometers and piezometers. The purposes of the inclinometers were to monitor horizontal

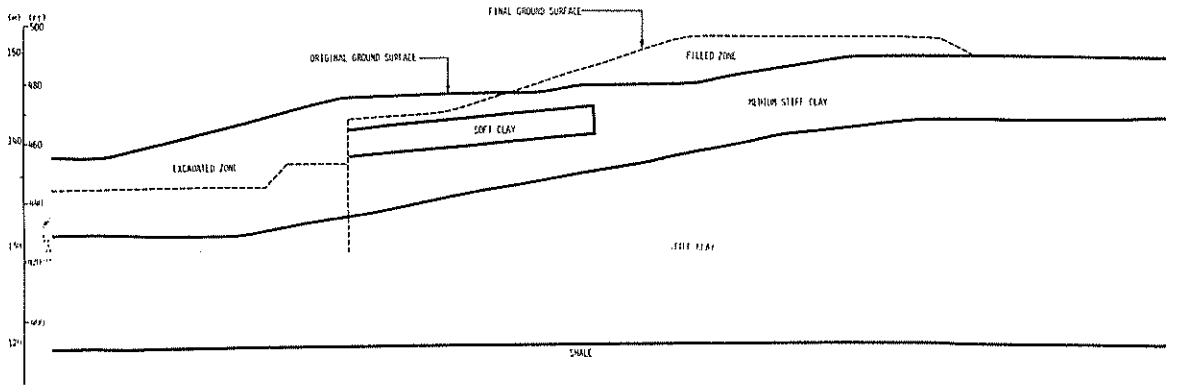

Figure 2 Generalized Subsurface Profile

ground movements during construction, and to detect any incipient development of large shear movements. The functions of the piezometers were to monitor pore pressure changes during construction.

5 STABILITY ANALYSES

5.1 General

Two methods of analysis were used to evaluate the stability of the retaining wall-embankment system. The first was a limiting equilibrium analysis based on the simplified Bishop method of slices. The second method was based on the Finite Element method.

5.2 Limiting Equilibrium Analysis

Both the short-term and long-term stability were a matter of concern.

During and immediately at the end of the embankment construction, stability of the slope would be governed essentially by the undrained shear strength of the clay formations. The low permeability of the clays, and the compressed nature of the construction schedule, would permit little or no strength gain due to consolidation.

Two modes of failure were identified as possible. The first mode would involve a sliding surface exiting between the toe of the embankment and the top of the retaining wall at Elevation +142.7 m (+468 ft). The second mode of failure would be related to a deep-seated sliding surface passing below the toe of the retaining wall. Stability analyses were performed using the simplified Bishop method of slices. The undrained shear strength parameters used in the analyses are presented in Table 1.

Results of the analyses for the stability of the embankment at the end of construction are summarized in Figure 3. It can be seen that the computed factor of safety with respect to a shallow slide is approximately 1.5, and that with respect to a deep-seated slide is approximately 1.2. These computed factors of safety, while low, were regarded as adequate for the end of construction (undrained) case.

TABLE I

STRENGTH PROPERTIES USED IN DESIGN ANALYSIS

Soil Type	Unit Weight gm/cc (pcf)	Undrained Shear Strength kN/m² (psf)	Drained Strength Parameters C kN/m² (psf)	Φ
Compacted Fill	2.00 (125)	59.9 (1250)	14.4 (300)	35°
Soft Clay	1.86 (116)	24.0 (500)	0°	30°
Medium Stiff Clay	1.89 (118)	38.3 (800)	4.8 (100)	30°
Stiff Clay	2.00 (125)	57.5 to 71.9 (1200 to 1500)	4.8 (100)	30°

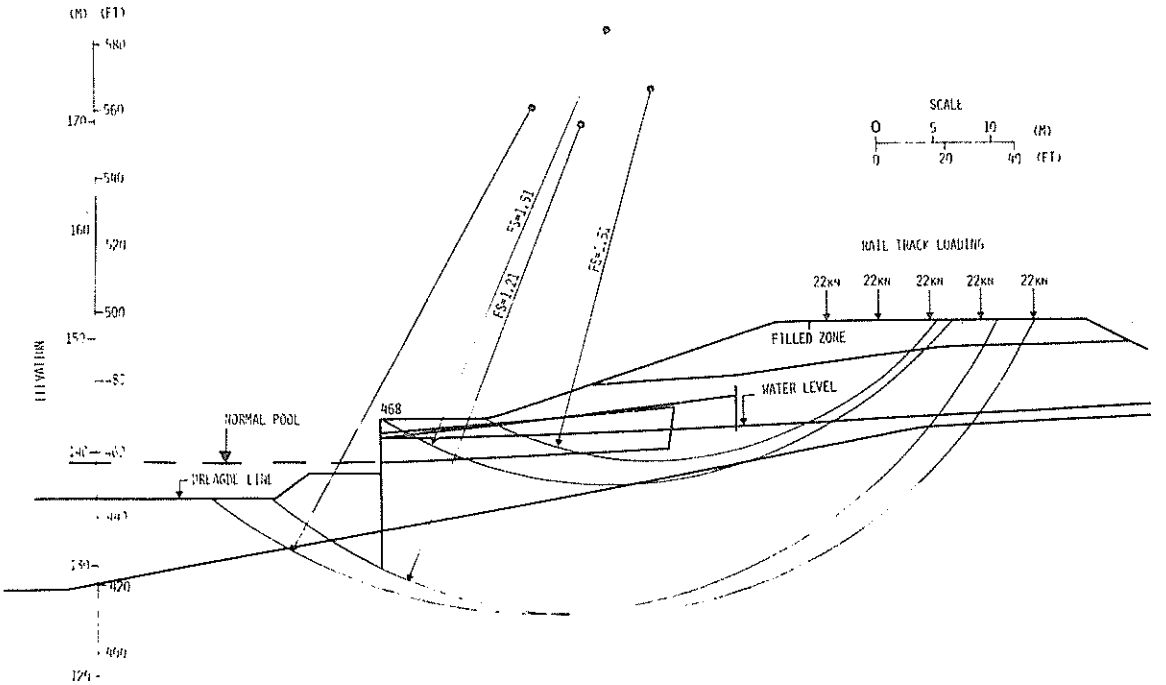

Figure 3 Embankment Stability at End of Construction (Undrained Case)

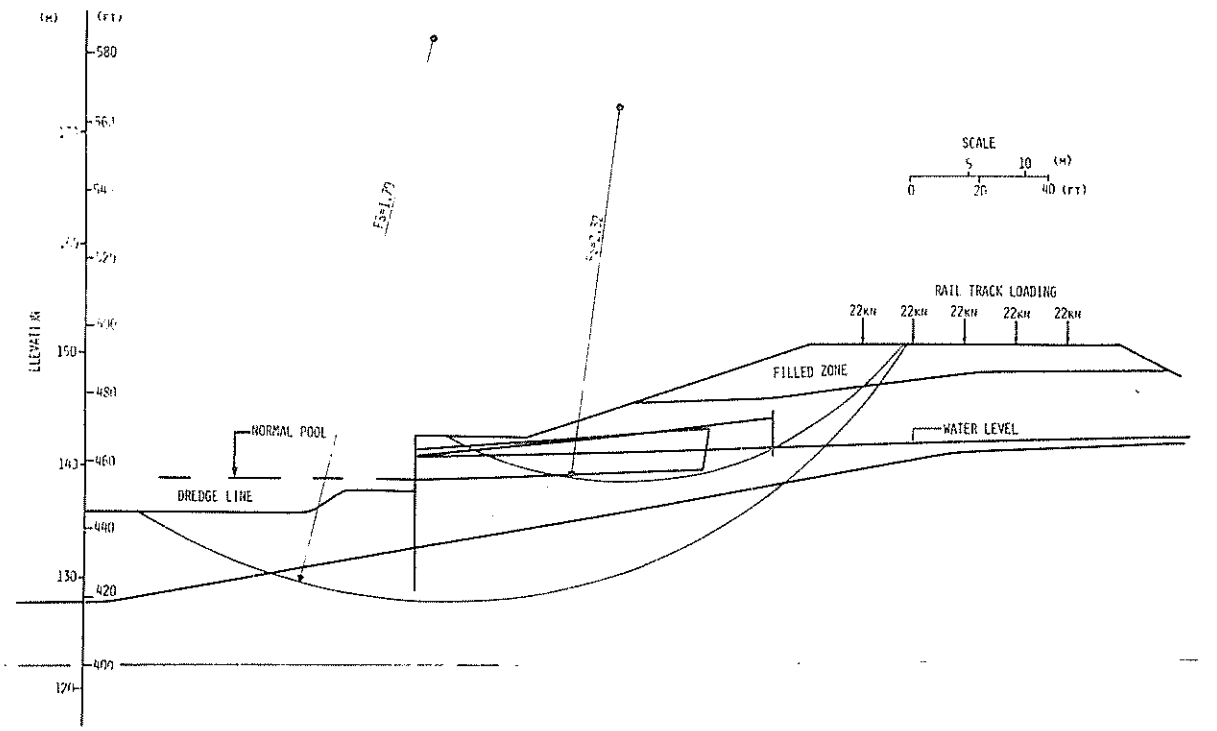

Figure 4 Long Term Embankment Stability (Drained Case)

Dredging in front of the retaining wall would result in an unloading process. Dissipation of the negative pore pressures following the unloading process could result in a loss of strength of the clay layer beneath the dredge line. In order to estimate the long-term stability of the embankment after the negative pore pressures have been dissipated, stability analyses, using the Bishop method of slices and effective stress parameters, were performed. The drained strength parameters used are presented in Table 1. Results of the analyses presented in Figure 4 indicate that the computed factor of safety with regard to long-term stability was about 2.3 for the shallower slide, and 1.8 for the slip circle passing below the toe of the retaining wall. These were considered adequate.

5.3 Finite Element Analysis

Limiting equilibrium analyses such as the Bishop method of slices provided an estimate of the factor of safety with respect to total failure. They did not provide an idea regarding the amount of movement of the embankment that was likely to occur at loading levels less than those required to cause failure.

The finite element analyses were used for estimating the deformations of the embankment. This method has been successfully applied to the analyses of retaining wall problems (e.g., Palmer and Kenney, 1972; Clough and Tsui, 1974; Wong, 1971), and embankment problems (e.g.,Kulhawy and Duncan, 1972).

5.3.1 Analysis Procedures

The analysis performed for this study was based on a computer program developed by Clough and Tsui (1974). The soil mass and the wall were represented by isoparametric linear strain quadrilateral elements developed by Doherty et al (1969).

Construction procedures that were to be followed in the field were simulated in the analyses. The construction procedures and operation loads included the following steps:

1. Excavation
2. Retaining wall and anchor deadmen installation
3. Prestressing of tieback rods
4. Placement of embankment fill
5. Dredging in front of the retaining wall
6. Railroad track loading

The finite element mesh used in the analyses is shown in Figure 5.

5.3.2 Material Properties Used in Finite Element Analyses

A completely nonlinear stress-strain behavior was simulated, based on the method recommended by Duncan and Chang (1970). This model assumes that as shear stresses increase, the soil behavior is nonlinear, but that upon a decrease in shear stresses in a soil element, the soil behavior is linearly elastic. For saturated clays the model requires as input, unit weights, initial tangent moduli, Poisson's ratios, and undrained strengths.

The undrained shear strengths used in the analyses are shown in Table 1. The initial tangent modulus of the clays was taken to be approximately 500 times the undrained shear strength. The proportion of initial tangent modulus to undrained shear strength reported in the literature varied from 300 to approximately 1,200 (Skempton, 1958; D'Appolonia & Lambe, 1972; D'Appolonia et al, 1971; and Murphy et al, 1975). The ratio of initial tangent modulus to undrained shear strength of 500 was judged to be reasonable for analysis purposes. The Poisson's ratio for the clay formation was taken to be 0.49, in consideration of the limited drainage expected of the clay formations during construction.

Before excavation, the initial stresses were assumed to correspond to an "at rest" condition, where the lateral stresses were computed as equal to k_o times the vertical stresses. For the compacted fill a k_o value equal to unity was used. For the in situ clay layers, it would appear that a k_o value of 0.5 would be appropriate from the equation $k_o = 1 - \sin\Phi$. However, as an expediency in the analysis, k_o of the soil layers located below the water table was converted to an equivalent total stress k_o of 0.75, relating the total lateral stress to the total vertical stress.

The sheet pile retaining wall, the tie rod, and sheet pile deadmen were assumed to remain fully linearly elastic. The elastic material properties of these steel members were based on values recommended by the manufacturers.

5.3.3 Results of Finite Element Analysis

Horizontal displacements predicted in the finite element analysis along the bulkhead wall are shown in Figure 6. Figure 6 shows the predicted wall movements both at the end of embankment construction itself and after the imposition of rail track loads. The predicted wall movements for the two cases are 18 cm (7 in.) and 25 cm (10 in.). This magnitude of horizontal displacement was considered to be acceptable during design analyses.

Figure 7 shows the ratio of the maximum shear stress to the undrained shear strength of the soil mass at the end of construction. Regions in the soil mass where this ratio exceeds 0.90 are shown in Figure 7. It can be seen that at the end of construction a substantial portion of the soil mass has been stressed to near its ultimate shear strength. This development of the highly stressed zones seemed consistent with the low factors of safety computed from the limiting equilibrium analyses.

6 DISCUSSIONS AND CONCLUSIONS

During design analyses, results of the finite element analyses provided a useful insight into the likely performances of the embankment. These results provided confidence, despite the low computed factor of safety obtained using the method of slices, that the embankment could be built. The horizontal displacements predicted by the finite element analyses provided a valuable basis for interpreting the measured horizontal movements obtained using the inclinometers.

The analysis procedures followed in the finite element program attempted to simulate all the major construction sequences in the field, including retaining wall construction, fill placement, and dredging. However, relatively simple soil properties inputs were required for the analyses. For undrained behavior of cohesive soils, both the unit weights and the undrained shear strengths could be obtained with relative ease in most commercial laboratories. Values of Poisson's ratios could be assumed with confidence to be close to 0.5 for clay subject to undrained shear. Taking it as a multiple of the undrained shear strength, no special testing is needed in the determination of the modulus.

Piezometer readings indicated that the pore pressure responses were essentially undrained. This, therefore,

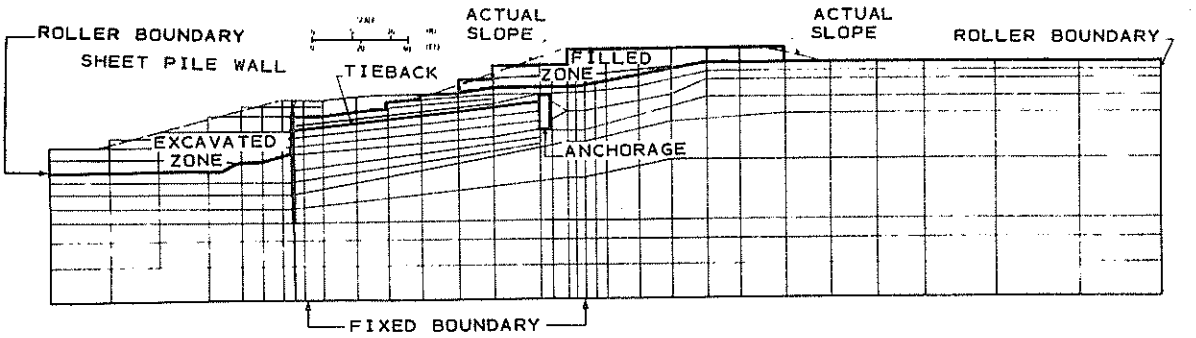

Figure 5 Finite Element Mesh

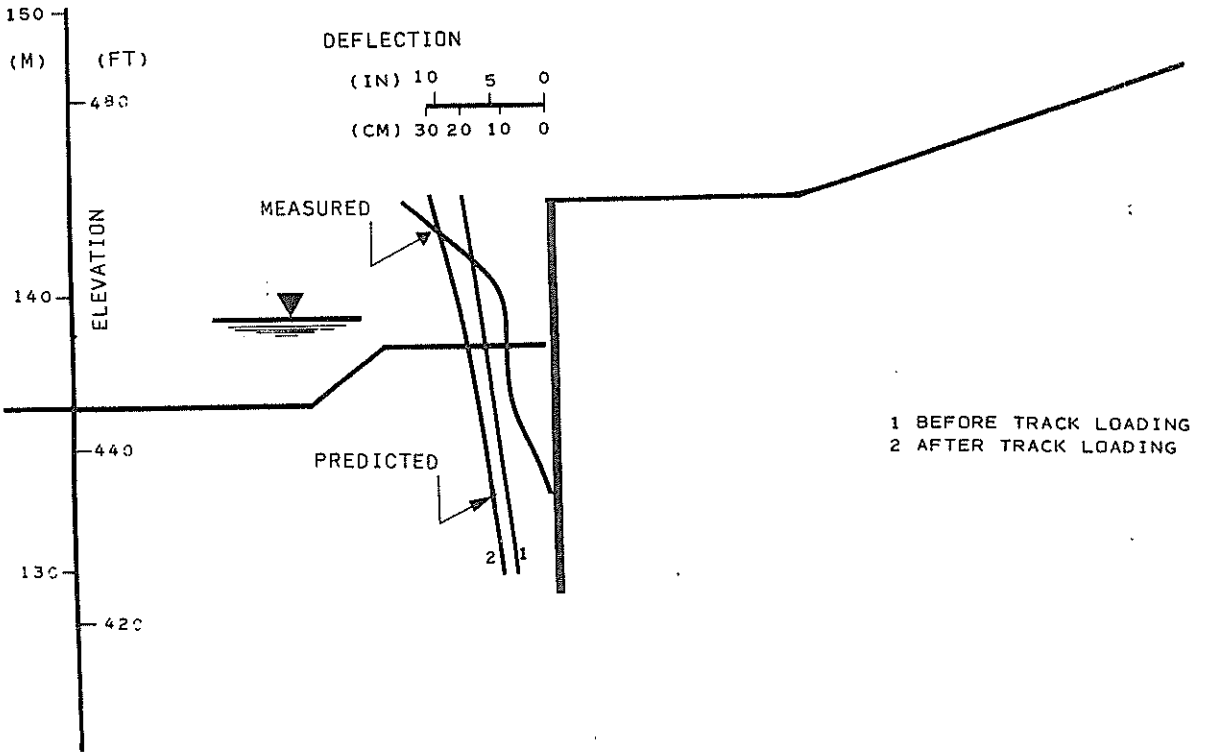

Figure 6 Deflections of Sheetpile Wall

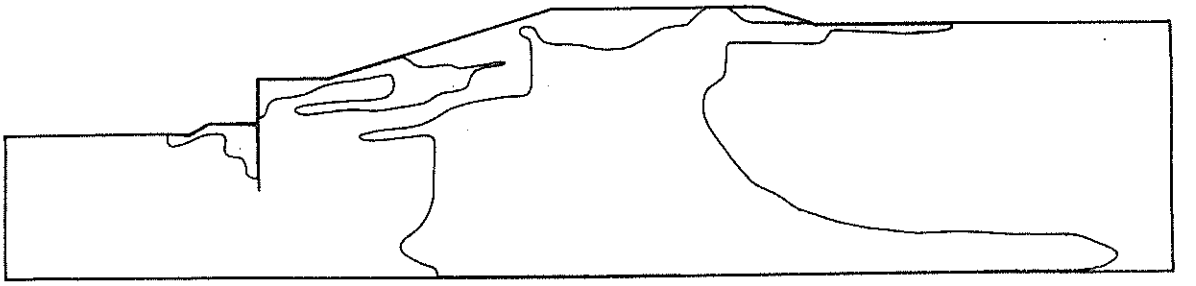

YIELDED ZONES WHERE RATIO
OF MAXIMUM SHEAR STRESS
TO UNDRAINED SHEAR STRENGTH
IS AT LEAST 0.9

Figure 7 Highly Stressed Zones from Finite Element Analysis

confirmed the design assumption that little or no strength increase could be counted on during the construction time involved. Horizontal displacements of the retaining wall before truck loading, measured using the inclinometers and shown in Figure 6 were within the range predicted.

Slope stability analyses indicated that short-term stability during or immediately at the end of construction was the most critical. Despite the unloading processes induced by dredging operations, the overall long-term factor of safety was computed to be substantially higher than the factor of safety during undrained shear. In this regard the decision to accept a low computed factor of safety of 1.2 for undrained shear was justified in economic terms.

The entire coal transfer facility was constructed on schedule, and has been functioning satisfactorily for three years.

7 ACKNOWLEDGEMENTS

The authors acknowledge Mr R Goettle of Richard Goettle, Inc., Cincinnati, Ohio, the Contractor for the retaining wall installation for providing the slope indicator measurements and for helpful discussions, Dr Y Tsui of Duke University for performing the finite element analyses, and Mr A Bradfish of Oglebay Norton, Inc., the Owner, for permission to publish the data.

The work described in this paper was performed when both authors were with Dames & Moore.

8 REFERENCES

Clough, G W and Tsui, Y, "Behavior of Tied-Back Walls in Clay," presented at the ASCE National Meeting on Structural Engineering held at Cincinnati, Ohio, April, 1974.

D'Appolonia, D J and Lambe, T W, "Method for Predicting Initial Settlement," *Journal of the Soil Mechanics and Foundations Division*, ASCE, Vol 96, March, 1970.

D'Appolonia D J, et al, "Initial Settlement of Structures on Clay," *Journal of the Soil Mechanics and Foundations Division*, ASCE, Vol 97, October, 1971.

Doherty, W P et al, "Stress Analyses of Axisymmetric Solids Utilizing Higher Order Quadrilateral Finite Elements," *Report No. SESM 69-3, Structural Engineering Laboratories*, University of California, Berkeley, California, January, 1969.

Duncan, J M, and Chang, C Y, "Nonlinear Analyses of Stress and Strain in Soils," *Journal of the Soil Mechanics and Foundations Division*, ASCE, Vol 96, September, 1970.

Kulhawy, F H, and Duncan, J M, "Stresses and Movements in Oroville Dam," *Journal of the Soil Mechanics and Foundations Division*, ASCE, Vol 98, July, 1972.

Murphy, D J et al, "Temporary Excavation in Varved Clay," *Journal of the Geotechnical Engineering Division*, ASCE, Vol 101, March, 1975.

Palmer, J H L, and Kenney, T C, "Analytical Study of a Braced Excavation in Weak Clay," *Canadian Geotechnical Journal*, Toronto, Canada, Vol 9, May, 1972.

Skempton, A W, "Bearing Capacity of Clays," *Building Research Congress*, England, 1951.

Tsui, Y and Clough, G W, "Plane Strain Approximations in Finite Element Analyses of Temporary Walls," *Proceedings*, ASCE Geotechnical Engineering Division Specialty Conference on Analysis and Design in Geotechnical Engineering, Austin, Texas, Vol 1, 1974.

Wong, I H, "Analyses of Braced Excavations," thesis presented to the Massachusetts Institute of Technology, Cambridge, Massachusetts in 1971, in partial fulfillment of the requirements for the degree of Doctor of Science.

Reinforced Earth Applications in Australia and New Zealand

M. S. BOYD
Engineer, Reinforced Earth Pty Ltd, Sydney

SUMMARY Reinforced Earth was introduced to Australia and New Zealand relatively recently and has since been adopted for many projects.

Design procedures have been based on the work of Vidal and others at the LCPC and recognise the composite nature of the Reinforced Earth block. Basic design criteria are described.

Practical application has resulted from the inherent simplicity and flexibility of the Reinforced Earth system coupled with significant economies in many cases. The basic Reinforced Earth costs for some Australian projects are tabulated.

1 INTRODUCTION

Reinforced Earth was introduced to Australia in 1975 and New Zealand in 1979. Design procedures and systems used are based on those which have been developed by Vidal in conjunction with the Laboratoire Centrale des Ponts et Chaussées (LCPC) and others.

The extensive use of Reinforced Earth in many applications around the world have highlighted the advantages of Reinforced Earth over more traditional construction techniques

- simplicity (both technically and practically).
- flexibility (both in application and in ability to accept large movement).
- economy.

Instrumentation of both full scale structures and extensive model testing have confirmed the pioneering theories of Vidal and show Reinforced Earth as being what it is, viz, a composite material of (granular) earth and (linear, metallic) reinforcements which together form a monolithic yet flexible mass gravity structure.

2 REINFORCED EARTH THEORY

2.1 Vidal And The LCPC

Between 1958 and 1963, Henri Vidal conceived and developed the theory of Reinforced Earth and checked its validity with extensive model tests and prototype structures. In 1965 he introduced the technique as "a new material for public works" (1966) providing a simple, economic alternative to traditional construction techniques.

Basically, Vidal saw that the introduction of flexible, linear (metallic) elements into a cohesionless (granular) earth material produced a composite structure which behaved as a coherent gravity block.

The significant factors of this behaviour which he recognised were:

- the friction at the earth/reinforcement interface
- the secondary (structural) importance of the outside skin or facing.
- the flexibility of the structure and its components.

Methods of analysis and design were thus proposed on the basis of both elemental or unit properties and overall block stability (e.g. analysis of reinforced bodies cut by an assumed surface).

In 1969, Schlosser and Vidal showed that the composite behaviour resulted in an apparent cohesion which could be simply observed in triaxial tests on reinforced sand specimens (Long et al 1972). The effect of this apparent cohesion was to induce a curved (potential) failure surface, differing from the straight Coulomb line predicted by classical retaining wall theory. At working loads this curved failure surface is manifested as a curved locus of maximum tension, separating active and resistant zones within a Reinforced Earth block.

2.2 Recent Developments

As the use of Reinforced Earth became more widespread so has the research. The Vidal concept of a coherent gravity structure in which the earth and the reinforcement act compositely has been challenged by the hypothesis that Reinforced Earth (retaining) structures are analagous to tie-back or anchored walls. McKittrick (1978) suggested that proponents of this apparently neglected or basically misunderstood the basic mechanics of the material or the significant and substantial documentation that has existed for several years that should eliminate the tie-back or anchor approach as a conceivable failure mechanism. McKittrick cites field experience which strongly supports the coherent gravity structure theory - at Aguadilla, Puerto Rico and Roseburg, Oregon, U.S.A. where gross foundation failures under structures resulted in a demon-

stration of the coherence of the Reinforced Earth block.

The fundamental difference in the two approaches is reflected in the dimensions obtained - for the same earth pressure coofficients, K, Vidal's approach requires more reinforcements to resist higher stresses but results in a reduced maximum reinforcement length compared with that predicted by the anchor theory (Fig. 1)

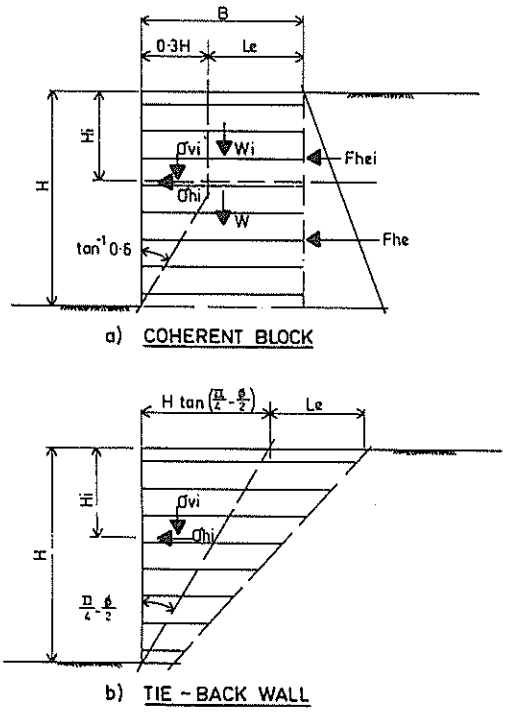

Fig. 1 Design Hypotheses

Consider a coherent block structure of height, H and block width, B. At any level, Hi below the top of the wall the horizontal pressures range from K.γ. Hi near the top of the coherent block to 1.33 K.γ.Hi near the base (assuming the eccentricity of the base resultant = B/8) due to overturning effects. In the upper part of the block, the block width provided is then checked with respect to 0.3 H + Le.

In a tie back wall structure, at any level, Hi below the top of the wall the horizontal pressures are K. γ.Hi . The reinforcement length is then checked with the adherence length Le provided beyond the Coulomb failure line which at the top of the wall yields a total length H tan$\left(\frac{\pi}{4} - \frac{\phi}{2}\right)$+ Le.

Thus, the coherent gravity block may yield reinforcement tensions up to 1/3 greater than a tie back wall, whereas, if $\phi = 30^0$, the maximum reinforcement length required for adherence is 0.3 H + Le and 0.58 H+Le, respectively.

3 DESIGN

3.1 Static Design Procedures

Reinforced Earth design procedures in Australia are derived from those recommended by the LCPC (1974, 1979). External stability criteria are based on the concept of the monolithic yet flexible Reinforced Earth block and checked against suitable minimum factors of safety. In particular, the bearing capacity at the foundation takes into account the total block width (as reduced for eccentricity effects) and a factor of safety of 2 is adopted (instead of 3 for traditional structures) due to the flexibility of the structure.

Internally, for plain (smooth) reinforcement strip, the basic internal design procedures assumed that

a) at the limit, an active (K_a) state of stress existed within the Reinforced Earth block.

b) the horizontal pressure at each level resulted in a tension in each reinforcement strip dependant on its area of influence.

c) the friction factor (earth/reinforcement) was constant with depth.

d) the resistant zone within the Reinforced Earth block (to resist pullout) was not less than one half the block width.

The allowable tension in each reinforcement was based on 2/3 yield stress on the nett section (i.e. after deduction of a corrosion allowance) and checked with respect to its weakest point (usually reinforcement/facing connection).

Friction or bond failure in each level was checked with respect to the maximum tension in each reinforcement and its minimum resistant length or half block width (for a factor of safety greater than 1.0).

Empirical data at that stage suggested that to satisfy both external and internal stability as well as to achieve the observed composite behaviour, a rectangular block of width/height ratio greater than 0.8 was required.

Recent availability of more extensive data on the performance of both model and full scale structures, both at working stress levels and at failure have allowed some refinement of the design procedures. The introduction of a ribbed reinforcement strip has also resulted in a more efficient use of material but its behaviour is more complex (Schlosser and Elias, 1978).

Design procedures now take into account that

i) the state of stress within the Reinforced Earth block evolves from an at rest (K_o) condition at the surface to an active (K_a) condition at depths greater than 6 m.

ii) the friction factor (earth/reinforcement) for plain reinforcement (usually 0.4 for mild steel) is constant with depth whereas for ribbed reinforcement there exists an apparent friction factor (f*) greater than

tan ϕ at depths less than 6 m.

iii) the line of maximum tension is defined by a line at a distance 0.3 x height of the structure behind the face and a line at $\tan^{-1}$ 0.6 from the toe (Fig. 2)

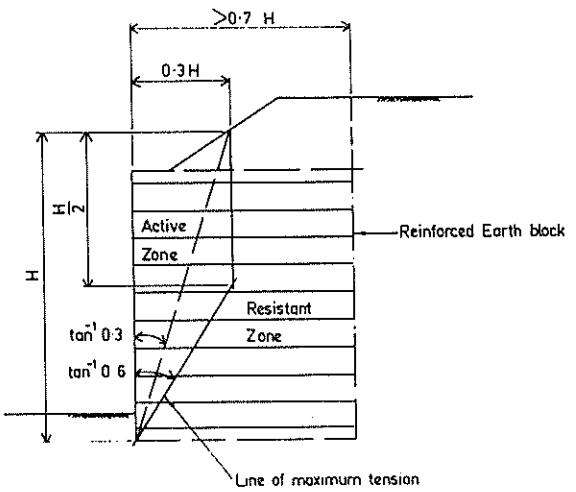

Fig. 2 Block Geometry

Friction is therefore checked with respect to the maximum tension line and resistant length available (i.e. reinforcement length - 0.3 x structure height) using a minimum factor of safety of 1.5.

Recent data has also suggested that a reduction in the minimum block width/height ratio to 0.7 is possible.

The evolution of these parameters and design criteria is described by Schlosser (1978, 1979) and they are incorporated in the comprehensive Guide, Specifications and Code of Practice for Reinforced Earth Structures issued by the LCPC and SETA in France (1979).

3.2 Aspects of Seismic Design

The introduction of Reinforced Earth to New Zealand has necessitated the adaption of the static design procedure to the dynamic conditions resulting from seismic design criteria.

Reinforced Earth structures, like other flexible earth structures, have the advantages of

a) a high degree of structural damping

b) an ability to accept large movement without loss of stability.

Richardson (1978) and others at UCLA have developed design procedures which are based on the response of a Reinforced Earth structure to dynamic loading and the effect of overall geometry, reinforcement distribution and damping. These procedures have been applied to the design of Reinforced Earth walls supporting the storage terminal for the Trans Alaska pipeline at Valdez which have a maximum height of 17 metres and are designed to withstand the following earthquake conditions:

- magnitude, 8.5 Richter
- ground acceleration, 0.6 g
- duration of strong motion, 50 seconds.

Basically, seismic design procedures involve the following considerations with respect to static design

i) the determination of an additional dynamic lateral earth pressure distribution based on the calculated stiffness and dynamic response of the structure. This generally results in an augmented reinforcement density in the upper region of the structure.

ii) the checking of tensile capacity of the reinforcement under static + dynamic loads and taking reinforcement to yield.

iii) the checking of capacity of the reinforcement for an adequate factor of safety under static loads only. Because of the cyclic nature of the dynamic loads, pull-out "failure" due to static + dynamic loads would only result in slight movement.

3.3 Durability

The corrosion of buried metals is a complex subject affected by many variables. Romanoff (1957) summarised the problem by stating that it was not possible to predict the rate or extent of corrosion from any single soil property, however, it was possible to qualitatively associate soil characteristics and properties (which are frequently interrelated) with the corrosion of particular metals.

Basically, in the presence of water, corrosion is fundamentally electrochemical. Long term studies by the National Bureau of Standards showed that, in well drained soils having a high resistivity, the corrosion rate of ferrous metals decreased after a few years from an initial high rate to an insignificant rate.

Analysis of NBS 10 year tests for relevant soil types (i.e. non organic soils with a resistivity greater than 2000 ohm.cm.) shows that 95% of increased corrosion rates for galvanised steels fall below 0.01mm/year (Boyd et al, 1978). Applying this figure to a corrosion allowance of 0.5mm/face leads to a conservative lower bound service life estimate of 80 years.

Darbin et al (1978) report on similar studies of long term corrosion and more recent research in France.

The corrosion allowance requirements for various service lives and environments adopted for the French code are summarised in Fig. 3

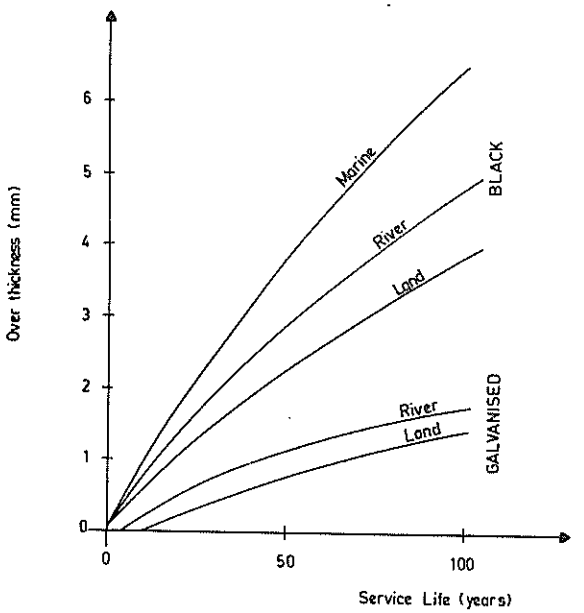

Fig. 3 Corrosion Allowances

4 AUSTRALIAN AND NEW ZEALAND PROJECTS

4.1 Applications

In Australia and New Zealand some 83 structures have been constructed or are under construction (at July, 1979). By far the major application is in the area of public road and highway retaining walls for grade separation or embankment support (TABLE I). The use of Reinforced Earth for bridge abutments, however, is a novel and spectacular example of the properties of the technique. It provides a simple, economic solution, particularly for overpass/underpass structures and has been adopted by many local and state authorities.

TABLE I

REINFORCED EARTH APPLICATIONS IN AUSTRALIA AND NEW ZEALAND.

Application	No. of Structures	Area (m^2)	Proportion (%)
Retaining Walls			
- road (public)	51	22 763	77
- road (mining)	6	695	2
- rail	7	1 140	4
- marine	1	430	1
Bridge Abutments			
- public	14	3 731	13
- mining	2	495	2
Loading Stations			
- industrial	1	150	0.5
- mining	1	153	0.5
Total	83	29 557	100

The first marine wall has been constructed at Bluff in New Zealand while in Australia, the mining industry has adopted Reinforced Earth for road embankment support near dump bridges (Comalco, Weipa) and at rear dump stations (Kandos).

In Queensland, the Railways Department undertook the first structures which physically support railway tracks at the Lutwyche Road widening project in Brisbane.

4.2 Technical Characteristics

4.2.1 Reinforcement

Tie strip, reinforcement and connection strengths are based on AS.1250 for the structural grade reinforcement and precision bolts (strength grade 8.8) adopted. Properties of the reinforcement material used are shown in TABLE II.

TABLE II

REINFORCEMENT PROPERTIES

Property	Plain	Ribbed
Material	Zincform G300 mild steel sheet to AS. 1397	Hot rolled mild steel flats to AS 1204
Galvanising	Hot dipped 600 g/m^2	Hot dipped 600 g/m^2.
Sizes (mm)	80 x 3	40 x 5 60 x 5 (60x6)
Min. yield stress (MPa)	300	275
Min. ultimate strength (MPa)	370	410
Elongation	18%	20%
Friction Factor	0.4	tan ϕ (min.)
Allowable tension (kN)	26.4 (80x3)	24.0 (40x5) 42.5 (60x5)

In terms of wall face area, or Reinforced Earth block volume, the amount of reinforcement required is very small. For the structures described in this paper, reinforcement density varies from 20 to 60 kg/m^2 of wall face or 0.17 to 0.33% by weight, earth/reinforcement (0.04 to 0.08% by volume).

4.2.2 Select backfill

The physical, chemical and electrochemical characteristics specified for the select backfill in a Reinforced Earth block are summarised as follows:

a) Free from organic or other deleterious matter.

b) Grading limits

i) nothing over 350mm

ii) not more than 25% (by weight) larger than 150 μm

iii) not more than 15% (by weight) smaller than 75 μm

Where ribbed reinforcement is used, the lower grading limit may be extended to not more than 15% (by weight) smaller than 13.5 μm, providing that the angle of internal friction is not less than 25°.

c) Chemical limits

i) pH between 5 and 10

ii) not more than 200 ppm, Cl

iii) not more than 1000 ppm, SO_3

d) Electrochemical limit

Resistivity under saturated conditions not less than 3000 ohm.cm.

Very fine clayey materials are specifically excluded on the basis of reduced service life potential with respect to the buried reinforcement and variability of soil properties (friction, cohesion) at different moisture contents.
In addition, creep characteristics of reinforcement in very fine grained soils may lead to reduced long term stability.

Materials used in Australia and New Zealand have ranged from sands (reclaimed, dune), sandstone (ripped and crushed) and gravels (river, quarry or minesite overburden).

4.2.3 Facing

The two facing panel systems used have been the articulated precast concrete panel system, 1 500 mm x 1 500 mm by 180 or 220 mm thick or the flexible rolled steel panel system, 333 mm high, 3mm thick and up to 9 000 mm long.

Both systems provide the necessary flexibility required for the facing or skin of a Reinforced Earth block so that the composite block behaviour can develop. Both facing systems have the ability to accept differential settlements of at least 1% without distress.

4.3 Construction

Construction of Reinforced Earth structures is primarily an earthworks operation. Experience has shown that overall construction rates achieved are generally controlled by the rate of supply and placement of the backfill, not the erection of the Reinforced Earth components.

A basic team of four men (one foreman, three labourers) can erect precast concrete facing panels (and lay reinforcement) at an average rate of four panels/hour (72 m^2 per day). Peak rates of up to 46 panels (103.5 m^2) per day have been reported in New South Wales (Leece, 1978) and 40 panels (90 m^2) per day in South Australia (Boyd and Thomas, 1980).
The construction procedure is cyclic with placement of a facing panel course, backfilling to level of reinforcement, placement and connection of reinforcement and backfilling to base of next panel course following in succession to the top of the structure. All construction can be carried out from within the wall alignment and the structure is stable during all phases of the operation.

5 ECONOMICS

The simplicity and economy of Reinforced Earth construction is highlighted in TABLE III where the labour content and in-place cost of three forms of retaining wall constructed by the Department of Main Roads in New South Wales is compared (Leece, 1978).

TABLE III

RETAINING WALL COMPARISON

Technique	Labour Content (manhours/m^2)	Cost ($/$m^2$)
Reinforced Earth	4.1	121
Reinforced concrete (1)	11.5	300
Crib wall	13.3	200

Note (1) Includes skilled labour (e.g. carpenters, steel fixers, riggers and scaffolders).

The breakdown of costs reported by Leece (1979) on six New South Wales road retaining wall projects and Boyd and Thomas (1980) on two South Australian bridge abutment projects is shown in TABLE IV.

The use of Reinforced Earth has resulted in savings of up to 45% over alternative retaining wall systems. For single span, road and rail overpasses using Reinforced Earth abutments this has resulted in overall structure economies of between 10 and 25%.

6 CONCLUSION

Reinforced Earth design is based on normal, practical procedures which recognise the unique composite behaviour of the monolithic Reinforced Earth block.

Reinforced Earth has become accepted as a simple, economic and practical alternative to the more traditional construction techniques for many applications in Australia and New Zealand.

Construction costs reported highlight the economy of Reinforced Earth structures.

7 REFERENCES

VIDAL, H. (1966). "La Terre Armée (Un materian nouveau pour Travaux Publics)" Annales de L'Institute Technique du Batiment et des Travaux Publics.

SCHLOSSER, F. and VIDAL, H. (1969) "La Terre Armée" Bulletin de Liaison des Laboratoires Routiers - Pont et Chaussées.

LONG, N.T., GUEGAN, Y. and LEGEAY (1972) "Etude de la terre armée a l'appareil triaxial" Rapport de recherche No. 17., Laboratoire Centrale des Ponts et Chaussées, Paris.

McKITTRICK, D.P. (1978) "Reinforced Earth: Application of Theory and Research to Practice". Proc. Symposium on Soil Reinforcing and Stabilising Techniques in Engineering Practice, Sydney.

LCPC (1974) "Dimensionnment des Ouvrages en Terre Armée - Murs et Culées de Ponts" Paris.

LCPC/SETA (1979) "Ouvrages en Terre Armée : Guide, Specifications et Regles de l'Art Final Draft, Paris.

SCHLOSSER, F. and ELIAS, V. (1978) "Friction in Reinforced Earth" Recherche Technique No. 11, la Terre Armée, Paris.

SCHLOSSER, F. (1978) "History, Current and Future Developments of Reinforced Earth" Proc. Symposium on Soil Reinforcing And Stabilising Techniques in Engineering Practice, Sydney.

RICHARDSON, G.N. (1978) "Earthquake Resistant Reinforced Earth Walls" ASCE, Symposium on Earth Reinforcement, Pittsburgh

ROMANOFF, M. (1957) "Underground Corrosion" Circular 579, National Bureau of Standards.

BOYD, M.S., VERGE, G.C. and REID, J.B.(1978) "Practical Application of Reinforced Earth Theory". Proc. Symposium on Soil Reinforcing and Stabilising Techniques in Engineering Practice, Sydney.

DARBIN, M., JAILLOUX, J.M. and MONTVELLE, J. (1978) "Performance and Research on the Durability of Reinforced Earth Reinforcing Strips". ASCE, Symposium on Earth Reinforcement, Pittsburgh.

LEECE, R. (1978) "Reinforced Earth Construction at Bondi Junction Bypass". Proc. Symposium on Soil Reinforcing and Stabilising Techniques in Engineering Practice, Sydney.

BOYD, M.S. and THOMAS, A.I. (1980) "The Design and Construction of Reinforced Earth Bridge Abutments in South Australia" Institution of Engineers, Australia, Annual Conference (in print).

LEECE, R. (1979) "Reinforced Earth Highway Retaining Walls in New South Wales". Proc. Conference on Soil Reinforcement, Paris.

TABLE IV

REINFORCED EARTH COSTS

Date	Project	Type	Max. Height	Area	Supply (1)	Erection (2)
			(m)	(m^2)	($/$m^2$)	($/$m^2$)
76	F5 Freeway, New South Wales	Retaining wall at abutment	6.0	450	75	43
76	Seven Hills, New South Wales	Retaining walls	8.25	1 000	88	19
77	North Parramatta, New South Wales	Retaining walls	8.25	2 300	82	19
77	Bondi Junction, New South Wales	Retaining walls	8.25	3 730	101	29
77	Epping Road, New South Wales	Retaining walls	10.50	3 310	95	24
77	Swanport Deviation, South Australia	Bridge abutments	6.00	400	104	19
78	Botany Road New South Wales	Retaining walls and abutments	7.50	3 350	98	32
78	Pt. Germein, South Australia	Bridge abutments	6.75	660	107	15

Note: (1) Includes supply of facing panels, reinforcement etc.
(2) Erection of facing panels, reinforcement etc. including labour and plant.
(3) Prices quoted are in Australian dollars.

Measurement of Soil/Reinforcement Interaction

M. R. HAUSMANN
Deputy Head, The New South Wales Institute of Technology
G. J. RING
Lecturer, The New South Wales Institute of Technology

SUMMARY Parameters of soil/reinforcement friction and adhesion are generally determined in direct shear tests or pull-out tests, or are deduced from the interaction of the behaviour of models or full-scale structures. The results obtained show a large variation and are significantly affected by the placement condition of the soil, the geometry of the reinforcement and the method of testing. Direct shear tests performed allowed measurements of the thickness of the shearing zone, the relative slip and the rate of dilatancy. Preliminary results presented indicate that this type of experiment can contribute to the understanding of the mechanism of soil/reinforcement interaction.

1 INTRODUCTION

The evaluation of the friction or adhesion between soil and structural elements has always been a significant problem in civil engineering. It is of particular importance in the design of pile foundations, caissons, conventional retaining walls, tie-back anchors and, most recently, reinforced earth and similar construction techniques.

The analysis of the internal stability of reinforced earth structures considers two basic causes of failure: slippage between the soil and the reinforcement and rupture of the reinforcement. Both cases require an estimate of horizontal earth pressures. Field measurements have shown that these generally correspond to at-rest pressures near the top of a wall and active pressures further down, reflecting the wall deformations which occur during construction. Since the strength properties of the reinforcements are known, the rupture mode of failure can be analysed with reasonably reliable data for the predominantly cohesionless soils used.

Considerably greater uncertainties are involved in the evaluation of failure by soil/reinforcement slippage, also interpreted as failure by pull-out. Many designers and researchers are of the opinion that values of the soil/material friction angle δ as obtained in a modified standard shear box give a conservative assessment of the potential shear resistance between granular material and reinforcement. However, some experimental data appears conflicting and it is the aim of this paper to present and discuss recent findings from laboratory and field studies and indicate avenues of further research, with special consideration given to the direct shear test.

2 DETERMINATION OF SOIL/MATERIAL FRICTION ANGLE

2.1 Direct Shear Tests

Most commonly soil/material or "skin"-friction characteristics are evaluated in a direct shear box. Although the state of stress in the soil is not completely known in this form of testing, its results have generally been adopted as reference values for comparing data obtained from other laboratory or field investigations and for specifying design criteria. For preliminary design purposes, the friction angle between soil and construction materials is often assumed to be between 1/2 and 2/3 of the internal friction angle.

Figure 1a shows the typical arrangement of materials for measuring skin friction such as used in the original comprehensive work by Potyondy (1961) and more recently by Schlosser and Long (1975) in an effort to establish basic design criteria for reinforced earth. Particularly for testing the friction between soil and flexible fabric-type reinforcement, the choice of support material in the lower half of the box is important, as demonstrated by Delmas, Gourc and Giroud (1979).

In an attempt to simulate the development of shear resistance along cylindrical anchors, Wernick (1978) developed a direct shear box where the two halves

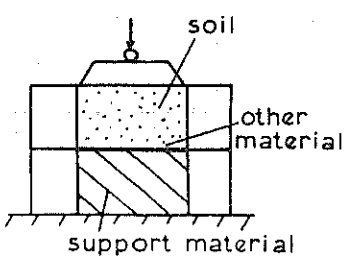

Fig. 1a Standard direct shear box

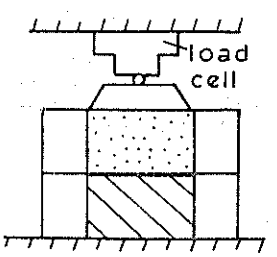

Fig. 1b Constant volume type shear box

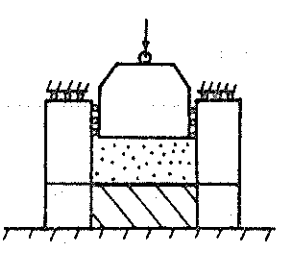

Fig. 1c "True shear" apparatus after Wernick (1978)

Figure 1 Typical direct shear test arrangements

are forced to move exactly parallel to each other and where the vertical force is induced by a non-tilting loading cap block (Figure 1c). The kinematic conditions in Wernick's "true shear apparatus" are similar to that in a conventional ring shear apparatus but unequal rates of shear strain in the failure plane are avoided. This apparatus proved particularly useful to measure dilatancy characteristics of sand.

Using an apparatus similar to that shown in Figure 1b, Guilloux, Schlosser and Long (1979) were able to monitor the variation of σ during direct shear at constant volume. A medium to fine dense sand which yielded an internal friction angle $\phi = 43^0$ in the standard test with σ = constant indicated a friction angle $\phi_c = 34^0$ at constant volume shear, while the normal stress increased more than twentyfold. However if the shear resistance was related to the original normal stress σ_0 = 50 kPa, an apparent friction angle of $\phi^* = 85^0$ was obtained. The difference between ϕ and ϕ_c was attributed to dilatancy.

For sand sliding on reinforced earth type smooth steel, the skin friction angle determined with σ = const. was $\delta = 26.5^0$. At constant volume, in contrast to the sand only tests, the skin friction angle increased slightly to $\phi_c = 31^0$. Guilloux et al concluded that in this case dilatancy was insignificant.

Apparent friction angles ϕ^* as computed by Gilloux et al lend themselves to be compared to friction angles backfigured from pull-out tests, where the normal stress is assumed to be equivalent to the overburden pressure. As indicated by Fig. 2 the ϕ^*-values decrease with increasing normal stress and appear to give an upper bound to friction angles computed from full-scale pull-out tests.

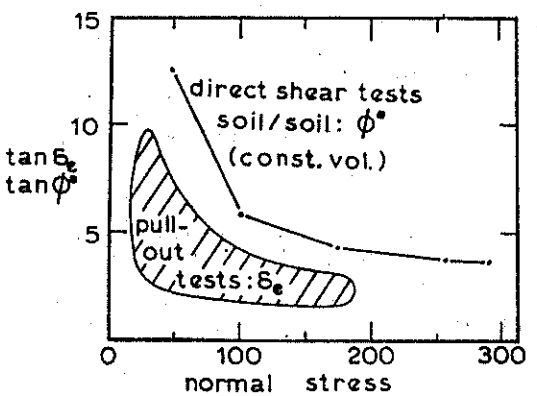

Figure 2 Apparent friction for constant volume conditions (Guilloux et al, 1979)

2.2 Pull-Out Tests

Vidal (1969) conceived reinforced earth as a new composite material in which a perfect bond between soil and reinforcement exists prior to failure. Reflecting this view, early design methods for reinforced earth walls assumed that frictional resistance developed along the entire length of the reinforcing strips contributes to the internal stability of the wall. In contrast, Lee et al (1973) thought that the earth pressure acting on the face elements is balanced by the pull-out resistance of the strips (or "ties") over that part of their total length which is beyond the potential failure wedge in the soil mass. Lee's concept of reinforced earth action led to a comprehensive program of pull-out tests in laboratory conditions and full-scale structures in the field.

A large range of results are now available, from small scale tests with less than 0.6m overburden to pull-out tests of dummy strips embedded in the backfill during the construction of full-size walls. Tie materials tested include standard reinforced earth galvanized steel strips, conventional reinforcing bars, bar mesh, mylar tape, geotextiles and other experimental materials. Tie dimensions, overburden pressure and soil characteristics are the principal variables in this research work. Pull-out resistance was also found to be affected by soil vibration. In some types of tests, the peak pull-out force required was significantly higher than the ultimate (or residual) resistance. In some large scale tests, the distribution of tie forces was recorded during pull-out.

Pull-out test results can be interpreted in terms of an "equivalent" (or "apparent") surface friction angle δ_e if it is assumed that the shear resistance is uniformly distributed along the strips and that the normal stress corresponds to the weight of the overburden plus any surcharge applied. This interpretation neglects the possible significance of relative strains between the soil and the reinforcing material and the possibility of arching.

Typical test arrangements are shown in Fig. 3. Most laboratory tests have been carried out by pulling strips out of a simple box as shown in Fig. 3a. Strips can be pulled through a rigid or flexible wall, or even without any restraint in front of the box (Chang et al, 1977), out of a soil mass of carefully controlled density, with or without surcharge on top. A sleeve may be provided to reduce any wall influence. Pull-out forces have also been measured on strips attached to a wall rotating outwards during the test (Hausmann and Lee, 1978) as shown in Fig. 3b. Delmas et al (1979) pulled fabrics through a modified direct shear box (Fig. 3c) in order to evaluate soil/fabric interaction.

An informative test series was conducted by Alimi et al (1977) who pulled out standard size Reinforced Earth strips from an experimental embankment with up to 2.5m overburden, using a pipe sleeve to avoid edge effects (Fig. 3d).

Fig. 3e gives typical dimension of the test sections of the Californian wall on Highway 39 (Chang et al, 1977) where pull-out of dummy strips was achieved without breakage for lengths of up to 7m under 5.5m overburden.

Generally researchers confirm that pull-out resistance is significantly affected by the placement conditions of the soil, the geometry of the strips and the mechanical arrangement of the experiments. French engineers concluded that the direct shear box yields conservative values of skin friction angles. In contrast, many American laboratory test results show that average shear resistance in pull-out can be substantially less than would be estimated from direct shear tests.

2.3 Indirect Methods

Soil/reinforcement interaction parameters can be backfigured from the results of model tests, the performance of full-size structures or from strength measurements in more basic tests such as triaxial or plane strain shear tests. Frictional properties are usually expressed in terms of angle

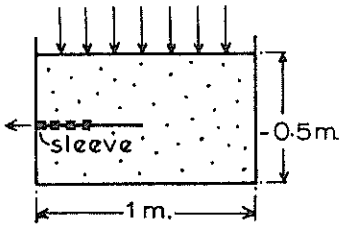

Fig. 3a Box pull-out test

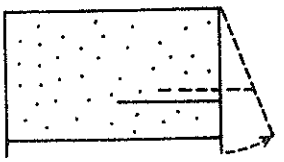

Fig. 3b Moving wall test

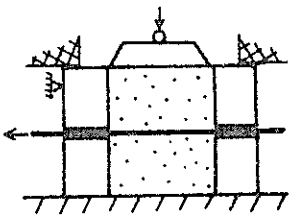

Fig. 3c Modified direct shear test

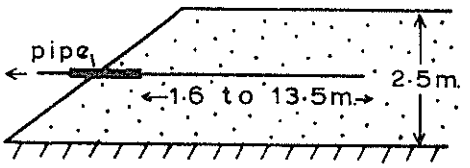

Fig. 3d Large prototype test

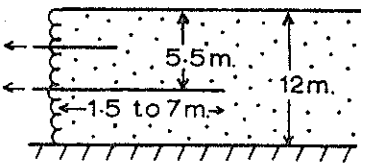

Fig. 3e Field tests on dummy strips

Figure 3 Typical pull-out test arrangements

δ of skin friction (Alternatively called surface friction or bond stress) or a friction factor $f = \tan \delta$. For cohesive soils, adhesion s_a may be calculated and, as with δ, is often presented as fractions (or multiples) of the strength parameters of the soil alone (internal friction angle ϕ and cohesion c).

The computed values of δ or s_a are only as good as the basic assumption made in the method of analysis proposed. Actually most researchers start by assuming the validity of a particular value of δ, say as determined in a standard shear box test. In order to fit experimental data to theoretical results, it may then be hypothesised that a certain lateral stress coefficient K (usually within the range K_a to K_o) or a particular distribution of normal stress σ_v or shear stress τ (based on assumed relative displacements) applies to the soil/reinforcement interface. On the other hand, if K, σ_v and τ are seen or made to follow a specific pattern, δ (and/or s_a) can be back-figured from the test. An additional complication arises in the interpretation of laboratory size model tests, where soil may be sheared at very low confining stresses. In these conditions, the angle of internal friction ϕ of a sand may be significantly higher, say, by 10^0, than the value obtained in standard triaxial tests using more "practical" higher cell pressures. A variation in ϕ has a significant effect on the values of K. Still unable to explain certain test results, researchers may then take recourse to concepts of dilatancy, arching, collapse of granular soil structure or progressive failure (emphasising the difference between peak and ultimate shear strength parameters).

Fig. 4 qualitatively compares typical shear stresses developed between mylar reinforcing material and sand in three different tests at the same overburden pressure: in strips attached to a rotating model wall, in a laboratory pull-out test and a direct shear test. Obviously the friction angles δ_e backfigured from these three tests will differ markedly, so does the general stress-strain behaviour. Fig. 4 is however only typical for the particular materials used. For rough or ribbed reinforcement, e.g., pull-out tests will likely show resistance in excess of that exhibited in direct shear.

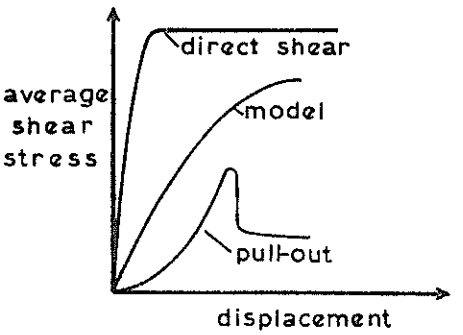

Figure 4 Shear stress between mylar and sand (typical results)

3 INTERNAL DEFORMATIONS IN DIRECT SHEAR TESTS

From the previous discussions, it can be seen that dilatancy and relative strains are significant factors affecting soil reinforcement friction. Dilatancy has already been subject of research by numerous investigators, notably Rowe (1969), Davis (1969), and Oda (1975), but experimental data is still limited.

In order to further study the dilatant properties of cohesionless soils, the authors devised a series of direct shear tests which allowed measuring the thickness of the shear zone and relative strains at the interface with another material.

3.1 Test Details

The sand used in following tests was a uniform fine sand with a sub-rounded grain. Cylindrical columns of dyed sand were formed in the shear box using drinking straws. After testing, a gelatine solution was poured into the shear box and allowed to set. The sand could then be removed and dissected to reveal the deformation pattern within

the box. Most tests were carried out for two cases: (1) shear box full of sand and (2) sand sliding on a roughened plate. This plate was formed by glueing a layer of the same sand to a metal plate.

considered rather than the rate. Finally, in Figure 9, the rate of dilatancy is plotted against normal stress. The results shown include the skin friction angle δ. Its value corresponding to 1 kPa

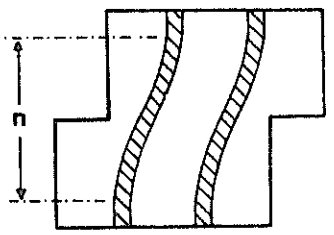

Fig. 5a Loose sand

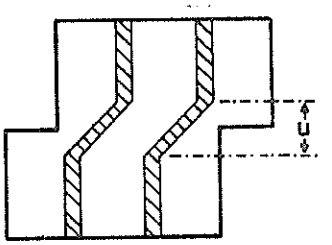

Fig. 5b Dense sand

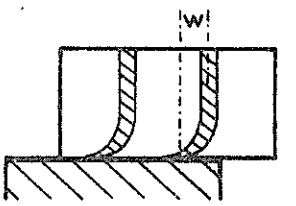

Fig. 5c Sand/plate

Figure 5 Deformation patterns in direct shear test

3.2 Test Results

The results clearly showed a marked difference between the deformation patterns obtained with a loose sand and a dense sand. Typical examples are shown in Figure 5a and 5b.

Similar patterns were found for sand sliding on a roughened plate. This is illustrated in Figure 6 where the thickness of the zone of shearing, u, is plotted against relative density. This figure shows that u for the full sand case is approximately double that for sliding on a roughened plate. The deformation pattern for this condition was found to be virtually symmetrical about the central horizontal plane of the box. Further, for the plate case, measurements of the horizontal shift as defined in Figure 5c can be used to give the relative strains at the soil/plate interface. The distance w was found to equal the shear movement applied during the test, as it would be expected for a rough plate. Rough interface behaviour was also confirmed by the friction angles computed from these tests, which are plotted in Figure 7.

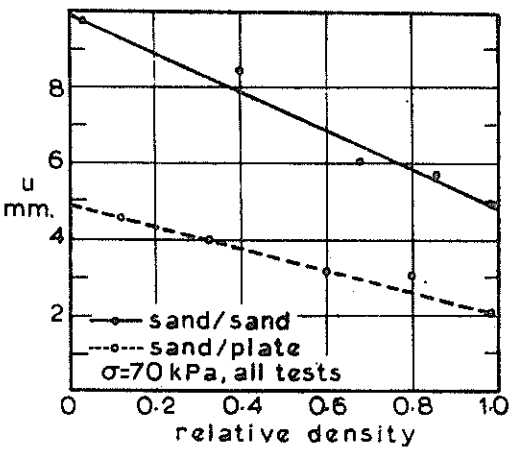

Figure 6 Variation of thickness of shear zone with density

The measure of the rate of dilatancy was taken as the maximum value of dv/dh where dv is the increment in vertical movement of the loading cap and dh the corresponding increment in shear displacement. The rate of dilatancy is plotted against relative density in Figure 8. It is interesting to note that the rate of dilatancy was approximately equal for both series of tests. The same conclusion is reached if the absolute magnitude of dilatancy is

normal stress is likely to be unreliable because of the small value of shear stress obtained in this test. Also indicated is the relative amount of slip which occurred at the sand plate interface; it varies from all slip at low stresses to no slip at higher stresses.

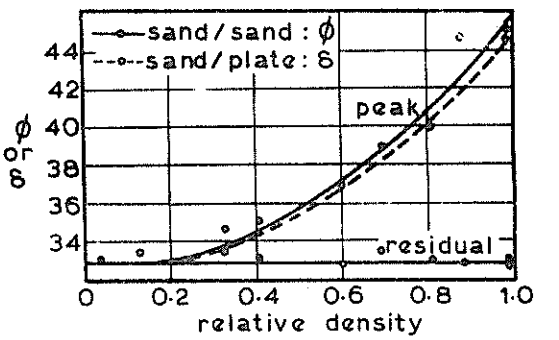

Figure 7 Friction angles as a function of density

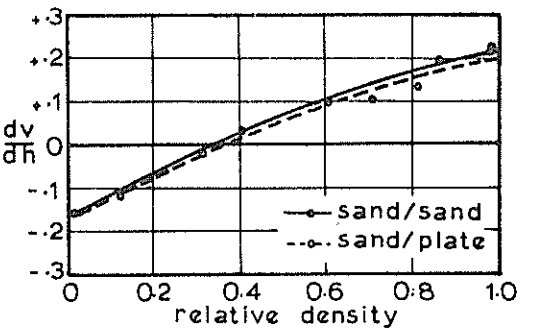

Figure 8 Variation of vertical rate of movement with density

3.3 Discussion of Results

The test results suggest that the amount or rate of dilatancy is not a function of the width of the shear zone but must be a property of the material itself and its state of density (Figures 6 and 8). Such a conclusion was theoretically reached by Oda, 1975.

If no slip occurs at the soil material interface, the skin friction angle is equal to the friction angle of the soil itself (Figure 7).

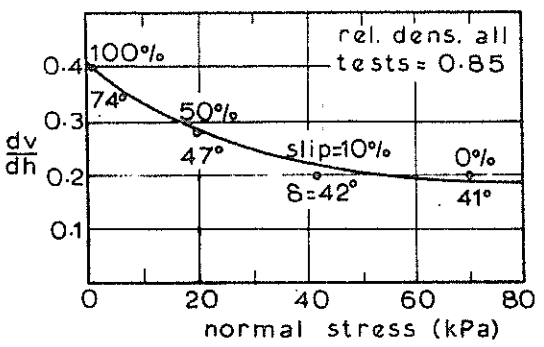

Figure 9 Variation of dilatancy, slip and friction with density

As a normal stress at the soil material interface is decreased, the amount of slip and the rate of dilatancy both increase (Figure 9). Rather surprisingly, the skin friction angle computed for low normal stresses is higher than the angle of internal friction, despite the fact more slip appears to occur. The question which must be asked is why failure does not occur within the soil itself at a lower shear stress. Kinematic restrictions of the shear box do not appear to be the answer because at higher normal stresses failure does occur within the soil. Further investigations are needed of this important low stress situation as many laboratory model tests are carried out at low stress levels.

There is a basic difference in the failure mechanism which occurs in a loose and a dense cohesionless material.

4 CONCLUSIONS

Parameters describing soil/reinforcement interaction have been obtained from direct shear tests, pull-out tests and from the interpretation of the behaviour of laboratory models and full-scale structures. The variation of the results obtained suggests that this interaction cannot be described by unique values of skin friction and/or adhesion.

Direct shear tests performed did not indicate any relationship between the thickness of the shearing zone and the rate of dilatancy. However it is felt that observing these characteristics will lead to better understanding of soil/material interface problems. The magnitude of relative strains in zones of interaction appears to be of prime importance for the interpretation of model tests and for the formulation of laws of interaction for the purpose of analysis by means of the finite element method.

5 ACKNOWLEDGEMENTS

The work described forms part of an ongoing research project carried out at the New South Wales Institute of Technology. The support and encouragement by Dr. G.J. Haggarty and Professor A. Pattison is gratefully acknowledged. Mr. T. Mathai assisted in the experimental programme.

6 REFERENCES

ALIMI, I., BACOT, J., LAREAL, P., LONG, N.T. and SCHLOSSER, F. (1977). Adherence between soil and reinforcements - In-situ and laboratory tests. Proc., 9th I.C.S.M.F.E., Vol. 1, pp. 11-14.

CHANG, J.C., HANNON, J.B. and FORSYTH, R.A. (1977). Pull resistance and interaction of earthwork reinforcement and soil. Paper presented at the T.R.B. Meeting, Washington, January.

DAVIS, E.H. (1969). Theories of plasticity and the failure of soil masses. Ch. 6 of Soil Mechanics, Ed. I.K. Lee, Sydney, Butterworths.

DELMAS, P., GOURC, J.P. and GIROUD, J.P. (1979). Analyse expérimentale de l'interaction mécanique sol-géotextile. Proc. Int. Conf. on Soil Reinforcement, Paris, Vol. 1, pp. 29-34.

GUILLOUX, A., SCHLOSSER, F. and LONG, N.T. (1979). Etude du frottement sable-armature en laboratoire. Proc. Int. Conf. on Soil Reinforcement, Paris, Vol. 1, pp. 35-40.

HAUSMANN, M.R. and LEE, K.L. (1978). Rigid model wall with soil reinforcement. Proc. ASCE Symposium on Earth Reinforcement, pp. 400-426.

LEE, K.L., ADAMS, B.D. and VAGNERON, J.M.J. (1973). Reinforced earth retaining walls. J.S.M.F. Div. ASCE, SM10, October, pp. 745-764.

ODA, M. (1975). On stress dilatancy relation of sand in simple shear test. Japanese Soc. Soil Mech. and Fndn. Eng., Vol. 15, No. 2, pp. 17-29.

POTYONDY, J.G. (1961). Skin friction between various soils and construction materials. Geotechnique, Vol. 11, No. 4.

ROWE, P.W. (1969). The relation between the shear strength of sands in triaxial compression, plane strain and direct shear. Geotechnique, Vol. 19, No. 1, pp. 75-86.

SCHLOSSER, F. and LONG, N.T. (1975). Choix du matériau de remblai. Dimensionnement des ouvrages en terre armée, murs et culées de ponts. Paris. L.C.P.C., pp. 141-148.

VIDAL, H. (1969). The principle of reinforced earth. Highway Research Record. Vol. 282, pp. 1-16.

WERNICK, E. (1978). Tragfähigkeit zylindrischer Anker in Sand unter besonderer Berücksichtigung des Dilatanzverhaltens. Publ. by The Institute for Soil and Rock Mechanics of the University of Karlsruhe, Karlsruhe.

Design of Reinforced Earth for New Zealand Conditions

B. B. PRENDERGAST
Design Engineer, Ministry of Works and Development, Wellington, N.Z.
G. RAMSAY
Design Engineer, Ministry of Works and Development, Wellington, N.Z.

1 INTRODUCTION

Reinforced Earth (R/E) is a patented system for the construction of earth retaining structures, which has been developed and is used extensively overseas. The system is now available in New Zealand, the licence holder being Reinforced Earth Limited.

This paper briefly reviews the uses, advantages, disadvantages, design methods, patented components and construction techniques associated with R/E retaining structures.

Seismic design of R/E structures is discussed in general and a particular seismic design method is considered in detail. The paper also describes the design of a large R/E retaining wall, of 1800 m^2 area and 13 m maximum height, in a seismically active area of New Zealand.

A simplified empirical seismic earth pressure loading is proposed for approximate design.

2 NOTATION

γ Bulk weight density of backfill
ϕ Effective angle of internal friction of backfill
K_o Coefficient of at-rest earth pressure
K_a Coefficient of active earth pressure

3 REINFORCED EARTH : PRINCIPLES & APPLICATIONS

3.1 History

The effect of embedded material in improving the strength of soil has been recognised by man since early history. The use of faggots, logs and rope for strengthening earth dykes, embankments and road subgrades is an application of the reinforced earth principle.

Engineers in the last 100 years have used materials such as wire mesh and wooden beams to improve the stability of earth dams, retaining walls and other earth structures. While several such systems have been patented, a method of analysing and adequately designing reinforced earth structures was not developed until the 1950s and 60s when the French engineer, Henri Vidal, carried out research and development work which culminated in his patenting and marketing the retaining wall system now known as Reinforced Earth (the capital letters indicating a registered trade name) or Terre Armee. Between 1966 and 1979 a total of 2249 structures with a combined face area of 1.3 million square metres were constructed in countries using the Vidal system. (McKittrick and Darbin, 1979).

3.2 Principles

Soil materials are basically strong in compression or shear, but weak in tension, as indicated by the normal Mohr-Coulomb failure envelope. Introduction into the soil of a material which has tensile strength, bonds to the soil and is orientated across potential tension failure planes, results in a new composite material with significant tensile strength, represented on the Mohr-Coulomb envelope as increased cohesion. Methods normally employed in designing R/E structures utilise earth pressure distributions and failure zones modified from normal limiting equilibrium earth pressure theories. The use of such empirically determined criteria disguises the fact that the R/E system results in fundamental changes to the soil mass behaviour.

While retaining wall applications of R/E require a facing wall to prevent fretting and erosion of the cohesionless soil, the R/E principles can be used in applications where facing is not required, such as in R/E mats for subgrade strengthening (Walkinshaw, 1975) and perhaps within embankments where a R/E section could provide additional tensile strength (cohesion) to inhibit formation of slip surfaces.

The principles of R/E and static design procedures are comprehensively reviewed by McKittrick (1979).

3.3 Vidal Reinforced Earth System

The R/E system developed by Vidal employs galvanised steel strips distributed in layers throughout a cohesionless backfill and connected to facing panels which are either elemental steel units, or more commonly precast concrete panels. The precast panels are of a cruciform shape and are interconnected and sealed by spigots and corbels. The reinforcing strips are normally of a rolled 60 x 5 mm thick ribbed steel sections, hot-dip galvanised for corrosion protection. An alternative 3 mm thick plain strip, cut and punched from galvanised sheet was used extensively in earlier applications, but this has largely been superseded by the ribbed strip. The ribs enhance the pull-out resistance by mobilising the full soil frictional resistance, as opposed to the lower strip/soil resistance of the unribbed strip (McKittrick, 1979). Galvanised bolts are used to connect the strips to the facing panel. A single bolt, double shear connection used with the ribbed strips, enables the full strip tensile capacity to be developed at the connection.

For the earlier plain strips, multiple bolt connections were sometimes required to reduce bearing pressures on the thinner strips.

To achieve adequate soil/strip friction a cohesionless backfill is generally used, and suitable backfill grading properties have been determined (McKittrick, 1979). In areas where such materials are uncommon, for example where softer shale rocks such as New Zealand papa predominate, the cost of importing suitable backfill may seriously affect the economics of R/E structures. Field and laboratory studies reported by Chang (1977) examined the use of an alternative reinforcing element consisting of panels of galvanised welded mesh, which appears to be suitable for use with some backfill materials containing a higher proportion of silt and clay particles than is recommended for the galvanised strip reinforcement.

3.4 Applications

R/E has been predominantly used in retaining structures for roading applications (road retaining and bridge abutments), industrial applications (material processing and storage facilities), and hydraulic applications (sea walls and sedimentation basins).

For bridging applications, it is common for the abutments to be entirely in R/E construction, thus avoiding the need for expensive piled foundations.

Applications of R/E construction are extensively reported in trade literature, which also indicates the variations in finish and appearance which are possible. While standard cruciform shape panels are normally used, variable and pleasing architectural effects can be achieved by varying the concrete surface texture and applying rib and other patterns in the moulds.

Walls up to 10 m high are common. Construction is carried out in lifts, with successive layers of facing panels, strips and backfill being placed from behind the wall line without falsework which is an advantage at congested sites. Other advantages of R/E wall construction are the vertical face which permits maximum use of the land in front of the wall, and the flexibility of R/E walls, which makes them particularly suitable for sites with poor ground conditions where some settlement is anticipated.

In general, the block of R/E has a depth of 0.8 times the height of the wall, and this can be a disadvantage as it prevents the use of the system at sites where a wall is to be constructed close to a natural steep slope which cannot be excavated.

4 DESIGN PRINCIPLES

4.1 Basic Mechanism

Generally R/E structures are designed using a tie-back analogy with Rankine limiting equilibrium earth pressures as shown in figures 1 and 2. Empirical adjustments are made to allow for the strips altering the behaviour of the soil. The strips and the soil form a composite material which acts as a gravity retaining structure.

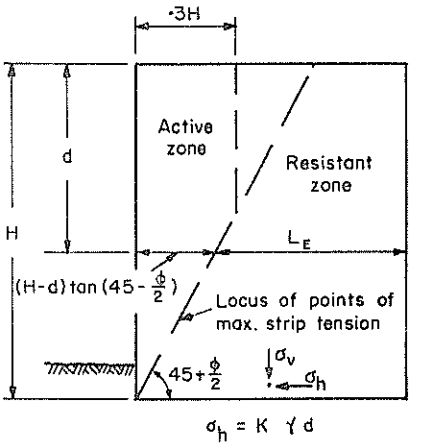

Figure 1 : Tie-back Analogy

Instrumentation of R/E structures has shown that the tensile forces in the strips are not a maximum at the facing (tie-back analogy), but at a distance behind the facing (McKittrick, 1979). For design it is often assumed that the locus of points of maximum tension in the strips follows the Coulomb wedge line ($45 + \frac{\phi}{2}$ to horizontal) except that the maximum wedge width is limited to .3H as shown in figure 1. This line defines two zones, the active zone and the resistant zone. If one imagines the active zone (or Coulomb wedge) trying to separate itself, then the strips are held in the resistant zone by friction between the strips and the soil. The length of the strips in the resistant zone is termed their effective length L_E. The strips are also held in the active zone by friction (as the maximum tensile force is some distance back from the facing), but there is probably also some tie-back effect from the panels. In practice the panels are designed for the full earth pressure (ie, as tie-backs). The tensile force in the strips is computed from this earth pressure on the panels.

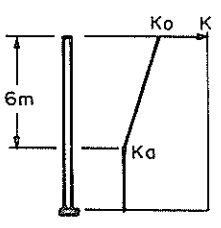

Figure 2

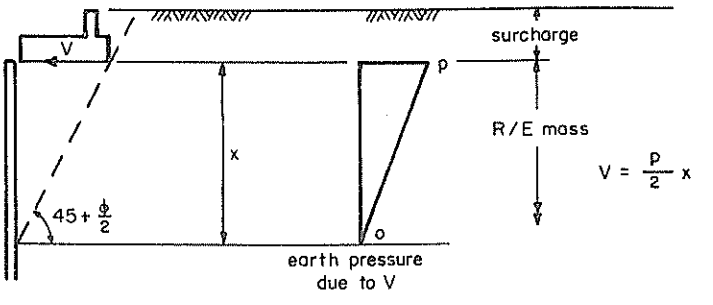

Figure 3 : Horizontal Load Distribution to R/E Mass

4.2 Earth Pressure

For the determination of lateral earth pressures in a R/E structure, the empirical relationship shown in figure 2, based on instrumentation of R/E structures, is often used.

4.2.1 Live load surcharge

The lateral earth pressure due to a live load surcharge, h_{LL}, is determined in the normal way. This amounts to a constant earth pressure of KYh_{LL} over the full height of the wall.

4.2.2 Horizontal shear load

Any horizontal shear load, V, is usually distributed to the R/E mass using the empirical relationship shown in figure 3 (Boyd et al, 1978).

4.3 Soil/Strip Friction

The frictional relationship between the soil and the ribbed strips has been investigated by means of pull-out tests (McKittrick, 1979). Ribbed strips pull-out when the soil itself shears, rather than by slippage occurring along the soil/strip interface. An apparent friction coefficient of $\tan\phi$, with some increase for soil dilation, is therefore appropriate. Pull-out tests also indicate that with continued pulling the apparent coefficient of friction drops to a residual value of about three-quarters this initial value.

4.4 Internal Stability

A R/E mass has two modes of internal failure: it can fail by strip breakage, which is sudden and catastrophic, or it can fail by strip pull-out, which will cause only a redistribution of stress and a slow deformation of the mass. A ductile failure is therefore achieved if failure is by strip pull-out, rather than by strip breakage.

4.5 External Stability

The external stability of a R/E structure is checked as for a gravity wall. The structure is considered as a rigid body, and overturning stability, bearing capacity and slip circle failure in the foundation material should be analysed.

4.6 Strip Corrosion

Corrosion of the hot-dipped galvanised steel strips is possible, but if there is sufficient data available, a cross-section and coating weight of galvanising to ensure a minimum specified service life may be selected.

This calculation of anticipated weight loss is based on laboratory or field measured values of resistivity and pH of the select backfill in saturated conditions. Experience with the corrosion of buried galvanised steel culverts gives a guide, although it should be remembered that in general these are in a more corrosively aggressive environment. In practice, when calculating the tensile capacity of the strips, 1 mm of their thickness is discounted to allow for loss of metal due to corrosion. This is then considered to give a minimum service life of at least 120 years. (McKittrick, 1979).

4.7 Select Backfill

R/E requires a select backfill which is free draining, cohesionless, and chemically and biologically inert. These properties ensure that a high shear strength is developed and that corrosion of the strips is minimised. An excessive fine grained content increases the danger of plastic deformation due to creep under working stresses, particularly during construction when the water content could be high. Research has shown that with ribbed strips the grain size which separates this fine grained portion from the granular portion is 15 μm (McKittrick, 1979).

Specifications vary, but an example of a suitable backfill would be:

Sieve Size	% Passing
150 mm	100
75 mm	75-100
80 μm	0-25

sand	60 to 2000	μm
silt	2 to 60	μm
clay	<2	μm

Plasticity Index <6
pH 6 to 10
minimum resistivity 5000 ohm.cm

More recent specifications for fill to be used with ribbed strips allow more than 25% finer than 80 μm, provided that not more than 15% is finer than 15 μm and that $\phi \geq 25^0$.

4.8 Facing Panels

Generally R/E facing panels have been unreinforced, utilising the tensile strength of concrete. Standard panel thicknesses usually vary from 180 mm at the top of the wall to 220 mm and 240 mm for higher earth pressures lower down. Some designers have reinforced the panels to maintain the 180 mm thickness throughout, and the MWD requires, in any case, some temperature and shrinkage reinforcement throughout the panels.

4.9 Panel/Strip Connection Detail

The standard panel/ribbed strip connection detail uses one 12 mm diameter high tensile bolt in double shear. The ribbed strip is sandwiched and bolted between two similar strips which protrude from the precast facing panels. Tests carried out at Auckland University show that the bearing stress on the ribbed strip can be ignored, probably owing to the confining action of the protruding strips.

5 EARTH PRESSURE DUE TO SEISMIC LOADING

The development of quantitative methods for assessing seismic earth pressures on R/E walls is relatively recent, and in the authors' opinion, as yet no completely satisfactory design method is available.

The methods available have been developed by Richardson and his co-workers from laboratory and field tests correlated to seismic analysis techniques. In the first instance Richardson and Lee (1975) examined the response of model walls excited sinusoidally on a shaking table. An earth pressure diagram shape was determined and the magnitude related to backfill properties, the natural frequency of the wall and excitation frequency. To enable the model test results to be extrapolated to full size walls under random earthquake excitation, a modal participation analysis approach was proposed. In this method a response acceleration obtained from the modal participation analysis is used as a base input acceleration in an equation for earth pressure from the model tests. The effect of amplification of the base imput is thus allowed for twice.

The excessive conservatism of the approach was illustrated in results obtained from blast excitation tests carried out on a full-scale wall (Richardson et al, 1977). While the excitation from a single blast is an impulse rather than the normal cyclic earthquake excitation, the tests provided data on material and geometric damping and on the increase in natural period with dynamic strain amplitude. Low strain natural frequencies obtained for a number of walls have provided data for the prediction of low strain first and second natural periods.

Using data obtained from the model tests and full-scale wall tests, Richardson (1978) has proposed a revised design method which yields seismic earth pressures of the order of half those predicted by the earlier model and adjusts the shape of the seismic earth pressure diagram according to the "stiffness", i.e. density of reinforcing strips in the wall.

The modal participation approach adopted allows for variation of the damping and the natural frequency for the anticipated dynamic strain level. This method was used to compute seismic earth pressures for the Ngauranga wall (see Section 7 of this paper) and appeared to give realistic answers. However, the method can be simplified further and in the authors' opinion can still yield results within the accuracy required for design purposes, considering the uncertainty of the actual earthquake response. A suggested approximation based on the Richardson method is presented in Section 7. As yet there appears to be no evidence of the location of maximum strip tensile stress under seismic loading, although this information is necessary for accurate computation of strip length.

While the methods proposed by Richardson are appropriate for major structures and those requiring a high level of seismic resistance, for minor or low-risk structures the methods may be unreasonable and may penalise R/E in comparison with other retaining wall types.

It is useful to consider basic seismic design philosophy in New Zealand. Seismic design for structures generally assumes that, for the design earthquake, major structural damage cannot be avoided and the emphasis is placed on ensuring that local failures occur where the structural integrity will not be impaired, and that such failures are ductile rather than brittle. Thus less emphasis is given to predicting member stresses exactly, and more emphasis, both in research and practice, is directed to ensuring that adequate ductility and energy absorption occurs at the predetermined failure locations.

For conventional retaining walls the traditional approach has been to use the Mononobe-Okabe limiting state equilibrium analysis which allows for a pseudo-static horizontal force to represent the earthquake. Design codes, such as that of the MWD (1978), set values for the pseudo-static force level appropriate to seismic activity zones and structure importance. These levels are set on a relatively arbitrary basis. Current research by Richards and Elms (1979) into gravity walls, has examined the significant but previously unallowed for effect of wall inertia, and the degree of movement of walls designed for varying pseudo-static force coefficients and subjected to actual earthquake type base excitation. Their results suggest that a more logical design approach for minor walls would be to set acceptable movement levels rather than attempt to arbitrarily reduce the design forces. A similar approach may be desirable for minor or low-risk R/E walls.

Because of the difficulty in predicting a "design" earthquake, the authors believe it is desirable to ensure as far as possible that in the event of a larger than design earthquake occurring, "failure" of the wall will be ductile and the wall will remain serviceable, even if permanently deformed, after the event. The model tests of Richardson and Lee (1975) indicated that where the R/E failed by strip breakage, catastrophic and complete collapse resulted, whereas when strips failed by pull-out (bond failure) the wall remained intact and fully load bearing, despite deformation of the facing. The precast cruciform panels normally used have inherent flexibility, with a significant outwards movement of the top relative to the base being possible.

It is considered desirable to detail strips to fail by pull-out rather than breakage. This may not be quite so important near the base of the wall, where, in the event of strip breakage, arching action between the foundation and higher intact areas could result in redistribution of the earth pressures.

6 THE NGAURANGA WALL

The Ngauranga wall will be a part of a major interchange of the Wellington-Foxton Motorway. It will retain the fill for the off-ramp from an overbridge structure, and will support traffic loading on the fill, but not loading from the overbridge. It will lie on a gentle horizontal curve, will be 160 m long and vary in height from 7 m to 13 m at the overbridge structure.

The sea (Wellington Harbour) is about 80 m from the toe of the wall.

6.1 Foundation Materials

The foundation materials consist of sandy gravels with some shell and silt content down to basement greywacke rock at approximately 16 m below ground level. Raymond N values indicate firm material at the surface (N = 50), a loose layer at a depth of around 5 m (N = 9), and then materials progressively firming with depth (N = 25 at 9 m). Groundwater level is approximately 3.8 m below the surface and appears to be slightly tidal.

6.2 Seismic Protection

The wall is in an area with a high level of seismicity, and the Wellington Fault runs parallel to it and in its close vicinity. The importance of the motorway which the wall supports demands a high level of seismic protection.

6.3 Alternatives Considered

At the design report stage, three basic types of wall were considered. A crib wall was not considered viable for this height of wall.

The following estimates exclude the cost of fill, but they do, however, include a cost differential for the R/E alternative to allow for the extra cost involved in a select backfill. CF represents the seismic design coefficient.

	CF	$/m²
Counterfort	.24	370
Tie-back	.24	350
R/E	.30	265

The R/E estimate was based on a quotation from Reinforced Earth Limited for a MWD preliminary design, and the cost was assumed to be spread between the various materials and operations in the following percentages:

R/E Ltd	(RC facing panels	25%
	(ribbed steel strips	25%
	(other	10%
	site labour and plant to erect	20%
	fill	20%

The R/E wall was adopted for the following reasons:

(a) it was considered the best technical solution to accommodate the anticipated settlement;

(b) it was practical to design it for a high level of seismic protection and to ensure a ductile failure;

(c) it was the most economical.

7 DESIGN OF THE NGAURANGA WALL

7.1 Design Policy

In general the detailed design was done in accordance with the loading combinations, allowable stresses and safety factors set out by MWD (1973, 1978). The working stress method was used throughout, apart from the design of the concrete facing panels where the strength method was used. Wherever possible Reinforced Earth Limited standard components were used.

Two loading combinations governed the design: (MWD, 1978). Static earth pressure + live load surcharge (equivalent to a height of 0.6 m) with normal allowable stresses; static + seismic earth pressures with a 33% increase in allowable stresses.

7.2 Select Fill Parameters

A good quality clean granular greywacke fill is available close to the site, and for this the following design parameters were adopted:

$\gamma = 19$ kN/m³, $\phi = 35^0$, $K_A = .27$, $K_o = .43$ (MWD, 1973)

7.3 Seismic Earth Pressure

The method described by Richardson (1978) was used to determine the pseudo-static seismic earth pressure loading on the R/E mass. This method represents the design earthquake by its Richter magnitude. A Richter magnitude of 7.5 was used to represent El Centro N-S 1940, which was considered to be appropriate for New Zealand earthquake code requirements.

The Richardson method assumes that R/E acts as a strain softening material, with natural period and damping increasing with increase in strain. The greater the density of reinforcing strips the stiffer the wall, and the varying stiffness of walls is taken into account by a factor I, where

$$I = \frac{\text{stiffness of wall}}{\text{stiffness of reference wall}} \quad \text{and } 1 \leq I \leq 2$$

Seismic earth pressure reduces with increase in value of I.

The Richardson method relies on empirical adjustments to correlate theory with model observations. Although calculations suggested a value of I close to 2 for the Ngauranga wall, a more conservative value of I = 1.5 was, in fact, adopted. It was found that, for a given Richter magnitude and I value, the seismic earth pressure varied directly with h (over the range h = 6 to 12 m considered), as shown in figure 4, where h is the free height of wall above ground level.

As shown in figure 4, the approach for R/E walls compares reasonably well with the Mononobe-Okabe approach usually adopted for ordinary retaining walls; it should be borne in mind that the stiffer R/E wall would be expected to induce lower earth pressures, and the ordinary retaining wall example with CF = .24 is probably designed to a lower seismic design level.

An approximate seismic earth pressure, conservatively based on these results, is also shown in figure 4. It is suggested that except for major structures, this would be appropriate for R/E structures in New Zealand seismic zone A, with the usual reductions to 75% and 50% for zones B and C respectively. (MWD, 1978).

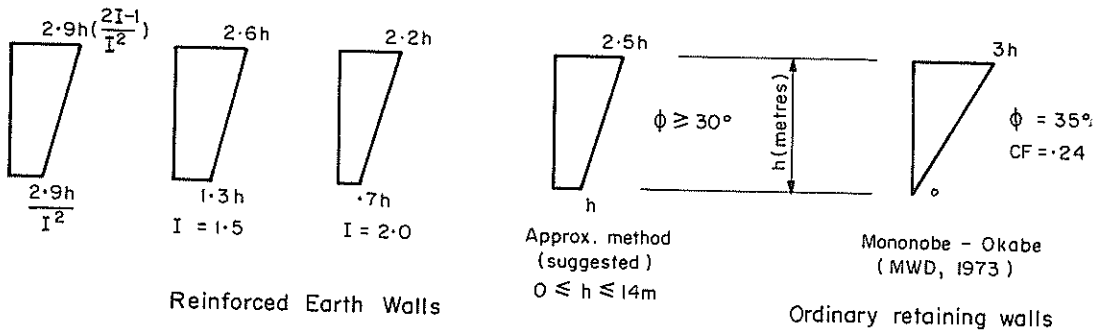

Figure 4 : Seismic Earth Pressure (kN/m²)

7.4 Strip Design

7.4.1 Strip density

The number of strips per panel was determined by considering the strip breakage failure mode and by practical considerations. It is not practical to have less than 4 strips per panel, and common standard panels have arrangements of 4 or 6 strips per panel. The design earth pressures for the governing loading combination taken over a panel area gave the total tensile force in the strips, and the number of strips required was determined by dividing this by the allowable tensile force per strip. As the design earth pressures increased with depth so did the theoretically required density of strips. However, it was found in this case that 4 strips per panel were sufficient throughout.

The static pressure + live load surcharge load combination governed for strip density.

7.4.2 Strip length

The length of strips at each level was determined by considering the strip pull-out failure mode. The static + seismic pressure load combination governed for strip length. The apparent coefficient of friction used for both load combinations was $\mu_{allowable} = .65 \tan\phi$. This was based on a value of soil shearing of $\tan\phi$, safety factors for sliding from MWD (1973) and a reduction factor of .75 to obtain the residual apparent coefficient of friction (McKittrick, 1979) which is appropriate for seismic loading.

From the tensile force per strip (7.4.1), overburden pressure ($= \gamma d$), the strip width (using both faces) and $\mu_{allowable}$ ($= .65 \tan\phi$) the effective strip length was calculated.

The length of strips extending over (H-d) tan $(45-\frac{\phi}{2})$, as shown in figure 1, was taken as being ineffective. This ineffective length was not limited to the maximum of 0.3H assumed in static design, as it was considered that insufficient testing under dynamic conditions had been done to justify this.

In theory, without any surcharge, required strip lengths approach infinity at the top of the wall. Consequently R/E specifications normally require a minimum depth of fill of 1 m above the strips. Also at a certain distance back from the facing panels the top layer of strips is often draped down to increase the depth of fill above it.

Because of the seismic earth pressure loading at the top of the Ngauranga wall, the strip lengths required were excessive. This problem was overcome by increasing the minimum fill depth on the strips in two ways:

(a) The design incorporated a 1 m high precast L-shaped cantilever wall, placed on top of the facing panels. The shear from the earth pressure on this 1 m height was distributed to the R/E mass as indicated in figure 3.

(b) Behind the facing panels the top two layers of strips were draped down 750 mm and 375 mm respectively.

Strip lengths for the Ngauranga wall are shown in figure 5. Although for strip breakage considerations, four strips per panel were adequate throughout, at the highest part of the wall geometric limitations restricted the length of strips to 13.5 m and this necessitated the use of 6 strips per panel in this region.

7.5 External Stability

The overturning and sliding safety factors required by MWD (1973) were easily achieved and did not affect the design.

The maximum foundation bearing pressure (during seismic loading) under the R/E mass, was approximately 400 kN/m^2. This was considered acceptable for a R/E structure founded on the materials at this site. Normally quoted allowable bearing pressures for cohesionless soils are governed by settlement considerations, so are very conservative for R/E structures which can readjust internally.

7.6 Facing Panel Reinforcement

Generally MWD design policy does not allow unreinforced concrete in a structural member. However, it was considered that the minimum amount of temperature and shrinkage reinforcement normally required did not necessarily apply to these panels. All the panels were made 180 mm thick and reinforced in one layer. It was possible to use the same amount of reinforcement in all the panels, as the design for the maximum earth pressure still only required about 70% of the amount normally required for temperature and shrinkage reinforcement, and this seemed a reasonable minimum quantity of reinforcement to use. A layer of 663 mesh (150 x 150 mm, 205 mm^2/m) located at one third the depth of the section, was specified. An alternative was considered using

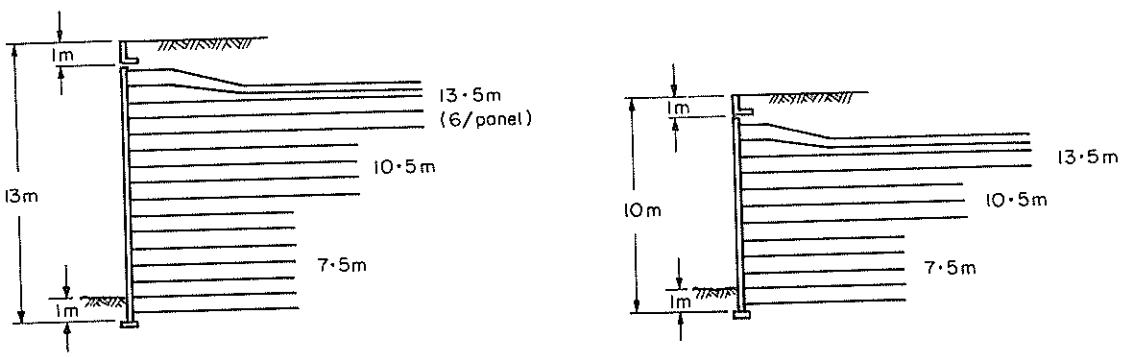

4 strips per panel unless indicated otherwise

Figure 5 : Ngauranga Wall Cross-Sections

12 mm diameter bars, the standard 1.5 m square panel requiring 5 bars horizontally and 4 vertically. It was found that with 4 strips per panel, strip spacings of 750 mm, both vertically and horizontally, optimised the bending moments in the panel, using yield line theory for the analysis.

The standard panel/ribbed strip connection detail was adopted after its strength was tested and confirmed at Auckland University, as discussed in sub-section 4.9.

7.7 Ductile Failure

An attempt was made to ensure that at each strip level internal failure due to overloading would be by strip pull-out rather than strip breakage. This required that at each strip level the minimum probable safety factor against breakage (SF_b) should be greater than the maximum probable safety factor against pull-out (SF_p).

SF_b was determined using the minimum tensile strength of the strips, this being approximately 50% greater than yield strength. To determine SF_p, values of $\mu_{allowable} = \tan\phi$ and $\phi = 40^0$ were used.

Because, in general, a 4 strip per panel arrangement was used throughout the wall height, the value of SF_b was high near the top of the wall but reduced lower down the wall. Consequently, the criterion of $SF_b > SF_p$ was easily satisfied at the top of the wall, but became progressively more difficult to satisfy lower down. In fact, some strips at lower levels had to be shortened to satisfy this criterion. (In practice, to limit the number of different strip lengths on the job, many strips are longer than they theoretically need to be.

So, in general, ductility was easily achieved towards the top of the wall, but due to the many assumptions made in the calculations and the fact that the SF_p could, on occasion, be much higher than calculated, it was not so certain that a ductile failure towards the base of the wall was ensured. However, it was considered that the pull-out requirement was not so essential at the base, due to the arching action of the fill at this level, as discussed in Section 5.

8 CONCLUSIONS

The R/E system has provided a satisfactory and economical solution for the design of a major retaining wall, where the depth of fill and foundation conditions would have made conventional solutions difficult and costly to construct.

R/E is already being used in New Zealand and the partly empirical design methods are being applied.

Seismic loading can be taken into account with R/E structures, and will in practice usually result only in longer strips being required towards the top of the structure. In general, ductility is automatically achieved near the top of the structure and can, to a lesser extent, be achieved lower down with minor detailing changes.

Except for major structures, the approximate seismic earth pressure loading shown in figure 4 may be used, as this is consistent with the design appr approach and loading generally adopted for conventional retaining structures in New Zealand.

9 ACKNOWLEDGEMENTS

The permission of the Commissioner of Works, to publish this paper, is acknowledged.

10 REFERENCES

BOYD, M.S., VERGE, G.C. and REID, J.B. (1978). Practical application of Reinforced Earth theory. Symposium on Soil Reinforcing and Stabilising Techniques, Sydney, pp 83-109.

CHANG, J.C. (1977). Pull resistance and interaction of earthwork reinforcement and soil. TRB, TRANSPORTATION RESEARCH RECORD 640. pp 1-7.

McKITTRICK, D.P. and DARBIN, M. (1979). Worldwide development and use of Reinforced Earth structures. Ground Engineering. March, pp 15-21.

McKITTRICK, D.P. (1979). Reinforced Earth : application of theory and research to practice. Ground Engineering. January, pp 19-31.

N.Z. MINISTRY OF WORKS AND DEVELOPMENT (1978). Highway bridge design brief. Civil Division Publication 701/D.

N.Z. MINISTRY OF WORKS AND DEVELOPMENT (1973). Retaining wall design notes. Civil Division Publication 702/C.

RICHARDS, R. and ELMS, D. (1977). Seismic behaviour of retaining walls and bridge abutments. Civil Engineering Research Report No.77-10. University of Canterbury

RICHARDSON, G.N. and LEE, K.L. (1975). Seismic design of reinforced earth walls. Journal of the Soil Mechanics and Foundations Division, ASCE, Vol 101, No GT2, February.

RICHARDSON, G.N., FEGER, D., FONG, A. and LEE, K.L. Seismic testing of Reinforced Earth walls. Journal of the Geotechnical Engineering Division, ASCE, Vol 103, No GT1, January.

RICHARDSON, G.N. (1978). Earthquake resistant reinforced earth walls. ASCE Spring Convention and Exhibit, Pittsburgh, April.

WALKINSHAW, J.L. (1975). Reinforced Earth construction. Department of Transportation Report No FHWA-DP-18.

The Water-jet Penetration Test — A Field Test of Loess Erodibility

S. P. A. HARRISON
Post Graduate Student, Department of Geology, University of Canterbury, N.Z.
J. K. HILL
Consulting Engineering Geologist, Christchurch, N.Z.

SUMMARY The development of a water-jet penetration test for measuring the erodibility of loess is described. The advantages of the test as a rapid and reproduceable means of measuring erodibility are shown. Two applications of the test are given as examples.

1 INTRODUCTION

A number of tests exist to estimate the erodibility of loess. These tests include the qualitative or semi-quantitative examination of loess samples in the pinhole, drop, crumb, and field dispersion tests; and quantitative examination in chemical tests and surface flume tests. All of these tests require considerable laboratory and field time. Most of the tests are subjective and evaluate the occurrence of dispersion or slaking. None is performed in situ and they do not always simulate realistically the field conditions affecting erodibility. Little is known in quantitative terms of the areal distribution of erodible loess, and without the investment of excessive time and effort none of the current laboratory tests can give a sufficient number of measurements to determine the distribution. Because of this limitation and various procedural limitations of available tests, there is a need for a rapid, reproduceable field test for erodibility.

2 THE APPARATUS

The water-jet penetration apparatus, developed in 1978 at the University of Canterbury, comprises a high pressure air source driving water from a pressurised tank through a nozzle designed to give a fine laminar jet (see Figure 1). An alloy diving cylinder of 27 cubic metres capacity provides the air source. Air is fed via a pressure regulator to a stainless steel water reservoir at 689 KiloPascals. The 5 litre capacity water reservoir is designed for fast filling and has a pressure relief valve. A WEBSTER Model "147" air dusting gun controls the water flow, which is also at 689 KiloPascals. A 0.6 millimetre welding nozzle attached to the gun gives a fine liminar jet of water. The apparatus is mounted on a pack frame with a flat base enabling it to be placed upright on level terrain. The apparatus, when full, weighs approximately 23 Kilograms.

A measurement is made by aiming the water-jet normal to an in situ loess surface (see Figure 1) and the penetration is measured under standard conditions, including time of application, air pressure, and distance from the surface. A provisional set of standard conditions was established during a series of trials in 1978. The conditions optimise the erosive force of the jet and make efficient use of the capacity of the water reservoir. They are: duration of jet - 10 seconds; distance from nozzle tip to the loess surface - 100 millimetres; water pressure - 689 KiloPascals. Penetration is measured using a wire depth gauge and a millimetre rule (see Figure 1 inset).

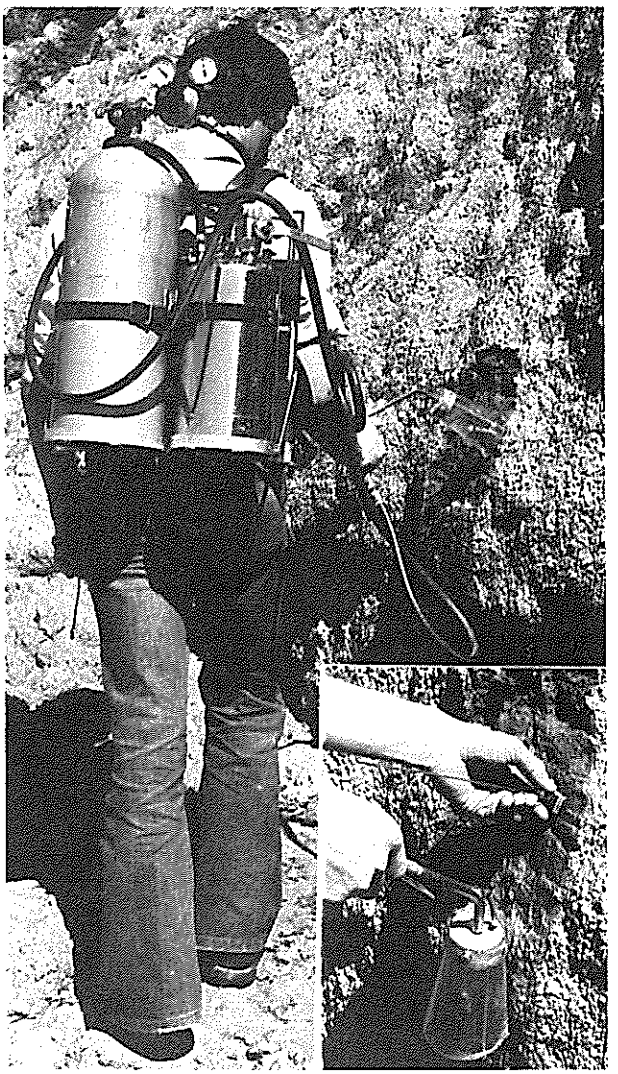

Figure 1 Apparatus in use, inset shows sample measurement

3 TWO APPLICATIONS

The water-jet penetration test was applied to a fresh-cut loess bank to see if layers of different erodibility in the loess profile could be distinguished. Eight groups of 15 measurements were made at 300 millimetre intervals down the bank. Five different penetration responses were distinguished at the 90 percent confidence level using the Mann-Whitney U-Test for non-parametric data. These different responses corresponded visually to identifiable layers in the loess profile. The water-jet penetration test thus showed there are layers in a loess profile with significantly different penetration values, which correspond to visual changes in loess character.

Another application tested the ability of the water-jet penetration apparatus to distinguish zones of different penetration resistance surrounding a subsurface tunnel. Ninety-two measurements were made on a grid pattern normal to the tunnel axis at its point of efflux. A contour diagram of the penetration data revealed zones of increased penetration, possibly associated with the tunnel opening. Further work is necessary to determine which loess properties are controlling water-jet penetration.

4 CONCLUSIONS AND FUTURE WORK

Preliminary investigations show that the water-jet penetration test could prove a satisfactory field test of loess erodibility. The test has the following characteristics:

a. It is a rapid test in which a sample measurement takes only seconds to obtain.

b. Very little, if any, laboratory work is required.

c. An in situ measure of loess characteristics is provided, and drill cores could be quickly tested if necessary.

d. The method has proved statistically valid and does not suffer from the limitations of low sample numbers as do many laboratory tests.

e. The test is a more objective approach to measuring loess erodibility than some other tests.

Future work will include an impirical examination of some of the geotechnical parameters which may control water-jet penetration in loess. These parameters include grainsize distribution and packing, water content, Atterberg Limits, clay mineralogy and exchangeable cations, and local factors such as lo loess type, slope angle, and aspect. A comparison will be made with existing erodibility tests.

Compaction Properties of Bay of Plenty Volcanic Soils, New Zealand

I. M. PARTON
Director, Mandeno, Chitty and Bell Ltd
A. J. OLSEN
Senior Geotechnical Engineer, Mandeno, Chitty and Bell Ltd

1 INTRODUCTION

The extraordinary physical properties of soils of volcanic origin were significant in the construction of a 3.3 km earthlined headworks canal for the 20 MW Ruahihi hydro-electric power project. The scheme is the final stage of hydro-electric development on the Wairoa River for the Tauranga Joint Generation Committee.

Soils at the site were found to have high natural water content, high plasticity, high sensitivity and low bulk density. These physical properties gave rise to problems during earthworks construction; namely, difficulties in excavation and compaction. These problems have since been attributed to the presence of the clay mineral allophane; similar difficulties have been reported by Northey and Schafer (1974). Perhaps the most perplexing property is that the soils undergo irreversible changes on drying. Hence compaction control values were found to be dependent on the treatment of the soils before testing.

This paper describes the engineering characteristics of the soils encountered at the site and the work carried out to establish parameters for compaction control. A range of laboratory tests were carried out to investigate the effects of pre-treatment of the soils encountered.

2 THE CANAL

The canal passes through rugged topography, traversing ridges and deeply incised river gorges necessitating cuts of 40 m depth and embankments of up to 15 m in height. At the downstream end, the canal is constructed on the top of a narrow ridge and structural fills are required on either side for stability. The canal is 8 m deep with 1 on 2 side slopes (in both cut and fills) and has a 4.5 m wide invert. The flow under maximum operating conditions is 28 cumecs. Earthworks design required the utilisation of all 2 million cubic metres of cut material.

3 GEOLOGICAL SETTING

The dominant feature of the project area is a broad plateau (the north-western margin of the Mamaku Plateau) that has been deeply incised by the Wairoa River and its tributaries. The ignimbrite forming the basement in the region is the middle Pleistocene Waiteariki Ignimbrite. Overlying the ignimbrite is a massive grey pumice breccia. This pyroclastic flow material was extensively eroded and redeposited within small lakes and rivers giving rise to highly variable and discontinuous lacustrine/alluvial sedimentary units. A further ignimbrite flow overlying the pumice breccia has been deeply weathered into a cream to reddish-brown silty clay. The present topography mantles the upper surface of these deposits.

Two sequences of volcanic tephras form a covering deposit 2 - 4 m thick, over the whole region. The older tephras are the highly weathered andesite Hamilton ash beds (approx. 0.3 my) while the younger tephras range in age from 41,000 years (Rotoehu Ash) to the present.

4 WEATHERING OF ALLOPHANE SOILS

Allophane soils are products of weathering of parent volcanic material. Fieldes (1966) has shown that the occurrence of allophane in soils is favoured by conditions that lead to the formation and persistence of random structural hydrous alumnosilicates such as:

i) Weathering of basic silicate material.
ii) Weathering of glasses in rhyolitic and andesitic volcanic ashes.
iii) Weathering of feldspars.

This weathering produces disordered structures with no discernible regular arrangement. The materials known collectively as allophanes appear under X-Ray diffraction as disordered fluffy formless substances termed gels.

Fieldes (1966) and Fieldes and Furkert (1966) state that the properties of these gels depend upon the extent to which dehydration has progressed. In their hydrous condition the allophane consists of gel-like fragments of alumnosilicates held together by random cross-linking at a small number of points. Large amounts of water are often enclosed in the open structure and these allophanic substances are termined hydrogels. Upon dehydration progressive isometric shrinkage occurs as increasing condensation and cross-linking leads to more compact structures termed xerogels. This process is largely irreversible and air drying of these fine grained cohesive soils tends to produce non-plastic silty sands. The effect of this irreversible drying is discussed further in Sections 5 and 6.

Fieldes and Furkert (1966) report great differences in the physical properties of allophane soils that are permanently wet and those which have been dried. This is very marked at the Ruahihi site where the surface ash is more friable due to periodic wetting and drying while the lower ignimbrites, which are permanently beneath the ground water level, exhibit a characteristic greasy consistency due to the presence of hydrogels.

Mineralogical analyses have been undertaken by the Geological Survey of the DSIR on typical samples of

both soils (see Table 1). The absence of recognisable volcanic glass in samples P26 and P27 is probably the result of more intense weathering of these soils and is consistent with the relative quantities of allophane and halloysite present. Fieldes (1955) distinguishes between the various forms of allophane and indicates that with increasing age clays derived from the weathering of parent volcanic material pass through a typical sequence allophane B → allophane AB → allophane A → meta-halloysite → kaolinite. This mechanism is consistent with the data contained in Table 1. Other minerals recorded in small amounts were quartz, plagioclase feldspar, cristobalite, illite and gibbsite.

TABLE 1

MINERALOGICAL ANALYSIS

Sample	Glass	Allophane	Halloysite
P17 Ash	Present	Abundant	Minor
P18 Ash	Present	Abundant	Minor
P20 WI	Present	Abundant	Minor
P26 WI*	-	Abundant	Common
P27 WI	-	Common	Abundant

*Weathered Ignimbrite

5 CLASSIFICATION TESTS

5.1 Atterberg Limits

A number of Atterberg Limit tests have been performed on soils recovered during the preliminary investigations and subsequently during construction (see Table 2). These tests were performed on materials which had not been subjected to drying before testing and the data relate only to samples on which liquid and plastic limit tests were performed. Many other water content tests have been performed and values in the ash as high as 221% have been measured.

TABLE 2

ATTERBERG LIMIT VALUES

Material	Index	Average	Range
Brown Ash	ω (%)	63	45-85
	LL (%)	85	64-115
	PL (%)	67	42-97
	PI	18	7-37
	< 75 μm (%)	56	32-84
Weathered Ignimbrite	ω (%)	86	36-240
	LL(%)	83	44-170
	PL(%)	68	31-130
	PI	15	2-57
	< 75 μm (%)	58	45-72

Note: ω = natural water content

5.2 Presence of Allophane

The test for presence of allophane as described in Test 13 NZS 4402P Pt 1: 1976 has been carried out on a number of samples. In general the test results indicate that few samples contain less than 5% allophane, while approximately equal numbers of tests show allophane contents in the range 5% - 7% or exceeding 7%.

5.3 Particle Size Distribution

A number of wet sieve tests were carried out according to Test 9A of NZS 4402P Pt 1: 1976 to investigate the effect of pre-treatment by drying back from the natural water content. Samples were washed through a nest of sieves down to the 63 μm sieve. For this comparative work the hydrometer test was not carried out.

Test results presented in Figure 1 show a marked change in particle size distribution depending upon whether the soils have been maintained at their natural water content before testing or pre-treated by drying.

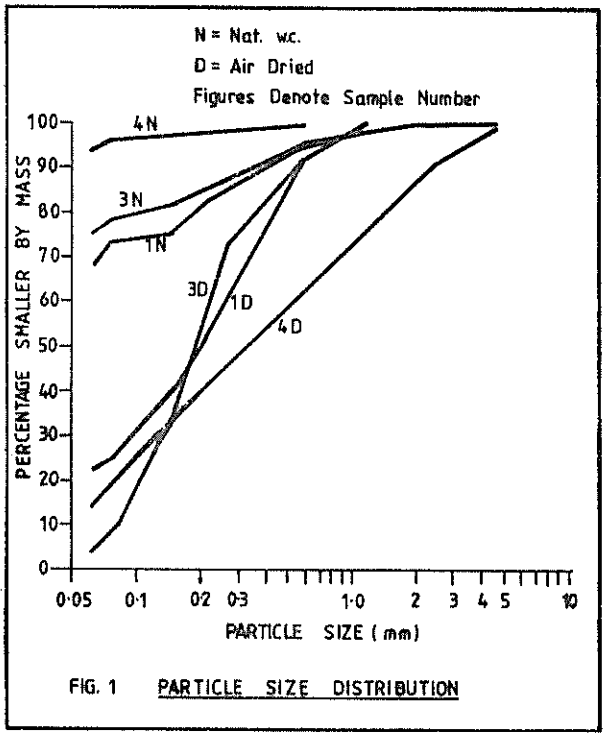

FIG. 1 PARTICLE SIZE DISTRIBUTION

6 COMPACTION CHARACTERISTICS

The physical properties of the *in-situ* soils have been described briefly in the preceding sections. In essence, the soils exist at relatively high water contents with high void ratios and low bulk densities.

Substantial drying of the soils is necessary to produce satisfactory earthfill materials. Table 3 presents average data compiled from laboratory compaction testing during construction. The ash had to be dried from an average water content of 63% to an optimum value of 46% while the weathered ignimbrite from 96% to 52% to achieve maximum dry densities of 1.09 and 1.06 tonnes/m^3 respectively.

The characteristic irreversible changes brought about by drying the allophane soils were significant in establishing the compaction properties of the soils at Ruahihi. Test results were found to be very dependent on the pre-treatment of the soils. In many cases, if specimens for compaction testing were prepared by drying back from their natural water contents, an ill-defined relationship between water content and maximum dry density was found with no clearly defined optimum water content

TABLE 3

Soil Type	Property	Average	Range
Volcanic Ash	ω (%)	63	36-123
	ρ_d (t/m^3)	1.09	0.83-1.55
	OWC (%)	46	23-66
Weathered Ignimbrite	ω (%)	96	33-178
	ρ_d (t/m^3)	1.06	0.72-1.42
	OWC (%)	52	32-88

ω = Natural water content
ρ_d = Maximum dry density
OWC = Optimum water content

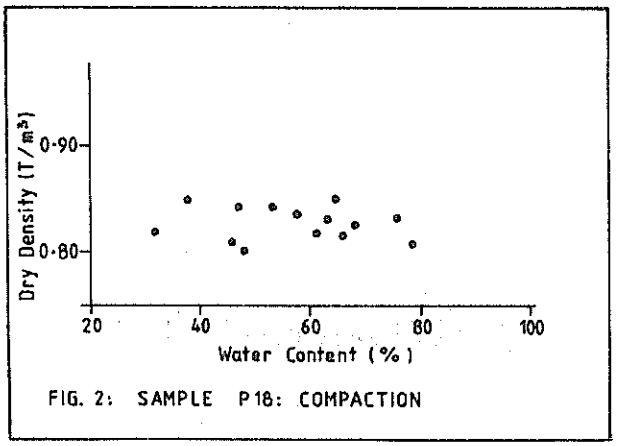

FIG. 2: SAMPLE P18: COMPACTION

as shown in Figure 2.

Wesley (1973) reported that optimum water contents of two allophane soils found in Indonesia were not well defined if the soils were prepared in this manner. He also showed that if the soils were air dried to various water contents and then prepared for compaction by wetting up from those intermediate values, any value of optimum water content and maximum dry density could be obtained. An illustration of Wesley's data is given in Figure 3 where decreasing initial water contents result in decreasing optimum water contents and increasing maximum dry densities.

Curve	Pretreatment
A	Natural Water Content
B	Air-dried to 65 %
C	Air-dried
D	Oven-dried

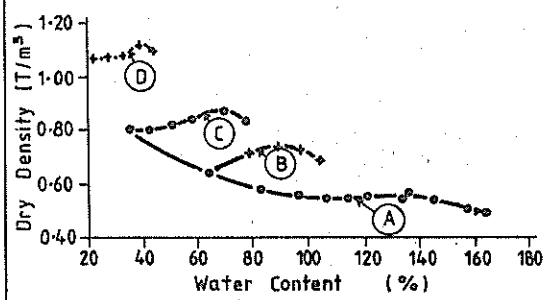

FIG. 3: COMPACTION CURVES FOR ALLOPHANE SOILS (from WESLEY 1979)

Frost (1967) has reviewed the behaviour of a number of tropical soils and examined the behaviour of some soils found in Papua New Guinea. His work showed that soils containing allophane, halloysite and gibbsite, exhibit irreversible changes in normal air drying which can significantly affect the engineering properties of the soils.

The same trends have been observed in the ash and ignimbrite soils found at Ruahihi. In one particular case (shown graphically in Figure 4), three samples were allowed to partially dry in the field during earthworks operations. Sample E was then subjected to complete air drying in the laboratory before preparation of specimens by wetting up and curing. Samples F and G were prepared by wetting up from the partially dry state. Sample E, which has been air dried, shows a significantly higher maximum dry density and lower optimum water content than samples F or G.

Curve	I W C* %	O W C %	ρ_d (Max.) T/m³
E	<5	45·5	1·07
F	64·5	57·5	0·98
G	75·3	64·0	0·93

* initial water content

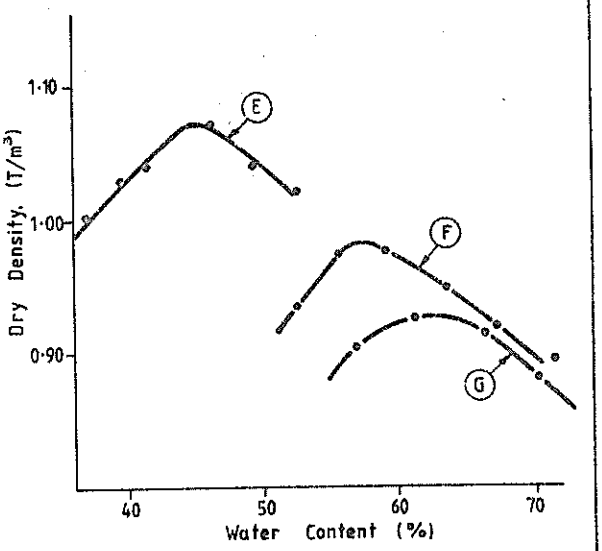

FIG. 4 COMPACTION CURVES AT DIFFERENT INITIAL WATER CONTENTS

Further studies were undertaken to investigate the effects of drying and curing in the pre-treatment of soil for compaction testing. The drying effect described above was investigated by comparing pre-treatments according to two standard test methods. The draft New Zealand Standard (DZ 4402P Pt. 2:1978, Tests 14 and 15) precludes a drying and wetting cycle prior to compaction. This is in recognition of the changes allophane soils can undergo when subjected to cyclic drying and wetting. In this standard test method specimens are prepared by drying back or wetting up from the "as received" water content with no other cyclic changes in water content. This method is referred to hereafter as the drying back method.

On the other hand Test 12 of BS 1377: 1975 allows complete air drying of the soil in certain circumstances and the specimens are further prepared by wetting up to the required water contents. This method is referred to hereafter as the air drying method.

Figure 5 presents data from compaction tests on sample P29, a weathered ignimbrite. Compaction tests using the 2.5 kg rammer have been carried out using both the drying back and air drying methods. The effects of curing have also been investigated. Samples H and I were prepared by drying back. Sample H was compacted immediately after drying, whilst sample I was cured for 24 hours after drying before compaction. The difference between the two curves is negligible and is to be expected as the drying process in this case was slow and curing took place essentially as the sample was drying.

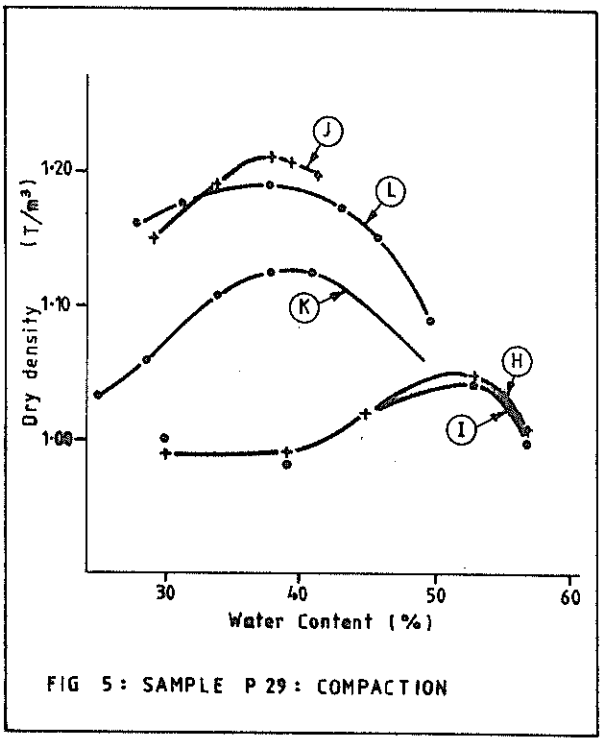

FIG 5: SAMPLE P 29: COMPACTION

Further tests were carried out by complete air drying, wetting up and then compacting immediately or curing prior to compaction. The resulting curves labelled J and K in Figure 5 show the non-cured specimens, J,gave a substantially higher dry density and lower optimum water content than the cured specimens, K.

Figure 5 also shows the curve L, for specimens prepared by drying back from the natural water content and compacting with the 4.5 kg rammer without curing. The increased energy of compaction is reflected in a higher maximum dry density and lower optimum water content than specimens prepared in the same manner but compacted according to the 2.5 kg rammer method.

Similar series of tests carried out on sample P38 are shown in Figure 6 and the trends above are again evident.

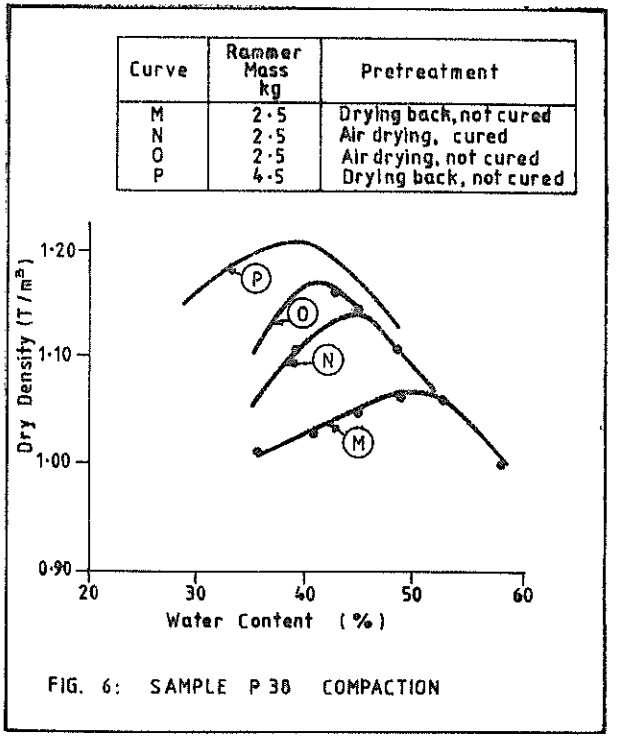

FIG. 6: SAMPLE P 38 COMPACTION

7 COMPACTION CONTROL

The most widely used and accepted method of earthfill compaction control is based on the comparison of the dry density and water content of the field compacted soil with the laboratory determined values of maximum dry density and optimum water content. A certain proportion of the maximum dry density must be achieved in the fill and the water content of the soil must lie within a specified range, which usually encompasses the optimum water content.

The main shortcomings of such a method for use in highly variable soils is that each time a new soil type is exposed in the cut or borrow area, a new laboratory compaction curve must be obtained, which could result in unacceptable time delays in the earth works.

Other methods of compaction control were considered at the time the earthworks specification was prepared. Control based on minimum shear strength and maximum air voids criteria such as reported by Pickens (1978) has certain advantages. Perhaps the main advantage of the method is that even in soils of variable compaction characteristics the need to establish compaction curves for each material type is eliminated. The air voids determination depends mainly on the field dry density and is insensitive to small variations in the solid density of soil particles.

This latter parameter was assessed during investigations and is checked from time to time during construction. At Ruahihi however, even values of solid density of soil particles were found to vary widely. This would have necessitated providing new values of solid density of soil particles for each soil type and hence the advantage of the method over the conventional dry density/water content method of control would have been largely negated.

A control method based on the 'compaction ratio', where field densities are compared with the laboratory density of the soil compacted at the field water content (an attempt to negate the irreversible changes on drying) was rejected because of its lack of general acceptance.

The specification for compaction control of the earthworks contracts at Ruahihi was written to BS 1377: 1967, as the draft New Zealand Standard (DZ 4402: Part II: 1978) was not published at that stage. Preliminary compaction testing of the soils adhered strictly to Test 11 BS 1377: 1967. To obtain consistent results the following procedures were adhered to as allowed with the BS test method:

a) the soil was air-dried to zero water content;
b) sub-samples for compaction testing were wet up to the required water contents;
c) sub-samples were cured for a minimum of 16 hours prior to testing;
d) the soil was not re-used;
e) at least 300 g mass of each compacted specimen was taken for water content determination.

This practice has been adhered to for all construction phase testing. It is recognised that the air drying method (not allowed by Test 14, DZ 4402, Pt. 2: 1978) changes many of the physical properties of the soil, but it is considered that this change is somewhat irrelevant to the question of compaction control as the laboratory testing merely sets the standard against which values achieved in the earthfill are compared. In addition, the values of maximum dry density and optimum water content achieved by the air drying method are conservative when compared with values obtained by drying back.

8 CONCLUSIONS

The irreversible changes allophane soils undergo on drying from their natural water contents were significant in establishing the compaction properties of volcanic soils encountered at a site in the Bay of Plenty. In many cases if specimens for compaction testing were prepared by drying back or wetting up from the natural water content, an ill-defined relationship between water content and maximum dry density was found with no clearly defined optimum water content.

To overcome this problem, and to establish unique values for compaction control, specimens were prepared for compaction testing by complete air drying prior to wetting up and curing before compaction. It has been shown that air drying to intermediate water contents, between the natural and air dried states, results in a range of compaction curves lying under the zero air voids line with no clearly defined maximum dry density or optimum water content.

The method evolved for determination of the dry density/water content relationship at the Ruahihi site is as follows:

- air dry soil completely and pass through 19 mm sieve;
- wet up to range of desired water contents and cure for 16 hours minimum in sealed containers;
- compact without re-using the soil.

It was found that the most practical method of compaction control was the comparison of water contents and dry densities of the field compacted soil (using the core cutter method) with laboratory determined values of maximum dry density and optimum water content. The main shortcoming of this method is the time delay in preparing a compaction curve when new soils are exposed in borrow areas. However, by maintaining close control on earthworks operations it has been possible to foresee changes in material types in sufficient time to avoid delays in obtaining control values from the laboratory.

9 ACKNOWLEDGEMENTS

The permission of the Taurang Joint Generation Committee to publish this paper is gratefully acknowledged.

10 REFERENCES

FIELDES, M. (1955). Clay mineralogy of New Zealand soils. Pt. 2, Allophane and related mineral colloids New Zealand Journal of Science and Technology Vol. 37, No. 3, pp 336-350.

FIELDES, M. (1966). The nature of allophane in soils. Part 1, Significance of structural randomness in pedogenesis. New Zealand Journal of Science Vol. 9, No. 3, pp 599-607.

FIELDES, M. and FURKERT, R.J. (1966). The nature of allophane in soils. Part 2, Differences in composition. New Zealand Journal of Science. Vol. 9, No. 3, pp 608-622.

FROST, R.J. (1967). "Importance of correct pre-testing preparation of some tropical soils." Proc. First South-East Asian Regional Conference on Soil Engineering, Bangkok, pp 43-53.

NORTHEY, R.D. and SCHAFER, G.J. (1974), Lime Stabilisation of New Zealand Soils. New Zealand Journal of Science, Vol. 17, pp 131-150.

PICKENS, G.A. (1978). "A practical method of compaction control." Proc. 2nd Conference of the Road Eng. Assn. of Asia and Australasia, Manila, pp36-43.

WESLEY, L.D. (1973). Some basic engineering properties of halloysite and allophane clays in Java, Indonesia. Geotechnique. Vol. 23, No. 4, pp471-494.

Friction and Cohesion Parameters for Highly and Completely Weathered Wellington Greywacke

M. J. PENDER
Senior Lecturer in Civil Engineering, University of Auckland

SUMMARY Data from five site investigations in central Wellington are pooled. Results of more than 190 consolidated undrained triaxial tests on highly and completely weathered greywacke are analysed statistically. The analysis shows the effective stress cohesion parameter is highly uncertain.

1 INTRODUCTION

Between 1969 and 1973 the Central Laboratories of the New Zealand Ministry of Works and Development were involved in five site investigations in the central Wellington area. At all the sites profiles of greywacke, weathered in situ, were encountered. The strength parameters for the completely and highly weathered material were of importance for the structures under design, which included multi-storey buildings, bridge foundations and cut slopes. Specific investigation work was done at each site. Subsequently the opportunity was taken to examine the results of all the laboratory tests on the material.

The properties of the weathered greywacke encountered at one site and the method of classification are described by Pender (1971). Both completely weathered and highly weathered greywacke have a buff brown colour, the relict joint surfaces are evident by the presence of a deposit of black manganese dioxide. The completely weathered material is easily crumbled to sand and silt sizes under finger pressure. The highly weathered material is more difficult to crush under finger pressure and at least some of it cannot be crushed to sand and silt sizes.

The various sites are fairly close, as shown in Figure 1. From the point of view of visual classification the material at all the sites was similar. Thus all the data were pooled and analysed as a group. No detailed statistical analysis was done comparing the strength parameters from one site with another, there was not enough data for this. No site appears to have test results greatly different from others, Figures 2 to 7.

Continuous cores, 100 mm in diameter, were recovered with a triple tube rotary coring barrel. This gives good quality undisturbed core. A total of 193 triaxial tests were done on 100 mm diameter specimens from the five sites. The tests were all consolidated undrained with pore water pressure measurement.

The earlier paper (Pender, 1971) provided a detailed examination of the results from the Public Trust Office Site in Lambton Quay. This suggested that the void ratio of the weathered material was a useful independent variable for correlating the values of various physical properties.

The results of the statistical analysis show that the effective stress friction angle is a most reliable parameter, the 95% confidence limits on ϕ' are close to the best estimate of ϕ'. On the other hand the cohesion intercept is a much more variable parameter. The 95% confidence limits are very wide and in all cases the lower confidence limit on c' is zero.

2 REGRESSION ANALYSIS

A complete tabulation of the individual triaxial test results is given by Pender (1977) as well as the output from the statistical analysis. The data were pooled and sorted into common void ratio ranges. The test results subjected to a linear regression analysis to give best fit values of c' and ϕ'. The 95% confidence limits for the predicted shear stress at each normal effective stress were also calculated. The correlation coefficient for the best fit line is very close to unity. This has the consequence that the 95% confidence limit values also suggest a straight line. Thus further linear regression analyses were done on the 95% confidence values to

1 Bolton Street Overbridge
2 Aurora Terrace Overbridge
3 Public Trust Office
4 Herbert Gardens
5 Southern Portal, Terrace Tunnel

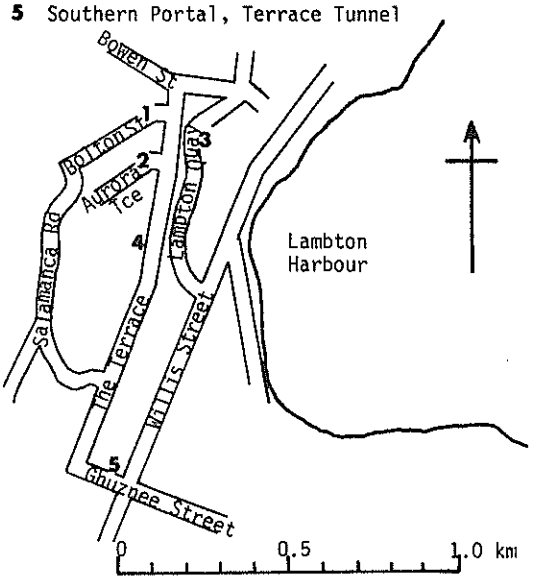

Figure 1 Locality of the five sites in Central Wellington from which the weathered greywacke samples were taken

give 95% confidence limits for ϕ' and c'. The results of this analysis are given in Table I.

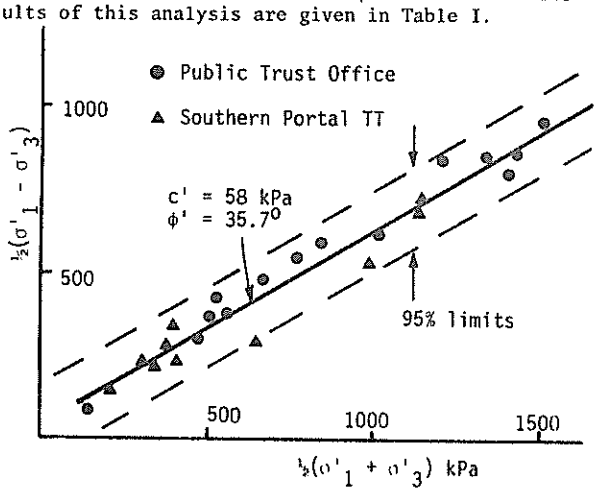

Figure 2 Triaxial results for the void ratio range 0.25-0.40

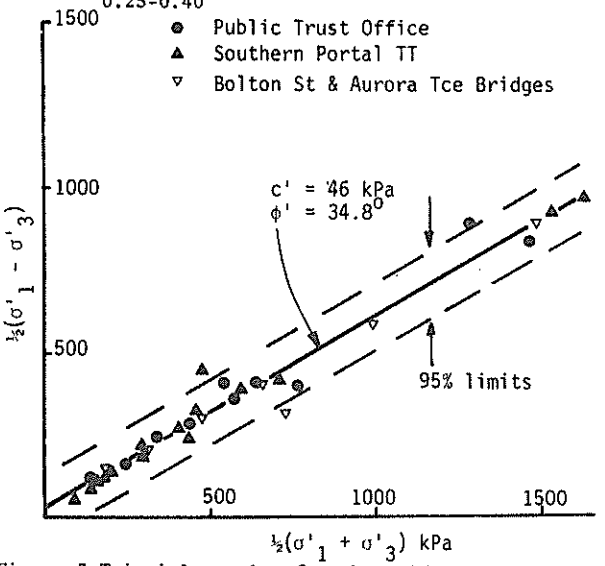

Figure 3 Triaxial results for the void ratio range 0.40-0.50

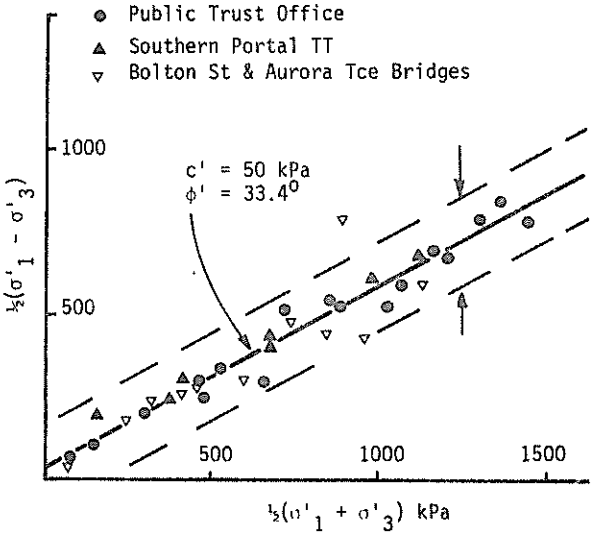

Figure 4 Triaxial results for the void ratio range 0.50-0.60

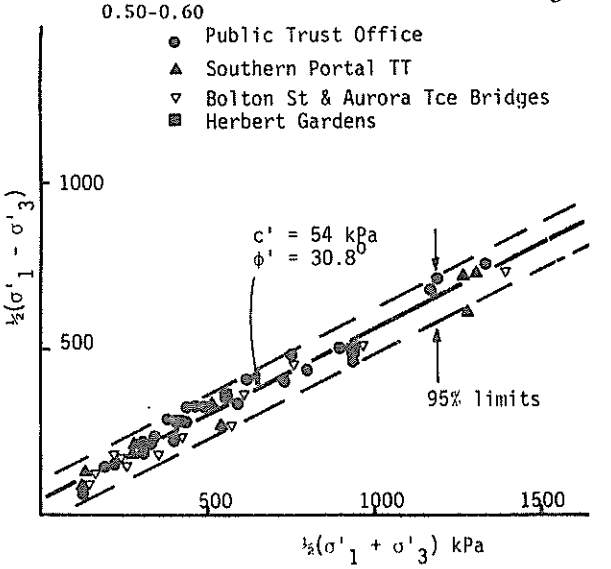

Figure 5 Triaxial results for the void ratio range 0.60-0.70

The lower 95% confidence limit value calculated for c' by this process was always negative. An additional option available in the statistical package used was the ability to perform a linear regression analysis in which the best fit straight line was forced through the origin. This option was tried with the intention that a more realistic lower limit for c' might be given. The result is shown in Figure 8. The lower 95% friction angle then diverges from the data. Thus the unconstrained option was adopted for the calculation of the lower 95% limits. The resulting ϕ' values appear in Table I, the c' values are assumed to be zero.

Careful examination of the data in Figures 2 to 7 shows, that at the low normal stress end of the data, all the data points lie on or beneath the best fit line. This suggests that the linear approximation for the failure envelope may no longer be valid at low normal stresses. In this region the failure envelope may curve down towards the origin. As insufficient data are available in this range the possibility cannot be investigated further.

In Figures 9 and 10 the results given in Table I are plotted. It is clear from Figure 10 that there is a good correlation (although nonlinear) between void ratio and the effective friction angle. On the other hand the effective cohesion, Figure 9, is much less reliable.

3 DISCUSSION

In Figure 7, for the void ratio range 0.80-0.90, there are only seven data points. As a consequence the confidence limits are wide. Figure 5, for the void ratio range 0.60-0.70, has sixty data points. In this case the 95% confidence limits are much narrower, but even so the limits on the cohesion are still rather wide. Figure 7 then raises a query about the conventional testing procedures that are used to determine c' and ϕ'. A typical number of test results on which c' and ϕ' would be determined is 4, 5 or 6. A worthwhile procedure would be to evaluate the 95% confidence limits on c' and ϕ' as a routine matter in soil testing. This would lead to a rather more caution in choosing cohesion values for analyses.

The fact that no data points are found in the very low normal stress range in Figures 2 to 7 is a consequence of performing consolidated undrained

TABLE I

SUMMARY OF REGRESSION ANALYSIS

Void Ratio Range	Number of Specimens	Best Fit Straight Line			95% Confidence Limits		
					Upper		Lower
		ϕ' (Degrees)	c' (kPa)	Regression Coefficient	ϕ'	c'	ϕ'
0.250-0.400	24	35.7	58	0.979	35.8	201	34.5
0.400-0.500	32	34.8	46	0.984	35.0	162	34.6
0.500-0.600	39	33.4	50	0.968	33.5	39	33.2
0.600-0.700	60	30.8	54	0.986	30.9	128	30.7
0.700-0.800	31	28.6	48	0.969	28.7	132	28.5
0.800-0.900	7	27.1	36	0.907	27.3	209	26.8

triaxial tests on material that would be classed as dense or heavily overconsolidated. Because of the negative pore water pressure response of such material the effective stress path approaches the failure envelope by moving up to the right. Thus even with a very low initial effective consolidation pressure there is a large increase in normal stress before failure is reached. For a cut slope problem the long term stress path approaches the failure envelope by moving to the left. Thus a drained constant axial stress triaxial test might be more appropriate for the determination of strength parameters for the long term stability of cut slopes.

The degree of saturation of the specimens before testing was generally high (greater than 90%). For some of the specimens saturation was ensured by the application of back pressure but generally no special measures were taken to ensure saturation. Saturated behaviour represents the worst possible condition in situ. Using the values for c' and ϕ' quoted in this paper it would be possible to show that many apparently stable cuttings around Wellington should have failed. This is probably because the material is not saturated, the suction in the pore water gives a larger effective stress and hence strength. During wet conditions this suction is relieved leading to greatly increased numbers of failures.

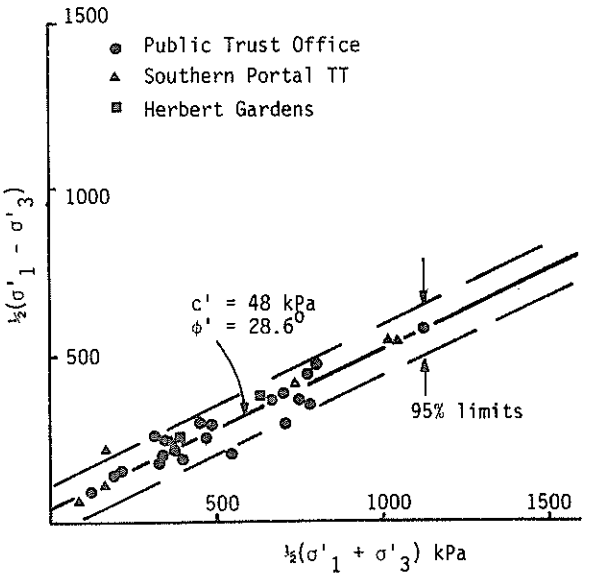

Figure 6 Triaxial results for the void ratio range 0.70-0.80

As the highly and completely weathered greywacke can be crumbled under finger pressure, stability analysis based on soil behaviour is appropriate, despite the presence of the relict joints in the material. It is difficult to decide how to handle the uncertainty in the cohesion parameter, particularly as the conventional limiting equilibrium stability analyses show that cohesion has a great effect on the maximum stable slope height. For an important structure one could argue that cohesion should be neglected and the slope designed on the basis of frictional behaviour only. Slopes steeper than the friction angle then require a support system such as ground anchors. Alternatively the large variations in c' can be considered by conducting a probabilistic analysis to find the probability of failure rather than the factor of safety. To simplify the calculations several assumptions are required about the variation of soil properties through the soil mass. Nevertheless the insight gained is sufficiently different from that given by the factor of safety approach to make the analysis of considerable interest. Such a series of calculations was done for the Southern Portal of the Terrace Tunnel (Pender 1976) which was constructed in a soil profile consisting mainly of greywacke weathered in situ.

Each test result plotted in Figures 2 to 7 represents

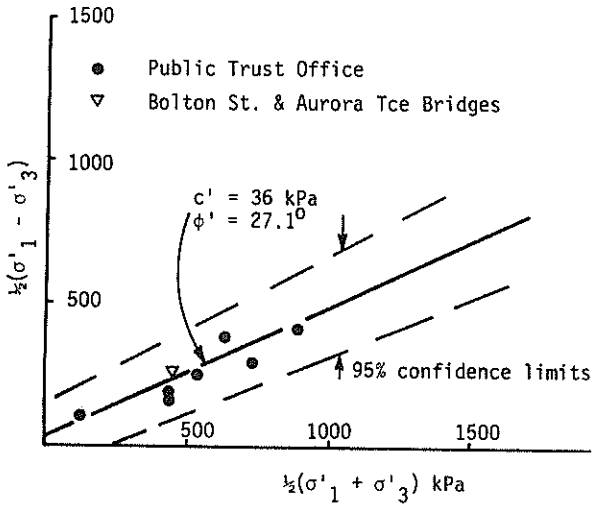

Figure 7 Triaxial results for the void ratio range 0.80-0.90

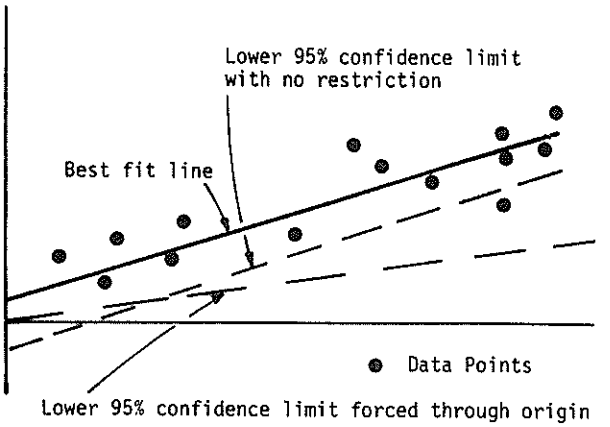

Figure 8 Regression analysis for lower 95% confidence limit on cohesion

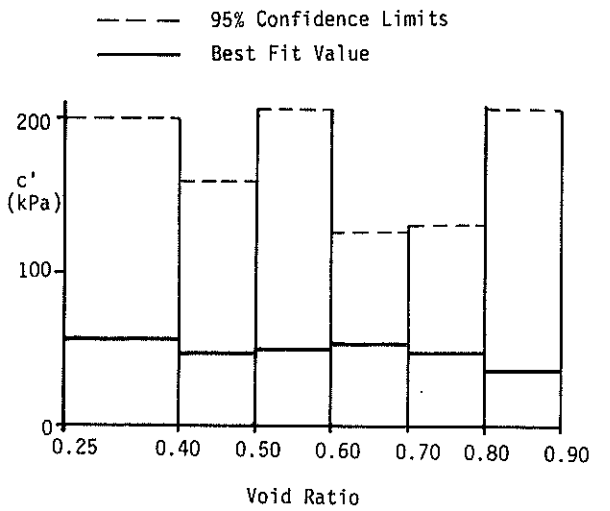

Figure 9 Variability of the effective stress cohesion parameter as a function of void ratio

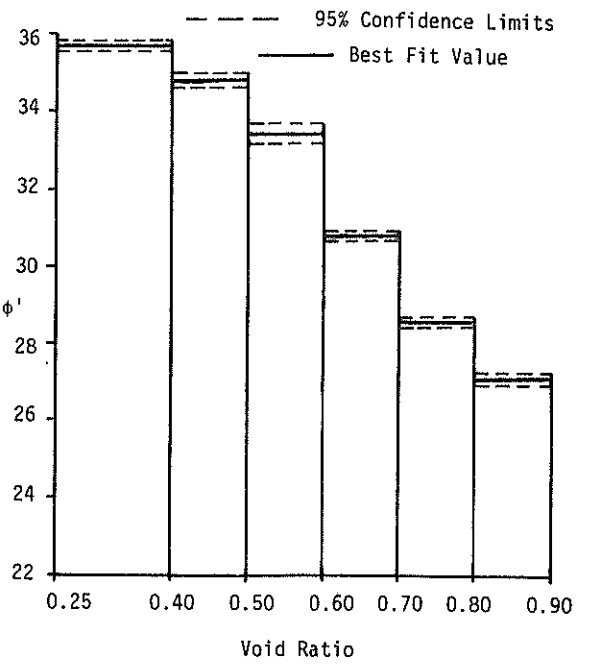

Figure 10 Variability of the effective stress friction angle as a function of void ratio

the behaviour of a volume of material that is small in relation to the volume of soil mobilised in civil engineering projects. Is the soil mass in situ to be modelled as a large number of small units about the size of a triaxial specimen all having different properties? Or is it to be regarded as a large mass of homogeneous material with an uncertain cohesion? The first of these possibilities would seem to be more likely, the second provides a simpler model for the purposes of the probabilistic analysis mentioned above. If the first of these ideas is correct it suggests that the appropriate cohesion for the completely and highly weathered greywacke is the best fit value obtained from a large number of tests. The cohesion for some elements of the soil mass will be greater than this and the cohesion for others less. However with such a distribution of cohesion values it is not necessary that the best fit or average value would control the strength of the soil mass. Perhaps a 'weakest link' mechanism operates leading to a type of progressive failure. The apparent cohesion would then be less than the best fit value.

4 CONCLUSIONS

The results plotted in Figures 2 to 7 suggest that the properties of the completely and highly weathered greywacke from the five central Wellington sites are a function more of void ratio than locality in the city. Figure 10 then provides a ready means of predicting the likely friction angle for the material if the void ratio is known. However, Figure 9 does not provide a similar means of estimating the effective cohesion of the material.

The statistical analysis of the test results emphasizes very clearly the uncertain nature of the effective cohesion parameter. The test results show that the cohesion can be expected to vary between wide limits from point to point in the soil mass. The choice of the appropriate cohesion value, even with the benefit of a large number of test results, is not a simple matter.

5 REFERENCES

PENDER, M.J. (1971). Some properties of weathered greywacke. Proc. 1st Aust.-N.Z. Conference on Geomechanics, Melbourne. Vol. I, pp 423-429, Vol. II, pp 573-574.

PENDER, M.J. (1976). Probabilistic assessment of the stability of a cut slope. N.Z. Engineering, Vol. 31, pp 239-241.

PENDER, M.J. (1977). Friction and cohesion parameters for highly and completely weathered Wellington greywacke. M.W.D. Central Laboratories Report 2-77/7.

The Behaviour of a Compacted Tertiary Siltstone Under Seismic Loading

D. V. TOAN
Senior Geotechnical Engineer, Beca Carter Hollings & Ferner Ltd
J. P. BLAKELEY
Director, Beca Carter Hollings & Ferner Ltd

SUMMARY: A comprehensive laboratory testing programme including both monotonic loading triaxial tests and stress controlled dynamic triaxial tests has been carried out to assess the suitability of fine sandy siltstone as fill material in the construction of a 72m high earth dam. The grading suggests that the compacted siltstone can provide high frictional resistance as well as low permeability. The monotonic triaxial tests indicated that the material tends to compact under load and this may lead to build up in pore pressure under cyclic earthquake loading. However, the dynamic triaxial tests subsequently showed that the compacted siltstone will provide a high resistance to liquefaction. It was concluded that the compacted siltstone will provide a satisfactory fill material for the proposed dam.

1 INTRODUCTION

This paper summarises the work carried out during the feasibility study for the Patea Hydro Electric Scheme for the Egmont Electric Power Board. The construction of a large (1 million cubic metre volume) earthfill dam was proposed on the Patea River (and is now in the detailed design stage). The selected dam site is situated in a deep sided valley. The meanders are deeply incised in near horizontal layers of sedimentary Tertiary Sandstone. The materials considered for use in the dam were the Tertiary Sandstone (which underlies the whole area) or silts and gravels deposited by various means on the river terraces.

The silts (volcanic ash) deposited on the old elevated river terraces were considered not suitable due to the high in-situ moisture content. The old terrace gravels found beneath the volcanic ash were variable in degree of weathering and were a long distance from the dam site. The river gravel would require costly dredging and hauling due to the difficult terrain. Comparative studies indicated that the most economical source of fill material would be the Tertiary Sandstone obtained from the high ground adjacent to the dam site.

Preliminary work indicated that the Tertiary Sandstone deposit consists of thick layers of mudstone, siltstone and sandstone interbedded with thinner layers of limestone. The mudstone layer was found to be suitable as core material but could not be readily quarried due to excessive depth of overlying material. Grading tests showed the sandstone layer to be an almost uniform fine sand which is not suitable due to its likely high permeability.

The siltstone layer is evenly graded and was observed to be readily available in large quantities adjacent to the dam site.

The Patea dam site is situated in a seismic zone. Doubt has been previously expressed regarding the competence of the sands and silts derived from these Tertiary deposits as an earth dam material. The near uniform particle size suggested that saturated compacted siltstone in the dam shoulders may liquefy or become mobile if subjected to severe earthquake shaking.

A laboratory testing programme consisting of both monotonic loading triaxial testing and dynamic triaxial testing was carried out to assess the behaviour of the saturated compacted siltstone under earthquake shaking.

2 LABORATORY STUDY

2.1 Volumetric Strain Behaviour

A simple approach to the study of liquefaction potential of a granular material is to postulate that for a certain effective confining pressure there exists a critical density above which the material will tend to dilate under loading and below this critical density the material will tend to compact. A saturated sand compacted to a density below its critical density will develop positive pore pressures under undrained conditions

when loaded to failure, while above this critical density the pore pressure developed will be negative. The development of positive pore pressures may lead to liquefaction if the pore pressure accumulates as a result of repeated loading and approaches the level of the confining pressure.

In order to study the variation of volumetric strain behaviour of the Tertiary siltstone proposed to be used in the dam with different degrees of compactive effort the siltstone was compacted as follows:-

(i) standard effort : 2.5 kg hammer falling 300mm 25 blows/50mm layer

(ii) heavy effort : 4.5 kg hammer falling 458mm, 25 blows/50mm layer

(iii) extra heavy effort : 3 times the heavy effort.

The maximum dry densities achieved are shown in Table 1.

move horizontally towards the steady state line as load is applied. This denser material would tend to dilate at failure under drained test conditions and develop negative pore pressure under undrained conditions.

However, even for a dense material (as defined by Lee and Seed, 1967), the material tested as described above will tend to contract under a confining pressure higher than the critical confining pressure (point E, figure 4).

The volume change records shown in Fig 1 indicate the critical effective confining pressure to be about 150 kPa. According to the critical void ratio theory, the siltstone compacted using the "standard" compaction effort may liquefy when sheared under an effective confining pressure in excess of 150 kPa.

Figs 2 and 3 indicate that for the siltstone compacted using the "heavy" compactive effort, the critical confining pressure would be about 250 kPa and for the "extra heavy" compactive effort in excess of 500 kPa.

TABLE 1

RESULTS OF MONOTONIC TRIAXIAL (CD) TESTS

Compaction Effort	Optimum Moisture Content %	Maximum Dry Density t/m^3	Effective Cohesion C' = kPa	Effective Friction Angle ϕ' = degrees
"Standard"	16	1.76	55	29
"Heavy"	13	1.91	186	32
"Extra Heavy"	11	2.01	210	38

100mm diameter samples compacted at optimum moisture content were loaded monotonically in a conventional triaxial cell. Consolidated drained triaxial tests were carried out with continuous volume monitoring. These were carried out as staged triaxial tests in order to study the volumetric behaviour of the material over a wide range of effective confining pressures.

Results of the stress and strain and volume change curves as shown in Fig. 1, 2 and 3 indicate that the siltstone tends to contract initially under the range of confining pressures used for all three levels of compacted densities. The level of volume reduction is greatest in the "standard" sample and decreases for the samples compacted with greater effort. No dilation was noted at failure in the "standard" sample, however some dilation occurs at failure in the "heavy" and "extra heavy" samples (following initial contraction).

It was noted that for small levels of strain, the siltstone will tend to contract, even if it was compacted to 114% of standard compaction ("extra heavy"). Castio and Poulos (1977) state that liquefaction only occurs in materials that are highly contractive, i.e. their effective confining stresses and density must lie above the steady state line (point A in figure 4). The material would then reduce in volume under drained test conditions or develop positive pore pressure under undrained conditions.

A material whose density and stress state lie below the critical line, (point C in figure 4) may tend to contract slightly at first but then it will

The practical level of compaction achievable in dam construction using sandy material is in the order of 95% to 100% of the "standard" compactive effort and hence the "heavy" and "extra heavy" compactive efforts would not be economically achievable in the field.

The effective confining pressure under a 72m high dam would be in excess of 700 kPa. Therefore it is concluded from the test results obtained that the compacted siltstone will develop positive pore pressures under earthquake loading. However, this may not necessarily mean that liquefaction will occur under earthquake as liquefaction will depend on the magnitude of the pore pressure rise during an earthquake load cycle, its rate of dissipation and the eventual build up due to the accumulation of the residual pore pressure at the end of each load cycle.

The next step was to study the pre pressure behaviour under cyclic loading which simulates earthquake loading.

2.2 Pore Pressure Build up Under Cyclic Loading

Stress controlled dynamic triaxial tests were carried out in the Civil Engineering Department of the University of Auckland. The samples were 100mm diameter and compacted to a range of densities, similar to those used for the monotonic load tests described above. The cell pressure was kept constant, the pore pressure was continuously monitored and the cyclic loading was applied axially. Full details of the dynamic triaxial apparatus have been published (Taylor, 1967).

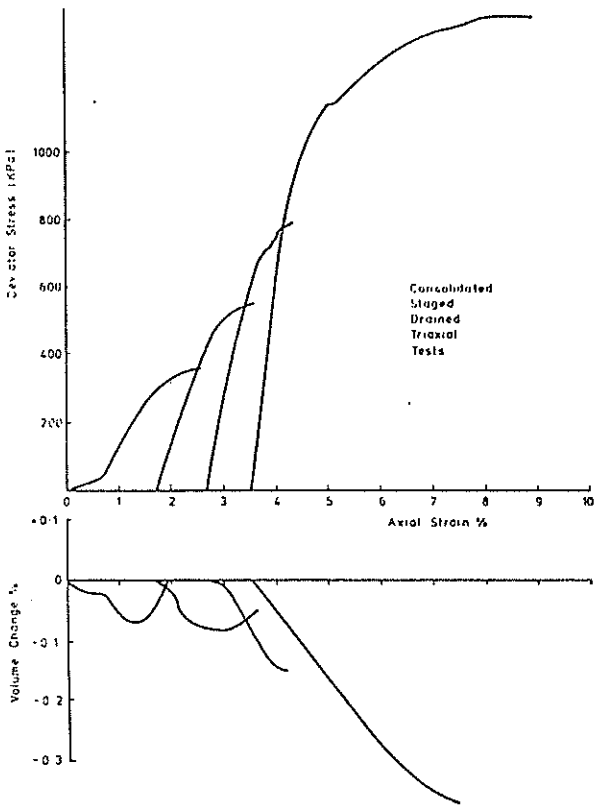

Fig. 1 Compacted Siltstone - "Standard" Effort

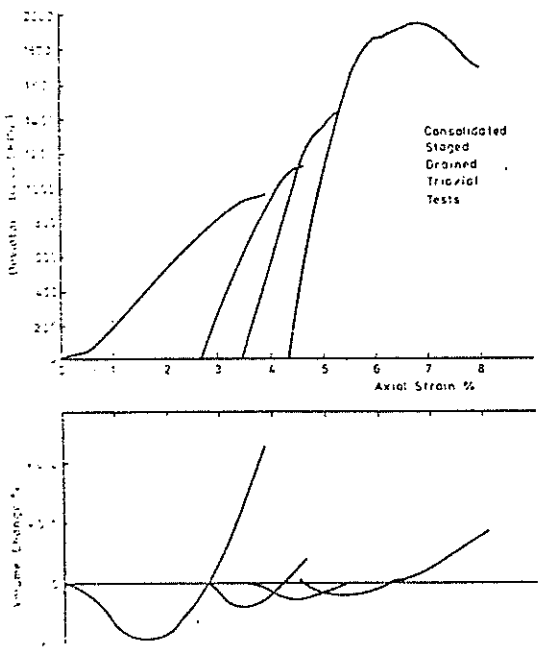

Fig. 2 Compacted Siltstone - "Heavy" Effort

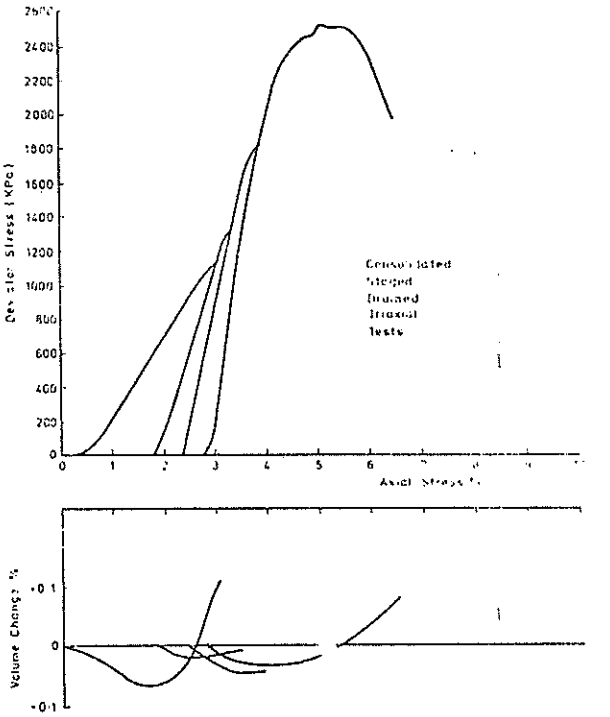

Fig. 3 Compacted Siltstone - "Extra Heavy" Effort

Each of the samples was subjected to varying levels of cyclic shear stress ratio for up to 500 cycles or 5% strain. Once 5% strain is reached, the sample was then failed under monotonic loading and the final pore pressure recorded. Table 2 summarises the data obtained from the series of dynamic triaxial tests and Table 3 shows some typical relationships between earthquake magnitude and expected cyclic stress ratios.

Cyclic stress ratio is defined as the ratio between the cyclic deviator stress and two times the initial effective confining stress ($\sigma_{dc}/2\sigma_{3i}$).

Fig. 5 shows the grading of the siltstone material compared to the grading envelope of material which are generally regarded as being susceptible to liquefaction. Also shown on Fig. 5 is the grading of a fine sandstone (also available at the dam site but judged to be unsuitable). The grading curve for the siltstone shows it has basically a granular nature so that when compacted the material has a high frictional shearing strength. Table 1 indicates an effective angle of internal friction of 29° is readily achievable. In addition it has sufficient clay content to give it the desirable low permeability (in the order of 10^{-5} cm/sec) and the effective cohesion of a clayey soil (about 55 kPa). The clay and silt content in the compacted siltstone will also provide high resistance to liquefaction when subjected to earthquake shaking.

Fig. 6 shows the comparison of results of dynamic triaxial test on the compacted siltstone with results of similar tests obtained from construction materials for dams (Selig et al, 1978) with known performance during strong earthquake shaking and other laboratory compacted materials (Seed, 1979).

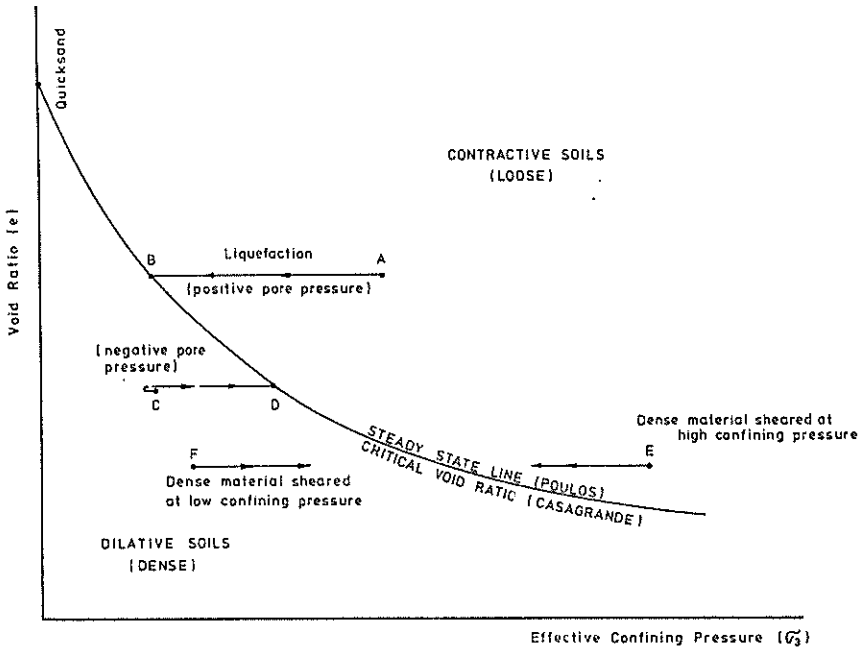

Fig. 4 Steady State Line Concept (After Castro & Poulos, 1977)

TABLE II

RESULTS OF DYNAMIC TRIAXIAL TESTS

Compaction Effort	Dry Density (t/m^3)	Test No.	Shear Stress Ratio	No. of Cycles	Cycles to 5% Strain	Initial Confining Pressure (kPa)	Increase in Pore Pressure (kPa)	Monotonic Failure Effective Confining Stress (kPa)	Monotonic Failure Effective Vertical Stress (kPa)
Heavy	2.02	1	.125	500	>500	500	28		
		2	.206	500	>500	462	35		
		3	.332	500	>500	423	79	702	3955
Heavy	2.04	4	.122	500	>500	500	20		
		5	.215	500	>500	480	40		
		6	.277	500	>500	440	35	795	2545
Standard	1.82	7	.118	500	>500	500	48		
		8	.184	500	>500	452	32		
		9	.258	500	>500	420	165		
		10	.529	100	68	255	200	420	1380
Standard	1.80	11	.125	500	>500	500	70		
		12	.176	500	>500	430	27		
		13	.241	500	>500	403	50		
		14	.338	500	385	353	303	360	1220
Standard	1.78	15	.530	8	7	300	275	265	1067
Standard	1.76	16	.300	600	525	300	275	255	1135

The concept of equivalent number of shear stress reversals has been generally used (Seed, 1979) to represent earthquakes of varying magnitude. Table 3 shows relationships between earthquake magnitude, number of equivalent cycles at 65% of the peak stress and typical range of cyclic stress ratios. The numbers of equivalent shear stress cycles shown in Table 3 are the result of statistical study of the representative number of cycles for a number of different earthquake motions and the effects of typical irregular stress history of earthquake vibrations.

This concept of equivalent number of uniform stress cycles allows simple cyclic shear tests to be performed and the results compared with records of past performance. Due to the inherent inaccuracies contained in this simplified approach, considerable judgement is required in the assessment of the liquefaction potential.

Fig. 6 includes cyclic load test data on relatively loose sand with a relative density of 54% (Dr = 54%) and also dense sand with a relative density of 82% (Seed, 1979). Sands compacted under different methods were studied by Mori, et al (1977).

Pouring sand through water (hydraulic fill) achieved rather low degree of compaction.

Tamping produced a much higher degree of compaction giving densities closer to Dr = 80%. High frequency vibration compaction was effective in producing a very dense material with high resistance to liquefaction. The test data points shown in Fig. 6 indicated that the compacted siltstone (using "standard" compaction effort) achieved a relatively high resistance to cyclic loading. Referring to Tables 2 and 3, it can be seen that the compacted siltstone may resist a magnitude 8 earthquake at a distance of the order of 30 km or an earthquake of magnitude 6.5 at a distance of about 5 km.

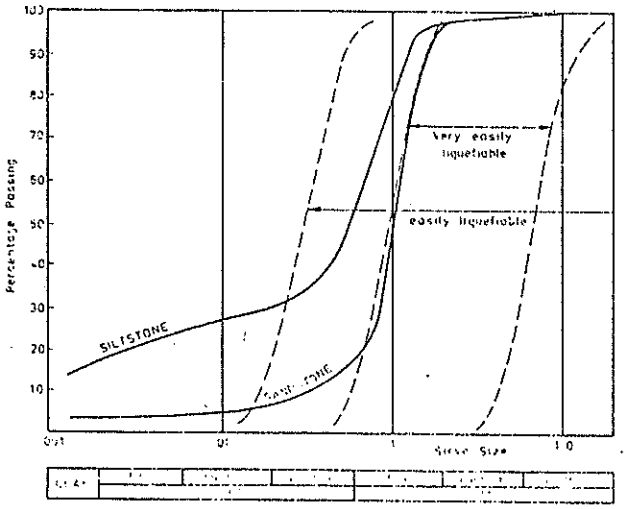

Fig. 5 Material Grading Curves

The data points obtained from the dynamic triaxial tests carried out on the compacted siltstone showed (Fig. 6) that this material performs in a manner representative of typical compacted soils used in dams with proven good performance during known strong earthquake shaking. For example, the Chabot Dam survived a magnitude 8¼ earthquake at a distance of 20 miles (0.4g max horizontal acceleration) with no apparent damage and would probably survive a magnitude 7 earthquake at a distance of 2 miles (0.6g max. horizontal acceleration). The Lower Franklin and Fairmont dams survived a magnitude 6½ earthquake at a distance of 20 miles (0.2g max. horizontal acceleration) with no apparent damage.

Fig. 7 showed the results of monotonic loading carried out on the dynamic triaxial sample after the conclusion of the cyclic shear test. In the cases of tests 10, 14, 15 and 16, the monotonic loading was carried out after 5% strain was achieved. It was also noted that the compacted siltstone sample retained its cylindrical shape, even though the pore pressure had reached up to 92% of the initial confining pressure. The effective shear strength recorded was still equivalent to that measured in conventional triaxial tests. This suggested that the compacted siltstone material did not become "liquefied" (and hence with no residual resistance) but conditions of cyclic mobility had occurred and that the soil would stabilise under the applied loads once the pore pressure dropped.

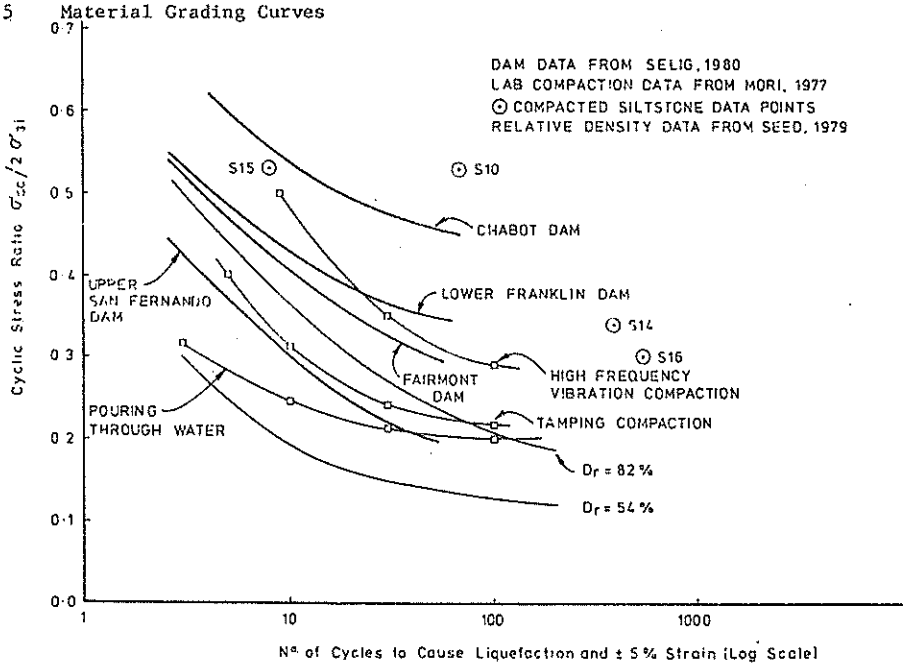

Fig 6 Comparison of Compacted Siltstone with Existing Liquefaction Data

TABLE III

EARTHQUAKE INDUCED LIQUEFACTION DATA

EQ Magnitude	No. of Equivalent Cyclics (*)	Typical Cyclic Stress Ratio (+)	Duration of Strong Shaking (*) (secs)	Typical Acceleration at 20 km (⁂) (%g)	Typical Acceleration at 5 km (⁂) (%g)
5½-6	5	0.1 - 0.25	8	0.12	0.35
6½	8	0.12- 0.35	14	0.18	0.46
7	12	0.15- 0.40	20	0.25	0.56
7½	20	0.20- 0.45	40	0.35	0.68
8	30	0.35- 0.50	60	0.45	0.80

Note: (*) Seed et al, 1976
(+) deduced from Mori et al, 1977
(⁂) Donovan et al, 1978

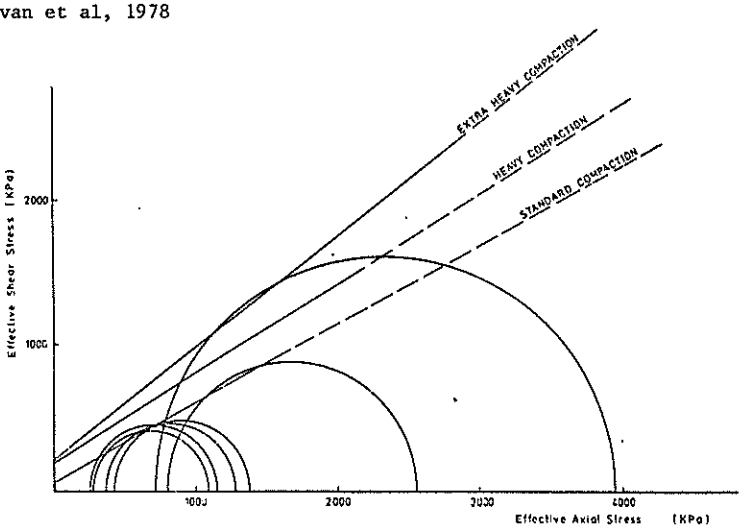

Fig 7 Compacted Siltstone Strength After Dynamic Triaxial Testing

3 CONCLUSIONS

The laboratory testing programme described in this paper has established that:-

(i) the tertiary siltstone material selected for use in the construction of the earth dam after quarrying and compaction into place is a fine sand/silt mixture with high frictional strength. The siltstone also contains silt and clay content to give the compacted material effective cohesion and good potential resistance to liquefaction.

(ii) Drained triaxial tests indicated that the compacted siltstone tend to contract under monotonic loading at low strains even at very high level of compactive effort which is not readily achievable in field conditions. Hence it is expected that pore pressure may build up during earthquake loading.

(iii) Stress controlled dynamic triaxial tests have shown that the compacted siltstone performs well under repeated cyclic shear even at high cyclic stress ratios in a manner representative of typical compacted soils used in dams with proven good performance. The pore pressure was found to increase under repeated cyclic shear loadings but the test sample retained its cylindrical shape and still retained unaltered effective shear strength under monotonic loading following the dynamic tests.

It was concluded that the compacted siltstone will provide a competent material for the construction of an earth dam despite the observed fact that this material contracts under monotonic loading at compactive efforts which are readily achievable under field conditions.

4 ACKNOWLEDGEMENTS

The results described in this paper were obtained in the course of feasibility study investigations for the Patea Scheme carried out by Beca Carter Hollings & Ferner Limited on behalf of the Egmont Electric Power Board. The main laboratory testing programme was carried out by Laboratory Testing Ltd under the direct control of Mr B. E. Coker and the programme of dynamic triaxial testing was carried out at the Civil Engineering Department of the University of Auckland by Mr G. G. Duske, under the overall supervision of Professor P. W. Taylor. The results of the testing programme have been reivewed by Dr James L. Sherard, Consulting Engineer of Devonshire, Bermuda. The authors gratefully acknowledge the assistance which they have received from those named above.

5 REFERENCES

CASTRO, G and POULOS, S.J. (1977). Factors Affecting Liquefaction and Cyclic Mobility. Proc. ASCE, Vol. 103, No. GT6, pp 501-516.

DONOVAN, N.C. and BORNSTEIN, A.E. 1978). Uncertainties in Seismic Risk Procedures. Proc. ASCE, Vol. 104, No. GT7, pp 869-887.

MORI, K., SEED, H.B. and CHAN, C.K. (1977). Influence of Sample Disturbance on Sand Response to Cyclic Loading. University of Berkeley, California. Report No. UCB/EERC-77/03.

LEE, K.L. and SEED, H.B. 1967). Drained Strength Characteristics of Sands. Proc. ASCE, Vol. 93, No. SM6, pp 117-141.

SEED, H.B., MARTIN, P.P. and LYSMER, J. (1976). Pore Water Pressure Changes During Soil Liquefaction. Proc. ASCE, Vol. 102, No. GT4, pp 323-346.

SEED, H.B., MAKDISI, F.I. and De ALBA, P. (1978). Performance of Earth Dams During Earthquakes. Proc. ASCE, Vol. 104, No. GT7, pp 967-994.

SEED, H.B. (1970). Soil Liquefaction and Cyclic Mobility Evaluation for Level Ground During Earthquakes. Proc. ASCE, Vol. 105, No. GT2, pp 201-255.

TAYLOR, P.W. (1967). Design of Spread Footings for Earthquake Loading. 5th ANZ Conference on Soil Mechanics and Foundation Engineering, pp 221.

The Effects of Drainage Conditions and Confining Pressures on the Strength of Melbourne Mudstone

H. K. CHIU
Research Student, Department of Civil Engineering, Monash University
I. W. JOHNSTON
Lecturer, Department of Civil Engineering, Monash University

SUMMARY This paper describes the results of a series of triaxial compression tests conducted on saturated specimens of Melbourne mudstone under drained and consolidated undrained conditions with special reference to volume and porewater pressure response. The results obtained showed that the mudstone displayed characteristics very similar to those of conventional soils. The relevancy of the strength parameters is discussed with regard to current foundation design practice.

1 INTRODUCTION

Mudstone of the Silurian era forms a major part of the geology of the entire Melbourne Metropolitan area. Consequently, it is this formation which forms the bearing stratum for a considerable proportion of the major structures of Melbourne. Over recent years there have been some significant developments in the design and construction of foundations in mudstone, especially concerning rock socketed piles.

However, despite these practical advances in technology, the designs adopted have generally been based on mudstone properties derived from somewhat arbitrary testing techniques, procedures and conditions. The first recognised attempts to determine the engineering properties of the mudstone were in connection with the King Street Bridge Project (Wilson, 1960; Parry, 1970). These investigations examined the relationships between shear strength and moisture content and elastic modulus and moisture content. The correlations were obtained from triaxial compression tests carried out on unconsolidated specimens at a confining pressure of 0.69 MPa under undrained conditions. The confining pressure of 0.69 MPa was adopted for this project on the basis of it corresponding "roughly with the overburden pressure".

Since these initial investigations, the design parameters for a number of construction projects have been determined in a similar manner using unconsolidated undrained tests with a confining pressure of 0.69 MPa. In all these investigations, it has been assumed that classical undrained behaviour applies with $\phi_u = 0$ leading to the adoption of a c_u value equal to half the applied deviator stress at failure. However, as pointed out by a number of workers (Fletcher and Parker, 1973; Parkin and Donald, 1975), ϕ_u for mudstone may be appreciable as a result of the porewater pressure parameter B being less than unity, even for a fully-saturated rock. Indeed, Adachi and Mesri (1973) reported a B value as low as 0.2 for a sandstone even after applying substantial back pressures before testing. Furthermore, as discussed by Parkin and Donald (1975), since the degree of saturation of the specimen tested was largely uncontrolled, it is likely that B values could vary greatly. This implies that the so-called "undrained" tests could vary from almost undrained for highly weathered saturated (B=1) specimens to virtually drained for fresh unsaturated (B=0) specimens. These factors may account for the wide scatter of strength and modulus values recorded when correlated with moisture content (Donald, 1977).

For the design of foundations in cohesive soils, it is conventional to adopt an undrained analysis. This is based on the premise that the porewater pressures induced by the dead loading due to foundation and superstructure are relatively slow to dissipate with the result that an undrained analysis represents a lower bound solution generally safer and possibly more representative than a drained analysis. However, there is strong evidence that the rates of consolidation of the Melbourne mudstone are rapid with the result that drained analyses may be more appropriate although considerably more difficult to apply.

Therefore as part of a comprehensive programme investigating the overall engineering properties of the Melbourne mudstone, the authors examined the effects of drainage conditions and confining pressures on the strength parameters of one particular type of saturated mudstone with particular reference to the effective stress parameters. This study was directed towards a clearer understanding of the basic mechanisms involved, including volume change characteristics during drained tests and porewater pressure variations during undrained tests.

2 MUDSTONE SPECIMENS AND EXPERIMENTAL TECHNIQUES

The mudstone samples were obtained from a very limited area using an NX core barrel, 0.5 m long with a diamond drill bit, and could be classified as moderately to highly weathered with a saturated moisture content of 14 ± 0.5%. Particle size analyses indicated that the samples were made up of about 75% silt and 25% clay. Each test specimen was prepared with smooth parallel ends and an L/D ratio of at least 2. Prior to testing, the specimens were vacuum saturated in a desiccator for two days.

In order to examine comprehensively the properties of the mudstone over a necessarily wide range of pressures, a high pressure triaxial cell was designed and built by the authors. The cell was essentially the same in principle as a high quality multi-purpose low pressure soil testing cell with the exception that it could accommodate confining pressures of up to 35 MPa and the porewater pressure measuring system had an extremely low compressibility.

Since the vacuum saturation method was not completely effective, once the specimens had been mounted in the triaxial cell, a back pressure saturation

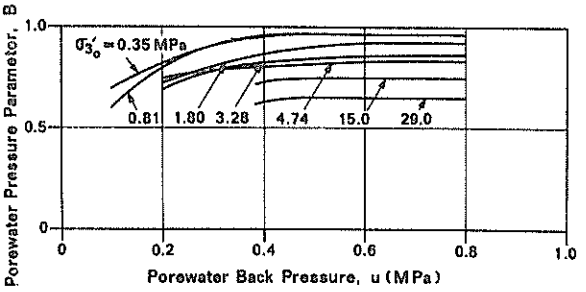

Figure 1 Variation of B parameter with porewater back pressure for a range of effective confining pressures.

technique, similar to that described by Wissa (1969), was used. Figure 1 shows the effects of this technique on the B parameter for a range of effective confining pressures. Generally, for saturated specimens, the higher the effective confining pressure, the lower is the B parameter. It appeared that a back pressure of 0.7 MPa was sufficient to fully saturate all specimens.

In order to remove strain rate effects on the measured strength of the specimens, to ensure that drainage was complete at all stages of drained tests, and to ensure that induced porewater pressures in the specimens were uniform during undrained testing, an investigation was undertaken to establish a suitable rate of strain for the testing. Although not reported herein, it was found that for the range of conditions of the test programme, a strain rate of 2 x 10^{-5}/minute was appropriate and this rate was in general agreement with the recommendations of Gibson and Henkel (1954).

3 RATES OF CONSOLIDATION

A series of hydrostatic triaxial consolidation tests were conducted in the high pressure cell with drainage in one direction to a back pressured burette. Figure 2 shows the typical relationship obtained between the coefficient of consolidation, c_v, for a range of effective isotropic confining pressures.

For effective stresses below about 1 MPa, c_v was found to be in excess of 100 m^2/year, decreasing to about 30 m^2/year for an effective stress of 30 MPa. Intact clay specimens, tested in an identical fashion yielded c_v values of about 1 m^2/year for

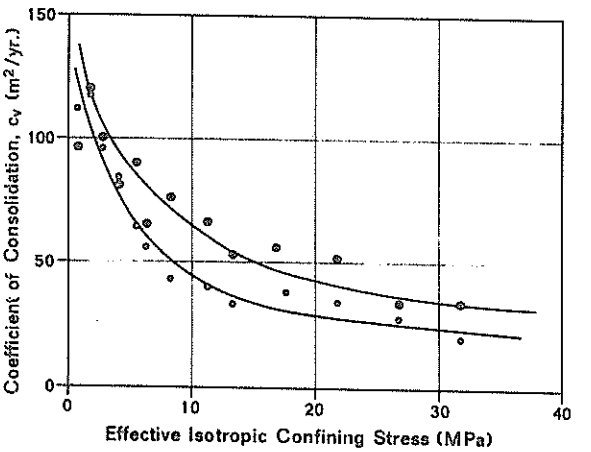

Figure 2 Variation of coefficient of consolidation with confining pressure.

effective stresses considerably lower than 1 MPa, with a further reduction at higher effective pressures. However, as discussed by Rowe (1972), while smaller intact specimens may produce certain c_v values in the laboratory, because of the presence of defects in the naturally occurring mass, in-situ rates of consolidation are often two or three magnitudes greater. It follows that if small intact, defect-free mudstone specimens yield c_v values of about 100 m^2/year in the laboratory, then when considering the presence of joints, fissures and regular continuous beds of sandstone in-situ, it is likely that the mass in-situ coefficients of consolidation for mudstone are many times greater, and more representative of a relatively free draining material than a slow draining one such as clay.

Furthermore, as reported by Cole *et al.* (1968), it would appear that the clay content of Melbourne mudstone rarely exceeds 30%, and therefore the above laboratory determined values of c_v may be considered representative of the lower range of likely c_v values for this type of mudstone.

4 STRESS-STRAIN RELATIONS

Figures 3 and 4 show typical stress-strain curves for drained and consolidated undrained tests respectively to failure for a range of initial effective confining pressures, σ'_{3_o}. These figures show that for both testing conditions, the higher the value of σ'_{3_o}, the higher was the deviator stress at failure. This general trend is to be expected and will be discussed in more detail below.

It is also interesting to note that the strain at failure increases with initial effective confining pressure indicating that the brittleness of the

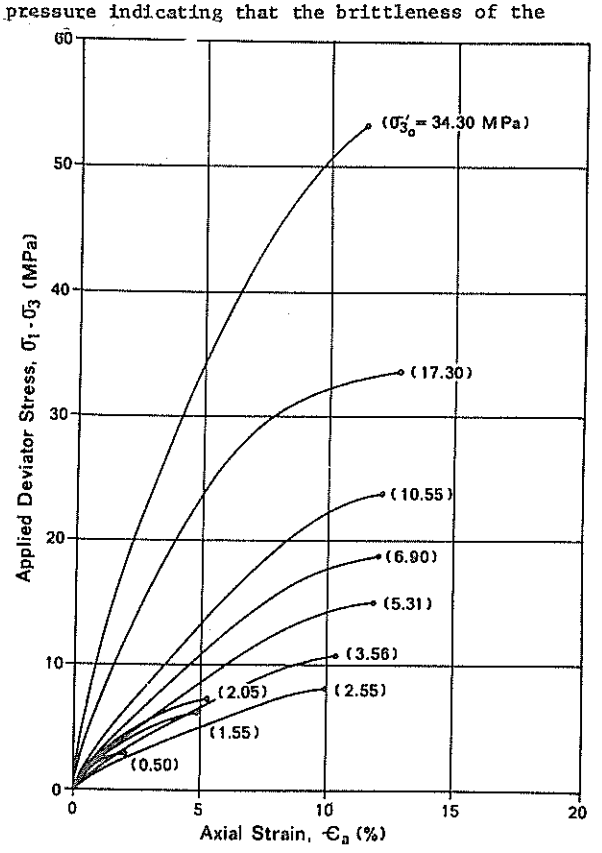

Figure 3 Stress-strain curves for drained triaxial tests.

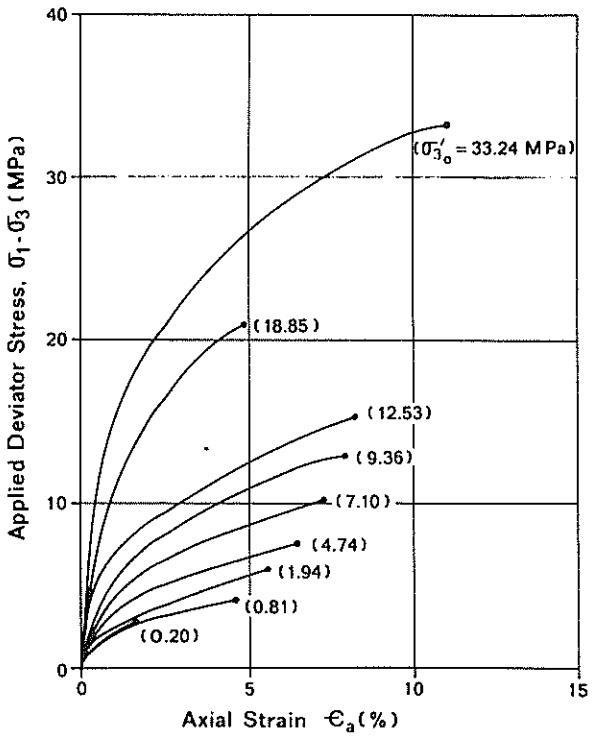

Figure 4 Stress-strain curves for consolidated undrained triaxial tests.

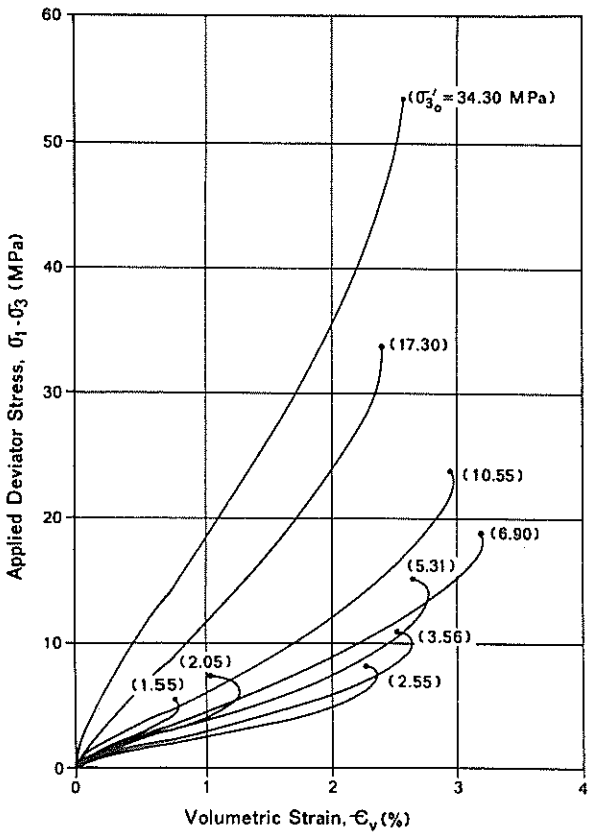

Figure 5 Stress-volumetric strain curves for drained triaxial tests.

mudstone decreased. Also worthy of note is the general shape of the curves for which, for any given value of σ'_{3_o}, the modulus up to about half the failure deviator stress was greater in the undrained tests than in the drained tests.

5 VOLUMETRIC AND POREWATER PRESSURE RESPONSE

5.1 Volumetric response

For the drained tests, the volume of water entering or leaving the saturated specimen was measured during testing. Figure 5 shows the relationship between volumetric strain and deviator stress for a range of initial effective confining pressures. This figure shows that for specimens tested at low initial effective confining pressures, dilation occurred before failure was reached. For specimens of higher σ'_{3_o}, the dilation effect was much less pronounced. Indeed the specimen tested at σ'_{3_o} = 34.3 MPa did not display a net dilation at all.

The rate of dilation at failure is examined more closely in Figure 6, in which it is represented by the ratio of $(d\epsilon_v/d\epsilon_a)_f$, in which $d\epsilon_v$ and $d\epsilon_a$ are the changes in volumetric and axial strain respectively at failure. This is plotted against log p_f' in which p_f' is the mean effective normal stress.

The result shows that for values of p_f' greater than about 35 MPa, dilation was effectively suppressed.

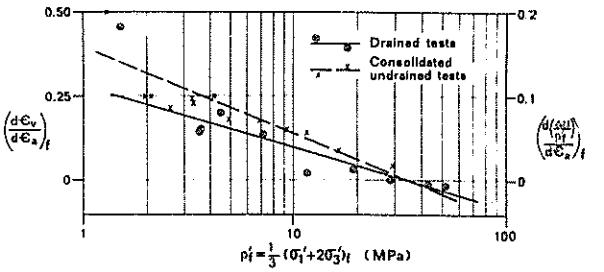

Figure 6 Rate of dilation with mean effective normal stress.

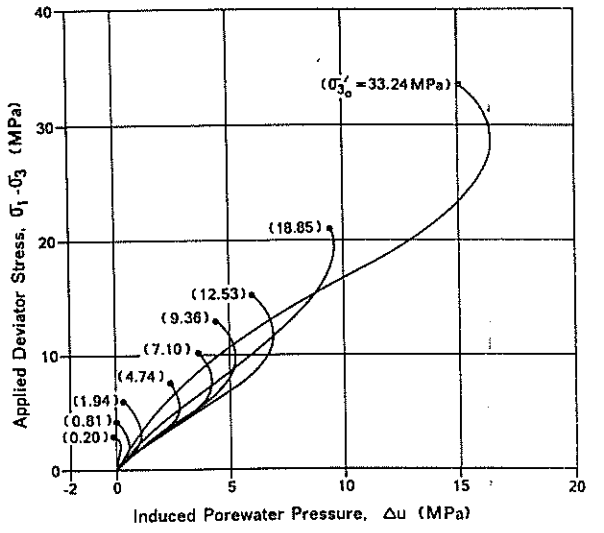

Figure 7 Stress-induced porewater pressure curves of consolidated undrained triaxial tests.

5.2 Porewater pressure response

Figure 7 displays the relationship between induced porewater pressure and deviator stress for a range of σ'_{3_o} values for the consolidated undrained tests. The results show the same characteristics as displayed by the drained tests. Tests conducted with low σ'_{3_o} showed dilational characteristics with the initially positive induced porewater pressures decreasing significantly before failure. Tests conducted with high σ'_{3_o} showed a much reduced tendency to dilate. Figure 6 shows the rate of dilation at failure in terms of $[d(\Delta u/p_f')/d\epsilon_a]$ against log p_f' in which it may be seen that dilation was again effectively suppressed for values of p_f' greater than about 35 MPa.

6 STRENGTH

Effective stress Mohr's circles are plotted in Figure 8(a) and 8(b) for the drained and consolidated undrained tests respectively. The resulting effective stress envelopes are essentially identical for both conditions of testing. For normal stresses up to about 10 MPa, ϕ' is constant at about 34° with $c' = 0.45$ MPa. At greater normal stresses, ϕ' decreases giving at about 60 MPa normal stress, $\phi' = 22°$.

Figure 8(b) also shows the envelope for the total stress circles obtained from the consolidated undrained tests. This envelope is essentially linear for the range of total stresses employed giving approximate values of $\phi_{cu} = 18°$ and $c_{cu} = 0.75$ MPa.

7 DISCUSSION OF RESULTS

Despite the fact that the Melbourne mudstone is generally referred to as a rock, and requires a much higher range of testing pressures than soils to obtain a general overview of its properties, it would appear that the mudstone does share a wide range of performance characteristics with soils, in particular with overconsolidated clays. It has been shown that the porewater pressure response to isotropic stress conditions is governed by the B parameter although, because of significant skeleton rigidity, this parameter can often have values significantly less than unity. On the application of a deviator stress, the mudstone showed dilatancy characteristics typical of overconsolidated clays. For low mean effective confining pressures, the dilatancy characteristics for both drained and undrained conditions were well marked whereas, for mean effective confining pressures greater than about 35 MPa, dilatancy characteristics were effectively suppressed. This relationship was noted by Parry (1958) for London and Weald clays, and indeed these same relationships have subsequently formed

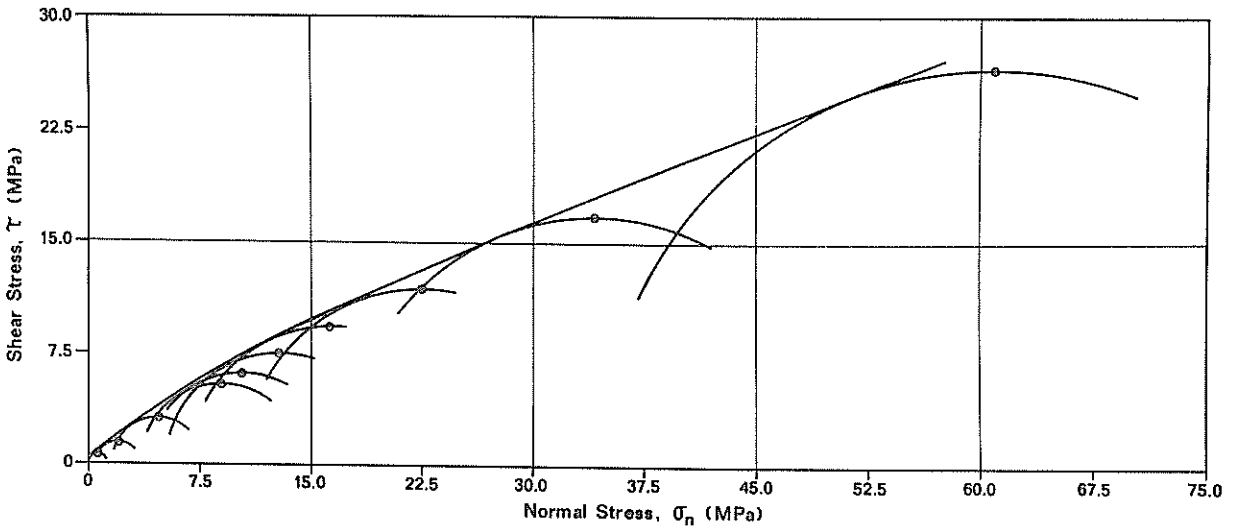

(a)

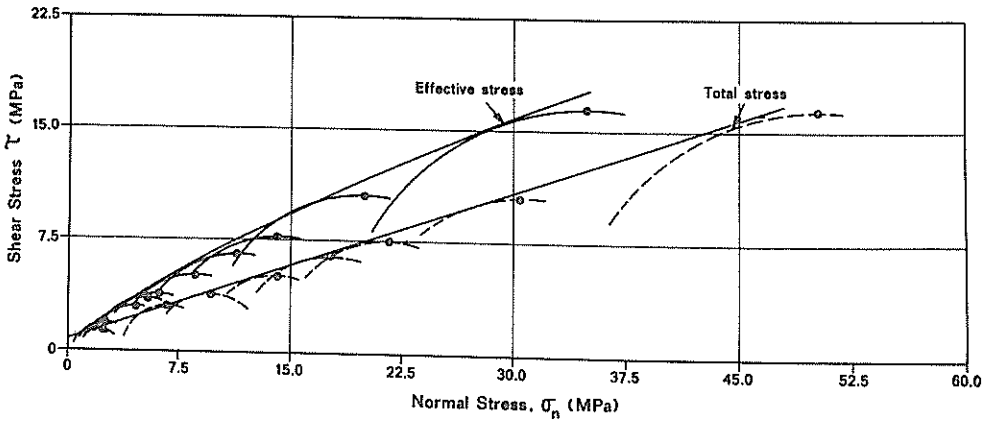

(b)

Figure 8 Mohr's circle plots for (a) drained and (b) consolidated undrained triaxial tests.

one of the basic building blocks for the application of critical state soil mechanics to the behaviour of clays (Atkinson and Bransby, 1978). It follows then that critical state techniques may be applied to the behaviour of Melbourne mudstone thereby removing the artificial and poorly defined division between soils and rocks!

The effective stress parameters based on both drained and undrained test techniques have shown quite definite soil-like behaviour with, for the mudstone tested, $c' = 0.45$ MPa and $\phi' = 34°$ for normal stresses up to about 10 MPa. For greater normal pressures, the value of ϕ' appears to decrease but this phenomenon has been noted by many workers for soils and rocks alike.

With the mudstone, however, it would appear that rates of consolidation are very much greater than for clays. Indeed, when considering the usual rates of structural dead load application, it would appear that full drainage of the mudstone would take place during the construction period. Certainly for unsaturated mudstone foundations, the mudstone would behave as a drained material. It follows then that effective stress parameters may be more appropriate and relevant to the design of foundations on mudstone. The conventional testing technique involving unconsolidated undrained triaxial compression tests at a total confining pressure of 0.69 MPa is not therefore strictly relevant to such processes.

As pointed out by Donald (1977), for less weathered mudstone, especially that approaching the fresh classification, the drained cohesion is likely to form a major component of the effective strength for the range of foundation pressures commonly encountered. Therefore the conventional unconsolidated undrained approach is likely to be a reasonable approach for design purposes. However, for the more weathered mudstones, represented by the type examined herein and of higher moisture content, the drained or indeed the apparent undrained cohesive component becomes only a minor component of the total available shear strength for typical foundation loads. Therefore, the use of an undrained testing approach is likely to lead to overconservative design parameters since the frictional component, although possibly significant, is basically ignored. It follows then, that if drained behaviour is considered for the apparently poorer quality mudstones, these may prove to be significantly superior founding materials than has been generally believed.

It should be emphasised, however, that in all the foregoing discussion, the overall influence of discontinuities on the mass strength of the mudstone have not been considered.

8 CONCLUSIONS

A series of drained and consolidated undrained triaxial compression tests, conducted on saturated Melbourne mudstone have been reported. The results obtained have shown that for the range of testing conditions investigated, the mudstone exhibits characteristics very similar to conventional soil behaviour, particularly with regard to overconsolidated clays. The principal difference encountered, however, was that the intact mudstone exhibited rates of consolidation that were considerably higher than typically displayed by overconsolidated clays. Therefore, whereas classical undrained testing techniques and analysis may be more appropriate to foundation dead loads on clays, for Melbourne mudstone it would appear that an effective stress approach is more relevant if a rational testing and design philosophy is to be developed.

9 REFERENCES

ADACHI, K. and MESRI, G. (1973). Influence of Pore Water Pressure on the Engineering Properties of Rock. Dept. of Civil Engineering, Univ. of Illinois, Urbana, Illinois.

ATKINSON, J.H. and BRANSBY, P.L. (1978). The Mechanics of Soils; An Introduction to Critical State Soil Mechanics. McGraw-Hill, U.K.

COLE, W.F., LANCUCKI, C.J. and NICKSON, N.M. (1968). Ceramic Clays and Shales from the Melbourne Area I. Minerology and Particle Size Distributions. C.S.I.R.O. Div. of Build. Res., Tech. Paper No. 22.

DONALD, I.B. (1977). Compression Test Properties, in Workshop on the Engineering Properties of Melbourne Mudstone. Australian Geomechanics Society, Victoria Group.

FLETCHER, S.J. and PARKER, R.J. (1973). Investigation of the Strength Properties of Melbourne Mudstone. Internal Report, Dept. of Civil Engineering, Monash University.

GIBSON, R.E. and HENKEL, D.J. (1954). Influence of duration of tests at constant rate of strain on measured 'drained' strength. Geotechnique, 4, pp. 6-15.

PARKIN, A.K. and DONALD, I.B. (1975). Investigations for Rock Socketed Piles in Melbourne Mudstone. 2nd Aust.-N.Z. Conf. on Geomechanics, I.E. Aust., Brisbane, pp. 195-200.

PARRY, R.H.G. (1958). Discussion on "On the Yielding of Soils", Geotechnique, 8, pp. 183-186.

PARRY, R.H.G. (1970). Triaxial Tests on Melbourne Mudstone. Jour. I. E. Aust., 42: 1-2, pp. 5-8.

ROWE, P.W. (1972). The Relevance of Soil Fabric to Site Investigation Practice. Geotechnique, 22, pp. 195-300.

WILSON, C. A. (1960). King Street Bridge Project - Part IV. Foundation Investigations. Jour. I.E. Aust., 32: 9, pp. 173-182.

WISSA, A.E.Z. (1969). Pore-Pressure Measurement in Saturated Stiff Soils. Proc. A.S.C.E., SMFD 95, SM4, pp. 1063-1073.

Cement and Lime Stabilisation of Melbourne Pavement Subgrade Soils

J. E. HOLLAND
Principal Lecturer, Swinburne College of Technology
C. GRIFFIN
Post-graduate Student, Swinburne College of Technology

SUMMARY A laboratory and field study of the properties and behaviour of three weak subgrade soils treated with cement and lime is outlined. From this study a pavement design procedure incorporating a stabilised soil subbase is presented.

INTRODUCTION

In the City of Melbourne, Victoria, Australia, three low strength road pavement subgrade soil conditions are commonly encountered. The three general problem subgrade soil conditions are; expansive clay, silty clay and loose silty sand overlying stiff sandy clay. In the expansive and silty clays, C.B.R. values of 1.5 to 2.0 percent at subgrade level commonly occur during the wetter winter and spring months. When a perched water table develops, the silty sand becomes very wet and weak with only extremely low insitu C.B.R. values of from 1 to 1.5 percent.

Past practice with these problem subgrade soils was simply to remove them until a stronger soil was encountered. The unsuitable soil was then replaced by coarse rock filling. This procedure has now become very expensive, and has led to pavement failures on the silty clay soils in particular. In parts of the eastern suburbs of Melbourne, this silty clay has been removed and replaced by rock filling to depths of 1200 mm. However, within a year, these deep pavements have failed because of the inevitiable wetting up of the underlying silty clay. Once this occurs the silty clay softens dramatically and tends to be forced up into the overlying pavement by the traffic movement over it. This in turn greatly increases the deflection of the pavement and quickly leads to pavement breakdown. In the loose silty sand soil areas it is often necessary to remove up to 1000 mm of this material to found pavements on the underlying stiff sandy clay.

In recent encounters with these three problem subgrade soils, lime and cement stabilisation has been used as an alternative to replacement for a number of residential estates. In the main this technique has been successful if the likely subgrade soil moisture conditions at the time of stabilisation are considered when selecting the percentages of lime and cement, and if the road contractor keeps construction traffic off the stabilised layer until it is protected by compacted crushed rock. The stabilised subgrade, however, is generally more expensive than the replacement approach, unless it is considered as a structural part of the pavement. The incorporation of the stabilised subgrade soil as a sub-base of the pavement rather than a construction expedient has been strongly advocated by McDOWELL (1972) in U.S.A..

At the beginning of 1978, a research project was commenced in the Civil Engineering Department of Swinburne College of Technology, aimed at developing a pavement design approach in these three troublesome soils. The design method would incorporate a lime and cement stabilised sub-base as part of the pavement.

This paper will briefly outline the field and laboratory testing of the soil from five trial pavement areas established in these three weak subgrade soil areas. The design basis and behaviour of these trail pavements will be presented and discussed. Finally, a pavement design approach incorporating a lime and cement stabilised sub-base will be outlined.

SITE SUBGRADE SOIL PROPERTIES

Five representative trial residential and industrial pavement sections in these three weak soil subgrade areas were selected. Extensive field and laboratory soil testing was conducted at each site. The field testing included soil profiling, insitu moisture content and dynamic C.B.R. testing using a falling weight type penetometer. Numerous soil identification tests were conducted. A brief summary of all this testing is given in Table I.

LABORATORY SOIL STABILISATION STUDIES

For the five sites, large composite samples of the proposed stabilised sub-base soils were collected and subjected to full C.B.R. and indirect tension testing with a range of cement and lime additive percentages. The samples were mixed at five to six initial moisture contents which were selected to cover the likely seasonal range at the particular site. The full C.B.R. soil tests were conducted in accordance with the appropriate Australian Standard procedure (AS1289.F1.1-1977), while the indirect tension tests were conducted on the full C.B.R. samples after this test was completed. The major results from this set of tests are tabulated in Table II. The points of interest from this Table are as follows.

(1) The need to introduce cement even into expansive clay soils if high stabilised C.B.R's are desired. In Figure 1 this point is clearly demonstrated by the series of tests on the Werribee expansive clay with 4% lime and 3% cement and 3% lime and 4% cement giving far greater stabilised C.B.R. test results than the series conducted with 6% lime only.

Obviously, one must expect that uniform mixing of the cement into this very impermeable clay soil prior to stabilisation will be more diffi-

TABLE I

SOIL PROPERTIES OF TRIAL SECTIONS

SITE	CRANBOURNE	CROYDON	ENDEAVOUR HILLS	PAKENHAM	WERRIBEE
General Subgrade Soil Type	Tertiary Basaltic Clay	Very Silty Clay	Loose Silty Sand over Sandy Clay	Silty Clay	Quaternary Basaltic Clay
Soil Profile	Darkgrey sandy loam topsoil to between 0.1 & 0.45 m Grey & Brown Silty Sandy Clay to between 0.5 & 1.2 (P.I.24%-42%) Stiff Mottled grey & orange brown sandy clay (P.I.0% 41%) to at least 1.5m	Grey Silty Topsoil & Clay silt to between 0.25 and 0.40m Orangey brown and red grey very silty clay (P.I. 18%-36%) to at least 1.5m	Dark brown sandy topsoil to between 0.2 & 0.4m Light brown silty sand to between 0.6 & 1.2m (P.I. 0% 22%) Orangey brown sandy silty clay (P.I. 22%-50%) to at least 1.5m	Grey silty topsoil to between 0.1 and 0.25m Grey & Brown Clayey Silt to between 0.55 & 0.95m Mottled Brown and Grey Silty Clay to at least 1.5m	Topsoil to between 0.05 and 0.1m Red Clay Interface at between 0.35 and 0.65m (P.I.22%-51%) White Clay (P.I. 32%-40%) Rock at between 1.3 and 1.4m
In Situ C.B.R. Range over stabilised layer %	3.5 - 20.0	2.0 - 7.5	Sand 2.0 - 10.0 Sandy Clay 3.5 - 10.0	2.0 - 10.0	2.0 - 15.0
In Situ Moisture Content Range %	10.0 - 30.0	16.0 - 32.0	Sand 10.0 - 20.0 Sandy Clay 17.0 - 31.0	[illegible]	24.0 - 42.0

TABLE II

STABILISED SOIL TEST RESULTS

SITE	CRANBOURNE	CROYDON	ENDEAVOUR HILLS	PAKENHAM	WERRIBEE
General Subgrade Soil Type	Tertiary Basaltic Clay	Very Silty Clay	Loose Silty Sand over Sandy Clay	Silty Clay	Quaternary Basaltic Clay
Stabilised Soil C.B.R.	%	%	%	%	%
Initial Moisture Content on compaction	17 17 22 27 32	12 16 20 24 28 32	Sandy Clay 12 16 20 24 28 32	12 16 20 24 28 32	12 16 20 24 28 37
Additives:					
3 % lime	35 35 30 11 6				
4 % lime	29 50 15 16 7				
5 % lime	16 [illegible]				
6 % lime					
2 % lime & 2 % cement	35 60 45 30 19			36 42 45 23 15 11	
2 % lime & 3 % cement					
2 % lime & 4 % cement	65 75 90 70 35			37 30 28 19 9	34 45 38 44 54 46
3 % lime & 2 % cement					
3 % lime & 3 % cement	55 100 80 55 30		57 25 28 57 40 35	53 48 36 28 12	35 34 32 35 62 24
3 % lime & 4 % cement				66 66 54 31 19	28 30 54 61 77 56
3 % lime & 5 % cement			41 51 76 55 36 16		
4 % lime & 2 % cement					39 46 48 79 66 58
4 % cement			28 32 48 46 11 13		
5 % cement			28 42 56 68 62 46		
			Silty Sand		
4 % cement			4 6 8 10 12 14		
8 % cement			140 [illegible]		
			125 [illegible]		
Indirect Tensile Strength Range (kPa)	29 - 52	[illegible]	16 - 74	14 - 25	19 - 75

cult in the field than in the laboratory. It would therefore be impractical not to use a substantial percentage of lime in conjunction with the cement to ensure that reasonable field mixing of the cement into the clay could be obtained after the lime was introduced to make the clay much more friable. Therefore it was considered that at least 4% lime should be adopted to achieve this.

(2) The areas where loose silty sand over sandy clay subgrade conditions are encountered in Melbourne are quite undulating and typically, pavements are founded transversely and longitudinally in both areas of loose silty sand and sandy clay. It was therefore important to adopt a stabilising system that could be used for the loose silty sand and the sandy clay. For the loose silty sand, lime was found to have a detrimental effect on the action of cement, so the use of cement, and cement and lime stabilisation for the sandy clay was investigated. The testing results obtained for the silty sand and the sandy clay are presented in Figures 2 and 3.

From Figure 2, it is obvious moisture control is essential in the silty sand, to ensure its initial moisture content before stabilisation

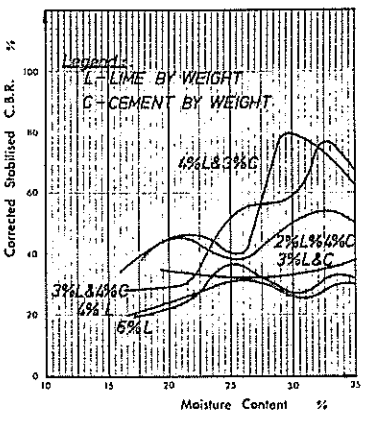

Figure 1 Werribee stabilised C.B.R. results

is less than 8 to 10 percent. If the moisture content can be lowered by good site drainage, or later summer or early autumn construction, then very large C.B.R.'s of at least 200% will be obtained. For the sandy clay the use of 4 and 5 percent cement were found to give equally as good C.B.R. values as the use of lime and cement (Figure 3). Again, one must consider the relative efficiency of field mixing of this cement into a sandy clay in comparison to that achievable in the laboratory. It was in fact considered necessary to use 5% cement in the field, even though 4% cement would have been sufficient based on the laboratory testing.

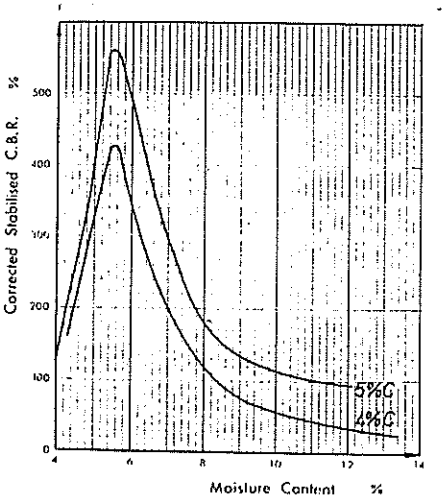

Figure 2 Endeavour Hills silty sand stabilised C.B.R. results

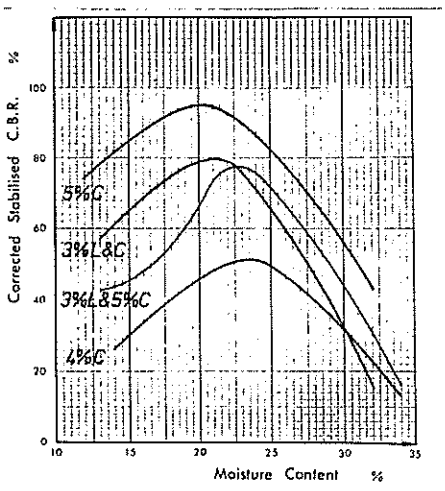

Figure 3 Endeavour Hills sandy clay stabilised C.B.R. results

(3) In Figure 4, the stabilised C.B.R. test results are presented for the Croydon silty clay site. They clearly show the importance of keeping the field moisture content prior to stabilisation as low as possible, if high C.B.R. values are to be obtained.

(4) As expected, the indirect tensile test results were very variable and it was difficult to distinguish a consistent pattern of behaviour with increasing initial moisture content. However, the indirect tension values increased as

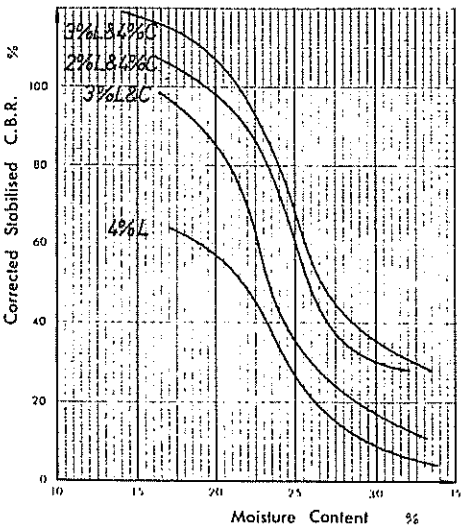

Figure 4 Croydon stabilised C.B.R. results

the additive percentages (especially cement) increased.

FIELD TESTING OF TRIAL PAVEMENTS

McDOWELL's (1972) procedure incorporating the stabilised soil layer as an integral structural part of the pavement was used to design pavements for these five trial sections. Details of these designs, including the initial moisture conditions assumed and the cement and lime additives recommended based on laboratory testing and the components of the pavement, are listed in Table III. In most cases the pavement details were also partly influenced by the particular local authority or Council who controlled the five particular sites.

At each of the test sites it is planned to monitor the soil before, during, and after pavement construction. Dynamic penetrometer C.B.R. testing until the final bitumen courses were laid and Benkelman beam testing was considered the simplest and most appropriate monitoring.

Unfortunately, because of the present over supply of residential and industrial land, only two of the trial sections have been constructed. Both of the sections are areas of silty clay at Pakenham and Croydon.

In Table IV, the field monitoring results are briefly presented, while in Figure 5 and 6 the C.B.R. and Benkelman beam values of the sub-base zone respectively at Pakenham are plotted.

A significant increase in the C.B.R. after stabilisation occurred at both sites (3.5 to at least 20%) with a further increase to about 40% occurring after the next few months. It is likely that the stabilised soil sub-base layer will continually increase in strength for many more months. A final C.B.R. in this layer of at least 60 percent would appear to be likely. Table IV clearly shows the dramatic reduction in the Benkelman beam deflections after treating the unstabilised silty clay. The deflections were marginally reduced after the compact-

TABLE III

PAVEMENT DESIGN FOR THE TRIAL SECTIONS

SITE	CRANBOURNE	CROYDON	ENDEAVOUR HILLS	PAKENHAM	WERRIBEE
General Subgrade Soil Type	Tertiary Basaltic Clay	Very Silty Clay	Loose Silty Sand over Sandy Clay	Silty Clay	Quaternary Basaltic Clay
Design Field Moisture Content	< 26 %	< 29 %	Sand < 9.0 % Sandy Clay < 20 %	< 26 %	< 0%
Recommended % Design Additives	3 Lime and 3 Cement by weight	3 Lime and 4 Cement by weight	4 Cement by weight	2 Lime and 3 Cement by weight	4 Lime and 4 Cement by weight
Design C.B.R. %	From 4.0 to > 40	From 2.5 to > 40	From 1.5 to > 40	From 3.0 to > 40	From 2.5 to > 40
Design Indirect Tensile Strength	34 kPa	45 kPa	37 kPa	48 kPa	48 kPa
Recommended Pavement Cross Section	20mm MS 40mm BB 300 mm FCR 150mm SSS	Industrial Roads 20mm MS 40mm BB 300 mm FCR 200 mm SSS	20mm MS 50mm BB 100mm FCR 150mm SSS	Country & Minor Streets 20mm MS 40mm BB 150mm FCR 150mm SSS Minor through Roads 20mm MS 40mm BB 150mm FCR 150mm SSS	Country & Minor Streets 20mm MS 40mm BB 100mm FCR 150mm SSS Minor through Roads 20mm MS 40mm BB 150mm FCR 200mm SSS

TABLE IV

FIELD MONITORING RESULTS

SITE	CROYDON	PAKENHAM
General Subgrade Soil Type	Very Silty Clay	Silty Clay
Average In Situ C.B.R. of Subbase zone prior to stabilisation	3 %	3.5%
Average In Situ C.B.R. of Stabilised Subbase zone	45 days after stabilisation 25 140 days after stabilisation 45	15 days after stabilisation 20 45 days after stabilisation 40
Average Deflection :-Subgrade Stabilised Subgrade Fine Crushed Rock Bituminous Course	0.92 mm 0.34 mm 0.26 mm 0.22 mm	0.09 mm 0.06 mm 0.31 mm 0.23 mm

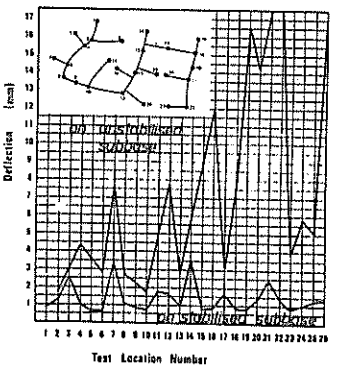

Figure 6 A Pakenham subbase deflection results

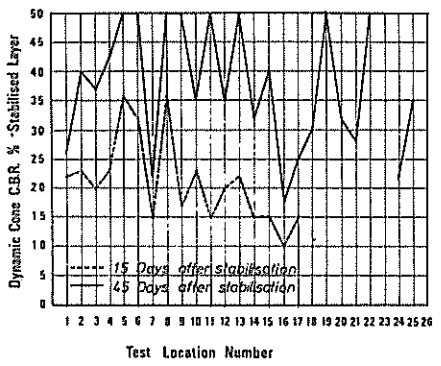

Figure 5 Pakenham insitu C.B.R. results for stabilised layer

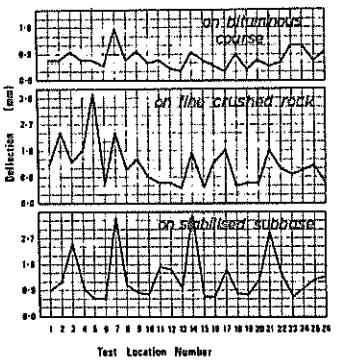

Figure 6B Pakenham deflection results

ed crushed rock and bituminous surface seal were placed. In Table V the allowable Benkelman beam deflections for various types of pavements recommended by the Victorian Country Roads' Board (1975) are tabulated. Based on this Table the deflections measured at Croydon and Pakenham indicate satisfactory pavement performance.

TABLE V
ALLOWABLE PAVEMENT DEFLECTIONS

Tolerable Pavement Deflections	
Number of commercial vehicles per day (Gross mass over 3 tonnes)	Flexible Pavement Asphalt surfacing Deflection (mm)
0 – 50 *	1·0
50 – 150 °	0·9
150 – 450 '	0·8

* DESIGN CURVES A & B
° DESIGN CURVE C
' DESIGN CURVE D

SWINBURNE STABILISED SUB-BASE PAVEMENT DESIGN METHOD

Adopting a laboratory C.B.R. of 40% and an indirect tensile strength of 40 kPa on soil tested at the estimated initial moisture content just prior to field stabilisation, McDOWELL'S (1972) method has been simplified to produce two pavement design charts (Figures 7 & 8). These charts consider the stabilised layer as part of the pavement.

To obtain the high stabilised C.B.R. values required to use these charts, both lime and cement will need to be used. These high C.B.R. values should ensure that the stabilised sub-base does not break down under any undesirable initial heavy construction traffic loading. It is essential if these high values are to be obtained, to keep the soil moisture content immediately prior to stabilisation reasonably low. It may be necessary to install pavement subgrade drainage a few months prior to stabilisation. This will undoubtedly be the case if winter or spring pavement construction is planned, especially in the areas of loose silty sand over sandy clay and silty clays.

CONCLUSIONS

For the three general groups of weak pavement subgrade soils commonly encountered in Melbourne, cement and lime can be shown in the laboratory to increase their C.B.R. and indirect tensile strength at the field moisture content to over 40 percent and 40 kPa respectively.

Five trial pavement sections were then designed using stabilised sub-bases, the cement and lime percentage being based on the laboratory testing at the likely field moisture content just prior to stabilisation. Field monitoring of two of these trial pavement areas during and after construction has supported strongly the incorporation of the stabilised sub-base as a structural component of the pavement.

Finally, McDOWELL'S (1972) pavement design procedure incorporating a stabilised sub-base has been simplified to two design charts. These charts require that the stabilised layer must have a C.B.R. and indirect tensile strength greater than 40 percent and 40 kPa respectively. To get these large soil strength increases by stabilisation it will be necessary to use from 3 to 5 percent cement and lime in clayey soils.

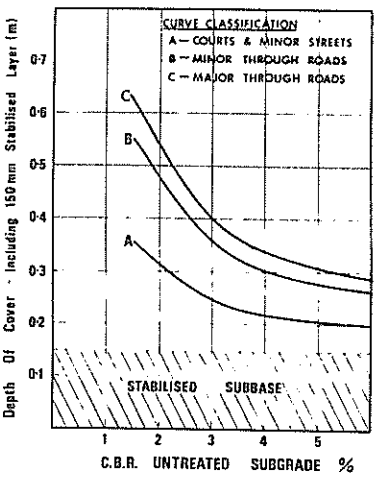

Figure 7 Stabilised pavement design chart

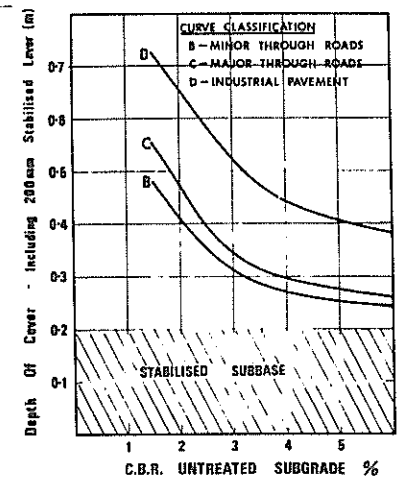

Figure 8 Stabilised pavement design chart

ACKNOWLEDGEMENTS

The financial support of the following companies and authorities made this study possible.

Australian Portland Cement, Blue Circle Southern Cement Ltd, David Mitchell Estate Ltd, Endeavour Hills Pty. Ltd, Housing Commission of Victoria, Jennings Industries Ltd, & Road Stabilisers Ltd.

REFERENCES

COUNTRY ROADS BOARD (1975). Pavement deflection testing using the benkelman beam. Country Roads Board, Technical Bulletin No.29.

McDOWELL,C. (1972). Flexible Pavement Design Guide. Bulletin 327, National Lime Association, Washington, D.C.

STANDARDS ASSOCIATION OF AUSTRALIA (1977). Determination of the California Bearing Ratio of a Soil. Standard Laboratory Method for a Re-Moulded Specimen, (AS1289.F1.1). Standards Association of Australia, North Sydney, Australia.

The Relationship Between Matrix and Solute Suction, Swelling Pressure, and Magnitude of Swelling in Reactive Clays

K. C. PILE
Senior Lecturer, School of Civil Engineering, South Australian Institute of Technology

SUMMARY The results of a series of one-dimensional swelling tests on reactive clays are reported, in which chemical analyses of salts in the porewater were first carried out to enable control of solute suction during testing. It is shown that for saline clays, the magnitude of swelling is dominated by solute suction changes. Total and solute suction values for the soils are compared, and comments are made on the significance of salt diffusion in measuring volume changes in reactive soils.

1 INTRODUCTION

The prediction of vertical movement of reactive (or expansive) clay soil profiles resulting from soil moisture changes is of concern to many geotechnical engineers. The problem arises in those parts of the world where the climate is arid for all or part of the year. Such a climate exists over large regions of Australia, and considerable damage to road pavements and light structures is the result. In particular, wall cracking in masonry domestic houses is often severe, and has attracted wide public interest.

Experience has shown that soil movement may be caused by

(i) Seasonal moisture changes, that is, due to natural rainfall and to drying by sun and wind.

(ii) Wetting of a soil profile by man-made or artificial effects, such as garden watering, leaking pipes, discharge of roof run-off close to footings, and build-up of moisture beneath impervious floors and pavements.

(iii) Drying of a soil profile as a result of ventilation under floors, air conditioning, heated areas, or moisture extracted from the soil by trees.

In Adelaide, South Australia, which has a Mediterranean climate, case-studies indicate that artificial wetting and drying are the major causes of cracking of masonry houses (Fargher, 1979, Aitchison et al, 1977).

This paper reports the results of a laboratory investigation into the swelling characteristics of soils from three sites near the City of Adelaide. The approach differs from any previous studies, in that chemical analyses for the solutes in the pore-water were carried out first, and then pairs of swelling tests using oedometers were made, in which the solute suction was kept constant in one test but allowed to vary in the other. It is postulated that these two cases represent extremes of possible wetting states beneath, say, a light building with a concrete floor. The first four causes of wetting in (ii) above will result in a dilution of solutes in the soil, or a lowering of osmotic pressure (solute suction). The last cause, i.e. build-up of moisture below an impervious floor, is likely to be due to rising saline moisture, and will result in a smaller or zero change in solute suction.

In each pair of oedometer tests, the one with distilled water in the cell measured swelling pressure and magnitude of swell due to a change in both solute and matrix (or capillary) suction, whereas that with saline water measured the effects of change in matrix suction alone.

2 EXPERIMENTAL WORK

2.1 Soil Profiles

Three soil profiles were selected for study:

- At the South Australian Institute of Technology Levels Campus, 14 km north of Adelaide, a red brown earth of pedological profile RB9b.
- At the Arboretum, Waite Agricultural Institute, 5 km south of Adelaide, a red-brown earth type RB3.
- From O'Halloran Hill, 18 km south of Adelaide, a black earth overlying Hindmarsh clay.

The annual rainfall is 500 - 600 mm.

Descriptions of soil profiles and average moisture contents are shown in Figure 1. The upper 3 m of Levels clay has nodules containing lime surrounded by relatively lime-free clay. Moisture contents may vary by $\pm 3\%$ from the values plotted.

2.2 Total Suction

It is now recognized that total suction, that is, the sum of solute and matrix suction, is a more useful parameter than moisture content in studying the swelling of reactive clays. (Peter, 1979). Total suction determinations were made on samples from each site using a thermister psychrometer similar to that described by Peter and Martin (1973). The results are shown in Figure 2. The pF scale has been used for plotting total suction values, where $pF = \log_{10} h$, and h = equivalent capillary rise in centimeters.
Figure 2 also plots the results of comparison tests done on Levels soil using three other psychrometers, with the kind co-operation of their owners. Considering the technical difficulties of measurement, the results must be regarded as in good

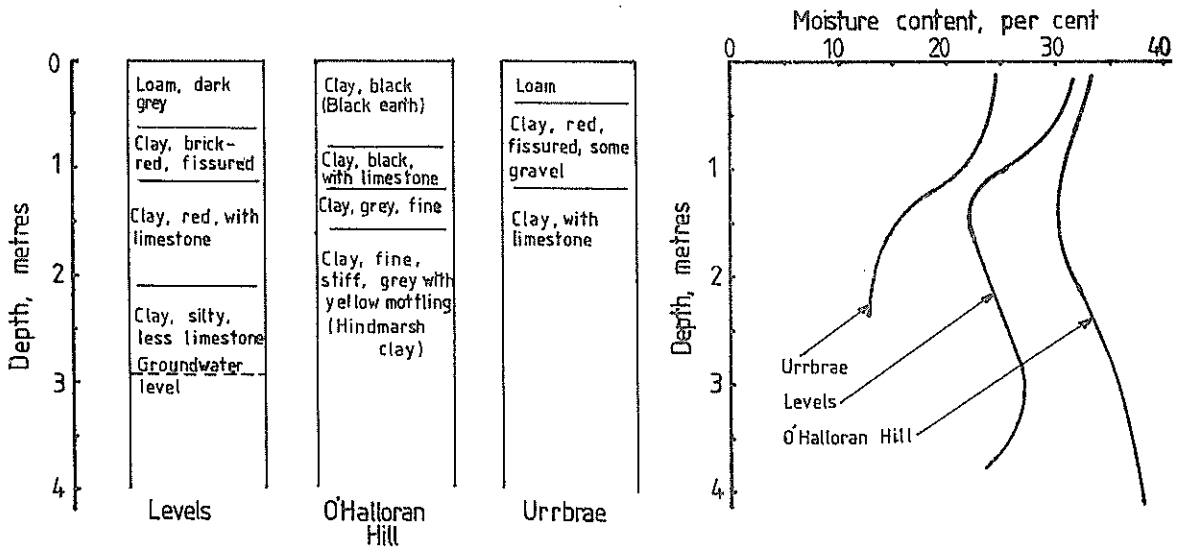

Figure 1. Soil Profiles and Moisture Contents

agreement.

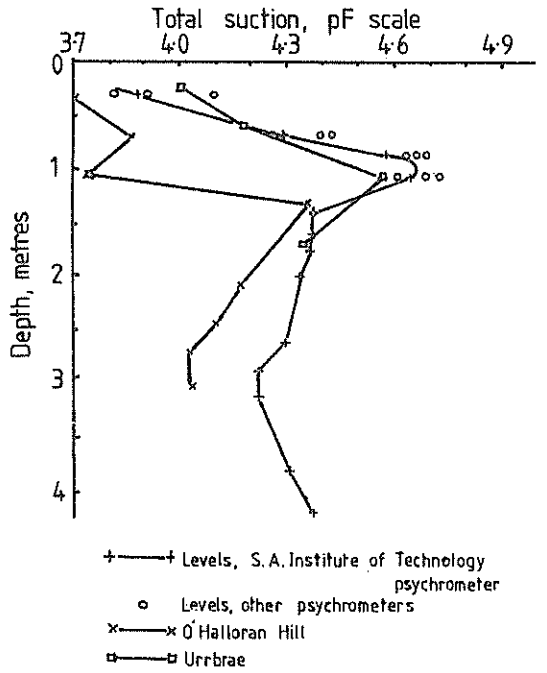

Figure 2. Suction Profiles

2.3 Chemical Analyses

Chemical analysis for salts in the pore-water involved firstly extracting moisture at several depths and then carrying out a series of chemical tests. Both were done with substantial help from the C.S.I.R.O., Division of Soils, Adelaide, South Australia.

2.3.1 Moisture extraction

Initially, three methods of extraction were tried on Levels soil samples:

- Standard 1:5 extraction as used by soil scientists, i.e. mixing 1 part of soil to 5 parts of weight of water, and using end-over-end mixing.
- Mixing soil and water to approximately the liquid limit and extracting some water using suction with a Buschner funnel.
- For a depth of 0.9 m, extraction by all-round pressure of 45 mPa in a high pressure triaxial cell.

Fine suspended matter was removed by centrifuging, and chemical testing carried out. Allowing for the dilution in the first two extraction methods, all gave the same amounts of solutes in the soil. For the Urrbrae and O'Halloran Hill soils, only 1:5 extraction was used, chiefly because it is the easiest and quickest method.

2.3.2 Methods of chemical analysis

For metal ions in solution, the atomic absorption spectro-photometer (AAS) was used. This device is now widely used in analytical chemistry, although its application to soils appear to be not widely known to engineers. A brief description of the AAS was given in Engineers Australia, May 4, 1979, p.27. Basically, it depends on spraying diluted soil pore-water into a hot flame and observing the absorption of selected wave lengths of light. The AAS is capable of measuring the concentration of metal ions accurately and quickly. It does, however, require some experience to use properly.

For non-metal ions, the methods of analyses were:

- Chlorides - titration with silver nitrate, using an electrometric method for precise determination of the null point.
- Carbonates and bicarbonates - titration with hydrochloric acid.
- Sulphates - gravimetric method as described in Australian Standard 1289 - Testing Soil for Engineering Purposes.

Figure 3 shows the concentration of salts (or rather ions) in solution in the pore-water. The concentration is given in milli-equivalents per litre (m.e/l). A normal solution is 1000 m.e/l.

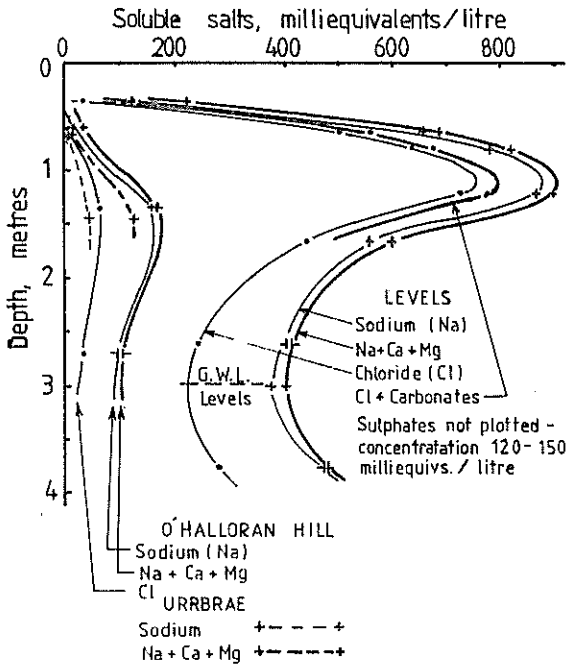

Figure 3. Solutes in pore-water

2.4 Oedometer Tests

Table 1 shows the results of tests carried out following the chemical analyses. The procedure was to prepare pairs of specimens, load to overburden pressure, and then add distilled water to one cell and water of the same salinity as the soil moisture to the other. As swelling commenced, vertical load was added in small steps to just prevent net vertical heave. The swelling pressures in Table 1, based on no volume change, were reached in a few hours.

Following the swelling pressure being reached, the vertical load on each specimen was reduced to approximately overburden pressure and the magnitude of resultant heave was observed. For the saline Levels clay, the tests with distilled water showed heave for several weeks, and of magnitude significantly greater than in the test with saline water. It became obvious that salt from the soil was diffusing out of the voids into the initially salt-free water, even though the sample was swelling.

In Table I the column for solute suction shows either 0 for distilled water or the normality of saline water used, chiefly sodium chloride. Test No. 3 was an attempt to examine the consequence of using a very dilute solute, and test No. 10 used a salt concentration of twice that in the soil water.

2.5 Pressure Plate and Vacuum Desiccator Tests

An attempt was made to measure matrix suction using pressure plates set at 1, 4 and 15 bars. These experiments did not lead to reliable results, probably because of lack of good contact with the Visking membrane.

It was attempted to check total suction determinations by placing Levels soil in vacuum desicators at pF 4.0, 4.5 and 5.0, using the null point technique. After 1 - 2 months, psychrometer check tests showed that the soil had reached equilibrium at pF 4.5 and 5.0, but not at pF 4.0, which would have required a moisture increase. It was also found that the moisture content changes for pF 4.5 and 5.0 were too erratic to enable the original soil pF to be determined accurately.

2.6 Solute Suction

Efforts were made to measure solute suction independently. For the Levels clay at 0.9 m, undiluted pore-water extracted by pressure (Section 2.3.1) was found by psychrometer testing to have a pF of 4.62, virtually the same as the total soil suction shown for 0.9 m in Fig. 2. The implication is that matrix suction is very small.

The known concentration of solute salts may also be used to calculate solute suction using vapour pressure tables. The method has been described by Aitchison and Richards (1965). At 0.9 m, Fig. 3 shows that Levels clay has a normality of about 0.9, mostly due to dissolved sodium chloride. The corresponding osmotic pressure calculated from tables is pF 4.61

2.7 Salt Diffusion

When the oedometer tests were found to exhibit long-term heave, additional testing was done on sample 6, table I. The water in the consolidation cell was syphoned out at the end of the test (35 days) and its salinity determined by the A.A.S. method. The specimen itself was tested for total suction in the psychrometer.

It was found that the pF of the specimen had been reduced from 4.37 (2300 kPa) to 3.7 (500 kPa), suggesting that more than 75% of the salt had moved from the soil into the surrounding water.

The measured salinity of the surrounding water confirmed that about 70% of the salts in the soil had indeed diffused into the cell water. The diffusion was not assisted by consolidation at any stage, as the specimen had swelled continuously during the test.

3 ANALYSIS OF RESULTS

Consideration of the experimental results suggests that

(1) The existence of a high total suction is not in itself an indication that a soil is reactive. Tests 8 and 9, Table I, show that Levels clay at 2.65 m has no capacity to swell under overburden pressure despite its pF of 4.25, whereas tests 18 and 19 on O'Halloran Hill clay at 2.75 m indicate a capacity to swell against a vertical pressure of over 150 kPa, despite an initial suction of only pF 4.03.

(2) Comparing pairs of tests, Table I, the swelling pressure appears to be relatively independent of the solute used, but the magnitude of swelling under reduced load is greater for the distilled water test which involves a lowering of solute suction due to ingress of fresh water into the voids, and salt diffusion.

TABLE I - RESULTS OF OEDOMETER SWELLING TESTS

Test No.	Location	Depth metres	Initial moisture content, %	Initial dry density grms/ml	Solute used - Normality	Duration of test, days	Swelling pressure, kPa	Heave data			Initial total suction	
								Field overburden, kPa	Vert. pressure during swelling kPa	% heave	pF	kPa
1	Levels	0.4	30.2	1.49	0 *	44	60 approx.	7	26	3.1%	3.9	800
2	"	0.4	34.4	1.38	.066 N	44	40 approx.	7	26	0.2		
3	"	0.4	34.4	1.42	.0001 N	50	>80	7	26	3.5		
4	"	0.7	36.6	1.33	0	24	40 approx.	10	7	0.5	4.30	2000
5	"	0.7	34.0	1.36	0.67 N	24	20 "	10	7	0.1		
6	"	1.4	22.5	1.63	0	35	>25	27	7	0.6	4.37	2300
7	"	1.4	21.8	1.65	0.8 N	21	21 approx.	27	7	0.1		
8	"	2.65	24.2	1.54	0	13	48 approx.	50		Zero - not reactive	4.25	1750
9	"	2.65	23.5	1.58	0.4 N	13	45 "	50				
10	"	2.65	23.0	1.61	0.8 N	13	45 "	50				
11	O'Halloran Hill	0.5	27.9	1.36	0	16	100 "	10	12	1.4	3.7	500
12	"	0.5	27.1	1.35	0.04 N	16	100 "	10	12	1.4		
13	"	1.3	25.8	1.32	0	21	120 "	25	60	2.0	4.38	2350
14	"	1.3	28.4	1.32	0.166 N	21	100 "	25	60	0.5		
15	"	1.65	30.0	1.33	0	10	>200	33	-	-	4.28	1900
16	"	1.65	31.3	1.35	0.166 N	10	>200	33	-	-		
17	"	2.75	39.9	1.26	0	22	200 "	50	50	3.75	4.03	1050
18	"	2.75	38.0	1.24	0.1 N	22	150 "	50	50	1.0		
19	Urrbrae	0.7	29	1.58	0	10	120 "	13			4.15	1400
20	"	0.7	29	1.52	0.03 N	10	<80	13				
21	"	1.5	30	1.56	0	10	>30	28			4.45	2800
22	"	1.5	30	1.58	0.06 N	10	120?	28				

* 0 indicates distilled water

(3) Comparison of Figs. 2 and 3 suggests that for the Levels soil, the psychrometer was really measuring solute suction. Matrix suction appears to be small.

(4) It cannot be inferred from (3) that matrix suction is low in all reactive soils. For example, in test 18 of Table I, the solute was constant at 0.1 Normal, corresponding to a solute suction of 450 kPa. Hence the matrix suction was initially 600 kPa. It appears that the high swelling pressures in tests 15 - 18 are associated with high initial matrix suctions.

(5) The above suggests that the existence of some matrix suction is essential to initiate swelling. Tests (8) and (9) were on clay close to the ground-water level, and must have had virtually zero matrix suction. The mechanism appears to be that once swelling starts, solute suction changes become significant.

(6) In Table I, the heaves reported for the tests with no solute change are due to matrix suction. The additional heaves in the comarison test with distilled water are due to changes in solute suction.

(7) The separate measurement of matrix suction is a difficult problem. Reactive clays generally have micro-fissures, and matrix suction probably varies greatly from fissures to intact groups of soil particles.

(8) The magnitude of swell in Table I is a function of the quantity of distilled water surrounding the soil. The swell figures in themselves have no absolute value, only comparative. In future work, it appears desirable to measure the pF of soil specimens at the beginning and end of oedometer tests involving swelling.

(9) The salts reported in the pore-water, Fig. 3, are soluble salts and do not take any account of exchangeable salts in the clay particles.

4 RECOMMENDATIONS

(a) Both matrix and solute suction have been shown to be important in reactive clays. In design of footings on such soils, possible variations of both must clearly be allowed for.

(b) It is apparent that in oedometer testing of saline soils, the consequences of any change in solute suction due to salt diffusion must be considered. Current laboratory practice appears to ignore this problem.

5 ACKNOWLEDGEMENT

The assistance is acknowledged of Dr. W.W. Emerson, Senior Research Scientist of the C.S.I.R.O., Division of Soil, Adelaide, South Australia.

6 REFERENCES

AITCHISON, G.D. and RICHARDS, B.G. Moisture Equilibria and Moisture Changes in Soil Beneath Covered Areas. Symposium in Print. Butterworths, Australia. 1965. pp 184-232

AITCHISON, G.D., PETER P. & POWER, R.F. Stress-deformation Mechanisms in Clays as Determinants of Design Requirements for Small and Large Structures. Annual Conference, Institution of Engineers, Australia, 1977.

FARGHER, P.J. Footings and Foundations for Small Buildings in Arid Climates. The Institution of Engineers, Australia, South Australian Division, June 1979. pp. 1-19.

PETER, P. and MARTIN, R. A Simple Psychrometer for Routine Determinations of Total Suction in Expansive Soils. Third International Conference on Expansive Soils, Haifer, Israel, 1973.

PETER, P. Footings and Foundations for Small Buildings in Arid Climates. The Institution of Engineers, Australia, South Australian Division, June 1979. pp 46-62.

Looking for Expansive Minerals in Expansive Soils; Experiments with Dye Absorption Using Methylene Blue

G. S. XIDAKIS
Visiting Scholar, Department of Civil Engineering, University of Leeds, England
I. J. SMALLEY
Soil Bureau, DSIR, Lower Hutt, New Zealand

1 INTRODUCTION

According to Chen (1975, p.16) there are three different approaches to the problem of classifying potentially expansive soils. The first, mineralogical identification, can be useful in the evaluation of the material but is not sufficient in itself when dealing with natural soils. The second includes the indirect methods such as the index property, the PVC method and the activity method which are valuable tools in evaluating the swelling property; and the third is direct measurement which offers the most useful data for a practicing engineer.

Chen lists five techniques for mineral identification; these are X-ray diffraction, differential thermal analysis (DTA), dye adsorption, chemical analysis and electron microscopy. He comments that the test results require expert interpretation and the specialised apparatus required is costly and often not available in soil testing laboratories.

The purpose of this paper is to report on some investigations which bear on Chen's claim of impracticality for the mineral identification methods. In particular we have studied the information which can be produced by dye adsorption tests on soils. The dye adsorption method did get some approval from Chen, and he stated that "the relatively simple testing procedure and speed of dye staining tests compared with X-ray diffraction and DTA justify wider application of the colour method." One of the contending dyes for use in the method is methylene blue and this does seem very suitable for investigations on soils for engineering purposes.

The dye adsorption method gives a measure of the surface area (S.A.) of the soil, and it appears that there is a very good correlation between surface area and swelling behaviour, although the presence of allophane may disturb this assertion. The clay minerals which are really dangerous from a swelling point of view are the high surface area smectites or montmorillonites, and these can be difficult to detect and measure. We investigated eight soils: four smectite-containing soils from north Greece (Gr1-Gr4); a black cotton soil from Kenya supplied by the Transport and Road Research Laboratory, England; two soils from the Adelaide area (Modbury & Adelaide) supplied by R. Martin and P. Peter of CSIRO Applied Geomechanics Division, and a vertisol from Transvaal, South Africa (Mngazi soil) supplied by Dr R.W. Fitzpatrick of Natal University. The swelling minerals content of these soils ranges from 10 to 60% of the whole soil. The last four soils are known to be highly expansive soils.

2 METHYLENE BLUE ADSORPTION METHOD

When methylene blue dye is adsorbed by clay, the dye molecules first form an irreversibly adsorbed monolayer over all the accessible clay surface (internal and external). Dye continues to be adsorbed from solution until this monolayer is formed, leaving a clear solvent on sedimentation of the clay. Further adsorption is reversible and the dye molecules superimposed on the monolayer are in equilibrium with the dye molecules in solution, leaving a coloured solution on sedimentation of the clay. (The actual technique used in the test is described in the appendix.)

When a monolayer has just been formed, any excess of dye will give a colouration to the supernatant liquid; the 'end-point' is considered to have been reached when enough dye has been added to a given amount of clay in suspension to produce this first permanent colouration. This is a little higher than the 'optimum flocculation point' used by Hang and Brindley (1970).

We need to relate the amount of dye used to reach the end-point to the surface area of the clay in the soil under test. The total area of the dye molecules at the end-point can be calculated by taking the effective area of the dye molecule as 107 $\AA^2$. This area is defined as the 'Apparent Surface Area' (ASA) of the clay; the units are m^2g^{-1} clay. The value of 107 $\AA^2$ is a compromise between the theoretical site area of a dye molecule and the fact that the dye behaves slightly differently with respect to the various types of clays (see Xidakis, 1979 for some discussion and justification).

The dye used was methylene blue hydrochloride, supplied by Hopkin and Williams Ltd, Chadwell Heath, Essex, England. The ASA of the clay or soil is calculated from the formula:

$$ASA = \frac{Vd}{C} \times N \times Ad \times 10^{-25} \ m^2/g \qquad (1)$$

where Vd is the volume of 0.01 M methylene blue standard solution required to reach the end-point, in cm^3; C is the mass of clay or soil present in the test-tube in grams; N is Avogadro's Number (6.02×10^{23}) and Ad is the effective area of the dye molecule in $\AA^2$.

Substituting for N and Ad in formula (1) it reduces to:

$$ASA_{107} = \frac{Vd}{C} \times 6.45 \ m^2/g$$

3 SUPPORTING TESTS AND RESULTS

To provide data for the important correlations a set of supporting tests was carried out on the eight soils. We report here tests on liquid and plastic limits, free swelling of dry disaggregated soil and linear shrinkage. The free swelling test was considered to give an indication of the expansiveness of the soil (and thus a measure of the geotechnical hazard) and this was related to the dye adsorption measurements and to the more conventional soil properties indicated by Atterberg limit and shrinkage determinations. To show how the methylene blue method relates to other methods of surface area determination some comparative tests were carried out with ethylene glycol and glycerol, on the fine clay (<1 μm) fractions of the eight soils. Table 1 shows the results of the surface area determinations.

TABLE I

SURFACE AREA (m^2g^{-1}) OF CLAY FRACTIONS OF EIGHT EXPANSIVE SOILS
(SIMPLIFIED FROM XIDAKIS, 1979)

Method \ Soil	Gr1	Gr2	Gr3	Gr4	Kenya	Adelaide	Modbury	Mngazi
Ethylene glycol	485	530	490	437	674	589	610	575
Glycerol	384	514	480	430	670	616	607	615
Methylene Blue (ASA_{107})	426	480	440	414	656	574	571	585

Table 2 is a matrix of correlation coefficients between the various properties of the eight soils. It should be noted that the ASA value has a correlation coefficient of 0.991 with respect to the free swelling capacity (although it must be admitted that the number of specimens is rather meagre).

TABLE II

MATRIX OF CORRELATION COEFFICIENTS BETWEEN VARIOUS PROPERTIES
OF EIGHT EXPANSIVE SOILS
(SIMPLIFIED FROM XIDAKIS, 1979)

		1 LS	2 LL	3 PL	4 PI	5 Cf	6 Fr.Sw	7 ASA
1	LS	1						
2	LL	0.992	1					
3	PL	0.527*	0.606*	1				
4	PI	0.985	0.983	0.449*	1			
5	Cf	0.794	0.862	0.754*	0.794	1		
6	Fr.Sw	0.989	0.998	0.617*	0.978	0.854	1	
7	ASA	0.968	0.989	0.623*	0.957	0.895	0.991	1

Significance level (S) <0.01 except values with asterisk (*);
LS = linear shrinkage (%); LL = liquid limit; PL = plastic limit; PI = plasticity index; Cf = % fine clay (<1 μm);
Fr.Sw = % free swelling; ASA = surface area of untreated whole soils (m^2/g - determined by methylene blue adsorption).

4 SURFACE AREA

It is apparent from the correlation matrix that the measured surface area of the untreated soil is reasonably well correlated with most of the other properties of the soils examined (r >0.95). The surface area used for the correlations was that obtained on the untreated natural soils, by the methylene blue dye method. It represents the dye adsorption by the untreated soil and not the true surface area of the soil i.e. the apparent surface area (ASA). When the surface area of the treated soil (i.e. after the removal of carbonates and organic matter) was used, the correlations were lower (data not shown).

This is not unexpected since in principle the treated soil must behave differently from the untreated one in which the carbonates and organic matter can act as cementing agents and reduce the surface area of the clay. The treated soil is expected to swell more (Rimmer & Greenland, 1976). However the use of the ASA or dye adsorption value of the untreated soil is preferable because firstly it simplifies the dye adsorption method since no pretreatment of the soil is required, and secondly it possibly simulates more closely the water adsorption system in a natural soil which is responsible for the swelling. In this case, where the soil is aggregated, part of the soil surface accessible to water molecules may be inaccessible to dye ions which are up to ten times as large (Lafleur, 1972). Nevertheless this difference is believed to be small and may be neglected.

The high correlation of the ASA with the liquid limit and plasticity index (r >0.95) means that the ASA (or dye adsorption value) may possibly be useful in determining the latter in soils and clays, after proper calibration or redefinition. Thus the plasticity of clays and soils might be defined by an intrinsic and not an arbitrary property. Many authorities have obtained good correlations between

surface area and Atterberg limits (Fairbairn & Robertson, 1956, Farrar & Coleman, 1967, Warkentin, 1972) or surface area and swelling properties (De Bruyn *et al.*, 1956, Greene-Kelly, 1974, Ross, 1978).

From the above results it appears that the best parameters for an indirect determination of the swelling potential of expansive soils are the Atterberg limits (LL and PI), linear shrinkage and the ASA of the untreated soil.

5 THE USE OF SURFACE AREA FOR CLASSIFYING SOILS

Some advantages of using surface area as an indicator of soil properties are presented below:

(a) The ASA appears to be as good as the other parameters often used for this purpose, i.e. LL, PL, etc.

(b) It is a basic and well defined property of the soil or clay and not an empirical one like the Atterberg limits.

(c) It can be determined in a much shorter time than even the consistency limits. For example, using the methylene blue dye method the time required for a test on a natural untreated soil is less than an hour, compared with the 48 hours necessary to complete the Atterberg limit tests.

(d) The methylene blue dye method appears to have a greater reproducibility than the consistency tests. The precision of the dye method is ±5-8% (Xidakis, 1979) whereas with the Atterberg limits it hardly exceeds ±10%. The effect of the operator's judgement can be more pronounced in the consistency limits operation than in the dye test. The method has possible application for soil classification in road works where there is the need for quality control of large amounts of earth-works. Also it could be used during site investigation for quick evaluation of soil samples obtained as drill cores.

(e) Surface area is an indicator of many other properties of a soil or clay, such as CEC, mineralogy, clay content, water adsorption, retention of phosphates and nutrients, green sgrength, etc. Thus it can be used in the evaluation of clays and soils for agricultural, engineering and ceramic purposes. It also provides information for soil genesis and evolution in pedological studies, for oil genesis and migration in the petroleum industry, and for catalyst preparation in the chemical industry.

(f) It can be shown by theoretical considerations that the surface area is directly related to both swelling pressure and volume change of soils (Xidakis, 1979).

However there are also some shortcomings to the dye method. For example, the dye adsorption is influenced by the nature of the surface, charge density, exchangeable ions, particle aggregation and other factors which have been discussed in more detail by Xidakis (1979). Nevertheless all these disadvantages are believed to be of minor importance when the method is employed for engineering purposes, where absolute accuracy is not of paramount importance.

6 DISCUSSION & CONCLUSIONS

The surface area is a basic soil property, directly related to swelling and other properties of soils, and can be adequately determined by dye adsorption methods. Therefore it can be used for evaluation and classification of expansive soils, and for the grading of such soils we suggest the boundaries: <100, 100-150, 150-200, >200 m^2g^{-1} as demarcating the low, medium, high and very high expansiveness classes.

The methylene blue dye method is a simple and versatile method of looking for expansive minerals in expansive soils, and it is also possible that the same method after proper calibration may be used to determine the Atterberg limits of expansive soils.

7 ACKNOWLEDGMENTS

G.X. would like to acknowledge the State Scholarships Foundation of Greece for sponsoring the research. We thank Drs R.D. Northey and R.J. Furkert for their copious comments on early drafts of this paper.

8 REFERENCES

CHEN, F.H. (1975). *Foundations on Expansive Soils.* Elsevier (Dev. Geotech. Eng. no. 12) Amsterdam, 275p.

DE BRUYN, C.M.A., COLLINS, L.E. and WILLIAMS, A.A.B. (1956). The specific surface, water affinity and potential expansiveness of clays. *Clay Min. Bull.* 3, 120-128.

FAIRBAIRN, D.E. and ROBERTSON, R.H.S. (1956). Liquid limit and dye adsorption. *Clay Min. Bull.* 3, 129-136.

FARRAR, D.M. and COLEMAN, J.D. (1967). The correlation of surface area with other properties of nineteen British clay soils. *J. Soil Sci.* 18, 118-124.

GREENE-KELLY, R. (1974). Shrinkage of clay soils: a statistical correlation with other soil properties. *Geoderma* 11, 243-257.

HANG, P.T. and BRINDLEY, G.W. (1970). Methylene blue adsorption by clay minerals: determination of surface areas and cation exchange capacities. *Clays Clay Miner.* 18, 203-212.

JONES, F.U. (1964). New fast accurate test measures bentonite in drilling mud. Oil & Gas J. *62*, (22) 76-78.

LAFLEUR, K.S. (1972). Some differences among soils of diverse clay mineralogy. *Soil Sci.* 113, 124-129.

RIMMER, D.L. and GREENLAND, D.J. (1976). Effects of calcium carbonate on swelling behaviour of a soil clay. *J. Soil Sci.* 27, 129-139.

ROSS, G.J. (1978). Relationship of specific surface area and clay content to shrink-swell potential of soils having different clay mineralogical compositions. *Can. J. Soil Sci.* 58, 159-166.

WARKENTIN, B.P. (1972). Use of the liquid limit in characterizing clay soils. *Can. J. Soil Sci.* 52, 457-464.

XIDAKIS, G.S. (1979). *Assessment of the engineering and other properties of expansive soils by various methods.* Thesis (Ph.D.) University of Leeds.

APPENDIX

Outline of the methylene blue dye method (for laboratory use or field test).

1. Take a few grams of <2 mm air dry soil and disaggregate it carefully to give about 5 g passing a BS 200 sieve (74 μm). Dry the soil in an oven at 105°C to give dry mass.

2. Make a suspension (2-5% by weight) preferably with distilled water. The concentration of the suspension should be adjusted depending upon the kind and amount of the clays in the soil; i.e. the greater the amount of swelling minerals in the soil the more dilute the suspension should be. This can easily be determined by a trial test.

3. Add 'Calgon' or Na_4EDTA solution to give 0.5-1.5 me Na per gram of dry soil. Excess of dispersing agent, within reasonable limits, does not affect the results.

4. Stir the suspension with a commercial stirrer for about 15 min. If no stirrer is available shake vigorously for 2-3 mins by hand. If the soil contains no more than small amounts of carbonates and/or soluble salts it will disperse easily by hand shaking.

5. Prepare a standard 0.01 M methylene blue dye solution (dissolve 3.65 g of dye in a litre of distilled water). Keep the standard dye solution away from the direct sunlight and in a polythene bottle to avoid fading of the solution.

6. Pipette an aliquot of the soil suspension (10-20 cm^3) into a Pyrex test-tube or a conical flask with stopper. The initial suspension can be prepared directly in a conical flask (200 cm^3 recommended). Avoid the use of soda glassware since it absorbs the dye. Perform the 'spot' test (Jones 1964): i.e. titrate the standard 0.01 M methylene blue dye solution by burette. For field tests a 2-10 cm^3 disposable plastic medical syringe without needle can be used both for pipetting the soil suspension and titrating the dye solution. The dye should be added to the suspension 1 cm^3 at a time; after each 1 cm^3 dye addition shake the container vigorously for a few seconds; then, using a glass rod, place one drop of suspension on a medium soft filter paper (e.g. Whatmans No. 1 or 40).

7. The 'end-point' is indicated when excess dye appears as a sky-blue (possibly greenish) colouration radiating away from the normally deeply dyed solid in the centre. This is confirmed as the true end-point if the titrated suspension still shows excess dye when the spot test is repeated after a two minute period.

8. With the spot-test an accuracy of ±0.5 cm^3 of dye can easily be obtained under normal conditions and this is quite satisfactory for engineering purposes. Having found the end-point from the spot test the ASA is obtained from the formula:

$$ASA_{107} = \frac{Vd}{C} \times 6.45 \ m^2/g \ soil$$

where Vd is the volume of the 0.01 M methylene blue standard solution required to reach the end point; C is the mass of the soil in the test container in grams.

Strength and Deformation Behaviour of Sand under General Stress System

B. SHANKARIAH
Lecturer in Civil Engineering Regional Engineering College, Warangal (A.P.), India
T. RAMAMURTHY
Professor of Civil Engineering, Indian Institute of Technology, Delhi

SUMMARY Drained shear tests have been conducted on fully saturated Ottawa sand specimens under axisymmetric compression and extension and general stress system. All the tests have been conducted in Universal Triaxial Apparatus. The specimens have been prepared under different inclinations to study the effect of structural anisotropy. The various factors which affect the strength and deformation properties under general stress system are discussed. The effect of intermediate principal stress on peak strength, linear and volumetric strains in discussed.

1 TESTING OF SOIL UNDER GENERAL STRESS SYSTEM

During the past four decades several apparatuses have been developed for subjecting a cuboidal specimens to general stress system. When the pressure was applied through rigid platens on all the six faces, the edge interference at the junctions posed problems. To avoid this, when undersized plates were used the soil squeezed into the gaps. In case of an apparatus using flexible bags on all six faces, edge interference again posed problems and the magnitude of pressure that could be applied was limited. Compared to the devices employing exclusively either rigid platens or flexible bags, a combination of these two poses lesser mechanical problems. The Universal Triaxial Apparatus developed by Ramamurthy (1970) and Rawat and Ramamurthy (1978) belongs to this category of mixed boundary conditions. In this the lateral pressures are applied through flexible bags and the vertical pressure through enlarged and lubricated rigid platens. The problem confronting the flexible bags of the possibility of applying a limited stress level has largely been overcome by confining the rubber bags in metallic guides. The edge interference has been overcome by providing side vanes to the metallic guides and reinforcing the vertical edges of bags applying higher lateral pressure with prismatic sponge pieces.

2 STRENGTH OF SOIL UNDER GENERAL STRESS SYSTEM

In theory of plasticity the effect of intermediate principal stress is accounted for by Lode's stress parameter μ given by

$$\mu = \frac{(\sigma_2' - \sigma_1') + (\sigma_2' - \sigma_3')}{(\sigma_1' - \sigma_3')} \qquad (1)$$

Where σ_1', σ_2' and σ_3' are the major, intermediate and minor principal stress respectively. Habib (1953) introduced a parameter b, which is the ratio of the deviator stresses, that is

$$b = \frac{\sigma_2' - \sigma_3'}{\sigma_1' - \sigma_3'} \qquad (2)$$

It may be observed that $\mu = (2b-1)$. In axisymmetric compression test, $(\sigma_2' = \sigma_3')$, $\mu = -1$, $b = 0$. In axisymmetric extension test $(\sigma_1' = \sigma_2')$, $\mu = 1$, $b = 1$. These being the two extreme cases betwen which the intermediate principal stress can vary, the range of μ is from -1 to 1 and that of b is from zero to one.

Most of the investigators agree that peak strength of a soil increases with increase in the value of b upto a particular point (possibly upto plane strain compression). These results mostly belong to compression zone. But most of the controversy centres around the peak strength in extension tests. Reported results show that the values of peak strength beyond plane strain compression may increase, remain constant or decrease. Attempts have been made to attribute these divergencies to equipment defects disregarding many other factors which effect the results. These are briefly discussed here.

2.1 Material Properties

The response of a soil to various stress paths depends upon the properties of the material. Pearce (1970) reported that σ_2' has no influence on the strength of clay he has tested. Shankariah (1977), investigated the strength and deformation behaviour of two cohesionless soils, namely, (i) Ottawa sand which is uniform material with hard, well rounded, nearly spherical and smooth textured grains and (ii) crushed stone consisting of hard, disc shaped subangular and rough textured particles. The ϕ' Vs b(or μ) curves were found to be strickingly different in two materials. Figure-1 is reproduced from Lomise et al (1969). These results are obtained from tests on various soils tested under similar conditions in a single apparatus developed by them. It may be

observed that these results incorporate many type of divergencies. Since many of the factors affecting the results are invariant in these tests, a large part of the divergence cannot but be attributed to the differences in the properties of the materials.

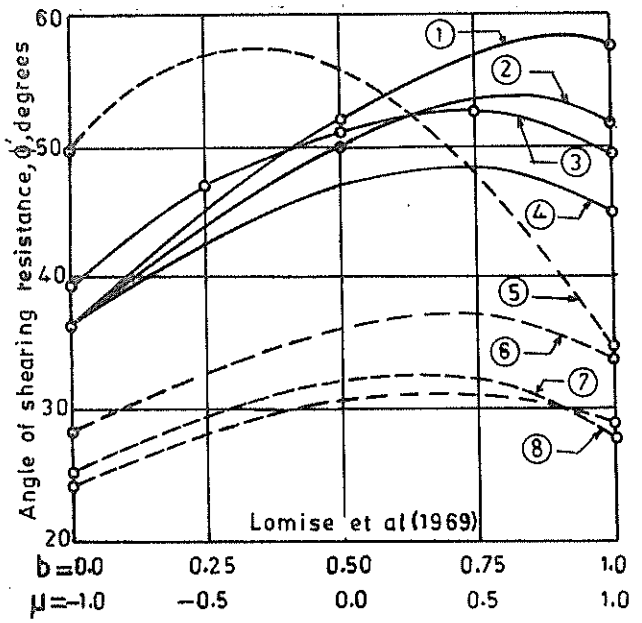

Figure 1 Effect of Material Properties on Peak Strength

2.2 Shape of the Specimen

Reades (1972) and Rawat (1976) among others reported practically identical results in cylindrical and cubical samples under axisymmetric compression. But higher peak strengths in cuboidal specimen in axisymmetric extension have been reported by Green (1971) and Reades (1972). It was suspected that this higher strength in cuboidal specimens could be due to corner effects. But when the strains were monitored accurately using X-ray method, no nonuniform strain conditions due to corner effects were noticed in a cuboidal specimen in extension. Therefore higher strengths in cuboidal specimens cannot be attributed definitely to corner effects. Thus, it cannot, at present, be said how the shape of the specimen affects the results.

2.3 Consolidation Pressure

Results of Marachi et al (1969) indicate that the increase in the value of peak strength from axisymmetric compression to plane strain compression decreases with increase in cell pressure (σ_3') at which the samples have been tested. They reported that the difference in the peak value of ϕ' between axisymmetric compression and plane strain compression was 7° in dense specimens at $\sigma_3' = 68.95$ KN/m^2, 4.5° at $\sigma_3' = 551.6$ KN/m^2 and zero at $\sigma_3' = 3447.5$ KN/m^2. This reduced difference in ϕ' could be due to restricted movement of particles at high cell pressures and/or due to grain crushing.

2.4 Stresspath Followed During Shearing

A given set of stress conditions at failure can be reached by following different stresspaths. The value of b (or μ) at failure depends on the values of three principal stresses, which may be attained by proceeding in several ways. The stresspath followed during shearing may effect the results.

2.5 Mean Normal Stress at Failure

Generally it is a normal practice to choose the consolidation pressures in extension tests such that the value of either σ_{1f}' or σ_{3f}' are comparable to those in compression. In either case the mean normal stress at failure will be higher in extension tests than those in compression, since in axisymmetric compression $\sigma_1' > \sigma_2' = \sigma_3'$, and in axisymmetric extension $\sigma_1 = \sigma_2 > \sigma_3$. It is fairly well established fact that principal stress ratio σ_1'/σ_3' of a given material decreases with increase in mean normal stress at failure (σ_{mf}').

2.6 Porosity - Basis of Compression

Whatever may be the basis on which the consolidation pressures are chosen (keeping constant either σ_{1f}' or σ_{3f}' or σ_{mf}') they are normally higher in extension tests. Therefore for a given initial porosity, the post consolidation porosity is lower in extension tests than that in compression tests. The results of extension and compression tests are compared based on initial porosities by some investigators and post consolidation porosities by others. This factor should be kept in view while comparing the results of different investigators.

2.7 Equipment Defects

There is no ideal equipment which can subject specimens of all types of soils, to all types of stress paths and stress levels. Equipment defects include, among other things, end restraints, undersized or oversized platens or bags, corner interferences, limited stress levels and so on. Hither to there has been a tendency to attribute most of the divergencies in the results exclusively to equipment defects. Though this may be unfair, many times the equipment defects contribute a major part in the divergencies of test results.

2.8 Type of Deposition and Compaction

The structural anisotropy of a specimen depends upon the method of deposition and subsequent compaction. The structural anisotropy of the specimen may lead to nonuniform deformation and directional variation of strength. However, not much is known about the directional variation of strength due to structural anistoropy of the material under various stress paths. The present investigation is an attempt in this direction.

3 EXPERIMENTAL WORK

The tests were conducted on standard Ottawa sand (18-52 B.S. sieves) consisting of hard,

well rounded, nearly spherical and smooth textured particles. Fully drained tests were conducted on freshly boiled, saturated cubical specimens of nominal size 76 mm specimens were prepared at three densities by vibrating in a sample former, the relative density varying from 50 to 100 per-cent. To study the directional variation of strength, samples were prepared at eight different angles of deposition θ namely 0, 15, 30, 45, 60, 70, 80 and 90 degrees, where θ is the angle made by the direction of deposition with the vertical axis of the specimen (Figure-2). The method of specimen preparation is explained in detail elsewhere (Shankariah, 1977).

All the specimens were consolidated isotropically. The consolidation pressures in other stress paths were so chosen that, for a given porosity, the mean normal stress at failure would be comparable to that in axisymmetric compression. This procedure was adopted to eliminate the possible effect of variation in mean normal stress at failure on the values of peak strengths obtained in different stress paths.

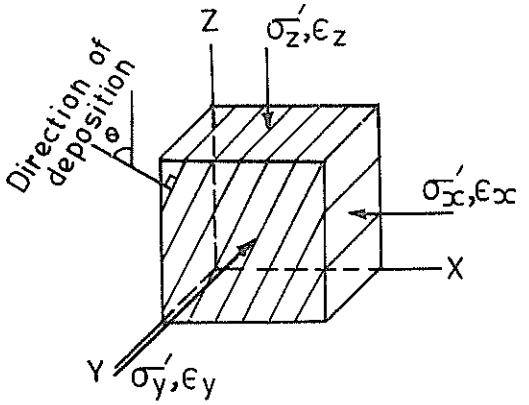

Figure 2 Reference Directions

The samples were sheared following five different stress paths

i) Axisymmetric compression ($\sigma_z' > \sigma_x' = \sigma_y'$); the lateral pressures were kept constant and the axial stress was increased during shearing.

ii) General compression ($\sigma_z' > \sigma_x' > \sigma_y'$): σ_y' was kept constant during shearing and both σ_x' and σ_z' was increased to failure.

iii) Plane strain compression ($\sigma_z' > \sigma_x' > \sigma_y'$ and $\epsilon_x \approx 0$): Samples were sheared by keeping σ_y' constant and increasing both σ_x' and σ_z'. σ_x' was increased continuously at such a uniform rate so as to prevent lateral deformation on those faces ($\epsilon_x \approx 0$).

iv) General Extension ($\sigma_x' > \sigma_y' > \sigma_z'$): During shearing σ_y' was kept constant, σ_x' was increased and σ_z' was reduced. Tests were repeated with three different values of σ_x' at failure so that each test will provide a different point on ϕ' vs b (or μ) diagram.

v) Axisymmetric extension ($\sigma_x' = \sigma_y' > \sigma_z'$) Samples were sheared by keeping the lateral pressures constant and reducing the vertical stress.

4 PRESENTATION AND DISCUSSION OF RESULTS

4.1 The Angle of Shearing Resistance

The angle of shearing resistance is found to be constant in the regions $0 < \theta < 30°$ and $60° < \theta < 90°$, there being a discontinuity in the region $30° < \theta < 60°$. This phenomenon was observed at all the three porosities of the specimens. Therefore the results of tests with $\theta = 0°$ and $60°$ which represent two distinct groups are presented here.

Figure-3 shows the variation of maximum angle of shearing resistance with b (or μ) It may be observed that, with increase in the value of b, the peak strength increases up to a value of b equal to about 0.3, which, corresponds to plane strain condition and then decreases continuously upto

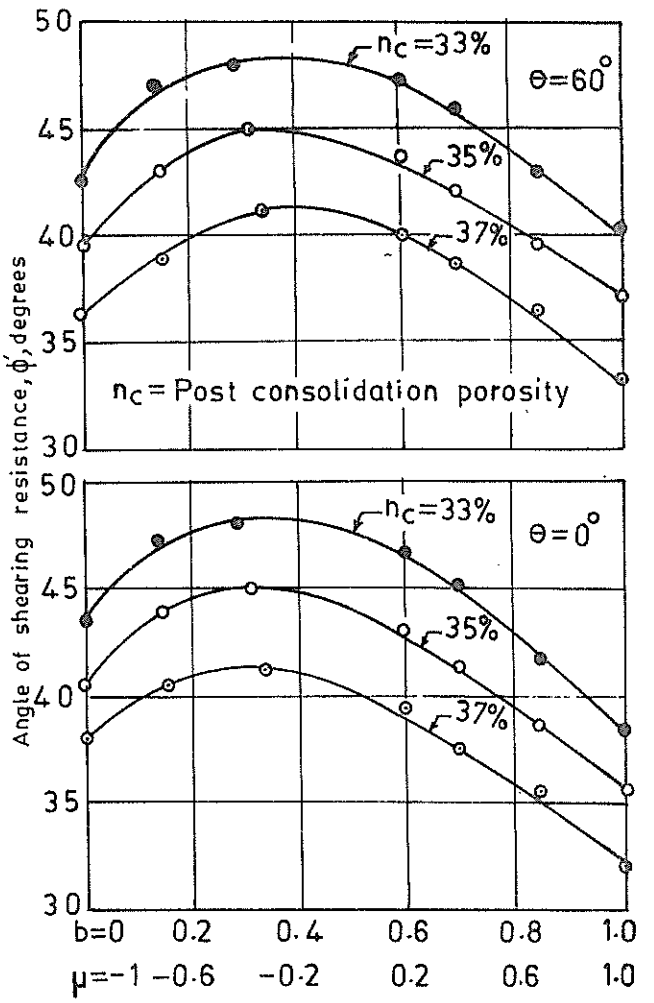

Figure 3 The Angle of Shearing Resistance

b=1 (axisymmetric extension). The curves pertaining to three porosities are nearly parallel.

When $\Theta = 0°$, the increase in the value of ϕ' from axisymmetric compression to plane strain compression is 4.5° in dense and medium dense state and 3.9° in loose state. In axisymmetric extension the values of ϕ' are lower by about 5° than those in axisymmetric compression.

When $\Theta = 60°$ the values of ϕ' in plane strain compression are higher by about 5.5° than those in axisymmetric compression at all the three porosities. The values of ϕ' in axisymmetric extension are lower by 2° to 3° than those in axisymmetric compression.

In axisymmetric compression the angle of shearing resistance is higher when $\Theta = 0°$ than when $\Theta = 60°$ by about 1.1° to 1.7°. This difference decreases with increase in the value of b and vanishes at plane strain condition. In extension the value of ϕ' is lower when $\Theta = 0°$ than when $\Theta = 60°$ by 1° to 2°. This difference which is zero at plane strain condition, increases with increase in the value of b beyond plane strain condition and attains its peak value under axisymmetric extension.

When $\Theta = 0°$ the direction of deposition coincides with the vertical axis of the specimen. The plane of preferred orientation of particles, which is the plane normal to the direction of deposition, is a major principal plane in compression tests where as it is a minor principal plane in extension tests. It may be observed from the above results that when the plane of preferred orientation is normal to the major principal stress (in compression) the material offers maximum resistance, where as it develops lesser resistance when the plane of preferred orientation is normal to the minor principal stress (in extension).

When the value of Θ increases from 60° to 90°, the direction of deposition approaches to the direction of the normal to the vertical axis of the specimen. Under these conditions the plane of preferred orientation is nearly normal to the minor principal stress in compression while it is nearly normal to the major principal stress in extension. Therefore the values of ϕ' are lower in compression and higher in extension than the corresponding values when $\Theta = 0°$.

It may also be concluded that material enjoys maximum freedom of movement under axisymmetric conditions and hence develops maximum strength anisotropy. As the deviation from axisymmetric conditions increases the freedom of the particles is increasingly restricted and hence the strength anisotropy is restricted more and more, culiminating finally in plane strain condition wherein the particles have least freedom for movement and strength anisotropy is almost completely suppressed. However, because of the restricted movement, the particles develop higher resistance and hence shows maximum strength under plane strain conditions.

The angle of deposition, Θ did not show appreciable influence on the pattern of variation of linear and volumetric strains with b. Therefore the results of only one deposition angle $\Theta = 0°$ are presented below.

4.2 Lateral Strain ϵ_{xf}

The lateral strain at failure ϵ_{xf} is nearly zero in plane strain compression. As μ increases numerically the value of ϵ_{xf} increases in compression zone, reaching its maximum value in axisymmetric compression (Fig.4). As we move from plane strain compression towards axisymmetric compression, the value of σ_x' decreases relatively and hence the lateral strain ϵ_{xf} increases with numerical increase in the value of μ. In axisymmetric compression ϵ_{xf} decreases with increase in porosity. In plane strain compression the value of b decreases with decrease in porosity. Therefore the curves in compression cross in the zone of general compression before reaching plane strain condition.

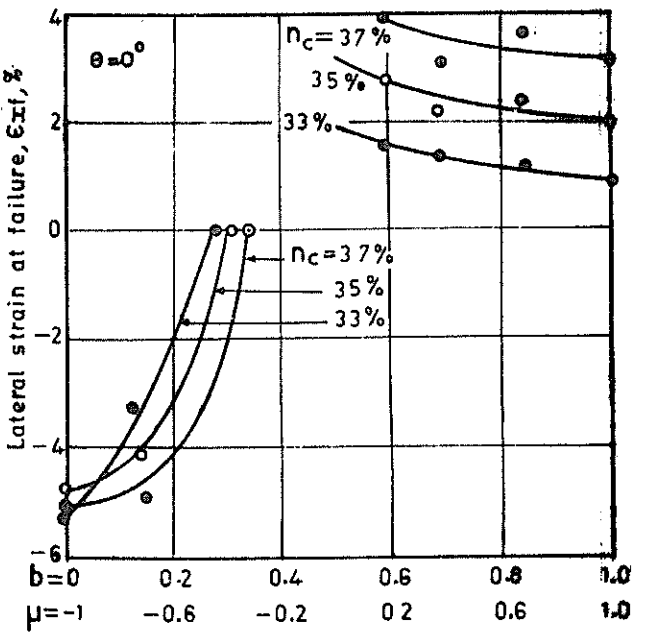

Figure 4 Lateral Strain ϵ_{xf}

In extension, the value of ϵ_{xf} decreases with increase in μ, the value being least in axisymmetric extension. With increase in the value of μ, σ_x' decreases relatively and ϵ_{xf} (which is compressive) also decreases.

4.3 Lateral Strain ϵ_{yf}

Figure-5 shows the variation of lateral strain at failure ϵ_{yf} with b. Both the lateral strains in conjucture with the axial strains have to respond to the volume

changes taking place in the specimen. Therefore, the variation of ϵ_{yf} has to be considered keeping in view the variations in other strains.

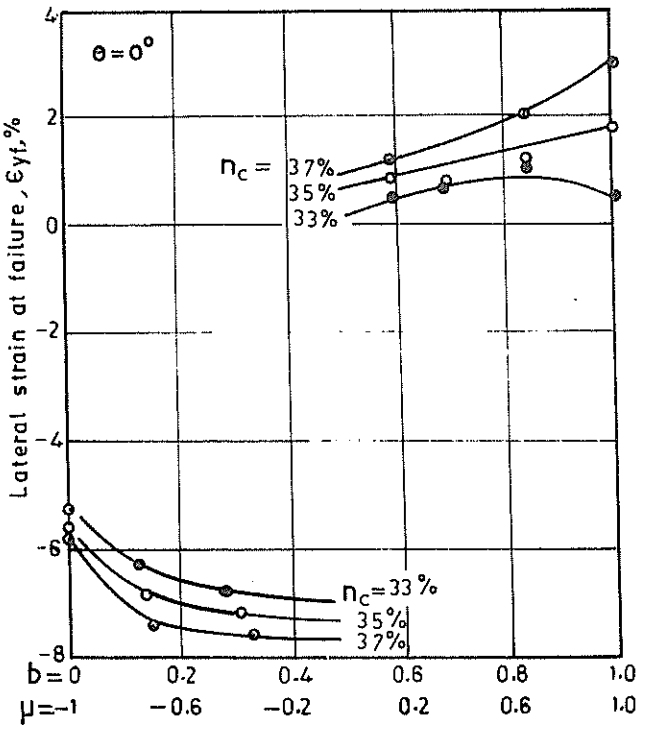

Figure 5 Lateral Strain ϵ_{yf}

It was observed earlier that, in compression, as b increases ϵ_{xf} decreases tending to attain a zero value in plane strain condition. The axial strain is always compressive. Therefore most part of the dilation is taken care of by ϵ_{yf}. Therefore, as b increases, ϵ_{yf} increases.

In extension as b decreases, ϵ_{yf} decreases approaching a zero value, that is a plane strain condition in extension. It will be interesting to compare the results of plane strains in compression and extension tests. As can be seen from Figures 4 and 5 that there exists a discontinuity in the relationship of linear strains Vs b between compression and extension test results. If compression and extension tests are conducted upto plane strain condition and beyond, the relationship of linear strains Vs b will be confirmed in the discontinuous region.

4.4 Axial Strains ϵ_{zf}

The axial strain at failure is maximum under axisymmetric conditions both in extension and compression (Figure 6). With increasing deviation from axisymmetric conditions the axial strain at failure decreases. It may be concluded from this that the brittle nature of failure increases with increasing deviation from axisymmetric conditions.

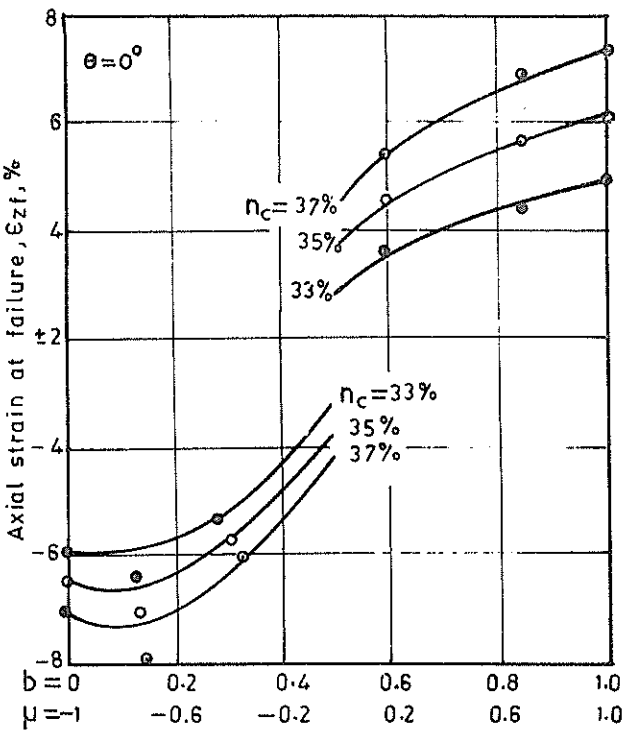

Figure 6 Axial Strain ϵ_{zf}

4.5 Volumetric Strain ϵ_{vf}

The material dilates at all porosities (Fig. 7). The dilation is maximum under axisymmetric conditions. With increasing deviation from axisymmetric conditions the volumetric strain at failure decreases. As has been mentioned earlier, the particles have maximum freedom of movement under axisymmetric conditions and hence produce higher dilation. As the deviation from this state increases, the freedom of the particles is restricted resulting in lesser dilation.

5 CONCLUSIONS

The angle of shearing resistance increases with increase in the value of b upto plane strain condition and then decreases continuously upto axisymmetric extension. However, the shape of the curve is not unique for all materials and under all type of test conditions. The structural anisotropy of the material effects the shape of the curve. The material exhibits maximum strength anisotropy under axisymmetric conditions and as the deviation from the axisymmetric conditions increases, the anisotropy decreases, ultimately vanishing at plane strain condition. With increase in the value of b, ϵ_{xf} decreases in compression culminating in plane strain condition when $\epsilon_x \approx 0$. In extension also ϵ_{xf} decreases with increase in b. ϵ_{yf} increases both in compression and

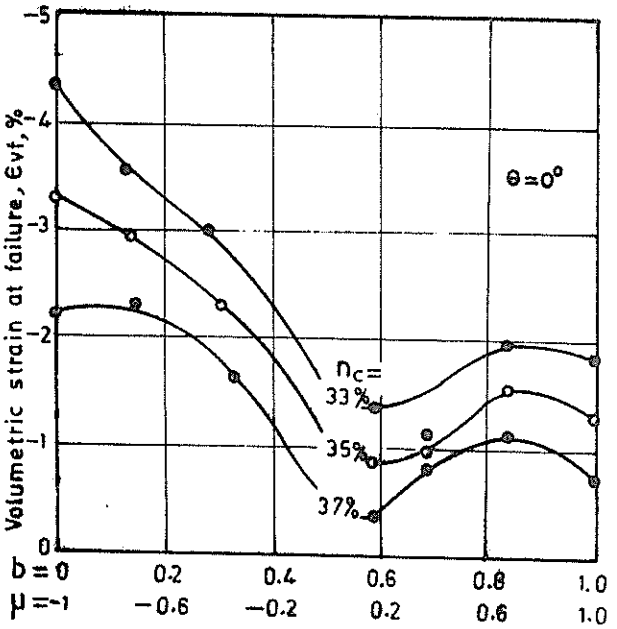

Figure 7 Volumetric Strain ϵ_{vf}

extension with increase in the value of b. The axial and volumetric strains are maximum under axisymmetric conditions and with increasing deviation from axisymmetric conditions both of them decrease.

If General Compression and extension tests are carried out to reach plane strain conditions and beyond, the results of compression and extension in the overlapping region of b could be compared.

6 REFERENCES

GREEN, G.E. (1971). Strength and deformation of sand measured in an independent stress control cell. Proc. Roscoe Memorial Symposium, Cambridge, pp 285-323.

HABIB, P. (1953). Influence of the variation of average principal stress upon the shearing strength of soils. Proc. 3rd Int. Conf. SMFE, Zurich, Vol. I, pp 131-136.

LOMIZE, G.M., KRYZHANOVSKII, A.L., VORONTSOV E.I. & GOLDIN, A.L. (1969). Study on deformation and strength of soils under three-dimensional state of stress. Proc. 7th Int. Conf. SMFE, Vol. I, pp 221-224.

MARACHI, N., CHAN, C.K., SEED, H.B. & DUNCAN, J.M. (1969). Strength and deformation characteristics of rockfill materials. Report TE-69-5 to State of Calif. Dept. of Water Resources, Univ. of Calif. Berkley.

PEARCE, J.A. (1970). The behaviour of soft clay in a new true triaxial apparatus, Ph.D. Thesis, Cambridge University.

RAMAMURTHY, T. (1970). A Universal triaxial apparatus. JSMFE India, Vol. 9, No. 3 pp 251-269.

RAWAT, P.C. (1976). Shear Behaviour of Cohesionless materials under generalised conditions of stress and strain. Ph.D. Thesis, I.I.T. Delhi.

RAWAT, P.C. & RAMAMURTHY, T. (1978). Shear Behaviour of Sand under Generalized conditions of Stress and Strain. Ind. Geo. Jnl. Vol. 8, No. 4, pp 235-269.

READES, D.W. (1972). Stress-Strain characteristics of a sand under three dimensional loading./Ph.D. Thesis (2 volumes) London University.

SHANKARIAH, B. (1977). Behaviour of anisotropic granular media under general stress system. Ph.D. Thesis, Indian Institute of Technology, Delhi.

Effect of Stress-Path on the Stress-Strain-Volume Change Relationships of a River Sand

A. VARADARAJAN
Assistant Professor, Civil Engineering Department, Indian Institute of Technology, Delhi
S. S. MISHRA
Research Scholar, Civil Engineering Department, Indian Institute of Technology, Delhi
G. L. WADHWA
Formerly Graduate Student, Civil Engineering Department, Indian Institute of Technology, Delhi

SUMMARY The effect of stress-path on the stress-strain-volume change relationships of a river snad is presented. It is shown that these relationships are very much a function of stress-paths. Modulus values are evaluated for different stress-paths and relationships between stress-paths and modulus values are established. A procedure for using these relationships in the analyses of field problems using finite element method is indicated.

1 INTRODUCTION

The current integrated analyses of movements and failure in soil masses using finite element method incorporate in them stress-strain volume change relationships of soil. The results obtained from such analyses are as realistic as the soil parameters used in the analyses. The stress-strain behaviour of soils is a complex function of many factors such as soil type, structure, confining pressure, stress-history, drainage condition, stress-path etc. (Lambe and Whitman, 1969; Duncan and Chang, 1970; Yudhbir and Varadarajan, 1975; Lade and Duncan, 1975, 1976). Considerable research work is now directed towards developing analytical models for describing the soil behaviour (Desai, 1977). Research work is in progress at IIT Delhi in developing an analytical model for granular soils. This paper deals with one of the major factors influencing the stress-strain volume change behaviour of soils, viz. stress-path. Experimental results for a local river sand are presented and discussed. Evaluation of parameters based on theory of elasticity for different stress paths is indicated. A procedure for using these parameters in the analyses of field problems is also dealt with in the paper.

2 TESTING PROGRAMME

Two test series were carried out using standard triaxial testing equipment. In the first series the samples were consolidated isotropically and sheared to failure using standard triaxial compresion tests. Three consolidation stresses σ_c, 1.05, 2.11 and 3.16 kg/cm^2 were used.

In the second series, the samples were anisotropically consolidated with a stress ratio K=0.42 to approximate the insitu state of stress condition. The samples were then sheared using six stress-paths (Figure 1), (i) vertical stress, σ_1 constant and lateral stress, σ_3 increasing (ii) σ_1 and σ_3 increasing such that $\sigma_3/\sigma_1 = 0.42$ (iii) σ_3 constant and σ_1 increasing (iv) σ_3 decreasing σ_1 constant (v) σ_1 and σ_3 decreasing such that $\sigma_3/\sigma_1 = 0.42$ and (vi) σ_3 constant and σ_1 decreasing. The stress-levels $p_c = (\sigma_1 + \sigma_3)/2$, 1.97, 3.94 and 5.91 kg/cm^2 were adopted.

2.1 Soil Used

Jamuna river sand was used for experimental investigations. River Jamuna is located near Delhi and is a major tributory to the famous river Ganga in the northern region of Indian subcontinent. The sand was of uniform size with ninety per cent of the soil having grain sizes between 0.1 mm and 0.4 mm. The sand contained mica flakes and was grey in colour. The specific gravity of sand material was 2.66. A single batch of sand was used for all the tests.

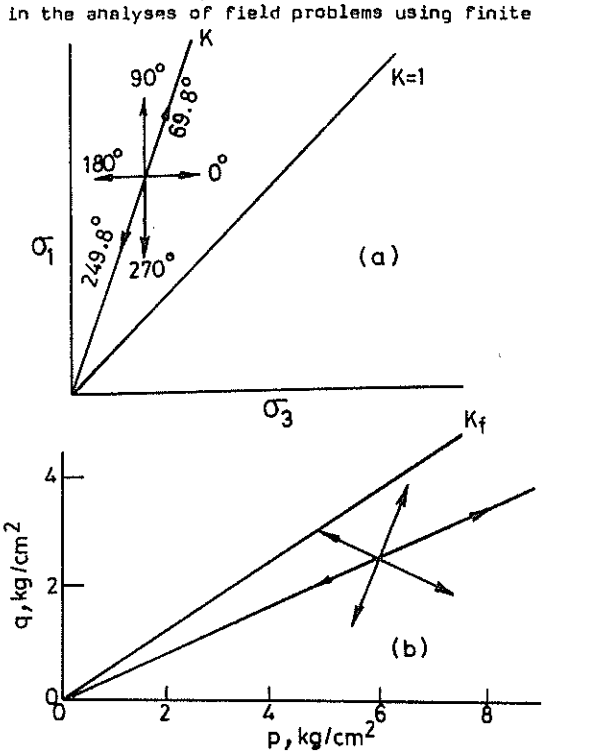

Figure 1 Stress-paths used for the tests in σ_3-σ_1 and p-q plots

2.2 Experimental Procedure

Standard triaxial compression testing equipment was used for all the tests. 3.81 cm diameter and 7.62cm long cylindrical samples were used. The samples were prepared under saturated condition (Bishop and Henkel, 1957). A uniform procedure of tamping the mould was used to achieve the same density of the samples. Cell pressure was applied by the self compensating mercury pot system and the vertical loading was applied through the loading frame-proving ring system. For tests with σ_3 constant, strain controlled loading was applied. For other stress-

path tests cell pressure and the vertical loading were applied by manual control in small increments. The loading to be applied was estimated at every increment after using appropriate area correction for the sample. For speedy calculations during experiment a standard programme was used with the aid of a 200 step programmable calculator. Vertical displacement and volume change readings were noted after steady condition was reached for each increment of loading. Smaller increments of loading were used as failure was reached. The vertical displacements and volume changes were measured to the accuracy of 0.000254 cm and 0.05 cc respectively.

3 EXPERIMENTAL RESULTS

3.1 Consolidation and Rebound

Figure 2 shows consolidation and rebound curves for isotropic and anisotropic stress conditions. Both the curves show similar behaviour. Very small amount of particle crushing was observed at higher pressure levels and this appears to have also contributed for the curvature of loading curves at those pressure levels. The rebound curves for the two stress conditions show that the irrecoverable volumetric strain is more in the case of isotropic unloading condition.

3.2 Stress-Strain-Volume Change Relationships

3.2.1 Isotropically consolidated samples

Figure 3 shows stress-strain-volume-change relationship of σ_3 constant stress-path test. All the tests indicate increase in vertical failure strain with higher consolidation pressures. Volume expansion is noted for all the tests near failure state.

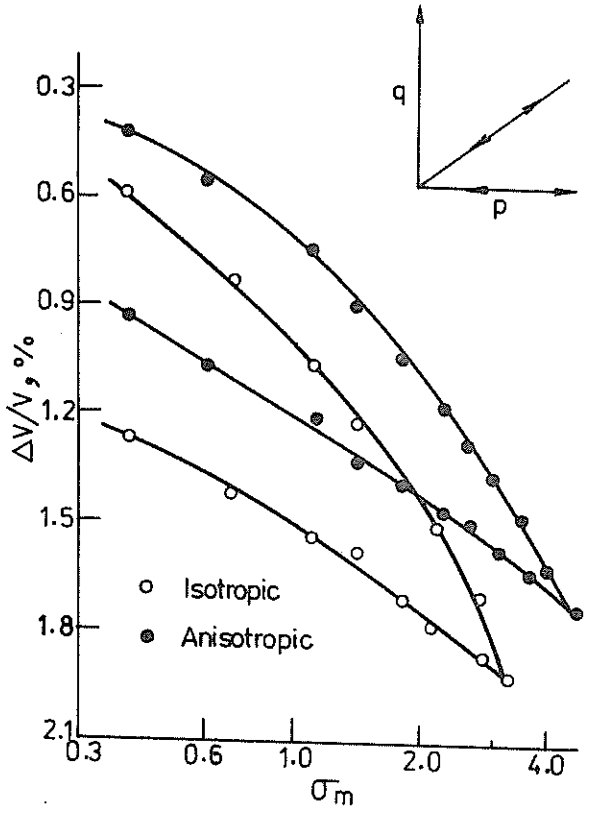

Figure 2 Isotropic and anisotropic loading and rebound curves

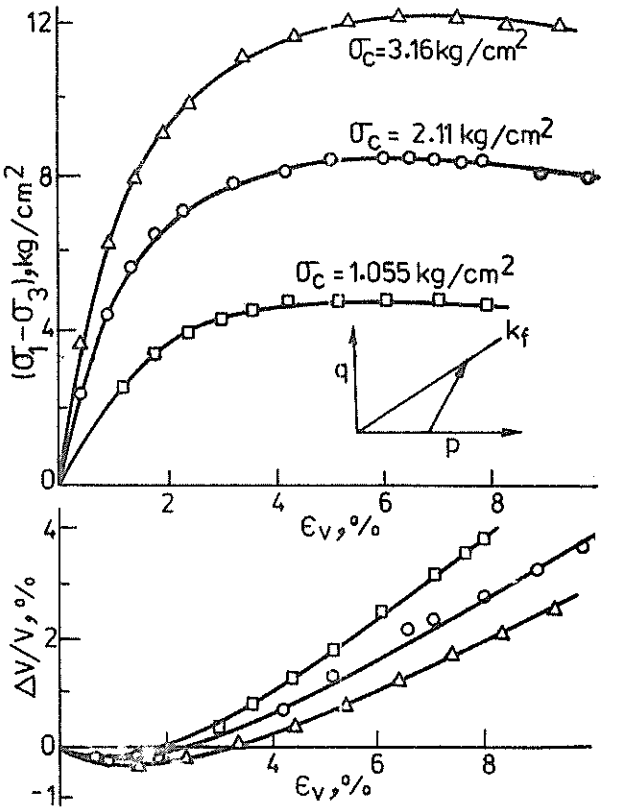

Figure 3 Stress-strain-volume change relationships of standard triaxial compression test (σ_3 constant).

3.2.2 Anisotropically consolidated samples

Figure 1a shows the stress-paths used in $\sigma_3 - \sigma_1$ stress-space. The stress-paths are designated as ASP0, ASP69.8, ASP90, ASP180, ASP249.8 and ASP270, the numbers indicating the angles with respect to horizontal in the counter clockwise direction. ASP indicates anisotropically consolidated samples.

In Figures 4 and 5 are shown the stress-strain volume-change relationships for ASP90 and ASP180 tests. These tests were carried out till failure was reached. In both the cases higher vertical failure strains are observed for higher pre-shear stress level

$$p_c \left(= \frac{\sigma_1 + \sigma_3}{2}\right)$$

Volume compression is observed only in the initial range of loading in ASP90 test and in the higher loading range volume expansion is noted whereas in ASP180 test volume expansion is noted from the very beginning of the test. Figures 6 and 7 show stress strain-volume-change relationships for ASP69.8 and ASP249.8 tests. These are loading and unloading tests along the K-line. The relationships are almost linear. As expected ASP69.8 shows compres-

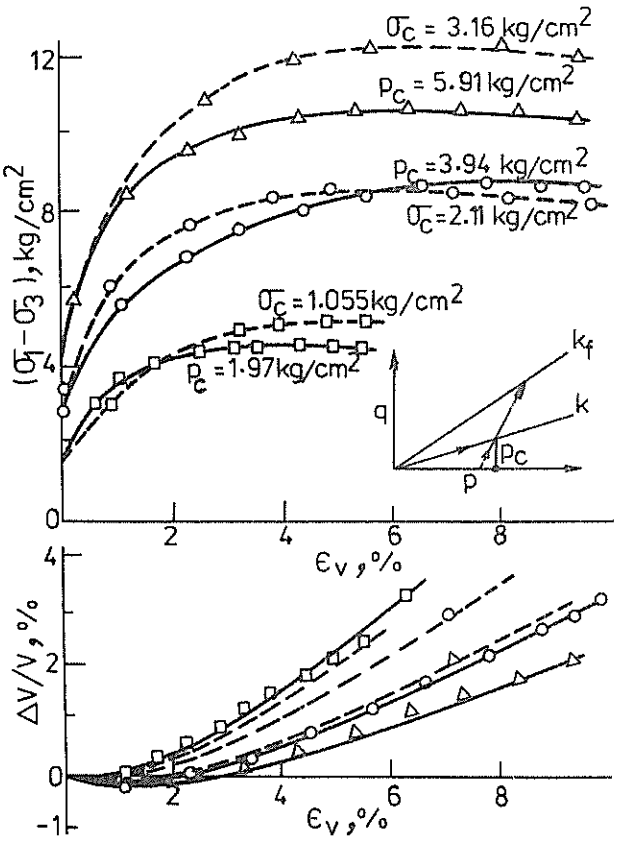

Figure 4 Stress-strain-volume change relationships of ASP90 and ISP90 tests

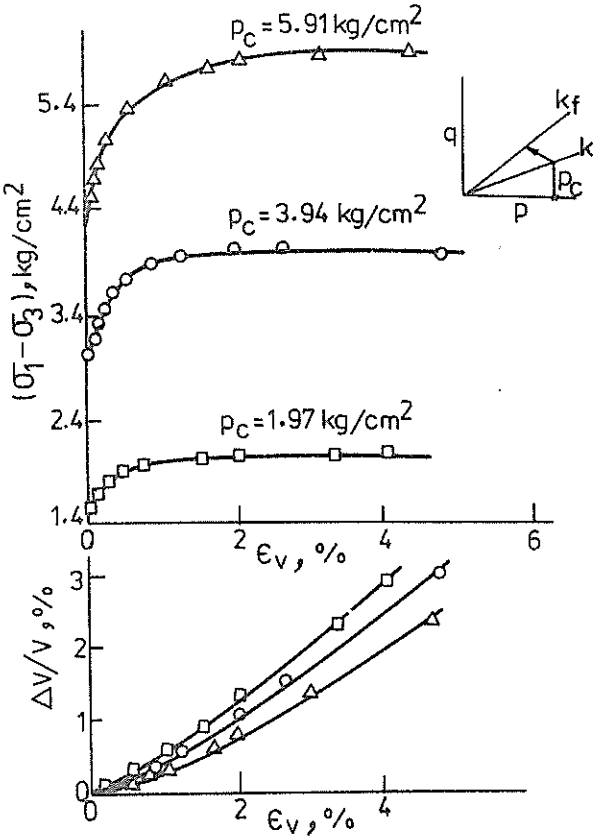

Figure 5 Stress-strain-volume change relationships of ASP180 tests

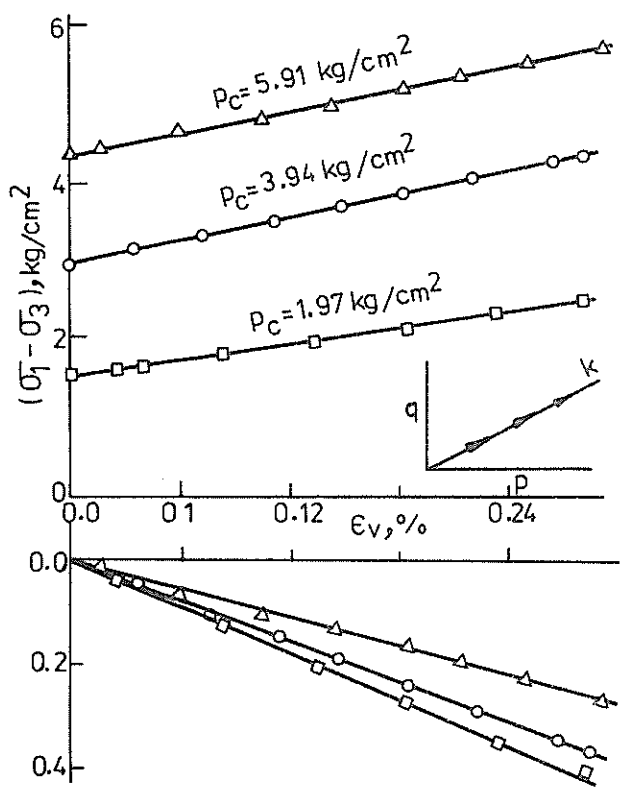

Figure 6 Stress-strain-volume change relationships of ASP69.8 tests

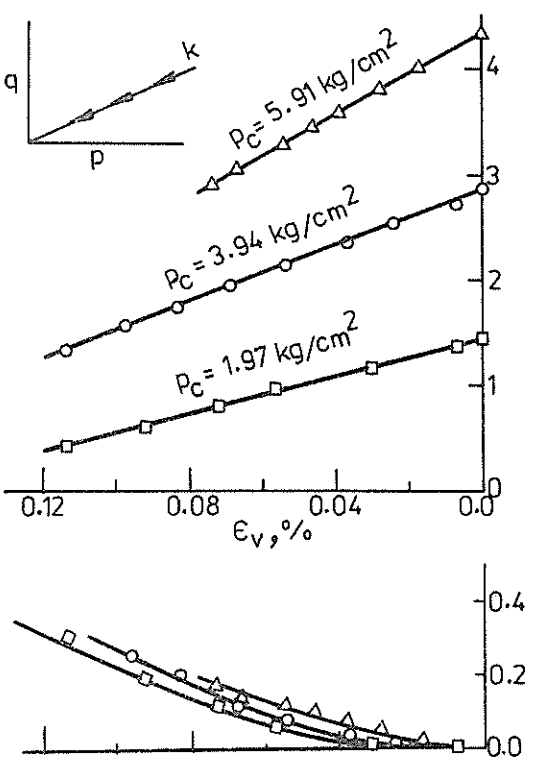

Figure 7 Stress-strain-volume change relationships of ASP249.8 tests

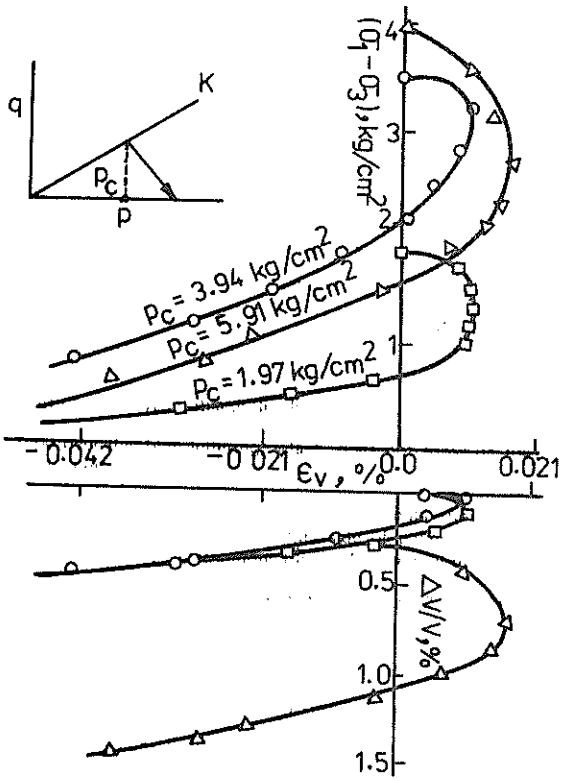

Figure 8 Stress-Strain-Volume change relationships of ASP0 tests

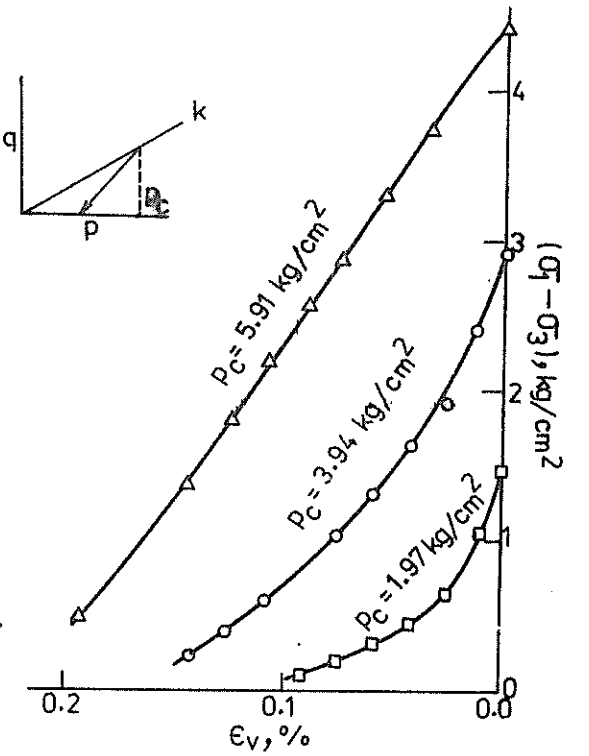

Figure 9 Stress-Strain relationships of ASP270 tests.

sion and ASP249.8 indicates expansion. Stress-strain-volume change relationships for ASP0 are shown in Figure 8. In these tests shear stress was decreased up to zero value only (due to limitations of standard triaxial cell). In the initial stages of loading small increase in vertical strains and for subsequent loading reduction in vertical strains are observed. During all stages of loading tests show volumetric compression.

Figure 9 shows stress-strain relationships for ASP 270. Negative vertical strain is indicated all through the test. For all the stress ranges negligible volume expansion is observed (not shown in Figure).

A comparative stress-strain-volume change relationships for all the stress-paths are presented in Figure 10 at p_c = 3.94 kg/cm². For ASP0, ASP270 and ASP249.8 tests, the shear stress is decreased and for ASP180, ASP90 and ASP69.8 the shear stress is increased. Whereas for the stress-paths ASP0, ASP270 and ASP249.8 vertical strains are negative, for the stress-paths ASP180, ASP270 the vertical strains are positive.

The ASP0 and ASP69.8 volume contraction is noted whereas for ASP80 and ASP249.8 volume expansion is observed. For ASP90 volume contraction is noted at initial loading range and volume expansion is indicated at higher loading range. Negligible volume change is observed for ASP270.

In Figure 4 are also shown the portions of stress-strain-volume change relationships of standard triaxial compression tests in addition to those of anisotropically consolidated samples. Though the stress conditions before shearing (with σ_3 constant) are same for both cases the relationships are

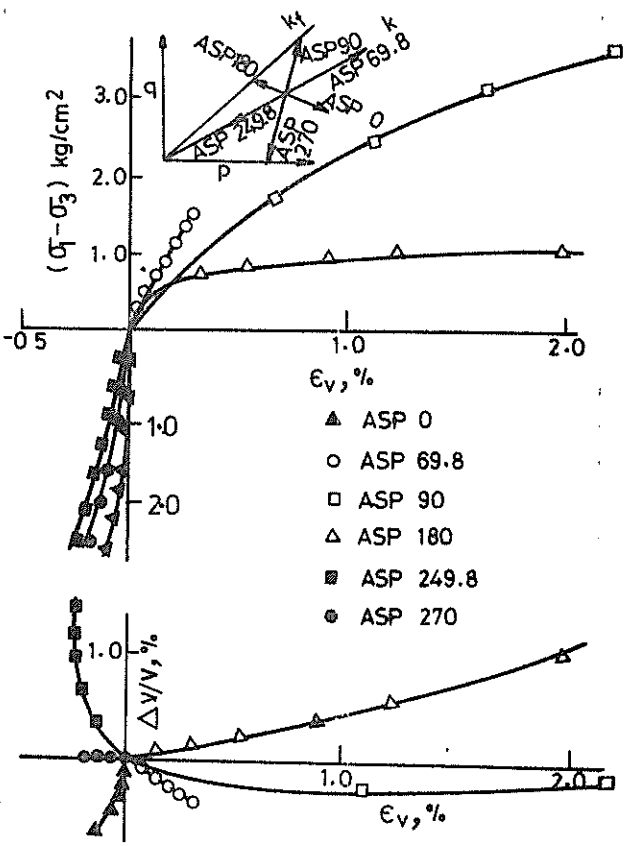

Figure 10 Comparison of stress-strain volume change relationships of different stress-path tests

markedly different.

4 STRENGTH ENVELOPE

The Mohr-Coulomb envelope obtained from the test results show slight curvature for high stress levels. The angle of shearing resistance at lower stress range is 42^0 and it is 39^0 at higher stress range.

5 ELASTIC STRESS-STRAIN PARAMETERS

To study the effect stress-path on the stress-strain-volume change relationships the Young's moduli, E and Poisson's ratios, ν, were calculated using the stress-probe level (n = 0.2) following Lewin and Burland(1970) as

$$\sigma_n = \sqrt{\sigma_1^2 + \sigma_2^2 + \sigma_3^2} \qquad (1)$$

$$\Delta\sigma_n = 0.2\ \sigma_n = \sqrt{\Delta\sigma_1^2 + \Delta\sigma_2^2 + \Delta\sigma_3^2} \qquad (2)$$

$\Delta\sigma_1$ and $\Delta\sigma_3$ values were calculated for this stress-level and corresponding values of strains $\Delta\epsilon_1$ and $\Delta\epsilon_3$ values for each stress-path were obtained from the experimental results and these E and ν values were obtained using theory of elasticity (Lambe and Whitman, 1969) as follows

$$E = \frac{(\Delta\sigma_1 + 2\Delta\sigma_3)(\Delta\sigma_1 - \Delta\sigma_3)}{\Delta\epsilon_3\,(\Delta\epsilon_1 - 2\Delta\epsilon_3) + \Delta\sigma_1\,\Delta\epsilon_1} \qquad (3)$$

and

$$\nu = \frac{\Delta\sigma_3\,\Delta\epsilon_1 - \Delta\epsilon_3\,\Delta\sigma_1}{\Delta\sigma_3\,(\Delta\epsilon_1 - 2\Delta\epsilon_3) + \Delta\sigma_1\,\Delta\epsilon_1} \qquad (4)$$

where,

$\Delta\sigma_1$ and $\Delta\sigma_3$ = change in σ_1 and σ_3

ϵ_1 and ϵ_3 = corresponding change in vertical and lateral strains.

The effect of consolidation pressure on E values was expressed using Janbu's (1963) relationships

$$E_i = K\,p_a\,\left(\frac{\sigma_m}{p_a}\right)^n \qquad (5)$$

where,

k = modulus number

n = exponent determining rate of variation of E with σ_m

p_a = atmospheric pressure expressed in the same unit as E and σ_m

$$\sigma_m = \frac{\sigma_1 + 2\sigma_3}{3}$$

E_i = initial tangent modulus

Within the stress ranges considered, it was observed that K, n vs σ_m relationships were bilinear.

K and n relationships for the two stress ranges are presented in Table 1. It may be observed that the K value which is also equal to E value at σ_m=1 kg/cm^2 is very much a function of stress path. Between the minimum and maximum value of K the ratio is in the order of about 10. The Poisson's ratio shows a wide variation for different stress-paths (not shown in the Table). Thus, the E and values are a function of stress level and stress-path. In analysing field problems it is, therefore,necessary to use appropriate modulus values.

Table 1

Stress-path	m	1.54-3.08 kg/cm^2		3.08-4.62 kg/cm^2	
		K	n	K	n
ASP0		681	0.987	1554	-0.315
ASP69.8		542	0.64	1167	-0.61
ASP90		292	0	87.2	1.62
ASP180		84	0.92	154.3	-0.21
ASP249.8		1156	0.65	2677	-0.33
ASP270		2023	1.05	8437	-1.21

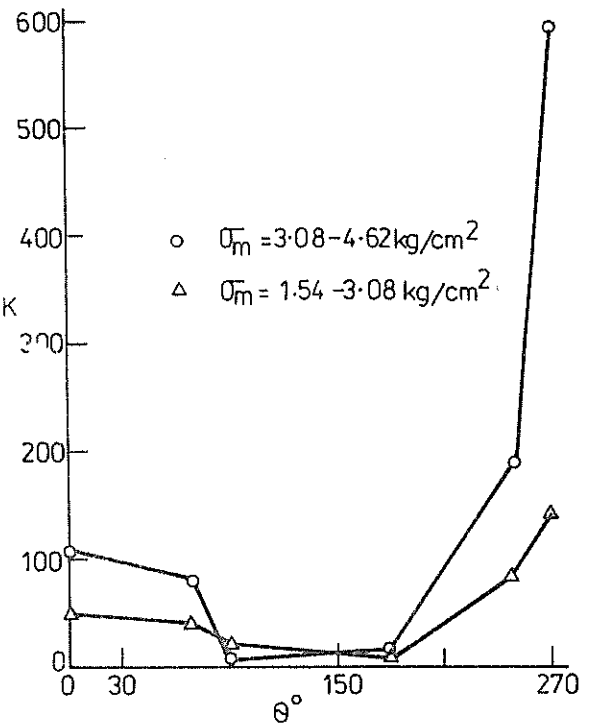

Figure 11 K - θ relationship

6 USE OF ELASTIC PARAMETERS

K and n vs stress-paths expressed quantitatively as θ in $\sigma_1 - \sigma_3$ stress space are shown in Figures 11 and 12. From these figures, equations can be developed between K and n and θ values.Values of K and n can be conveniently obtained from the figures or equations.

For realistic analysis of field problems with finite element method at higher factors of safety, the modulus values evaluated by this procedure may be advantageously used. To start with the analyses of any field problem may be carried out using K and n values of a stress-path which is representative for the field problem (for example, for the footing problem σ_3 constant stress path is the representative one). The stress paths for each element may be evaluated in terms of θ from the stresses

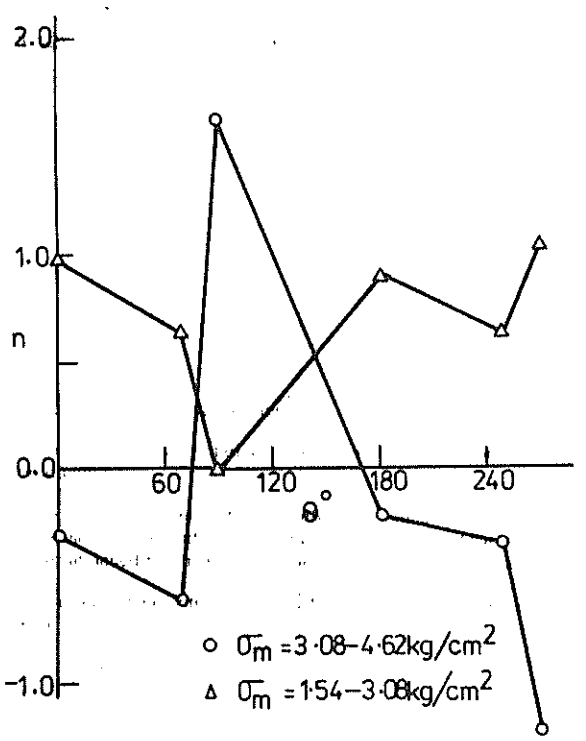

Figure 12 n – θ relationship

obtained. Knowing the θ values, the analysis may be repeated using appropriate values of K and n in each element. Two or three such iterations may be necessary before the modulus values used are consistent with the stress-paths. Either an average value of Poisson's ratio or appropriate values of Poisson's ratio obtained from similar relationships as for E may be used.

7 CONCLUSIONS

On the basis of the limited experimental investigations carried out on Jamuna sand, it is observed that the stress-strain-volume change relations are very much a function of stress-path. Stress-paths can be quantified and the relationships so established. This relationships may be used for the realistic analyses of field problems using finite element method.

8 REFERENCES

BISHOP, A.W. and HANKEL, D.J. (1957). The measurement of soil properties in triaxial test. Edward Arnold (Publishers) Ltd., London.

DESAI, C.S.(1977). Constitutive law for geologic media, In C.S. Desai and J.T. Christian (ed.), Numerical Methods in Geotechnical Engineering, McGraw-Hill Book Company, New York.

DUNCAN, J.M. and CHANG, C.Y.(197). Nonlinear analysis of Stresses and strain in soil, Jnl.of soil mechanics and foundation division, ASCE,Vol.96, pp.1629-1653.

JANBU, N.(1963). Soil compressibility as determined by Oedometer and triaxial tests, European Conference on soil mechanics and foundation engineering, Germany, Vol.1, pp.19-25).

LADE, P.V. and DUNCAN, J.M.(1975). Elastoplastic stress-strain theory for cohesionless soil. Jnl. of the geotech. engng. divn., ASCE, 101, pp.1037-1054.

LADE, P.V. and DUNCAN, J.M.(1976). Stress-path dependent behaviour of cohesionless soil, Jnl. of the geotech. engng. divn., ASCE, 102,pp.51-68.

LAMBE, T.W. and WHITMAN, R.V.(1969). Soil mechanics, John Wiley and Sons, Inc., New York.

LEWIN, P.I. and BURLAND, J.B.(1970). Stress probe experiments on saturated normally consolidated clay, Geotechnique, Vol.20, pp.38-56.

YUDHBIR and VARADARAJAN, A.(1975). Stress-path dependent of deformation moduli of clay, Jnl. of the geotechnical engng. divn., Proc. ASCE,Vol.101, pp.315-327.

The Nature of Anisotropy in Soft Clays

L. D. WESLEY
Tonkin and Taylor, Consulting Engineers, Auckland

1 INTRODUCTION

This paper presents the results of a study of the undrained strength anisotropy of a soft clay and relates the results to measurements of such anisotropy in other similar clays. The clay involved is a soft sedimentary clay which occurs along the north coast of the Thames estuary in the county of Essex. The clay is believed to have been deposited over the last 10,000 years during the gradual rise of the sea level from its low levels during the last ice age. Properties of the clay are as follows:

Natural Water Content	51%
Plastic Limit	25
Liquid Limit	54
Clay Fraction	30
Sensitivity	6
Undrained Shear Strength (approximately)	15 kPa

The tests presented in this paper form a small part of a much wider study described fully by Wesley (1975). The tests were performed as part of an investigation of the properties of these coastal clays carried out to assist in the design of higher stopbanks being planned as part of the London flood protection scheme.

The samples used in the study were taken from a depth of just over 3 m in a wide test pit, using large diameter steel cylinders. These cylinders were 250 mm (10 in) in diameter and 300 mm (12 in) high. The cylinders were pushed into the soil using a dead weight pressing on a plate resting on the upper rim of the cylinder. When full the cylinders were dug out by hand. It is believed that the degree of disturbance using this procedure was considerably less than that which result from normal sampling with a relatively small diameter tube in a borehole.

2 MEASUREMENTS OF SOIL SKELETON STIFFNESS

As a starting point to this study of the anisotropy of soft clays we will look at the results of some measurements of soil skeleton stiffness made in drained tests of various types. The simplest such test is the conventional oedometer test and it is easy to perform these tests on both vertical (i.e. compression axis in the vertical direction) and horizontal samples. The results of such tests on the Mucking clay are given in Fig.1 (a). It is seen that in the initial stages of loading the soil is substantially more compressible in the horizontal direction than in the vertical direction. At higher stress levels the curves become identical. Also shown in Fig.1 (b) are the strains measured in an isotropic (all round) compression test. The initial stress in this test was the pore water tension in the sample. The strain in the horizontal direction is initially much greater than in the vertical direction, but at higher stress levels the strains become the same (and the curves become parallel).

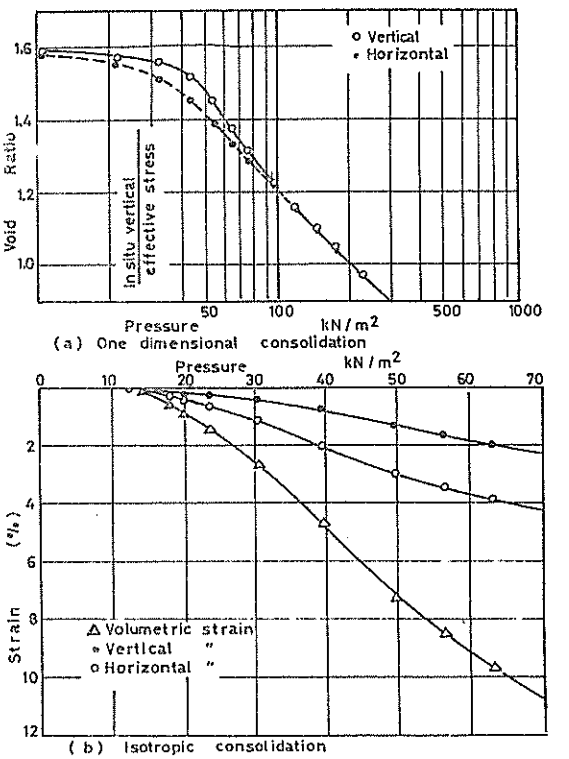

Figure 1 Skeleton Stiffness in the Horizontal and Vertical Directions

In Fig.2 the initial portions of stress strain curves from drained triaxial tests on vertical and horizontal samples are shown. These curves also show that the soil skeleton is less stiff in the horizontal direction than in the vertical direction. It is of interest to note that the volume change is almost identical regardless of the direction of stress application.

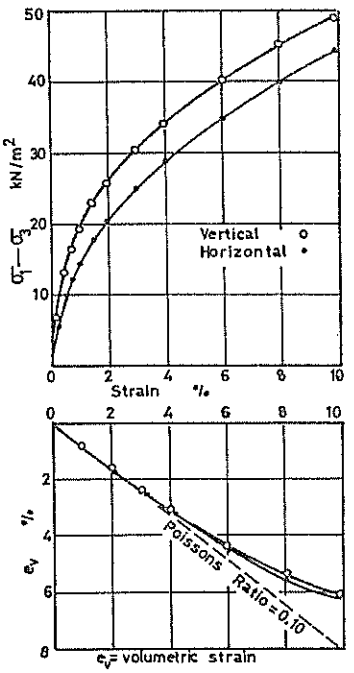

Figure 2 Drained Triaxial Tests on Vertical and Horizontal Samples

A careful analysis of the above test results suggest that the soil skeleton stiffness in the horizontal direction is about half that in the vertical direction. It is not known how representative the above results are of soft sedimentary clays as data from such clays is not available.

3 INFLUENCE OF SOIL SKELETON STIFFNESS ON BEHAVIOUR IN UNDRAINED LOADING

The behaviour of the soil in undrained loading will clearly be influenced by the differences in stiffness of the soil skeleton. To gain some idea of what this influence is likely to be we can make use of elastic theory and the assumption that the soil is transversely isotropic. The simplest means of evaluating the influence which anisotropy may have on undrained strength is by examining its influence on pore pressure response to various types of loading. If the assumption is made that the Mohr-Coulomb failure envelope is isotropic then differing pore pressure responses will lead to differences in undrained strength. We will therefore examine the value of the pore pressure parameter A ($A = \Delta u/\Delta\sigma_1 - \Delta\sigma_3$) for different loading conditions.

Using the same nomenclature as Bishop and Hight (1977) for the elastic parameters we can obtain the following values of A for the following loading conditions:

Loading Condition	A
Triaxial Vertical	$\dfrac{E_x/E_y - 2\mu_{xy}}{E_x/E_y - 4\mu_{xy} - 2\mu_{xx} + 2}$
Triaxial Horizontal	$\dfrac{1 - \mu_{xy} - \mu_{xx}}{E_x/E_y - 4\mu_{xy} - 2\mu_{xx} + 2}$
Plain Strain Vertical	$\dfrac{E_x/E_y - \mu_{xy} - \mu_{xy}^2 - \mu_{xx}\,\mu_{xy}}{E_x/E_y + 1 - 2\mu_{xy} - 2\mu_{xy}\,\mu_{xx} - \mu_{xx}^2 - \mu_{xy}^2}$
Plain Strain Horizontal	$\dfrac{1 - \mu_{xy} - \mu_{xy}\;\mu_{xx} - \mu_{xx}^2}{E_x/E_y + 1 - 2\mu_{xy} - 2\mu_{xy}\,\mu_{xx} - \mu_{xx}^2 - \mu_{xy}^2}$

The term "triaxial vertical" refers to a triaxial compression test on a sample prepared with its axis in the vertical direction. See Fig.3

Tests carried out on the Mucking clay led to the following values for the elastic parameters.

$$\frac{Ex}{Ey} = 0.5 \quad , \quad \mu xy = 0.05 \quad , \quad \mu xx = 0.15$$

and inserting these values in the above expressions leads the following values of A.

Loading Condition	Pore Pressure Parameter A
Triaxial Vertical	0.20
Triaxial Horizontal	0.40
Plane Strain Vertical	0.33
Plane Strain Horizontal	0.66

These values show that higher pore pressures are to to expected from horizontal loading than from vertical loading, and that plane strain loading will result in higher pore pressures than triaxial loading (as with the isotropic case). If we assume that the Mohr-Coulomb failure envelope for the material is defined by $c' = o$ and $\phi = 30^0$, and that the initial state of stress is the same, then the above A values imply a strength for horizontal triaxial loading about 73% of that for vertical triaxial loading, and a similar ratio for the two plane strain loading conditions. The plane strain strengths would be expected to be about 80% of the triaxial strengths respectively.

The above indictation is intended as a guide only to expected behaviour. It is widely recognised that soils do not behave elastically although it is perhaps not unreasonable to expect them to approximate to elastic behaviour at small strains beginning from in situ stress levels.

4 UNDRAINED TRIAXIAL AND PLANE STRAIN TESTS

We will now look at the results of undrained tests to see whether these are in agreement with expectations from the above analysis. These tests include triaxial and plane strain tests on samples prepared at varying inclinations. The full range of test types is indicated in Fig.3. Samples trimmed with their axis vertical, horizontal, and inclined at 45^0 were tested in both triaxial and plane strain compression. In addition a fourth type of plane strain sample was tested; this was a sample trimmed so that the plane strain axis was the vertical axis in situ.

It should be noted that in the plane strain tests the planes on which failure can occur are much more restricted than in the triaxial tests. For example, in a triaxial test on a horizontal sample failure could occur on planes vertical in situ, or on planes which in situ dip at approximately 30^0, or on any intermediate planes. In plane strain tests, however, failure could only occur on planes dipping at approximately 30^0; failure on planes vertical in situ, is not possible. This point is of some importance when attempts are made to relate

compressive strengths to strengths on particular planes. Each test was carried out several times and the results presented are averaged from the several results. The tests were carried out in a triaxial apparatus or plane strain apparatus and a cell pressure equal to the overburden pressure applied in each case.

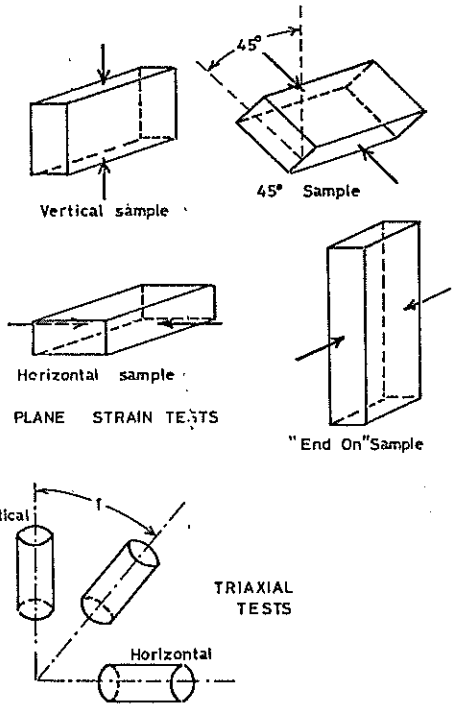

Figure 3 Types of Undrained Tests

The results of these tests are shown in Figs.4 and 5 in the form of stress strain curves. The most significant features of the results are the following:

(a) These is a steady decrease in strength as the angle of inclination changes from vertical to horizontal

(b) The curves from the vertical samples show a much sharper peak than those from the horizontal samples

(c) The initial slope of the curves is reasonably similar in all tests

Similar triaxial and plane strain tests were carried out on a range of samples taken from different depths,with similar results to those in Figs 4 and 5, except for the strength difference between triaxial and plane strain tests. The data in Figs. 4 and 5 suggests that the strength in plane strain tests was significantly lower than in triaxial tests. However, taken as a whole, the test series indicated that the strength in plane strain was only marginally lower than in triaxial compression.

In Fig.6 the data is summarised in the form of a polar diagram. The ratio of the strength in horizontal compression to that in vertical compression varied between 0.64 and 0.78.

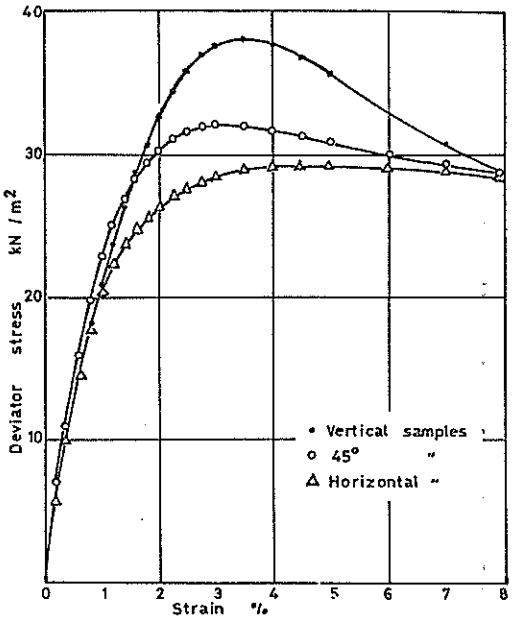

Figure 4 Undrained Triaxial Tests

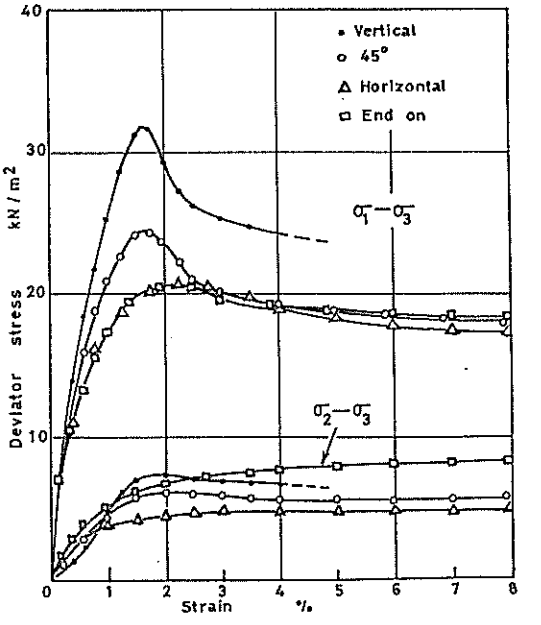

Figure 5 Undrained Plane Strain Tests

These undrained test results are similar to those obtained by Lo (1955) from tests on a similar clay. They are also in agreement with the predictions made earlier in this paper from considerations of the anisotropy of the soil skeleton stiffness. Of particular significance are the results from the plane strain tests on horizontal samples and "end on" samples. Despite the fact that failure is forced to take place on entirely different planes in these two tests, the strength obtained is the same. These suggest strongly that the strength is not related to the orientation of the failure planes, but to the direction of the stress application since the direction of stress application in these two tests is the same.

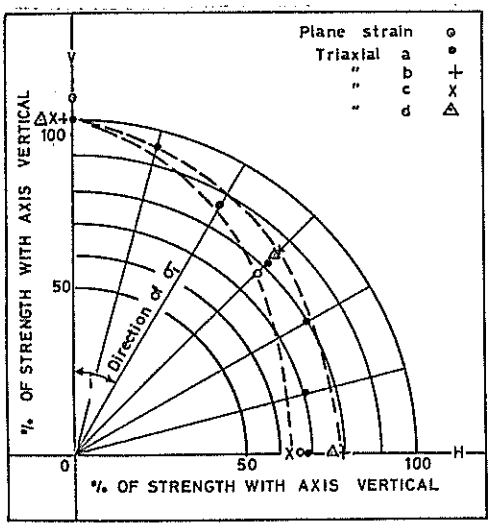

Figure 6 Polar Diagram of Strength With Inclination

5 CONSOLIDATED UNDRAINED TESTS

In the above sections it has been suggested that the anisotropy in undrained strength results from differing pore pressure responses during loading, rather than from anisotropy in the Mohr-Coulomb failure envelope (i.e. in the c' and Ø' values). To check the actual pore pressure response during loading, and the nature of the Mohr-Coulomb envelope, several series of different types of test have been carried out. These have included the following:

(a) Triaxial compression tests on vertical and horizontal samples

(b) Triaxial extension tests on vertical and horizontal samples

(c) Triaxial compression and extension tests on samples prepared at intermediate inclinations to the vertical

(d) Plane strain compression tests on vertical and horizontal samples

Before testing, all samples were consolidated to the mean in situ stress level. This was necessary as sensible comparisons of pore pressure response could only be made if the initial stress states were the same. Full details of these tests are given by Wesley (1975) and only the results of direct relevance to the present paper are presented here.

In Fig.7 all of the failure values are plotted on a conventional plot of $\frac{\sigma_1 - \sigma_3}{2}$ Versus $\frac{\sigma_1' + \sigma_3'}{2}$.

The values plotted in each case are the averages from four identical tests. It is seen that all the values lie close to a single line and demonstrate clearly that anisotropy in the values of c' and Ø is negligible. It was expected intuitively that the c' and Ø values may have been greater on the horizontal plane, since this was the plane of maximum effective stress in situ, and also the plane of bedding, but the tests on inclined samples showed no evidence of this.

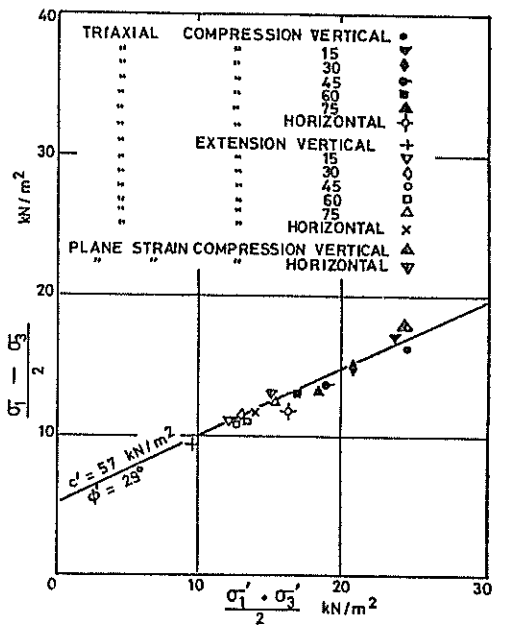

Figure 7 Failure Envelope from Differing Test Types

It is of interest to make a specific comparison of behaviour in undrained tests that predicted from drained tests using elastic theory. In Fig.8 the predicted stress paths and the actual experimental stress paths are shown for four different test types. These test types were:

Triaxial compression and extension on vertical samples

Triaxial compression and extension on horizontal samples

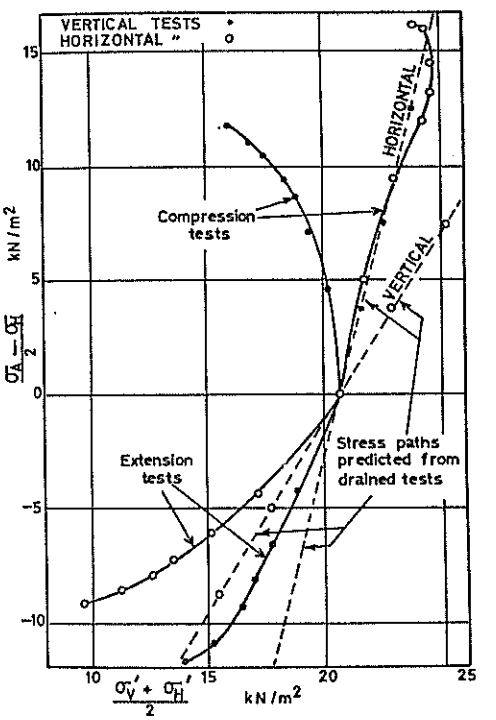

Figure 8 Undrained Stress Paths in Triaxial Tests

It is seen that the stress paths are in agreement with the general trend predicted by elastic theory, but are displaced to the left of the theoretical paths. This means that the actual pore pressures are higher than the theoretical values.

6 OTHER MEASUREMENTS OF UNDRAINED STRENGTH ANISOTROPY

An examination will now be made of measurements of anisotropy reported in the literature and the interpretations which have been placed on such measurements. The simplest, and most common method of measuring undrained strength anisotropy is by carrying out undrained compression tests on cylindrical samples cut at varying inclinations to the vertical. A comprehensive set of such tests was done by Lo (1965) and the results were very similar to those presented in Figs.4 and 6. As Bishop (1966) has pointed out there is considerable ambiguity associated with this type of test when attempts are made to relate particular values of undrained strength to particular planes.

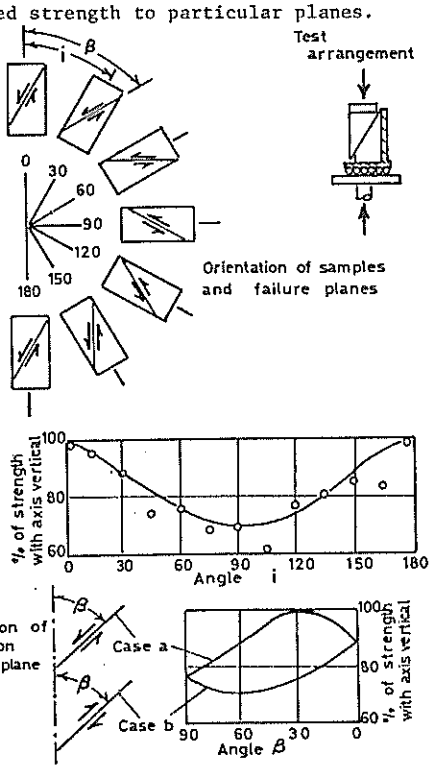

Figure 9 Evidence of Semi-Confined Tests

To overcome this ambiguity, De Lory and Lai (1971) carried out tests on block specimens which they called semi-confined as they used an arrangement (see Fig.9) which restricted failure to one particular plane. Samples were tested at values of i varying from 0 to 180°, and the results are shown in Fig.9. When plotted as strength versus the angle i the results show an identical trend to Lo's tests and the tests presented in this paper, i.e. maximum strength when the axis is vertical and minimum strength when the axis is horizontal. However the results can also be plotted against β, the angle of the failure plane to the vertical, and with this plot two curves are obtained as seen in Fig.9. The upper curve (case a) applies when shear is occurring in the same direction as the existing shear stress in the ground, and the other (case b) when the direction of shear is reversed. Dr.Lory and Lai believe their results support a hypothesis put forward by Bjerrum (1972,1973) that the soil structure has a greater resistance to shear in one direction than the other. However it is not at all established that unique values of undrained strength (dependent only on the direction of shear) can be associated with particular planes. A simpler explanation of De Lory and Lai's results is that suggested in this paper, namely that the values of c' and ϕ' are not influenced by orientation, but that the pore pressure is, the response increasing as i increases from 0^0 to 90^0.

A further method which has been used to measure undrained strength anisotropy is by carrying out field vane tests using vanes of varying height to diameter ratios. Tests by Aas (1965 and 1967) showed the strength on the horizontal plane to be generally greater than the vertical plane and Aas suggests that this results from the differing in situ effective stresses acting on the planes. The results of these vane tests do not appear compatible with the results of compression tests at varying inclinations. If in a normally consolidated clay the minimum strength is found on vertical planes, then it follows that in tests on cylindrical specimens, the specimen cut with the axis inclined at 30^0 to the vertical should have the lowest strength as failure would occur on a plane originally vertical in the ground.

Finally, mention should be made of work done by Bjerrum and co-workers at the N.G.I., who have proposed undrained triaxial compression and extension tests as a method of measuring undrained strength anisotropy. Bjerrum and Kenney (1967) present results of compression and extension tests which show a large difference in strength, and put forward their hypothesis to explain this difference. Their hypothesis is that the soil skeleton has developed a greater resistance to shear when the shear stress acts in the same direction as it does in situ than when it acts in the reverse direction (which is the case in an extension test). Bjerrum (1973) and Berre and Bjerrum (1973) further develop this hypothesis and use the ratio of extension to compression strength as a measure of the anisotropy.

Both the hypothesis and the use of extension and compression tests as a measure of anisotropy are open to serious criticism. There is no clear explanation of what is meant by the hypothesis; in particular whether the "greater resistance to shear" in one direction than the other is because of higher c' and ϕ' values, or because of lower pore pressures due to some sort of increased resistance to the development of pore pressures in one direction.

The use of undrained triaxial extension and compression tests as a means of measuring anisotropy does not appear valid, as theory predicts and experiment shows that undrained extension tests will give lower strengths than undrained compression tests even with an isotropic soil. Fig. 10 shows the results of undrained extension and compression tests on isotropic sand and clay samples. It is seen that the extension tests give a substantially lower strength than compression tests, the difference being greater with sands than with clays.

This review of other measurements of undrained strength anisotropy has been very brief but sufficient to indicate that such measurements are compatible with the explanation for anisotropy put forward in this paper. The explanation offered in this paper appears to provide a better

basis of understanding undrained strength behaviour than do the various hypothesies put forward by the authors.

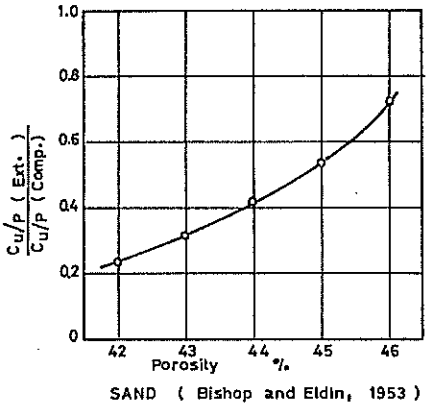

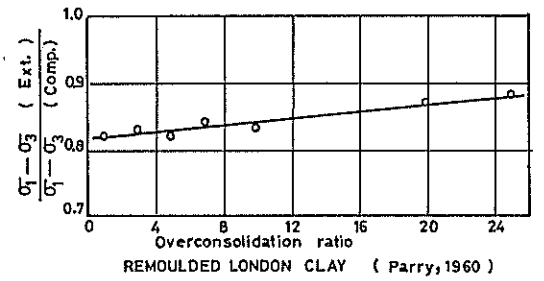

Figure 10 Extension and Compression Test on Isotropic Samples

7 CONCLUSION

An explanation has been put forward to account for the undrained strength anisotropy of soft clays. The key to this explanation is the difference in the stiffness of the soil skelton in the vertical and horizontal directions. That such a difference should exist is not surprising since the effective stress to which the skeleton is subjected in situ is about half in the horizontal direction what it is in the vertical direction.

It follows from the above explanation that it is not possible to associate unique values of undrained strength with planes at particular orientations. In taking account of undrained strength anisotropy in stability estimates it is the directions of the principal stresses which should be investigated rather than the angle of the failure plane. Lo (1965) in taking account of anisotropy starts from the position of the slip surface and assumes that the principal stresses are inclined to it at a fixed angle. A more logical procedure would be to determine the principal stress directions (by such a method as finite element analysis) and then to assign strength values to each point throughout the soil mass making use of the laboratory test data. This procedure would lead to some differences with Lo's assumptions.

The purpose of this paper has been to make a contribution to the understanding of undrained strength anisotropy rather than to analyse its effect in practice. It should be mentioned however that the effect in practical situations is not great. For slip circle stability analysis, a very close approximation to the true effect of anisotropy will be obtained simply by using the average of vertical and horizontal strengths in a conventional analysis.

8 REFERENCES

AAS G. (1965) A study of the effect of vane shape and rate of strain on the measured values of in situ shear strength of clays. Proc.6th Int.Conf. on Soil Mech. Toronto.Vol 1, 141-145

AAS G. (1969) Vane tests for investigation of anisotropy of undrained shear strength of clays. Proc. Geotechnical Conf.Oslo. Vol 1, 3-8.

BERRE,T.AND BJERRUM,L (1973) Shear strength of normally consolidated clays. Proc.8th Int.Conf.on Soil Mech. Moscow. 1.1, 39-40.

BJERRUM,L.AND KENNEY T.C. (1967) Effect of structure on the shear behaviour of normally consolidated quick clays. Proc.Geotechnical Conf. Oslo. Vol 2, 19-27

BJERRUM (1973) Problems of soil mechanics and construction on soft clays. Proc.8th Int.Conf. on Soil Mech. Moscow.

BISHOP,A.W. AND ELDIN,G. (1953) The effect of stress history on the relation between Ø and porosity in sand. Proc.3rd Int.Conf. on Soil Mech. Zurich Vol 1, 100-105.

BISHOP,A.W. AND HIGHT (1977) The Value of Poisson's ratio in saturated soils and rocks stressed under undrained conditions. Geotechnique 27,No3,369-384

BISHOP,A.W. (1966) The strength of soils as engineering materials Sixth Rankine Lecture. Geotechnique 10:2, 89-129

DE LORY,F.A.AND LAI,H.W. (1971) Variations in undrained shearing strength by semi-confined tests. Canadian Geotech.Journal 8, 538-545

LO,K.Y. (1965) Stability of slopes in anisotropic soils. ASCE Journal Soil Mech and Found.Eng. Vol 91,SM4,85-106

PARRY,R.H.G. (1960) Triaxial compression and extension tests on remoulded saturated clay. Geotechnique Vol 10, No 4, 166-180.

WESLEY (1975) Influence of stress path and anisotropy on the behaviour of a soft alluvial clay. Ph.D. Thesis, Imperial College.

An Impact Soil Test as Alternative to California Bearing Ratio

B. CLEGG
Senior Lecturer in Civil Engineering, The University of Western Australia

SUMMARY A case is presented for the use of an Impact Soil Test as an alternative to CBR. A comparison of the two methods in both terms of concept and procedure is made and a correlation based both on general observations and on a series of laboratory tests is indicated.

1 INTRODUCTION

In the field of pavement technology, particularly flexible pavements, California Bearing Ratio or CBR has become one of the most widely used and recognised soil strength parameters. Its use extends from a general classification "index property" to the basis of sophisticated design procedures. Although it has little basis as a theoretical or rational test its world wide acceptance speaks for itself. At the time of its introduction in the 1920's there was clearly the need for a practical test to meet the rapidly growing demand for pavement design. From time to time numerous alternatives, such as penetrometers, have been introduced but these have not had the same facility for application in both laboratory and field. Recently the author introduced the concept of an Impact Test based on the standard or "Proctor" compaction test. This device is being considered as an appropriate alternative to CBR. It appears to be comparable with the CBR concept in that it is also a simple meaningful test applicable to both laboratory and field situations over a wide range of soils and conditions.

It is the intention of this paper to examine the concept of CBR and to make a comparison between the CBR and Impact Test and to illustrate how by making the CBR value so much simpler to obtain, the CBR concept can be extended and given even wider application.

2 THE CBR CONCEPT

To understand the CBR philosophy one needs to consider the "state of the art" at its time of inception. This may be judged to some extent from the papers presented to the symposium on "Development of CBR flexible pavement design method of Airfields". In his paper at this symposium Porter (1949a) describes the background to the original elementary pavement design curves. The use of a model scale bearing test appears logical. So also does the original use of static compaction since laboratories at the time would have been oriented towards concrete testing, and compression testing machines would have been available. From its inception the CBR seems to have crept into most road and airfield pavement studies. For example both the Stockton, Porter (1949b) and Barksdale (Hansen 1949) test tracks used CBR as the basic soil strength parameter, and it was also included in the well known WASHO (1954) and AASHO (1962) pavement performance studies. With the entry of USA into World War II and the need for rapid expansion of airfields throughout the world the CBR became the basis of design of emergency airfields.(War Department 1942). With the kind of expediency that probably only wars can bring,design curves were extrapolated from truck loads to bombers by the application of simple elastic theory. (Middlebrooks and Bertram 1949).

As stated by Porter (1949) "To predict the probable behaviour of materials underlying the pavement, it was desired to have a simple quick test that would evaluate the quality of subgrade, sub-base, and base course material". With CBR appearing to meet these basic requirements it is not surprising that it found its way into general application as, for example, in classification charts such as Casagrande's along with the now well known and recognised Group Symbols. (See Table I)

TABLE I

EXTRACT FROM UNIFIED SOIL CLASSIFICATION SYSTEM

Group Symbol	CBR (field)
GW	60-80
GP	25-60
GM	40-80
GC	20-40
SW	20-40
SP	10-25
SM	20-40
SC	10-20
ML	5-15
CL	5-15
OL	4-8
MH	4-8
CH	3-5
OH	3-5

The obvious correlation between CBR and general soil index properties led in due course to procedures for estimating CBR's based on multiple regression equations. These have proven popular in Australia and may be similar to the equations given in Table II.

The advantage of inferring CBR from index properties appears to be the avoidance of problems associated with performing the CBR test as will be discussed in a later section of this peper. It should be noted that density and moisture content are not included and the need for good compaction and appropriate moisture content is therefore assumed. In many respects the CBR is to the pavement engineer what the Standard Penetration Test or SPT test is to the foundation engineer. Whatever alternative one might suggest it must of necessity show at

TABLE II

EMPIRICAL EXPRESSIONS USED TO RELATE THE SOAKED/STANDARD C. B. R. VALUE WITH THE SOIL CLASSIFICATION PARAMETERS:

$$\log_{10} C_s = 1.667 - 0.005056\, P_{0.425} + 0.001855\, P_{0.075} - L(0.01676 + 0.0003848\, P_{0.075})$$

$$\log_{10} C_s = 1.886 - 0.003717\, P_{2.36} - 0.004495\, P_{0.425} + \frac{P_{0.075}}{P_{0.425}}\left(5.153 - 0.4562\,\frac{P_{0.075}}{P_{0.425}}\right)10^{-3} - 0.01429\, I$$

where C_s is the C.B.R. value at the Soaked condition of moisture content and density.

$P_{2.36}$ is the percentage by weight of particle passing the 2.36 mm sieve

$P_{0.425}$ is the percentage by weight of particles passing the 0.425 mm sieve

$P_{0.075}$ is the percentage by weight of particles passing the 0.075 mm sieve.

L is the percentage Linear Shrinkage

I is the Plasticity Index

The two values of C_s are combined in the following manner:

$$C'_{ss} = (3\, C_s^{\min} + C_s^{\max})\ 0.25$$

where C'_{ss} is the calculated estimate of the subgrade C.B.R. at the Soaked/Standard condition.

$C_s^{\min}$ is the less of the two values calculated by Equations 2.03 and 2.04

$C_s^{\max}$ is the greater of the two values calculated by Equations 2.03 and 2.04. (N.A.A.S.R.A. 1977)

least some relationship to the "basic yard stick". By this means access is made to the great wealth of empirical data relating to design, construction and performance. Thus, for example, although the California Department of Public Works, Division of Highways changed to Hveem's stabilometer-cohesiometer method (Hveem and Carmany 1948) one suspects that this "new rational method" had as its basis, at least initially, earlier performance data based on CBR. As another example, Scala (1960) in proposing the use of a penetrometer for strength evaluation reported correlations with CBR for the lower end of the strength scale.

Although the CBR concept was based on comparing the material under consideration with a standard crushed rock giving 100% its use has not been confined to materials under 100%. In the case of stabilised materials values of several hundred percent are obtained. (Ingles and Metcalf, 1972) and it has been used to evaluate such materials. It has also been used to estimate a Young's Modulus for theoretical analysis and the modulus of subgrade reaction for application to rigid pavement design.

Thus the CBR has become the common basis for "talking" and evaluating pavement material strengths and may be considered as having fully justified the aspirations of those who introduced the concept.

3 IMPACT TEST CONCEPT

The concept of a simple impact test based on the common dynamic laboratory compaction tests was presented by the author at the 8th ARRB Conference (Clegg 1976). An observant operator performing drop hammer type of compaction test knows that as compaction proceeds the nature of the impact changes, varying from a dull thud with some materials at certain conditions to a solid bounce at others. The Impact Soil Test system enables the strength changes indicated by these differing responses to be quantified.

The basic principle of this particular impact test is that the peak deceleration of the compaction hammer when it is brought to rest is directly related to the resistance offered at contact resulting from the stiffness and shearing resistance of the material. This resistance may be seen as deriving largely from particle interraction leading either towards densification or resulting in shear deformation. Using appropriate assumptions as to the shape of the time vs acceleration curve, Millar (1977) carried out the appropriate integrations to obtain depth of penetration. Since from the deceleration and mass the peak force can also be obtained the peak deceleration is a very convenient parameter to use. The main difficulty from the electronics point of view relates to the "hash" that is produced at impact requiring carefully designed filtering.

The concept of dynamic testing of pavement materials using a falling weight has of course been developed in numerous other contexts such as, for example, the experiments of Asai (1960), Forssblad (1965), Orrje and Broms (1970) and others. All of these support the soundness of the concept of using in some way the deceleration to indicate the soil properties. By introducing this to the common laboratory compaction procedure and in such a way as to make it possible to use the CBR test mould (as will be discussed later) a system that meets all the basic requirements of a simple quick test to cover the full range of materials as set down by Porter (1949) and previously quoted, is evolved.

4 THE CBR TEST PROCEDURE

The CBR laboratory test has changed little since its inception in 1929. The mould size 150 mm (6") diameter, 125 mm high specimen, 1935 mm^2 (3 sq.ins) plunger, 1 mm (.05 ins)/min. rate of penetration have become standard. However, there have been some variations in sample preparation such as:

- the original static compaction has been generally replaced by dynamic compaction e.g. "modified AASHO" or similar
- The soaking procedure is not always carried out
- the surcharge weights are not always used
- top and or bottom of the specimen may be tested.
- a correxion is commonly made to allow for initially excessive penetration.

With regard to the first variation listed above this was apparently introduced because of the need for "field compaction" which really meant that a compression test machine of adequate capacity was not available to produce the required 14 MN/m^2 . Although impact compaction is now commonly employed it should be noted that the British Standard Test procedures permit static compaction, and in view of the possible difference in CBR due to the method of compaction it would seem desirable to keep this in mind when quoting a CBR value.

In the case of soaking, this was introduced to produce "realistic" field conditions. This in effect means worst conditions, namely the wettest. In the case of drier climates it is now common to test at expected field conditions.

The surcharge weights were added to provide confinement around the piston area. The amount of surcharge is related to the expected pavement thickness. It apparently makes a significant difference in the case of cohesionless soils, particularly clean rounded sands.

The difference between top and bottom CBR's can be quite considerable. Both the Australian Standard (AS 1289.F1.1-1977) and the British Standard (BS 1377: 1975) permit testing at both ends if desired and the result for each case should be noted.

With respect to the corrections to the force penetration curves and the derivation of the CBR value from the data it appears that differences in interpretation can be important. While the value at 2.5 mm (0.1 ins) penetration appears to be the common choice when 5 mm penetration gives a higher CBR the British Standard requires this to be reported while the Australian Standard requires the test to be repeated.

From the foregoing it may be seen that when a CBR value is quoted it needs to be recognised that there are variations in test conditions that may need to be considered. In the application of the CBR value to design these test variations may be insignificant and are commonly ignored. However, they do not appear to have lessened the CBR's wide general acceptance, either as a "precise" design parameter or as a general notional parameter.

5 THE IMPACT TEST PROCEDURE

The Impact Test being considered in this paper consists essentially of a laboratory compaction hammer, a guide tube and a meter. It is operationd as follows :- Loose material is removed from the surface to be tested, the instrument is placed in position and held down by the operator's foot, the hammer is raised in one hand with the meter in the other, the meter is cleared, hammer dropped and impact reading obtained, the meter is cleared again and the blow repeated the desired number of times.

The test may be performed in a CBR mould or in the field. Variations that have been used in addition to those that might be considered with respect to sample preparation as previously discussed in relation to the CBR test are :-

- changing the mass of the hammer
- changing the height of drop
- the number of blows
- use of surcharge
- direct measurement of residual penetration
- shape of the hammer end
- method of field calibration

The first variation of changing the mass has been found to be a convenient way of changing scale. The use of a lighter, say 0.5 kg hammer increases the deceleration and may therefore be used with softer materials. Similarly the light compaction hammer 2.5 kg may be used. However, it is considered doubtful whether this is really warranted or provides any significant advantage since the instrument appears to be still capable of valid readings at very low strengths such as CBR's less than 5 even with the 4.5 kg hammer. The heavy hammer has the advantage that it may be used for materials up to several hundred percent CBR. Increasing the mass to say 20 kg requires a diameter of about 150 mm to produce the same order of decelerations but has been tried as a means of testing to a greater depth and for possible correlation with Benkelman Beam deflections.

With regard to the second point the impact value tends to increase with height of drop. Quite early in the development of the device the height of drop was kept to that used for the compaction test,450 mm for the 4.5 kg hammer. Experience suggests that this height of drop is preferable since it leads to a more rapid flattening of the surface with successive blows.

The fact that the Impact Value increases with successive blows appears to be inconvenient but in some respects it is essential to the technique. Should the surface be so strong that there is virtually elastic rebound from the first blow it is more difficult to observe stiffness differences. The desirable mechanism appears to be that a wad of compacted material is projected into the body of the material. The recommended practice is to use the 4th blow reading. The first one or two blows flatten and compact. Too many blows pulverise and loosen the immediate surface or may continue to densify the material. Early in the use of the device rubber pads were used on the ground surface but later abandoned as an unnecessary encumberance and a modest number of successive blows are used instead.

The direct measurement of the residual penetration was at one stage considered as possibly providing useful information. While there does seem to be some correlation between Impact Value and the depth of the indentation it is awkward to measure,and also it may be influenced by heaving around the perimeter.

Experiments with a hemispherical end were an early innovation. Rounding in this way may reduce unwanted frequencies and perhaps more desirable characteristics from the measurement point of view. However its use was not pursued in favour of developing the cone or dome within the material itself. Simplicity of construction also favoured the square end.

Surcharge weights have been used around the test area similar to those used with the CBR test and for essentially the same reason. The guide tube is in fact recessed so that there is no surcharge immediately around the hammer. It is made of plastic

weighing only 1.02 kg and the operator's foot holds it in place rather than applying any great amount of pressure that might be considered surcharge. For the sake of simplicity, surcharge weights have not been used for general application.

The need for field calibration of the instrument as distinct from its laboratory electronic calibration led to the design of a plastic calibrating ring. This ring is placed on a solid surface such as a concrete floor and the hammer dropped as in a normal test. The impact Value so obtained is recorded and may then be checked from time to time.

From the foregoing it can be seen that when the Impact Value is quoted it would be well to qualify this by commenting on the mass, height of drop, blow number, surcharge, hammer shape when these are different from the standard 4.5 kg, 450 mm drop, 4th blow, square ended hammer.

6 CORRELATION : CBR vs IMPACT VALUE

The initial research on the Impact Test concentrated on observations in relation to different materials at varying densities and moisture contents (Clegg 1976), pavement performance observations and for compaction control (Clegg 1977). However, evidence began to accumulate that a correlation with CBR would be obtained. For instance the performance studies showed that an Impact value of 50 corresponded to "satisfactory" while 30 represented "doubtful". These values could be seen in relation to a minimum CBR of 80 for light traffic and general consensus that 50 CBR was the lowest acceptable. The laboratory studies suggested that for a well graded crushed rock at optimum moisture which could be seen as having a CBR of around 100 the Impact Value would be about 40.

To obtain a direct comparison, Millar (1978) performed a series of Impact Tests on samples that had been previously tested for CBR and Texas Class numbers. The results were sufficiently encouraging to warrant the author carrying out a series of laboratory tests covering a range of material and test conditions to give CBR's from 2 to 200. No soaking, no surcharge conditions were adopted. The data from these tests are plotted on Figure 1.

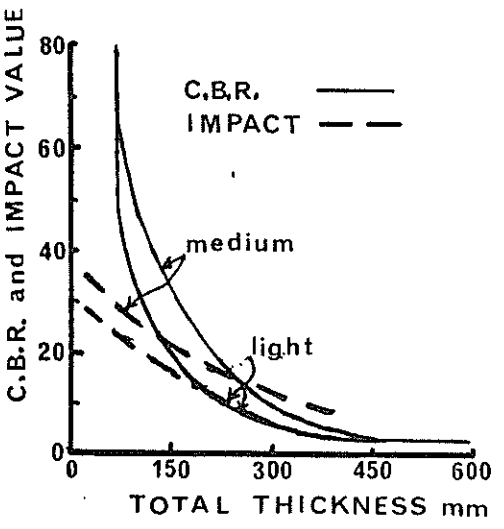

Fig.2. Total thickness of base and surfacing in relation to C.B.R. and Impact Values [Based on Porter, (1949)]

Subsequently Hill (1978) also carried out such tests quite independent of the author and obtained what might be seen as identical results. Millar(1978) also carried out a theoretical analysis producing the relationship indicated on this figure. It should be noted that this relationship is for unsoaked, no surcharge and laboratory tests. At the time of writing only limited studies had been made to see whether this relationship also holds for these variations in test conditions but it looks possible.

Thus it appears from these observations that the original impression of a correlation is certainly substantiated and that the relationship is of the form $CBR = .07\ (IV)^2$.

7 COMPARISON

The correlation presented in the previous section needs to be seen in relation to the overall comparison between the two methods with respect to concept and test convenience. The following summarises their similarities :

- approximately the same area and volume of soil tested.
- applicable to both laboratory and field.
- cover the full range of materials encountered.
- produce "force-penetration" parameters.
- respond to the same variations in sample preparation and test conditions.

Their major differences may be seen as follows :

- static vs dynamic loading
- single load application vs repeated load application.
- method of correction for surface irregularities.
- portability of the apparatus.
- degree of skill required to perform the test.
- time and cost of performing the test.

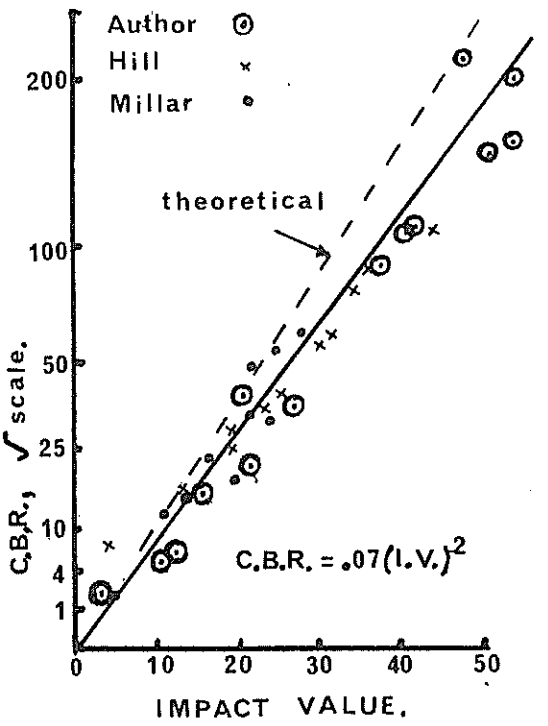

Fig.1. Laboratory correlation between C.B.R. and Impact Value. (No surcharge, no soaking).

Thus the Impact Soil Test as developed is similar in many important respects to the CBR and it may be seen as a reasonable alternative compatible with the overall concept. However its unique aspect of dynamic action and direct read out of the test result in a fundamental unit (gravities x 10) suggest that Impact value may be more appropriate than CBR. It has been suggested that a scale of CBR should be added to the Impact Meter and while this may have some logic it implies that an acceptable correlation has been established but this may in fact need to be modified from time to time.

The Impact value may also be considered in relation to the two main areas of application of CBR viz pavement thickness and base course strength. There are many variations of the pavement thickness charts based on CBR. It is of interest to take the original curves of California Highways presented by Porter (1949) and by converting on the basis of the previously presented correlation, an approximately linear relationship is obtained. (See Fig.2) If extrapolation is permitted an Impact Value of around 40 seems appropriate for zero thickness of asphalt concrete and this is in accord with the values obtained from field observations of performance. (Clegg 1976). It should be noted however, that this correlation is for unsoaked and no surcharge conditions and its acceptance for other conditions of test has still to be confirmed.

With respect to base course strength, as mentioned previously, CBR is frequently specified to define strength and stability of these materials. A value of 80 is often set with a minimum of 50 being considered the lower limit. With stabilised materials values of several hundred may be required. The corresponding Impact Values would be in the order of 34 and 27 respectively with 200 CBR corresponding to an Impact Value of around 50. It has been found that Impact Values of 70 or more are common on traffic compacted materials that have some dry cohesion or are stabilised.

One of the desirable features of the CBR concept is with respect to its application to field in-situ testing. The Impact Test makes this more feasible in that it is portable and takes less than a minute to perform. (See Figures 3(a) and 3(b). Many more tests can thus be carried out and more adequate data can be obtained readily for future comparison with performance and strength re-evaluation may be performed from time to time at minimum cost.

Both the CBR and the Impact Test have been considered as possible compaction control devices. Truesdale and Sellig(1967),report a field test to evaluate various procedures for rapid compaction control purposes. The CBR was included for comparative purposes only, presumably due to the degree of difficulty involved in carrying out the test. It was also noted that the use of any in-situ strength was complicated by the influence of moisture content when density in some form is the desired control parameter. This question of using strength measurement for compaction control needs further consideration. If minimum in-situ strength, say in terms of CBR, is specified and is the prime objective it seems logical to monitor this parameter during and subsequent to construction. Shackel (1976) further developed this concept of "strength objective" rather than "density objective" and concluded that control based merely on the latter does not represent good practice. While the required moisture content for compaction in relation to the appropriate optimum moisture content is generally specified the final moisture requirement is not usually specified but in fact needs to be considered if a specific strength condition is to be obtained. It seems logical therefore to monitor the strength during a specified compaction process requiring a certain strength at optimum moisture content and a final acceptance strength after "drying back" with or without more compaction.

Fig.3. (a) Field C.B.R. being carried out, 1954.

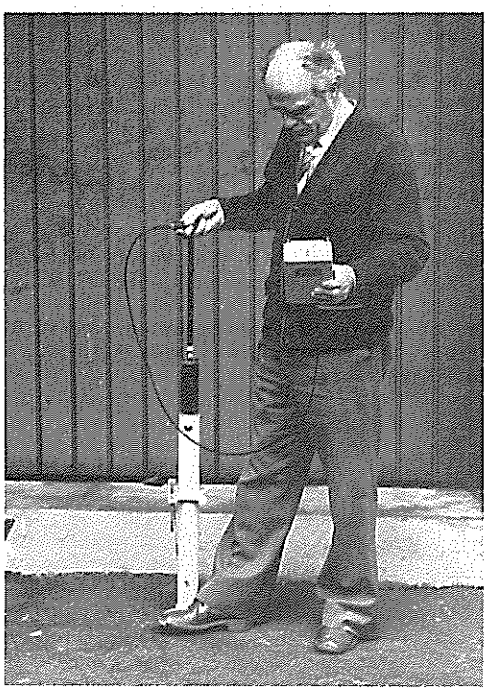

Fig. 3(b) Impact Test, 1979

8 CONCLUSIONS

From the foregoing it may be seen that the Impact Soil Test as described herein is similar to the CBR both conceptually and in terms of general test procedure.

While the CBR has gained wide acceptance as laboratory test its application as in in-situ strength test has been limited. The portability and simplicity of operation of the Impact Test gives the possibility of extending the concept in a meaningful way, particularly to the area of compaction control.

The sensitivity of the CBR test to higher strengths is overcome by the Impact Test without any apparent detrimental loss in sensitivity at the lower end of the scale. One of the consequences of this is to linearise the strength pavement thickness relationshop. Another is to make it possible to observe the effect of such factors as traffic compaction and stabilisation.

As a simple low cost test procedure the Impact test as described herein has considerable advantages and, while different to CBR in certain important aspects,such as that it is "dynamic" rather than "static", an excellent correlation has been obtained and it should therefore provide a viable alternative.

9. REFERENCES

A.A.S.H.O. (1962).The A.A.H.S.O. road test. Highway Research Board Special Report 61.

ASAI, S. (1960). Measurement of bearing capacity of subgrade by drop impact method. Soils and Foundations, Japan Soc. of Soil Mech. and Found. Engg., Vol. 1, No.1., p 42.

BRITISH STANDARDS INSTITUTION (1975). Methods of testing soils for Civil Engineering purposes. B.S. 1377, Test 16.

CLEGG, B. (1976). An impact testing device for in-situ base course evaluation. Proc. 8th A.R.R.B. Conf. Perth ,Session 8, pp 1-6.

CLEGG, B. (1976). Field assessment of the impact soil tester. A.R.R.B. Res. Report No. 76.

FORSSBLAD, L. (1965). Investigations of soil compaction by vibration. A.C.T.A. Polytechnica Scandinavia, Building and Construction, Series No. 34.

HANSEN, R. (1949). Service behaviour tests, Barksdale Field, Shreveport, L.A. Proc. A.S.C.E., Vol. 75, No.1., pp 45-55.

HILL, T.W. (1978). An assessment of Clegg's impact tester. Capricornia Inst. of Adv. Ed., Dept. Civil Engg., Final year project. Unpublished.

HVEEM, F.N. and CARMANY, R.M. (1948). The factors underlying the rational design of pavements. Highway Research Board. Proc. Vol.27, pp 101-136.

INGLES, O.G. and METCALF, J.B. (1972). Soil Stabilisation: Principles and Practice, Sydney, Butterworths.

MIDDLEBROOKS, T.A. and BERTRAM, G.E. (1949). Adaption to the design of airfield pavements. Proc. A.S.C.E., Vol.75, No.1, pp 18-21.

MILLAR, L.R. (1977). Application of the soil impact tester to road pavement construction. Univ. West. Aust., Hon. Thesis. Unpublished.

N.A.A.S.R.A. (1977) Pavement thickness design manual. The Nat. Assoc. of Aust. Road Auth. Draft Standard. Unpublished.

ORRJE, O., and BROMS, B., (1970). Strength and deformation properties of soils as determined by a free falling weight. Proc. Swedish Geotechnical Inst.,No.23

PORTER, O.J. (1949a). Development of the original method of highway design. Proc. A.S.C.E., Vol.75, No.1., 99 11-17.

PORTER, O.J. (1949b). Test Section No.1., Stockton Field, California. Proc. A.S.C.E., Vol.75., No.1, pp 35-44.

SCALA, A.J. (1956). Simple methods of flexible pavement design using cone penetrometers. Proc.2nd. A.N.Z. Conf. Soil Mech. and Found. Engg., Christchurch, N.Z. pp 73-84.

SHACKEL, B., (1976). Factors to be considered in the drafting of compaction specifications for soils. Proc. 8th A.R.R.B. Conf. Session 8, pp 23-34.

STANDARDS ASSOCIATION OF AUSTRALIA (1977). Methods of testing soils for engineering purposes. AS 1289 F1.1.

TRUESDALE, W.B. and SELIG, E.T. (1967). Evaluation of rapid field methods for measuring compacted properties. Highway Res. Board, Highway Res. Record No.177, pp 58-76.

U.S.A. WAR DEPARTMENT (1942). Technical Manual, Aviation Engineers, TM 5-255 Washington.

W.A.S.H.O. (1954). The W.A.S.H.O. road test. Highway Res. Board. Special Report 18.

Alternative Compaction Specifications for Non-uniform Fill Materials

G. A. PICKENS
Principal, Tonkin & Taylor, Consulting Engineers, Auckland

SUMMARY *The difficulties that arise in enforcing standard compaction specifications where the fill materials are not uniform, are described. A case is made for alternative specifications that permit much more straightforward and reliable control testing in non-uniform soils. The alternative air voids - strengths approach is described for soils ranging in type from clays to sands.*

1 INTRODUCTION

We excavate, prepare and compact a wide range of natural materials to alter the landscape in civil engineering works. In most cases we handle fine grained soils, natural gravels or processed aggregates. The compaction specifications for these materials are extensively expressed in standard terms related to one laboratory compaction test method, despite the wide variety of materials handled and the varying service conditions of the compacted fill. A tradition of standard specification use has been built up that discourages many of us from seeking alternative compaction specifications that may be more appropriate in certain circumstances.

Situations are often encountered where the material covered by the compaction specification does not have uniform compaction characteristics, or in effect comprises a range of different materials. Large difficulties can arise in interpretation of control test results and in these circumstances the standard specification approach is inadequate. Effort has been put into developing field testing techniques that attempt to ease the problem of interpretation but surprisingly little effort has been put into developing alternative specifications that allow accurate or more practical interpretation of field control tests.

The desire to set rational and readily enforceable compaction specifications has led to experience in New Zealand in the use of alternative compaction specifications, principally covering clays, silts and sands. This experience is generally known but many engineers still persist with standard type specifications in circumstances where they are better avoided. It seems appropriate to describe some of the alternative specification methods that can be used successfully and remaind all engineers that we do not fulfill our proper technical role if we become hidebound to outdated traditions.

2 STANDARD SPECIFICATIONS AND REFERENCE TESTS

Most compaction specifications follow much the same pattern and relate to a standard laboratory compaction test method which is usually the Proctor test or a modified version of it. The criteria laid down may vary from case to case but the terms used are usually consistent and specifications of this form may be termed standard specifications. They require the fill material to be compacted so that its dry density exceeds a certain percentage of the maximum dry density obtained in the standard test, and the fill water content to be confined within limits referenced to the standard test optimum water content.

What is the justification for these particular standards? We nearly always seek high strength and low compressibility, and to aim for a dense state of packing of the soil particles referenced to the maximum dry density, will help achieve these objectives. We know from experience that if the fill is too dry it will be difficult to compact to the specified dry density, and if it is too wet, the desired strength may be too low even if the specified dry density is achieved; hence we also impose compaction water content limits.

We know that the standard laboratory test, involving a particular compactive effort and procedure, does not uniquely describe the compaction performance of a soil: a particular piece of field equipment operated in a certain way will have its own water content/dry density relationship, possibly significantly different from the standard test results. Although there are logical reasons for setting specification criteria in the terms that are used, it is basically empirical evidence that supports expression of compaction standards in terms of the standard test for a wide range of materials. If standard specifications have been developed in this way, the door must be wide open for alternative and improved approaches.

3 ENFORCEMENT OF STANDARD SPECIFICATIONS IN PRACTICE

To establish whether fill complies with a standard type specification, it is necessary to establish the as-compacted dry density and water content and be able to compare these results with the maximum dry density and optimum water content for the particular soil being tested. Testing for field density and water content is a relatively straightforward matter for a wide range of material types, using several techniques: compacted aggregates are not physically easy to test other than by nuclear test methods. However, the field measurements are of little practical use unless they can be readily

related to a previously determined dry density/ water content relationship.

Some sites or portions of sites do have essentially uniform fill material with consistent maximum dry density and optimum water content as measured in the standard test, and use of standard specifications is acceptable. However, at least in New Zealand, these circumstances are the exception rather than the rule and even very small sites can contain highly varied soils, such that a scraper may uplift and deposit in one pass a mixture of materials with no characterising standard compaction properties. Fig 1 illustrates the order of variation that can be met.

A further complication arising with some soils (especially those of volcanic origin containing allophane), is that their compaction properties vary depending on the history of wetting and drying and any manipulation prior to final compaction. For these soils there is less relevance between the field results and the laboratory results unless the laboratory test models the field sequence of water content adjustment and soil manipulation. This difficulty does not preclude the use of, or prejudice the contractural validity of standard specifications based on a standard test, but adds further to the complications of assessing variable fill specified this way.

Under the conditions outlined, the controlling engineer has either to abandon the strict terms of the specifications and employ subjective judgement of fill standards, or to prove the case, must perform a standard compaction test on the particular material tested in the field to obtain reliable reference properties. Use of subjective judgement is contracturally unacceptable and to undertake a large number of standard compaction tests is too costly and time consuming to be regarded as a practical solution.

4 BASIC SPECIFICATION REQUIREMENTS

A satisfactory specification is one that adequately describes the designer's requirements, is understood by the parties to the contract, is practically capable of being enforced, and is not unnecessarily costly or time consuming in enforcement.

The key properties we wish to achieve for compacted fill are low compressibility, high strength and long term stability. These properties and how they may vary depending on the initial state of compaction may be described, perhaps in an over simplified manner, by reference to the saturation or zero air voids line that exists for a soil of constant solid density.

Compressibility, stability and strength are all principally governed by the density of packing of the soil particles. Compare points A & B on figure 2 which represent two initial states of compacted fill. The more densely compacted material represented by point A would achieve a state represented by A_1 if saturation can occur by compression at constant water content, and would reach A_2 if saturation were to occur without changing the soil density, say as a result of seepage forces: B representing a less dense initial state of compaction could similarly move to B_1 or B_2.

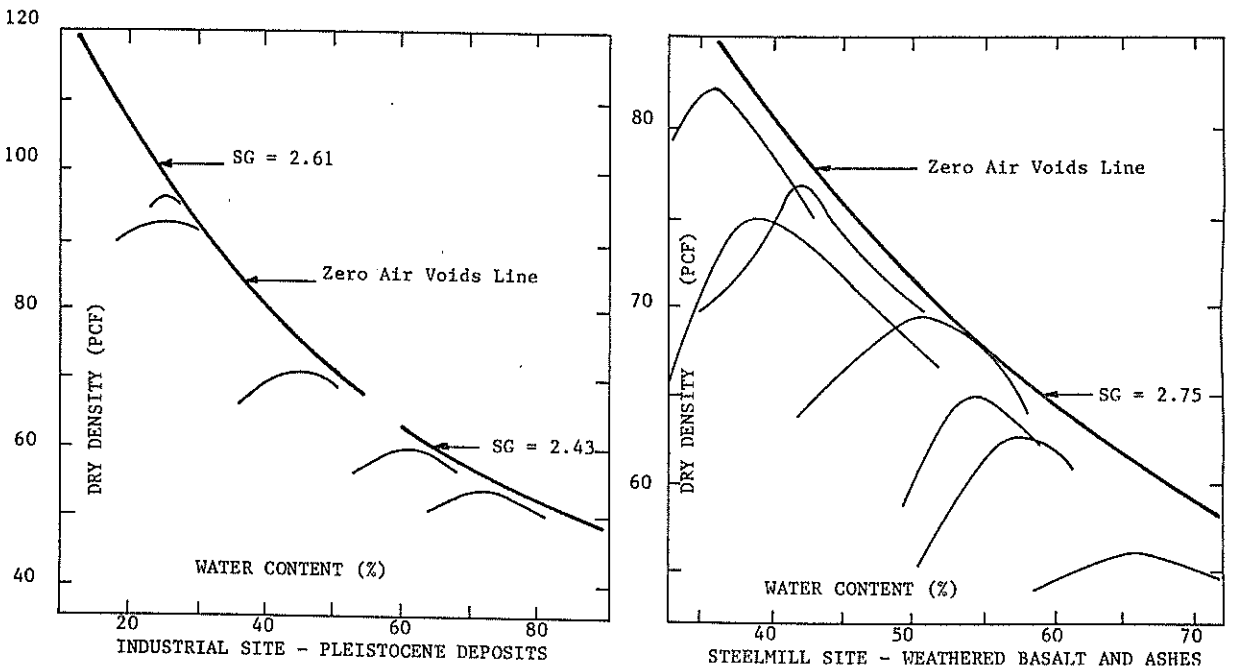

Figure 1 Illustration of Variable Fill Materials

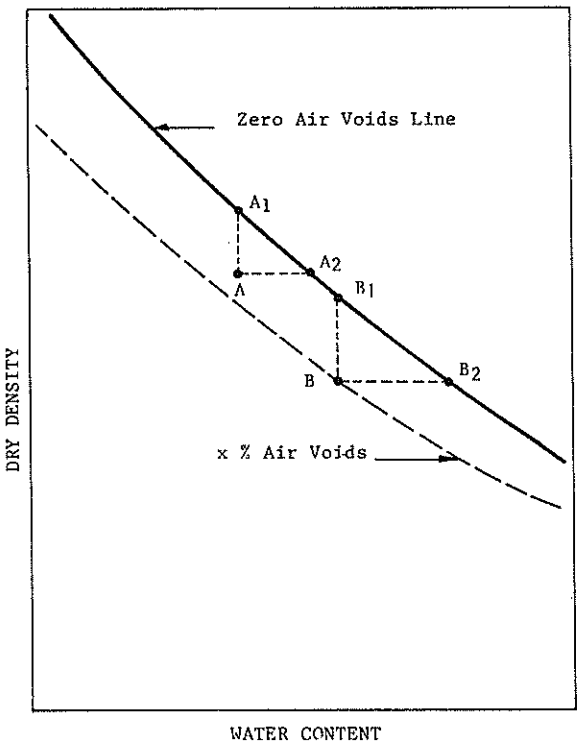

Figure 2 States of Compaction

If the intervals AA_1 and BB_1 are regarded as a measure of potential compressibility (setting aside questions of elasticity and consolidation properties), fill represented by condition A would be expected to be less compressible than B type fill. The stability of the A type fill, expressed in terms of the reduced potential for water content increase and consequent softening (A_1 A_2), is better than that of the B type fill (AA_1 $<BB_1$).

Based on experience, we know that the soil strength at point A_1 will be higher than at point A_2, and at A_2 will be higher than at B_1 and B_2; similarly, the initial strength at A will exceed that at B unless the A material is dried to a water content that is unacceptably low.

Developing a feel for the properties of compacted fill in relation to the zero air voids line is believed to be more useful than understanding compaction curves, and assists in understanding the workings of the alternative specifications described below.

The compaction standards specified and the related control testing should eliminate reliance on personal judgement in measuring the adequacy of construction. The control tests should be kept simple and inexpensive if possible, and permit quick response on site to avoid difficulties such as having to reject fill placed three days previously and now buried below another two metres of fill.

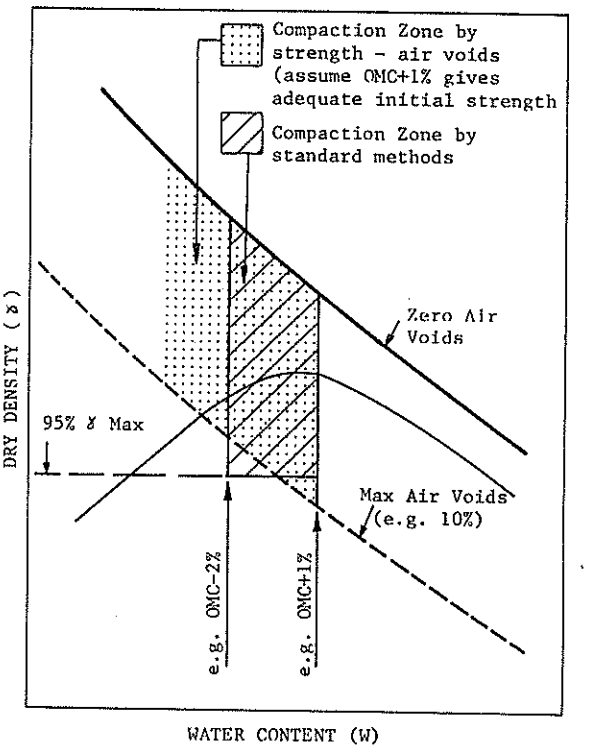

Figure 3 Comparison Alternative Specifications

5 AN ALTERNATIVE APPROACH FOR COHESIVE FILL MATERIAL

5.1 Description

A specification and control test approach based on air voids and soil strength has been proved suitable for variable cohesive soils. A maximum tolerated air voids is specified together with a minimum undrained shear strength after compaction. Strength is usually defined and measured by unconfined compaction, C.B.R., or in-situ vane with the latter preferred where the fill behaves as a clay. The pre-specification soil testing necessary before the particular limits are set depends on the nature of the project.

The differences in state of compaction resulting from use of strength-air voids and standard specifications are illustrated in Figure 3.

Specifications in terms of strength and air voids permit the reliable measurement of fill standards and removal of the use of personal judgement commonly employed where the soils are variable. Generally when earthmoving jobs are running in an orderly manner, low air voids are easily met and the largest problem encountered is avoidance of excessively wet fill that leads to low density and low strength. The strength-air voids approach is particularly useful here in that the low strength can be demonstrated in a matter of moments using field vane apparatus and the contractor can be notified immediately that the fill does not meet the specified requirements.

5.2 Field Control

In order to measure air voids, it is necessary to know the field density, the field water content and the specific gravity or solid density of the soil particles. Density and water content are measured by usual methods. The specific gravity is a factor that does not require frequent measurement. It varies by only a small amount within a locality where the soil is of uniform geological origin, even though the compaction properties of the local soils may vary considerably, and the effect of small variations of specific gravity on the position of the zero air voids line is not significant. Usual practice is to do several specific gravity tests at the design stage, select an average value and write into the specification that this value shall be adopted until such time as specific gravity tests done during construction, show that a change in average value is warranted. Check specific gravity tests are done on an infrequent basis as a part of control testing.

This specification method does not reduce the problems of rapid evaluation of water content and dry density which form part of the measurements. Interim results obtained via rapid water content test methods and involving possible inaccuracies have to be used as necessary. However, with the specific gravity pre-established and described in the specification, no further tests are required to identify fundamental soil characteristics and the air voids control test result can be confirmed with confidence and related to the specification requirements regardless of the standard compaction characteristics of the soil.

Strength, the other parameter, is measured directly and quickly. Where the in-situ vane method is used, small hand operated vane apparatus with about 19 x 29 mm blade dimensions has been found suitable on fills of lesser importance, whereas a landrover mounted vane with 47 x 94 mm blade and torsion spring measuring device has been used on a major earthfill dam.

In practice, the field supervisor begins with a large scale graph sheet on which the zero air voids line and relevant per cent air voids lines are drawn. Each measured dry density/water content point is then plotted to see whether it falls within the specified air voids zone. The corresponding strength result is generally unimportant providing it exceeds the minimum value specified: more often than not where the fill standard is high and vane strength is being used the supervisor will just record, "too hard to penetrate".

5.3 Standards and Examples

Experience in New Zealand with a wide range of cohesive soils has shown that sufficiently low compressibility is obtained if the air voids of the fill are less than 10% and the fill has a reasonable initial undrained shear strength (say not less than 100 kPa). The minimum strength should be sufficient to ensure safety of typical fill slopes and also support the earthmoving equipment without excessive deformation occurring. Special studies are required to determine appropriate values for critical fills such as in earth dams.

The strength below which the excessive deformation or overcompaction phenonemon occurs, varies with soil type and construction machinery, but has been observed to be about 70 kPa for light equipment on plastic clays and about 100 kPa for heavy equipment on very silty, low plasticity clays.

Therefore a typical specification for cohesive type general fill, based on experience rather than a comprehensive testing programme, would read;

average air voids < 10% (10 consecutive tests)

maximum air voids 12% (any one test)

average undrained > 150kPa(10 consecutive tests) shear strength

The strength air voids approach is being used increasingly in the north of New Zealand where soils are particularly variable. It has been used predominantly for general purpose earthworks but has been used successfully on larger projects where high compaction standards are important. Three cases involving important fills located in the Auckland region are described in summary form by way of illustration.

A Earth Dam

Eighty metre high earthfill dam of 3,000,000 cubic metre fill volume, built from residual greywacke and argillite origin materials varying in type from plastic clay to moderately weathered rock. Construction period 1973 - 1977.
Central fill zones comprising cohesive type materials specified and controlled in accordance with the following:

maximum air voids single test result		10%
average air voids for 10 consecutive tests	≯	8%
minimum vane shear strength, single test result		69 kPa
average vane shear strength for 10 consecutive tests	≮	103 kPa

Supplementary test requirement, used where judged necessary, was maximum compaction water content, optimum plus 3%

B Steelworks Site Development

Basic site levelling for steelworks expansion,1977-1978, involving 500,000 cubic metres of fill comprising weathered basalt and ashes.

General filling carried out in accordance with the following:

maximum air voids,single test		10%
average air voids	≯	8%
minimum vane strength,single test		110 kPa
average vane strength	≮	150 kPa

C Urban Motorway Extension

3.5 kilometres motorway extension involving 800,000 cubic metres of fill, mainly consisting of weathered volcanic ash, built 1973 - 1974. Specification as follows:

embankment fills:	
maximum air voids	12%
minimum C.B.R.	10
subgrade:	
maximum air voids	10%
minimum C.B.R.	15

Specific gravity for interpretation taken at 2.8. Proctor needle permitted for control in place of C.B.R.

(Construction tests showed that most fill was compacted to about 5% air voids: specific gravity varied between 2.7 and 2.8 and was re-adjusted to 2.75 for test interpretation).

6 AN ALTERNATIVE APPROACH FOR SANDY SOILS

Variable soils of a sandy and silty nature can be encountered that also present considerable difficulties in enforcement of standard specifications. Extensive variations in materials of this type within a site may be more common in New Zealand than Australia. For example, the centre of the North Island contains volcanic ashes and lapilli that are often closely banded and variable in grain size. In some districts weathered sandstone with variable silt content occurs below a shallow zone of weathered clays and silts and earthmoving work can involve the sandstone or sandstone mixed with overburden.

The strength-air voids specification approach can be used for these sandy materials in a similar manner to that described for cohesive clays and silts. However, the simple in-situ shear vane cannot be used with reliability and it may not always be feasible to prepare unconfined compression samples. In these circumstances it is necessary to measure strength by means of methods such as C.B.R. or Scala dynamic penetrometer. The Scala penetrometer (Scala, 1956) appears to be a satisfactory control test tool and has advantages over the C.B.R. in the scale of equipment required and ease and cost of test. The following two recent examples of specifications based on use of the Scala penetrometer for sandy fills illustrate the approach.

In the first project, some 150,000 cubic metres of volcanic ashes were required in two small dams and a large canal. During investigations Scala penetrometer tests were conducted in the laboratory on material compacted at different water contents within the proposed air voids limits. From these tests a minimum penetration value was determined corresponding with the lowest acceptable fill strength and stiffness. The blows required to penetrate the top 50 mm were discounted to allow for likely disturbance at the top of each layer after compaction. The final specification was expressed in the following terms:

maximum air voids single test		10%
average air voids	$\geq$	8%
average Scala value	$\leq$	7 blows (50 - 200mm penetration)
lowest single Scala value	$\leq$	5 blows (50 - 200mm penetration)

It should be noted that the material on the project generally had the consistency of a silty sand after handling: for clean sands a higher air voids value may have to be adopted.

In the second project, weathered silty sandstone was used in a foreshore reclamation. In this case, provision was made in the contract to calibrate Scala blows against undrained shear strength during the early stages of earthmoving. Subsequent control testing for strength relied on the Scala penetrometer alone. The specification and results of the calibration testing were as follows:

maximum air voids single test		12%
average air voids	$\geq$	10%
average undrained compressive strength	$\leq$	300 kPa by triaxial test at 15 kPa confining pressure
established minimum corresponding Scala value		9 blows (100mm - 250mm penetration)

7 CONCLUSIONS

Non-uniform fill materials are found in practice, that present large difficulties in the evaluation and enforcement of compaction specifications expressed in terms of standard laboratory compaction test results. Such specifications do not have a rigorous scientific base and are in part empirically based. There is justification for adopting alternative specifications if they are equally well based, and those that reduce the problems of controlling variable fills are particularly valuable.

Specifications that relate to the density of packing of the soil particles and the actual compacted strength of the soil are felt to describe desired fill properties better than current standard specifications. Specifications in terms of air voids and strength are of this type and cope satisfactorily with variable soils ranging from clays to sands without involving extensive reference testing. Shear vane testing is convenient for materials that behave as clays after compaction and the Scala penetrometer is suitable for sandy fills.

8 REFERENCES

PICKENS,G.A. (1978). A Practical Method of Compaction Control.Proc. Second P.E.A.A.A. Cont., Manila.

SCALA,A.J. (1956). Simple Methods of Flexible Pavement Design, Proc. Second A.N.Z. Conf. Soil Mech and Fond Engg., Christchurch.

Geotechnical Testing for Leigh Creek Coalfield

R. L. CAVAGNARO
Senior Geotechnical Engineer, Coffey & Partners Pty Ltd, Adelaide

SUMMARY This paper presents the results of some of the field and laboratory testing undertaken in providing geotechnical mine planning constraints at the Leigh Creek Coalfield, South Australia. The approach adopted to systematically test large amounts of drill core is described. Correlations developed between the basic classification test, the Point Load Strength Index, and other more sophisticated tests used in geotechnical analysis are presented. In particular the difficulties of testing material transitional between strong "soils" and weak "hard rocks", the characteristics of rock defects with very low residual strengths; and the simplification of a test used in assessing diggability of bucketwheel excavators are described.

1 INTRODUCTION

The Leigh Creek Coalfield is situated in the northern Flinders Ranges of South Australia some 600 km north of the capital Adelaide. The mine provides sub bituminous coal for use in generating the State's electricity supply in power stations located at Port Augusta about midway between Leigh Creek and Adelaide. Coal was first mined underground at Leigh Creek in the 1890's. Since 1943 coal has been mined by open cut methods to depths of about 30 m. Planning studies are now under way to extend the life of the mine into the twenty-first century with maximum depths increasing to 150 m. Mining is relatively difficult due to both the geometry of the deposit and low rock substance and defect strengths.

Between 1975 and 1978 three major geotechnical drilling programmes have been carried out as an adjunct to mine exploration drilling with some 9700 m of HQ size core being recovered for geotechnical purposes. The programme was instigated in order to:

1. Further define the geology and stratigraphy of the basin
2. Define regimes with similar geotechnical characteristics
3. Quantify through laboratory testing both substance and defect properties
4. Carry out analysis and make recommendations for mine planning
5. Monitor trial sections of the mine to confirm and upgrade predictions based on drilling and testing of laboratory samples

Items 1 to 4 have largely been completed whilst item 5 is just commencing. This paper describes the approach used and results of some of the laboratory testing undertaken and illustrates how they were incorporated into the analyses.

2 COALFIELD GEOLOGY

2.1 Stratigraphy

The Leigh Creek Coalfield consists of four separate deposits as shown on Fig. 1. The largest of these Lobe B has been the subject of the geotechnical studies undertaken to date. Lobe B is a remnant, asymmetric saucer-shaped basin of Triassic and Jurassic coal measures unconformably overlying Precambrian basement rocks of siltstone and limestone. Three separate sequences of coal have been identified (Coffey & Partners Pty. Ltd. 1975, 1979) and named the Lower Series, Main Series, and Upper Series, as shown on Fig. 1. The intervening overburden strata have been named after the coal seams which they cover. The units, their composition and typical strength range are given in Table 1. Strength ranges have been defined using the Point Load Strength Index (Broch & Franklin 1972).

Thin bands of rock of high to extremely high strength called "hardbars", are also encountered in some units. Hardbar thicknesses are often less than 100 mm although a significant number with thicknesses up to 500 mm have been encountered. They appear to be continuous over distances of one to several kilometres.

2.2 Defects

Defects in the rock mass include joints, sheared and crushed zones clay seams, and faults. Their distribution is however quite variable. In the Upper Series and to a lesser extent in the Main Series Overburden there are large volumes of rock where joints are often spaced greater than 10 m. In contrast the Lower Series Overburden and Main Series Coal have substantial zones where spacings are under 1 m and the remainder in the 3 to 10 m range. There is a concentration of defects subparallel to the bedding plus two other, steeply dipping concentrations which strike parallel and perpendicular to the bedding dip. Many of the joints in all units are polished and slickensided, showing evidence of past movements along them.

In addition to joints a number of clay seams exist. The seams are of medium to high plasticity ($w_L \simeq 40$ to 60%) and vary from about 5 to in excess of 200 mm thick. Samples from clay seams had residual angles of friction down to 8°. The clay seams are believed to be the product of extensive shearing of the rocks along planes of extreme movement and thus low residual shear strengths were anticipated.

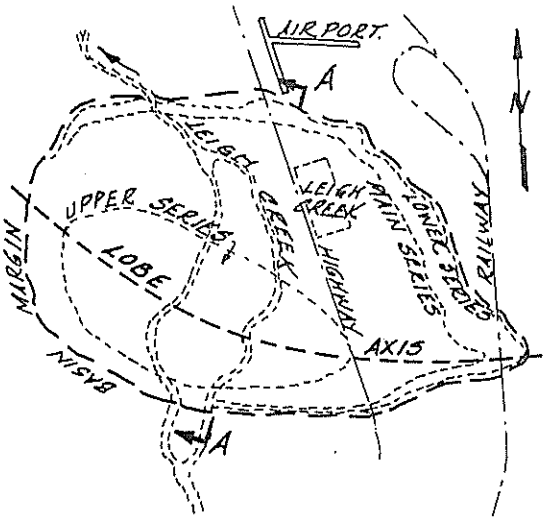

PLAN OF LOBE B

0 1 2 3 4 5

km

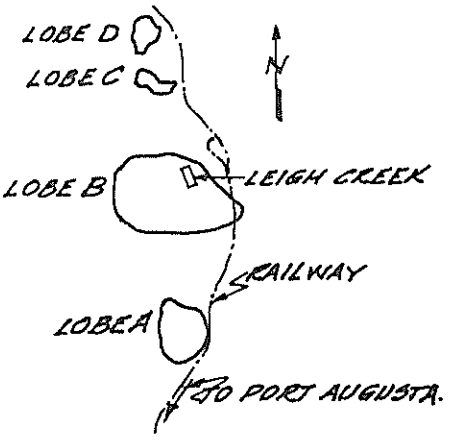

LEIGH CREEK COALFIELD

LOCATION MAP

0 5

km

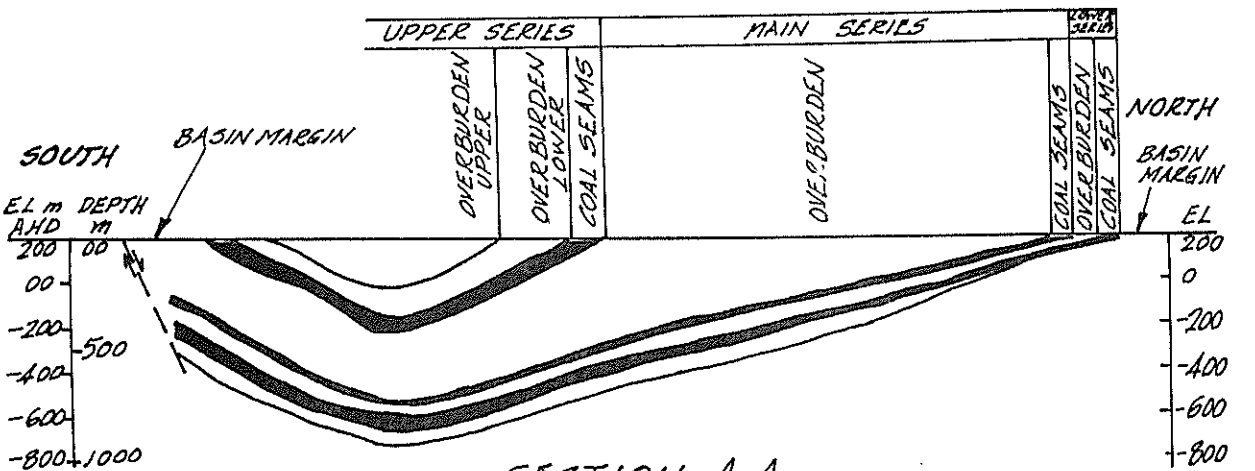

SECTION A-A

0 0.5 1.0 1.5 2.0

km

Figure 1 Plan and Section of Leigh Creek Coalfield

TABLE 1

Lobe B - Stratigraphic Sequence		
Unit	Principal Composition	Strength Range
Upper Series Overburden		
Upper	Mudstone and Siltstone	EL-L
Lower	Weakly cemented sand and Sandstone	EL & VL-L
Upper Series Coal	Coal with siltstone partings	L-M
Main Series Overburden	Mudstone	L-M
Main Series Coal	Two thick coal seams minor partings	L
Lower Series Overburden	Mudstone. some siltstone	L-M
Lower Series Coal	Thin coal seams and siltstone partings	L-M
EL = Extremely Low VL = Very Low L = Low M = Medium Strength		

They have also been observed to be continuous over very large areas beneath and parallel to the mine low wall. A number of low wall failures have been attributed to sliding along clay seams, particularly when associated with groundwater seepage.

3 APPROACH TO TESTING

The extended nature of the project and the large amount of core which had to be assessed for geotechnical properties required that a systemmatic approach to testing be developed. Further difficulties were evident due to the remoteness of the site limited transportation facilities to an established geotechnical laboratory and the harsh semi-arid climate. The approach adopted was:

1. Establishment in Leigh Creek of a fully equipped geotechnical testing laboratory capable of conducting both classification and some strength tests

2. Logging and classification testing all core on site within 24 to 48 hours of drilling

3. Carry out both on site and, for more sophisticated tests, on samples returned to Adelaide a more limited testing programme to determine strength and other required properties

4. Correlate the classification and other tests so that the latter could be applied to the entire deposit.

4 CLASSIFICATION TESTS

4.1 The Point Load Strength Index - $I_s(50)$

The Point Load Strength test shown on Fig. 2 was selected as the basic classification test and all drill core was tested progressively as it was recovered during the drilling. The Point Load Strength which is a measure of tensile strength and was developed at the Imperial College, London (Broch & Franklin 1972 and subsequently adopted by the International Society for Rock Mechanics (ISRM 1972) was selected as the standard test because it is a simple and rapid one which is readily carried out using portable testing equipment thus making it suitable for field use. Further since a large number of tests can be carried out a much more statistically significant interpretation of rock strengths may be obtained. Tests were carried out on a systemmatic basis every 5 to 10 m along all core plus on the remains of other test samples e.g. unconfined compression tests. Fig. 3 presents the correlation obtained between Point Load Strength Index and Unconfined Compressive Strength.

5 SHEAR STRENGTH OF DEFECTS

5.1 Testing Equipment

The Leigh Creek rocks whilst not unique, are difficult to test in that their strengths are often in the transition range between strong "soils" and weak "hard rocks". Thus tests conducted with equipment designed along classical "soil mechanics" or "rock mechanics" lines may be either inappropriate or susceptible to inaccuracies. Shear strength tests were carried out using two types of equipment:

a) A Hoek shear box designed for testing defects in hard rock and

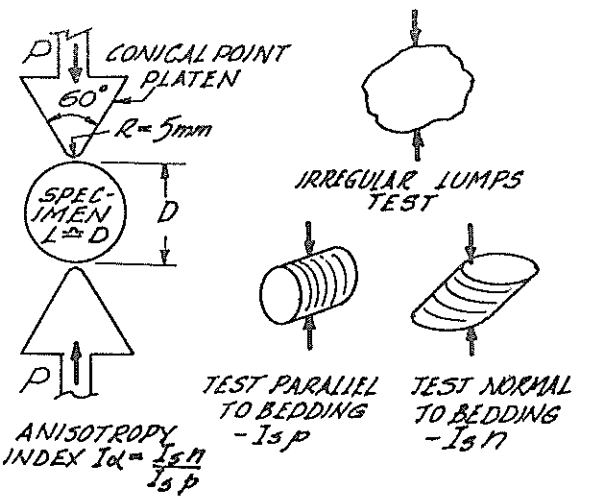

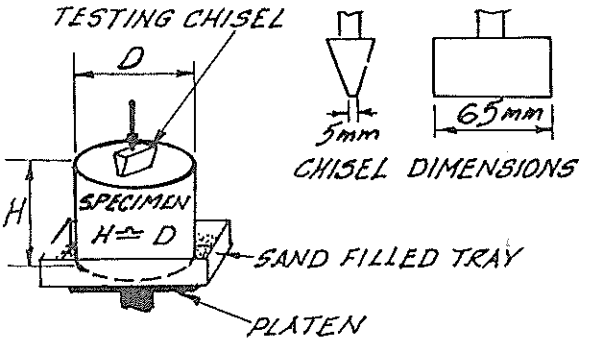

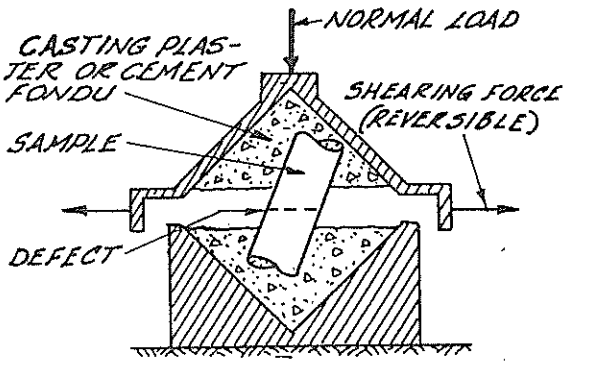

Figure 2 Description of Rock Strength tests

b) A conventional soil shear box

The two machines differ greatly in characteristics. The Hoek Shear Box (Hoek & Bray 1974) is designed to test defects in very strong rock and is very rigid and stiff in operation. Loading is by hand pumped hydraulic jacks which are difficult to operate accurately at very low strain rates. Accurate measurement of low shearing forces.

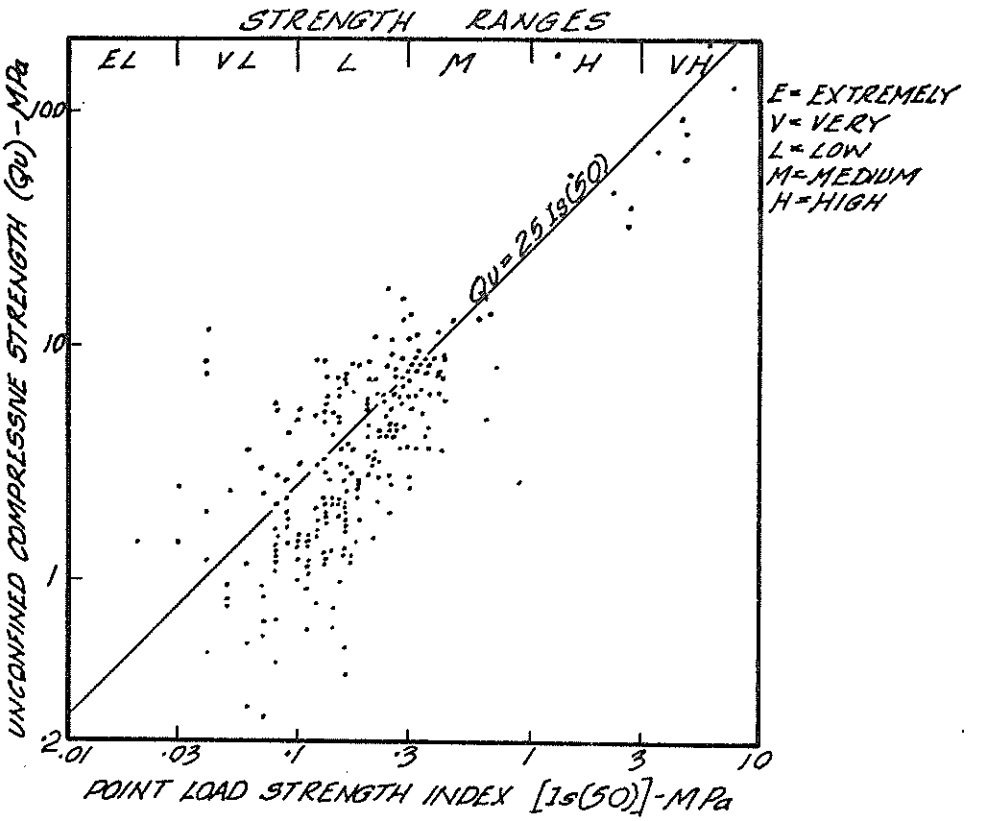

Figure 3 Unconfined Compressive Strength vs Point Load Strength Index

particularly when coupled with low normal loads is difficult and requires careful and detailed calibration of individual jacks. The sample (a length of core containing the defect) is first cast in a diamond shape mould and then sheared across the diagonal as shown on Fig. 2.

The soil shear box was a conventional Farnell constant strain type box with automatic mechanical feed . By use of a lever system normal pressures up to the equivalent of 30 m overburden could be applied. Preparation was by trimming into the box in the usual manner.

The strain rate used in the soil shear box was 10 mm/h. The Hoek shear box strain rate was between about 100 to 150 mm/h it being extremely difficult to hold steady normal and shearing loads at lower loading rates. Both boxes were capable of having the shearing force direction reversed so that repeated shearing cycles could be carried out in order to obtain residual strength parameters. Between 4 and 6 shearing operations were required at each normal pressure to obtain a repeatable minimum value.

5.2 Clay Seam Strengths

Typical shearing force-displacement curves for successive shearing cycles at the same normal pressure are presented in Fig. 4. The peak shear strength obtained in the first cycle is only slightly higher than the residual value after six cycles. This characteristic of peak strengths being little higher than residual values was common for most of the Leigh Creek defects and suggests that sufficient displacement and shearing has already occurred along the defects for their strengths to have approached residual values.

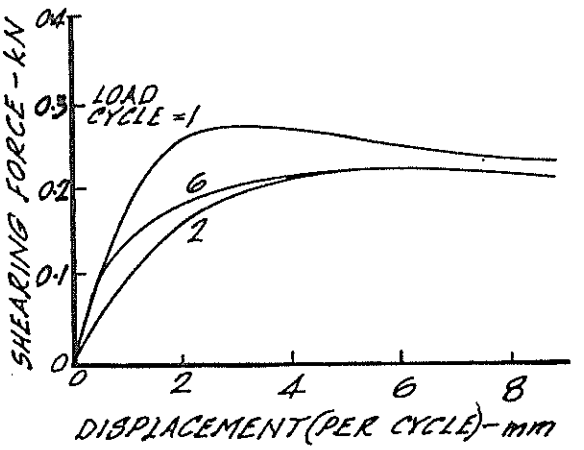

Figure 4 Typical load displacement curves on clay seam

The clay seams represent the weakest defects tested with residual friction angles down to 8 degrees and most values under 15 degrees. Residual angles of friction and apparent cohesion are summarised in the upper portion of Fig. 5. It is clear that the Hoek shear box gives significantly higher apparent residual cohesion values than the soil shear box for similar friction angles. It is considered that the apparent high cohesions are due to an excessive rate of shearing which does not allow sufficient time for pore pressure dissipation in the high plasticity, low

permeability clays.

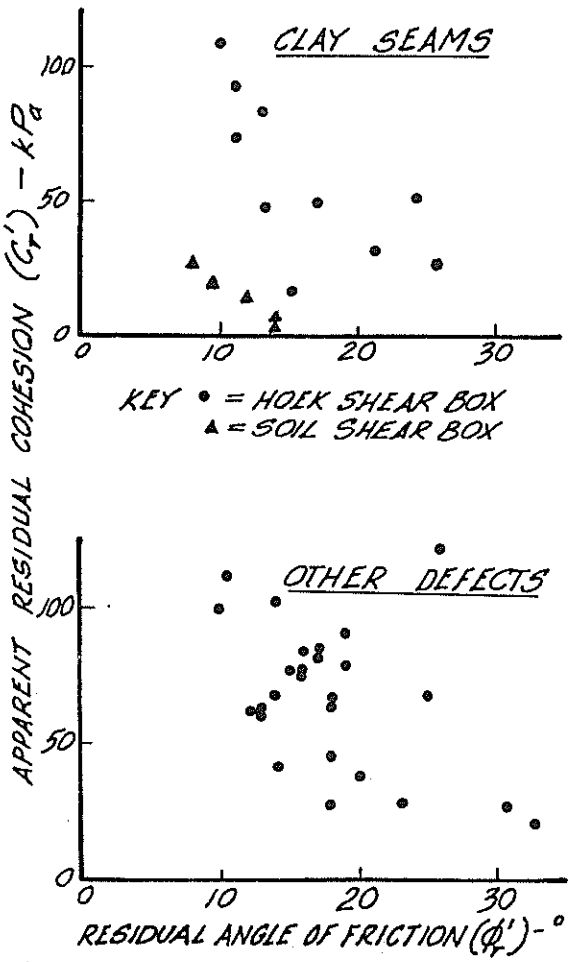

Figure 5 Summary residual shear strength tests

5.3 Other defects

Other defects which were strength tested included mainly slickensided and polished joints and sheared zones in mudstone and siltstone with some cemented sand/sandstone, and intact shale and coal also being tested. As shown on the lower portion of Fig. 5 the residual angles are higher than for the clay seams but still relatively low with most being under 20°. Apparent residual cohesion values are similar to the Hoek shear box results for clay seams. They should however be viewed with caution since most of the defects tested were in fine grained rocks where it is still possible for pore pressures to develop on the failure surface during shearing. Examination of the samples after completion of the tests often revealed the development of a layer of silt or clay material on the failure surface.

5.4 Application of Results

Low wall dips typically vary between about 10 and 30° which is considerably greater than the residual angle of friction of the clay seam. The effect of cohesion is relatively minor both because of the low values and the size of the failure mass. Clay seams have been found to be generally parallel to the bedding and to extend over considerable areas, thus as shown on Fig. 6 the bottom of the low wall contains a "plug" of rock which is placed in compression. A limiting depth is reached when failure occurs by crushing or buckling of the plug. The major constraints to mine planning identified to date have thus been:

a) that the dumping of overburden spoil on the low wall, thereby placing additional load on the plug, is not feasible except in limited cases without seriously reducing the allowable depth of mining, and

b) that there is a limiting depth to which mining may proceed before further flattening of the low wall is required.

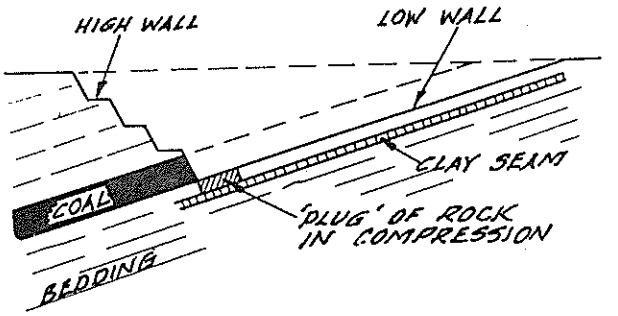

Figure 6 Low wall failure mechanism

6 DIGGABILITY

Part of the planning at Leigh Creek included a review of the most suitable type of excavation equipment for future use as the economic limit of mining with existing draglines was being approached. One alternative is the use of large bucketwheel excavators for overburden and coal removal. One of many tests developed by bucketwheel manufacturers is the chisel cutting resistance (Rasper 1975) which consists of loading a 150 mm cube to failure with a chisel as shown on Fig. 2. Obtaining such large size samples at depth is both difficult and expensive. Samples were obtained at shallow depths by diamond coring in existing mine pits with right circular cylinders being judged sufficiently similar to cubes to not adversely affect results. Considerable care must be exercised in trimming the ends of the cylinders to be smooth and parallel.

It has been recognised (Coleman & Fitzhardinge 1979) that from the geotechnical viewpoint there is considerable similarity between the chisel cutting test and the top half of the point load test as may be seen from Figure 2.

Figure 7 presents a comparison of chisel cutting resistance and Point Load Strength Index. Also shown in the figure are the theoretical correlation obtained between the chisel and point load tests assuming different load conditions applied by the bottom platen in the chisel test. It may be seen that assuming the platen in the chisel test acts as the point of symmetry (applies UDL) of a point load test given a reasonable upper bound for cutting resistance by use of the much simpler and more economical point load strength index which may be carried out on core recovered at any depth.

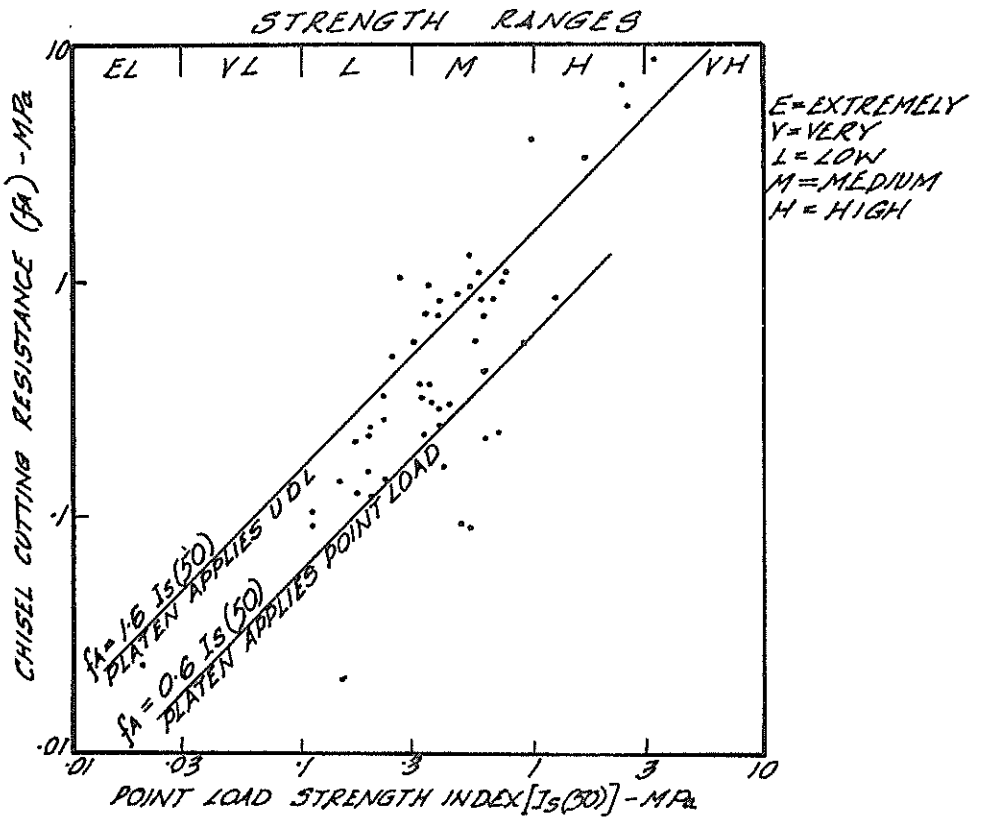

Figure 7 Chisel cutting resistance vs Point Load Strength Index

7 CONCLUSIONS

1. For a large and extended programme such as was carried out at Leigh Creek it is essential to systematically and progressively test all core with a simple and economical classification test which is capable of being correlated with more sophisticated, and usually expensive, tests for use in geotechnical analysis. The Point Load Strength Index has been found to be suitable as such a classification test. It may be readily carried out with portable equipment.

2. Many of the rocks at Leigh Creek are transitional in strength between strong clays and weak rocks and conventional shear boxes designed for soft soils or hard rocks are not ideally suited for determination of residual shear strength parameters. In particular the effect of strain rates needs to be carefully considered.

3. Sufficient movement has occurred along most defects at Leigh Creek to reduce their shear strength value to very close to residual strength and the latter are considered appropriate for use in stability analyses.

4. Correlations between Point Load Strength Index versus Unconfined Compressive Strength and chisel cutting resistance are presented.

8 ACKNOWLEDGEMENT

The Author gratefully acknowledges the permission of the Electricity Trust of South Australia to publish this paper.

9 REFERENCES

BROCH E. & FRANKLIN J.A. (1972). The Point Load Strength Test. Int. J. Rock Mech. Min. Sci. Vol. 9 pp 669-697

COFFEY & PARTNERS PTY. LTD. (1975). South-eastern margin - Report on Geotechnical Studies for Slope Design, Report No. A183/1-1 to Electricity Trust of South Australia. Unpublished.

COFFEY & PARTNERS PTY. LTD. (1979). Results of Geotechnical Investigations (1978), Report No. A183/4E to Electricity Trust of South Australia. Unpublished.

COLEMAN, J.R. and FITZHARDINGE, C.F.R. (1979) The Geotechnology of Excavation Equipment Selection with Particular Emphasis on Bucket Wheel Excavators. Int. Conf. Min. Mach., Brisbane, pp 139-146

HOEK E. & BRAY W. (1974). "Rock Slope Engineering", The Institution of Mining & Metallurgy. London.

I.S.R.M. (1972). International Society for Rock Mechanics Commission on Standardisation of Laboratory and Field Tests suggested methods for determining the Uniaxial Compressive Strength of Rock Material and the Point Load Strength Index - Committee on Laboratory Tests Document No. 1.

RASPER, L. (1975). "The Bucket Wheel Excavator". Trans. Tech. Publications.

Development of a High Pressure Pressuremeter for Determining the Engineering Properties of Soft to Medium Strength Rocks

J. M. O. HUGHES
Director Situ Technology Inc, Vancouver
M. C. ERVIN
Senior Geotechnical Engineer, Coffey & Partners, Sydney

SYNOPSIS

This paper gives some of the details of a pressuremeter developed to work at high pressures in soft to medium strength rocks. It has been used in a wide variety of materials. As the displacements and pressures are measured very accurately using electrical transducers, the modulus and strength characteristics of the rock can easily be measured. Further because the displacements are separately recorded at four positions the anistropic stiffness behaviour can be assessed.

1 INTRODUCTION

This paper outlines the details of an instrument developed for testing soft to medium strength rocks in situ. This instrument is particularly useful in determining the properties of weathered or jointed rock where core recovery is particularly difficult. It is often rocks of this nature which are of prime concern to the geotechnical engineer.

The instrument is placed down a predrilled borehole which in rock does not result in as much adverse disturbance from stress relief as in the case for bore holes in soil. Once in place a flexible membrane clamped to the instrument is expanded radially against the sides of the bore hole, shearing the surrounding rock. Accurate measurements of the displacement allow the rock modulus and the shear strength to be determined.

2 DETAILS OF THE INSTRUMENT

The instrument is very similar in principle to the selfboring pressuremeter developed at Cambridge in the early 1970's (Hughes 1973). It consists of a heavy steel cylinder on which is clamped a flexible membrane, as shown in Figure (1) and Photograph (1). The instrument is placed down a NMLC size hole (76 mm in diameter). When lowered to the appropriate depth the flexible membrane is expanded against the sides of the bore hole by oil. The oil is pumped from the surface by a hand pump. Using this technique pressures as high as 20 mPa (3000 psi) can be reached. This pressure is sufficient to allow rock strengths of up to about 7 mPa to be measured.

The pressure of the instrument is recorded electrically at the instrument and again via a mechanical pressure gauge at the surface. The pressure gauge is at the end of a hydrostatic oil line, hence the pressure recorded is unaffected by the head losses in this line.

With the use of two lines running from the instrument the membrane can be maintained in a collapsed state, even in a dry hole where the balancing hydrostatic forces of the drilling fluid are not present.

The displacements are again recorded electrically by sensors located around the centre of the instrument. Each sensor is recorded separately and can record radial displacement corresponding to an expansion of the bore hole to 85 mm diameter.

If the displacement sensors just record and displacement at points on the membrane the results could be misleading as the sensors could be opposite an anomalous hard or soft spot or even a hole or defect on the borehole wall. The displacement sensors are designed to measure the average displacement over a section 110 mm long and 10 mm wide at four positions 90° apart on the centre line. As each gauge is recorded separately the anisotropic stiffness characteristic of the rock can be assessed.

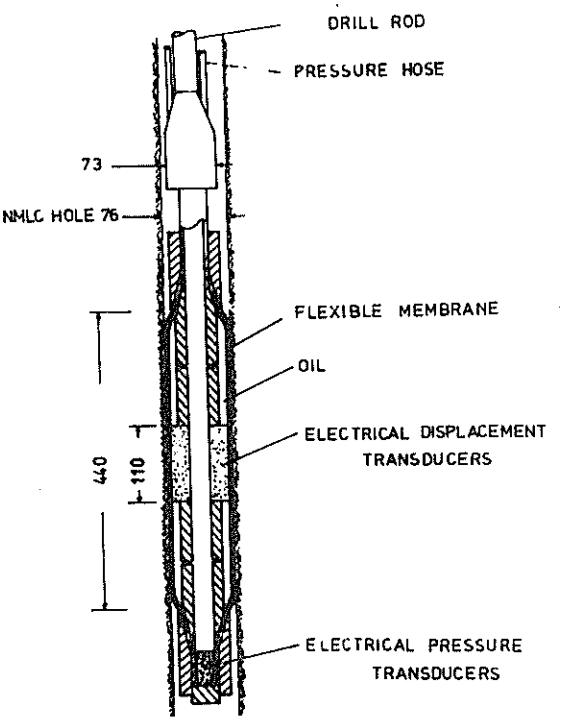

FIGURE (1) - Schematic Details of High Pressure Pressuremeter

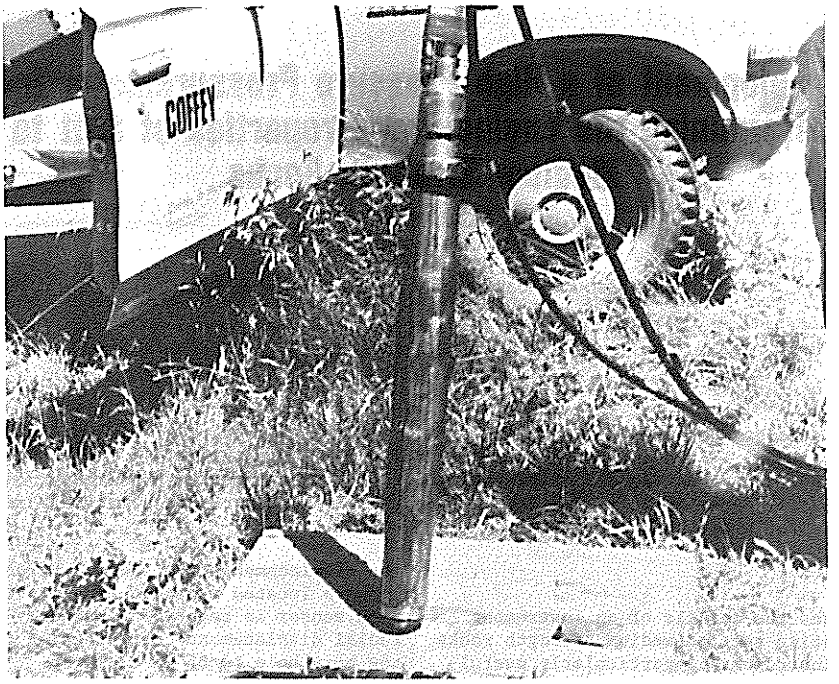

PHOTOGRAPH (1) - General View of Instrument

3.1 TYPICAL RESULTS

If the rock is perfectly homogeneous then the displacement pressure curve for the average of the "north-south" and the "east-west" displacement sensors will be similar and follow the typical form shown in Figure (2).

The curve is divided into three sections as is typical with most pressuremeter results. The membrane expands quickly until it comes in contact with the sides of the bore hole, somewhwere near point B. After this is reached the bore hole tends to expand linearly as the pressures are increased, i.e. B-C.

Beyond this region the strains increase more quickly. At this stage a close watch is kept on the volume of the fluid which is pumped into the instrument. For instance if the membrane is expanded into a cavity in the bore hole wall, remote from the sensors, the membrane could rupture. However, by following both the volume expansion and the displacement sensors a close check can be kept on the behaviour of the membrane expansion.

The result of the pressuremeter test are ideally suited to analysis, probably much more than any other in situ device for the reason that the boundary conditions are very simple. The boundary stresses are uniform and radial as shown in Figure (3a). This is not the case with instruments in which rigid plates are jacked against the sides of a bore hole, such as a Goodman Jack (Goodman et al. 1968), although the force and displacements of the plates in the jack can be accurately measured this does

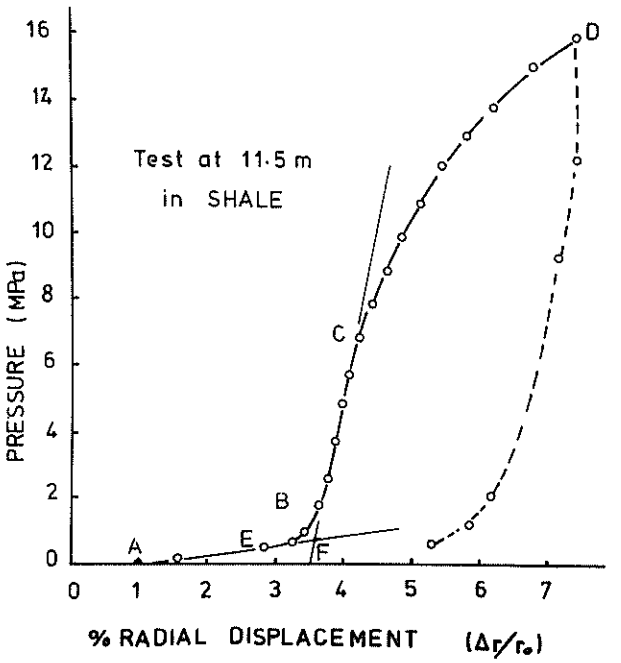

FIGURE (2) - Typical Pressure Displacement Curve. Displacement shown in "N-S" Direction only

not necessarily give a measure of the stresses and displacements in the soil on the boundary of the hole because the geometry of the plates does not match with the geometry of the borehole (Figure (3(b)).

A further consideration is that the pressuremeter tends to shear the soil while the hole expands. In contrast the rigid plate test tends to compress the soil. The typical stress paths for rock elements such as A and B on the borehole wall indicated in Figure (3(a) and (b)) are shown in Figure (4(a) and (b)).

The pressure required to initiate failure for the Jack test in the rock under the plates is very high, i.e. where the stress path CE intersects the failure surface. However, before this pressure is reached failure probably initiates as splitting in the region C, midway between the plates.

In contrast in the pressuremeter test all elements of the rock follow along stress paths such as CF and the pressure required to initiate failure is in the vicinity of point F.

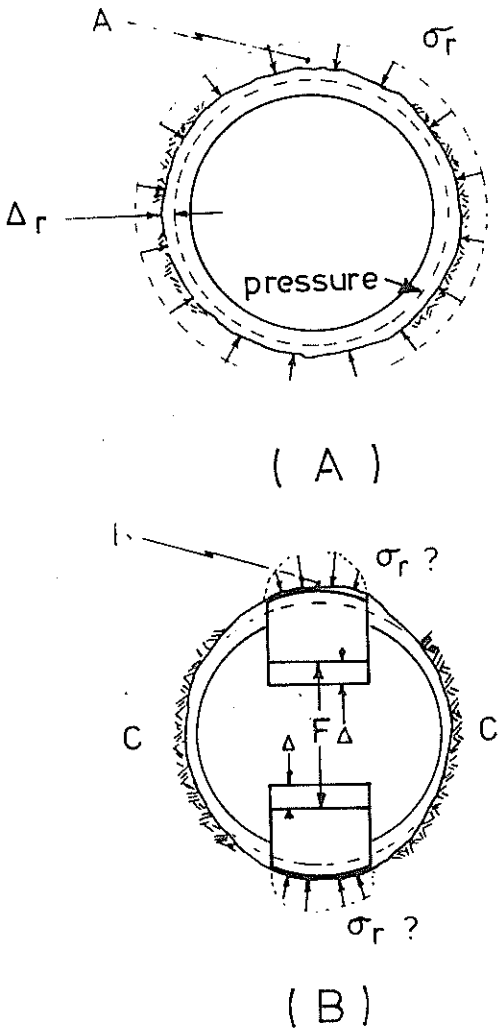

FIGURE (3) - Boundary Conditions on the Wall of the Borehole from (a) Pressuremeter Test (b) Expanding Plate Test

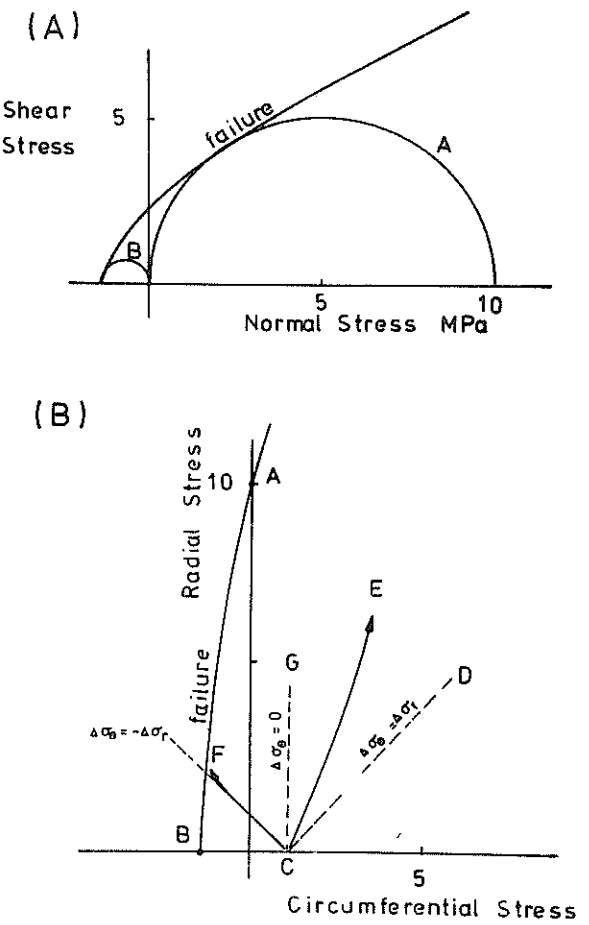

FIGURE (4) - Typical Stress Paths followed for Elements A and B on the Boundary of the Borehole shown in Figure (3(a) and (b))

3.2 MODULUS DETERMINATION

If the rock is considered to be an elastic material then the Young's modulus can be determined by evaluating the slope of the straight sections of the pressure expansion curve.

The Young's modulus is given by:

$$E = (1 + \mu) \frac{dp}{d\ \Delta r/r_o}$$ (Gibson Anderson 1961)

It must be appreciated however that the slope of the curve BC shown in Figure (2) on first loading may well be softer than subsequent unloading. The initial loading represents the "mass" modulus in which joints are closing whereas subsequent unloading and reloading curves indicate a substantially higher modulus, e.g. Figure (5). This higher modulus is probably much more representative of the intact material. The difference between the two moduli give a qualitative indication of the extent of the jointing. The intact modulus can be obtained from laboratory tests on good core samples however it is exceedingly difficult to obtain a "mass" modulus from samples alone.

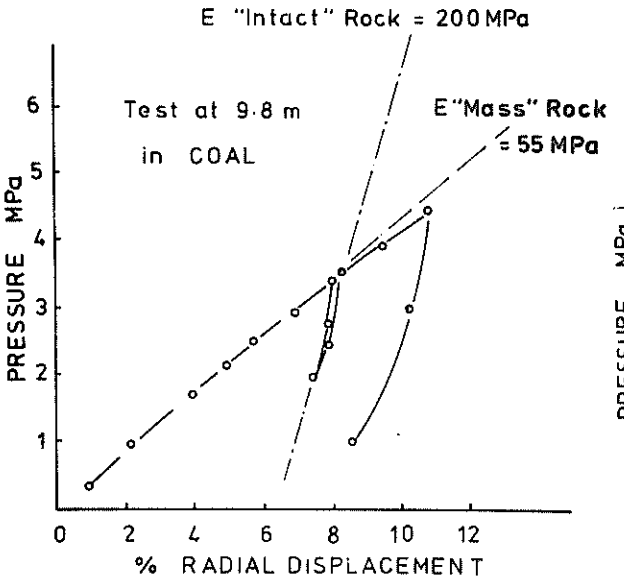

FIGURE (5) - Loading and Unloading Pressure Expansion Curves

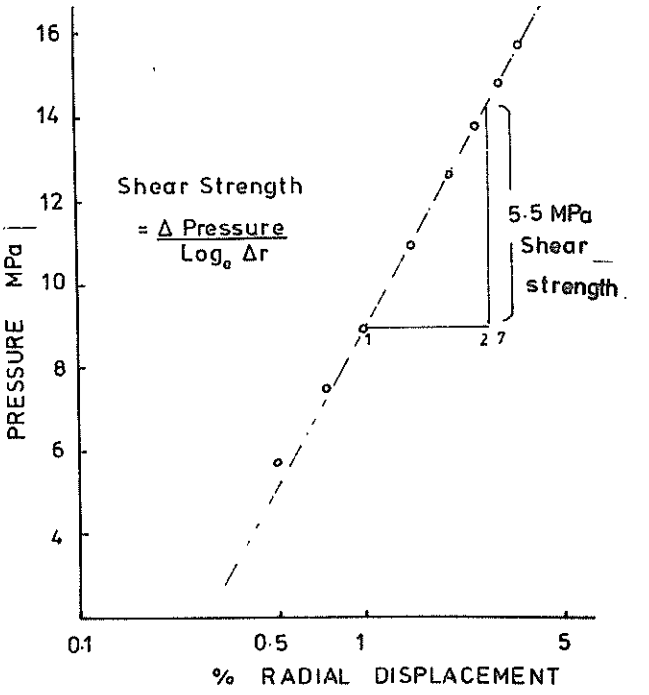

FIGURE (6) - Pressure against Log Expansion for the Test Shown in Figure (2)

3.3 SHEAR STRENGTH

The pressure-displacement response of the rock near failure is governed by three effects:

(a) the shear strength of the intact rock or the shear roughness of the joints;
(b) the dilation or expansion of the rock or joints on shearing;
(c) the modulus.

If a rock shears at constant volume then the pressure required to expand the cavity to a given radius will be considerably different from that required to expand rock of the same shear strength but which dilates on shearing.

Unless there is a unique relationship between the shear strength characteristics and the dilation characteristics it is difficult to separate the two components (Hughes, 1977).

If the pressure expansion curves are analysed on the assumption that the rock fails at a constant shear stress and at constant volume then the shear strength can be determined by the technique developed by Gibson and Anderson 1961. In this method the pressure is plotted against the log of the strain using the in situ stress as the strain origin. For the purposes of this analysis this strain origin is considered to be the point interaction of lines CB and AE, i.e. by the point F in Figure (2).

The slope of this curve is a measure of the

The results of many tests in Silurian Age mudstone and sandstone at a site in Melbourne have been compared with confined compression tests carried out in a Hoek Triaxial cell on corresponding core samples (Figure (7)). The samples are all taken from between 20 and 50 m in depth and during the triaxial tests a constant confining pressure of (690 kPa) has been used in all cases.

It was observed that the measured in situ shear strength was always in excess of the laboratory results. This probably indicates that the rock is expanding while it is shearing or perhaps a very high in situ stress is present in this rock than assumed for the determination of the confining pressure for the laboratory tests.

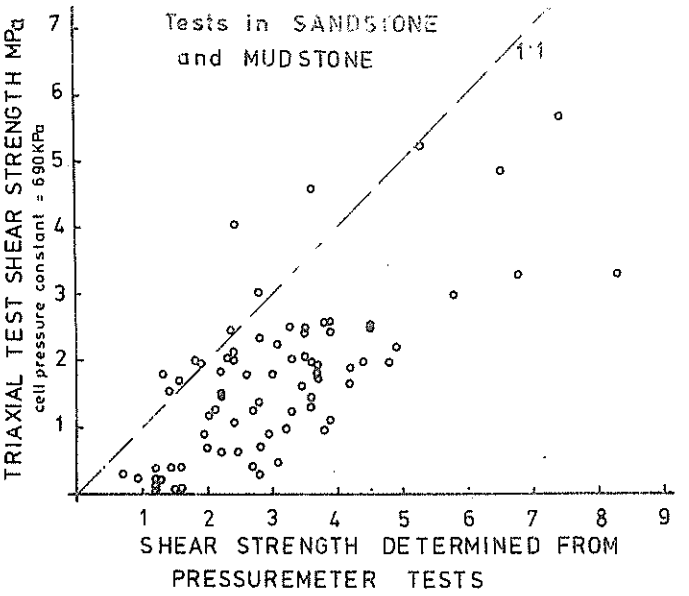

FIGURE (7) - Comparison between the Shear Strength determined from Lab. Tests using a Hoek Cell and the Analysis of the Shear Strength from the Pressuremeter assuming Constant Volume Shearing

3.4 ANISOTROPIC BEHAVIOUR OF THE ROCK

As discussed in Section 2 the displacement can be measured separately at four locations 90° apart on the centre line of the instrument. With this capacity it is possible to observe the anisotropic behaviour of the rock by comparing the average displacement in the "north-south" and the "east-west" directions. The result of a typical test in shale is shown in Figure (8). Clearly there is a distinct difference in the behaviour of the rock in the two directions.

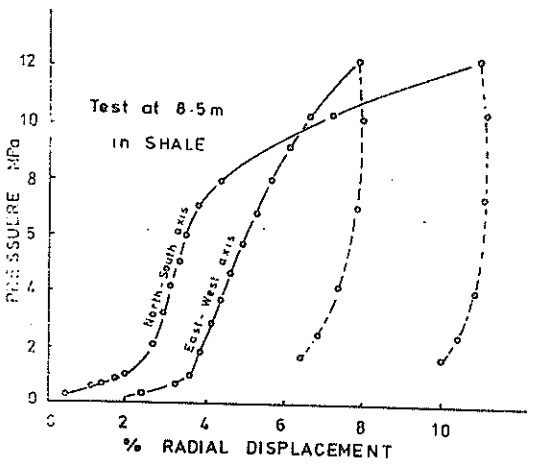

FIGURE (8) - Pressure Expansion Curves showing the Effect of Anisotropy

It is interesting to note that in almost all the tests conducted to date there has been distinct difference between the displacements recorded in the two sensor directions. To determine the true magnitude and orientation of the anistropic behaviour would require a displacement to be observed in at least three directions.

4 CONCLUSION

This paper gives some details of an instrument which was developed to work at high pressures in soft to medium strength rock. In the first year of operation, since the instrument went into commercial use in October 1978 some 800 tests have been performed to depths of up to 60 metres in different parts of Australia and Canada. The instrument has been used in a range of sedimentary rocks, coal, very stiff clays, and very dense sands.

The results have proved particularly successful in determining the modulus and strength characteristics of these materials which, in general may have been difficult to obtain by other in situ methods.

5 REFERENCES

HUGHES, J.M.O. (1973), "An Instrument for the In Situ Measurement of the Properties of Soft Clays", Ph.D Thesis, University of Cambridge

GOODMAN, R.E., VAN, J.K. and KENZE, F.E. (1968), "Measurement of Rock Deformability in Boreholes", Proc. 10th Symp. on Rock Mechanics, Austin, Texas

GIBSON, R.E. and ANDERSON, W.F. (1963), "In Situ Measurements of Soil Properties with the Pressuremeter", Civil Engineering and Publ. Wks. Rev. 56 No. 658, pp. 615-618

HUGHES, J.M.O., WROTH, C.P. and WINDLE, D. (1977), "Pressuremeter Tests in Sands", Geotechnique, Vol. 27, No. 4, pp. 455-477

HOEK CELL, ASTM STANDARD D 2664-67

Determination of the Engineering Properties of the Coode Island Silts using a Self Boring Pressuremeter

J. M. O. HUGHES
Director Situ Technology Inc, Vancouver (formerly Auckland University)
M. C. ERVIN
Senior Geotechnical Engineer, Coffey and Partners, Sydney
J. C. HOLDEN
Senior Materials Engineer, Country Roads Board of Victoria
R. J. HARVEY
Senior Geotechnical Engineer, Coffey and Partners, Sydney

1 INTRODUCTION

The eastern approaches of Melbourne's West Gate Bridge are being constructed as an elevated freeway some 2 km long. For the most part this freeway is being supported on large diameter cast in situ reinforced concrete piles. These piles range in diameter from 1.1 to 1.5 m and are socket ed into Silurian mudstone and sandstone. These piles are generally in excess of 40 m in length. The upper 30 m to 35 m is in alluvial deposits ranging from dense gravels to soft silty clays. The upper 10 m to 20 m of these deposits are in the so-called Coode Island Silts, which are in fact predominantly soft to firm silty clays.

These piles must resist the heavy vertical loads from the dead and live loads of the freeway structures as well as lateral loads imposed by thermal stresses in the bridge deck and substantial construction loads resulting from the prestressing of the deck.

The vertical loads are all assumed to be carried in the mudstone. The method of analysis of these pile sockets is described by Williams (1980). The in situ strength and moduli, required for this analysis, have been determined by pressuremeter testing. A significant portion of this testing has been carried out using a high pressure pressuremeter described by Hughes and Ervin (1980).

The lateral resistance of the piles must be provided by the strength of the Coode Island Silts, particularly the material near the surface. Hence the assessment of the stiffness properties as they relate to the lateral behaviour of the piles is of critical importance to the action of the piles. In view of the importance of understanding the action of these piles, full-scale lateral load pile tests were conducted by the Country Roads Board of Victoria, under the direction of Mr. P. McDonald. As part of this pile load testing programme, an extensive series of in situ tests was undertaken. These tests were conducted in two parts:

Part (A) The determination of the in situ, undisturbed, properties of the Coode Island Silts.

Part (B) The determination of the in situ properties of the Coode Island Silts as they relate to the particular pile installation process.

The lateral load pile tests were conducted on four prototype piles, 1.5 m in diameter, which were loaded by pulling them together and jacking them apart. The results of these full-scale tests and the comparisons with the predictions based on the in situ tests are described by McDonald and Scott (1980) The results reported in this paper relate to the determination of the modulus and the undrained strength of the Coode Island silty clays and their stiffness in relation to the behaviour of the lateral loading of the pile.

2 GENERAL SITE CONDITIONS

The general area of the West Gate Bridge site and the location of the West Gate Freeway in South Melbourne are shown in Figure 1. A simplified geological profile along the line of the freeway is shown in Figure 2. Essentially the Silurian age bedrock is overlain by Tertiary and Quaternary age alluvial deposits, of which the near surface deposits are known as the Coode Island Silts.

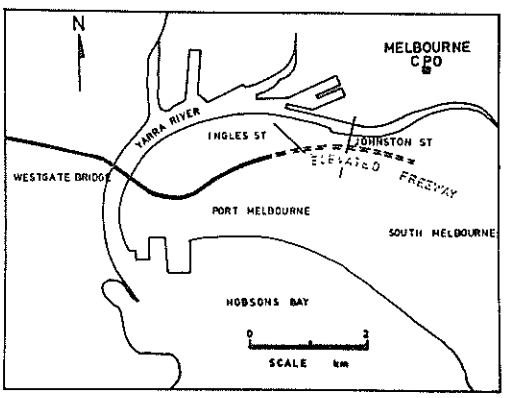

Figure 1 - Location of the West Gate Freeway Project

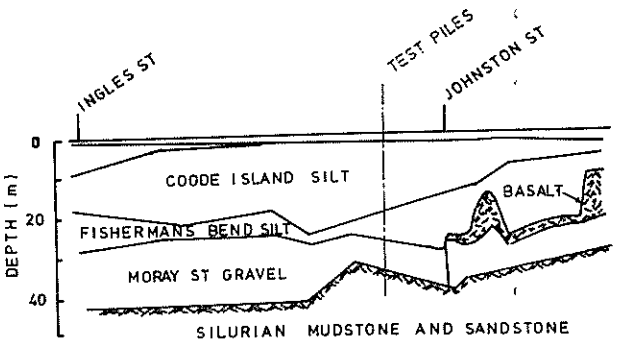

Figure 2 Simplified Geological Section along part of the Freeway

In some areas, generally in the middle of the elevated freeway, some Tertiary age Basalt flows are present within the alluvial deposits. For most of the length of the freeway the lateral resistance to the piles is provided by the soft silty clays in the top 10 metres of the soil. These soils are recent deposits and from Geological evidence they would appear to be normally consolidated. However, the results of both laboratory and field tests indicate they are slightly overconsolidated, probably as a result of dessication, fluctuation in groundwater level and/or aging.

The average moisture content for the silty clays of the Coode Island Silts range from 49-82% and the Liquid Limit and Plastic Index range from 58-103 and 35-80 respectively.

Further, although the material in the top 20 m is described as Coode Island Silts it also contains shell beds and lenses of silt and sand.

3 SITE INVESTIGATION AT TEST PILE SITE

Part (A) The determination of the in situ, undisturbed properties of the Coode Island Silts

This investigation was done using the electrical friction cone penetrometer developed at the Country Roads Board by Holden (1974), a Ménard pressuremeter and a self boring pressuremeter.

The penetrometer does not give a direct measure of either the shear strength or the modulus, however, it does give a measure of the consistency of the material. The results of a typical penetration test are shown in Figure 3. The average cone resistance increases almost linearly until a depth of 14 to about 20 m is reached. The interfingering of numerous sand or shell lenses shows up clearly as spikes on the penetration records. Even though the penetrometer does not give a direct measure of the modulus or the shear strength, numerous authors have made correlations with the penetration resistance Most of these have been summarised by Sangleret (1972)

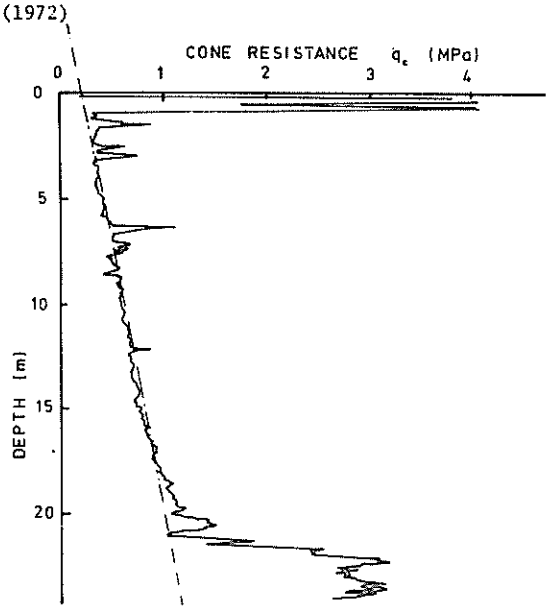

Figure 3 - Cone Resistance against Depth for Piles A and B at Pier 302

For a normally consolidated clay - the generally accepted correlation is:

$$c_u = q_c/10 \text{ to } q_u/15$$

and

$$E = 150 \text{ to } 400\ c_u$$

Using the above correlations with the cone resistances shown in Figure 3 gives the shear strength and modulus graphs in Figure 9a and b. It is interesting to note that the average increase in cone resistance with depth in the upper 12 m for all the tests, which were about 50 m apart, is very similar.

In contrast with the penetrometer, the Ménard-pressure meter is designed to give a direct measure of the modulus and shear strength. The Ménard pressuremeter (Ménard 1957), which is placed down a predrilled hole, is expanded radially against the sides of the borehole during the test. A typical result is illustrated in Figure 4.

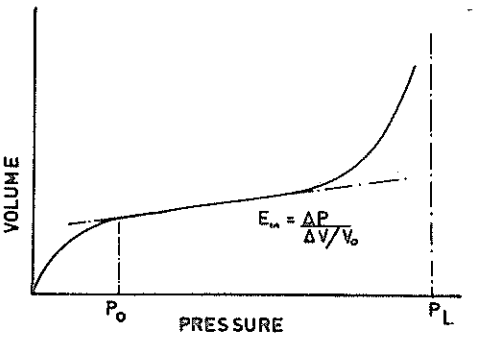

Figure 4 - Typical Ménard Pressuremeter Curve

The modulus is obtained from the flat section of the curve and the shear strength is conventionally evaluated from the difference in pressure between the limiting pressure P_L and the in situ pressure P_o

$$c_u = (P_L - P_o)/5.5$$

The results of the Youngs modulus and undrained shear strength obtained from the Ménard test are shown in Figures 5a and b.

The third instrument which was used extensively at this site was a self boring pressuremeter. The instrument used here is a modified version of the self-boring pressuremeter (Camkometer) which was developed at Cambridge in the early 70's. (Hughes 1973). This instrument essentially consists of a thick walled tube which is slowly jacked into the ground. (Figure 6) The material displaced by the instrument is removed by the action of a central rotating cutter; water or drilling mud is pumped down the central rotating cutter rod and the mud and cuttings return to the surface in the annular space between the cutter rod and the body of the instrument.

Using this technique the instrument can be placed in the ground with the soil surrounding the instrument suffering very little disturbance.

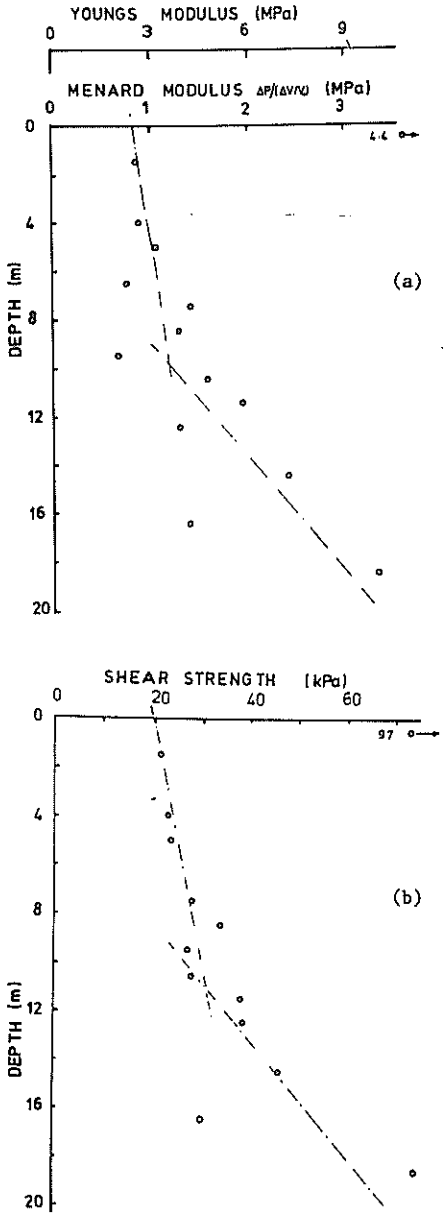

Figure 5 - (a) Modulus and (b) Shear Strength obtained from a Ménard Pressuremeter

Once the instrument is in place the membrane on the outside of the thick-walled tube can be expanded against the undisturbed soil (Figure 6). The pressure required to expand the membrane and the radial displacement of the membrane are recorded electrically with transducers inside the instrument.

The instrument used at the West Gate test site was developed by the first author in conjunction with Coffey and Partners for commercial use, where ease of operation is essential. The instrument can be placed in the ground using virtually any rotary drilling rig.

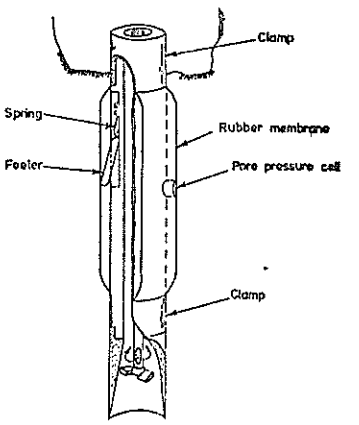

Figure 6 - Self-Boring Pressurementer (Camkometer)

A typical result of a self-boring pressuremeter test is shown in Figure 7. Several features of the behaviour of the soil can be determined from this test. In particular, the in situ lateral stress, the Young's modulus and the undrained stress/strain curve. The in situ lateral stress is considered to be the pressure at which the membrane expands from the body of the instrument. In the test shown on Figure 7 this would correspond to 130 kPa. The in situ Young's modulus is more difficult to determine because the soil in almost all cases is non linear hence the modulus shown is the secant modulus at 1% radial displacement. Clearly if a larger displacement was considered a reduced modulus would be obtained.

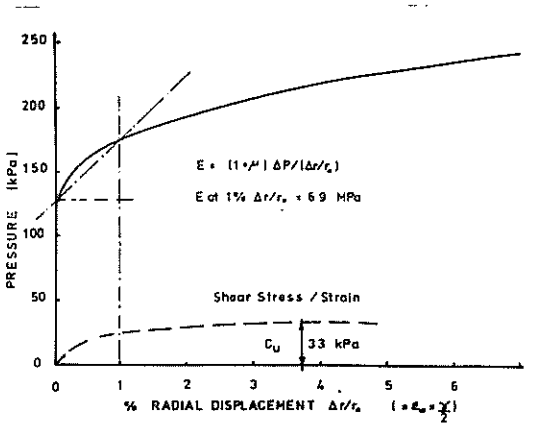

Figure 7 - Typical Pressure Expansion Curve from a Self Boring Pressuremeter

The undrained stress/strain curve is calculated by the method of Palmer (1972). This simple method only requires that the soil deforms radially at constant volume. The stress/strain curve and hence the undrained shear strength is shown on the bottom of Figure 7. The results of the in situ lateral stress, 1% secant modulus and undrained shear strength are shown in Figures 8a, b and c.

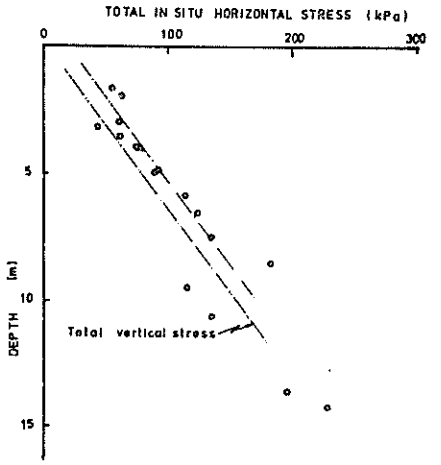

(a)

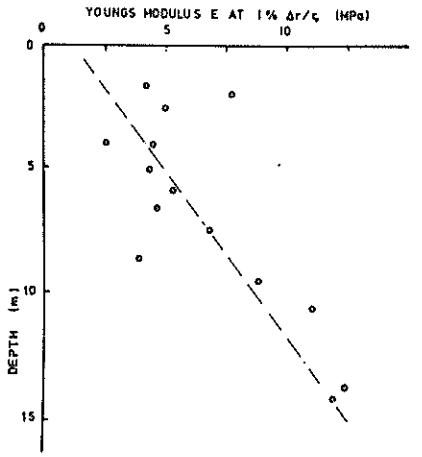

(b)

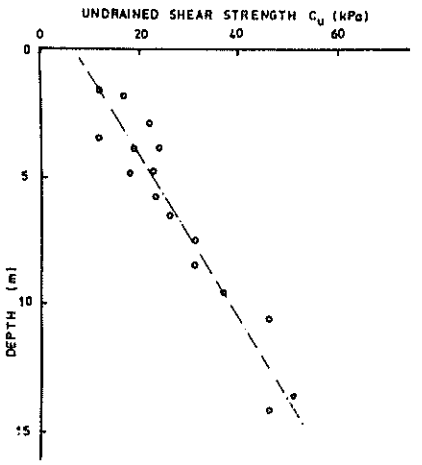

(c)

Figure 8 - (a) Results of the In Situ Lateral Stress (b) 1% Secant Modulus and (c) the Undrained Shear Strength for Tests at Pier 302 from a Self-Boring Pressuremeter

The average modulus and shear strengths for all three methods of in situ test are combined in Figures 9a and b. It would appear that the shear strengths obtained from the various in situ field techniques do not vary too much. However, there is considerable variation in the values and the trend of the moduli obtained from the different techniques. Hence the use of one particular method alone for determining the modulus should be viewed with caution.

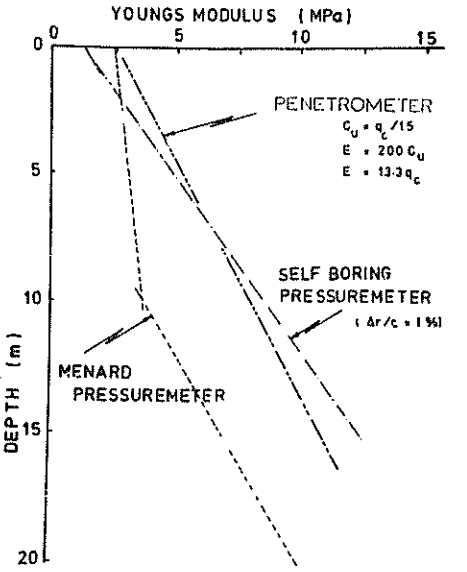

(a)

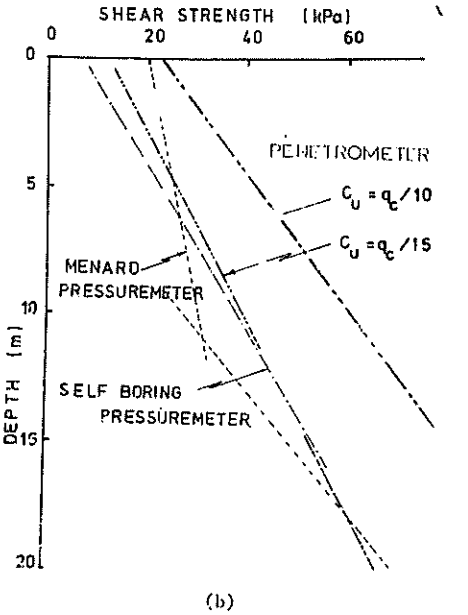

(b)

Figure 9 - (a) Average Moduli and (b) Shear Strengths obtained from a Penetrometer, Ménard Pressuremeter and a SBP

Part (B) The determination of the in situ properties of the Coode Island silty clays as they relate to the particular pile installation process

The piles at this site were constructed by driving casing through the upper layers of soft materials then into the top of the mudstone. The steel casing had a reinforcing shoe which was 25 mm proud of the casing. This construction enabled the inside diameter of the casing to remain constant for ease of construction of the pile sockets, however, it did mean that, in theory at least, a void could be left around the outside of the casing into which the soft soils would flow as shown in Figure 10. In view of the fact that the 25 mm radial gap was large in terms of the shear stresses which would be imposed on the soil as it moved back, it was considered that this effect should be examined in more detail.

(The 25 mm gap is equivalent to a radial displacement of about 3%. If the soil closes back in an undrained state it would experience a 6% shear strain.)

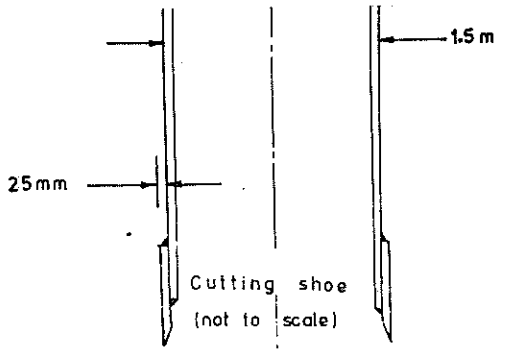

Figure 10 - Details of the Cutting Shoe on the Bottom of the Casing

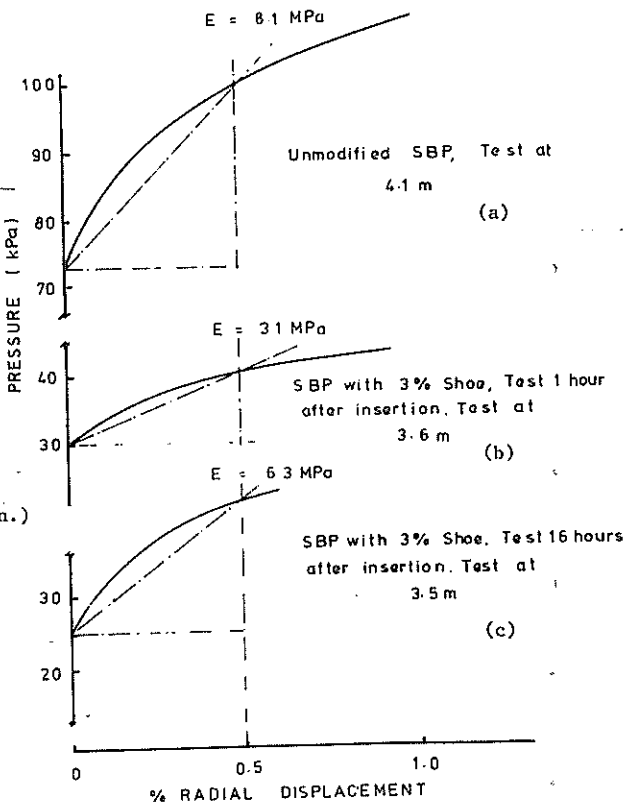

Figure 11 - (b) and (c) Pressure Expansion Curves obtained from a Modified SBP (3% Shoe) Compared with the Unmodified Instrument, (a) for tests at 3.5 - 4 m depth

The self-boring pressuremeter used in the previous study was modified by constructing an instrument with an enlarged cutting shoe which would directly model the geometry of the casing. Two model studies were undertaken. In the first study a 3% enlarged shoe was used and in the second a 6% shoe.

In the first study the instrument was drilled into the ground then either within a few minutes or within 16 hours of insertion the membrane was expanded. This study was to examine the behaviour of the soil on the "front" face of the pile (i.e. the side which is pushed towards the soil). In the second series of tests the instrument was drilled in with the 6% shoe and with the membrane expanded to 3%. After insertion the membrane was allowed to collapse under controlled conditions, thus modelling the behaviour of the "back" face of the pile.

The results of three tests done at about the same depth (around 3.5 - 4 m), but in different holes, are shown in Figure 11a, b and c. The first figure represents the initial in situ undisturbed properties as discussed in Part (A), the second figure represents the pressure expansion curve obtained using the 3% shoe and expanding the instrument within an hour of insertion. The soil has moved back on to the instrument; however, it is much softer. The third figure is the pressure expansion curve obtained about 16 hrs after insertion. Clearly the soil has moved back on the instrument and become much stiffer, almost back to the undisturbed level. However, it is interesting to note that the in situ lateral stress has not been restored in that time. The same pattern of behaviour has also occurred in the results from other depths. Unfortunately only a limited series of testing was done, and further it was not possible to run the tests over a longer period; nevertheless, the trends would appear to show that

(a) the soil quickly moves back against the pile;

(b) the stiffness of the soil is restored within a reasonably limited period of time, although the time taken for the soil to "flow" back about the 1.5 m caisson could well be different from that taken with the 75 mm diameter self-boring pressuremeter;

(c) the in situ lateral stress does not seem to be restored, at least over the above time period.

In the second series of tests in which a 6% oversize shoe was used, the membrane was generally collapsed under controlled conditions within a short time after insertion. These results indicate that the soil had moved back against the membrane but was now considerably softer and of low modulus. Figure 12 shows the results obtained at 5.7 m.

In two tests the membrane was left inflated to 3% overnight and then allowed to collapse. From these tests a considerably higher modulus was observed than for the "immediate" tests.

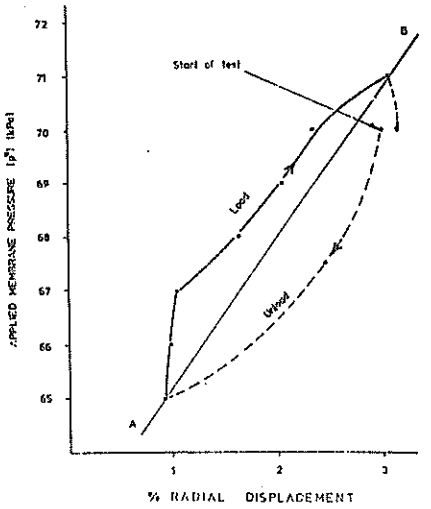

Figure 12 - Pressure Collapse Curves for a 6% to Model the Soil Behaviour on the "Back" Face of the Pile

In conjunction with the above tests, creep or consolidation tests were run in which the pressure in the membrane was kept constant and the strain recorded with time. Two distinct types of results occurred as shown in Figure 13. If the pressure applied was greater than the in situ pressure then the pressure expansion curve followed curve A whereas if the pressure applied was less the in situ pressure expansion curve followed curve B

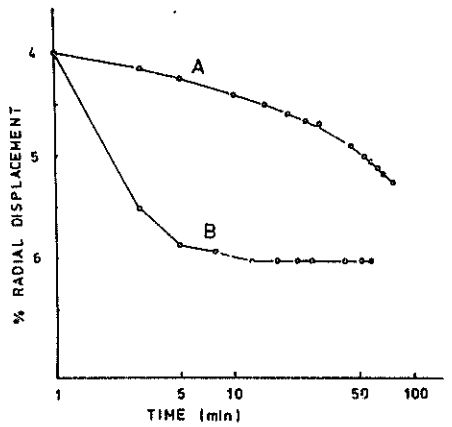

Figure 13 - Consolidation Curves

4 CONCLUSION

The results reported in this paper are all from commercial testing and therefore are perhaps not as precise as those which could be obtained under careful research procedures. Nevertheless the results show that the determination of the modulus of the soil obtained from self-boring pressuremeter tests is promising. Further more for the detailed examination of the behaviour of the actual caisson geometry, a self-boring pressuremeter can be a particularly powerful tool since the boundary conditions are more clearly understood.

5 ACKNOWLEDGMENT

This paper is published with the kind permission of the Chairman of the Country Roads Board of Victoria, Mr. T.H. Russell to whom the authors are grateful for the co-operation received on this project

6 REFERENCES

Williams, A.F. (1980), "The design of piles socket ed into soft rock", Proc. Int. Conf. on Structural Foundations on Rock, Sydney

Hughes, J.M.O., Ervin, M.C. (1980), "Development of a high pressure pressuremeter for determining the engineering properties of soft to medium rocks", Third Aust. N.Z. Geomechanics Conference, Wellington

McDonald, P.. and Scott, G., (1980)- Paper to be presented for publication to ASCE Geotech. Division

Palmer, A.C. (1972), "Undrained plane-strain expansion of a cylindrical cavity in clay : a simple interpretation of the pressuremeter test", Geotechnique, Vol. 22, No. 3, pp. 451-457

Holden, J.C. (1974), "Penetration Testing in Australia - State-of-Art-Report, Proc. European Symposium on Penetration Testing, Stockholm, Vol. 1, p. 155

Sangleret, G. (1972), "The Penetrometer and Soil Exploration ", Elsevier, Amsterdam

Menard, L. (1957), "Measures In-Situ des proprietes Physique des Sols. Annls. Ponts Chauss. 127 No. 14

Hughes, J.M.O. (1973), "An instrument for the in situ measurement of the properties of soft clays", Ph.D Thesis, University of Cambridge

A Down Hole Plate Load Test for Insitu Properties of Stiff Clays

J. NEIL KAY
Senior Lecturer, University of Adelaide
PETER W. MITCHELL
Director, Kenneth W. G. Smith and Associates, Adelaide

SUMMARY The screw plate load test is proposed as a method for field testing of stiff clays. The plate is advanced beyond the bottom of the borehole in a manner that minimizes soil disturbance. Values of undrained modulus, drained modulus, undrained shear strength and coefficient of consolidation are determined in a straightforward test procedure. The fundamental nature of the test as well as preliminary results suggest that extremely valuable data may be obtained at relatively low cost.

1 INTRODUCTION

Because of the difficulties associated with soil sampling and laboratory testing for efficient evaluation of soil properties, investigators have frequently sought suitable field testing procedures. Indeed, under ordinary circumstances, for determination of engineering properties of coarse-grained soils, field testing is the only viable procedure. The disturbance associated with a proper sampling process for soft insensitive clays is not particularly severe but frequent use of field testing procedures such as vane shear tests and Dutch cone penetrometer tests has been made. The methods have tended to become more popular in commercial testing of the latter soil types particularly because of economic advantages to be gained. On the other hand, in the case of stiff clays, there appears to have been a preference for laboratory testing and relatively little effort has been expended on the development of field testing procedures. This situation has prevailed in spite of the fact that it is well established (Hooper and Butler, 1966) that as far as borehole sampling is concerned even the most careful techniques cause considerable disturbance in these soils. Apart from possible direct physical disturbance of the soil structure the relief of high levels of insitu stresses may lead to development of fissures not present in the natural state. Although the original insitu stress conditions may be re-established in the laboratory in conjunction with proper stress path testing techniques the planes of weakness will remain. The test values obtained for strength and deformation parameters may be seriously affected. This has been demonstrated for Adelaide clays by Woodburn (1972). Furthermore, determination of the magnitude of horizontal stress may involve considerable uncertainty, and even when a reasonable prediction of horizontal stress can be made, few laboratories are equipped for testing in accordance with stress path procedures where the coefficient of earth pressure at rest, K_o, is greater than unity. In areas where high levels of solute suction prevail the influence of diffusion of incompatible test fluid may be significant. These arguments appear to indicate a need for a procedure that can economically measure the properties under field conditions before any significant change in the insitu stress condition has occurred. One recent development in this direction has been the self-boring pressuremeter but with this tool there is a question of economic viability for many projects. In this paper an adaption of the screw plate load test is proposed as an alternative.

2 PREVIOUS SIMILAR WORK

The screw plate load test has been used in sands and sandy soils by Janbu and Senneset (1973), Schmertmann (1970) and Dahlberg (1974) and in soft clay soils by Schwab and Broms (1977). In these tests a single pitch helical plate of diameter generally in the range 150 to 250 mm is screwed from the ground surface to the test depth. The load is applied through a hydraulic system to a piston near the plate. At regular intervals of load application the resulting deflection is measured and either or both of compressibility and strength parameters are obtained.

In the United Kingdom load tests using large diameter flat plates have recently been conducted on carefully prepared surfaces in shafts and large diameter boreholes in stiff clay. The Building Research Station (Marsland 1971, 1974) has used 865-mm diameter plates mainly as a control test for evaluation of other methods such as triaxial and cone penetration tests. A smaller version has been used as a commercial test procedure to some extent. Deflection control rather than load control has been the basis of the British tests and considerable attention has been given to test rate. For the 865-mm plate a penetration rate of 2.5 mm/min has generally been used. Tests conducted at rates several times higher and several times lower have shown little change in undrained property values.

3 TEST DESCRIPTION

The test developed at the University of Adelaide incorporates some aspects from both of these test types as well as some additional features. The plate, 88 mm in diameter, is of a low pitch helical form and, for tests in stiff clays, is advanced approximately 100 mm beyond the bottom of a 90-mm diameter pre-drilled hole. The rate of advance per revolution of the plate is controlled by a screw at the surface whose pitch is precisely the same as the underside of the test plate. In this way the axial distortion of the undisturbed soil is minimized during advancement of the plate. The leading edge of the helical test plate is chisel shaped so that the soil is cut and forced upwards into the open hole. Experience has shown that a solid plug of soil forms above the plate. This is significant in that it forms a seal above the plate and minimizes changes in water content or soil suction

during the test period.

The test is in a form that essentially permits the concurrent measurement of undrained modulus, drained modulus, coefficient of consolidation and undrained shear strength. Both a lever arm system and a geared drive are incorporated to enable either load or settlement control as desired. The test unit is shown in Figure 1. The procedure used in the test method is as follows:-

(a) The plate at test depth, 100 mm below the bottom of the drillhole, is loaded to the estimated value of the overburden stress. If movement occurs no further loading is applied until movement is less than 0.0005 mm/min.

(b) An estimate is made of the ultimate capacity of the plate based on the torque required to advance the plate to the test position. A correlation obtained from previous experience is used for this estimate.

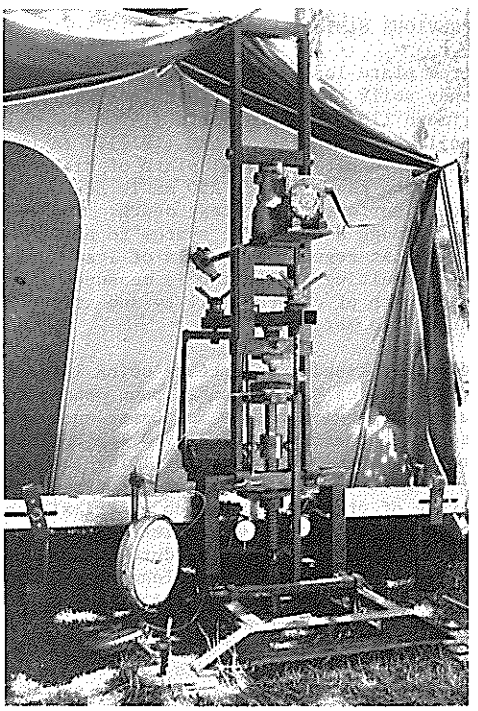

Figure 1 Test Apparatus at Constant Rate of Settlement Stage

(c) A load equal to one third of the estimated net ultimate capacity is applied to the plate through the lever arm system. Deflection readings are taken with time until the deflection is less than 0.0005 mm/min.

(d) The system is then operated in a settlement-controlled mode and the plate is advanced at a rate of 0.25 mm/min until a peak stress level or, alternatively, 2 percent of the plate diameter is reached. Records are taken of both load and settlement.

4 INTERPRETATION OF TEST DATA

4.1 General Load - Settlement Behaviour

The theory used for determination of an equivalent elastic modulus has been reviewed by Selvadurai and Nicholas (1979). They give the relationship for the settlement, $\Delta\rho$, of a loaded horizontal disc in an elastic medium as

$$\frac{\Delta\rho}{\Delta\sigma D/E} = \frac{(1+\upsilon)\sqrt{3-4\upsilon}}{4[1+\{\ln(3-4\upsilon)\}^2/\pi^2]} \qquad (1)$$

where $\Delta\sigma$ is the plate stress increment, D is the plate diameter, and E and υ are the elastic parameters of the medium. The disc is assumed to be rigid, to be bonded to the medium on its underside but to be unbonded on its upper surface.

Finite element studies made by the authors have shown that the effects of an unlined vertical shaft no nearer than one diameter above the disc are negligible. A possible additional source of error in applying the model to soil is the onset of local yield. D'Appolonia et al (1971) have investigated this matter and have shown that, whereas local yield may occur at lower stress levels in normally consolidated clays, such a condition is unlikely at less than 50 percent of the ultimate bearing stress in overconsolidated soils. In the proposed test modulus measurements are restricted to approximately the lower third of the stress range.

4.2 Undrained Modulus - E_u

The substitution, $\upsilon = 0.5$, in Equation 1 for the undrained case yields the equation for undrained elastic modulus, E_u.

$$E_u = 0.38 \frac{\Delta\sigma D}{\Delta\rho} \qquad (2)$$

4.3 Drained Modulus - E_s

Little information is available for υ for the stiff Adelaide clays but the general similarity with London clay in many respects suggests that similar υ values would be reasonable. Wroth (1971) has indicated a value of 0.16 and on this basis the rounded value of 0.2 is chosen. Substitution in Equation 3 leads to:

$$E_s = 0.42 \frac{\Delta\sigma D}{\Delta\rho} \qquad (3)$$

4.4 Coefficient of Consolidation - c_r

Janbu and Senneset (1973) have proposed a version of the square root of time approach for determination of a radial component of the coefficient of consolidation, c_r. According to these authors the time factor, T_{90}, is 0.335 so that

$$c_r = \frac{T_{90} R^2}{t_{90}} = 0.335 \frac{R^2}{t_{90}} \qquad (4)$$

where R is the plate radius and t_{90} the time to 90 percent consolidation.

4.5 Undrained Shear Strength - c_u

For conversion of the ultimate capacity of the plate to an undrained shear strength value Marsland (1974) has used a bearing capacity factor, N_c, of 9.6 for stiff London clays. He cites theoretical values of

about 5 for E_u/c_u ratios near 20 and between 9 and 10 for E_u/c_u greater than 500 obtained from the expansion of a spherical cavity and approximate solutions by Meyerhof (1951, 1961). For Adelaide clays as for London clays the higher figure appears to be more appropriate (Cox, 1970) and the equation used by Marsland is proposed. That is:

$$c_u = q_u/9.6 \qquad (5)$$

where q_u is the net ultimate capacity of the plate.

5 RESULTS OF PRELIMINARY FIELD TESTS

5.1 Tea Tree Plaza Test Site

The first series of tests were conducted in the undrained mode only. (See Figure 2). Both field tests and consolidated (isotropic) undrained triaxial tests on 35 mm diameter samples were conducted on soils from Tea Tree Plaza, an Adelaide shopping centre site. These soils consist of a stiff, highly plastic, pleistocence clay. The deflection rates used were relatively high and 20 percent of the plate diameter was used as the failure criterion. In these tests the bearing stress continued to rise at a relatively rapid rate after the initial yield period and it was only in later tests that the slower penetration rate compatible with that of Marsland (1974) was adopted. The undrained shear strength values obtained are likely to be high because of the high settlement rate and the 20 percent failure criterion. However, the relative results are of considerable interest. A rapid consistent linear increase in strength with depth is observed. There is a similar trend in the results of the triaxial tests but more scatter is apparent. The results for undrained modulus are less decisive but a constant ratio appears likely between modulus and strength. A factor of 4 to 5 appears to exist between laboratory and field results for undrained modulus.

5.2 Victoria Square Test Site

At this site the combined drained - undrained loading procedure was adopted. The soil is a typical Adelaide city soil profile - a stiff, highly plastic, grey-green Hindmarsh clay. The undrained shear strength based on the stress at a deflection of 2 percent of the diameter and a bearing capacity coefficient of 9.6 is indicated in Figure 3. Two of the ten tests, those at 7.5 and 9 metres depth were entirely deflection controlled. The values obtained for undrained shear strength for these cases appear to indicate that an intervening consolidation phase has little influence on the measured undrained shear strength value.

5.3 University of Adelaide Campus Site

For the tests in a brown silty clay at the University of Adelaide campus site, improvement in the apparatus enabled measurement of the additional drained soil parameters in what appears to be a reliable manner.

Figure 4 represents the settlement-time and stress-settlement graphs, respectively, for a typical test at 4.5 metres. The total time for the test including extension of the borehole was about 2 hours. In Figure 4(a) settlement was plotted in terms of square root of time with detailed construction as proposed by Janbu and Sennesett (1973). This enabled determination of undrained modulus, drained modulus and coefficient of consolidation. Drained

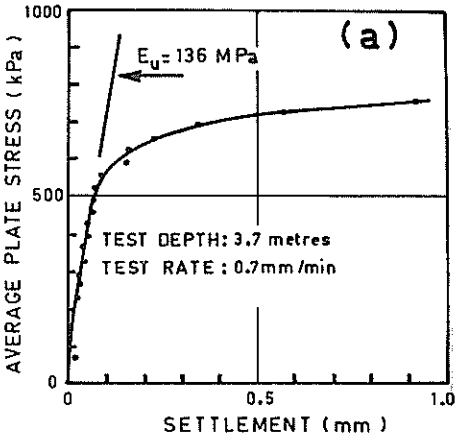

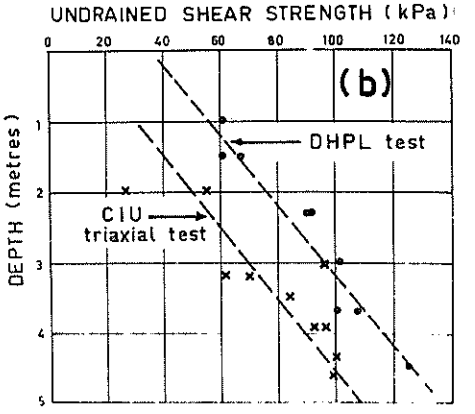

• Indicates result from DHPL test
x Indicates result from CIU triaxial test

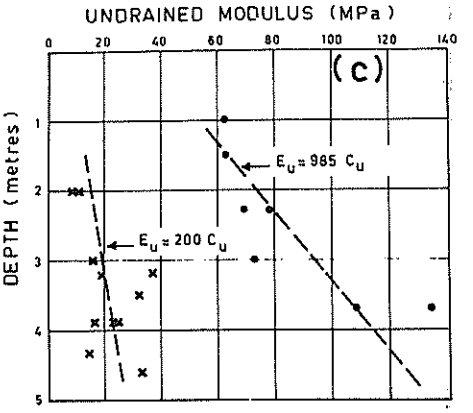

Figure 2 Tea Tree Plaza Controlled Settlement Results

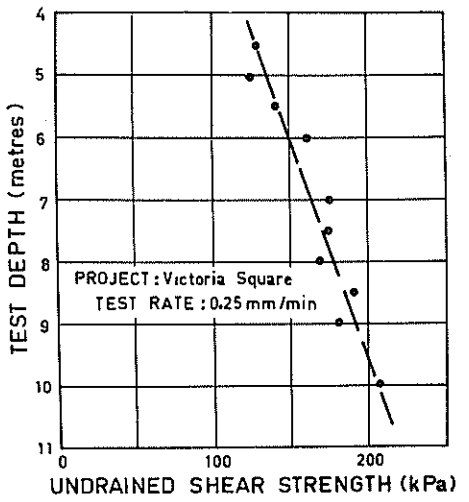

Figure 3 Undrained Shear Strength - Depth Profile for Victoria Square Site

and undrained moduli were found to be 28.3 and 105.7 MPa, respectively. The stress-settlement plot in Figure 4(b) produced the values E_u = 48.9 MPa and C_u = 35.9 kPa. The discrepancy between the two E_u values highlights the arbitrary nature of the usual definition of E_u. It is to be expected that the value for E_u interpreted in an instantaneous sense from the $\sqrt{t}$ plot will be higher than that from a strain controlled test.

6 ADVANTAGES OF THE PROPOSED TEST

6.1 K_o Conditions

Simons and Som (1973) have discussed the influence of lateral stresses on deformation characteristics of London Clay. In particular they indicate that the axial compressibility in a triaxial test is greatly influenced by the ratio of lateral to vertical effective stress. The difficulties associated, firstly, with determining the insitu K_o conditions and, secondly, with reproducing these conditions in the laboratory for stiff clays would tend to indicate that this is likely to be a large source of error in compressibility estimation. The nature of this field test ensures that the true K_o conditions exist at the test start.

6.2 Approximation of True Stress History

The usual aim of the first part of reproduction of the insitu stress history in a laboratory programme is automatically achieved as discussed above. The next step in the laboratory test is to reproduce the stress conditions at representative point at working load (Davis and Poulos, 1968). To apply stresses that correspond to about one third of those associated with the failure stress level is frequently considered appropriate. This is the procedure used in this test. However, there is no control over the horizontal stress in-

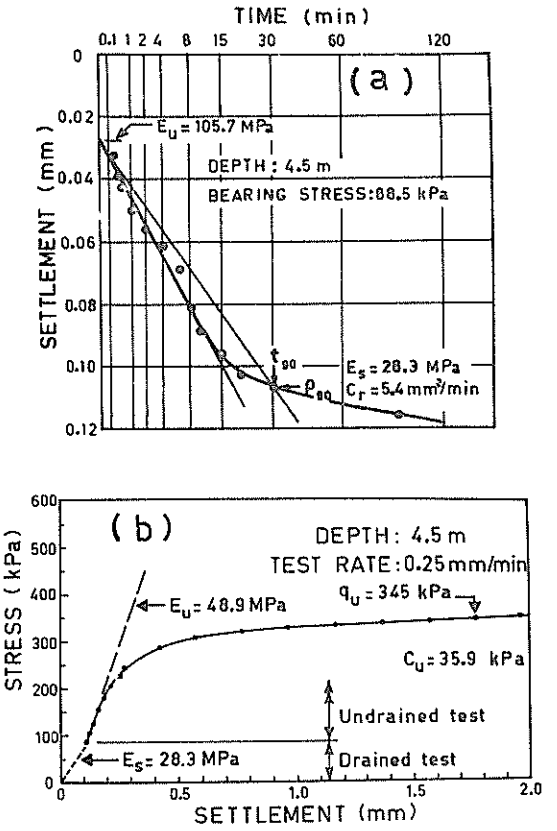

Figure 4 Settlement-Time and Stress-Settlement Results for University of Adelaide Site

crease as in the triaxial test and in this regard the stress path is not entirely reproduced as desired. Nevertheless, the approximation to the required stress path is far superior to that in many test types and certainly to all currently used field tests.

6.3 Test Orientation

The proposed test essentially models a large scale structure and in doing so automatically accounts for some of the complexities. Many other tests fail to do this, and, in these cases, possible effects of anisotropy of soil properties need careful consideration. For most structures a vertical orientation of applied load is appropriate and this is the normal situation for this test. By applying theory appropriate to isotropic conditions, as is usual, it is likely that an equivalent rather than a true property value is obtained. Because of the appropriate orientation of the down hole plate load test it is likely that the equivalent value as obtained in this test is quite appropriate for design.

6.4 Physical Disturbance

The nature of the penetration of the plate ensures little disturbance of the insitu soil.

6.5 Natural Porewater and Temperature Environment

Particularly in the Adelaidearea where soils of high expansion potential are associated with high

solute suctions there is considerable doubt associated with the validity of conventional oedometer and triaxial test procedures. The use of back-pressure testing in conjunction with tap water or distilled water is not possible under these conditions. A field test procedure is a logical alternative where natural porewater conditions appear to be necessary. Proper temperature conditions are sometimes of considerable importance and these too are automatically provided by the insitu test.

6.6 Range of Soil Properties

The single test arrangement can be used to provide a valuable set of engineering properties all of which are potentially more realistic than values obtained by present methods. These include the undrained shear strength, the undrained elastic modulus, the drained elastic modulus and the coefficient of consolidation.

6.7 Economics

Experience to date indicates that a two man crew supported by equipment at a capital cost of about $4000 could complete 3 tests per day including the measurement of drained properties. This would seem to be a viable commercial operation when it is considered that the associated laboratory time would be almost eliminated.

The plate size in use at present is smaller than that used in European practice and much smaller than the British plates. This aspect must be further studied in relation to Adelaide clays as it is likely that lower strengths will be obtained for larger plates as has been the case in Britain due to natural fissures. However, in terms of volume of soil tested, the present size of plate is superior to most laboratory tests and many field tests. Equipment for drilling 90-mm diameter holes exhibits much greater convenience and lower cost. In addition, the reaction requirements are very reasonable even for very stiff soils. This convenient size means that a larger number of tests may be run and better representation of the overall conditions may be obtained. The limitations on test depth are essentially the same as those associated with conventional drilling equipment.

7 SUMMARY AND CONCLUSIONS

Preliminary results obtained from the down hole plate load test apparatus specially developed at the University of Adelaide for testing of stiff clays appear to indicate that it has some potential as both a research and commercial testing tool in these types of soils. In particular, the capability for measurement of drained modulus and coefficient of consolidation in a reasonable test time period is a valuable one. Much work remains to be done to further improve interpretation procedures and to consider the influence of variables such as the test plate diameter. However, there is good reason to believe that the parameters as presently obtained exhibit a higher level of reliability than those associated with many currently used test methods.

8 ACKNOWLEDGEMENT

Financial assistance for the work presented herein was obtained by the first author from the Australian Research Grants Committee.

9 REFERENCES

COX, J.B. (1970) "A Review of the Geotechnical Characteristics of the Soils in the Adelaide City Area", Proceedings of the Symposium on Soils and Earth Structures in Arid Climates, Adelaide, pp. 72-86.

DAHLBERG, R. (1974) "Penetration, Pressuremeter and Screw Plate Tests in a Preloaded Natural Sand Deposit", Proceedings, European Symposium on Penetration Testing, Stockholm, pp. 69-87.

D'APPOLONIA, D.J., POULOS, H.G. and LADD, C.C. (1971) "Initial Settlement of Structures on Clay", Journal of the Soil Mechanics and Foundations Division, ASCE, Vol. 97, No. SM, 10 Oct., pp. 1359-1377.

DAVIS, E.H. and POULOS, H.G. (1968) "The Use of Elastic Theory for Settlement Prediction under Three-Dimensional Conditions", Geotechnique, Vol. 18, No. 1, March, pp. 67-91.

HOOPER, J.A. and BUTLER, F.G. (1966) "Some Numerical Results Concerning the Shear Strength of London Clay", Geotechnique, Vol. 16, No. 4, pp. 282-304.

JANBU, N. and SENNESET, K. (1973) "Field Compressometer - Principles and Applications", Proceedings, 8th International Conference on Soil Mechanics and Foundation Engineering, Moscow, Vol. 1-1, pp. 191-198

MARSLAND, A. (1971) "The Use of In-situ Tests in a Study of the Effects of Fissure on the Properties of Stiff Clays", Proceedings, 1st Australian-New Zealand Conference on Geomechanics, Melbourne, Vol. 1, pp. 180-189.

MARSLAND, A. (1974) "Comparison of the Results from Static Penetration Tests and Large In-Situ Tests in London Clay", Proceedings, European Symposium on Penetration Testing, Stockholm, pp. 245-252.

MEYERHOF, G.G. (1951) "The Ultimate Bearing Capacity of Foundations", Geotechnique, Vol. 2, No. 4, pp. 312-316.

MEYERHOF, G.G. (1961) "The Ultimate Bearing Capacity of Wedge-Shaped Foundations", Proceedings, 5th International Conference on Soil Mechanics and Foundation Engineering, Vol. 2, pp. 105-109.

SELVADURAI, A.P.S. and NICHOLAS, T.J. (1979) "A Theoretical Assessment of the Screw Plate Test", Proceedings, International Conference on Numerical Methods in Geomechanics, Aachen, pp. 1245-1252.

SCHWAB, E.F. and BROMS, B.B. (1977) "Pressure-Settlement-Time Relationship by Screw Plate Tests Insitu", Proceedings of the 9th International Conference on Soil Mechanics and Foundation Engineering Tokyo, pp. 281-288.

SIMONS, N.E. and SOM, N.N. (1973) "The Influence of Lateral Stresses on the Stress Deformation Characteristics of London Clay", Proceedings, 8th International Conference on Soil Mechanics and Foundation Engineering.

WOODBURN, J.A. (1972) "Consolidation and Shear Strength of Swelling Clay Soils", Proceedings, Symposium on Physical Aspects of Swelling Clay Soils, Armidale, pp. 75-80.

WROTH, C.P. (1971) "Some Aspects of the Elastic Behaviour of Overconsolidated Clay", Proceedings, Roscoe Memorial Symposium, University of Cambridge, pp. 347-362.

Author Index